


# Advancing the physical chemical understanding of coffee foam

**by**

**Christos Papageorgiou**

**Thesis submitted to the University of Nottingham for the Degree of Doctor of Philosophy**

**Division of Food, Nutrition and Dietetics**
**School of Biosciences**
**University of Nottingham**

**November 2023**

To my father,
Michalis

# ABSTRACT

Coffee foam is one of the important sensory characteristics of brewed coffee and defines the quality of a cup of coffee. However, there are no published mechanisms that describe the stability of the coffee foam system. The present PhD thesis aimed to advance the physical-chemical understanding of coffee foams in the pursuit of manufacturing high quality coffee beverages.

Firstly, the foam quality of 41 instant coffee was assessed and their performance was compared with a control instant coffee sample. It was found that 21 instant coffee samples were significantly ($p<0.05$) different from the control instant coffee in terms of foam quality. Foaming assessment experiments on coffee extracts from beans roasted to a range of degrees (0,2,4,6 minutes) showed that foam ability was significantly ($p<0.05$) increased only after 6 minutes of roasting. It was concluded that roasting degree plays a significant role in foam quality performance, and it was hypothesised that roasting generates foam-promoting compounds.

Chemical differences among the 21 instant coffee samples and control were established by employing targeted and untargeted metabolomic techniques via high resolution LC-MS-MS. The relative abundance of each chemical entity and foam quality performance parameters were correlated, in order to find which chemical compounds in coffee are associated with good foam quality. Six chemical compounds (Mannotetraose, Cyclo(Phe-Val), Cyclo(Pro-Val), Cyclo(Phe-Phe), Cyclo(Leu-Phe) , Cyclo(Phe-Phe)) were found to be strongly correlated with foam quality performance (Pearson's $R>0.87$) and can be considered as good foam quality markers in the instant coffee process.

The role of 6 key foam compounds on foam quality was investigated by spiking each chemical compound at various amounts in a poor foaming coffee and assessing the foam quality. Cyclo(Pro-Val) was found to influence foam performance by increasing the bubble count per $mm^2$. Therefore, Cyclo(Pro-Val) may reduce the coalescence rate during the aeration step or contribute to lowering the foam disproportionation rate. The dynamic surface tension of Cyclo(Pro-Val) over 30 minutes at 20˚C showed that it was similar to the surface tension of water at 20˚C. Hence, it was hypothesised that Cyclo(Pro-Val) might not be adsorbed on the air/beverage interface but interact with other molecules in coffee and influence foam quality through synergy.

Finally, comparison of the chemical profile of coffee brews across different degrees of roasting, showed that Cyclo(Pro-Val) along with the rest of the cyclopeptides are indeed generated during roasting, probably by the reported breakdown of proteins. Untargeted metabolomic analysis on the same coffee brews showed that the oligopeptide N-[(R)-3-[(**L-Val-L-Pro-)**Amino]-1,2-dioxopentyl]-D-Leu-L-Val-OH, which is associated with good foam quality performance, is generated during roasting and it might be the precursor compound for Cyclo(Pro-Val).

The utilization of key foam compounds as foam quality markers in the instant coffee process may assist in maintaining or improving the quality of the manufactured coffee products.

# ACKNOWLEDGEMENTS

I would like to express my sincere gratitude to my academic supervisors, Dr. Tristan Dew, and Dr. Jo Gould for their guidance, encouragement, and invaluable support through the project.

I would like to express my sincere gratitude to my industrial supervisor Borja Roman Corrochano, Robert Farr, and Joe Welsh, whose contribution, guidance, and expertise were instrumental for completing this thesis.

Within University of Nottingham, I would like to express my appreciation to the technical team of School of Biosciences for their hard work, and for making the required adaptations to make the laboratories a safe working environment, especially during the pandemic. Special thanks go to Louise Williams for her encouragement and for being a great lab companion.

Within Jacobs Douwe Egberts, I would like to thank Cameron Duhig and Mark Al-Shemmeri for organising the roasting trials and acquiring the coffee samples of the present thesis. My sincere thanks go to Dirk Jan Steenbeek for his excellent collaboration and assistance during my laboratory time in Utrecht.

I would be ungrateful, if I have not expressed my appreciation to Prof. Serafim Bakalis and Sian Henson. Their contribution, support, and guidance - especially at the first stages of this journey - are most acknowledged.

I would like to thank my beloved friends, Theocharis, Eleni, Yiannis, Kostas, and Simos for their true friendship and for the good times we have together. Special thanks go to Alexandra for always being there for me, for her unconditional support and for making the days of this journey a little brighter.

Last but not least, I want to thank my parents, Michalis, and Despoina and my sister Anastasia for being there for me, for their emotional support and for always being proud of me.

# TABLE OF CONTENTS

ABSTRACT ..... II
ACKNOWLEDGEMENTS ..... IV
TABLE OF CONTENTS ..... VI
LIST OF FIGURES ..... IX
LIST OF TABLES ..... XVI
LIST OF EQUATIONS ..... XIX
NOMENCLATURE ..... XX
Chapter 1: Introduction ..... 1
1.1 Background and objectives ..... 2
1.2 Relevance to Jacobs Douwe Egberts ..... 3
1.3 Thesis layout ..... 4
Chapter 2: Literature Review ..... 6
2.1 Introduction ..... 7
2.2 Coffee production process ..... 7
2.2.1 Coffee cultivation ..... 7
2.2.2 Coffee harvesting ..... 8
2.2.3 Coffee processing (Unwashed and Washed method) ..... 8
2.2.4 Roasting ..... 9
2.2.5 Instant coffee process ..... 10
2.3 Coffee chemistry and foam stability ..... 11
2.3.1 Carbohydrates ..... 11
2.3.2 Lipids ..... 19
2.3.3 Phenolic acids ..... 23
2.3.4 Nitrogen Compounds ..... 29
2.3.5 Melanoidins ..... 33
2.4 Beer foam stability ..... 41
2.5 Aspects of coffee foam stability ..... 45
2.6 Conclusions ..... 47
Chapter 3: Foam Quality of Coffee ..... 48
3.1 Introduction ..... 49
3.2 Materials and Methods ..... 49
3.2.1 Materials ..... 49
3.2.2 Moisture content determination of instant coffee samples ..... 53
3.2.3 Lipid content determination – Soxhlet extraction ..... 53
3.2.4 Heat treatment of instant coffee samples ..... 56
3.2.5 Sample Preparation for foam ability and foam stability experiments ..... 56
3.2.6 Roasting of green coffee beans ..... 57
3.2.7 Freezer milling and sieving of whole coffee beans ..... 58
3.2.8 Coffee extraction protocol ..... 58
3.2.9 Total solids determination ..... 59
3.2.10 Aeration protocol ..... 60
3.2.11 Foam ability and foam stability experiments ..... 60
3.2.12 Data analysis ..... 60
3.2.13 Statistical analysis on the volume of foam ..... 61
3.2.14 Correlation Analysis ..... 61
3.3 Results and Discussion ..... 62
3.3.1 Aeration protocol development ..... 62
3.3.2 Foam quality – Screening process ..... 64
3.3.3 Evaluation of Foam Stability ..... 69
3.3.4 Foam quality and Lipid content ..... 77

3.3.5 Foam assay on defatted instant coffee samples ..... 87
3.3.6 Foaming assay on the heat-treated instant coffee samples ..... 90
3.3.7 Grinding, sieving and extraction of green and roasted whole beans. ..... 97
3.3.8 Effect of roasting degree and instant coffee process on foam quality. ..... 104
3.4 Conclusions ..... 117

Chapter 4: Screening of polyphenols in coffee via LCMS ..... 118

4.1 Introduction ..... 119
4.2 Materials and Methods ..... 120
4.2.1 Chemicals ..... 120
4.2.2 Instant coffees ..... 121
4.2.3 Instant coffee sample preparation for chemical analysis ..... 122
4.2.4 Chemical reference standard preparation for MSI Level 1 Metabolite Identification ..... 122
4.2.5 Chemical analysis with high-resolution liquid chromatography-mass spectrometry method ..... 123
4.2.6 Data analysis ..... 126
4.2.7 Level 2 identification of chemical compounds via MS2 analysis ..... 127
4.3 Results and discussion ..... 129
4.3.1 Method development of targeted chemical analysis ..... 129
4.3.2 Results of targeted chemical analysis ..... 147
4.4 Conclusions ..... 158

Chapter 5: Untargeted chemical analysis of coffee samples of differing foam quality ..... 159

5.1 Introduction ..... 160
5.2 Materials and Methods ..... 160
5.2.1 Chemicals ..... 160
5.2.2 Instant coffees ..... 161
5.2.3 Instant coffee sample preparation for chemical analysis ..... 161
5.2.4 Chemical analysis with high-resolution liquid chromatography-mass spectrometry method. ..... 161
5.2.5 Data analysis ..... 162
5.3 Results and discussion ..... 164
5.3.1 Correlation analysis ..... 164
5.3.2 MSI Level 2 identification of chemical compounds via MS2 analysis ..... 169
5.3.3 Validation of key foam target identities ..... 179
5.4 Conclusions ..... 186

Chapter 6: Influence of key foam compounds on foam quality ..... 189

6.1 Introduction ..... 190
6.2 Materials and Methods ..... 190
6.2.1 Chemicals ..... 190
6.2.2 Instant coffee ..... 190
6.2.3 Fine quantitation of candidate molecules in coffee samples via high-resolution liquid chromatography-mass spectrometry ..... 191
6.2.4 Instant coffee sample preparation for surface tension measurement and foam analysis via KRÜSS Dynamic foam analyser 100 ..... 191
6.2.5 Density measurement of instant coffee solution ..... 192
6.2.6 Surface Tension measurement ..... 192
6.2.7 Foam quality assessment via KRÜSS Dynamic Foam Analyser 100 ..... 192
6.2.8 Data analysis ..... 193
6.2.9 Statistical analysis ..... 193
6.3 Results and Discussion ..... 194
6.3.1 Quantification of candidate compounds in coffee samples with standard addition method 194
6.3.2 What is the effect of coffee matrix on ionisation of cyclo dipeptides? ..... 204
6.3.3 Estimating the concentration of Mannotetraose ..... 207
6.3.4 Assessing the foam quality of spiked instant coffees with key foam metabolites. 210
6.3.5 Dynamic surface tension of instant coffee ..... 230

6.4 Conclusions ..... 238

Chapter 7: Comparing the chemical profile of aqueous coffee brews across the roasting process and instant coffee manufacture ..... 240

7.1 Introduction ..... 241
7.2 Materials and Methods ..... 241
7.2.1 Chemicals ..... 241
7.2.2 Coffee samples ..... 242
7.2.3 Sample preparation for chemical analysis via high-resolution liquid chromatography-mass spectrometry ..... 242
7.2.4 Fine quantitation and screening of polyphenols and key foam compounds in coffee samples via high-resolution liquid chromatography-mass spectrometry ..... 243
7.2.5 Untargeted chemical analysis of coffee samples via high-resolution liquid chromatography-mass spectrometry ..... 243
7.2.6 Statistical analysis ..... 243
7.2.7 Correlation analysis ..... 244
7.3 Results and discussion ..... 244
7.3.1 Fine quantitation and screening of polyphenols and key foam compounds in coffee samples via high-resolution liquid chromatography-mass spectrometry ..... 244
7.3.2 Untargeted chemical analysis of coffee samples via high-resolution liquid chromatography-mass spectrometry ..... 259
7.4 Conclusions ..... 280

Chapter 8: Conclusions and Future Work ..... 282

8.1 General conclusions ..... 283
8.2 Future work ..... 287

Reference ..... 290

Appendix A: Foam height curves fit ..... 305

Appendix B: Find by Formula Parameters ..... 317

Appendix C: Chromatography column vs non-polar mobile phase system. ..... 320

Appendix D: Initial list of polyphenols reported in coffee. ..... 332

Appendix E: List of phenolic compounds found by Find by Formula function in control instant coffee. 339

Appendix F: Extracted ion chromatographs from Polyscreen mk1 to mk6. ..... 343

Appendix G: MS2 annotation results of polyphenols ..... 373

Appendix H: Recursive extraction parameters ..... 393

Appendix I: Mass Profiler Professional settings ..... 397

Appendix J: MSI Level 2 annotation results of untargeted chemical analysis ..... 402

Appendix K: MS1 and MS2 spectra of key foam targets ..... 423

Appendix L: Standard curves of key foam compounds prepared with standard addition method 437

Appendix M: Standard curves of key foam compounds prepared without standard addition method 440

Appendix N: Standard curves for major polyphenols in coffee samples. ..... 442

Appendix O: MSI Level 2 annotation of chemical compounds significantly affected by roasting degree or instant coffee manufacture. ..... 445

Appendix P: Relative abundance values of MS2 annotated polyphenols in coffee ..... 475

Appendix Q: Foam quality assessment of centrifuged and ultracentrifuged control instant coffee ..... 480

# LIST OF FIGURES

Figure 2-1 (a) Proposed structure of green coffee bean arabinogalactan-protein. Adapted from (Nunes *et al.*, 2008), (b) (i) Proposed structure of AGP from Acacia senegal gum polypeptide backbone which is substituted with AG moieties, (b) (ii) Proposed structure of the polypeptide backbone and the AG polymer enlarged. Adapted from Fincher, Stone and Clarke (1983). ..... 16
Figure 2-2 Quinic acid and hydroxicinamic acid esterified to form chlorogenic acids. Picture adapted from Bee et al. (2005). ..... 24
Figure 2-3 Possible reactions of chlorogenic acids during roasting: (a) lactonization, (b) water elimination, (c) water addition, (d) trans-cis isomerisation, (e) epimerization, (f) oxidation, (g) acyl-migration. Image adapted from Jaiswal et al. (2012). ..... 27
Figure 2-4 Chemical reactions during roasting of coffee bean. Figure adapted from Viani, Rinantonio; Petracco (2012). ..... 34
Figure 2-5 Structure of CROSSPY 1,4-bis-(5-amino-5-carboxy-1-pentyl) pyrazinium radical cation. Figure adapted from Hofmann, Bors and Stettmaier (1999a). ..... 36
Figure 2-6 Chemical reaction paths of CROSSPY as intermediate for brown coloured material generation. Figure adapted from Hofmann and Schieberle (2002). ..... 37
Figure 3-1 Control's coffee foam aerated at different stirring speeds and aeration times. n=5. Different letters indicate a significant difference between samples at $p<0.05$. ..... 63
Figure 3-2 Foam ability of instant coffee samples (% on foam ability of control instant coffee). n=5 Samples marked with * were significantly different from control in terms of foam ability. ..... 65
Figure 3-3 Foam height of Control at 0 min (left) and 30 min (right) after aeration. ..... 66
Figure 3-4 (a) & (b) Example of bubble disproportionation. (c) &(d) Example of bubble coalescence ..... 67
Figure 3-5 Foam stability evaluation. (a) Volume of foam vs time for JDE pilot plant samples, (b) JDE freeze-dried commercial samples , (c) JDE freeze-dried commercial samples, (d) JDE spray-dried commercial samples, (e) Nescafe Gold Blend series, (f) Nescafe Original and Nescafe Azera series ..... 68
Figure 3-6 Fitted curve on foam height of control coffee. ..... 70
Figure 3-7 Calculated foam stability parameters for foam height curves ..... 71
Figure 3-8 Volume of liquid vs time data points for control coffee sample (n=5). ..... 72
Figure 3-9 Volume of liquid retained in foam structure vs time for control instant coffee (n=5). ..... 73
Figure 3-10 Calculated liquid retention parameters for instant coffee samples. ..... 74
Figure 3-11 Comparison of B and D parameter for foam height and liquid height data points 75
Figure 3-12 Foam quality parameters of instant coffee samples that are significantly different from the control coffee. ..... 77
Figure 3-13 Lipid content of instant coffee samples which are significantly different from control in terms of foam ability. (n=3) ..... 78
Figure 3-14 Correlation analysis of lipid content against the foam quality parameters (i.e. Foam Ability, Drainage rate, Disproportionation/Coalescence rate) ..... 79
Figure 3-15 Cluster analysis technique (left side: Elbow Method, right side: Silhouette Scores) for (a) Foam Ability vs lipid content data set, (b) Drainage rate vs lipid content data set, (c) Disproportionation/Coalescence rate vs lipid content data set. ..... 83
Figure 3-16 Cluster analysis of each data set (i.e. Foam Ability vs lipid content, Drainage rate vs lipid content, Disproportionation/Coalescence rate vs lipid content) ..... 84
Figure 3-17 Lipid content and foam quality of native and defatted instant coffee samples. Number of replicates for foam quality=5, Number of replicates for lipid content=3 ..... 88
Figure 3-18 Defatted control coffee which is contaminated with cellulosic material from the filter paper. ..... 89
Figure 3-19 Proposed metabolic pathway of production of 4-vinylcatechol oligomers (1 to 9a/b) from 5-O-caffeoylquinic acid (A) and caffeic acid (B) via 4-vinylcatechol as an intermediate metabolite (C1). Image adapted from Frank et al., 2007. ..... 91
Figure 3-20 Heat-treated control instant coffee for 20 minutes at 150˚C (Top image), 185˚C (Middle image), 220˚C (Bottom image) ..... 93

Figure 3-21 Foam quality parameters of (top to bottom) native control and vacuum-dried, Control, heat-treated control (150˚C) and defatted control. Different letters indicate significant differences at p<0.05. (n=5)..... 94
Figure 3-22 Foam quality of native, heat treated at 150˚C and Defatted FD5 instant coffee sample..... 96
Figure 3-23 Bio - pulveriser..... 98
Figure 3-24 Punctured GF/C RTU glass microfiber filter paper-1.2 um pore size diameter (Cytiva, Sheffield, UK) ..... 102
Figure 3-25 Whatman Filter Paper Chart..... 103
Figure 3-26 Roasting profile, Colour, Mass of beans and Bulk density of roasted beans at 120,240 and 360 seconds..... 106
Figure 3-27 Total solid content (%) of coffee extracts at different roasting degrees for Arabica Nicaragua Washed, Arabica Brazil Unwashed, and Robusta Vietnam Unwashed (n=3). Coffee/Water ratio: 18g/300mL. Statistical analysis was performed on each bar plot separately. Different letters indicate significant differences at p=0.05 ..... 107
Figure 3-28 Foam quality parameters for Arabica Nicaragua Washed, Arabica Brazil Unwashed and Robusta Vietnam Unwashed green and roasted bean extract. Disproportionation/ Coalescence rate were determined only for samples with 6 minutes of roasting. Statistical analysis were performed throughout the sample set. Different letters indicate significant differences at p=0.05. Statistical analysis performed per column. ..... 108
Figure 3-29 Foam height vs time curve for Arabica Nicaragua Washed at 6-minute roast. The black arrow indicates the time when bubbles pop. .....113
Figure 3-30 Collapsed foam system of Arabica Nicaragua Washed R6 minutes. .....113
Figure 3-31 Foam quality parameters of green, roasted, and instant coffee products. Coffee samples concentration was normalised in 1.5% w/w. Different letters indicate significant differences at p=0.05. Statistical analysis performed per box .....114
Figure 4-1 Extracted ion chromatographs of C7H8O2 (i.e. 3-methylcatechol or 4-methylcatechol) for every combination of mobile phase B and column phase. (a) Biphenyl-Acetonitrile, (b) Biphenyl-Methanol, (c) C18-Acetonitrile, (d) C18-Methanol. The presented peaks indicate chemical entities where their molecular mass is equal to the molecular mass of C7H8O2. In three out of four extracted chromatographs (i.e. a,c,d) the tallest peak showed a shoulder effect, which means that the specific chemical compound was eluting at a close retention time with another compound. The methanol-biphenyl column solved this issue; therefore it was considered as the optimum combination for achieving good native separability. ..... 132
Figure 4-2 Summary heatmap of separability of each column-mobile phase system for every chemical entity. Legend: Y: Good Separability, N: Poor Separability, Grey tiles indicate that no extracted ion were found for all four combinations of mobile phase and column phase so no conclusion could be shaped. ..... 132
Figure 4-3 Left: Gradient of mobile phase A, Right: Gradient of mobile phase B. Legend applies to both plots. ..... 135
Figure 4-4 Separability of each Polycreen method for mono-feruloylquinic acid (C17H20O9). ..... 137
Figure 4-5 Summary heatmap of separability of Polyscreen method for every chemical entity. Legend: Y: Good Separability, N: Poor Separability ..... 138
Figure 4-6 Total Ion Chromatograph of instant coffee sample via Polyscreen mk5 method .. 139
Figure 4-7 Area of 38 chemical compounds at 3 different ionisation voltages. ..... 143
Figure 4-8 Twenty injections of QC in Polyscreen mk5. ..... 144
Figure 4-9 Magnified peaks of total ion chromatographs between 5 and 9 minutes. ..... 145
Figure 4-10 Chemical structure of Sinapic acid..... 146
Figure 4-11 Chromatograph of a control instant coffee along with a chromatograph of Sinapic acid, used as a chemical reference standard. The red arrow indicates the peak of the Sinapic acid. The blue arrows indicate the chemical entities that were found by searching the empirical formula C11H12O5 with the “Find by Formula” tool..... 147
Figure 4-12 Heatmap of normalised abundance values of 38 phenolic compounds throughout the 22 instant coffee samples of Table 4.1(number of replicates = 5). Reference coffee: Control – Coffee_V. ..... 148
Figure 4-13 Ratio of 3-Caffeoylquinic acid per 3,4-di-Caffeoylquinic acid for commercial instant coffees. Data retrieved by Mills et al., 2013 and Rodrigues and Bragagnolo, 2013 (blue and green bars respectively). ..... 149

Figure 4-14 Ratio of 3-Caffeoylquinic acid per 3,4-di-Caffeoylquinic acid for Nescafe gold beld and Nescafe gold blend Decaff. Direct comparison of data from targeted chemical analysis and data from Mills et al., 2013. ..... 150
Figure 4-15 Heatmap of p values for compounds which are significantly correlated ($p<0.05$) with at least one of the foam quality parameters. Grey tiles without annotated value mean that the given Foam quality parameter is not correlated significantly ($p>0.05$) with the given chemical compound. ..... 151
Figure 4-16 $R^2$ value of chemical compounds which are significantly correlated ($p<0.05$) with at least one of the foam quality parameters. Grey tiles without annotated value mean that the given chemical compound is not correlated significantly ($p>0.05$) with the given Foam quality parameter. ..... 152
Figure 4-17 Histogram of $R^2$ of Normalised abundance vs foam quality parameters. ..... 153
Figure 4-18 Pearson correlation analysis between the normalised abundance of 4-vinylguaiacol and each of the foam quality parameters. ..... 154
Figure 4-19 Pearson correlation analysis between the normalised abundance of p-Coumaroylquinic acid lactone and each of the foam quality parameters. ..... 155
Figure 4-20 Chemical structures of 4-vinylguaiacol and p-Coumaroylquinic acid lactone .... 156
Figure 4-21 Lactonization of p-Coumaroylquinic acid ..... 157
Figure 5-1 PCA plots of Total Ion Chromatographs for Negative (TOP) and Positive (BOTTOM) polarity mode. ..... 165
Figure 5-2 Histogram of $R^2$ of Normalised abundance vs foam quality parameters. TOP: Negative polarity mode. BOTTOM: Positive polarity mode ..... 166
Figure 5-3 $R^2$ as calculated by Pearson correlation analysis for the 44 chemical entities found by the untargeted chemical analysis in negative polarity mode. Grey tiles indicate that the specific chemical entity acquired $R^2<0.67$ with the given foam quality parameter. ..... 167
Figure 5-4 $R^2$ as calculated by Pearson correlation analysis for the 278 chemical entities found by the untargeted chemical analysis in positive polarity mode. Grey tiles indicate that the specific chemical entity had a correlation parameter $R^2<0.67$ with the given foam quality parameter. ..... 168
Figure 5-5 r of Foam Ability vs SIRIUS score vs CSI score for chemical entities from positive polarity mode which were annotated with high certainty. ..... 175
Figure 5-6 r of Drainage rate vs SIRIUS score vs CSI score for chemical entities from positive polarity mode which were annotated with high certainty. ..... 175
Figure 5-7 r of Disproportionation/Coalescence rate vs SIRIUS score vs CSI score for chemical entities from positive polarity mode which were annotated with high certainty. ..... 175
Figure 5-8 Histogram of Score A, Score B and Score C. Each score depicts the strength of correlation for each chemical entity with each of the foam quality parameters, along with the certainty of annotation. Score A is associated with Foam ability, Score B is associated with Drainage rate and Score C is associated with Disproportionation rate. Red dashed line and red arrow indicate that chemical compounds with Score A or Score B or Score C higher than were considered as most important. ..... 178
Figure 5-9 Two peaks detected for Cyclo(-Phe-Pro) chemical reference standard provided from Merck Life Science. ..... 182
Figure 5-10 Top: MS1 spectra of chemical reference standard of Cyclo(-Phe-Pro). Bottom: MS1 spectra of MS2 annotated Cyclo(-Phe-Pro) ..... 184
Figure 5-11 Two peaks detected for Cyclo(L-Phe-D-Pro) chemical reference standard provided by Santa Cruz Biotechnology Inc. ..... 185
Figure 5-12 6 key foam identified in instant coffee ..... 188
Figure 6-1 Area of sinapic acid as detected in instant coffee samples and standard curves in (a) Negative polarity mode and (b) Positive polarity mode ..... 195
Figure 6-2 Area of Sinapic acid in three different samples (n=3). Significant difference: * $p<0.05$, ** $p<0.01$, *** $p<0.001$ ..... 196
Figure 6-3 Theoretical bar plot which presents the peak area of compound x as identified in different samples. The intensity of each bar consists of the intensity of compound x that is native in the blank sample and the intensity of compound x that was spiked. C1 to C8 are theoretical concentrations of compound x. ..... 197
Figure 6-4 Area of sinapic acid as identified in negative and positive polarity mode for coffee samples and standard curve which were prepared via standard addition method (SAM). ..... 198

Figure 6-5 Standard curve of Cyclo(Pro-Val) prepared with Standard addition method (SAM) ..... 199
Figure 6-6 Standard curve points for Mannotetraose. Standard curve was prepared with standard addition method. ..... 200
Figure 6-7 Concentration of Cyclo(-Phe-Pro) alpha and beta, Cyclo(-Phe-Val), Cyclo(-Pro-Val), Cyclo(Leu-Phe) and Cyclo(Phe-Phe) for Control, Trial-FD5 and SD3-SR1/12 instant coffee (n=3). Statistical test was performed for each chemical entity separately throughout the coffee samples. Different letters indicate significant difference at p=0.05. + **symbol**: The concentration was calculated by extrapolation of standard curve. ┐ **symbol**: Concentration was calculated via linear regression in log-log scale plots. ┴ **symbol**: Concentration calculated under the assumption that Cyclo(-Phe-Pro) alpha/beta ratio was 96/4. ..... 203
Figure 6-8 Standard curve of Cyclo(Phe-Pro) beta prepared without Standard addition method (SAM). Concentration of x-axis were calculated under the assumption that Cyclo(-Phe-Pro) alpha/beta ratio was 96/4. ..... 204
Figure 6-9 Cyclo(Phe-Pro) beta determined in Control and SD3-SR1/12 with or without Standard Addition Method. (n=3). Statistical analysis was performed at each sample between two different conditions. Significant difference: * p<0.05 ..... 205
Figure 6-10 Chemical structure of key foam targets and internal standard ..... 206
Figure 6-11 Standard curve for Mannotetraose. Standard curve was prepared without standard addition method. ..... 207
Figure 6-12 Control's coffee foam aerated at different aeration times. n=3. Different letters indicate a significant difference between samples at p<0.05. ..... 210
Figure 6-13 Baseline concentration for Trial-FD5. ..... 212
Figure 6-14 Volume of foam vs time plot for Trial-FD5 blanks. ..... 213
Figure 6-15 Volume of foam vs time plots for Trial-FD5 spiked with Mannotetraose at different concentrations. Top left: Blank - Co, Top right: Spiked x2.5, Bottom left: Spiked x5, Bottom right: Spiked x7.5. ..... 215
Figure 6-16 Volume of foam vs time plots for Trial-FD5 spiked with Cyclo(Pro-Val) at different concentrations. Top left: Blank - Co, Top right: Spiked x2.5, Bottom left: Spiked x5, Bottom right: Spiked x7.5. ..... 215
Figure 6-17 Volume of foam vs time for Blank Trial-FD5 ..... 217
Figure 6-18 Principle of foam height detection for Dynamic Foam Analyser. Schematic adapted by Shankaran and Chinnaswamy (2019). ..... 218
Figure 6-19 Effect of illumination value for identifying the foam height level. ..... 219
Figure 6-20 Volume of foam vs time plot for Trial-FD5 spiked with Mannotetraose x2.5, x5 and x7.5 (n=3). Error bars estimated by the device shown in black. ..... 220
Figure 6-21 Bubble count per mm^2 vs time for Trial-FD5 instant coffee spiked x2.5 x5, x7.5 the initial concentration with Mannotetraose (n=3). Error bars estimated by the device shown in black. ..... 220
Figure 6-22 Volume of foam vs time plot for Trial-FD5 spiked with Cyclo(Phe-Pro) x2.5, x5 and x7.5. ..... 221
Figure 6-23 Bubble count per mm^2 vs time for Trial-FD5 instant coffee spiked x2.5 x5, x7.5 the initial concentration with Cyclo(Phe-Pro) (n=3). ..... 221
Figure 6-24 Volume of foam vs time plot for Trial-FD5 spiked with Cyclo(Pro-Val) x2.5, x5 and x7.5. ..... 222
Figure 6-25 Bubble count per mm^2 vs time for Trial-FD5 instant coffee spiked x2.5 x5, x7.5 the initial concentration with Cyclo(Pro-Val (n=3). ..... 222
Figure 6-26 Effect of 0.59% EtOH or 0.59% DMSO in foam quality of control instant coffee (n=3). ..... 223
Figure 6-27 Effect of 0.59% EtOH or 0.59% DMSO in bubble count per mm^2 of control instant coffee (n=3). ..... 224
Figure 6-28 Bubble count per mm^2 vs time for Control instant coffee spiked x10 the initial concentration with Cyclo(Leu-Phe) (n=3). ..... 225
Figure 6-29 Foam quality vs time for Control instant coffee spiked x10 the initial concentration with Cyclo(Leu-Phe) (n=3). ..... 225
Figure 6-30 Bubble count per mm^2 vs time for Control instant coffee spiked x5.9 the initial concentration with Cyclo(Phe-Val) (n=3). ..... 226
Figure 6-31 Foam quality vs time for Control instant coffee spiked x5.9 the initial concentration with Cyclo(Phe-Val) (n=3). ..... 226

Figure 6-32 Bubble count per mm^2 vs time for Control instant coffee spiked x10 the initial concentration with Cyclo(Phe-Phe) (n=3). ..... 227
Figure 6-33 Foam quality vs time for Control instant coffee spiked x10 the initial concentration with Cyclo(Phe-Phel) (n=3). ..... 227
Figure 6-34 Surface tension of ultra-pure water at 20˚C ..... 228
Figure 6-35 Dynamic surface tension of Cyclo(Pro-Val) and ultra-pure water at 20˚C (n=2). 229
Figure 6-36 Schematic of Cyclo(Pro-Val). Red dots indicate polar-polar or charge-polar interaction. Blue indicates nonpolar interactions. ..... 230
Figure 6-37 Dynamic surface tension for Control, SD3-SR1/12 and Trial-FD5 (n=2). ..... 231
Figure 6-38 Fitted data of surface tension vs$time$ for Control, SD3-SR1/12 and Trial-FD5 . 233
Figure 6-39 Diff and Surface tension at t=0 sec as calculated for Control, SD3-SR1/12 and Trial-FD5. ..... 234
Figure 6-40 Schematic representation of diffusion-controlled adsorption of surface-active compounds as introduced by Ward and Tordai (1946).Ward and Tordai (1946). Figure (a) and (b) represents a pure surfactant solution and coffee solution respectively. Between interface and subinterface, only adsorption/desorption of surface-active compounds occurs. The thickness between interface and subinterface is a few molecular diameters. Just below subinterface, diffusion of soluble compounds occurs towards the interface. Image adapted by Chang and Franses (1995). ..... 236
Figure 6-41 Surface tension of Control and Trial-FD5 for non-centrifuged samples (n=2).... 238
Figure 7-1 Normalised abundance of MS2 annotated polyphenols for Arabica washed, Arabica unwashed and Robusta unwashed coffee beans roasted for 0, 2, 4 and 6 minutes. White tiles indicate that the given compound was not detected at the given sample. The presented data were normalised to the abundance of the internal standard (i.e. Sinapic acid). Raw data are presented in Appendix P. ..... 252
Figure 7-2 Proposed metabolic pathway of production of 4-vinylcatechol oligomers (1 to 9a/b) from 5-O-caffeoylquinic acid (A) and caffeic acid (B) via 4-vinylcatechol as an intermediate metabolite (C1). Image adapted from Frank et al., 2007. ..... 254
Figure 7-3 Normalised abundance of (a) caffeic acid, (b) 4-vinylcatechol and (c and d) )roasted caffeic acid product alpha and beta in coffee samples roasted at different roasting degree. The presented data were normalised to the abundance of the internal standard (i.e. Sinapic acid) ..... 255
Figure 7-4 Normalised abundance of MS2 annotated polyphenols for Robusta and Arabica green bean, roasted and instant coffee. White tiles indicate that the given compound was not detected at the given sample. The presented data were normalised to the abundance of the internal standard (i.e. Sinapic acid). Raw data are presented in Appendix P. ..... 256
Figure 7-5 Foam Ability for Arabica Nicaragua Washed, Arabica Brazil Unwashed and Robusta Vietnam Unwashed green and roasted bean extracts. ..... 257
Figure 7-6 Effect of roasting degree (a) and effect of coffee process (b) on normalised abundance of key foam compounds. White tiles indicate that a given compound was not detected in a given sample. ..... 258
Figure 7-7 PCA plots of Total Ion Chromatographs for Negative (a) and Positive (b) polarity mode. ..... 260
Figure 7-8 PCA plot of Total Ion Chromatograph for Positive polarity mode ..... 261
Figure 7-9 Chemical entities significantly up regulated during roasting. The full name of compounds presented as *Neutral mass x@Retention time y* can be found in the Appendix O. ..... 264
Figure 7-10 Chemical entities significantly down regulated during roasting (1 of 2). The full name of compounds presented as *Neutral mass x@Retention time y* can be found in Appendix O. ..... 266
Figure 7-11 Chemical entities significantly down regulated during roasting (2 of 2). The full name of compounds presented as *Neutral mass x@Retention time y* can be found in Appendix O. ..... 267
Figure 7-12 Chemical entities with maximum abundance in green bean (1 of 2). The full name of compounds presented as *Neutral mass x@Retention time y* can be found in Appendix O. ..... 269
Figure 7-13 Chemical entities with maximum abundance in green bean (2 of 2). The full name of compounds presented as *Neutral mass x@Retention time y* can be found in Appendix O. ..... 270

Figure 7-14 Chemical entities with maximum abundance in roasted beans. The full name of compounds presented as *Neutral mass x@Retention time y* can be found in Appendix O. ..... 271
Figure 7-15 Chemical entities with maximum abundance in instant coffee (1/2). The full name of compounds presented as *Neutral mass x@Retention time y* can be found in Appendix O. ..... 273
Figure 7-16 Chemical entities with maximum abundance in instant coffee (2/2). The full name of compounds presented as *Neutral mass x@Retention time y* can be found in Appendix O. ..... 274
Figure 7-17 Log2 Normalised abundance of 5-O-Caffeylquinic acid ((MSI Level 1 Identification) and several MSI Level 2 annotated caffeoylquinic, Feruloylquinic and p-Coumaroylquinic acids. The MSI Level 2 compounds were in maximum abundance in instant coffee. ..... 276
Figure 7-18 Chemical structure of 5-O-Caffeoylquinic acid (a) and MS2 annotated isomers (b,c,d). ..... 276
Figure 7-19 Roasting profile and whole bean colour for Arabica Nicaragua Washed, Arabica Brazil Unwashed and Robusta Vietnam Unwashed..... 277
Figure 7-20 Histogram of $R^2$ of Normalised abundance vs whole bean colour.(a) Negative polarity mode. (b) Positive polarity mode ..... 278
Figure K-1(a) MS1 spectra of MS2 annotated Mannotetraose.(b) MS1 spectra of chemical reference standard of Mannotetraose..... 423
Figure K-2 (a) and (b) MS1 spectra of chemical reference standard of Cyclo(-Phe-Phe). (c) and (d) MS1 spectra of MS2 annotated Cyclo(-Phe-Phe) ..... 424
Figure K-3 (a,b,c) MS2 spectra of chemical reference standard of Cyclo(-Phe-Phe) at 10V,20V and 40V. (d,e,f) MS2 spectra of MS2 annotated Cyclo(-Phe-Phe) at at 10V,20V and 40V. ..... 425
Figure K-4 Cyclo(-Phe-Pro) MS2 spectra @13.08 min @10V ..... 426
Figure K-5 Cyclo(-Phe-Pro) MS2 spectra @13.08 min @20V ..... 427
Figure K-6 Cyclo(-Phe-Pro) MS2 spectra @13.08 min @40V ..... 428
Figure K-7 Cyclo(-Phe-Pro) MS2 spectra @13.55 min @10V ..... 429
Figure K-8 Cyclo(-Phe-Pro) MS2 spectra @13.55 min @20V ..... 430
Figure K-9 Cyclo(-Phe-Pro) MS2 spectra @13.55 min @40 ..... 431
Figure K-10 (a) MS1 spectra of MS2 annotated Cyclo(-Pro-Val). (b) MS1 spectra chemical reference standard of Cyclo(-Pro-Val)..... 432
Figure K-11 Cyclo(-Pro-Val) MS2 spectra @10V ..... 432
Figure K-12 Cyclo(-Pro-Val) MS2 spectra @20V ..... 433
Figure K-13 Cyclo(-Pro-Val) MS2 spectra @40V ..... 433
Figure K-14 (a) MS1 spectra of chemical reference standard of Cyclo(-Leu-Phe). (b) MS1 spectra of MS2 annotated Cyclo(-Leu-Phe). ..... 433
Figure K-15 Cyclo(-Leu-Phe) MS2 spectra @10V ..... 434
Figure K-16 Cyclo(-Leu-Phe) MS2 spectra @20V ..... 434
Figure K-17 Cyclo(-Leu-Phe) MS2 spectra @40V ..... 434
Figure K-18 (a) MS1 spectra of MS2 annotated Cyclo(-Phe-Val). (b) MS1 spectra of chemical reference standard of Cyclo(-Phe-Val) ..... 435
Figure K-19 Cyclo(-Phe-Val) MS2 spectra @10V, 20V and 40V. (a,b,c):Chemical reference standard,(d,e,f): MS2 annotated Cyclo(-Phe-Val) ..... 436
Figure L-1 Standard curve for Cyclo(Leu-Phe) prepared with standard addition method..... 437
Figure L-2 Standard curve for Cyclo(Phe-Phe) prepared with standard addition method. ..... 437
Figure L-3 Standard curve for Cyclo(Phe-Pro) alpha (log-log scale) prepared with standard addition method..... 438
Figure L-4 Standard curve for Cyclo(Phe-Pro) beta prepared with standard addition method 438
Figure L-5 Standard curve for Cyclo(Phe-Val) prepared with standard addition methods .... 439
Figure M-1 Standard curve for Mannotetraose prepared without standard addition method.. 440
Figure M-2 Standard curve for Cyclo(Phe-Pro) alpha in log-log scale prepared without standard addition method..... 440
Figure M-3 Standard curve for Cyclo(Phe-Val) prepared without standard addition method 441
Figure M-4 Standard curve for Cyclo(Pro-Val) prepared without standard addition method . 441
Figure N-1 Standard curve for 3-O-Caffeoylquinic acid prepared without standard addition method..... 442

Figure N-2 Standard curve for 5-O-Caffeoylquinic acid prepared without standard addition method ..... 442
Figure N-3 Standard curve for 3,4-diCaffeoylquinic acid prepared without standard addition method ..... 443
Figure N-4 Standard curve for 3,5-diCaffeoylquinic acid prepared without standard addition method ..... 443
Figure N-5 Standard curve for 4,5-diCaffeoylquinic acid prepared without standard addition method ..... 444

# LIST OF TABLES

Table 2.1 Monomer composition of polysaccharides from green coffee. Values expressed on dry weight ..... 14
Table 2.2 Degree of branching of Arabinogalactan-Proteins and Galactomannans from different types of arabica and Robusta green beans ..... 17
Table 2.3 Loss percentage of arabinose, galactose and mannose at light and dark roasting degree. ..... 17
Table 2.4 Concentration of organic acids in green coffee bean. ..... 25
Table 2.5 Concetration of CQA, FQA, diCQA and p-CoCA in green and dark roasted arabica and robusta beans. Table adapted by (Perrone *et al.*, 2008). a: Concentration expressed as mg/100g coffee dry weight. ..... 28
Table 2.6 Bound and free amino acids that are present in green bean ..... 32
Table 3.1 Instant coffee sample. FD: Freeze-dried, SD: Spray dried, ASD: Agglomerated spray dried ..... 51
Table 3.2 Green bean, Roasted bean, and Instant coffee series ..... 52
Table 3.3 Green whole beans ..... 52
Table 3.4 Empirical coefficients of Vapor pressure equation for n-hexane, 2-methylpentane, water. Tmin-Tmax is the minimum and maximum temperature that equation 3.3 is valid.(Perry and Green, 1997) ..... 55
Table 3.5 Vapour Pressure of nHexane, 2-methylpentane and water at T=343.15K ..... 56
Table 3.6 Optimum parameters for fitting control foam height curve to Equation 3.8. ..... 70
Table 3.7 Method to reduce the particle size of green and roasted beans ..... 101
Table 3.8 Photographs before and after aeration step of Arabica Nicaragua Washed extracts. 110
Table 3.9 Foam Ability of Instant coffee samples #1-5 of Table 3.1 and coffee samples of Table 3.2 R&G:Roast and Ground coffee (n=5) ..... 116
Table 4.1 Instant coffee samples which are significantly different from control. FD: Freeze Dried coffee, SD: Spray Dried coffee ..... 121
Table 4.2 Polyscreen mk5 (i.e. version 5) gradient. Mobile phase A: 100% Water. Mobile phase B: 100% Methanol ..... 124
Table 4.3 Source parameters in negative polarity mode for targeted chemical analysis ..... 125
Table 4.4 Negative polarity mode adducts. M: the neutral mass of the chemical compound of interest ..... 126
Table 4.5 SIRIUS parameters for MS2 annotation ..... 128
Table 4.6 Polyphenols that are reported both in coffee and cocoa. ..... 130
Table 4.7 Gradient for Polyscreen mk1 to mk6 ..... 135
Table 4.8 Chemical compounds that were identified with chemical reference standards ..... 139
Table 4.9 Level 2 annotation of Ferulic acid (C10H10O4) via MS2 analysis ..... 139
Table 4.10 Polyphenols identified in level 1 and level 2 in Polyscreen mk5 method. ..... 141
Table 5.1 Positive polarity mode adducts. M: the neutral mass of the chemical compound of interest ..... 162
Table 5.2 Recursive extraction feature parameters ..... 163
Table 5.3 Summary results from MS2 annotation workflow ..... 170
Table 5.4 Chemical entities annotated with high certainty in negative mode polarity ..... 171
Table 5.5 Compounds which appear amphiphilic in structure ..... 173
Table 5.6 Chemical entities which acquired Score A, Score B or Score C higher than 0.8 .... 179
Table 5.7 Chemical entities that were available in the market ..... 180
Table 5.8 Summary of compounds that were positively or negatively ID validated ..... 181
Table 6.1 Instant coffee samples that were used for the present chapter. SD3-SR1/12 and Trial-FD5 has the maximum and minimum foam ability, respectively. ..... 191
Table 6.2 Standard curve ranges of key foam compounds ..... 191
Table 6.3 Foaming and data acquisition parameters ..... 193
Table 6.4 Linear regression results for cyclo-dipeptides as analysed via standard addition method. ..... 201
Table 6.5 Estimated concentration of Mannotetraose in Control, SD3-SR1/12 and Trial-FD5 ..... 209
Table 6.6 Initial foaming and data acquisition parameters ..... 211
Table 6.7 Key foam compounds and preferred solvent ..... 213

Table 6.8 Partition coefficient values for key foam targets. Values of LogP were retrieved by https://pubchem.ncbi.nlm.nih.gov/ ..... 214
Table 7.1 Green bean, roasted bean and instant coffee series ..... 242
Table 7.2 Green and roasted whole beans ..... 242
Table 7.3 Concentration (mg/100 mL coffee solution) for major chlorogenic acids in Arabica Washed, Arabica Unwashed and Robusta Unwashed coffee beans roasted at 0, 2, 4 and 6 minutes. CQA: Caffeoylquinic acid, diCQA: Dicaffeoylquinic acid. Each solution was normalised in 1.5% w/w soluble solids. One-way ANOVA was performed for each column. Different letters indicate significant differences at level p=0.05. + symbol: The concentration was calculated by extrapolation of standard curve..... 246
Table 7.4 Concentration (mg/100 mL coffee solution) for major chlorogenic acids in Robusta and Arabica green bean, roasted bean and instant coffee extracts. CQA: Caffeoylquinic acid, diCQA: Dicaffeoylquinic acid. Each solution was normalised in 1.5% w/w soluble solids. One-way ANOVA was performed for each column. Different letters indicate significant differences at level p=0.05. + symbol: The concentration was calculated by extrapolation of standard curve The roasting time for each coffee was not provided. .. 247
Table 7.5 Reported values of 3-O-Caffeoylquinic acid (3-CQA), 5-O-Caffeoylquinic acid, 3,4-Dicaffeoylquinic acid (3,4-DiCQA), 3,5-Dicaffeoylquinic acid (3,5-DiCQA), 4,5-Dicaffeoylquinic acid (4,5-DiCQA) in green bean, roasted bean at various degrees of roasting and, instant coffee solutions. The concentration is expressed as mg/100 mL coffee solution of 1.5% w/w coffee solution. **i**- Coffee samples were clarified with Carrez's I & II solutions. **ii**-Polyphenols were extracted via Solid Phase Extraction (SPE). **a**-Diluent 100% water, **b**- Diluent 11.8% Ethanol/Water, **c**-Diluent - 15.8% Acetonitrile/Water.. 249
Table 7.6 Total solid (%w/w) of coffee brews as reported in the literature..... 250
Table 7.7 Chemical entities correlated with whole bean colour..... 279
Table C.1 Extracted ion chromatographs of chemical entities by using two mobile phases (Acetonitrile vs Methanol) vs two chromatography columns (C18 vs Biphenyl) ..... 320
Table D.1 Phenolic compounds reported in coffee ..... 332
Table E.1 Chemical entities found in control instant coffee..... 339
Table F.1 Extracted ion chromatographs for targets analysed via Polyscreen mk1 to m6 ..... 343
Table G.1 Ferulic acid - MS2 Results ..... 373
Table G.2 ,4 - Dimethoxycinnamic acid : 3,5- Dimethoxycinnamic - MS2 Results..... 374
Table G.3 Roasted caffeic acid products - MS2 Results ..... 375
Table G.4 p-Coumaroylquinic acid lactone - MS2 Results..... 376
Table G.5 Caffeoyl quinic acid lactone - MS2 results..... 377
Table G.6 p-Coumaroylquinic acid - MS2 Results ..... 378
Table G.7 Caffeoylquinic acid - MS2 Results..... 379
Table G.8 Roasted caffeic acid product - MS2 Results..... 380
Table G.9 Feruloylquinic acid lactone - MS2 Results..... 381
Table G.10 Feruloylquinic acid - MS2 Results ..... 382
Table G.11 Phenol - MS2 Results ..... 383
Table G.12 Catechol - MS2 Results..... 384
Table G.13 Pyrogallol - MS2 Results ..... 384
Table G.14 Quinic acid lactone - MS2 Results ..... 385
Table G.15 Quinic acid - MS2 Results..... 385
Table G.16 Salicylic acid - MS2 Results..... 386
Table G.17 Guaiacol - MS2 Results..... 386
Table G.18 4-ethylcatechol - MS2 Results..... 387
Table G.19 4-vinylcatechol - MS2 Results ..... 387
Table G.20 4-vinylguaiacol - MS2 Results ..... 388
Table G.21 p-Coumaric acid - MS2 Results ..... 388
Table G.22 Caffeic acid - MS2 Results..... 389
Table G.23 di-Caffeoylquinic acid lactone - MS2 Results..... 389
Table G.24 di-Caffeoylquinic acid - MS2 Results ..... 390
Table G.25 Caffeoyl-Feruloylquinic acid - MS2 Results..... 391
Table G.26 di-Feruloylquinic acid - MS2 results..... 392
Table J.1 Results from the annotation of ID of chemical entities found with negative polarity mode. ..... 402
Table J.2 Results from the annotation of ID of chemical entities found with positive polarity mode..... 405

Table O.1 Chemical entities significantly decreased during roasting. ..... 445
Table O.2 Chemical entities significantly increased during roasting. ..... 452
Table O.3 Chemical entities with maximum abundance in green beans ..... 457
Table O.4 Chemical entities with maximum abundance in roasted beans ..... 463
Table O.5 Chemical entities with maximum abundance in instant coffee ..... 465

# LIST OF EQUATIONS

Equation 3.1 Moisture content determination. ..... 53
Equation 3.2 Lipid content determination ..... 54
Equation 3.3 Vapor pressure equation ..... 55
Equation 3.4 Coffee mass equation ..... 57
Equation 3.5 Water mass equation ..... 57
Equation 3.6 Total solids equation ..... 59
Equation 3.7 Sum of square residuals of predicted vs measured values ..... 61
Equation 3.8 Foam height model ..... 69
Equation 3.9 Silhouette coefficient equation for each sample ..... 81
Equation 5.1Mathematical equation which calculates the Score A ..... 176
Equation 5.2 Mathematical equation which calculates the Score B ..... 177
Equation 5.3 Mathematical equation which calculates the Score C ..... 177
Equation 6.1 Time dependent surface tension ..... 232
Equation 6.2 Time depended surface tension equation, adapted for coffee samples. ..... 232
Equation 6.3 Slope of Equation 6.2 ..... 234

# NOMENCLATURE

| | |
|---|---|
| A,B,C,D | Fitting parameres for foam height and liquid retention curve |
| C1,C2,C3,C4,C5 | Empirical coefficients for each substance |
| $C_{Mannotetraose}$ | Concentration of Mannotetraose |
| Diff | Diffusivity |
| K | Kelvin |
| $k_d$ | diffusion coefficient |
| $M_1$ | Mass of dried dish |
| $M_2$ | Gross mass of dish with coffee after 4 hours of drying |
| $Mass_{flask\ after\ extraction}$ | Mass of dried flask after the soextherm analysis |
| $Mass_{flask\ and\ sones}$ | Mass of dried flask with 3 boiling stones before soextherm analysis |
| $Mass_{instant\ coffee}$ | The mass of instant coffee to be analysed |
| $M_{dried\ sample}$ | Mass of dried sample |
| $M_{extract}$ | Mass of extract |
| $M_{sample}$ | Mass of sample |
| n | mole |
| Pa | Pascal |
| R | Boltzman constant |
| T | Temperature in K |
| t | time |
| V | Volume |
| $V_P$ | Vapor pressure in Pa |
| $y_{measured}$ | values measured |
| $y_{predicted}$ | values calculated through fitted curve |

**Greek letters**

| | |
|---|---|
| $\sigma$ | Surface tension |
| $\sigma_o$ | Surface tension when t->0 |

**Abbreviations**

| | |
|---|---|
| AGP | Arabino Galactan Protein |
| ANOVA | Analysis of Variance |
| ASD | Aglomerated spray dreid |
| BS | British Standard |

| | |
|---|---|
| CEF | Compound exchange file |
| CFQA | CaffeoylFeruloylQuinic acid |
| CID | Compound ID |
| CPS | CYCLES PES SECOND |
| CQA | Caffeoylquinic acid |
| CQL | Caffeoylquinolactone |
| DFA | Dynamic Foam Analyser |
| diCQA | di-Caffeoylquinic acid |
| diCQL | di-Caffeoylquinolactone |
| DMSO | Dimethyl Sulfoxide |
| DP | Degree of polymerisation |
| EIC | Extracted Ion Chromatograph |
| ESI | Electospray ionisation |
| EtOH | Ethanol |
| FA | Foam Ability |
| FBF | Find By Formula |
| FD | Freeze dried |
| FFA | Foaming Fraction A |
| FFB | Foaming Fraction B |
| FQA | Feruloylquinic acid |
| FQL | Feruloylquinolactone |
| FS | Foam Stability |
| HMWC | High Molecular Weight Carbohydrate |
| HPLC | High Performance Liquid Chromatography |
| ICO | International Coffee Organisation |
| IS | Internal Standard |
| IUPAC | International Union of Pure and Applied Chemistry |
| JDE | Jacobds Douwe Egberts |
| KRR | Kenco Really Rich |
| KRS | Kenco Really Smooth |
| LC/Q-ToF | Liquid Chormatography/Quadrapole-Time of Flight |
| LCMS | Liquid Chromatography Mass Spectrometry |
| LMWC | Low Molecular Weight Carbohydrate |
| LTP | Lipid Transfer Protein |
| MBI | Mellanoidin Browning index |
| MS | Mass spectrometer |
| MSDS | Material Safety Data Sheet |
| MSI | Metabolomics Standards Initiative |
| MW | Molecular Weight |
| NA | Not Available |
| NIR | Near InfraRef |
| NMR | Nuclear Magnetic Resonance |

| | |
|---|---|
| p-CoCA | p-Coumaroylquinic acid |
| PAT | Profile Analysis Tensiometry |
| PCA | Principal Component Analysis |
| PCDL | Personal Compound Database and Library |
| p-CoQL | p-Coumaroylquinolactone |
| PFA | Profinder Archive File |
| PTFE | Polytetrafluoroethylene |
| QC | Quality Control |
| RPM | Revolutions Per Minutes |
| RSD | Relative Standard Deviation |
| SAM | Standard Addition Method |
| SD | Spray Dried |
| SPE | Solids Phase Extraction |
| TFF | Total Foaming Fraction |
| TIC | Total Ion Chromatograph |
| TS | Total Solids |
| UPLC | Ultra-performance Liquid Chromatography |

# Chapter 1: Introduction

## 1.1 Background and objectives

Coffee is one of the most popular beverages around the world (Ballesteros, Teixeira and Mussatto, 2014). The British Coffee Association reported that UK coffee industry's total output contribution to the UK economy was £17.7 billion in 2017 (British Coffee Association, 2018). According to the International Coffee Organisation (ICO), 168.5 million bags (60 kg per bag) were produced globally in 2021/22. The worldwide consumption of coffee for 2021/2022 was 175.6 million bags (60 kg per bag), while Europe accounts for 31.5% of the annual global consumption (International Coffee Organization, 2023).

Along with the increasing consumption of coffee beverages from COVID-19 years (International Coffee Organization, 2023), there is a constant demand from consumers for high quality products. The quality of a cup of coffee, like espresso is determined by its aroma and taste. However, another important characteristic that contributes to the consumer experience is the formation of crema, a layer of light-coloured foam that accumulates at the top of the coffee cup (Illy and Navarini, 2011). Consumers have associated a good cup of coffee with the presence of the crema. Foam also enhances the consumer experience because it assists in the controlled delivery of aromatic compounds upon consumption (Folmer, Blank and Hofmann, 2017).

There are several key factors involved in ensuring the quality and stability of coffee foam. Foam is defined as gas phase dispersed in a liquid continuous phase (Bikerman, 1973). In principle, three things are required to make a bubble: gas, liquid and surface-active compounds. These compounds typically are adsorbed

on the air/liquid interface and assist on the creation of the bubbles by decreasing the surface tension (Karakashev, 2017).

From a scientific perspective, little is known on the mechanisms that drive foam formation in coffee preparations and it is often considered more art than a science. Coffee foam-as any other liquid foam-attributes its existence to the surface-active compounds, while the surface activity of such compounds is determined by the physical-chemical properties (e.g. hydrophobicity-hydrophilicity) and therefore by the structure. Understanding the physical-chemical phenomena that occur during the formation of the foam may therefore contribute towards increasing quality of coffee and assisting the design of a more efficient instant coffee manufacturing process.

The overall aim of the present work is to advance the physical-chemical understanding of coffee foams. The present PhD seeks to answer the following research questions:

- Which chemical compounds in coffee are associated with foam quality and which actively play a role in foam stability mechanisms?
- At which point of a coffee bean's lifetime (i.e. from green bean to cup) do the foam promoting compounds occur and at what levels?
- What are the foam stability mechanisms in coffee?

## 1.2 Relevance to Jacobs Douwe Egberts

Jacobs Douwe Egberts (JDE), the industrial sponsor of the present project is subordinate company of JDE Peet's. Its net revenue for 2022 was increased to EUR 8.2€ billion. JDE Peets products are sold in more than 100 countries, and

in 43 of these the company is number 1 or 2 in terms of sales. The company has a market cap of €14 billion, 20710 employees (2022 figures), and sells 4200 cups of coffee every second. The brands in the portfolio include L'OR, Kenco, Jacobs, Tassimo, Moccona, Senseo and Pickwick. In order to continue being a successful company, it is very important to advance the understanding of coffee foam to maintain or optimise the coffee process in the pursuit of manufacturing high quality coffee products. The freeze-drying process (lyophilisation) can allow good retention of aromas in soluble coffee, so is used for many of JDE's instant coffee products. However, achieving a good crema layer with this technology has traditionally been a challenge. A deeper understanding of the foam chemistry of soluble coffee should therefore make a contribution to improving this aspect of coffee quality.

## 1.3 Thesis layout

The layout of the thesis is presented:

In Chapter 2, a literature review on coffee chemistry was conducted. Emphasis is given on chemical compounds and chemical families (e.g. melanoidins) that have been reported to influence foam quality performance. A short review on foaming mechanisms of beer foam is presented in order to acquire paradigms that may be applicable to coffee foam.

Chapter 3 includes the method development for a foam quality assessment, followed by the assessment of a range of instant coffee products. The influence of oil content and (further) heat treatment of instant coffee on foam quality performance is discussed. Finally, the influence of roasting degree on foam quality of coffee brews is examined.

Chapter 4 investigates the influence of coffee polyphenols on foam quality. A method is developed for chemical screening via LCMS, followed by a correlation analysis between the relative abundance of major and minor polyphenols in coffee against the foam quality performance. The relationship of polyphenols with foam quality is discussed.

In Chapter 5 the LCMS method that was developed in Chapter 4 is applied to an untargeted metabolomic workflow. The relative abundance of unknown chemical entities is correlated with foam quality performance in order to reveal which compounds are associated with foam. In this chapter, the key foam compounds which are associated with foam quality are identified via chemical reference standards.

In chapter 6, the key foam compounds from the previous chapter are spiked at a range of concentrations in a poor foaming coffee and the foam quality is assessed. The influence of key foam compounds on foam quality is discussed.

In Chapter 7, the effect of roasting and instant coffee manufacture on the chemical profile of coffee brews is investigated. A mixture of targeted and untargeted metabolomic analysis is performed in order to monitor the chemical changes. The influence of roasting degree on the abundance of key foam compounds in coffee brews is discussed.

Chapter 8 summarises the conclusions of the thesis, highlights the importance of the findings and suggests future work.

# Chapter 2: Literature Review

## 2.1 Introduction

The following review is focused on the chemistry of coffee and especially on the reported surface-activity of compounds that influence the foaming properties. Since the composition of coffee is dynamic and changes through the instant coffee process, it is also reviewed how the reported surface-active compounds are altered or generated. There are no published mechanisms that describe the stability of the coffee foam system. However, other food foam systems like beer, have been studied more extensively than coffee, and foam stability mechanisms have been suggested. It is hypothesised that the principles of the foam stability mechanisms in beer may describe the behaviour of the coffee foam system. Therefore, a review on the foam stability mechanisms of beer foam is conducted and similarities with the coffee foam system are proposed.

## 2.2 Coffee production process

### 2.2.1 Coffee cultivation

Commercial coffee production is based on two plant species, the Coffea Arabica L. (Arabica coffee) plant and the Coffea canephora Pierre ex Froehn plant. (robusta). A third species of plant, named Coffea liberica Bull ex Hiern (liberica or excels coffee) contributes less than 1% to coffee production worldwide. All species of the genus Coffea originate from the tropical zones of Africa and Latin America. Many hybrids of C. canephora occur in the equatorial lowland forest regions between Equatorial Guinea and Uganda, while populations of C. arabica occur only in the montane forests of southwestern Ethiopia(Anzueto *et al.*, 2005). Coffee trees thrive in areas characterized by frequent rains, an average annual temperature of 21°C and no frost. They grow at altitudes from sea level up to 2000 m and higher. The coffee tree from the time it is planted in the soil

takes about 5 years to produce the first crop and will be capable of producing crops for about 15 years (Murthy and Madhava Naidu, 2012).

### 2.2.2 Coffee harvesting

Harvesting the fruits of coffee tree is a very important stage in the overall processing of coffee. In Colombia, the hand-harvesting technique is traditionally used where the red ripe fruits of the tree are selected. The harvesting time depends on the weather conditions, which makes it difficult to plan the process. The maturity of coffee beans varies between trees located in different locations. Both unripe yellow or green beans and overripe soft beans are often encountered. A portion of the grain is on the ground or on specially designed sheets that have been placed under the plants to more easily collect the fruits that have fallen accidentally. Also, during the harvest, fruits are encountered that have cavities on their flesh, which are due to an attack on the grains by insects. In Brazil, specifically in the regions of São Paulo and Paraná, the harvest season coincides with the long dry season. In these areas the harvesting of overripe fruits is preferred, while techniques for mechanical harvesting of the coffee beans have been developed (Clarke and Macrae, 1985).

### 2.2.3 Coffee processing (Unwashed and Washed method)

Post-harvest processing aims to separate the bean from the rest of the coffee fruit. Also, the technique must be sufficient to protect the coffee from acquiring undesirable characteristics during the process. Coffee beans have five layers of protective material that must be removed to reveal the bean:

1. the skin: a monocellular layer covered with a waxy substance. When ripe it can be red, yellow or pink, depending on the variety of coffee

2. the pulp: consisting of fleshy pulp while in ripe fruits the pulp is covered by a gelatinous layer of mucous material (mucilage)
3. the parchment, a thin covering of polysaccharide.
4. the silverskin, a thin layer that directly covers the seed
5. two coffee seeds with elliptical shape

Two governing methods are used to reveal the coffee bean – the unwashed and washed method. In the unwashed method, the coffee beans are dried and then mechanically dehulled. This method is mainly used in Arabica varieties of Brazil, Ethiopia and Haiti, and in robusta varieties grown in all parts of the world. The unwashed method is carried out either naturally using the heat of the sun or mechanically with dryers. During the process, the coffee beans are detached from the parchment and after 3 to 4 weeks, depending on the drying conditions, the fruits are ready to peel. The washed method is a more advanced process compared to the dry method. It is based on removing the fruit flesh mechanically and fermenting them. The fermentation allows the disintegration of material that is attached on the coffee bean. Although the process requires abundant water and specific technical equipment, it generally allows the achievement of a final product of high quality and therefore of high economic value. This specific process is used for Arabica coffee varieties. (Alves *et al.*, 2017).

### 2.2.4 Roasting

Coffee roasting is a complex thermal process that transforms green coffee beans into the aromatic, flavourful coffee commonly consumed. This process involves a series of endothermic and exothermic reactions that occur as beans are heated to temperatures between 180°C and 250°C. Initially, beans undergo drying, losing moisture content and initiating Maillard reactions, which develop the

beans' characteristic flavours and aromas. As roasting progresses, caramelization of sugars and the breakdown of chlorogenic acids contribute to the complexity of the coffee's taste profile. The precise control of temperature and time during roasting is crucial to achieving the desired balance of flavours, ranging from light roasts with pronounced acidity to dark roasts with richer, more robust profiles. Chemical changes also result in the formation of volatile compounds and the release of carbon dioxide, which play essential roles in the coffee's aroma and crema formation in espresso (Clarke and Macrae, 1985; Bonnländer et al., 2005a; Al-Shemmeri et al., 2021).

### 2.2.5 Instant coffee process

The production of instant coffee involves several steps to convert roasted coffee beans into a soluble form. Initially, high-quality coffee beans are roasted and ground to the desired particle size. The ground coffee undergoes extraction using hot water under high pressure to produce a concentrated coffee solution. This extract is then aerated and subjected to one of two main drying methods: spray drying or freeze drying. In spray drying, the coffee extract is sprayed into a stream of hot air, rapidly evaporating the water and leaving behind fine coffee powder. In freeze drying, the coffee extract is frozen and then placed under vacuum, causing the ice to sublimate and leave a more granular coffee product. Both methods aim to preserve the coffee's flavour and aroma compounds while ensuring a stable, long-lasting product (Clarke, 2001; MacLeod *et al.*, 2006; S and Nisha, 2020).

## 2.3 Coffee chemistry and foam stability

### 2.3.1 Carbohydrates

**Carbohydrates on foaming properties**

Nunes et al. (1997) studied the functionality of carbohydrates and their contribution to foam properties in two different arabica espresso coffees. It was reported that during roasting the polysaccharide content of arabica espresso coffee increased to a maximum and then decreased (Nunes *et al.*, 1997). The same behaviour of carbohydrate content during roasting has been reported by (Wei *et al.*, 2012a), whereby the carbohydrates profile, structure and distribution are altered. The Foam Stability (FS) of espresso coffees showed a positive correlation with the neutral polysaccharide content. At the early stages of roasting, in arabica coffee beans, the increase of neutral carbohydrates by 1 mg per 40 g espresso increased the Foam Stability of crema for approximately 3.5 s, while for robusta beans the increase of 1 mg of neutral carbohydrates increased the FS by approximately 11 s. At the late stages of roasting the decrease of neutral carbohydrate content decreases dramatically the FS of arabica and robusta beans by 11 seconds and 43 seconds, respectively. The impact of neutral carbohydrate content on foam stability is not the same in the light and dark roasted coffee. The extended times of roasting process may produce surface active compounds that interact with neutral carbohydrates and affect the foaming properties of coffee samples. Moreover, this may indicate that carbohydrates play a significant but not the absolute role on foaming properties.

It is important to highlight that systems with increased carbohydrate content increase the viscosity of the bulk which thus affects the foam stability (Eugénie

*et al.*, 2014). D'Agostina et al. (2004) isolated a total foam fraction (TFF) of espresso coffee and separated in two subfractions. The first subfraction (foaming fraction A, or FFA) had high molecular weight, low nitrogen compound concentration, contained mostly polysaccharides and showed good foam stability. Whereas, the second fraction (FFB), had low molecular weight, higher nitrogen compound concentration and showed good foam ability (FA). In terms of carbohydrate content, the first fraction consisted of mannans and galactans while the second fraction of arabinose and galactose.

The functionality of pure green bean arabinogalactan-proteins on foam stability has been studied by Redgwell et al. (2005). Arabinogalactan-proteins with MW= 3.78 x $10^6$ Da were isolated and dispersed in deionised water (18.6 MΩ). The minimum concentration of AGP in order to build a self-supporting foam is 5 wt%. Ultimately, the minimum protein included in the AGP is 0.1-0.2%. The foam experiments showed that arabinogalactan protein is surface active and contributes to foam stability. The foam ability and foam stability were studied through a range of pH (pH=4-7). Whilst foam ability was not affected by pH, an increase of pH reduced the foam stability of arabinogalactan. The influence of pH on foam stability for coffee arabinogalactans was explained by the dissociation of carboxylic groups of glucuronic acid that are present as residues of the side chain. At low pH the dissociation is reduced and therefore the chains aggregate in the thin films of the foam structure. At high pH the opposite phenomenon occurs which reduces this stabilisation mechanism.

**Chemistry of coffee carbohydrates**

Green coffee bean carbohydrates vary between 40-65% on a dry weight basis and they consist of mono-, oligo- and polysaccharides (Clifford, 1985). The carbohydrate fraction can be divided in two groups: the low molecular weight carbohydrates (LMWC) and the high molecular weight carbohydrates (HMWC). Low molecular weight carbohydrates (LMWC) are monosaccharides and oligosaccharides, and they mainly consist of sucrose (90% of oligosaccharides), fructose, glucose, galactose, arabinose and traces of ribose, mannose and mannitol (Flament, 2002; Poisson *et al.*, 2017). Mono-, di- and oligosaccharides are present in higher levels in green Arabica than in green Robusta beans, at 6.2-9.5% vs 3-7% dry weight, respectively (Belitz, Grosch and Schieberle, 2009). Sucrose levels are slightly higher in green Arabica than green Robusta, at 5.4-8.1% vs 2.7-6.3% dry weight, respectively (Belitz, Grosch and Schieberle, 2009). However, total reducing sugars are typically lower in green arabica beans (0.10%) than in green Robusta beans (0.45%) on a dry weight basis (Flament, 2002). Low molecular weight carbohydrates contribute to the aroma formation (Bonnländer *et al.*, 2005a; Poisson *et al.*, 2017). After roasting almost all of the low molecular weight carbohydrates have been degraded because they take part in the Maillard reactions and to caramelization reactions (Bonnländer et al., 2005; Wei et al., 2012).

High molecular weight carbohydrates (HMWC) are polymers of mannose, galactose, glucose, arabinose, traces of xylose, rhamnose and galacturonic acid (Bee *et al.*, 2005; Poisson *et al.*, 2017). These compounds are combined with proteins and chlorogenic acids as they construct the cell wall and make up 50%

of green beans' dry weight (Clifford, 1985; Bradbury and Halliday, 1990; Fischer *et al.*, 2001; Redgwell and Fischer, 2006). The most abundant monomer of the polysaccharide fraction is mannose followed by galactose, glucose and arabinose (Table 2.1) (Bradbury and Halliday, 1990; Flament, 2002; Redgwell, Trovato, *et al.*, 2002).

Table 2.1 Monomer composition of polysaccharides from green coffee. Values expressed on dry weight

| Monomers | - | Robusta | Arabica Catimor CIFC | Arabica Yellow Caturra | Arabica Sarchimor |
|---|---|---|---|---|---|
| Mannose | 20.8 | 22.4 | 23.7 ± 0.33 | 23.58 ± 0.38 | 24.89 ± 0.68 |
| Galactose | 9.3 | 12.4 | 11.76 ± 0.45 | 12.10 ± 0.20 | 11.91 ± 0.07 |
| Glucose | 6.8 | 8.7 | 7.25 ± 0.12 | 7.09 ± 0.17 | 8.01 ± 0.09 |
| Arabinose | 1.8 | 4.0 | 3.96 ± 0.15 | 4.29 ± 0.13 | 3.74 ± 0.06 |
| Rhamnose | - | 0.3 | 0.135 ± 0.02 | 0.175 ± 0.02 | 0.155 ± 0.01 |
| Xylose | - | 0.2 | 0.22 ± 0.01 | 0.365 ± 0.06 | 0.26 ± 0.01 |
| Reference | (Flament, 2002) | (Bradbury and Halliday, 1990)0) | (Redgwell, Trovato, *et al.*, 2002) | | |

The cell wall of green coffee beans consists of long chain carbohydrates and can be divided in three main parts. The external layer of the cell wall consists of long chain β-mannan. Between the outer layers of cell wall, long microfibrils of cellulose construct the matrix of the cell wall and a continuous phase of lignin, pectin and hemicellulose fills the remaining space. The components of the cell wall are physically entangled and are held by secondary forces. In addition, they are linked together with primary covalent linkages (Clifford, 1985). The main HMW polymers are mannans or galactomannans, arabinogalactan proteins and cellulose. Small amounts of pectic polysaccharides and xyloglucans have also been reported (Redgwell, Curti, *et al.*, 2002; Oosterveld *et al.*, 2003).

The Arabinogalactan proteins (AGP) consist of 14-17% coffee dry weight (Bradbury and Halliday, 1987). The structure has been studied and the characteristics of the biopolymer are presented in Figure 2-1 (Fischer *et al.*, 2001; Nunes *et al.*, 2008)**.** Arabinogalactans are not a primary component for the structure of cell wall (Redgwell, Curti, *et al.*, 2002). The structure of AGPs consist of the backbone chain which is formed by 1-3 and 1-3,6 galactopyranose linkages**.** Attached on the O-6 position of the backbone chain there are side chains which consist of Arabinose in furanosidic form (5 – Araf), Galactose in pyranosidic form ((1-6)-Galp), Terminal Arabinose (T- Araf) and Terminal Glucuronic acid (6-10% of AGP) which is non-reducing sugar and provides negative charge to AGP. The average molecular weight of the polymer is 650 kDa (Range 150 - 2000 kDa ) (Redgwell, Curti, *et al.*, 2002). The degree of branching has been studied for green arabica and robusta bean (Redgwell, Trovato, *et al.*, 2002). The Gal/Ara ratio is of the same magnitude for arabica and robusta green bean (Table 2.2). 6-10% of AGP is glucuronic acid, which is a non-reducing sugar, occurs mainly as the terminal monomer of side chains, and provides negative charge to the polymer (Redgwell and Fischer, 2006). In order to determine the presence of proteins, the arabinogalactans have been tested with the a-glucosyl-Yariv reagent, a stain specific for arabinogalactan-proteins. The test results were positive (Redgwell, Curti, *et al.*, 2002). The protein component accounted for between 0.5 and 2.0% of the AGPs and contained between 7 and 12% hydroxyproline (Redgwell, Curti, *et al.*, 2002). The structure of the linkage between AG and protein is proposed by (Fincher, Stone and Clarke, 1983) (Figure 2-1). It is reported that the solubility of Robusta's arabinogalactan-proteins is higher from Arabica's. Comparing the degree of branching between

the Arabica and Robusta AGP, (Fischer *et al.*, 2001) reported that the latter is more branched with extended branches. The higher solubility of Robusta AGPs may be attributed to the increased degree of branching.

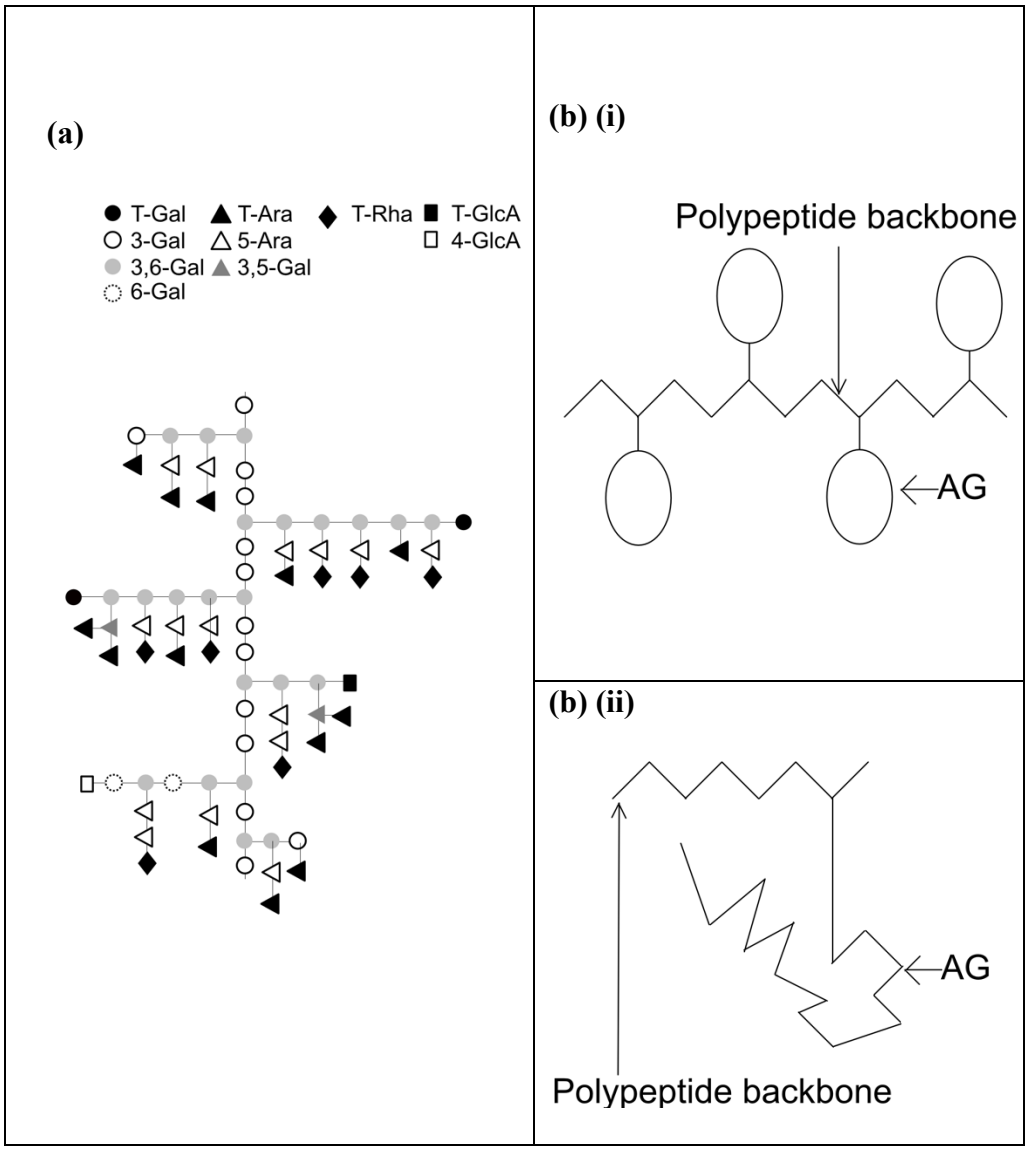



Figure 2-1 (a) Proposed structure of green coffee bean arabinogalactan-protein. Adapted from (Nunes *et al.*, 2008), (b) (i) Proposed structure of AGP from Acacia senegal gum polypeptide backbone which is substituted with AG moieties, (b) (ii) Proposed structure of the polypeptide backbone and the AG polymer enlarged. Adapted from Fincher, Stone and Clarke (1983).

Table 2.2 Degree of branching of Arabinogalactan-Proteins and Galactomannans from different types of arabica and Robusta green beans

| Arabinogalactan - Proteins | | | |
|---|---|---|---|
| Variety | | Gal/Ara Ratio* | Reference |
| Arabica | Caturra | 0.9-3.1 | (Redgwell, Curti, *et al.*, 2002) |
| | Catimor | 1.5-3.2 | |
| | Sarchimor | 1.2-3.0 | |
| Robusta | Indes | 0.9-3.1 | |
| | Conillon | 1.1-3.0 | |
| | Ivoire | 0.9-3.1 | |

| Galactomannans | | |
|---|---|---|
| Variety | Man/Gal | Reference |
| Arabica | 47:1 | (Wolfrom, Laver and Patin, 1961) |
| Robusta from Ivory Coast | 130:1 | (Bradbury and Halliday, 1990) |
| Arabica Caturra and Robusta ROM | 10:1 - 30:1 | (Fischer *et al.*, 2001) |
| Arabica Caturra from Ecuador | 7:1 and 40:1 | (Redgwell *et al.*, 2003) |
| Arabica from Columbia | 3:1 and 9:1 | (Oosterveld *et al.*, 2004) |

*Range of 5 different AGP fractions from the same source

During roasting, the arabinogalactans are highly susceptible to degradation (Table 2.3) (Redgwell and Fischer, 2006). At dark roast, the arabinogalactans are degraded by 60% (Redgwell, Trovato, *et al.*, 2002). The degradation is attributed to the debranching of arabinogalactans which releases free arabinose (Oosterveld et al., 2003; Wei et al., 2012). While the bean undergoes roasting, in addition to debranching of arabinosyl residues, fission of the galactan backbone also occurs (Redgwell, Trovato, *et al.*, 2002).

Table 2.3 Loss percentage of arabinose, galactose and mannose at light and dark roasting degree.

| Monomer | Degradation at light roast | Degradation at dark roast | Reference |
|---|---|---|---|
| Arabinose | 43-58% | 80% | (Redgwell, Trovato, *et al.*, 2002) |
| Galactose | 6%-30% | 50% | |
| Mannose | 10% | 30%-36% | |

Capek et al. (2010) isolated arabinogalactan-proteins from instant coffee and the changes of structure are significant compared to the structure of green bean AGP. The degree of branching is reported to be Gal/Ara = 9:1, which is in accordance with the findings by Matulová et al. (2011). The protein content of instant coffee AGP is ~1.6% and the Mw~5400 Da (Capek *et al.*, 2010). The instant coffee process consists of processes that are time and temperature related. Eventually, compounds like AGPs are exposed to high temperatures (180˚C-200˚C) during roasting and extraction (Clarke, 2001). As a result, the biopolymer suffers significant degradation which may have an impact on its functionality.

The Galactomannans comprise 19%-22% of dry green beans (Bradbury and Halliday, 1987; Poisson *et al.*, 2017). The structure of galactomannans consists of a backbone of mannosyl residues with β-1-4 linkages. The branches are a-1-6 linked galactose, acetyl groups, terminal arabinose (2% mole) and glucose (6% mole) (Nunes, Domingues and Coimbra, 2005).Researchers have studied the degree of branching (Table 2.2) and found a variety of Man/Gal ratios. Oosterveld et al. (2004) have isolated green *Coffea* arabica galactomannans extracted with hot water and separated them with anion-exchange chromatography. The galactomannans were eluted in two fractions, which differed in MW. The first fraction has MW of 20kDa while the second has MW 100 times larger, at 2000kDa. This indicates that there is more than one type of green coffee galactomannan.

During roasting, galactomannans suffer debranching and decrease of polymerization degree (Nunes and Coimbra, 2002a). Redgwell, Trovato, et al.

(2002) observed that there was no difference in the molecular weight of extracted galactomannans from green and roasted beans (10 kDa). However, there was a loss of 35% of mannose during roasting, while the galactose monomers are decreased by 6% and 50% at light and dark roast respectively (Table 2.3) (Redgwell, Trovato, *et al.*, 2002). These results indicate that the extracted mannans may not be representative of total galactomannans and that the average molecular weight of polymer decreases.

### 2.3.2 Lipids

**Lipids' effects on foaming properties**

Folmer, Blank and Hofmann (2017) have reported that sucrose fatty acid esters, which are obtained from green bean, are responsible for generating foam. Van Kempen et al. (2014) studied the surface activity of oligofructose fatty acids esters and it was found that mono- and di- fatty acids esters, which chain has more than 10 carbons, provide stability to generated foams.

The surface activity of coffee oils has been investigated by Ferrari et al. (2010). Coffee oil fractions have been extracted from different roasted arabica and robusta beans, and their surface activities have been determined by measuring the interfacial tension at the coffee oil/water interface. The results showed that coffee oil reaches an equilibrium interfacial tension (15.6±0.4 - 20.9±0.1 mN/m) which is lower than common vegetable oils such as corn (32.53±0.03 mN/m). Thus, the roasted coffee oil contains efficient surface-active compounds and can be used as an emulsifier.

The influence of coffee oil on foaming properties has been studied by Deotale et al. (2019). Coffee oil was analysed by means of NMR and LC-MS/MS. The results showed that coffee oil consists of hydrocarbons which act as lipophilic tails and chlorogenic acids which act as hydrophilic heads, and both groups are interacting and form micelles. The said coffee oil was spiked at 5 different concentrations into coffee beverages and the foaming properties were studied. The results showed that there was no impact on foam ability except that the sample with maximum coffee oil concentration (0.090% w/w), gave a foam volume smaller by 4.8% than of the control sample. Also, the foam stability was not influenced by addition of coffee oils and remained the same as the control sample.

Piazza, Gigli and Bulbarello (2008) studied the influence of lipids on foaming properties by following the previously described procedure to isolate total foaming fraction (TFF) from coffee (D'Agostina *et al.*, 2004). Their approach is based on the extraction of an oil fraction from TFF and determining the foaming properties of TFF without oils. The results show that absence of lipids contributes towards the foam stability as it increases the mean lifetime of foam. However, the absence of lipids decreases the maximum foam height.

Similar findings were presented by Padma Ishwarya and Nisha (2021). For arabica and robusta spent coffee grounds, native and defatted total foaming fraction was isolated, while a further step of ultrafiltration (3000 Da cut-off) was added. With regards to foam ability, all defatted samples produced larger foams than the native foaming samples. Also, the results show that molecules with MW

higher than 3000 Da have 2 to 4 times better foamability than the low molecular weight samples. When it comes to foam stability, the native samples were less stable than the defatted. Also, the defatted high molecular weight samples showed 1.25 to 1.6 better foam stability than the low molecular weight foaming samples. By the aforementioned results, it can be speculated that the presence of coffee oil interacts with the molecules that are attached to coffee bubble. However, it has been reported in the literature that coffee oil can either enhance or decreases the foam stability of coffee.

**Chemistry of coffee lipids**

The lipid fraction of Arabica and Robusta green beans represent the 15-18% and 8-12% respectively (Viani, Rinantonio; Petracco, 2012). The main chemical compounds that comprise the oil fraction are fatty acids, diterpenes, sterols and tocopherols (Clarke and Vitzthum, 2008).

Most of the fatty acids are esterified with glycerol in the triglycerides, while the 20% are esterified with diterpenes and a small portion are esterified with sterols. (Clarke and Vitzthum, 2008). The predominant fatty acids are C16:0, C18:0, C18:1 and C18:2 (Folstar *et al.*, 1975; Folstar, 1985; Sehat, Montag and Speer, 1993). Apart from the main fatty acids, (Sehat, Montag and Speer, 1993) identified 6 more free fatty acids, C18:3, C20:0, C20:1, C22:0, C24:0. Comparing the free fatty acids concentration in arabica and robusta, the former beans have lower content (Clarke and Vitzthum, 2008).

The main diterpenes that are identified in coffee oil fraction are Cafestol and Kahweol (Poisson *et al.*, 2017) and occur in free and esterified form with fatty

acids. 16-O-methylcafestol and 16-O-methylkahweol are also found in the fraction of diterpenes, while the latter only occurs in robusta coffee (Kölling-Speer and Speer, 2001). In arabica green beans, the concentration of cafestol is higher than kahweol, while robusta coffee oil contains more cafestol than 16-O-methylcafestol (Clarke and Vitzthum, 2008). The free diterpenes (Cafestol, Kahweol and 16-O-methylcafestol) are only found in traces. In addition, diterpenes occur as esterified compounds with palmitic, linoleic, oleic, stearic, arachidic and behemic acids and constitute the 98% of diterpene esters (Clarke and Vitzthum, 2008). Purified cafestol and kahweol are not stable when they are exposed to heat. During roasting, these diterpenes can be dehydrated and produce the dehydrocafestol and dehydrokahweol. It is observed that the raised roasting temperatures increased the concentration of these dehydrated diterpenes in coffee oil (Speer, Tewis and Montag, 1991; Tewis, Montag and Speer, 1993; Kölling-Speer, Kurt and Speer, 1997).

Sterols comprise the 1.5-2.4% of lipid fraction (Picard, Guyot and Vincent, 1984). Sterols occur either free (40%) or esterified (60%) (Bee *et al.*, 2005) The most abundant fraction of sterols are the desmethylsterols which mainly consist of beta-sitosterol (45.4 - 51.6% of desmethylsterols), stigmasterol (21.9 – 23.1% of desmethylsterols) and campesterol (15.8 – 16.9% of desmethylsterols) (Mariani and Fedeli, 1991).

The tocopherols that have been identified in green coffee are a-tocopherols (13.77-22.37 μg/g dry coffee bean) and beta & gamma tocopherols (28.30-74.31 μg/g dry coffee bean) (Clarke and Macrae, 1985). While the lipid fraction is

mainly located in the endosperm, the coffee wax, which is the 0.2-0.3% of green bean, covers the bean (Viani, Rinantonio; Petracco, 2012). The coffee wax is rich in saturated arachidic acid, behemic acid and lignoceric acid.

A typical arabica espresso cup contains 2.5 mg/mL of lipids while robusta contains 1.0 mg/mL (Petracco, 2005). Sehat, Montag and Speer (1993) reported that fine grinding enhances the yield of oil extraction during coffee beverage preparation.

### 2.3.3 Phenolic acids

**Phenolic acids' effects on foaming properties**

The contribution of chlorogenic acids to foaming properties is not clearly defined. During roasting, organic acids are degraded and are involved in reactions that produce Maillard products and melanoidins. The previously reported foaming fraction FFB, which had high foam ability, was reported to have antioxidant properties (D'Agostina *et al.*, 2004). This may indicate that chlorogenic acids are included with melanoidins. The findings of Bekedam, Schols, et al., (2008), showed indeed that chlorogenic acids are incorporated in coffee brew melanoidins. FFB may not derive its foaming properties only from the presence of chlorogenic acids, however, during roasting the degradation of caffeic acid produces low and high molecular weight 4-vinylcatechol oligomers (Frank *et al.*, 2007a), which increased the initial volume and stability of an espresso coffee foam. (Folmer, Blank and Hofmann, 2017)

**Chemistry of coffee chlorogenic acids**

The main groups of acids that are present in green coffee are phenolic acids, volatile aliphatic acids and non-volatile aliphatic acids (8% dry matter, in total)

(Poisson *et al.*, 2017). Acetic and formic acids comprise the volatile aliphatic fraction. (Viani, Rinantonio; Petracco, 2012). The non-volatile fraction consists of citric, malic, oxalic, quinic and phosphoric acid (Kampmann and Maier, 1982; Scholze and Maier, 1983, 1984; Viani, Rinantonio; Petracco, 2012). Another main type of acids that are present in green and roasted coffee are chlorogenic acids.

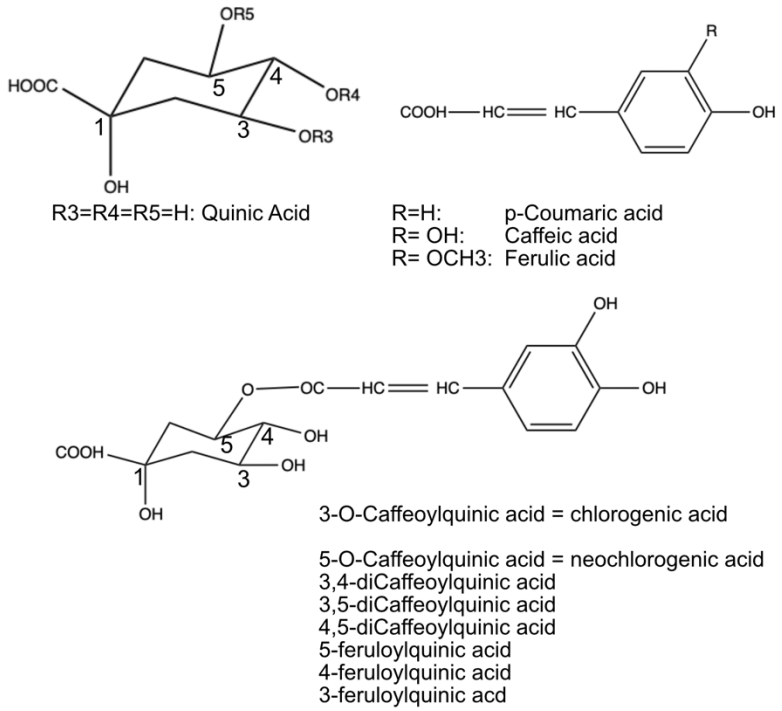



Figure 2-2 Quinic acid and hydroxicinamic acid esterified to form chlorogenic acids. Picture adapted from Bee et al. (2005).

Table 2.4 Concentration of organic acids in green coffee bean.

| | Concentration (% in dry matter) | | Reference |
|---|---|---|---|
| | Arabica | Robusta | |
| Volatile Acids<br>Acetic acid<br>Formic Acid | <0.1 | - | (Viani, Rinantonio; Petracco, 2012) |
| Non-volatile acids<br>Citric acid<br>Malic acid<br>Oxalic acid<br>Quinic acid<br>Phosphoric acid | 2-2.9 | 1.3-2.2 | (Kampmann and Maier, 1982; Scholze and Maier, 1983; Viani, Rinantonio; Petracco, 2012) |
| Chlorogenic acids | 3.4-4.8 | 8.0-14.4 | (Ky *et al.*, 2001; Flament, 2002; Perrone *et al.*, 2008; Viani, Rinantonio; Petracco, 2012) |
| CQA[a] | 80-84% | 67-76% | |
| diCQA[a] | 11-15% | 11-15% | |
| FQA[a] | 4-5% | 7-13% | |
| p-CoCA[a] | 1% | 0.6% | |
| CFQA[a] | 0.4% | 1.6% | |

[a] Calculated as % of total chlorogenic acids

A chlorogenic acid is formed by the esterification of a quinic acid with hydroxycinnamic acid (Flament, 2002; Bee *et al.*, 2005; Viani, Rinantonio; Petracco, 2012). When an ester bond is attached on the 5$^{th}$ position of quinic acid, the resulting chlorogenic acid is 5-caffeoylquinic acid (5-CQA) (Figure 2-2). In the same way, hydroxycinnamic acids attached on the 3$^{rd}$ or 4$^{th}$ position of quinic acid produce the chlorogenic acids 3-CQA and 4-CQA, respectively (Bee *et al.*, 2005; Viani, Rinantonio; Petracco, 2012). Other types of chlorogenic acids are dicaffeoylquinic acids (diCQA), Feruloylquinic acids (FQA), p-coumaroylquinic acids (p-CoQA) and Caffeoylferuloyquinic acids (CFQA) (Clifford, 1985; Bee et al., 2005).

The concentration of chlorogenic acids in green arabica bean is 3.4-4.8% in dry matter, while robusta green beans consist of 8-14.4% in dry mater (Ky *et al.*, 2001) (Table 2.4). Mono-CQAs comprise 80-84% of chlorogenic acids in green

arabica bean, while mono-CQAs in robusta green beans comprise 67-76% of chlorogenic acids (Ky *et al.*, 2001; Perrone *et al.*, 2008). It is reported that 5-CQA is the most abundant CQA (85%), followed by 4-CQA and 3-CQA (Flament, 2002; Perrone *et al.*, 2008). The second most abundant group of chlorogenic acids are diCQA, which comprise 11-15% of the chlorogenic acids in green arabica and robusta beans while FQAs comprise 4-5% and 7-13% of cholorogenic acids in roasted coffee (Perrone *et al.*, 2008). The most abundant isomer is 5-FQA, which comprises 85% of the class (Flament, 2002). The acid p-Coumaroylquinic comprises 1% and 0.6% of CGA in green arabica and green robusta, respectively (Perrone *et al.*, 2008). Caffeoylferuloyquinic acids comprise 0.4% and 1.6% of total chlorogenic acids in green arabica and green robusta beans, respectively (Perrone *et al.*, 2008).

Quinic acid occurs free in green arabica (0.55% dry matter) and green robusta beans (0.35% dry matter) (Viani, Rinantonio; Petracco, 2012). Also, the caffeic acids occur free in green beans (0.2-0.3%), while ferulic acids occur in trace amounts (Viani, Rinantonio; Petracco, 2012).

The roasting process affects the concentrations of organic acids in coffee beans (Farah *et al.*, 2005; Wei *et al.*, 2012a; Król *et al.*, 2020). Exposure of chlorogenic acids to high temperatures leads to many reaction pathways such as: lactonization, water elimination, water addition, trans-cis isomerisation, epimerization, oxidation, acyl-migration, polymerization, and reactions with sugars, like sucrose (Trugo and Macrae, 1984; Jaiswal *et al.*, 2012; Viani,

Rinantonio; Petracco, 2012). Some suggested pathways are presented in Figure 2-3.

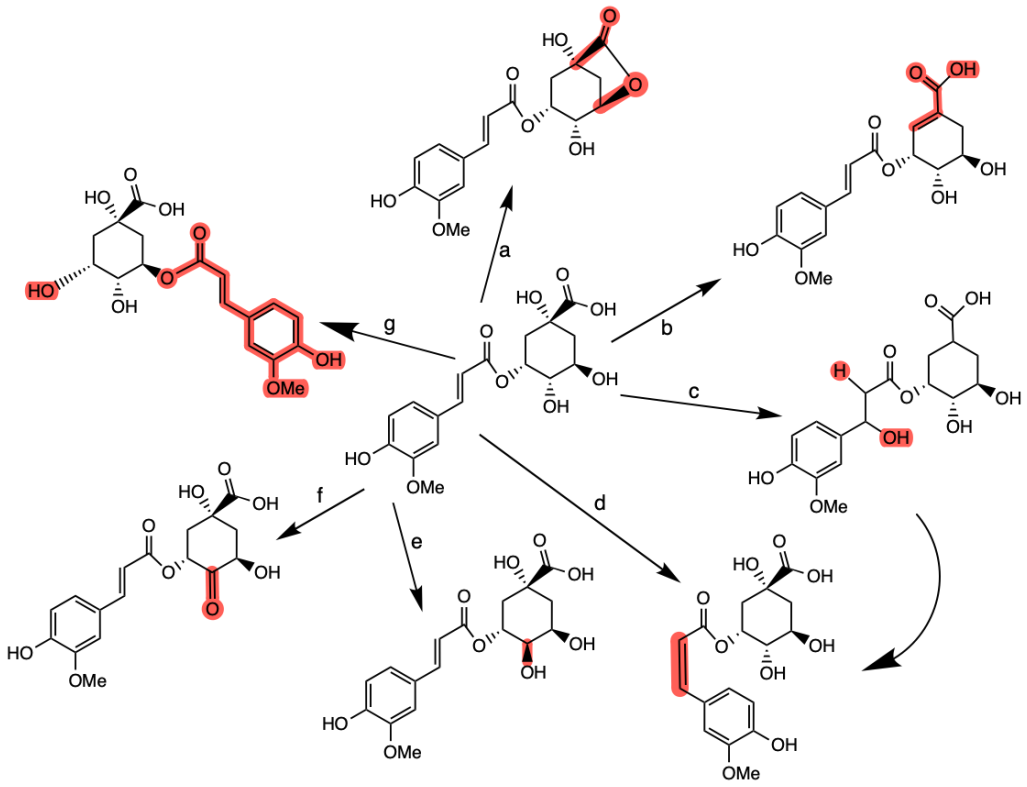



Figure 2-3 Possible reactions of chlorogenic acids during roasting: (a) lactonization, (b) water elimination, (c) water addition, (d) trans-cis isomerisation, (e) epimerization, (f) oxidation, (g) acyl-migration. Image adapted from Jaiswal et al. (2012).

Regarding degradation of 3,5-diCQA, it has been reported that during the first minutes of roasting the 5-CQA moiety is esterified with carbohydrates or proteins, forming so-called "bound chlorogenic acid". Next, the 5-CQA is hydrolysed to its moieties, quinic acid and hydroxycinnamic acid. Simultaneously, the ester bond of the remaining 3-CQA is hydrolysed (Leloup, Louvrier and Liardon, 1995; Viani, Rinantonio; Petracco, 2012). The increased heating stimulates reactions that transform the caffeic acid to 4-vinylcatechol and 4-ethylcatechol. The quinic acid is transformed to hydroquinone, catechol, phenol and pyrogallol (Leloup, Louvrier and Liardon, 1995; Frank *et al.*, 2007a).

During roasting, the concentration of the 5th isomer of CQA and FQA decreases continuously. However, at early stages of roasting the concentration of the 3rd and 4th isomer increases, reaches a peak before decreasing (Farah *et al.*, 2005; Perrone *et al.*, 2008). This can be explained by isomerization of chlorogenic acids (Trugo and Macrae, 1984; Leloup, Louvrier and Liardon, 1995; Farah *et al.*, 2005).

Table 2.5 Concetration of CQA, FQA, diCQA and p-CoCA in green and dark roasted arabica and robusta beans. Table adapted by (Perrone *et al.*, 2008). a: Concentration expressed as mg/100g coffee dry weight.

| | Variery | CQA[a] | FQA[a] | p-CoCA[a] | diCQA[a] |
|---|---|---|---|---|---|
| Green Bean | C.arabica cv. Mundo Novo | 5085.9±66.3 | 232.9±9.66 | 68.9±2.36 | 847.8±34.96 |
| | C. arabica cv. Catuai Vermelho | 4746.3±56.9 | 193.3±2.91 | 55.2±0.82 | 511.8±5.59 |
| | C. canephora cv. Conillon | 6456.8±43 | 609.8±6.09 | 52.4±6.21 | 1299±22.69 |
| Dark Roast bean | C.arabica cv. Mundo Novo | 200.3±3.02 | 34±1.40 | 0 | 3.6±0.5 |
| | C. arabica cv. Catuai Vermelho | 271.7±30.1 | 25±3.41 | 3±0.40 | 5.6±1.12 |
| | C. canephora cv. Conillon | 377.7±3.01 | 125.6±3.37 | 1.6±0.30 | 36.2±1.16 |

Chlorogenic acids are degraded during roasting (Perrone *et al.*, 2008). In dark roasts, the CQAs are degraded by 94-96%, FQAs by 79-85%, p-CoCAs are eliminated by 95-100% and diCQA are degraded by 97-99% (Table 2.5).

Another group of organic acids that is detected mostly in roasted beans is the lactones (Farah *et al.*, 2005; Perrone *et al.*, 2008). Lactones are formed due to

the loss of a water molecule from the quinic acid and the formation of an intramolecular ester bond. At the beginning of the roasting process, the concentration of lactones reaches a maximum and then decreases (Farah *et al.*, 2005; Perrone *et al.*, 2008). Seven lactones were detected in coffee (3-CQL, 4-CQL, 3-FQL, 4-FQL, 3,4-diCQL, 3-pCoQL and 4-pCoQL) (Farah *et al.*, 2005).

### 2.3.4 Nitrogen Compounds

**Nitrogen compounds' effects on foaming properties**

The degradation of protein material is associated with the formation of Maillard products, melanoidins and volatile compounds which define the aroma of coffee (Ali *et al.*, 2012; Hwang, Chen and Ho, 2012). The products of Maillard reactions are reported to lower the surface tension of the beverage (D'Agostina *et al.*, 2004). Conversely, Nunes et al. (1997) reported that the increased degree of roasting increases the extracted protein content in coffee beverages. It is also reported that the protein content has a strong positive correlation with foamability of coffee extracts. This indicates that protein content of coffee extracts is responsible for the initial foaming properties. In accordance with the previous hypothesis, Folmer, Blank and Hofmann (2017) report that material rich in protein is adsorbed on an isolated air bubble of crema of espresso from arabica coffee.

In another paper, Ferrari et al. (2010) examined the interfacial tension of coffee oils and found that oil from a decaffeinated coffee has higher surface tension than coffee oil from the original coffee. The hypothesis that is proposed is that caffeine may contribute to lowering the interfacial tension. However, the decaffeination process may not only remove caffeine but also affect other

surface-active compounds that are responsible for lowering the interfacial tension of coffee oil.

**Chemistry of coffee nitrogen compounds**

Nitrogen compounds comprise 13-16% of the dry matter of green beans (Macrae, 1985). This biomaterial consists of the protein fraction, which is bound and free amino acids, and the non-protein nitrogen compounds, such as caffeine and trigonelline (Homma, 2001; Belitz, Grosch and Schieberle, 2009).

The protein material comprises 8.7-12.2% of dried green beans (Flament, 2002; Bee *et al.*, 2005; Belitz, Grosch and Schieberle, 2009; Viani, Rinantonio; Petracco, 2012). Between 25-40% of total proteins are soluble proteins (Viani, Rinantonio; Petracco, 2012) and 85% of soluble proteins are globulins (Ludwig, Raczek and Kurrock, 1995) which belong to the 11S storage proteins family (Acuña *et al.*, 1999; Rogers *et al.*, 1999) . The remainder of the protein material is insoluble proteins (structural proteins), which are covalently linked with arabinogalactans and chlorogenic acids in the cell wall (Macrae, 1985; Viani, Rinantonio; Petracco, 2012).

The majority of proteins have molecular weights at least 150 kDa (Bee *et al.*, 2005) and they form chains that are bridged with cystine amino acids (Macrae, 1985). Nunes and Coimbra (2002b) determined the nitrogen content in green coffee extract and found that the protein fraction has two subfractions with molecular weights of 58 kDa and 38 kDa. The former fraction is possibly cross-linked with sulphur amino acids.

Although the protein content is the same for arabica and robusta, the protein profile is different. Robusta contains more sulphur amino acids, such as cystine and cystathionine, while alanine is more abundant in arabica (Macdonald and Macrae, 1985; Flament, 2002; Viani, Rinantonio; Petracco, 2012). The major green bean amino acids that constitute the proteins are glutamic acid, aspartic acid and leucine (Müller and Hofmann, 2005; Viani, Rinantonio; Petracco, 2012). Rawel, Rohn and Kroll (2005) report that chlorogenic acids of green bean are incorporated covalently in protein chains and provide an antioxidant activity to these biopolymers.

Free amino acids are also present in green coffee beans and comprise 1% of dry matter (Flament, 2002; Belitz, Grosch and Schieberle, 2009).The main free amino acid is glutamic acid (Poisson *et al.*, 2017) and minor amino acids are ornithine, hydroxyproline, beta-alanine, pipecolic acid and 3-methylhystidine (Homma, 2001). Concentrations of bound and free amino acids in green beans are presented in Table 2.6. The non-protein nitrogen compounds consist of caffeine and trigonelline. Robusta beans have a higher concentration of caffeine than arabica, 2.3% and 1.2% on dry basis, respectively (Bee *et al.*, 2005; Belay *et al.*, 2008). Trigonelline concentration is similar for both coffees (0.6-1.3%) (Bee *et al.*, 2005). Theobormine and theophylline are also present in coffee beans. In Arabica beans the theobromine and theophylline have concentrations 36-40 mg/kg and 7-23 μg/kg, respectively. The concentration of theobromine and theophylline in robusta beans are 26-82 mg/kg and 86-344 μg/kg, respectively (Belitz, Grosch and Schieberle, 2009).

Table 2.6 Bound and free amino acids that are present in green bean

| | % in dry matter of green bean | | |
|---|---|---|---|
| | Bound amino acids | Free amino acids | References |
| Alanine | 0.43-0.61 | 0.05-0.24 | |
| Aminobutyric acid | NA | 0.03-0.33 | |
| Arginine | 0.48-0.68 | <0.04 | |
| Aspartic acid | 0.71-1.00 | 0.05-0.33 | |
| Asparagine | NA | 0.05-0.3 | (Pokorný *et al.*, 1974, |
| Glutamic acid | 1.14-2.26 | 0.07-0.49 | 1975; Tressl, |
| Glycine | 0.56-0.78 | <0.03 | Holzer and |
| Histidine | 0.21-0.30 | <0.04 | Kamperschoer, |
| Isoleucine | 0.33-0.46 | <0.04 | 1982; Macrae, |
| Leucine | 0.54-1.20 | <0.03 | 1985; |
| Lysine | 0.56-0.79 | <0.07 | Flament, |
| Methionine | 0.21-0.29 | Traces | 2002; Viani, |
| Phenylalanine | 0.57-0.80 | 0.03-0.08 | Rinantonio; |
| Proline | 0.55-0.78 | 0.03-0.14 | Petracco, |
| Serine | 0.46-0.64 | 0.03-0.19 | 2012) |
| Threonine | 0.31-0.43 | <0.01 | |
| Tyrosine | 0.42-0.59 | <0.04 | |
| Valine | 0.43-0.60 | <0.08 | |
| Tryptophan | 0.87-1.2 | 0.01-0.05 | |
| 3-Methylhistidine | - | traces | |

Proteins are reported to be involved in many reactions during the roasting process. Due to increased heating, proteins are denatured and are decomposed by up to 80% (Nunes and Coimbra, 2001; Viani, Rinantonio; Petracco, 2012). The free amino acids are destroyed at very high degrees of roasting by pyrolysis and are involved in Strecker and Maillard reactions (Macrae, 1985). Wei et al (2010) identified L-glutamic acid, L-alanine, L-asparagine and γ-aminobutyrate in green coffee extract and reported that they are completely degraded after roasting (Wei *et al.*, 2012b). Homma (2001) reported that lysine contains ε-amino groups that allow the biopolymer to be involved in non-enzymatic browning reactions during roasting.

### 2.3.5 Melanoidins

**Melanoidins' effects on foaming properties**

As previously mentioned, melanoidin content was identified in a foaming sub-fraction (FFB) of a total foaming fraction (TTF) from espresso coffee extract (D'Agostina *et al.*, 2004). An investigation on fractions that contain a combination of polysaccharides and Maillard reaction products have also been reported from Padma Ishwarya and Nisha (2021). A foaming fraction from arabica and robusta spent coffee grounds was isolated. Ultrafiltration (3000 Da cut-off) was applied on each foaming fraction and the foam ability and foam stability were evaluated. With regards to foam ability, the results show that molecules with MW higher than 3000 Da have approximately 1.5 to 6 times better foam ability than the low molecular weight samples. When it comes to foam stability, the high molecular weight samples showed approximately 1.25-to-1.6-time better foam stability than the low molecular weight foaming samples. Also, the foam, which was formed with a low molecular weight fraction from robusta coffee, was completely ruptured after 30 minutes.

**Formation and chemistry of coffee melanoidins**

During the roasting process, coffee beans are exposed to high temperatures which initiate a series of chemical reactions that produce brown coloured pigments. As previously described, the most reactive compounds that are responsible for the formation of coloured compounds are carbohydrates, phenolic acids and free amino acids and proteins (Figure 2-4).

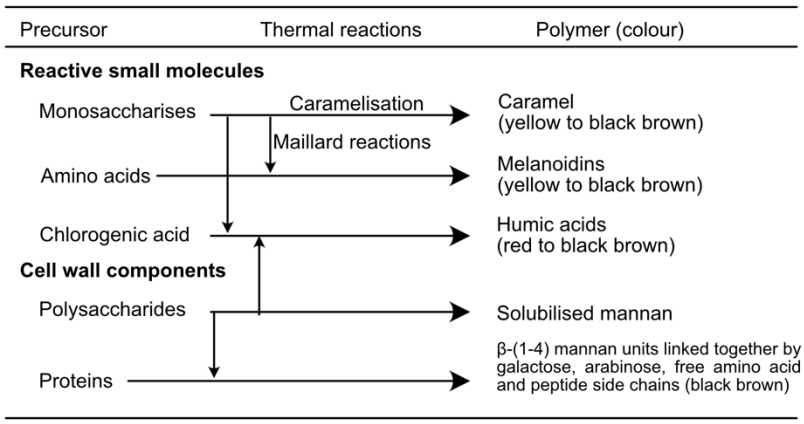



Figure 2-4 Chemical reactions during roasting of coffee bean. Figure adapted from Viani, Rinantonio; Petracco (2012).

The nature of compounds that derive from the thermal treatment of the beans depends on the chemical reaction path that is followed. The products of roasting are volatile aromatic compounds and polymeric brown pigments that are either produced by small molecules (caramelized monosaccharides, melanoidins) or by the reaction of cell wall components with chlorogenic acids and peptide chains (Bonnländer *et al.*, 2005a; Viani, Rinantonio; Petracco, 2012).

The formation of brown coloured material is attributed to four reactions. The main reaction that produces the brown pigments is the Maillard reaction. Carbohydrates are reacting with amino acids or peptides to produce high molecular weight brown material, the melanoidins (Friedman, 1996). Another source of brown compounds is the non-enzymatic oxidation of phenols. (Zamora and Hidalgo, 2005). Third, the incorporation of chlorogenic acids to melanoidin structures has been observed (Bekedam, Schols, *et al.*, 2008) and this work indicated the brown colour of roasted coffee can be attributed to oxidized phenols. A fourth reaction that contributes to the brown colour of the roasted beans is the caramelization of sugars (Kitts *et al.*, 2006). It has been reported that the caramelized products require more time to be formed than the Maillard products (Phongkanpai, Benjakul and Tanaka, 2006). Thus, there is a

competitive reaction between the molecules of sugars and a molecule of amino acid and a sugar (Bekedam, 2008). Also, this indicates that Maillard reaction contributes more to the formation of brown coloured material than the caramelization reactions. It has been reported that the lipid oxidation can lead to the formation of brown colour compounds (Zamora and Hidalgo, 2005; Adams, De Kimpe and Van Boekel, 2008). However, the lipid content of the coffee beans remains stable before and after the roasting process (Bonnländer *et al.*, 2005a), which means that lipid oxidation is not significant, so will not contribute to the brown colour of roasted beans (Bekedam, 2008).

The chemical structure of melanoidins is not yet clearly defined, due to the variation of the structures that are bound together to form the melanoidin compounds and the difficultly to fractionate and isolate such molecules (Nunes and Coimbra, 2010; Rufián-Henares and Pastoriza, 2015). Despite the fact that the melanoidin structure is not clearly understood, there are three main hypotheses proposed for melanoidin formation (Nunes and Coimbra, 2010; Rufián-Henares and Pastoriza, 2015):

1) During the advanced stages of Maillard reaction the furans and pyroles form the high molecular weight material via polycondensation reactions (Tressl, Wondark, et al., 1998; Tressl, Wondrak, et al., 1998; Hayase, Usui and Watanabe, 2006).
2) The high molecular weight material derives from the incorporation of coloured low molecular weight material to proteins. The proteins are linked

together through their reactive amino acids (e.g. lysine, arginine) (Hofmann, 1998a, 1998b; Hofmann, Bors and Stettmaier, 1999b).

3) At the early stages of Maillard reaction, sugar degradation products form a backbone via aldol-type reactions, branched with amino-acids (Cämmerer and Kroh, 1995; Cämmerer, Jalyschko and Kroh, 2002).

An important intermediate of Maillard reactions is the 1,4-bis-(5-amino-5-carboxy-1-pentyl) pyrazinium radical cation (CROSSPY) (Figure 2-5) (Hofmann, Bors and Stettmaier, 1999a; Hofmann and Schieberle, 2002). The CROSSPY radical is involved in the crosslinking of amino acid groups and may therefore participate in the formation of melanoidin backbones. CROSSPY is associated with the second of the three proposed structures of the melanoidins.

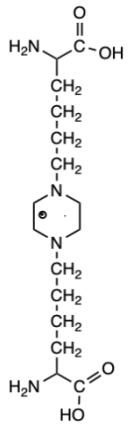



Figure 2-5 Structure of CROSSPY 1,4-bis-(5-amino-5-carboxy-1-pentyl) pyrazinium radical cation. Figure adapted from Hofmann, Bors and Stettmaier (1999a).

The possible reaction paths of CROSSPY in melanoidin formation are presented in (Figure 2-6). The CROSSPY is involved in a redox cycle and can form the pyrazinium ions. The pyrazinium ions either form the CROSSPY by the redox cycle or they form 2-hydroxy-1,4-dihydropyrazines with the addition of water. The mono-,bishydroxylated dihydropyrazines and dimers which are formed due to hydration are precursors of melanoidin compounds.

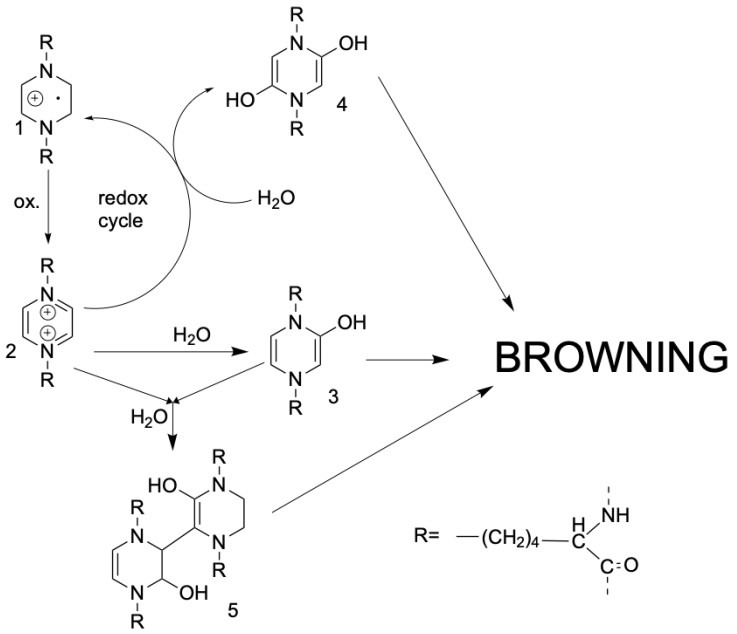



Figure 2-6 Chemical reaction paths of CROSSPY as intermediate for brown coloured material generation. Figure adapted from Hofmann and Schieberle (2002).

As previously mentioned, the coffee compounds that react and form the brown compounds are the carbohydrates, the chlorogenic acids and the amino acids-peptides. The melanoidin content is detected "by difference", which means that the content of "known" material is subtracted from the starting material (Bekedam *et al.*, 2006). Based on this approach the coffee melanoidin content is 25% of the dry roasted coffee bean (Borrelli *et al.*, 2002; Moreira *et al.*, 2012). Another proposed method to calculate the melanoidin fraction is by the absorbance of samples at 405 nm (Borrelli *et al.*, 2002). Bekedam et al. (2006), proposed the use of Specific Extinction Coefficient ($K_{mix}$, ($L\ g^{-1}\ cm^{-1}$)) which was calculated by the law of Lambert – Beer, by substituting the molar extinction coefficient ($\varepsilon$), with the specific extinction coefficient ($K_{mix}$) since the precise molecular weight of melanoidins is not defined and varies. An additional method that takes into consideration the aforementioned methods is the Melanoidin Browning Index (MBI) (Nunes, Cruz and Coimbra, 2012). The MBI is

calculated as the Specific Extinction Coefficient at 405 nm ($K_{mix}$) divided by the relative amount of "unknown material".

The molecular weight of the coffee melanoidins ranges from 2 to 100 kDa (Hofmann, Bors and Stettmaier, 1999a; Gniechwitz *et al.*, 2008). Bekedam et al. (2006) analysed high molecular weight material from coffee brew with the aim to determine the molecular weight distribution by size exclusion chromatography using the Sephadex G-25 column. It was found that the method is not reproducible, and this may be explained by the fact that certain coffee compounds interact with the material of the column and influence the run. The same authors overcame the obstacle of reproducibility by using TSKgel size exclusion columns on HPLC. However, the results showed that such columns do not separate molecules solely by size but with interaction with the material of the column. Thus, a distinct molecular weight distribution for high molecular weight melanoidins was not detected. Bekedam, Roos, et al. (2008) reported that 69% of coffee melanoidins have molecular weight greater than 12 kDa, while 29% of coffee melanoidins are low molecular weight.

The sugar content of high molecular weight material is 70-83% (w/w), while the low molecular weight material contains 16-17% (w/w) (Bekedam *et al.*, 2006; Bekedam, Roos, *et al.*, 2008). The main monomers of the carbohydrate fraction of high molecular weight materials are mannose (29%-43%), followed by galactose (26-36%) and arabinose (6-11%). It is reported that arabinogalactans are more likely to be involved in the formation of melanoidins (Bekedam, Loots, *et al.*, 2008). The main sugars that comprise the low molecular weight fraction are galactose (5-31%), arabinose (2-21%) and mannose (5-10) (Bekedam *et al.*,

2006; Bekedam, Roos, *et al.*, 2008). The presence of sucrose has been linked with the generation of brown colour material, which means that the Melanoidin Browning index is increased (Bekedam, Roos, *et al.*, 2008; Nunes, Cruz and Coimbra, 2012).

Amino acid analysis of the high and low molecular weight material revealed that 6% of each fraction comprises a small number of amino acids (Bekedam *et al.*, 2006). The most abundant amino acids of this material are Glutamic acid/ Glutamine, Glycine, Alanine, Aspartic acid/ Asparagine, Leucine and Proline; while hydrophilic Lysine, and Tyrosine are in low concentrations (Bekedam *et al.*, 2006; Nunes and Coimbra, 2010; Rufián-Henares and Pastoriza, 2015)**.** Bekedam, Loots, et al. (2008) report that the melanoidin content is positively correlated with both the nitrogen and protein content of the isolated brown coloured fractions.

Quinic acid is correlated with the melanoidin content, and this indicates that it is incorporated into melanoidin structures via ester bonds (Bekedam, Schols, *et al.*, 2008). It is reported that Quinic acid may contribute to the negative charge of melanoidins as its content is correlated with the ionic strength of melanoidins (Bekedam, Schols, *et al.*, 2008). Intact incorporation of CGAs in melanoidin structures via non ester linkages of caffeic acid has been observed (Bekedam, Schols, *et al.*, 2008) and comprise the 29% of total phenolic compounds that are incorporated in the brown coloured compounds (Perrone, Farah and Donangelo, 2012a). The phenolic compounds that are present in high molecular weight material showed positive correlation with the melanoidin concentration (Bekedam *et al.*, 2006)**.** Also, protein fragments that are incorporated in

melanoidin structures are mainly linked with the intact chlorogenic compounds (Bekedam *et al.*, 2006; Nunes and Coimbra, 2007).

The effect of roasting degree on melanoidin formation was measured by means of specific extinction coefficient and it is reported that $K_{mix\,405\,nm}$ of high molecular weight material of dark roasted coffee is 2.24 times greater than $K_{mix\,405\,nm}$ of high molecular weight material of light roasted coffee. Technically, this indicates that the extended exposure of coffee beans to heat increased the melanoidin content (Borrelli *et al.*, 2002; Bekedam, Loots, *et al.*, 2008). The roasting degree not only influences the melanoidin content, but also the molecular weight of such structures. It has been reported that with the increase of roasting degree the molecular weight is increasing, then reaches a maximum and then decreases (Borrelli *et al.*, 2002; Bekedam, Loots, *et al.*, 2008; Ripper, Kaiser and Perrone, 2020)**.** Also, it is reported that the increase of roasting degree decreases the antioxidant activity of melanoidin structures (Borrelli *et al.*, 2002)**.** The incorporation of chlorogenic compounds into melanoidin structures occurs at the first stages of the roasting process but the content is decreased later (Perrone, Farah and Donangelo, 2012a).

The physical chemical structures of melanoidins are significant for the foaming mechanisms in brewed coffee (D'Agostina *et al.*, 2004). In general, coffee melanoidins show a negative charge. But the high molecular weight material is more negatively charged than low molecular weight material (Bekedam *et al.*, 2007; Perrone, Farah and Donangelo, 2012a)**.** Although the negative charge of AGP derives from the branched glucuronic acids (Redgwell and Fischer, 2006), the negative charge of melanoidins is not attributed to the incorporated

arabinogalactan moieties but to the incorporated chlorogenic acids (Bekedam *et al.*, 2007; Bekedam, Schols, *et al.*, 2008)**.** Regarding the low molecular weight melanoidins there is contradictory information on the polarity of the molecules. While it has been reported that low molecular weight melanoidins have interacted with anion exchange columns, it has also been reported that through the roasting process melanoidins are altered and become non-polar compounds (Bekedam, Roos, *et al.*, 2008). This indicates that there is a range of charged and uncharged LMW melanoidins. Bekedam, Roos, et al. (2008) speculates the existence of polar and non-polar molecules through the involvement of chlorogenic acid in LMW melanoidin formation. Taking into account that the incorporation of whole chlorogenic acid into melanoidin structures occurs via a non-ester bond through Caffeic acid (Bekedam, Schols, *et al.*, 2008), the resulting structure is negatively charged due to the presence of quinic acid. Further roasting releases the quinic acid moiety while the caffeic acid is still bound and provides a non-polar character to the melanoidin structure (Bekedam, Roos, *et al.*, 2008). As a result, there is a variety of melanoidin structures which show very hydrophilic and partial hydrophobic character (Nunes and Coimbra, 2010; Rufián-Henares and Pastoriza, 2015).

## 2.4 Beer foam stability

While in the case of coffee foam there are no published mechanisms that describe the interaction between foam quality markers, other food foam systems like beer have been studied and suggest such foam stability mechanisms (Evans and Bamforth, 2009). The foam stability mechanisms of beer were selected to be compared with the mechanisms of coffee foam stability, because both products are beverages, and comprise similar chemical compounds. Both beverages have

non-starch polysaccharides, acids, lipids and melanoidins, which are reported to influence the foaming properties.

Beer is very popular beverage and it preferred to be consumed in different ways. Some consumers are more attracted to a pint with a good stable 'head', while others prefer no head at all, so they consume a larger amount of beer (Evans and Bamforth, 2009). Thus, the stability of a good 'head' in a pint of beer is a very crucial sensory attribute and it has been studied since the 1970s (Hudson, 1968). The main components that play a role in the stability and instability of beer foam are non-starch carbohydrates (e.g. beta-glucan, arabinoxylan oligosaccharides), proteins (e.g. Lipid Transfer Proteins (LTP), protein Z), hop-derived acids (e.g iso-humulone), melanoidin fractions, polyphenols, metal anions, pH and lipids (Evans and Sheehan, 2002; Evans and Bamforth, 2009).

Non-starch polysaccharides which can be found in beer, such as beta glucan or arabinoxylans are increasing the bulk viscosity and this may prevent the drainage of the foam system (Evans and Sheehan, 2002; Evans and Bamforth, 2009). The role of carbohydrates on beer foam stability was tested by Lusk, Goldstein and Ryder (1995) on model beer system. Independently, carbohydrates form less stable foam rather than carbohydrates and melanoidin fraction combined. Also Sarker, Wilde and Clark (1998) tested the contribution of arabinoxylans to foaming solutions of bovine serum albumin and Tween 20. Small addition of arabinoxylan (0.2-0.3 mg/mL) reduced the drainage rate and increased the surface elasticity. This may be attributed to the crosslinking of adsorbed proteins with arabinoxylan oligomers.

The beer derived proteins are playing the most significant role in the foam stability of beer. Early research on the foaming properties of proteins has shown that proteins with MW higher than 50 kDa give better foam retention than protein factions with MW of 30 kDa (Slack and Bamforth, 1983). Also, it has been proposed that the more hydrophobic a protein is, it tends to have more affinity for the air/liquid interface. The proteins interact with other substances on the liquid films of foam and contribute to the stability of the system (Slack and Bamforth, 1983; Onishi and Proudlove, 1994). The two most important proteins that have been proposed for foam stability are Protein Z and LTP1 (Kaersoaard and Hejgaard, 1979; Evans and Bamforth, 2009). The synergistic effect of LTP1 and Protein Z leads to stable and elastic air/liquid interfaces (Lu, Bergenståhl and Nilsson, 2020).

Also, it has been reported that proteins interact with hop derived acids (i.e. isohumulones) and the resulted complex enhances the foam stability of beer. The three main proposed mechanisms that contribute to foam stability are:

i. Interaction of epsilon-amino groups of lysine with the ketones of iso-alpha acids (Asano and Hashimoto, 1980).
ii. Ion-dipole interaction of primary amino groups with carbonyl and enolate groups of iso-alpha acids (Simpson and Hughes, 1994)
iii. Hydrophobic interaction between LTP protein and Iso-alpha acids (Euston *et al.*, 2008)

Euston et al. (2008) conducted a molecular dynamic simulation on the interaction of iso-alpha acids and LTP molecules when adsorbed on a vacuum-water interface. It was reported that iso-alpha acids have great surface activity and are adsorbed at high rates to the vacuum/water interface. The LTP molecules

showed higher affinity to interact with the already adsorbed acids, than to adsorb at the bare vacuum/water interface. In addition, Lu, Bergenståhl and Nilsson, (2020) reported that when LTP, protein Z and iso-alpha acids are adsorbed at the air/liquid interface, the surface pressure and elastic modulus increases. Thus, a more stable and elastic interface is formed.

Not only proteins, carbohydrates and acids play significant roles in beer foam stability, but also melanoidins, metal cations, polyphenols, lipids and pH have been studied for their contribution to bubble stability. It was reported that an isolated fraction of beer melanoidins has good foam stability (Lusk, Goldstein and Ryder, 1995). Lewis and Lewis (2003), reported that there is a positive corelation of phenolic acids with beer foam stability. This may imply that phenolic acids may act similarly to iso-alpha acids and crosslink proteins which leads to interface stabilization. In addition, Simpson and Hughes (1994) proposed that divalent and trivalent cations bind with iso alpha acids. The cation-hop acid complex crosslinks the adsorbed protein and leads to enhancement of beer foam stability. Kobayashi et al. (2002), reported that free fatty acids in beer interact with the hydrophobic and foam positive compounds on the air/liquid interface. The outcome of this competitive interaction is the destabilization and rupture of the film.

Depending on the isoelectric point of the foam positive protein and the pH value of the system, the amino acids can have positive or negative or no charge. If the foam stabilising mechanisms in a given system tend to rely on ionic interactions, then the pH values have a significant impact on stability of the interface. In the case of a North American Lager beer, it was showed that high pH values enhanced foam stability (Siebert, 2014). This could imply that the foam

stabilizing agents form ionic bond. However, it was shown that the stabilizing mechanisms in this system are more reliant on hydrogen bonding. Therefore, it can be concluded that there isn't one and only one type of interaction (i.e. hydrophobic, hydrophilic, ionic) that governs the stabilizing mechanisms of foam.

## 2.5 Aspects of coffee foam stability

When it comes to foaming stability mechanisms, what plays the most significant role is the intermolecular interactions between molecules that tend to stabilize or destabilize the foam system. In food foam systems, like beer and coffee, the types of intermolecular bonds that are of interest are the hydrophilic, hydrophobic and ionic interactions (Siebert, 2014). Apart from the type of bonds that are developed, what also plays a significant role is the molecular weight of the compounds that are involved in foam formation.

As can be concluded from the proposed mechanisms of foam stability of beer, there are high molecular weight proteins that are adsorbed on the air/liquid interface, which interact with other compounds and contribute to the stability of the interface. In common with coffee foam, it was observed that foaming fractions which contains high molecular weight material and are rich in melanoidins and carbohydrates show good foam ability and good foam stability (Padma Ishwarya and Nisha, 2021).

In addition, in the beer foam system it was observed that small molecules (e.g. iso-alpha-acids) are interacting with the adsorbed proteins and form a complex which provides more elasticity on the bubble interface. If this model can be

applied to the coffee foam system, then one possible type of molecule that may act similarly to iso-alpha acids are the 4-vinyl-catechol oligomers. There is no evidence which supports that 4-vinyl-catechol oligomers are interacting with melanoidin complexes. However, it has been reported that these oligomers are responsible for promoting the foaming properties of coffee (Folmer, Blank and Hofmann, 2017).

It is very important to take into account the structure and nature of compounds that are responsible for promoting the foaming properties. As described before, there is a variety of low molecular weight melanoidins that are either hydrophilic or hydrophobic, and this depends on the presence or absence of a quinic acid moiety on the compound. These types of low molecular weight compounds could possibly compete with 4-vinyl catechol oligomers and tend to destabilise the foam system.

Apart from the contribution of coffee molecules to the foam stability, it has been reported that also micron- and sub-micron-sized particles affect the foaming properties of coffee (Gmoser *et al.*, 2017). Instant coffee solutions were filtered with 0.2, 0.8 and 1.2 μm cut off and the foaming properties were assessed. The foam system which contained particles smaller than 0.2 μm in diameter tended to have good stability rather than an unfiltered coffee sample. However, the bubble growth rate and surface tension of an unfiltered instant coffee is lower than the filtered coffee with 0.2 μm cutoff. These findings are a very important contribution to the path of unlocking the mechanisms that drive particle stabilized coffee foams. However, the real contribution of particles to foam

stability will probably depend not only on the size but also on the shape and on the physical-chemical properties of the particle's surface (Robert J Pugh, 2016).

## 2.6 Conclusions

The coffee bean is a complicated food structure which undergoes many changes through the roasting and instant coffee process. From the information presented in this review, the main families of compounds (e.g. carbohydrates, acids, proteins) are degraded or bound together to form new materials (i.e. melanoidins). Technically, the foaming properties of a coffee sample are attributed to the composition, structure and functionality of the coffee chemical compounds. The surface activity and foam stability resulting from coffee compounds is not well investigated, and the main findings only highlight correlations between the content of chemical compounds and the foaming properties of coffee samples. Similar foam systems in the food sector, such as beer, can assist in understanding the foam stability mechanisms. The synergistic effect of LTP, protein Z and iso-alpha acids can promote the foam stability of bubble interface in beer. According to this mechanism, it can be proposed that there is not only one family of compounds that are responsible for the foam formation. Thus, the foaming properties of a system in the presence of a number of different surface-active compounds is still unknown. To conclude, further research is required to shed light on mechanisms that explain the foaming properties of coffee solutions.

# Chapter 3: Foam Quality of Coffee

## 3.1 Introduction

The aim of this chapter was to evaluate the foam quality performance of a range of coffee samples. For this reason, a foaming assay was developed to classify instant coffee samples into products with good or poor foaming behaviour. The method development is explained in the 3.3.1 section. The foam decay mechanisms are described by a proposed mathematical equation in section **Error! Reference source not found.**. In the rest of the sections, experiments were carried out to test the influence of i) lipid content ii) soextherm extraction process and iii) heat treatment on instant coffee samples that were found to be significantly different from a control sample in terms of foam ability. Also, experiments were conducted to examine the influence of roasting degree and instant coffee process on the foam quality of coffee extracts.

## 3.2 Materials and Methods

### 3.2.1 Materials

Foam quality performance was assessed for a total of 43 instant coffee products (Table 3.1). Samples #0-28 were kindly provided by Jacobs Douwe Egberts R&D GB Ltd. Sample #0 was assigned as the control sample. Samples #1-7 were the result of pilot plant trials conducted by Jacobs Douwe Egberts R&D GB Ltd. Samples #8-28 comprised the commercial instant coffee products of Jacobs Douwe Egberts R&D GB Ltd that have been produced in the UK. Samples #29-42 were commercial products of Nestlé, including Nescafe Original, Nescafe Gold Blend and the Nescafe Azera series of instant coffees and were obtained locally.

5 single origin and single variety series of green bean, roasted bean and instant coffee products were kindly provided by Jacobs Douwe Egberts R&D GB Ltd

(Table 3.2). Four single variety series were 100% Arabica and one was 100% Robusta. Trial-FD1 is instant coffee which was produced by roasted whole beans Trial-1. The same relationship connects Trial-5 and Trial-FD5. Samples Trial-FD2 and Trial-FD3 originated from whole roasted bean Trial-2/3, but different process parameters were applied during the instant coffee process. Further information on the instant coffee process parameters that were applied on Trial-FD2 and Trial-FD3 were not provided. Trial-4 was the roasted version of Green Bean Trial-4 and Trial-FD4 is the instant coffee product by processing Trial-4. Trial-6 is the roasted version of Green Bean Trial-6 and Trial-FD6 is the instant coffee product by processing Trial-6.

Unwashed arabica green whole coffee beans, washed arabica green whole coffee beans and unwashed robusta green whole coffee were also kindly provided by Jacobs Douwe Egberts R&D GB Ltd (**Error! Reference source not found.**).

Table 3.1 Instant coffee sample. FD: Freeze-dried, SD: Spray dried, ASD: Agglomerated spray dried

| Group | # | Sample | Coffee type | Variety | Roasting Degree |
|---|---|---|---|---|---|
| | 0 | Control | FD | 30% Brazil Arabica - 70 % Robusta | Medium Roast |
| JDE pilot plant samples | 1 | Trial-FD1 | FD | Central America 100% Arabica | Dark Roast |
| | 2 | Trial-FD2 | FD | Colombian 100% Arabica | Medium Roast |
| | 3 | Trial-FD3 | FD | Colombian 100% Arabica | Medium Roast |
| | 4 | Trial-FD4 | FD | Ethiopian Sidamo 100% Arabica | Medium Roast |
| | 5 | Trial-FD5 | FD | Kenyan 100% Arabica | Medium Roast |
| | 6 | Trial-SD1 | SD | 100% Arabica | Unknown |
| | 7 | Trial-SD2 | SD | 100% Arabica | Unknown |
| JDE commercial samples | 8 | FD-Kenco Smooth (KRS) | FD | 30% Brazil Arabica-70 % Robusta | Medium Roast |
| | 9 | FD-Kenco Rich (KRR) | FD | 50% Brazil Arabica-50% Robusta | Medium Roast |
| | 10 | FD-Kenco Decaff | FD | Unknown | Unknown |
| | 11 | FD-Kenco Colombia | FD | Colombian Arabica | Unknown |
| | 12 | FD-Millicano Americano | FD | Unknown | Unknown |
| | 13 | FD-Millicano Americano Decaff | FD | Unknown | Unknown |
| | 14 | FD-Millicano Americano Intense | FD | Unknown | Unknown |
| | 15 | FD-Douwe Egberts Gold (30/70) | FD | 30% Brazil Arabica-70 % Robusta | Medium Roast |
| | 16 | FD-Douwe Egberts Decaff | FD | Unknown | Medium Roast |
| | 17 | FD-Douwe Egberts Pure Indulgence | FD | Unknown | Dark Roast |
| | 18 | FD-L'or Classique | FD | Unknown | Unknown |
| | 19 | FD-L'or Decaff | FD | Unknown | Unknown |
| | 20 | FD-L'or Intense | FD | Unknown | Unknown |
| | 21 | FD-BQI | FD | 100% Robusta | Dark Roast |
| | 22 | SD-Mellow Birds | SD | 100% Robusta | Light Roast |
| | 23 | SD-Maxwell House mild (LRIC) | SD | 100% Robusta | Light Roast |
| | 24 | SD 3-SR1/12 | SD | 100% Robusta | Medium Roast |
| | 25 | SD4-SR10 | SD | 100% Robusta | Medium Roast |
| | 26 | SD5-SR11 B | SD | 100% Robusta | Dark Roast |
| | 27 | SD6-BIC CREMA | SD | 100% Robusta | Light Roast |

Table 3.1 cont.

| Group | # | Sample | Coffee type | Variety | Roasting Degree |
|---|---|---|---|---|---|
| | 28 | SD7-SR16 | SD | 100% Robusta | Dark Roast |
| Nescafe commercial samples | 29 | NESCAFÉ Original | ASD | Blend | Medium-Dark roast |
| | 30 | NESCAFÉ Decaff | ASD | Robusta | Medium Roast |
| | 31 | NESCAFÉ GOLD Blend | FD | Blend | Unknown |
| | 32 | NESCAFÉ GOLD Decaff | FD | Blend | Unknown |
| | 33 | NESCAFÉ GOLD Espresso | SD | 100% Arabica | Unknown |
| | 34 | NESCAFÉ GOLD Intense | FD | Blend | Dark Roast |
| | 35 | NESCAFÉ GOLD Smooth | SD | Blend | Light Roast |
| | 36 | NESCAFÉ GOLD Barista Style | FD | Blend | Unknown |
| | 37 | NESCAFÉ GOLD Origins Cap Colombia | FD | Colombian 100% Arabica | Unknown |
| | 38 | NESCAFÉ GOLD Origins Indonesian Sumatra | FD | Indonesian 100% Robusta | Unknown |
| | 39 | NESCAFÉ AZERA Americano | SD | Blend | Unknown |
| | 40 | NESCAFÉ AZERA Americano Decaff | SD | Blend | Unknown |
| | 41 | NESCAFÉ AZERA Intenso | SD | Blend | Unknown |
| | 42 | NESCAFÉ AZERA Espresso | SD | Robusta | Unknown |

Table 3.2 Green bean, Roasted bean, and Instant coffee series

| Green Bean | Roasted bean | Instant coffee | Variety | Origin |
|---|---|---|---|---|
| N/A | TD1 | FD1 | 100% Arabica | Central America |
| N/A | TD2/3 | FD2<br>FD3 | 100% Arabica | Colombia |
| T4 | TD4 | FD4 | 100% Arabica | Ethiopia Sidamo |
| N/A | TD5 | FD5 | 100% Arabica | Kenya |
| T6 | TD6 | FD6 | 100% Robusta | Vietnam |

Table 3.3 Green whole beans

| Origin | Variety | Process |
|---|---|---|
| Nicaragua | 100% Arabica | Washed |
| Brazil | 100% Arabica | Unwashed |
| Vietnam | 100% Robusta | Unwashed |

### 3.2.2 Moisture content determination of instant coffee samples

Aliquots (n=3) of 3 ± 0.0001 g of instant coffee sample (GR200-EC, A&D, Tokyo, Japan) were heated in a vacuum oven (Vacutherm, Thermo Fisher Scientific, Loughborough, UK) at 70˚C under reduced pressure (i.e. 5000 ± 100Pa) (Edwards 2 stage, Edwards Vacuum, Burges Hill, UK) for 16 hours as per BS 5752-6:1983 and ISO 3726-1993as per BS 5752-6:1983 and ISO 3726-1993. The mass of samples was weighed again, and the moisture content was determined by Equation 3.1:

Equation 3.1 Moisture content determination.

$$\text{Moisture content (\%)} = \frac{\mathrm{M_{sample}} - \mathrm{M_{dried\ sample}}}{\mathrm{M_{sample}}} * 100 \qquad \text{Equation 3.1}$$

### 3.2.3 Lipid content determination – Soxhlet extraction

Aliquots (n=3) of 2 ± 0.0001g of instant coffee granules were placed on 2 sheets of qualitative filter paper (Fisher Scientific UK Ltd, Loughborough, UK). The filter papers were folded and placed in a Whatman™ cellulose extraction thimble (GE Healthcare, Chicago, Illinois, USA). An extraction flask was placed in a draft oven (GPIS/100/CLAD/250/HYD, Leader Engineering, Merseyside, UK) at 105 ˚C for 1 hour to dry out. Then the flask was placed in a desiccator filled with self-indicating silica gel (Fisher Scientific, Loughborough, UK) to cool down. 3 boiling stones (C. Gerhardt GmbH & Co. KG, Königswinter, Germany) were placed in the flask and the weight of flask, and boiling stones was determined with a digital balance. The flask was filled with 50 mL of petroleum ether (Fisher Scientific UK Ltd, Loughborough, UK) and the thimble was placed into the flask. The flask was loaded into the Soexterm unit (C. Gerhardt GmbH & Co. KG, Königswinter, Germany) to commence the analysis. At the end of the analysis, the thimbles were removed from the flask and placed

in a fume hood overnight to dry out the remaining petroleum ether. The flask was placed in a draft oven at 105 ˚C for 1 hour to dry out the remaining petroleum ether before it was placed in a desiccator filled with self-indicating silica gel to cool down. Finally, the mass of flask was determined again, and the lipid content was determined by Equation 3.2:

Equation 3.2 Lipid content determination

$$\%\ \text{Lipids} = \frac{\text{Mass}_{\text{instant coffee}} * (100 - \text{Moisture content}(\%))}{\text{Mass}_{\text{flask after extraction}} - \text{Mass}_{\text{Flask+Stones}}} \quad \text{Equation 3.2}$$

Where:

| | |
|---|---|
| $\text{Mass}_{\text{instant coffee}}$ | The mass of instant coffee to be analysed |
| $\text{Moisture content}(\%)$ | Moisture content as defined by equation Equation 3.1 |
| $\text{Mass}_{\text{flask after extraction}}$ | Mass of dried flask after the soextherm analysis |
| $\text{Mass}_{\text{Flask+Stones}}$ | Mass of dried flask with 3 boiling stones before soextherm analysis |

Complete removal of the remaining petroleum ether on the defatted coffee was achieved in a vacuum oven at 70˚C for 16 hours at 5000 ± 100Pa.

BS 5752-6:1983 is a sufficient method to remove the moisture from the matrix of instant coffee granules. The removal of water is achieved as the temperature of the inside of the oven reaches 70 ˚C and the pressure 5000±100 Pa.

Any substance will freely create new surface area to change state from liquid to gas at a given temperature when its vapour pressure is equal to or higher than the surrounding pressure. In the given system of defatted instant coffee granules, there were water molecules due to the moisture of the material and remains of petroleum ether from the soextherm extraction. According to the MSDS of the

petroleum ether that was used for this method, its components are hydrocarbons, C6, isoalkanes and <5% n-hexane (ThermoFisher Scientific, 2021). A C6 isoalkanes is 2-methylpentane. To remove the water, n-hexane and 2-methylpentane from instant coffee matrix the oven's pressure must reach values lower than the vapour pressure of each substance at 70˚C. The vapour pressure of a given substance at a specific temperature can be determined according to Equation 3.3 (Perry and Green, 1997):

Equation 3.3 Vapor pressure equation

$$\frac{\mathrm{V_p}}{Pa} = \exp\left(\mathrm{C1} + \frac{\mathrm{C2}}{\frac{\mathrm{T}}{K}} + \mathrm{C3} * \ln\left(\frac{\mathrm{T}}{K}\right) + \mathrm{C4} * \left(\frac{\mathrm{T}}{\mathrm{K}}\right)^{\mathrm{C5}}\right) \qquad \text{(Equation 3.3)}$$

Where:

| | |
|---|---|
| $\mathrm{V}_p$ | Vapor pressure in Pa |
| T | Temperature in K |
| Pa | Pascal |
| K | Kelvin |
| C1,C2,C3,C4,C5 | Empirical coefficients |

The empirical coefficient of each substance and the temperature range that Equation 3.3 is defined are presented in Table 3.4.

Table 3.4 Empirical coefficients of Vapor pressure equation for n-hexane, 2-methylpentane, water. Tmin-Tmax is the minimum and maximum temperature that equation 3.3 is valid.(Perry and Green, 1997)

| Substance | C1 | C2 | C3 | C4 | C5 | Tmin- Tmax (K) |
|---|---|---|---|---|---|---|
| nHexane | 104.65 | -6995.5 | -12.702 | 1.24E-05 | 2 | 177.83-507.5 |
| 2-methylpentane | 77.36 | -5791.7 | -8.4912 | 7.79E-06 | 2 | 119.55-497.5 |
| Water | 73.649 | -7258.2 | -7.3037 | 4.17E-06 | 2 | 273.16-647.13 |

Substituting the C1, C2, C3, C4 and C5 coefficients to Equation 3.3 when T=273.15+70 K = 343.15 K the Vapor pressure of each substance is shown in Table 3.5.

Table 3.5 Vapour Pressure of nHexane, 2-methylpentane and water at T=343.15K

| Substance | Vapor Pressure (Pa) |
|---|---|
| nHexane | 105382.546 |
| 2-methylpentane | 136852.054 |
| Water | 31180.991 |

The vapour pressure of each substance at T=70˚C is higher than the pressure of the oven (5000±100 Pa) so by applying the parameters that BS 5752-6:1983 suggests it is feasible to boil off and remove not only the water but also a part of what remains of the petroleum ether form the defatted instant coffee matrix. In practice, some of the solvent will be molecularly adsorbed onto or into the coffee particles, so will require an (unknown) temperature to remove, depending on how strong the physical bonds are with the coffee material. The defatted coffee was vacuum packed with a vacuum packing machine (AUDIONVAC VMS 43, Audion Vacuum Packing Machines, Wessp The Netherlands) in foil bags (Fresherpack Limited, Brigg, UK) and stored at 4˚C for further analysis.

### 3.2.4 Heat treatment of instant coffee samples

Aliquots (20±0.1 g n=3) of a vacuum-dried instant coffee sample (70˚C for 16 hours, P=5000±100 Pa) were placed in a draft oven at 150˚C, 185˚C and 220˚C for 20 minutes. After heating, the sample was placed in a desiccator with self-indicating silica gel for 30 minutes, so the temperature of the sample was equilibrated with the ambient temperature. The heat-treated samples were vacuum packed as per 3.2.3 section.

### 3.2.5 Sample Preparation for foam ability and foam stability experiments

Each pre-weighed instant coffee sample was placed in a Duran bottle. Ultra-pure water (18.2 MΩ) (PurA-Q+ 18.2 MΩ, SLS Lab Pro, Nottingham, UK) was heated in a kettle (Russell Hobs, Spectrum Brands Ltd, Manchester, UK) until

the temperature reached 85˚C. The temperature of the water was monitored by a PT100 resistance thermometer submerged in the kettle (Fischerbrand, Pittsburgh, Pennsylvania, USA). The heated water was transferred into the bottle until the total mass of the solution reached 200±0.1g with final concentration 1.5% w/w in coffee solids. The bottle was gently shaken 10 times, and it was placed in a water bath at 4˚C until the temperature of the solution reached 20˚C. The mass of instant coffee and water were calculated based on the moisture content of instant coffee by Equation 3.4 and Equation 3.5:

Equation 3.4 Coffee mass equation

$$\text{Coffee(g)} = 0.0316 * \text{Moisture (\%)} + 2.9887 \qquad \text{Equation 3.4}$$

Equation 3.5 Water mass equation

$$\text{Water (g)} = -0.0003 * \text{Moisture (\%)} + 197 \qquad \text{Equation 3.5}$$

### 3.2.6 Roasting of green coffee beans

Roasting of unwashed arabica, washed arabica and robusta coffee (Table 3.3) was performed using an RFB-S Roaster (Neuhaus Neotec, Ganderkesee, Germany) under isothermal regimes. The inlet air temperature was 250˚C. The duration of roasting was 120, 240 and 360 seconds. The roaster's fan frequency was set to 48 Hz, with batch sizes of 500±0.1g (Lunar balance, Acaia, California, USA). Both inlet air and product temperature were measured using a Type-K thermocouple with a length of 100 mm and diameter of 1 mm (RS Components Ltd., Nottingham, UK) and logged with an 8-channel type-K temperature logger (TC-08, Pico Technology, Saint Neots UK). Ambient air was used to cool the beans for 60 s once the specified roasting endpoint was achieved. Whole bean surface colour was measured in duplicate using a ColorTrack Benchtop Device (R-100B, FreshRoastSystems, Inc., California, USA). The mass of the batch was

measured before and after roasting (Lunar Balance, Acaia, California, USA). Measurements after roasting were completed once the beans had equilibrated with ambient temperatures. Bulk density was calculated from the measured mass (Lunar balance, Acaia, California, USA) of coffee that occupies a 250 ml beaker, where beans settled freely. The top of the beaker was smoothed to ensure a level fill and measurements were repeated in triplicate using aliquots of each sample set. Whole bean moisture was measured in duplicate using a NIR Food Analyser (Infralab, NDC Technologies, Ohio, USA)

### 3.2.7 Freezer milling and sieving of whole coffee beans

A Spex 6875 Freezer/Mill (Antylia, Illinois, USA) was used to grind whole coffee beans under cryogenic conditions. A 20±0.1 g aliquot of whole coffee beans and a stainless-steel impactor (Antylia, Illinois, USA) were placed in a polycarbonate cylinder. The container was sealed with stainless steel end plugs, and it was loaded on the freezer mill. The freezer mill was filled with liquid nitrogen and the lid of the mill was closed. The grinding settings were Pre-cool:10 minutes, Run time: 2 minutes, Cool time:1 minute, Cycles:2, Rate: 10 CPS (or 20 impacts per second). Throughout each run, the polycarbonate container along with the coffee were submerged in liquid nitrogen. The ground material was sieved (pore size; 500um) using a horizontal sieve shaker AS 400 Control (Retch GmbH, Haan, Germany) upon the following conditions Amplitude: 2.00 mm/"g", Time: 20 min, Time intervals: 20 seconds. The freezer-milled and sieved coffee was vacuum packed as per 3.2.3 section.

### 3.2.8 Coffee extraction protocol

A weighed portion (18±0.01 g) of freeze-milled coffee beans and a magnetic agitator were placed in a 1000 mL beaker (Schott, Wolverhampton, UK). A 300

mL aliquot of ultra-pure water at 85˚C was decanted into the beaker. The temperature of water was monitored by a PT100 resistance thermometer submerged in the kettle. The beaker was placed on a magnetic stirring hotplate MR 3001 K (Heidolph, Schwabach, Germany). Several layers of tin foil covered the beaker during the extraction time to prevent the loss of water due to evaporation. The stirring speed was 500 RPM. The temperature of the slurry was monitored by a PT100 resistance thermometer submerged in the beaker. The agitation of the slurry lasted 5 minutes. Then, the beaker was removed from the hotplate, left to stand for further 5 minutes, and filtered in a Duran bottle with a stainless-steel mesh coffee filter (pore size of 200 um; Amazon, London, UK).

### 3.2.9 Total solids determination

The method is based on previously reported method (Castaño-Castrillón, Quintero and León Vargas, 2000). 10±0.0001 g of coffee extract was weighed in a dry and pre-weighted glass dish (inner diameter 5 cm; Schott, Wolverhampton, UK). The dish was placed in a draft oven at 105˚C for 4 hours. After 4 hours the dish was placed in a desiccator filled with self-indicating silica gel for 30 minutes and then weighed again. The number of replicates was n=3. Total solid content was determined with the following Equation 3.6:

Equation 3.6 Total solids equation

$$\text{TS}\ (\%) = \frac{M_2 - M_1}{M_{extract}} * 100 \qquad \text{Equation 3.6}$$

Where:

| | |
|---|---|
| TS (%) | Total solids expressed in % per unit of extract's mass |
| $M_2$ | Gross mass of dish with coffee after 4 hours of drying |
| $M_1$ | Mass of dried dish |
| $M_{extract}$ | Mass of extract |

### 3.2.10 Aeration protocol

Coffee foams (n=5 per condition) were generated by a stirring method with a VDI 25 disperser (VWE, Radnor, Pennsylvania, U.S.A) and a S 25 N - 18 G – ST dispersing tool (IKA, IKA®-Werke GmbH & CO. KG, Staufen, Germany). An aliquot of 20±0.01 mL (TS, Czech Republic) of a coffee solution was decanted in a 100 mL measuring cylinder (SLS, Nottingham, UK). The immersion depth of the dispersing tool into the coffee solution was 40 mm, stirred at 17500 RPM for 10 seconds.

### 3.2.11 Foam ability and foam stability experiments

Coffee foam was characterised in terms of the amount of foam that was generated and its stability through time. For the purpose of this project, foam ability was defined as the initial volume of foam immediately after cessation of the aeration process. The foam height and liquid height were recorded using a Canon 2000D digital SLR camera (Canon, Japan). Snapshots were taken every 10 seconds for 30 minutes; this data set was used to evaluate foam stability as described in the next section. The number of replicates was 5.

### 3.2.12 Data analysis

A script was developed in Python 3 to fit the foam height vs time data points in by mathematical equation. The aim was to quantify the foam stability parameters of a given coffee sample. The package that was used for fitting was scipy.optimize.curve_fit (Virtanen *et al.*, 2020). The input of the package requires the model function along with the defined model parameters, the independent variable where the data is measured and the dependent data. In the foam height vs time data points, the time was the independent variable, and the

foam height was the dependent variable. The package returned the optimal values (popt) for the parameters so that Equation 3.7 was minimised.

Equation 3.7 Sum of square residuals of predicted vs measured values

$$\min\left(\sum_{i=1}^{N}\left(y_{Predicted}-y_{Measured}\right)^2\right) \qquad \text{Equation 3.7}$$

The package also returned the estimated covariance (pcov) square matrix of optimal parameters (popt). The diagonal values of matrix indicate the parameter estimate's variance. Each parameter's standard deviation error was calculated by calculating the square root of each element from the diagonal of the covariance matrix.

### 3.2.13 Statistical analysis on the volume of foam

One-way ANOVA was performed through Python 3 scripts by using the package scipy.stats.f_oneway (Virtanen *et al.*, 2020). The level of significance was set at $p = 0.05$ for the statistical test.

### 3.2.14 Correlation Analysis

The correlation analysis between two independent variables was executed through Python scripts by using the package scipy.stats.linregress (Virtanen *et al.*, 2020). The input of the scipy.stats.linregress command is the two sets of independent variables. The package returned:

- the slope of the regression line, the intercept of the regression line
- the Pearson correlation coefficient
- the p-value for a hypothesis test whose null hypothesis is that the slope is zero, using Wald Test with t-distribution of the test statistic

- the standard error of the estimated slope, under the assumption of residual normality
- The standard error of the estimated intercept, under the assumption of residual normality.

## 3.3 Results and Discussion

### 3.3.1 Aeration protocol development

The aim was to develop an aeration protocol that incorporates the largest amount of air in the initial liquid by producing a foam system in minimum time. In this set of experiments, the aeration procedure was developed with consideration for the stirring method and the parameters considered were i) the impeller, ii) the vessel, iii) working volumes, iv) temperature, v) aeration time and vi) stirring speed.

It is important to highlight that the instant coffee samples were rehydrated in hot water in order to assist on the solubilisation but then the samples were cooled to ambient temperature prior the aeration protocol. The ambient temperature at aeration was selected because at higher temperatures there is an increased evaporation rate of water molecules from the bubble lamellae which will have instant effect on the foam structure. When evaporation occurs, the lamellae become thinner and more prone to rupture. On the other hand, the concentration of surface-active compounds increases and possibly make the film more elastic and less prone to rupture. These two counteractive mechanisms determine the fate of the lamella. In order to exclude such mechanisms when investigating the foam ability and foam stability mechanisms, the samples were aerated at ambient temperature.

The impeller that was selected was a rotor-stator mixer because it is reported that such devices can produce a high amount of foam with very small bubble sizes (Drenckhan and Saint-Jalmes, 2015). To find the optimal combination of aeration time and stirring speed, foam ability of control coffee was tested at different aeration times and different aeration speeds (Figure 3-1).

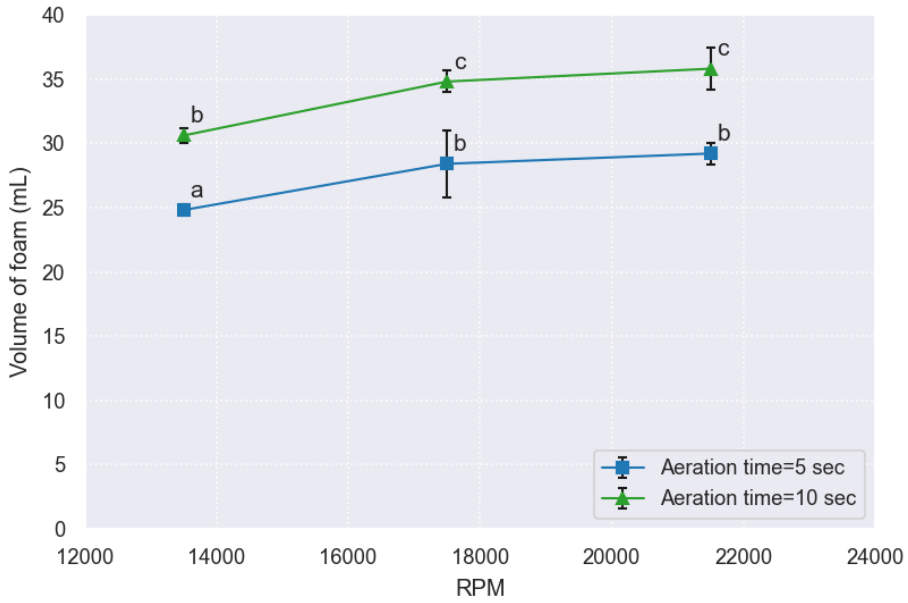



Figure 3-1 Control's coffee foam aerated at different stirring speeds and aeration times. n=5. Different letters indicate a significant difference between samples at $p<0.05$.

As per Figure 3-1, higher foam volume was achieved at an aeration time equal to 10 seconds for all the tested RPMs. The generated foam volume was increased with increasing RPM and reached a plateau at RPM higher than 17500 RPM. Thus, the optimal parameters identified in this experiment were aeration for 10 seconds and stirring speed at 17500 RPM.

Since foam generation in the present system is based on a combination of gas entrainment at the free surface and on the break-up of bubbles under shear, higher aeration time results in a larger amount of generated foam (Drenckhan and Saint-Jalmes, 2015). In the same manner, higher RPM transfers a higher amount of kinetic energy to the system, and the flow field tends to reach the

turbulent regime (Raju *et al.*, 2005) and this favours the disturbance of the free surface. At RPM higher than 17500 the foam volume did not change significantly, and this may be attributed to the fact that every low molecular weight surface active agent had been adsorbed on the interface and no other new, stabilised air/beverage interface could be generated. Another possible reason is that the rate of breaking up bubbles under shear equals the rate of bubble coalescence. At high RPM the bubbles may reach a critical velocity which means that the Weber number reaches its critical value. Under these conditions, if two bubbles collide, they will form a larger bubble (Karakashev, 2017).

### 3.3.2 Foam quality – Screening process

For the purpose of this project, the foam quality performance was defined by foam ability and foam stability. Foam ability was defined as the initial volume of foam immediately after cessation of the aeration process. Foam stability was evaluated by monitoring foam decay through the course of time. Detailed evaluation of foam stability is presented in section **Error! Reference source not found.**.

**Foam Ability**

The foam ability of instant coffee samples was normalised against the foam ability of the control instant coffee sample (Figure 3-2). The foam ability score for half of the samples was not significantly different to the control. However, pilot plant instant coffee (i.e Trials) and several other commercial coffees (e.g. Milicano, several Nescafe Gold Blend and several Azeta) exhibited lower foam ability.

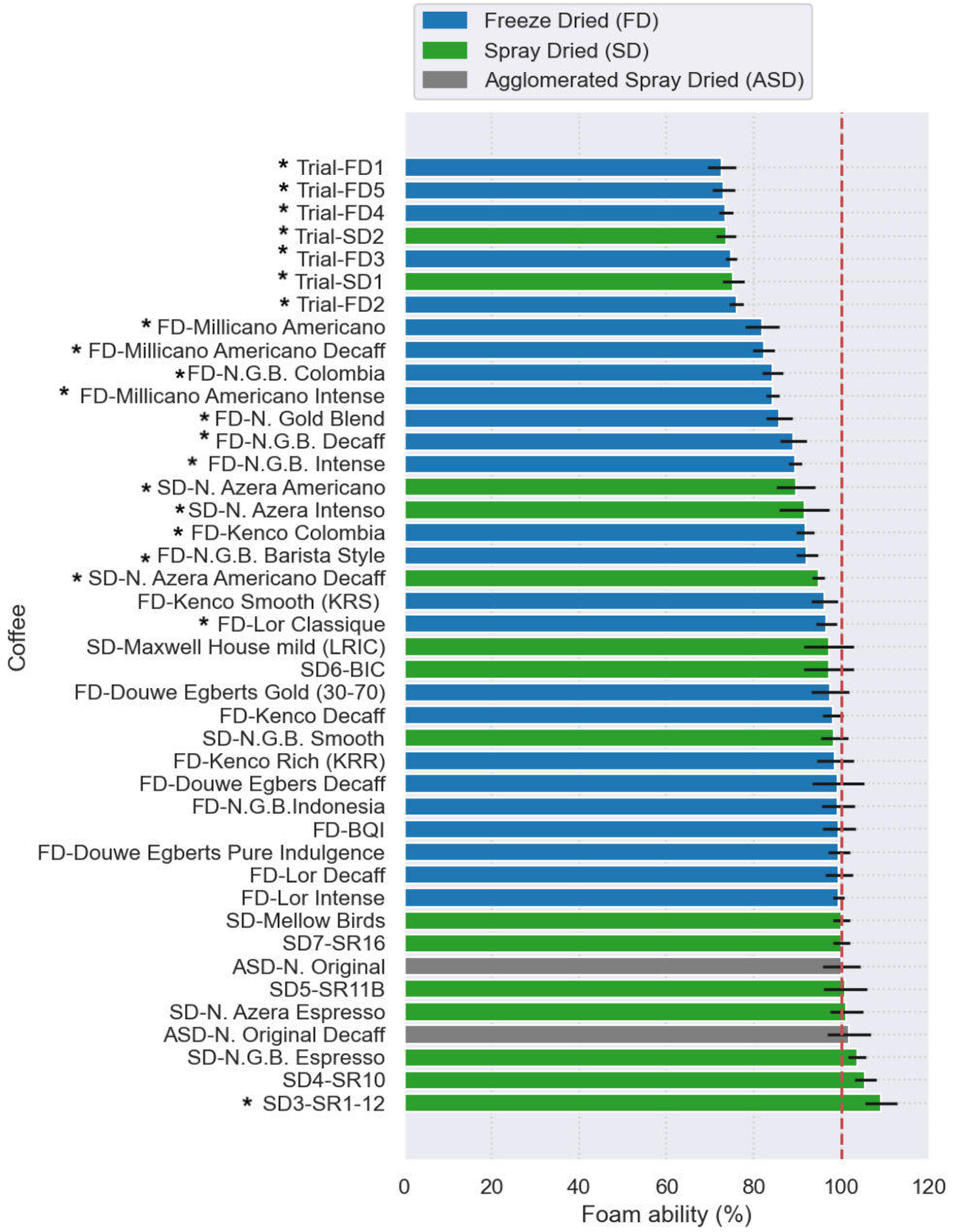



Figure 3-2 Foam ability of instant coffee samples (% on foam ability of control instant coffee). n=5 Samples marked with * were significantly different from control in terms of foam ability.

### Foam Stability

The foam was generated in a volumetric cylinder, and the foam height was measured at rest for 30 minutes. At t=0 min the foam height was at its maximum value. As the foam system rests, several destabilising phenomena occur simultaneously which led to foam decay (Figure 3-3). There are three primary

physical phenomena which occur during foam decay (Robert J. Pugh, 2016; Karakashev, 2017). The first phenomenon is gravitational drainage, where the liquid is drained between the bubbles and accumulates at the bottom of the vessel. The second destabilising mechanism is foam disproportionation, which causes bubble coarsening, and its driving mechanism is the different pressure across a foam film. Foam disproportionation can occur both within the foam and at the foam surface. In the first case, the phenomenon causes bubble coarsening, while in the second case the gas which diffuses to the air volume above the foam structure, reduces the volume of foam directly. The third phenomenon is coalescence where the foam films burst. Rupture can occur when external vibrations affect the film. It is important to highlight that the thinner is a bubble lamella the less energy through vibration is needed to rupture it. Similar to foam disproportionation, coalescence can occur within the foam structure between two neighbouring bubbles and cause foam coarsening. In addition, coalescence can occur between a bubble and the volume of air above the foam which can reduce the volume of foam.

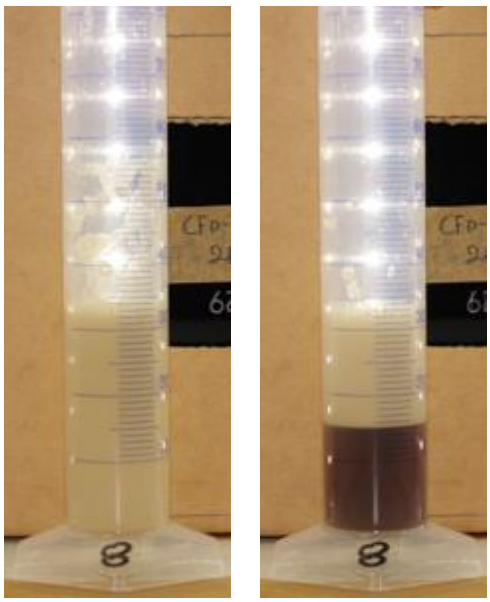


Figure 3-3 Foam height of Control at 0 min (left) and 30 min (right) after aeration.

In Figure 3-4a, bubble 1 has higher pressure than bubble 2 and this leads to air diffusion from bubble 1 to bubble 2. Then, bubble 1 vanishes to leave only a larger bubble 2 which in turn decays. The same mechanism applies in Figure 3-4b, where the pressure of "blue" bubble is higher than the atmospheric pressure. Figure 3-4c depicts the bubble coalescence within foam. The foam film between two bubble bursts and the two bubbles merge in one larger bubble. Figure 3-4d shows a specific form of coalescence between the "blue" bubble and the volume of air above the foam.

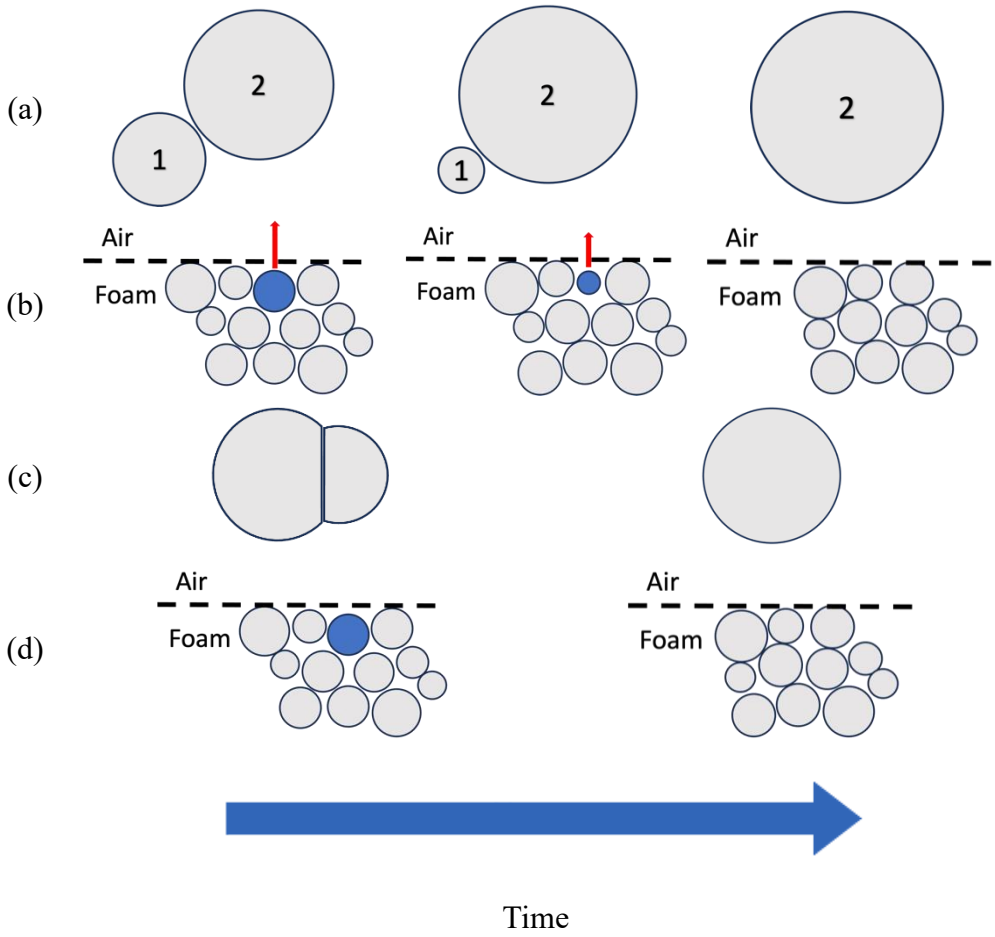



Figure 3-4 (a) & (b) Example of bubble disproportionation. (c) &(d) Example of bubble coalescence

The foam fractions that were measured through time are presented in Figure 3-5.

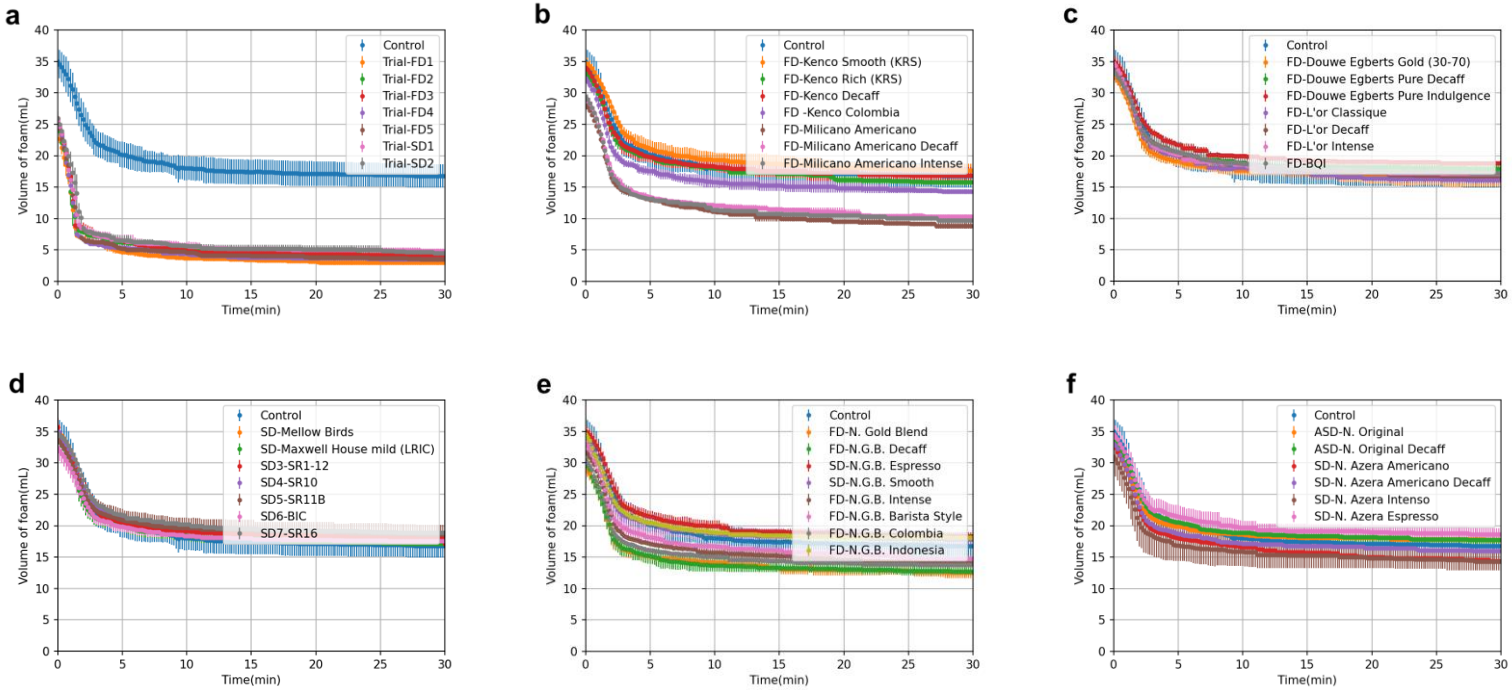



Figure 3-5 Foam stability evaluation. (a) Volume of foam vs time for JDE pilot plant samples, (b) JDE freeze-dried commercial samples , (c) JDE freeze-dried commercial samples, (d) JDE spray-dried commercial samples, (e) Nescafe Gold Blend series, (f) Nescafe Original and Nescafe Azera series

### 3.3.3 Evaluation of Foam Stability

To quantify and compare the foam curves of each sample, the data were fitted to Equation 3.8.

Equation 3.8 Foam height model

$$V_f = Ae^{-Bt} + Ce^{-Dt} \qquad \text{Equation 3.8}$$

Where:

| Parameter | Units | Description |
|---|---|---|
| $V_f$ | mL | Volume of foam |
| A | mL | Partial initial volume of foam |
| B | $min^{-1}$ | Decay constant |
| C | mL | Partial initial volume of foam |
| D | $min^{-1}$ | Decay constant |
| t | minutes | time |

The fitted curve for control coffee foam is presented in Figure 3-6. Along with fitted curve, 95% confidence band and 95% prediction band are displayed in the plot. The confidence band is the confidence region for the fitted equation. The prediction band is the region that contains approximately 95% of the measurements.

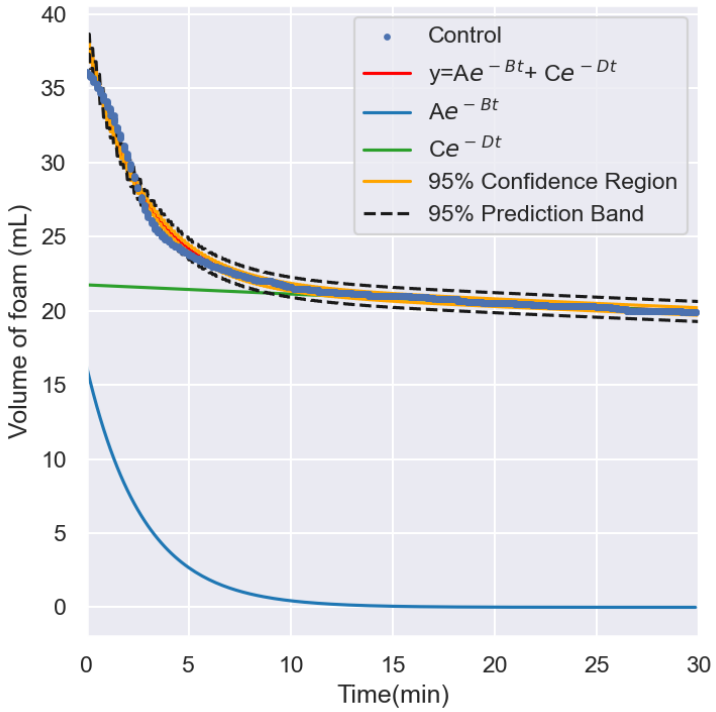



Figure 3-6 Fitted curve on foam height of control coffee.

Calculated parameters, standard deviation error and $R^2$ of fit for control coffee are presented in Table 3.6.

Table 3.6 Optimum parameters for fitting control foam height curve to Equation 3.8.

| Control coffee | |
|---|---|
| A (mL) | 16.23±0.08 |
| B($min^{-1}$) | 0.360±0.004 |
| C (mL) | 21.74±0.06 |
| D ($min^{-1}$) | 0.0029±0.0001 |
| $R^2$ | 0.99 |

The rest of the fitted curves of foam height are presented in the Appendix A. The calculated parameters for the rest of foam curves are presented in Figure 3-7.

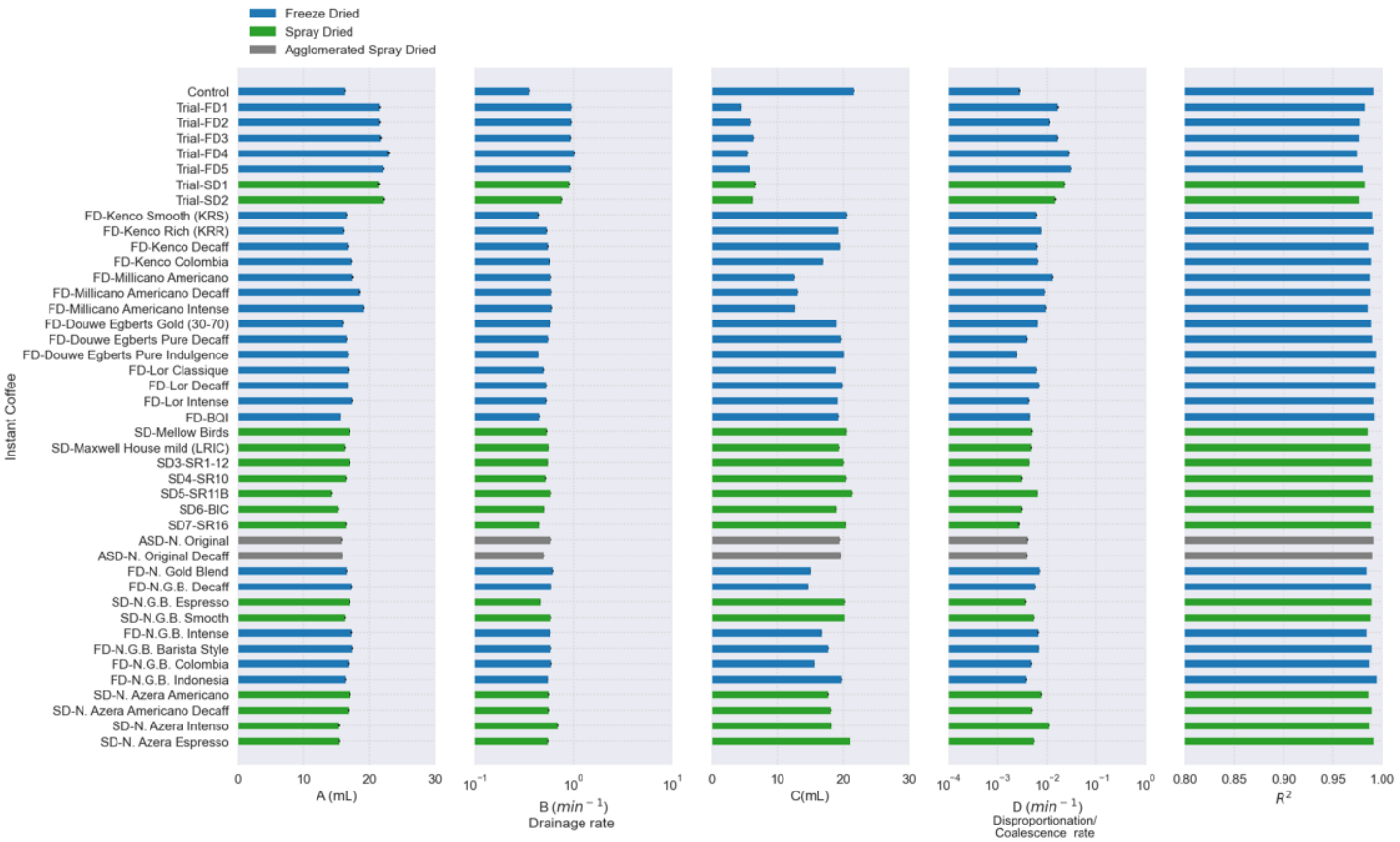



Figure 3-7 Calculated foam stability parameters for foam height curves

The model that was used for fitting consists of 4 parameters A (mL), B ($min^{-1}$), C (mL) and D ($min^{-1}$). The sum of parameters A and C represents the initial volume of foam. The values B and D represent the rate of foam decay (i.e. inverse lifetime). The two-stage foam decay is depicted in the fitted model. It is hypothesised that the first term of Equation 3.8, $Ae^{-Bt}$, describes the gravitational drainage, while the second term of Equation 3.8, $Ce^{-Dt}$, describes the bubble disproportionation and bubble coalescence within foam and at the open interface (i.e. interface of between the top layer of bubbles and air).

In order to test if the term $Ae^{-Bt}$ describes the gravitational drainage, it is important to verify if the value of supposed foam gravitational rate (i.e. B) is similar to the rate of liquid rise vs time. This could be achieved by fitting the liquid height vs time data in sum of two exponentials equation, similar to Equation 3.8.

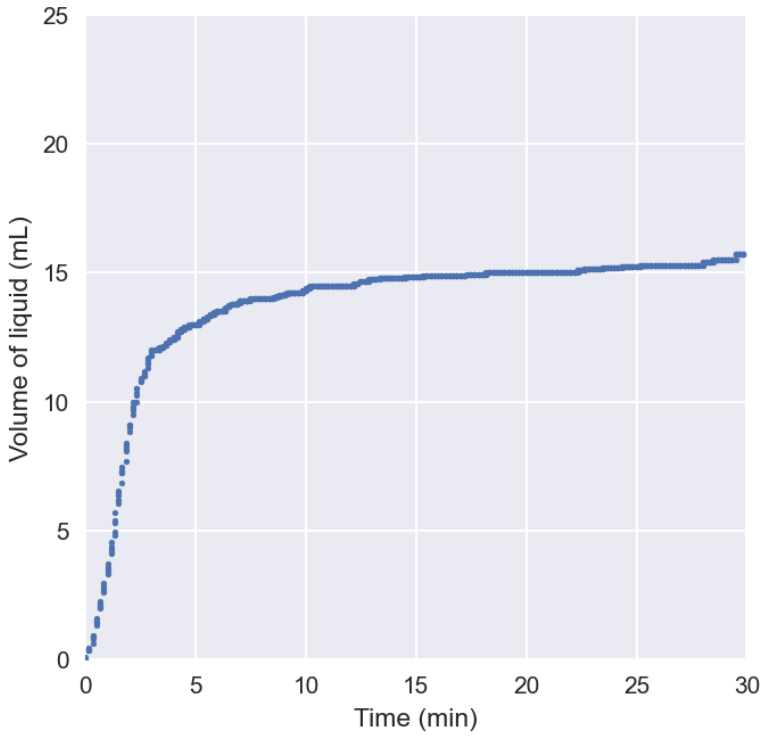



Figure 3-8 Volume of liquid vs time data points for control coffee sample (n=5).

An example of liquid height vs time data points is presented in Figure 3-8. It can be observed that at the first moments of the experiment (i.e. 0 min<time<5 min) the volume of liquid rose with high rate until it passed threshold (i.e. aprox. t=5 minutes) where the rate decreased. In order to achieve a good fit of an exponential equation to the volume of liquid data, it was important to "convert" the liquid height. As described in section 0 an aliquot of 20 mL of coffee liquid was used for the aeration experiments. With the applied aeration parameters (i.e. time, RPM) it was feasible to incorporate the maximum air in the volume of liquid. This means that at t=0 min the volume of liquid which was accumulated at the bottom of the vessel was 0 mL. Therefore, the data points of Figure 3-8 were subtracted from 20 mL. The converted data points expressed the volume of liquid which was retained in the foam structure vs time. At this point it was feasible to fit the Equation 3.8 to the data points of Figure 3-9.

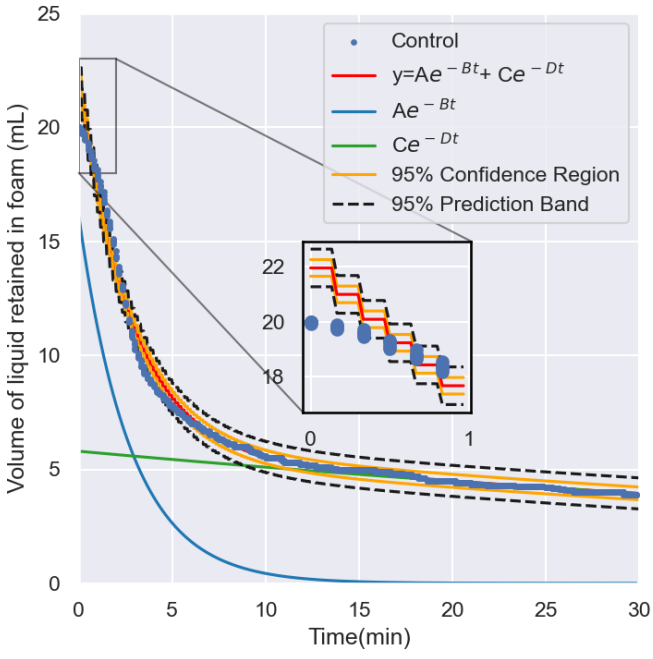



Figure 3-9 Volume of liquid retained in foam structure vs time for control instant coffee (n=5).

The calculated parameters and $R^2$ of control coffee and the rest of sample set are presented in Figure 3-10.

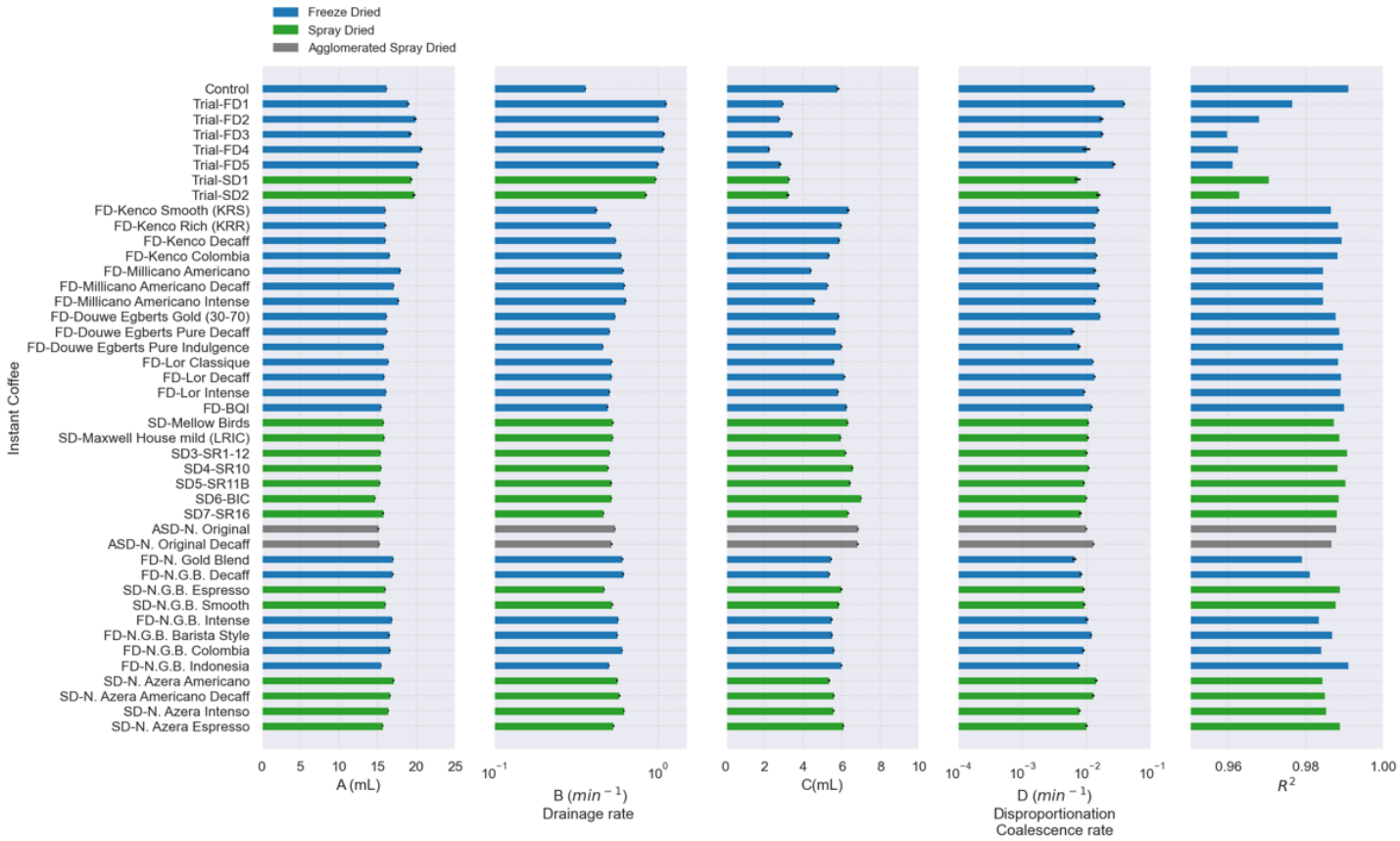



Figure 3-10 Calculated liquid retention parameters for instant coffee samples.

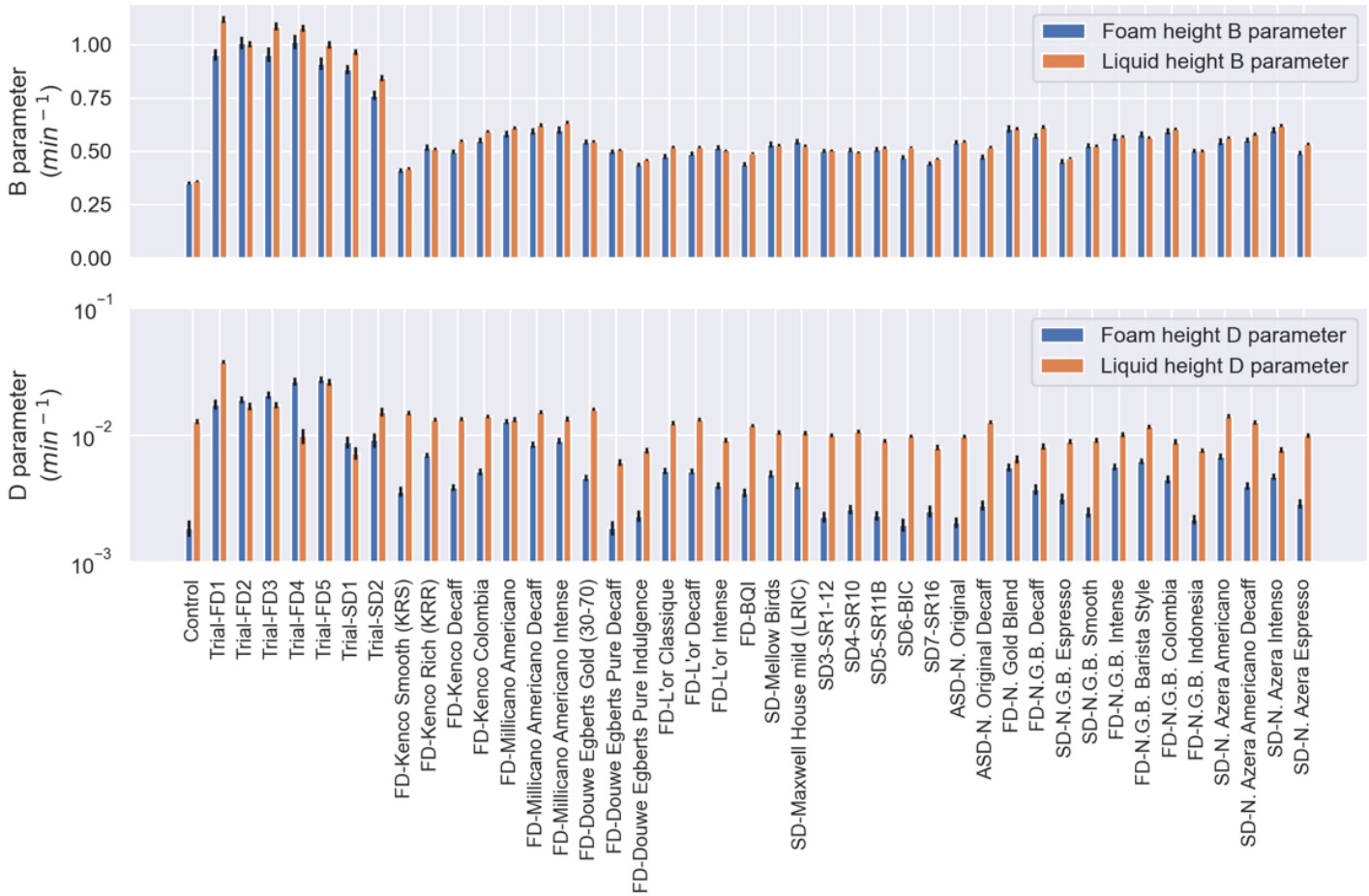



Figure 3-11 Comparison of B and D parameter for foam height and liquid height data points

In Figure 3-11, it is shown that there is a good agreement for the B parameter between the Foam height and Liquid height data and provides evidence that the foam-height B parameter describes the drainage rate.

At this point of analysis, it was important to identify which coffee samples were significantly different from control in terms of foam quality performance. For this reason, one-way ANOVA analysis was performed between the control coffee and each of the 41 instant coffee samples for the foam ability. Because both gravitational and disproportionation/coalescence rate were calculated by fitting Equation 3.8 to raw data, the standard deviation errors of gravitational and disproportionation/coalescence rate were estimated by the covariance (pcov) square matrix of optimal parameters (popt). For this reason, it was not possible to perform one-way anova analysis for drainage and disproportionation/coalescence rate. The analysis showed 21 instant coffee samples were significantly different from the control in terms of foam ability (Figure 3-12). The control's drainage rate was the lowest in the sample set, while its standard deviation error did not overlap with any of the rest of the coffee samples. The control's disproportionation/coalescence rate performed in the same way. The differences in foam quality potentially rely on the differences in the chemical profile of each coffee system.

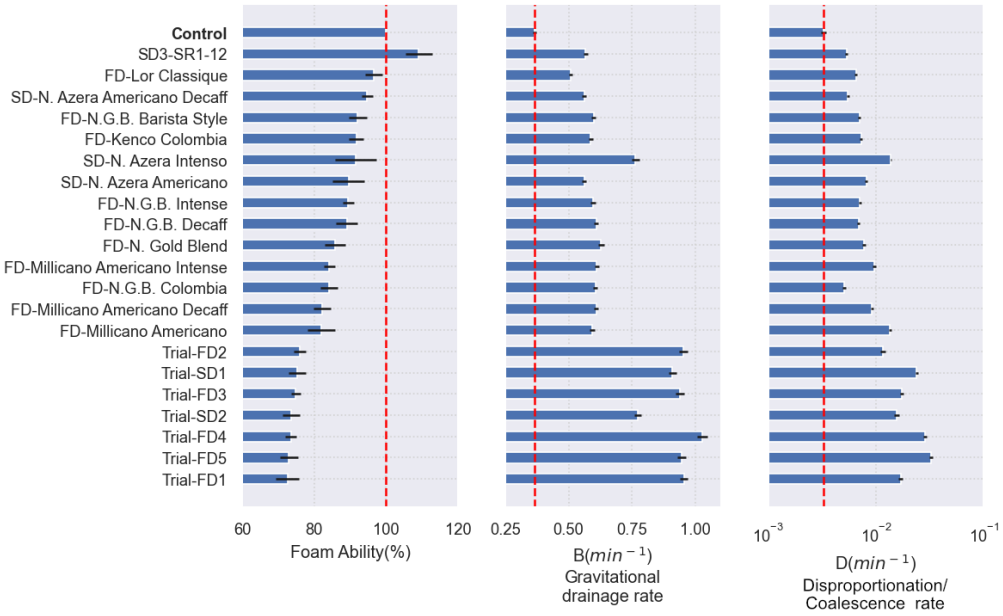



Figure 3-12 Foam quality parameters of instant coffee samples that are significantly different from the control coffee.

### 3.3.4 Foam quality and Lipid content

It was hypothesised that the lipid content of instant coffee samples affects the foaming behaviour. To test this hypothesis, the lipid content was determined with Soxhlet analysis (Figure 3-13). The present data were correlated with foam quality parameters that have been calculated from the screening process and the modelling of foam stability curves (Figure 3-12).

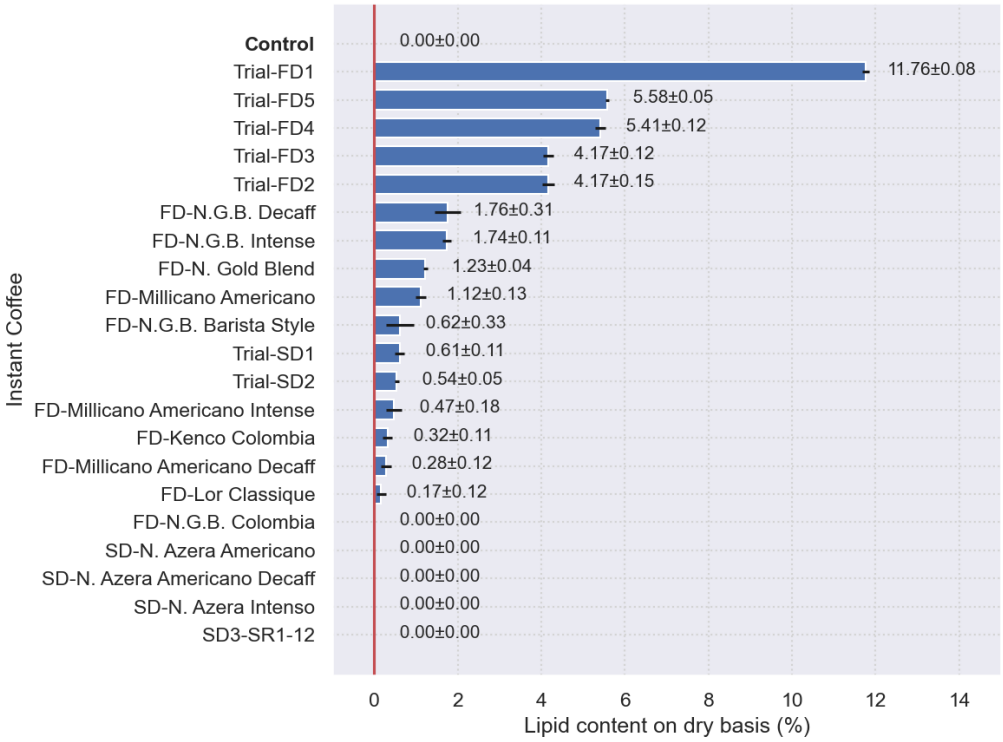



Figure 3-13 Lipid content of instant coffee samples which are significantly different from control in terms of foam ability. (n=3)

The lipid content data were correlated with the Foam Ability, Drainage rate and Disproportionation/Coalescence rate (Figure 3-14).

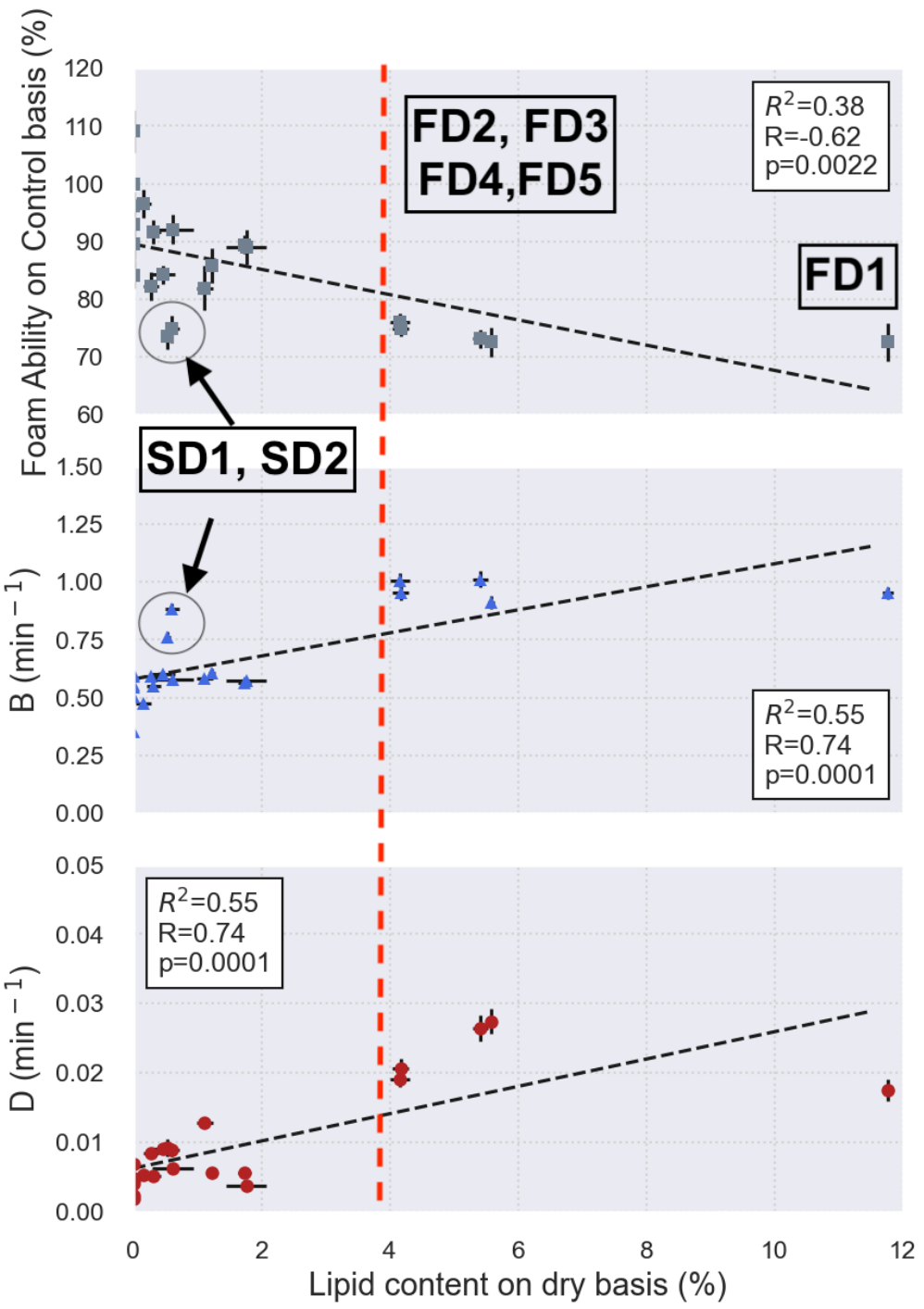



Figure 3-14 Correlation analysis of lipid content against the foam quality parameters (i.e. Foam Ability, Drainage rate, Disproportionation/Coalescence rate)

The correlation analysis between foam ability and lipid content showed that there was a significant correlation ($p<0.05$). The Pearson correlation coefficient was -0.62. So, there is a negative but moderate correlation between the two

values. Regarding the Drainage and Disproportionation/Coalescence rate, the p-value for both correlation analyses indicates that the correlation was significant ($p<0.05$). The Pearson correlation value was 0.74 and 0.74, so there is a positive correlation between the tested parameters. The data are not evenly distributed along the fitted line, in all the cases and Pearson's correlation analysis is very sensitive to extreme data values. This means that data with very high values can easily shift the slope of the fitted line and change the correlation coefficient.

It is important to comment that as the lipid content increases and exceeds the value of 4% on a dry basis, the foam ability tends to reach a plateau (see Figure 3-14). This is consistent for drainage rate and disproportionation/coalescence rate. This observation could indicate that lipid content is not correlated linearly with the foam quality parameters in the examined range of lipid content (i.e. 0-12 % on a dry basis). Therefore, it can be hypothesised that there is a critical concentration of lipid content where if the lipid content of a given system exceeds the critical value, then the foam quality parameters would not be influenced. It is also very important to acknowledge that the lipid fraction of a given system consists of several non-polar lipid molecules. To evaluate the addition effect of lipid content on the foam quality of instant coffee, then the chemical profile of the lipid fraction must remain the same (i.e. ratio of metabolites must remain constant) and the only parameter that should be changed is the amount of lipid content.

Since it was observed that there are extremes values of lipid content that influence the Pearson correlation coefficient it was important to perform a cluster analysis to the data set of each foam quality parameters agains the lipid

content. Cluster analysis techniques, such as the Elbow Method and Silhouette Scores, are critical for determining the optimal number of clusters. The Elbow Method, described in Christopher M. Bishop (2006) and Kaufman (1990), involves plotting the within-cluster sum of squares (WCSS) against the number of clusters and identifying the "elbow" point where adding more clusters yields diminishing returns. The Silhouette Score, introduced by Kaufman (1990) measures the consistency within clusters and identifies the optimal number of clusters as the point where the score is maximized.

The Elbow method is a technique used to determine the optimal number of clusters in a dataset by measuring the within-cluster sum of squares (WCSS). WCSS is the sum of the squared distances between each point and the centroid of the cluster to which it belongs. It quantifies the compactness of the clusters where lower WCSS indicates more compact clusters. The optimal number of clusters is often at the point where adding another cluster does not significantly reduce the WCSS. If the plot shows a clear elbow, the number of clusters at this point is considered optimal. Whil, if the plot is smooth without a clear elbow, other methods for validation should be considered (e.g., Silhouette Score).

The Silhouette Score is a metric used to evaluate the quality of clusters created by a clustering algorithm. It measures how similar each data point is to its own cluster compared to other clusters. The Silhouette Coefficient for each sample is calculates as:

Equation 3.9 Silhouette coefficient equation for each sample

$$s = \frac{(b - a)}{\max(a, b)} \qquad \text{Equation 3.9}$$

where:

- *a* is the mean distance between the sample and all other points in the same cluster.
- *b* is the mean distance between the sample and all other points in the nearest cluster (i.e., the cluster that the sample is not a part of, but is closest to).

The Silhouette Score ranges from -1 to 1. A score close to +1 indicates that the sample is far from the neighbouring clusters, implying well-separated clusters. A score close to 0 indicates that the sample is on or very close to the decision boundary between two neighbouring clusters. A score close to -1 indicates that the sample might have been assigned to the wrong cluster. The optimal number of clusters is typically the one that maximizes the average silhouette score. If the silhouette score is significantly higher for a certain number of clusters compared to others, that number is likely the optimal choice. If the silhouette scores are similar for several numbers of clusters, consider the simplest model (i.e., the smallest number of clusters).

Considering the aforementioned, the Elbow method and Silhouette Score was calculated for each data set (i.e. Foam Ability vs lipid content, Drainage rate vs lipid content, Disproportionation/Coalescence rate vs lipid content) and the results are presented in Figure 3-15. It evident that the optimal number of clusters was 3 for all three data sets.

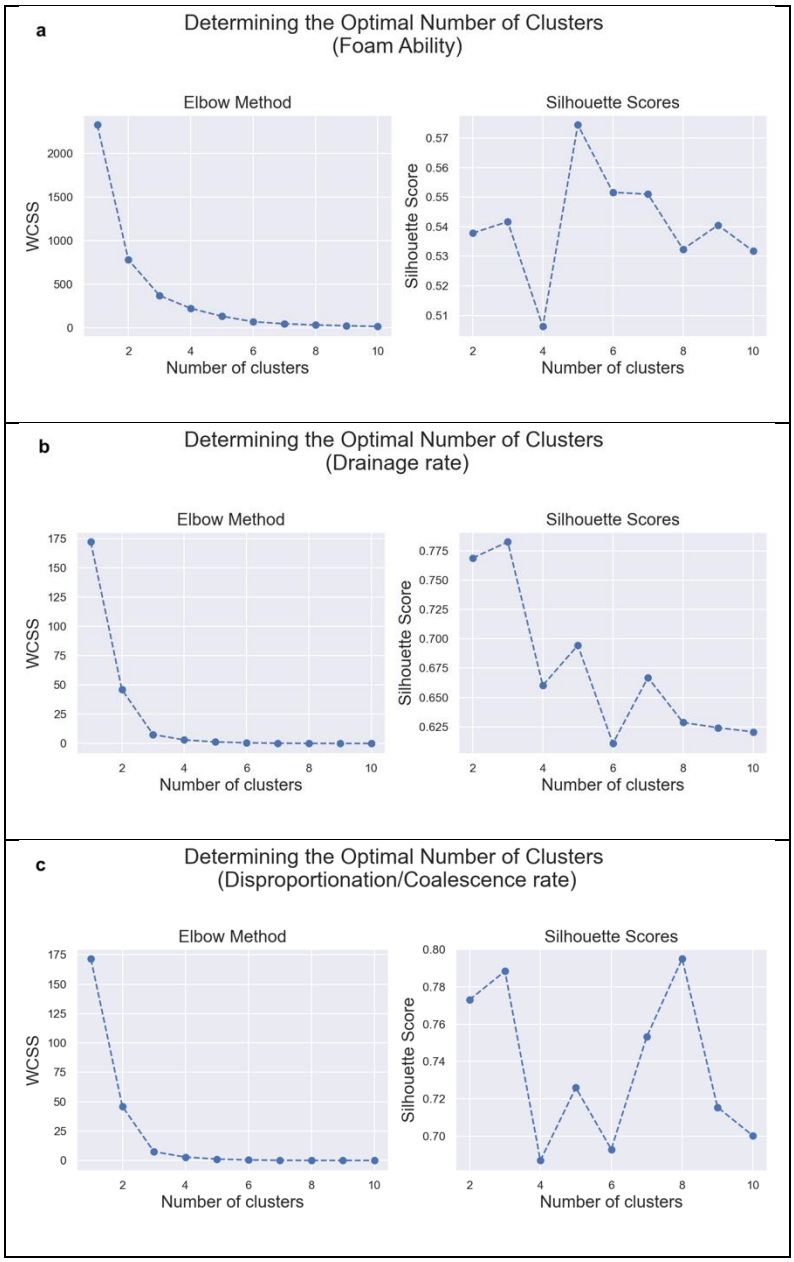



Figure 3-15 Cluster analysis technique (left side: Elbow Method, right side: Silhouette Scores) for (a) Foam Ability vs lipid content data set, (b) Drainage rate vs lipid content data set, (c) Disproportionation/Coalescence rate vs lipid content data set.

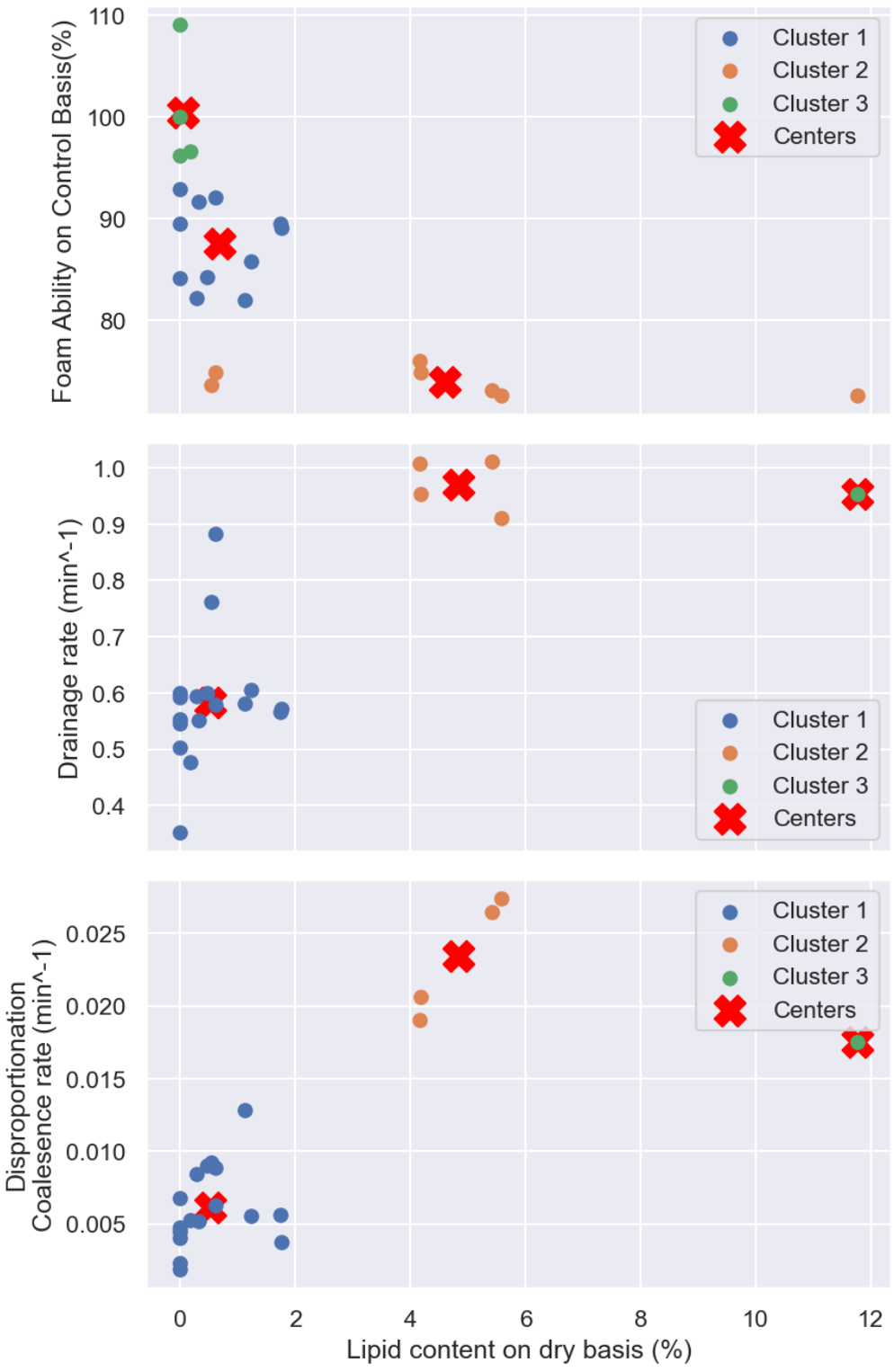



Figure 3-16 Cluster analysis of each data set (i.e. Foam Ability vs lipid content, Drainage rate vs lipid content, Disproportionation/Coalescence rate vs lipid content)

The Cluster analysis on the Foam Ability vs Lipid content data set, clustered the Trial FD1 to Trial FD5 along with Trial-SD1 and Trial -SD2 (i..e orange cluster). These samples were very low in Foam Ability but its lipid content varied from

0.54% to 11.56% d.b.The second cluster (i.e. green cluster) contains samples such as SD3-SR1/12. These samples did not contain any lipid and it's foaming ability varied between 95% to 110% on control basis. The rest samples were clustered (i.e. blue cluster) as samples with very low lipid content (i.e. 0 to 2% d.b.) and their foaming ability ranged between 80% to 95% on control basis.

The Cluster analysis of the Drainage Rate vs Lipid content data set clustered the Trial-FD2 to Trial-FD5 (i.e. orange cluster). This cluster comprised from samples that has very high drainage rate and the lipid content ranged between 4 to 6 % d.b. Trial -FD1 created its own cluster (i.e. green cluster; sample with high drainage rate and very high lipid content) and this indicates that indeed such sample can be considered an outlier while performing the pearson correlation analysis. The third cluster was comprised of the remaining samples. It is evident that while the lipid content was ranged between 0 to 2% d.b., the drainage rate ranged from 0.35 $min^{-1}$ to 0.9 $min^{-1}$. The cluster analysis of the Disproportion/Coalescence rate vs Lipid content data set created the exact same clusters as the Drainage rate vs Lipid content cluster analysis. It is observed that the cluster analysis results of Foam ability vs lipid content were not systematic when compared to the results of other two cluster analyses. However, this cluster analysis supports the argument that there is a relationship between the lipid content and each foam quality parameter but it may not be linear at the tested range of the sample set.

The effect of Arabica coffee oil and the evaluation of foam quality on a spray-dried instant coffee was investigated by Deotale et al. (2019). The coffee oil concentration that was examined ranged from 0 to 0.090% w/w and the results

indicate that there was a significant decrease in the maximum foam volume for a coffee solution spiked with coffee oil at a final concentration of 0.090% w/w. Instant coffee solutions with lower concentrations of coffee oil were not significantly different from the control. In the sample set that was examined in this chapter, the amount of coffee oil that was contained in the samples expressed in % w/w of the solution ranges from 0 to 0.1765% w/w. This concentration range is comparable with the range reported by Deotale et al. (2019). The maximum foam volume results of the two different sample sets are not directly comparable. In the cited paper the authors evaluated the foam ability of the samples with the sparging method, while in this chapter the foam quality was assessed by the stirring method. In principle, the mechanisms of bubble formation are different which can lead to different foam structures (Drenckhan and Saint-Jalmes, 2015). However, the cited authors determined the coalescence rate of instant coffee samples spiked with different concentrations of oil. It was observed that coffee samples with higher concentration in oil had increased coalescence rate. The same trend was observed (see Figure 3-14) for the disproportionation/coalescence rate vs lipid content plot in the sample set of instant coffees tested in this chapter.

Another important observation in Figure 3-14 is the lipid content of Trials SD1 and SD2. These samples were produced by pilot plant Trials (Table 3.1) and the foam quality of these was very poor (Figure 3-2, Figure 3-7). However, the lipid content of these samples was very low compared to the rest of the Freeze-dried pilot plant samples (i.e., FD1, FD2, FD3, FD4 and FD5). This could indicate the lipid content is not related to the foam quality of such samples. In conclusion,

the differences in foam quality throughout the tested sample set do not rely necessarily only on lipid content.

### 3.3.5 Foam assay on defatted instant coffee samples

To further investigate the effect of lipid content on foam quality, coffee solutions (1.5% w/w) of the defatted samples were prepared and the foam quality was assessed. It was hypothesised that the removal of lipid content will enhance the foam quality of samples. The lipid content and the foam quality of the native and defatted samples are presented in Figure 3-17.

Overall, the defatting process did not have the same effect on the foam quality of the samples. Removal of lipid content enhanced the overall foam quality for Samples FD1, FD5, FD4, FD3, FD2, FD-N.G.B. Barista Style and FD-Millicano Americano Decaff. However, the defatting process also enhanced the foam quality of samples like Nescafe Gold Blend Colombia, which normally have no measurable lipid content. Also, in the Control sample, the disproportionation/coalescence rate was increased and in SD3 the foam ability was increased, but again both of these coffees did not contain any coffee oil.

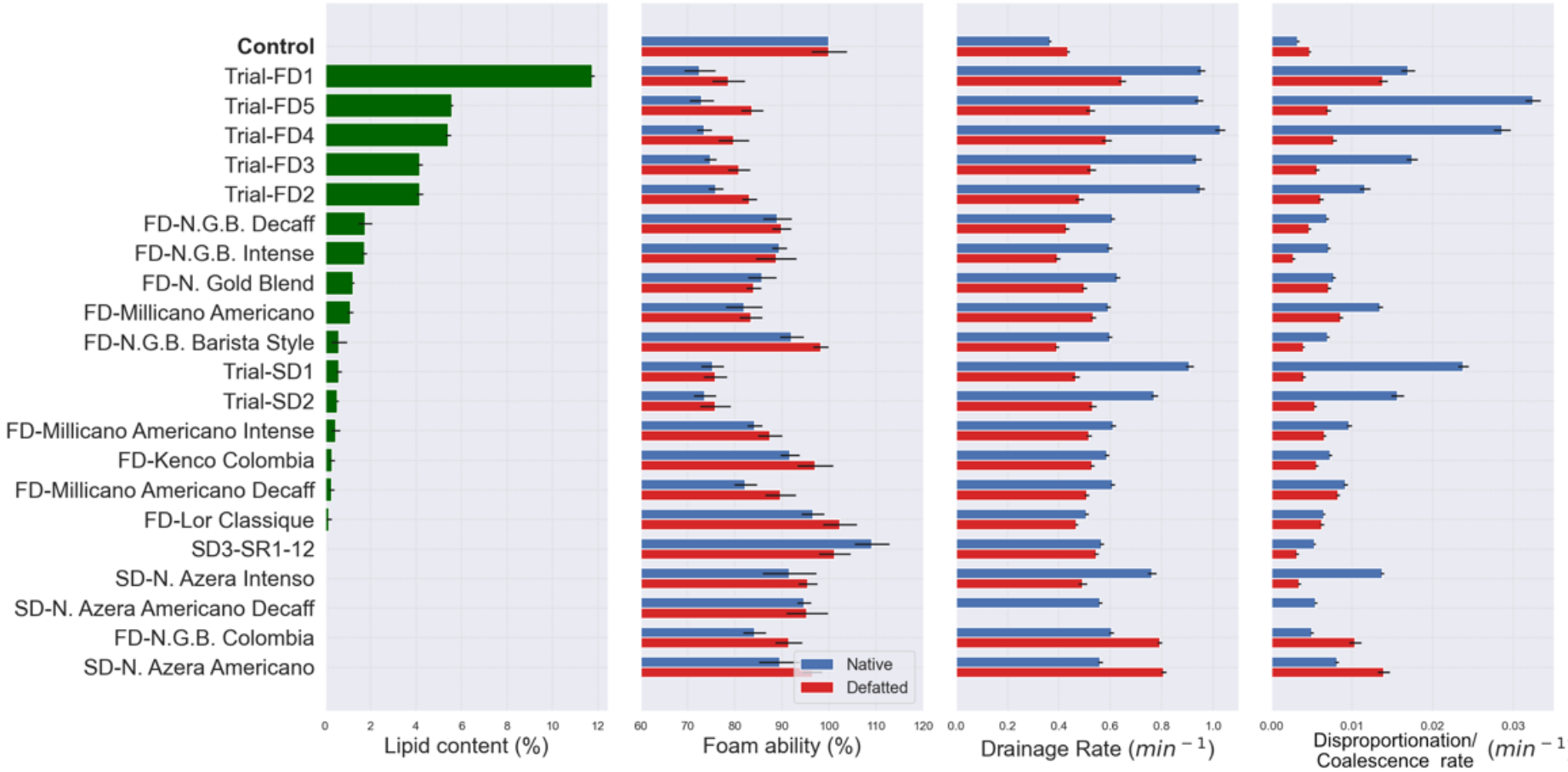



Figure 3-17 Lipid content and foam quality of native and defatted instant coffee samples. Number of replicates for foam quality=5, Number of replicates for lipid content=3

Enhancement of foaming properties by "defatting" fat free samples was an unexpected result and therefore it was essential to consider every phenomenon that occurs in the defatting process, and which may affect the abundance or structure of the metabolites, that could be associated with foaming behaviour. During the soextherm extraction, the analysed material is exposed to petroleum ether and to heat (150˚C for 2 hours). Also, a macroscopic investigation of samples revealed that defatted samples were contaminated in a non-controlled way with cellulosic material from the filter paper during the sample preparation step (Figure 3-18).



Figure 3-18 Defatted control coffee which is contaminated with cellulosic material from the filter paper.

The presence of cellulosic material may interfere with the foam quality parameters. It can be hypothesised that cellulosic material could increase the viscosity of the liquid continuous phase, and this would affect the drainage rate. Also, it can be hypothesised that surface active chemical molecules in coffee would interact with cellulosic material and form a complex structure which can be adsorbed on the air/beverage interface, and this might provide stability to the foam structure. A similar synergistic effect of small and big molecules towards the enhanced elasticity of foam films has been reported for beer foam, where

iso-alpha acid interacted with beer proteins (Lu, Bergenståhl and Nilsson, 2020). It appeared that the samples of the present work were contaminated at different level. Therefore, with such uncontrolled contamination, the defatting process on the foaming behaviour cannot be systematically investigated.

The application of heat during the defatting process may also alter the chemical profile and abundance of compounds that are associated with the foam quality. According to the literature, foam quality is correlated with the abundance of 4-vinyl catechol oligomers which are products of roasted caffeic acid (Frank *et al.*, 2007b; Folmer, Blank and Hofmann, 2017; LELOUP, Valérie Martine, Jeanine (CH) *et al.*, 2019). Caffeic acid can be found free or in the form of caffeoylquinic acid. The roasting process degrades the said metabolites and leads to the creation of bitter 4-vilylcatechol oligomers (Figure 3-19).

It was therefore hypothesised that the heating process of the soextherm extraction generated the amphiphilic compounds that are associated with the foam quality of coffee. The petroleum ether used in the soextherm protocol might then extract these amphiphilic and foam-promoting compounds.

### 3.3.6 Foaming assay on the heat-treated instant coffee samples

The effect of the heating process on the foam quality of instant coffee samples was examined by performing the foaming assay on heat-treated instant coffee samples. The defatting process decreased the foam quality of the control sample (increase of drainage and disproportionation/coalescence rate) and therefore the heat applied during defatting could also potentially be responsible for the change

in functionality alongside the action of petroleum ether; thus, the control instant coffee was selected for the heat-treatment experiments. It was predicted that if the petroleum ether removed the foam-promoting metabolites, then the foam quality of the heat-treated sample (no petroleum ether) would either remain the same as the native sample or it would be enhanced.

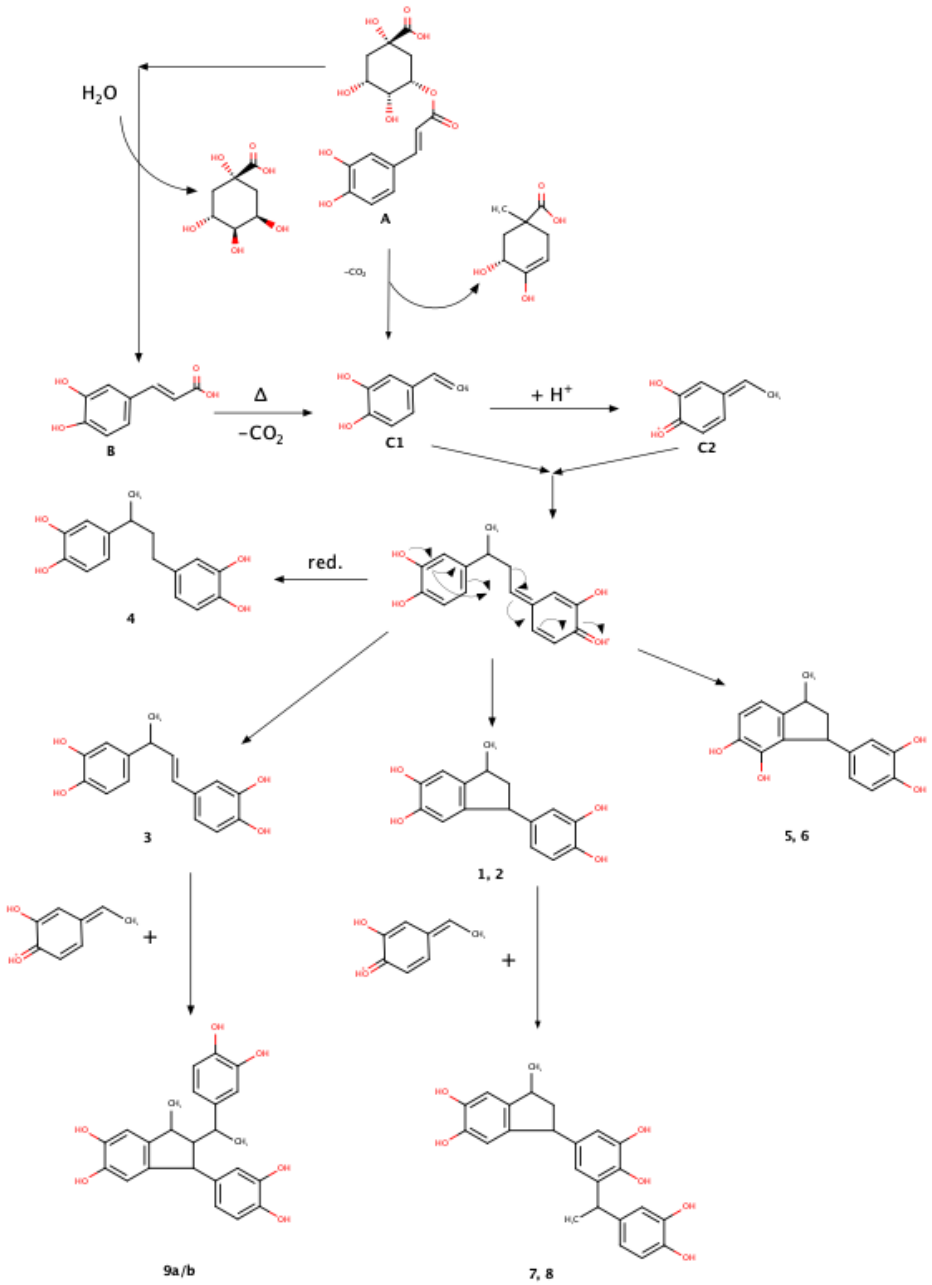



Figure 3-19 Proposed metabolic pathway of production of 4-vinylcatechol oligomers (1 to 9a/b) from 5-O-caffeoylquinic acid (A) and caffeic acid (B) via 4-vinylcatechol as an intermediate metabolite (C1). Image adapted from Frank et al., 2007.

Heat treatment of a native instant coffee sample would change moisture content in an uncontrolled way, so it would not be feasible to prepare an instant coffee solution with the desired concentration in solids. For this reason, moisture was removed from the instant coffee sample before the heat treatment (vacuum-dried sample). The method that was selected to remove the moisture content from the sample was drying at reduced pressure (i.e 5000±100 Pa) at 70˚C for 16 hours. The aim was to remove the remaining moisture from the material but keep intact the profile and abundance of the metabolites which are associated with foam quality. Afterwards, the vacuum-dried sample was heat treated at 150˚C, 185˚C and 220˚C for 20 minutes and the foaming quality was assessed through the foaming assay. The results were compared with the foaming quality of the defatted sample. The minimum temperature selected was 150˚C because this was the temperature that was applied in the soextherm extraction and the maximum temperature selected was 220˚C because at this temperature 4-vinyl catechol oligomers are produced (Frank *et al.*, 2007b).

A macroscopic investigation of heat-treated samples showed significant alteration to the matrix of the instant coffee product (Figure 3-20). The 185˚C and 220˚C samples were expanded after the heat treatment and formed a continuous solid foam structure. During the heating process, the coffee material may have reached the glass transition temperature. The instant coffee granules appeared to become less rigid and formed a continuous phase. The excess heat may have transformed the remaining bound water of the material into vapour. Expanded vapour due to increased heat, created cavities and expanded the overall structure. Instant coffee after treatment at 150˚C did not expand but the

granules were slightly accumulated together which may also be attributed to the glass transition. It has been reported that the glass transition temperature of green and roasted coffee beans ranges from 34.09±0.02˚C to 48.76±0.04˚C and from 40.15±0.10 ˚C to 45.73±0.05˚C respectively (Iaccheri *et al.*, 2019). To the best of our knowledge, the glass transition temperature of freeze-dried instant coffee granules has not been reported. Since the applied temperature in the heat-treating step is at least 150˚C then it is possible that instant coffee granules experienced glass transition. Also, it must be considered that the instant coffee process may affect the glass transition temperature. Since the instant coffee material was significantly changed after heating to 185˚C and 220˚C, the foaming behaviour was not assessed. However, the foaming assay was performed for the sample that was heat treated at 150˚C (Figure 3-21).




Heat treatment at 150˚C

Heat treatment at 185˚C

Heat treatment at 220˚C

Figure 3-20 Heat-treated control instant coffee for 20 minutes at 150˚C (Top image), 185˚C (Middle image), 220˚C (Bottom image)

The foam ability of the control sample was not affected by any of the processes. The drainage rate systematically increased from native to vacuum dried to heat treated instant coffee. The soextherm extraction increased (as detailed in the previous section), even more, the drainage rate compared to the rest of the samples, as shown in Figure 3-21.

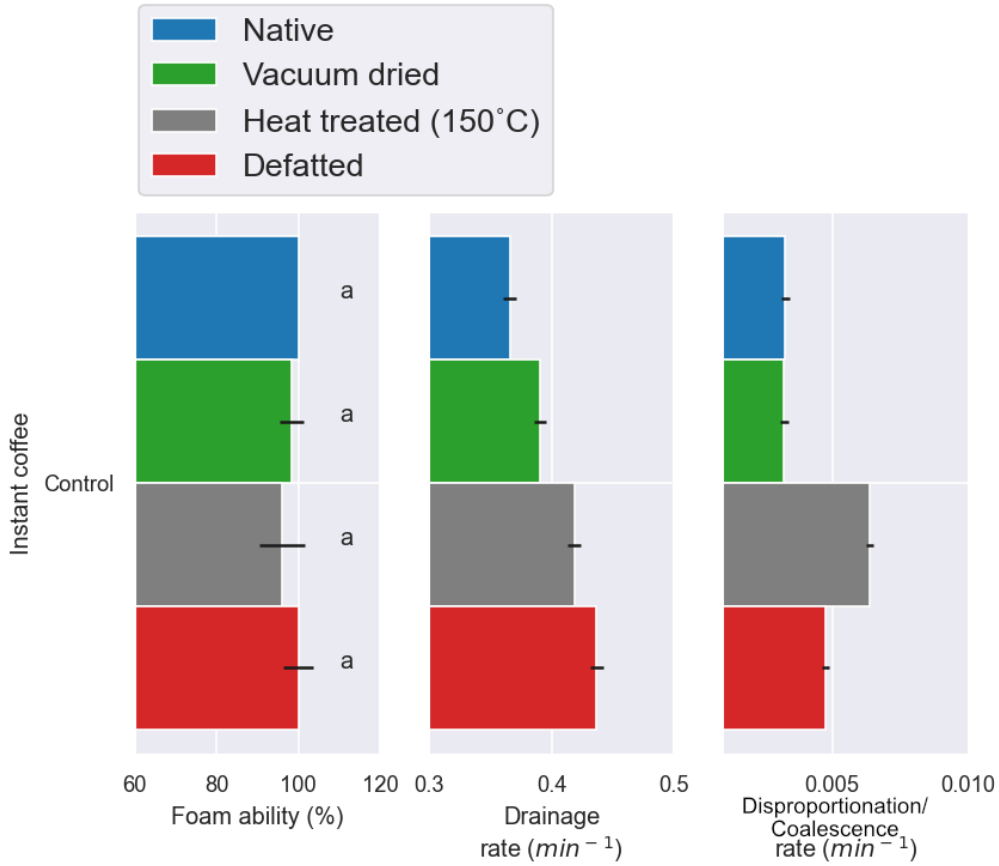



Figure 3-21 Foam quality parameters of (top to bottom) native control and vacuum-dried, Control, heat-treated control (150˚C) and defatted control. Different letters indicate significant differences at $p<0.05$. (n=5)

The disproportionation/coalescence rate of the vacuum dried sample stayed at the same level as the rate of the native sample; however heat treatment at 150˚C increased the disproportionation/coalescence rate. The disproportionation /coalescence rate of the defatted control coffee was also higher than the native and vacuum dried but lower than the heat-treated sample.

It was hypothesised in the 3.3.5 section that the increase in drainage and disproportionation/coalescence rates of the defatted coffee sample may be attributed to the removal of the foam-promoting amphiphilic compounds by petroleum ether during the soextherm extraction. In the case of drainage, this hypothesis was confirmed as the drainage rate of the defatted sample was more than the heat-treated sample, making the foam less stable. In the case of the disproportionation/coalescence rate, this hypothesis was not confirmed as the heat treatment increased the rate of disproportionation/coalescence to a greater rate than defatting, again making the foam system less stable. It is important to consider that the different response of drainage and disproportionation/coalescence rate of heat treated and defatted samples may be attributed to different time-temperature profiles applied in each treatment/process.

The same workflow of experiments was performed on the FD5 instant coffee sample (i.e. coffee sample with 5.58% w/w lipid content) (Figure 3-22). This sample was selected because the defatting process significantly increased the overall foam quality compared to the native one (Foam ability increased, drainage and disproportionation/coalescence rate decreased, see Figure 3-17). The foam quality of the heat-treated sample did not have the same response as the defatted sample. The heat treatment of FD5 instant coffee enhanced foam stability as the drainage rate was decreased. However, the disproportionation/coalescence rate did not change with the application of the heat treatment. Similar to the case of control coffee, the heat treated and defatted coffee samples differ in two points. First, both samples underwent heat

treatment, but the time scale was different. Second, the defatted coffee contained cellulosic material whereas the heat-treated sample did not. Therefore, the differences in foam quality could be attributed to process or material differences.

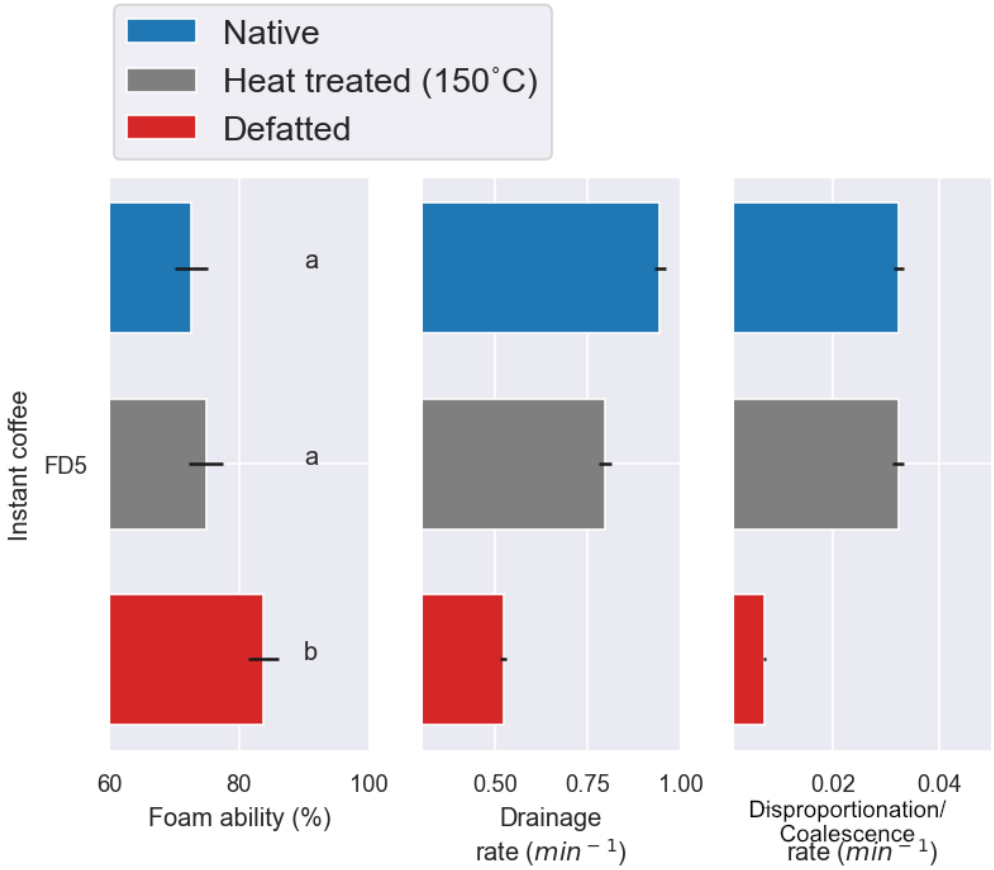



Figure 3-22 Foam quality of native, heat treated at 150˚C and Defatted FD5 instant coffee sample.

It is concluded that heat treatment and the application of petroleum ether along with a possible uncontrolled contamination of the instant coffee sample with cellulosic material can change the foam quality of an instant coffee sample. Also, it is concluded that heat treatment can have either a positive or negative effect on foam stability of an instant coffee, as evidenced by comparing results presented in Figure 3-21 and Figure 3-22, and at present this behaviour is difficult to predict. The positive or negative effect of the heat treatment on the foam stability of a coffee sample might be associated with the relative abundance

of metabolites which influence coffee foam, in the native system. To further understand the differences that occurred by the heat treatment of the samples, it would be essential to determine the relative abundance of compounds that are associated with the foam quality of coffee, such as 4-vinyl catechol oligomers (Figure 3-19).

### 3.3.7 Grinding, sieving and extraction of green and roasted whole beans.

**Grinding method development**

For advancing the understanding of foaming mechanisms in coffee, it was essential to investigate the foam quality not only of instant coffee samples but also on fresh extracts of green and roasted whole coffee beans. Before developing an extraction protocol for the coffee beans, several qualitative methods to reduce the particle size of coffee beans were investigated (Table 3.7).

Roasted coffee beans could have been ground via a high-end domestic or professional burr coffee grinder. Such machines have been proven for their consistency in the grinding size through many grinding sessions and it would have been an optimal solution. However, in the case of this research, the sample set contains green beans. In comparison with roasted coffee beans, green beans have higher density and increased water content, so it would be harder to reduce the particle size conventionally (Bonnländer *et al.*, 2005a) . Burr coffee grinders are designed to reduce particle size only on roasted coffee beans. Also, use of conventional coffee grinders increases the temperature of the beans. Because of this, there may be changes in the relative abundance and structure of key foaming metabolites.

The aim was to find a method to reduce the particle size of both green and roasted coffee beans with consistency between runs. Consistency in grinding size would help for consistency in the extraction rate during the extraction protocol. Also, the aim was to keep intact the chemical profile of the sample set. So, it was proposed to perform the grinding under cryogenic conditions. Cryogenic grinding can be beneficial for maintaining the profile of key metabolites during grinding. It was hypothesised that if green beans were frozen before the grinding, brittleness would be increased, and it would be easier to reduce the particle size.

The initial qualitative method attempted to reduce the particle size was by using a bio-pulveriser (Figure 3-23). Several grams of green coffee beans were placed into the bio-pulveriser. A small amount of liquid nitrogen was poured into the pot to freeze the green beans. Once the liquid nitrogen was evaporated, the lid of the bio-pulveriser was replaced, and the beans were smashed with a rubber hammer (Table 3.7). Freezing helped reduce the particle size of the beans, but the material was not ground to a fine powder. Also, the particle size reduction was not automatic but manual, so this method would not have been consistent between different runs.



Figure 3-23 Bio - pulveriser

The second qualitative method that was attempted was to use a Bead Mill 24 Homogeniser (Fisher Scientific, USA) with 2.8 mm ceramic beads (Fisher Scientific, USA). A whole green bean did not fit into the 2 mL mill tube. So, green whole beans were frozen with liquid nitrogen and the Bio-pulveriser was used to reduce the particle size. Then, several grams were frozen again and placed into the tube with ceramic beads. The repeated impact of beads on the beans provided a consistent grinding size but the temperature increased quickly, so the grinding was not yet considered cryogenic. Also, the ceramic beads were not strong enough to fracture the beans to a fine powder. So, the bead mill was proven insufficient for grinding green coffee beans.

The third qualitative method used was a high-duty metal blender (Model 35BL64, Waring, USA) with metal blades. It was hypothesised that employment of high torque would have been proven enough to reduce the green bean's particle size. Initially, several grams of green coffee beans were frozen with liquid nitrogen and placed into the metal blender. Several grinding times and spinning speeds were used for the grinding trial. The metal blender was more efficient than the Bio-pulveriser and bead mill. However, the beans' temperature increased rapidly due to the high friction from the blades. So, this method was not sufficient for grinding green coffee beans.

The last qualitative method that was employed utilised a Spex 6875 Freezer/Mill (Antylia, Ilinois, USA). Several grams of green beans were placed into the vial with a metal impactor. The sealed polycarbonate vial was submerged in liquid nitrogen for pre-cooling. The vial remained submerged in liquid nitrogen

throughout the whole grinding run. The advantage was that any amount of heat that was generated due to the repetitive impact of the impactor, was dissipated by the liquid nitrogen. The freezer mill was able to smash the green beans to a fine powder and keep the temperature of the material even below 0˚C due to the application of liquid nitrogen. In conclusion, the freezer mill was chosen as the appropriate method to reduce the particle size of green and roasted whole coffee beans.

Table 3.7 Method to reduce the particle size of green and roasted beans

| Method | Result | Advantages | Disadvantages |
|---|---|---|---|
| Bio-pulveriser |  | -Reduction of particle size | -Inconsistent result |
| Bead mill with ceramic beads |  | -Consistent grinding | -Increased heat<br>-Limit on reducing the particle size |
| High-duty metal blender |  | -Reduction of particle size<br>- Consistent grinding | -Increased heat |
| Freezer mill (Selected method) |  | -Cryogenic milling<br>-Consistent - grinding<br>-Powder | N/A |

**Sieving**

It has been reported that the particle size of coffee grounds plays an important role in coffee extraction kinetics (Cordoba *et al.*, 2020), so the aim was to

achieve consistency in the particle size distribution of the ground coffee beans. Thus, the sieving step with a 500-um sieving screen was included in the extraction protocol.

**Filtration method development**

It was essential to remove the milled coffee particles from the extract before assessing the foam quality. Initially, it was attempted to filter the coffee extract with a Buchner flask and funnel (Fisher Scientific, Loughborough, UK) and a LABOPORT® N 86 KT.18 vacuum pump (KNF, Witney, UK) with GF/C RTU glass microfiber filter paper-1.2 um pore size diameter (Cytiva, Sheffield, UK). These filter papers were proven unsuitable for filtration as they were not resilient enough and were punctured (Figure 3-24).




Figure 3-24 Punctured GF/C RTU glass microfiber filter paper-1.2 um pore size diameter (Cytiva, Sheffield, UK)

| Filter speed | Qualitative | Qualitative Wet-Strengthened | Ashless | Hardened | Hardened Ashless | Retention |
|---|---|---|---|---|---|---|
| Fast | 4 (20-25µm) | 114 (25µm), 113 (30µm) | 41 (20µm) | 54 (22µm) | 541 (22µm) | Coarse and Gelatinous Precipitates |
| Medium Fast | 1 (11µm) | 91, 93 (10µm) | 43 (16µm) | | | Medium Crystalline |
| Medium | 2 (8 µm) | | 40 (8µm) | 52 (7µm) | 540 (8µm) | Crystalline |
| Slow | 5 (2.5µm), 6 (3µm) | | 44 (3µm), 42 (2.5µm) | 50 (2.7µm) | 542 (2.7µm) | Fine Crystalline |
| Ash | 0.06% | 0.06% | 0.01% | 0.025% | 0.008% | |

| | | |
|---|---|---|
| No.3 | Thick, medium speed paper with high retention. | 6µm |
| GF/A | Standard laboratory glass microfibre paper. | 1.6µm |
| GF/B | Thicker, stronger version of GF/A. | 1.0µm |
| GF/C | Very fine glass microfibre paper. | 1.2µm |
| GF/D | Thick version ideal for membrane prefiltration. | 2.7µm |
| GF/F | Ultra-fine filter with retention down to 0.7µm in liquids. | 0.7µm |

Figure 3-25 Whatman Filter Paper Chart

The most suitable filter papers for the filtration were the ones that would allow low filtration times to minimise the residence time of the milled coffee beans in the slurry and thus minimise the extraction time. Also, puncturing during filtration could be prevented with hardened filter papers. According to the Whatman Filter paper chart (Figure 3-25), two filter papers were qualified the Qualitative Wet-strengthened 114 Whatman and the Hardened 54. The Hardened ashless 541 filter papers were not considered as these filter papers are specified for ash content determination. Further investigation towards selecting the optimum filter paper for the filtration between Whatman 114 (wet-strengthened) and Whatman 54 (hardened), revealed that the former contains a resin which contains nitrogen (*Whatman Grade 114 Qualitative Filter Papers*, 2022). Using these filters could lead to contamination of coffee samples with further nitrogen,

and this will potentially influence the foam quality of the extract. Thus, the Whatman 54 hardened was selected for the filtration of coffee extracts. Although the Whatman 54 hardened filter papers can provide fast filtration on coarse precipitates, this was not feasible for the coffee extracts. The green and roasted coffee beans were finely ground by the freezer mill, and this caused clogging of the Whatman 54 filters. The clogged filters increased the filtration time and therefore the retention time of ground beans in the liquid phase. The increase in retention time could lead to an uncontrolled extraction time and yield of coffee beans. For this reason, it was essential to find a way to separate fast the coffee beans from the coffee extract. Therefore, a 200-um metal sieve (TIMCOOK, Amazon, UK) was used for fast filtration.

### 3.3.8 Effect of roasting degree and instant coffee process on foam quality.

The foam screening process analysis on instant coffees showed that some coffee samples were significantly different from control in terms of foam ability and potentially these differences could be caused by differences in the chemistry of each system. The differences in the chemistry can be induced by the different process parameters, such as the roasting degree (Wei *et al.*, 2012a). According to the literature, the roasting degree affects the foam quality and more specifically affects the abundance of compounds that influence the foam quality (Nunes *et al.*, 1997). Therefore, it was essential to investigate the foam quality of coffee products at different degrees of roasting and different stages of production (i.e., green bean, roast bean, instant coffee).

**Effect of roasting**

The roasting profile, colour, mass, and bulk density of roasted beans at different roasting stages are presented in Figure 3-26. Regardless of the variety (i.e. Arabica vs Robusta), origin (i.e. Nicaragua, Brazil, Vietnam) or process method (i.e. Washed vs Unwashed), by increasing the roasting time up to 120 seconds, the surface colour value was decreased which is an indication that the coffee beans were slightly brighter than the green unroasted bean. Further roasting resulted in darker colour beans hence the increased whole colour value. The same behaviour of colour development during the early stages of roasting has been reported in the literature(Hernández, Heyd and Trystram, 2008a, 2008b). This colour development may indicate that the brown Maillard products start to be produced after 120 seconds of roasting. The mass of beans, bulk density and moisture content are shown to decrease with the increase in roasting time (Figure 3-26). It is also evident that by increasing the roasting time the total solid content of the extract increases systematically (Figure 3-27).

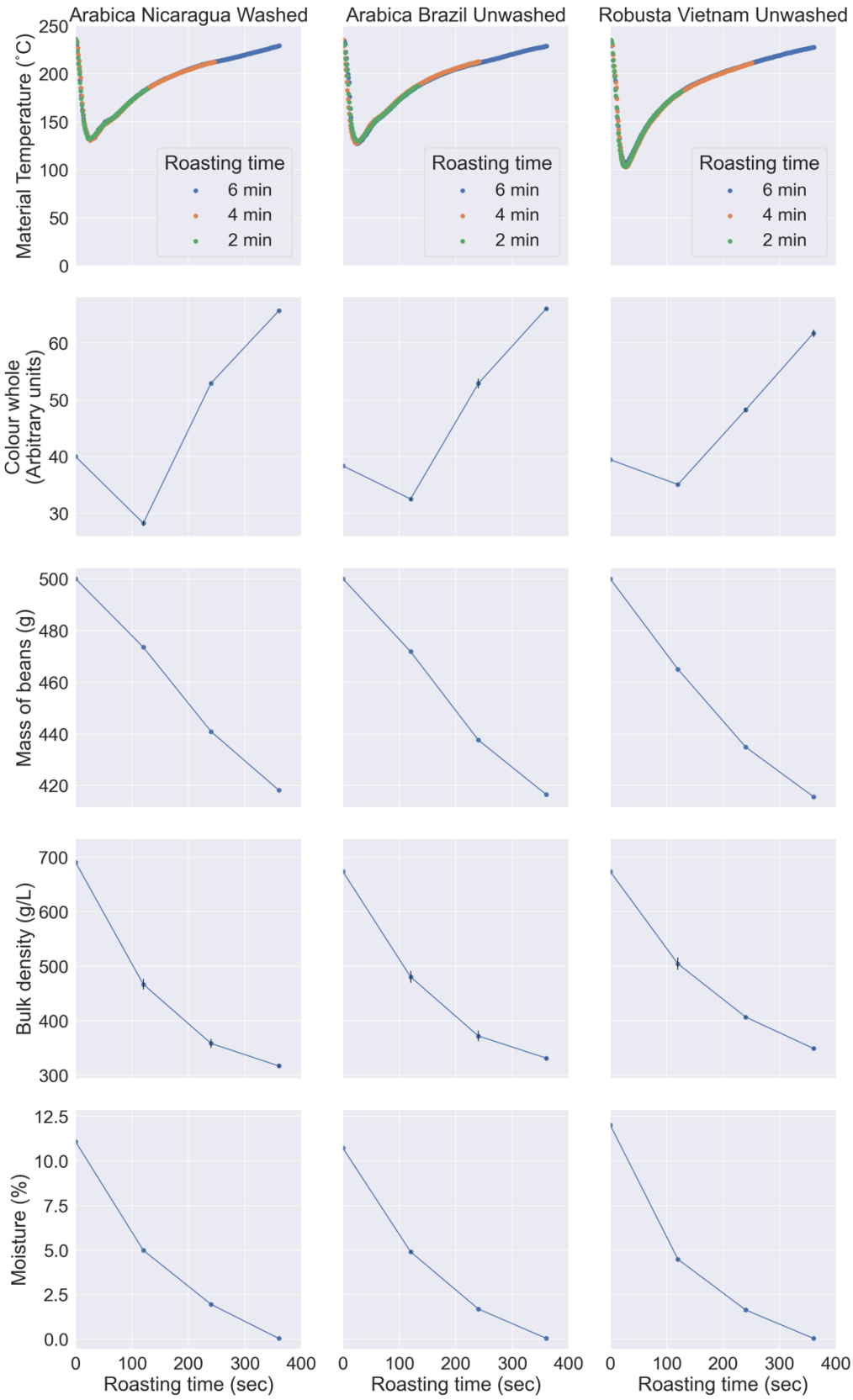



Figure 3-26 Roasting profile, Colour, Mass of beans and Bulk density of roasted beans at 120,240 and 360 seconds

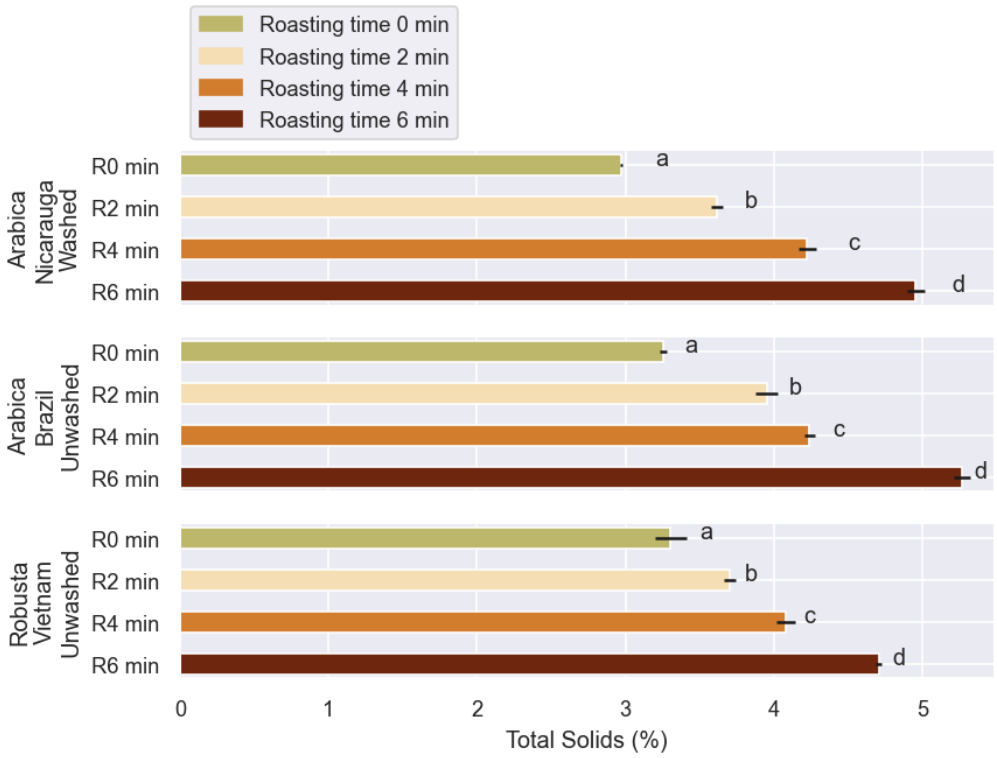



Figure 3-27 Total solid content (%) of coffee extracts at different roasting degrees for Arabica Nicaragua Washed, Arabica Brazil Unwashed, and Robusta Vietnam Unwashed (n=3). Coffee/Water ratio: 18g/300mL. Statistical analysis was performed on each bar plot separately. Different letters indicate significant differences at p=0.05

The foam quality of coffees at different roasting degrees was assessed, as shown in Figure 3-28. For all cases, the extracts of R0 min, R2 min and R4 min did not achieve total aeration (i.e. 100% foam system) whereas the R6 min extracts did (Table 3.8). It can be observed that the roasting degree affects the foam ability of the extracts but not linearly. For the Arabica Nicaragua Washed and the Arabica Brazil Unwashed, there is no significant difference from 0 to 4 minutes of roasting. However, coffee beans that were roasted for up to 6 minutes showed a significant increase in foam ability. In the case of Robusta Vietnam Unwashed, the 0- and 2-minute roasted extracts did not show any significant difference. Roasting at 4 minutes significantly enhanced the foam ability compared to the

less roasted coffee. Finally, roasted coffee beans for 6 minutes of roasting further increased the foam ability from 7.59±1.60 % to 65.69±1.46% on Control basis.

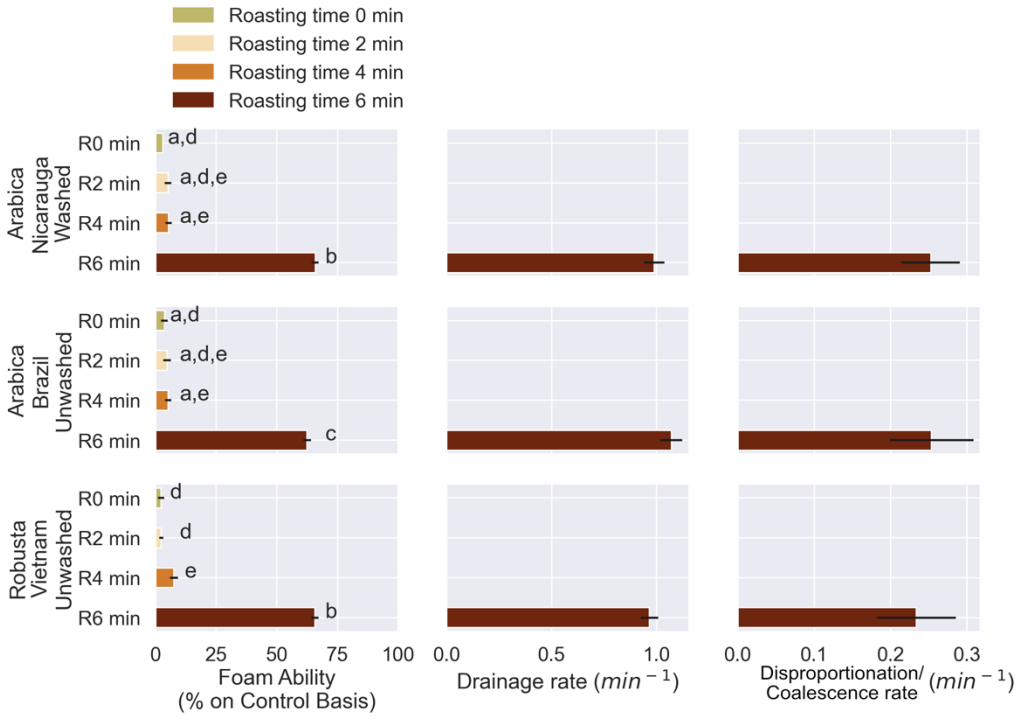
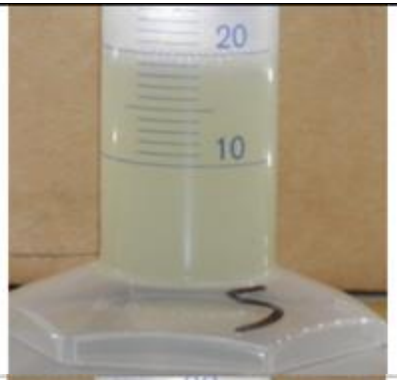
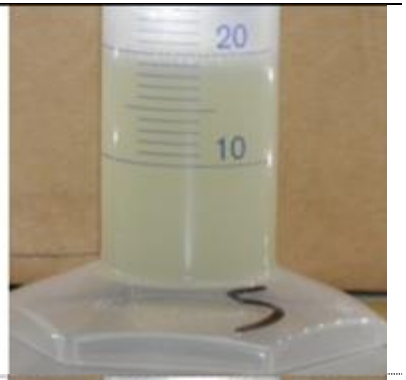
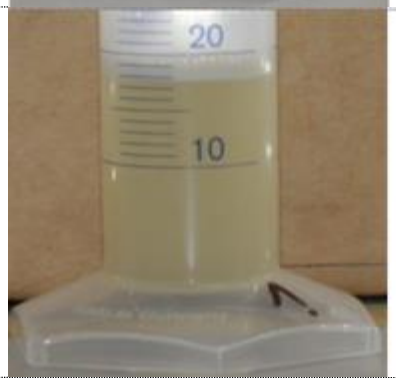
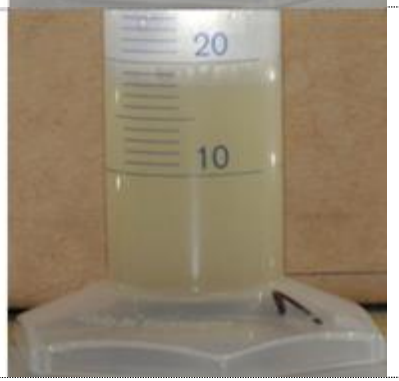


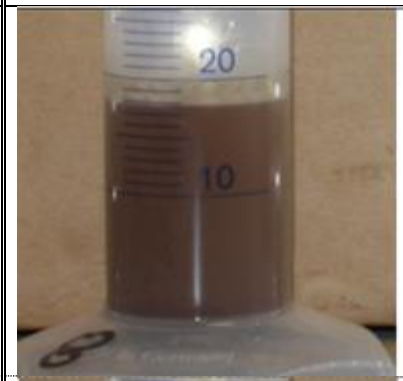
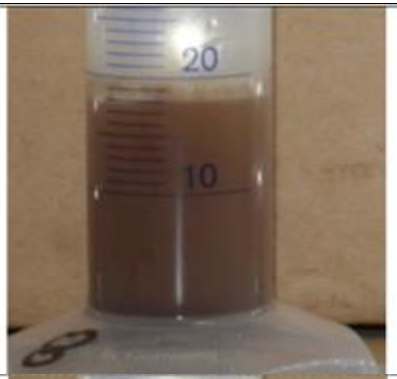
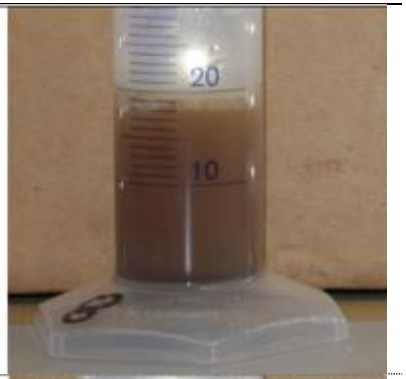
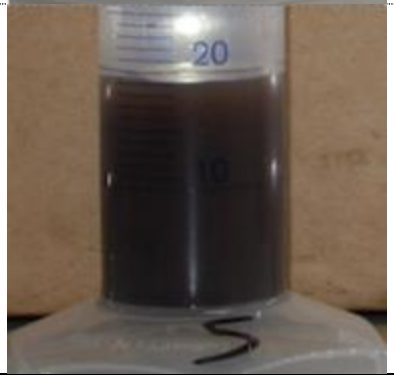
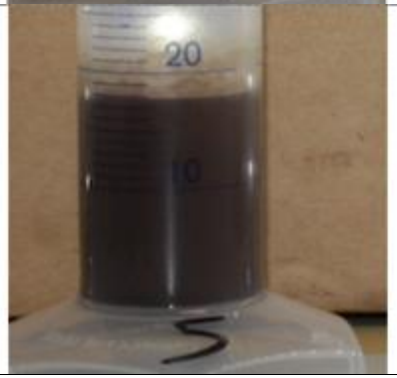
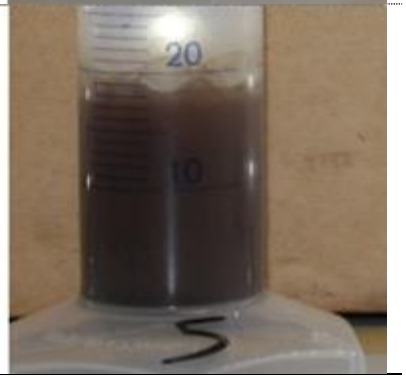

Figure 3-28 Foam quality parameters for Arabica Nicaragua Washed, Arabica Brazil Unwashed and Robusta Vietnam Unwashed green and roasted bean extract. Disproportionation/ Coalescence rate were determined only for samples with 6 minutes of roasting. Statistical analysis were performed throughout the sample set. Different letters indicate significant differences at p=0.05. Statistical analysis performed per column.

As described in Foam Stability section, the foam decay mechanisms which occur simultaneously are foam drainage and bubble disproportionation/coalescence. From t=0 minutes after the aeration step, it has been observed that samples which were roasted at 0, 2 and 4 minutes created a thin foam layer at the top of liquid (Table 3.8). As the time increased the foam height appeared not to change. In that case, the dominant foam decay mechanism was disproportionation/coalescence. Evolution of disproportionation/coalescence

effect could lead to the formation of monolayer of bubbles on top of the liquid. For this reason, the foam curve was not similar to the characteristic volume of foam vs time curve (i.e. Figure 3-6). Hence the fitting of the foam height vs time curve (Equation 3.8) was not feasible.

Table 3.8 Photographs before and after aeration step of Arabica Nicaragua Washed extracts.

| Roasting time (minutes) | Extract prior aeration | 0 minutes after aeration | 5 minutes after aeration | 10 minutes after aeration |
|---|---|---|---|---|
| 0 (R0 min) |  |  |  |  |
| 2 (R2 min) |  |  |  |  |

| Roasting time (minutes) | Extract prior aeration | 0 minutes after aeration | 5 minutes after aeration | 10 minutes after aeration |
|---|---|---|---|---|
| 4 (R4 min) |  |  |  |  |
| 6 (R6 min) |  |  |  |  |

The foam stability parameters (Drainage and Disproportionation/Coalescence rate) for the extracts roasted for 6 minutes are presented in Figure 3-28. It is important to highlight that the calculated error for Disproportionation/Coalescence rate for the roasted coffee extracts (Figure 3-28) is higher than the calculated error for any previous coffee sample assessed in this chapter (e.g. Figure 3-7, Figure 3-17, Figure 3-21, Figure 3-22). Disproportionation/Coalescence rate had a high error because the suggested two-exponential equation for the volume of foam vs time does not sufficiently describe the foam decay of these samples (Equation 3.8). By investigating the foam height vs time curve for R6 min of Arabica Nicaragua Washed (Figure 3-29), there is a point between 5 and 8 minutes where the foam height drops to zero. As described in section **Error! Reference source not found.**, after the foam drainage regime ceases to be the dominant decay mechanism, the foam decay is described as foam disproportion/coalescence. Essentially, the volume of foam decreased slightly, caused by the foam disproportion and bubble rupture at the open interface. At this stage, there is a change in the bubble size distribution as the foam becomes coarser. After a certain point, the few remaining large bubbles rupture which leads to total decay of foam and exposure of the top of the liquid continuous phase (Figure 3-30). The suggested mathematical model does not describe this phenomenon, so the Disproportionation/Coalescence rate has increased calculated error. Regarding the foam quality of the tested sample set, it is evident that there is a threshold between 4 and 6 minutes of roasting. Once the coffee beans pass this threshold, it is hypothesised that there is a sufficient amount and type of chemical compounds generated, which promote the creation of foam.

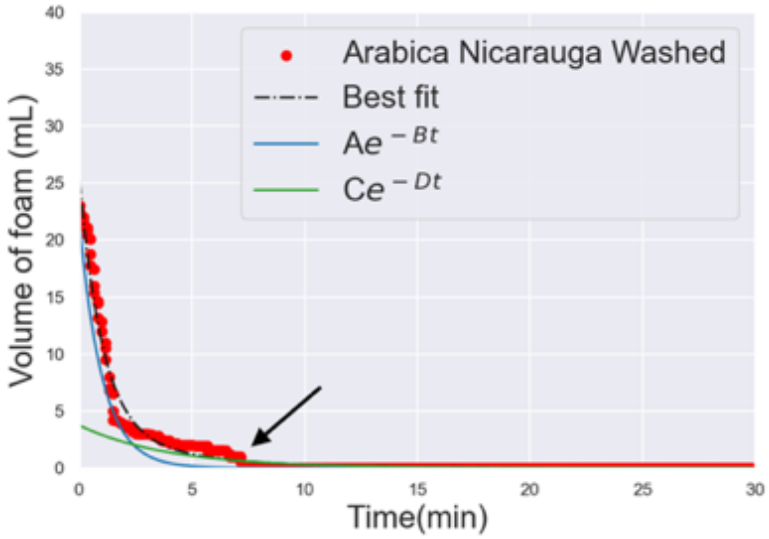



Figure 3-29 Foam height vs time curve for Arabica Nicaragua Washed at 6-minute roast. The black arrow indicates the time when bubbles pop.



Figure 3-30 Collapsed foam system of Arabica Nicaragua Washed R6 minutes.

**Foam quality assessment for Green bean, Roasted bean and Instant coffee**

The effect of the instant coffee manufacturing process on the foaming quality is discussed in this section. For this reason, sequential samples comprised by green bean, roasted bean and its instant coffee version have been used. The foam quality of the instant coffee samples #1-5 of Table 3.1 and the coffee samples of

Table 3.2 were assessed as per 0 section. The foam ability of each sample along with the fitted parameters of drainage and disproportionation/Coalescence rate are presented in Figure 3-31.




Figure 3-31 Foam quality parameters of green, roasted, and instant coffee products. Coffee samples concentration was normalised in 1.5% w/w. Different letters indicate significant differences at p=0.05. Statistical analysis performed per box

Regardless of the origin of the coffee bean, the foam ability of roast and ground extracts in most cases is significantly lower than the foam ability of the instant coffee version of the roasted bean. In the same manner, Drainage rate and Disproportionation/Coalescence rates were lower for the instant coffee products

compared to the roast and ground extract. Samples Trial-FD2 and Trial-FD3 were instant coffee versions of the same roasted bean Colombia Arabica R&G. As described in section 3.2.1, these instant coffee samples were prepared with different process parameters. However, there was not a significant difference in the foam ability. The overall enhanced foam quality of instant coffees against roast and ground extracts could be attributed to different chemical profile of each system. It could be hypothesised that instant coffee products were processed with a set of specific process parameters where the end product enriched in such chemical compounds that enhance the foam quality.

The foam quality was assessed for two different green coffee products, a 100% arabica from Ethiopia and a 100% robusta from Vietnam. Both green coffee extracts had very poor foam ability as maximum incorporation of air was not achieved to form a foam system. For this reason, Drainage rate and Disproportionation/Coalescence rate were not calculated. For the case of Ethiopia Arabica coffee, the roasting process increased the foam ability to 67.0±2.0 % and the instant coffee process further increased the foam ability by 6.1 percentage points. In the case of Vietnam Robusta coffee, the roasting process increased the foam ability to 66.0±2.0% and the instant coffee further increased the foaming ability by 30.48 percentage points (Table 3.9).

Table 3.9 Foam Ability of Instant coffee samples #1-5 of Table 3.1 and coffee samples of Table 3.2 R&G:Roast and Ground coffee (n=5)

| Sample | Foam ability(%) |
|---|---|
| Central America Arabica R&G | 68.42±1.60 |
| Central America Arabica Instant Coffee (FD1) | 72.6±3.3 |
| Colombia Arabica R&G | 62.57±2.62 |
| Colombia Arabica Instant Coffee (FD2) | 76.0±1.6 |
| Colombia Arabica Instant Coffee (FD3) | 74.9±1.3 |
| Ethiopia Arabica Green bean | 3.47±1.29 |
| Ethiopia Arabica R&G | 66.96±1.62 |
| Ethiopia Arabica Instant coffee (FD4) | 73.1±1.6 |
| Kenya Arabica R&G | 63.41±1.62 |
| Kenya Arabica Instant Coffee (FD5) | 72.6±2.6 |
| Vietnam Robusta Green bean | 2.37±1.5 |
| Vietnam Robusta R&G | 65.65±1.5 |
| Vietnam Robusta Instant Coffee (FD6) | 96.13±2.57 |

In conclusion, the foam quality results from Figure 3-28 and Figure 3-31 indicate that whilst instant coffees typically have the maximum foaming ability, the biggest change occurred from green bean to roasted bean. This shows the significant role of roasting process on the foaming properties of coffee – presumably through chemistry generated during roasting.

## 3.4 Conclusions

The established foaming assay proved sufficient to distinguish optimal from poor foaming behaviour of coffee samples. The proposed foam height vs time curve equation depicts very well the foam decay mechanisms for samples which generate a significant amount of foam, while estimating the rate of decay for each phenomenon (drainage and disproportionation/coalescence). Lipid content can be correlated with foam quality, but the chemical profile of the oil fraction must be considered. The application of heat either by roasting the coffee beans or by heat treating instant coffee samples (a second heat treatment) affects the foam quality, but in a way that depends on lipid content. It was evident that the roasting step was crucial for the formation of foam as it has the biggest effect on foam quality compared to the subsequent instant coffee process. This chapter strongly indicates the importance of the chemical profile of a given coffee system. To advance our understanding of the foaming mechanisms and get a deeper insight into the findings of this chapter, it is important to identify and establish chemical compounds that would represent foam quality markers.

# Chapter 4: Screening of polyphenols in coffee via LCMS

## 4.1 Introduction

Following the identification of 21 instant coffee samples that were significantly different from the control coffee in terms of foam ability, it was important to establish differences in the chemical profile of these samples. It has been reported that during roasting, caffeic acid is degraded in favour of several bitter-tasting 4-vinylcatechol oligomers (Frank *et al.*, 2007b), while the foam promoting nature of these oligomers has been reported in a patent (LELOUP, Valérie Martine, Jeanine (CH) *et al.*, 2019). For this reason, it was important to investigate the influence of polyphenolic acids on foam quality. A new targeted LC mass spectrometry method was developed to semi-quantitatively screen principal phenolics and a wider range of lower intensity phenolics in coffee (normalised to internal standard). The method that was utilised in this chapter is Liquid chromatography – Time of Flight Mass spectrometry. The principle of this method lies in the separation of chemical compounds (i.e. metabolites) in the chromatography column. Once the metabolites are eluted from the chromatography column, are ionised either positively (i.e. acquire a proton) or negatively (i.e. lose a proton). Then the ionised metabolites are oriented through a quadrupole magnet to the mass spectrometer where its mass is determined. The utilisation of LC-MS was superior to other chromatographic methods (e.g. HPLC) because the metabolite identification was achieved by measuring the mass of each metabolite with high precision. MSI (Metabolomics Standard Initiative) Level 1 Metabolite Identification (i.e. identification via chemical reference standards ; Sumner et al., 2007); Sumner et al., 2007) was performed for five principal (i.e. high concentration) phenolics. MSI Level 2 Metabolite Identification of the rest of the phenolics of interest was performed by acquiring

the MS2 spectra of the compounds and performing automated comparison to online metabolomics databases (e.g Pubchem, Natural Products) (Sumner *et al.*, 2007). Thereafter correlation analysis was performed to reveal which chemical entities were associated with foam quality performance.

## 4.2 Materials and Methods

### 4.2.1 Chemicals

Reference standards (>95% pure) of 3-methylcatechol, 4-methylcatechol, Caffeic acid and Sinapic acid were acquired from Merck life sciences Ltd (Gillingham, UK). 3-O-Caffeoylquinic acid, 3,4-Dicaffeoylquinic acid were acquired from Cambridge Biosciences Ltd (Cambridge, UK). Formic acid was acquired from Fisher Scientific (Loughborough, UK). Purine and Hexakis(1H, 1H, 3H-tetrafluoropropoxy)phosphazine were acquired from Agilent Technologies (Cheadle, UK). Acetonitrile HPLC grade, ethanol absolute >99.7% and Methanol HPLC grade were acquired from VWR International Ltd (Lutterworth, UK).

### 4.2.2 Instant coffees

The instant coffee samples which were significantly different from the control in terms of foam ability are presented in Table 4.1.

Table 4.1 Instant coffee samples which are significantly different from control. FD: Freeze Dried coffee, SD: Spray Dried coffee

| Code Name | Sample | Coffee type | Variety | Roasting Degree |
|---|---|---|---|---|
| Coffee_V | Control | FD | 30% Brazil Arabica - 70 % Robusta | Medium Roast |
| Coffee_A | Trial-FD1 | FD | Central America 100% Arabica | Dark Roast |
| Coffee_B | Trial-FD2 | FD | Colombian 100% Arabica | Medium Roast |
| Coffee_C | Trial-FD3 | FD | Colombian 100% Arabica | Medium Roast |
| Coffee_D | Trial-FD4 | FD | Ethiopian Sidamo 100% Arabica | Medium Roast |
| Coffee_E | Trial-FD5 | FD | Kenyan 100% Arabica | Medium Roast |
| Coffee_F | Trial-SD1 | SD | 100% Arabica | N/A |
| Coffee_G | Trial-SD2 | SD | 100% Arabica | N/A |
| Coffee_H | SD 3-SR1/12 | SD | 100% Robusta | Medium Roast |
| Coffee_I | NESCAFÉ GOLD Intense | FD | Blend | Dark Roast |
| Coffee_J | NESCAFÉ GOLD Blend | FD | Blend | N/A |
| Coffee_K | NESCAFÉ GOLD Decaff | FD | Blend | N/A |
| Coffee_L | NESCAFÉ GOLD Barista Style | FD | Blend | N/A |
| Coffee_M | NESCAFÉ GOLD Origins Cap Colombia | FD | Colombian 100% Arabica | N/A |
| Coffee_N | NESCAFÉ AZERA Americano | SD | Blend | N/A |
| Coffee_O | NESCAFÉ AZERA Americano Decaff | SD | Blend | N/A |
| Coffee_P | NESCAFÉ AZERA Intenso | SD | Blend | N/A |
| Coffee_Q | FD-Kenco Colombia | FD | Colombian Arabica | N/A |
| Coffee_R | FD-Millicano Americano | FD | N/A | N/A |
| Coffee_S | FD-Millicano Americano Decaff | FD | N/A | N/A |
| Coffee_T | FD-Millicano Americano Intense | FD | N/A | N/A |
| Coffee_U | FD-L'or Classique | FD | N/A | N/A |

### 4.2.3 Instant coffee sample preparation for chemical analysis

A 2 mL aliquot of the instant coffee solution (prepared as per 3.2.5 section) was filtered through a PTFE syringe filter (25 mm, 0.22 um; Jaytee Biosciences Ltd, Herne Bay, UK). The filtered coffee solution was placed in 1.5 mL Eppendorf tubes (Eppendorf, Hamburg, Germany) and ultracentrifuged at 18000 g for 10 minutes (Microfuge 22R Centrifuge, Beckman Coulter, CA, USA). The supernatant was transferred to an Eppendorf vial, spiked with an internal standard solution of Sinapic acid and the Eppendorf vial was vortexed for 10 seconds. The final concentration of Sinapic acid in the spiked solution was 0.07 mg/mL. A 200 uL portion of the spiked solution was transferred to amber vials of 300 uL (fused insert; Agilent Technologies Santa Clara, CA, USA) and sealed with silver crimp cap 11 mm PTFE (Agilent Technologies Santa Clara, CA, USA). A QC (Quality Control) sample was prepared by mixing 100 uL of each sample of the sample set. A 200 uL portion of QC was transferred and sealed to amber vials of 300 uL as per each coffee sample.

### 4.2.4 Chemical reference standard preparation for MSI Level 1 Metabolite Identification

A 1±0.1 mg portion of each chemical reference standard was weighed (Quintix 124-1s, Sartorius Lab Instrument, Göttingen, Germany) into 1.5 mL Eppendorf tubes. A 1000 uL aliquot of solvent (matched to the logP of each standard, typically ultra-pure water, ethanol, or methanol) was transferred in the Eppendorf tube and the tube was vortexed (Vortex genie 2, Scientific Industries, USA) for 10 seconds. The Eppendorf tube was placed in a floating foam rack (Heathrow Scientific, UK) and it was sonicated for 10 minutes in an ultrasonic water bath at 35˚C (Clifton, Nickel Electron Ltd, UK). A 200 uL aliquot was

transferred in crimp amber vials of 300 uL and sealed with silver crimp cap 11 mm PTFE.

### 4.2.5 Chemical analysis with high-resolution liquid chromatography-mass spectrometry method

**Mobile solvents for chemical analysis**

For mobile phase A, ultra-pure water (PurA-Q+ 18.2 MΩ ultra-pure water dispenser, SLS Lab Pro, Nottingham, UK) was decanted in a 1000 mL volumetric flask. The volumetric flask was almost half-filled. A 1.00±0.05mL aliquot of formic acid was transferred via a 2 mL glass pipette (FB50234, Fisherbrand, New Hampshire, USA) to the volumetric flask. The volumetric flask was gently shaken 10 times and topped up with ultra-pure water until the bottom of the meniscus touched the line on the neck of the volumetric flask. The volumetric flask was gently shaken 10 times and decanted into a 1000 mL glass solvent bottle (Agilent Technologies, Santa Clara, CA, USA). The bottle was degassed for 20 minutes. For mobile phase B, the same process was followed using LCMS-grade methanol.

**Reference mass solution for chemical analysis**

Reference mass solution was nebulised into the electrospray ionisation source throughout each analytical run to enable real-time correction of the mass axis. To prepare this solution, 950 mL of acetonitrile - HPLC grade and 50 mL of 18.2 MΩ ultra-pure water were decanted in a 1000 mL glass bottle. Then 2.0 mL of purine and 0.8 mL of Hexakis(1H, 1H, 3H-tetrafluoropropoxy)phosphazine were added to the solvent. The reference mass solution was degassed for 20 minutes.

**Chemical analysis method**

The samples were analysed with an Agilent 6546 LC/Q-TOF (Agilent Technologies, Santa Clara, CA, USA). Agilent MassHunter Workstation LC/MS Data Acquisition software (Version 10.1, Build 10.1.48; Agilent Technologies) was used to control the LC-MS system. The LC front end comprised a high-speed binary pump (G7120A), a multi-sampler with a chiller unit (G7167B), a multicolumn thermostat (G7116B) diode array detector (G7117B) and an isocratic pump (G7110B) for delivery of reference mass solvent at 2 mL/min. A splitter with a ratio of 1:100 was installed between the isocratic pump and the ionisation source; therefore 0.02 mL/min of reference mass solution was injected into the ionisation source and the remainder was recycled back to the reservoir bottle. All units of LC belong to the Agilent 1290 Infinity II series.

Each 1 uL of a sample was injected onto a Kinetex Biphenyl chromatography column (1.7 um, 30 x 2.1 mm; Phenomenex, CA, USA) fitted with a SecurityGuard ULTRA guard column, at 40˚C. The binary pump flowed at 0.3 mL/min, following the gradient as presented in Table 4.2. This chromatographic method was designed to separate polyphenols from cocoa, coffee, and tea – notes on the development of this method can be found in section 4.3.1

Table 4.2 Polyscreen mk5 (i.e. version 5) gradient. Mobile phase A: 100% Water. Mobile phase B: 100% Methanol

| Time (min) | Mobile phase A (%) | Mobile phase B(%) | Flow (mL/min) |
|---|---|---|---|
| 0 | 95 | 5 | 0.3 |
| 2 | 95 | 5 | |
| 8 | 81 | 19 | |
| 17 | 17.5 | 82.5 | |
| 18 | 0 | 100 | |
| 20 | 0 | 100 | |
| 22 | 95 | 5 | |
| 24 | 95 | 5 | |

The worklist commenced with ultra-pure water injection to wash the column, followed by 10 injections of QC for conditioning the ionisation source. Each sample was injected in replicates of 5 in random order. A QC injection was applied every 5 injections of coffee samples to check the stability of the instrument. The MS detector was an Agilent 6546 LC/Q-TOF fitted with a JetStream ESI source and experiments were performed in negative polarity mode. The source parameters are presented in Table 4.3.

Table 4.3 Source parameters in negative polarity mode for targeted chemical analysis

| Parameter | Units |
|---|---|
| Gas temperature | 320˚C |
| Drying gas rate | 8 L/min |
| Nebulizer pressure | 35 psi |
| Sheath Gas Temperature | 350 ˚C |
| Sheath Gas Flow rate | 11 l/min |
| Capillary voltage | 3500 V |
| Nozzle voltage | 1000 V |
| Fragmentor voltage | 110 V |
| Skimmer | 65 V |
| Oct 1 RF Vpp | 750 V |

The MS1 data acquisition parameters were as follows: acquisition rate; 5 spectra/s, m/z detection mass detection range; 50-1700 m/z. The Auto MS/MS experiments were performed with the same chromatographic method. The MS2 data acquisition parameters were as follows: acquisition rate; 6 spectra/s, m/z detection mass detection range; 50-1700 m/z, collision energies; 10V, 20V and 40V. The possible ionised adducts in negative polarity mode are presented in Table 4.4.

Table 4.4 Negative polarity mode adducts. M: the neutral mass of the chemical compound of interest

| Negative polarity adducts | Comment |
|---|---|
| [M-H]- | A proton was removed from neutral chemical compound |
| [M+CH2O2-H]- | Formate adduct |
| [M+C2H4O2-H]- | Acetate adduct. |

### 4.2.6 Data analysis

The acquired data were analysed by Agilent MassHunter Workstation Qualitative Analysis 10.0, Build 10.0.10305.0 (Agilent Technologies, Santa Clara, CA, USA). A built-in function named, Find by Formula (FBF), in Workstation Qualitative Analysis software allowed the extraction of target peaks from a Total Ion Chromatograph (TIC) against data for specific chemical species held in a Personal Compound Database and Library (PCDL). Each extracted peak was accompanied by its retention time, m/z, ionisation format (i.e. adduct), peak height and peak area. The development of the PCDL for targeted chemical analysis can be found in section 4.3.1 of this chapter. The FBF algorithm parameters were as follows: matches per formula (Isomer detection); 1, match mass tolerance; ± 10.00 ppm, match retention time tolerance; ± 0.350 minutes, possible ion species; [-H],[+HCOO],[+CH3COO], Extracted Ion Chromatograph (EIC) Peak filter; Absolute height >= 100 counts, Isotope model; Common organic (no halogens). Screenshots of the Find By Formula algorithm parameters can be found in Appendix B. The peak area of each chemical entity throughout the sample set was normalised against the peak area of Sinapic acid. The average and standard deviation values of normalised abundances of compounds were calculated for each coffee sample in the set. Correlation

analysis between the normalised abundance of each chemical compound vs each foam quality parameter was performed by using the package scipy.stats.linregress (Virtanen *et al.*, 2020) in Python 3. Details on the stats packages can be found in section 3.2.14

### 4.2.7 Level 2 identification of chemical compounds via MS2 analysis

Spectra for extracted ion peaks were exported as a Compound Exchange file (.CEF). and it was imported to SIRIUS software (Dührkop *et al.*, 2015, 2019, 2020; Djoumbou Feunang *et al.*, 2016; Hoffmann *et al.*, 2021; Kim *et al.*, 2021). SIRIUS software takes the MS2 spectra of a given compound as input, calculates the most likely empirical formulae and structural features and then compares the results to several online metabolomics databases (e.g. Pubchem, Pubmed, Natural Products etc.). Feasible identities for annotation of each compound are provided with two key scores of relative certainty:

a. SIRIUS score: The SIRIUS score depicts the certainty of annotating the unknown compound with an empirical formula (i.e.$C_xH_yO_zN_iP_j$). SIRIUS score can take any value between 0% and 100%. The higher the score the higher the certainty of annotation.
b. CSI score: The CSI score is associated with the structure of the chemical entity which is annotated. The CSI score can take any value up to 0. The closer the CSI score to 0 indicates that the proposed structure has higher certainty.

The detailed parameters of MS2 annotation via SIRIUS are presented in Table 4.5.

Table 4.5 SIRIUS parameters for MS2 annotation

| **Algorithm engaged for MS2 annotation** | | |
|---|---|---|
| **SIRIUS – Molecular Formula Identification** | **General** | |
| | Instrument | Q-TOF |
| | Filter by isotope pattern | Yes |
| | MS2 mass accuracy (ppm) | 10 |
| | MS/MS isotope scorer | SCORE |
| | Candidate stored | 10 |
| | Min candidates per Ion stored | 1 |
| | **Use Database formulas only** | None |
| | **Possible Ionizations** | [M-H]-<br>[M+CH2O2-H]-<br>[M+C2H4O2-H]- |
| | **ILP** | |
| | Tree timeout | 0 |
| | Compound timeout | 0 |
| | Use heuristic above m/z | 300 |
| | Use heuristic only above m/z | 650 |
| | **Elements and their range allowed in Molecular Formula** | |
| | H<br>C<br>N<br>O<br>P | 0-Infinity |
| **Predict Fingerprints & Search Databases** | **CSI:FingerID** | |
| | Fallback Adducts | [M-H]-<br>[M+CH2O2-H]-<br>[M+C2H4O2-H]- |
| | Structure Database Search | Bio Database, Biocyc, CHEBI, COCONUT, EcoCyc Mine, GNPS, HMDB,KEGG, KEGG Mine, KNApSAcK, Maconda, MeSH, Norman, Natural Products, Plantcyc, Pubchem, Pubmed, YMDB, YMDB Mine, ZINC bio |
| **Canopus-Compound Class prediction** | Parameter free | |

A good MS2 annotation was considered one where the SIRIUS score was close to 100, the CSI score was higher than a -180 and the suggested annotation was in the top 10 suggestions.

## 4.3 Results and discussion

### 4.3.1 Method development of targeted chemical analysis

A chromatographic method to separate, identify and quantify polyphenols commonly reported on coffee was developed. An optimum method for chromatographic chemical analysis is considered one where extracted ion peaks are sharp and base-to-base separation of peaks is achieved. The parameters that were considered during the method development were:

- Chromatography column
- Mobile phases
- The gradient of mobile phases during the chromatographic analysis
- Ionisation voltage of chemical entities

**Chromatography column and mobile phases**

The first step of method development was to investigate which chromatography column and which mobile phases would separate the peaks of interest and give chromatographs with sharp peaks. For the research purposes of the Molecular Phenomics group in the Division of Food, Nutrition and Dietetics, this method was developed with the aim of identifying and quantifying polyphenols that are present in coffee, cocoa and tea. The method was initially developed by chemically analysing a cocoa extract – a source of procyanidins (Oracz, Zyzelewicz and Nebesny, 2015) that are typically difficult to resolve via traditional C18 reverse phase chromatography. The list of targets of interest included polyphenols reported both in coffee and cocoa (Table 4.6).

Table 4.6 Polyphenols that are reported both in coffee and cocoa.

| Chemical Target | Empirical Formula | Reported in cocoa | Reported in coffee |
|---|---|---|---|
| Catechol- | C6H6O2 | Lang et al., 2006Lang et al., 2006 | Baeza et al., 2016; Król et al., 2020 |
| 3-methylcatechol- | C7H8O2 | | |
| 4-methylcatechol- | | | |
| 4-ethylcatechol- | C8H10O2 | | |
| Pyrogallol- | C6H6O3 | | |
| Caffeic acid- | C9H8O4 | Caprioli et al., 2016Caprioli et al., 2016 | |
| Phenol- | C6H6O | Serra Bonvehí & Ventura Coll, 1998Serra Bonvehí & Ventura Coll, 1998 | |
| Epigallocatechin gallate | C22H18O11 | Caldero N et al., 2009Caldero N et al., 2009 | |
| Quercetin | C15H10O7 | Andres-Lacueva et al., 2008Andres-Lacueva et al., 2008 | |
| Quercetin-3-glucoside | C21H19O12 | | |
| Chlorogenic acid-<br>Coumaric acid<br>Ferulic acid | C16H18O9<br>C9H8O3<br>C10H10O4 | Rusconi & Conti, 2010Rusconi & Conti, 2010 | |

For the optimal separation of polyphenols, reverse-phase liquid chromatography was performed. The separation ability of two different columns was investigated. One column was C18 Acquity UPLC HSS T3 1.8 µm (Waters, MA, USA) and the other column was Kinetex Biphenyl 1.7 µm (Phenomenex, CA, USA). Both columns were accompanied by a SecurityGuard ULTRA guard column (Phenomenex, CA, USA).

Binary gradients of water versus either methanol or acetonitrile (plus 0.1% formic acid) were investigated. The preparation of mobile phases is described in Mobile solvents for chemical analysis subsection of 4.2.5 section.

The initial chromatographic method was as follows. The method started with isocratic 5% solvent B for 2 minutes. Then, a gradient was applied, and B solvent reached 30% at 4 minutes. The slope of solvent B% became smoother and reached 100% at 12 minutes before reaching an isocratic flow at 100% B for 2 minutes. Finally, solvent B changed to 5% at 15 minutes and was kept isocratic flow for 3 minutes. The extracted ion chromatographs of chemical entities in Table 4.6 were extracted via Find by Formula function and the native separability of peaks for each column-non-polar phase system was examined.

Figure 4-1 depicts the native separability of each column-mobile phase system for C7H8O2 (i.e. 3-methylcatechol or 4-methylcatechol). It is evident that peaks are sharp in every case but are more spread in Biphenyl-Methanol system. The native separability of each chemical entity is depicted in the heatmap (Figure 4-2) and detailed extracted chromatographs are presented in Appendix C.

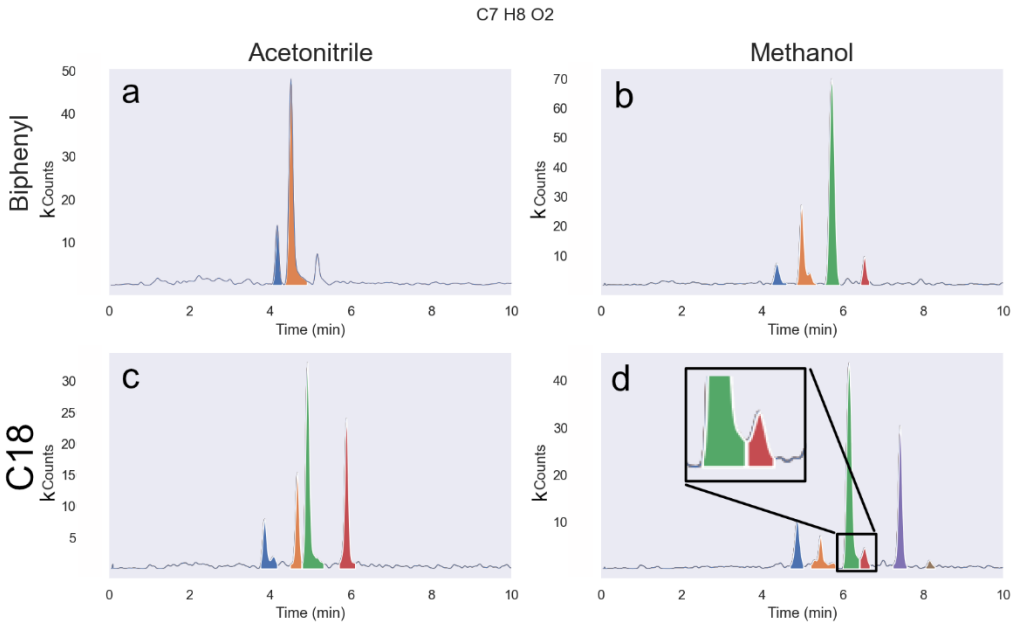



Figure 4-1 Extracted ion chromatographs of C7H8O2 (i.e. 3-methylcatechol or 4-methylcatechol) for every combination of mobile phase B and column phase. (a) Biphenyl-Acetonitrile, (b) Biphenyl-Methanol, (c) C18-Acetonitrile, (d) C18-Methanol. The presented peaks indicate chemical entities where their molecular mass is equal to the molecular mass of C7H8O2. In three out of four extracted chromatographs (i.e. a,c,d) the tallest peak showed a shoulder effect, which means that the specific chemical compound was eluting at a close retention time with another compound. The methanol-biphenyl column solved this issue; therefore it was considered as the optimum combination for achieving good native separability.

| Empirical Formula | Acetonitrile-Biphenyl | Acetonitrile-C18 | Methanol-Biphenyl | Methanol-C18 |
|---|---|---|---|---|
| C6H6O2 | N | N | Y | N |
| C7H8O2 | N | N | Y | N |
| C8H10O2 | | | | |
| C6H6O3 | Y | Y | Y | Y |
| C9H8O4 | N | N | Y | N |
| C6H6O | Y | N | Y | N |
| C22H18O11 | N | Y | N | N |
| C15H10O7 | N | N | Y | Y |
| C21H19O12 | | | | |
| C16H18O9 | N | N | Y | N |
| C9H8O3 | N | N | Y | N |
| C10H10O4 | Y | N | Y | N |

Figure 4-2 Summary heatmap of separability of each column-mobile phase system for every chemical entity. Legend: Y: Good Separability, N: Poor Separability, Grey tiles indicate that no extracted ion were found for all four combinations of mobile phase and column phase so no conclusion could be shaped.

It can be concluded that the Biphenyl column using methanol as an eluent had the optimum native separability for most of the targets compared to the rest of the column-mobile phase combinations.

**Gradient method development**

Taking into account the that the combination of Methanol-Biphenyl had the optimum native separability of the initial chemical targets, the next step involved broadening the list of polyphenols that have been reported in coffee and the gradient optimisation with the aim of optimum separability of peaks. A control instant coffee solution was prepared as per section 4.2.3 of this chapter and this was the sample that was used for the optimisation of the chemical analysis method, as described in section 4.2.5. Given the expense of acquiring reference standards for all possible coffee polyphenols, the chromatographic method was initially developed by comparing the separation of peaks matching the formulae of common coffee phenolics. MSI Level 1 or 2 Metabolite Identification was performed for principal phenolic compounds once the chromatography was established.

The broadened list of polyphenols was shaped from 5 references (Frank *et al.*, 2007b; Nunes and Coimbra, 2010; Wei and Tanokura, 2015; LELOUP, Valérie Martine, Jeanine (CH) *et al.*, 2019; Król *et al.*, 2020). The list included but was not limited to, ferulic acid, quinic acid, caffeic acid, p-coumaric acid, mono- and di-caffeoylquinic acids, mono- and di-feruloylquinic acids, mono- and di-p-coumaroylquinic acids, their lactones and roasted caffeic acid products. The number of chemical compounds was 175. Several compounds share the same empirical formula (i.e. isomers). For example, forms of mono-caffeoylquinic

acids (i.e 3-O-, 4-O- or 5-O-caffeoylquinic acid) share the same empirical formula of C16H18O9. Therefore, the number of empirical formulae in the list of polyphenols was 71. A detailed table of the 175 polyphenols is presented in Appendix D.

A control instant coffee solution was injected in the LC-MS with the gradient method as described in Chromatography column and mobile phases subsection of section 4.3.1 and the total ion chromatograph was acquired. 71 empirical formulae were searched for with the "Find By Formula" function and the algorithm returned the extracted ion chromatographs for 29 empirical formulae. The remaining 42 empirical formulae were not detected in the coffee sample. A detailed table of the 29 empirical formulae., which are equivalent to 66 different chemical compounds can be found in Appendix E.

At this point in the analysis, the aim was to optimise the gradient of the mobile phase to achieve sharp peaks with good base-to-base separation. Several gradients were tested and are presented in Figure 4-3 and Table 4.7. The general profile of the methods was to start with a more hydrophilic flow, change to more hydrophobic and then return to a hydrophilic flow. The differences between the applied methods (i.e. Polyscreen mk1 to mk6) was in how steep or smooth is the transition from hydrophilic to hydrophobic flow. The methods were named as Polyscreen because these were developed to for **Poly**phenol **screen**ing analysis.

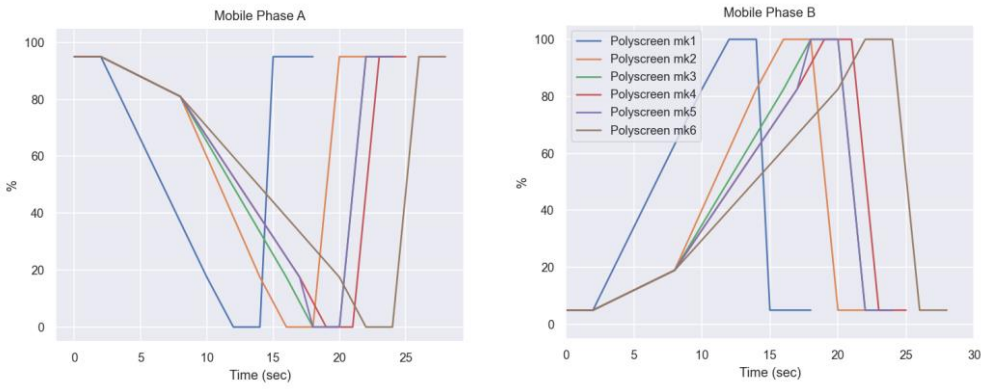



Figure 4-3 Left: Gradient of mobile phase A, Right: Gradient of mobile phase B. Legend applies to both plots.

Table 4.7 Gradient for Polyscreen mk1 to mk6

| Polyscreen mk1 | | | Polyscreen mk2 | | | Polyscreen mk3 | | |
|---|---|---|---|---|---|---|---|---|
| Time (min) | A (%) | B(%) | Time (min) | A (%) | B(%) | Time (min) | A (%) | B(%) |
| 0 | 95 | 5 | 0 | 95 | 5 | 0 | 95 | 5 |
| 2 | 95 | 5 | 2 | 95 | 5 | 2 | 95 | 5 |
| 10 | 17.5 | 82.5 | 8 | 81 | 19 | 8 | 81 | 19 |
| 12 | 0 | 100 | 14 | 17.5 | 82.5 | 16 | 17.5 | 82.5 |
| 14 | 0 | 100 | 16 | 0 | 100 | 18 | 0 | 100 |
| 15 | 95 | 5 | 18 | 0 | 100 | 20 | 0 | 100 |
| 18 | 95 | 5 | 20 | 95 | 5 | 22 | 95 | 5 |
| | | | 22 | 95 | 5 | 24 | 95 | 5 |
| Polyscreen mk4 | | | Polyscreen mk5 | | | Polyscreen mk6 | | |
| Time (min) | A (%) | B(%) | Time (min) | A (%) | B(%) | Time (min) | A (%) | B(%) |
| 0 | 95 | 5 | 0 | 95 | 5 | 0 | 95 | 5 |
| 2 | 95 | 5 | 2 | 95 | 5 | 2 | 95 | 5 |
| 8 | 81 | 19 | 8 | 81 | 19 | 8 | 81 | 19 |
| 17 | 17.5 | 82.5 | 17 | 17.5 | 82.5 | 20 | 17.5 | 82.5 |
| 19 | 0 | 100 | 18 | 0 | 100 | 22 | 0 | 100 |
| 21 | 0 | 100 | 20 | 0 | 100 | 24 | 0 | 100 |
| 23 | 95 | 5 | 22 | 95 | 5 | 26 | 95 | 5 |
| 25 | 95 | 5 | 24 | 95 | 5 | 28 | 95 | 5 |

The separability of each Polyscreen method for mono-feruloylquinic acids (i.e C17H20O9) that was applied is depicted in Figure 4-4. The "Find by Formula" function identified 8-10 peaks that could possibly be Feruloylquinic acid throughout the different methods. According to the literature, 3 different Feruloylquinic acids have been reported in coffee and it can be seen from Figure 4-4 that 3 major peaks appeared in each chromatograph. The identity of each peak would be ascertained later, either by using chemical reference standards or

via MS2 annotation techniques. However, at this point of analysis, it was important to investigate which gradient could best separate the peaks of interest. In Figure 4-4, sharp peaks were achieved from all applied gradients. A shouldering effect appeared at a peak at 11.365 min at Polyscreen mk3 (red arrow). The shouldering effect was resolved only after Polyscreen mk4. Therefore, Polyscreen mk4 to mk6 methods were sufficient to separate the peaks of interest. A summary of separability for each Polyscreen method on each chemical entity of interest is presented in Figure 4-5.

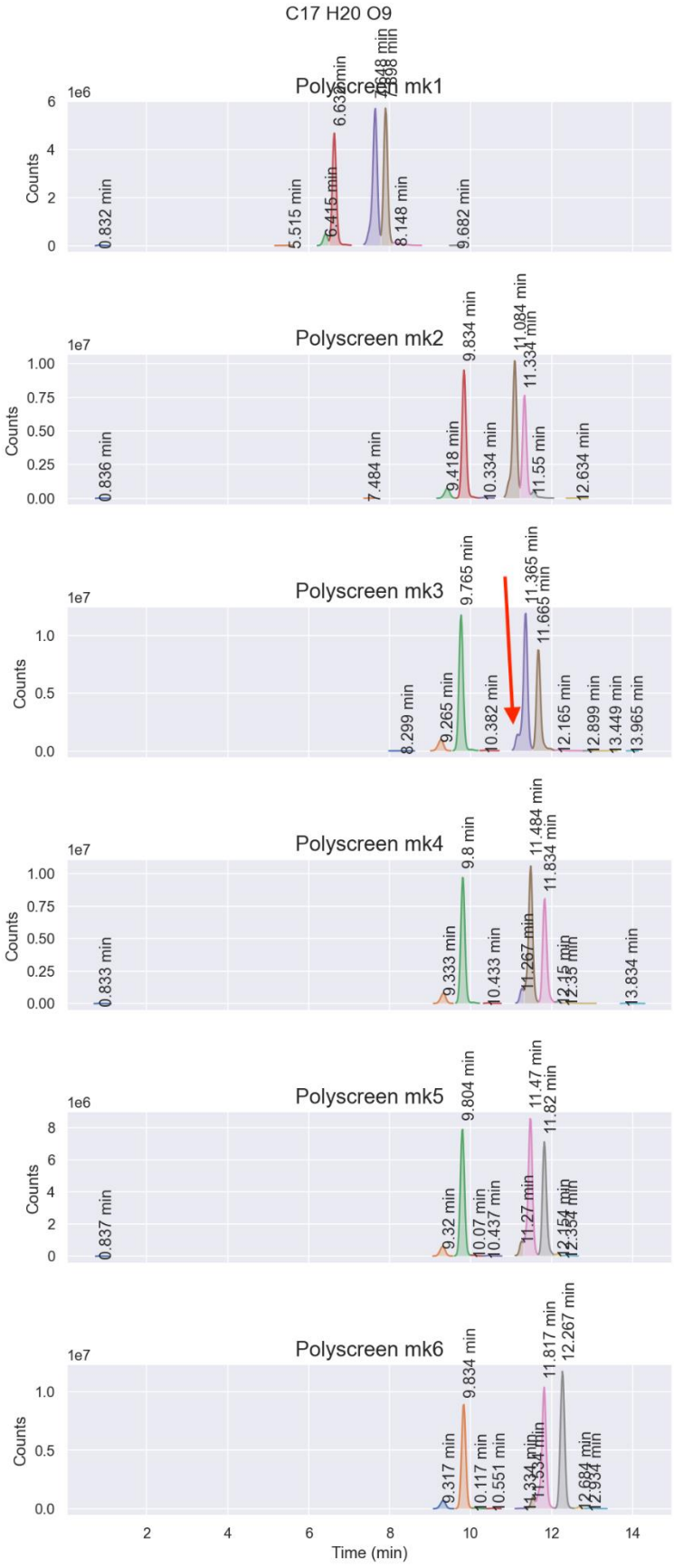



Figure 4-4 Separability of each Polycreen method for mono-feruloylquinic acid (C17H20O9).

| # | Empirical Formula | Polyscreen | | | | | |
|---|---|---|---|---|---|---|---|
| | | mk1 | mk2 | mk3 | mk4 | mk5 | mk6 |
| 1 | C10H10O4 | Y | Y | Y | N | N | N |
| 2 | C11H12O4 | N | Y | Y | Y | Y | Y |
| 3 | C16H16O4 | N | N | N | Y | Y | Y |
| 4 | C16H16O7 | N | N | N | Y | Y | N |
| 5 | C16H16O8 | N | N | N | N | Y | Y |
| 6 | C16H18O4 | N | N | Y | Y | N | N |
| 7 | C16H18O8 | N | N | Y | Y | Y | Y |
| 8 | C16H18O9 | N | N | N | N | Y | N |
| 9 | C17H16O6 | N | N | N | Y | Y | N |
| 10 | C17H18O8 | N | N | N | Y | Y | N |
| 11 | C17H20O9 | N | N | N | Y | Y | Y |
| 12 | C6H6O | N | Y | Y | Y | Y | Y |
| 13 | C6H6O2 | Y | Y | Y | Y | Y | Y |
| 14 | C6H6O3 | Y | Y | Y | Y | Y | Y |
| 15 | C7H10O5 | Y | Y | Y | Y | Y | Y |
| 16 | C7H12O6 | Y | Y | Y | Y | Y | Y |
| 17 | C7H6O3 | Y | Y | Y | Y | Y | Y |
| 18 | C7H8O2 | | Y | Y | Y | Y | Y |
| 19 | C8H10O2 | Y | Y | Y | Y | Y | Y |
| 20 | C8H8O2 | N | N | Y | Y | Y | Y |
| 21 | C9H10O2 | N | N | N | Y | Y | N |
| 22 | C9H8O3 | N | N | N | Y | Y | N |
| 23 | C9H8O4 | N | Y | Y | Y | Y | Y |
| 24 | C25H22O11 | N | N | Y | Y | Y | Y |
| 25 | C25H24O10 | N | N | N | Y | Y | N |
| 26 | C25H24O12 | N | N | N | Y | Y | Y |
| 27 | C26H26O12 | N | N | N | Y | Y | N |
| 28 | C27H26O12 | Y | Y | Y | Y | Y | Y |
| 29 | C27H28O12 | Y | Y | Y | Y | Y | Y |

Figure 4-5 Summary heatmap of separability of Polyscreen method for every chemical entity.
Legend: Y: Good Separability, N: Poor Separability

It is evident from Figure 4-5 that Polyscreen mk5 was the only applied gradient where the base-to-base separation and sharp peaks were achieved for most of the tested empirical formulas. Hence Polyscreen mk5 was used for all the types of chemical analysis in this thesis (Figure 4-6). Detailed extracted chromatographs for the rest of the chemical entities can be found in Appendix F.

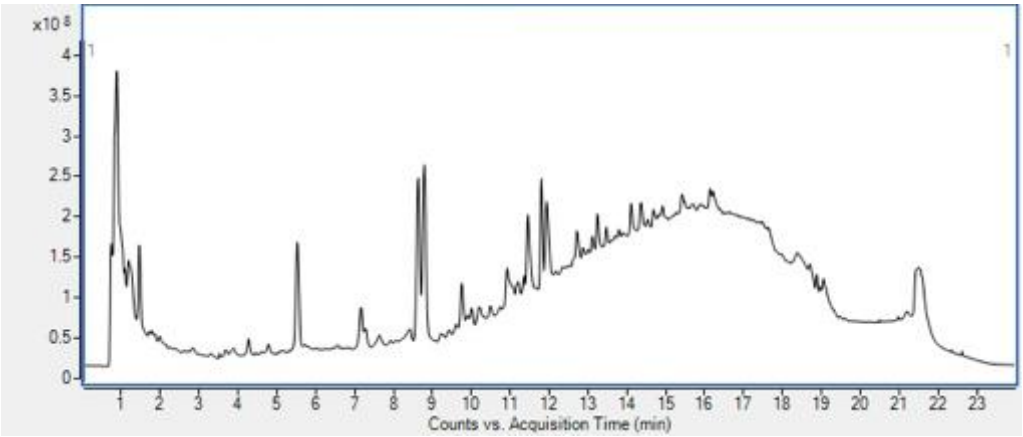



Figure 4-6 Total Ion Chromatograph of instant coffee sample via Polyscreen mk5 method

**MSI Level 1 and Level 2 identification of chemical entities**

At this point of method development, the aim was to identify 66 chemical compounds of interest in the Polyscreen mk5 method. Chemical reference standards were used to confirm the identity of 5 out of the 66 targets (Table 4.8).

Table 4.8 Chemical compounds that were identified with chemical reference standards

| Name | Empirical formula | Retention time (min) |
|---|---|---|
| 3-O-Caffeoylquinic acid | C16H18O9 | 8.832 |
| 3-methylcatechol | C7H8O2 | 8.897 |
| 4-methylcatechol | | 8.316 |
| Caffeic acid | C9H8O4 | 7.966 |
| 3,4-Di-O-caffeoylquinic acid | C25H24O12 | 12.729 |

The rest of the 61 targets were identified at MSI level 2 via MS2 annotation techniques as described in section 4.2.7. An example of MS2 annotation results is presented in Table 4.9.

Table 4.9 Level 2 annotation of Ferulic acid (C10H10O4) via MS2 analysis

| Empirical formula | Precursor m/z | Retention time (min) | Annotated name | CSI SCORE | SIRIUS SCORE | Comment |
|---|---|---|---|---|---|---|
| C10H10O4 | 193.050689 | 12.21785 | Ferulate | -196.406 | 33.33 | 100th suggestion |
| | 193.0506664 | 11.50117 | Ferulate | -185.646 | 33.33 | 75th suggestion |
| | 193.0506956 | 13.11787 | Ferulate | -179.346 | 33.33 | 45th suggestion |
| | 193.0507359 | 9.80113 | Ferulate | -121.8 | 33.33 | 7th suggestion |

For example, MS2 analysis pointed out that 4 chemical entities were initially suggested as possible hits for Ferulic acid. However, only 1 of these had CSI score>-150 and it was within the first 10 suggestions ($7^{th}$ from the top). Therefore, the chemical entity with retention time 9.80113 minutes and m/z 193.05 was annotated as Ferulic acid. The level 1 and level 2 identification steps annotated 38 chemical entities in Polyscreen mk5 method (Table 4.10). As described previously several compounds of interest were isomers. Sufficient distinction between the isomers was not feasible through the MS2 annotation. Therefore, the isomers were annotated as Isomer alpha, Isomer beta or Isomer gamma (e.g. Feruloylquinic acid alpha, Feruloylquinic acid beta). Detailed tables of level 2 identification for the rest of chemical entities can be found in Appendix G.

Table 4.10 Polyphenols identified in level 1 and level 2 in Polyscreen mk5 method.

| Target name | Empirical formula | Retention time (min) | Level of identification |
|---|---|---|---|
| Caffeic acid | C9H8O4 | 7.93 | 1 |
| 3-methylcatechol | C7H8O2 | 8.33 | 1 |
| 3-Caffeoylquinic acid | C16H18O9 | 8.82 | 1 |
| 4-methylcatechol | C7H8O2 | 8.98 | 1 |
| 3,4-di-Caffeoylquinic acid | C25H24O12 | 12.73 | 1 |
| Phenol | C6H6O | 0.88 | 2 |
| Pyrogallol | C6H6O3 | 3.32 | 2 |
| Caffeoylquinic acid gamma | C16H18O9 | 4.32 | 2 |
| Guaiacol | C7H8O2 | 4.35 | 2 |
| Salicylic acid | C7H6O3 | 5.37 | 2 |
| p-Coumaroylquinic acid beta | C16H18O8 | 7.65 | 2 |
| Caffeoylquinic acid beta | C16H18O9 | 8.45 | 2 |
| Quinic acid | C7H12O6 | 8.85 | 2 |
| 4-ethylcatechol | C8H10O2 | 9.17 | 2 |
| Feruloylquinic acid alpha | C17H20O9 | 9.32 | 2 |
| Ferulic acid | C10H10O4 | 9.80 | 2 |
| p-Coumaroylquinic acid gamma | C16H18O8 | 10.55 | 2 |
| Quinic acid lactone | C7H10O5 | 10.55 | 2 |
| p-Coumaroylquinic acid alpha | C16H18O8 | 10.97 | 2 |
| Feruloylquinic acid beta | C17H20O9 | 11.48 | 2 |
| Caffeoyl quinic acid lactone alpha | C16H16O8 | 11.92 | 2 |
| p-Coumaroylquinic acid lactone | C16H16O7 | 12.09 | 2 |
| 4-vinylguaiacol | C9H10O2 | 12.38 | 2 |
| Feruloylquinic acid lactone alpha | C17H18O8 | 12.73 | 2 |
| Caffeoyl quinic acid lactone beta | C16H16O8 | 12.88 | 2 |
| Catechol | C6H6O2 | 12.97 | 2 |
| di-Caffeoylquinic acid beta | C25H24O12 | 13.13 | 2 |
| Caffeoyl-Feruloylquinic acid gamma | C26H26O12 | 13.33 | 2 |
| di-Caffeoylquinic acid gamma | C25H24O12 | 13.48 | 2 |
| Roasted caffeic acid product beta | C16H16O4 | 13.72 | 2 |
| Caffeoyl-Feruloylquinic acid alpha | C26H26O12 | 13.80 | 2 |
| 4-vinylcatechol | C8H8O2 | 14.13 | 2 |
| Roasted caffeic acid product alpha | C16H16O4 | 14.45 | 2 |
| di-Caffeoylquinic acid lactone alpha | C25H22O11 | 14.47 | 2 |
| Caffeoyl-Feruloylquinic acid beta | C26H26O12 | 14.55 | 2 |
| di-Feruloylquinic acid alpha | C27H28O12 | 14.75 | 2 |
| di-Caffeoylquinic acid lactone beta | C25H22O11 | 14.82 | 2 |
| di-Feruloylquinic acid beta | C27H28O12 | 15.42 | 2 |

**Electro-spray ionisation (ESI) optimisation**

The final step of method development was the optimisation of ionisation voltage in the JetStream ESI source. The default ionisation voltage was 1000 V and it was investigated if higher or lower levels of voltage could increase the response of the mass spectrometer. A control instant coffee solution was injected in LC-MS and analysed via Polyscreen mk5. The peaks of interest were extracted from the Total Ion Chromatograph via the "Find by Formula" function by using a PCDL and the areas was calculated via integration. The area of peaks under 3 different ionisation voltages is presented in Figure 4-7. In most cases, there was little difference between areas at 500 V versus 1000 V, and as such the default ionisation voltage was retained.

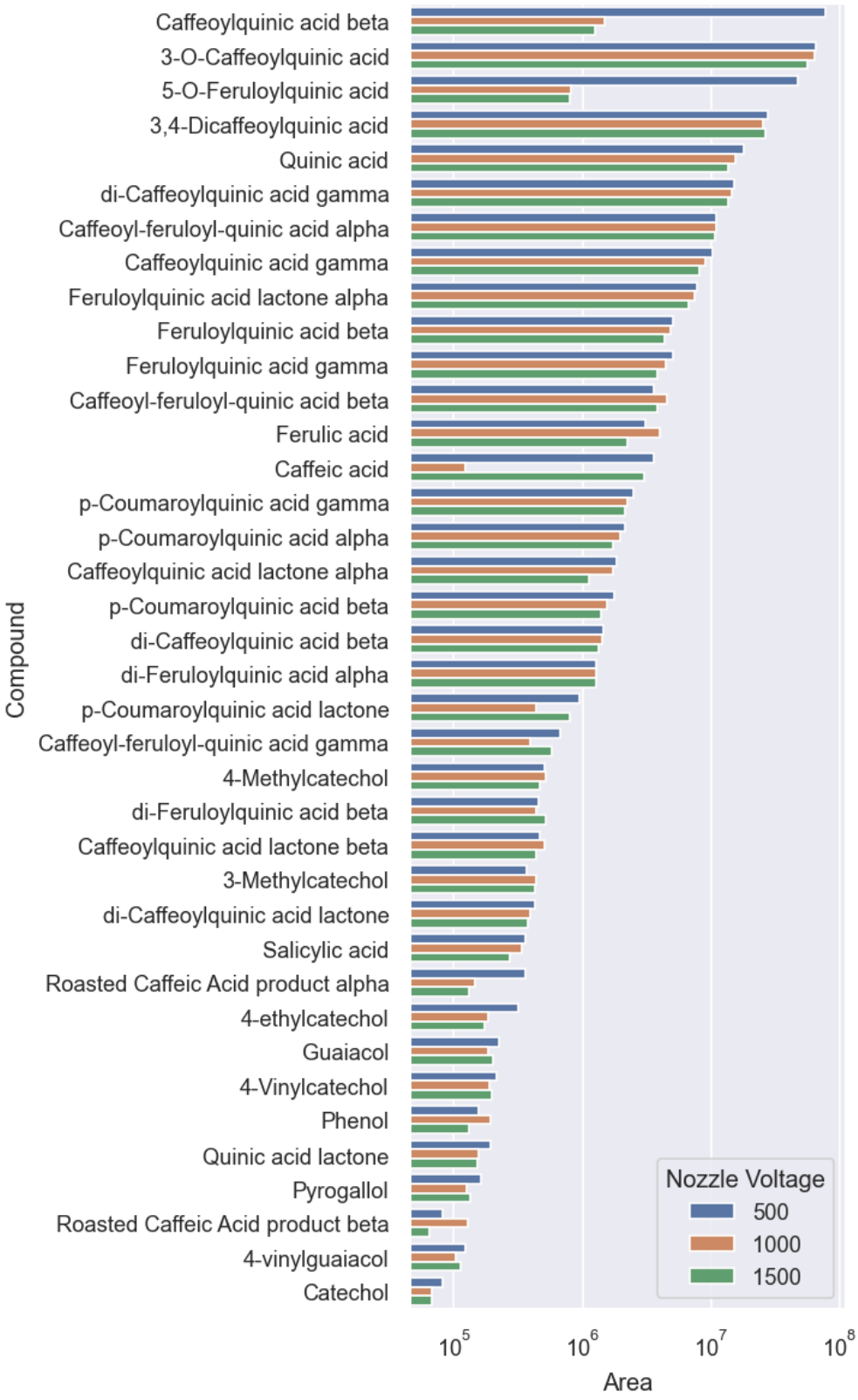



Figure 4-7 Area of 38 chemical compounds at 3 different ionisation voltages.

**Conditioning of source**

Prior to every chemical analysis of a sample, it is good practise to clean the ionisation source from debris resulting from previous runs. A dirty ionisation source would affect the response of the mass spectrometer and result in lower sensitivity. It is evident though that once the source is completely clean the Total Ion Count would decrease rapidly after each injection until it stabilises. It was important to determine the number of injections needed until the response is stabilised. A QC sample was injected 20 times in LCMS and analysed via the Polyscreen mk5 method, the total ion chromatographs were collected and are presented in Figure 4-8.

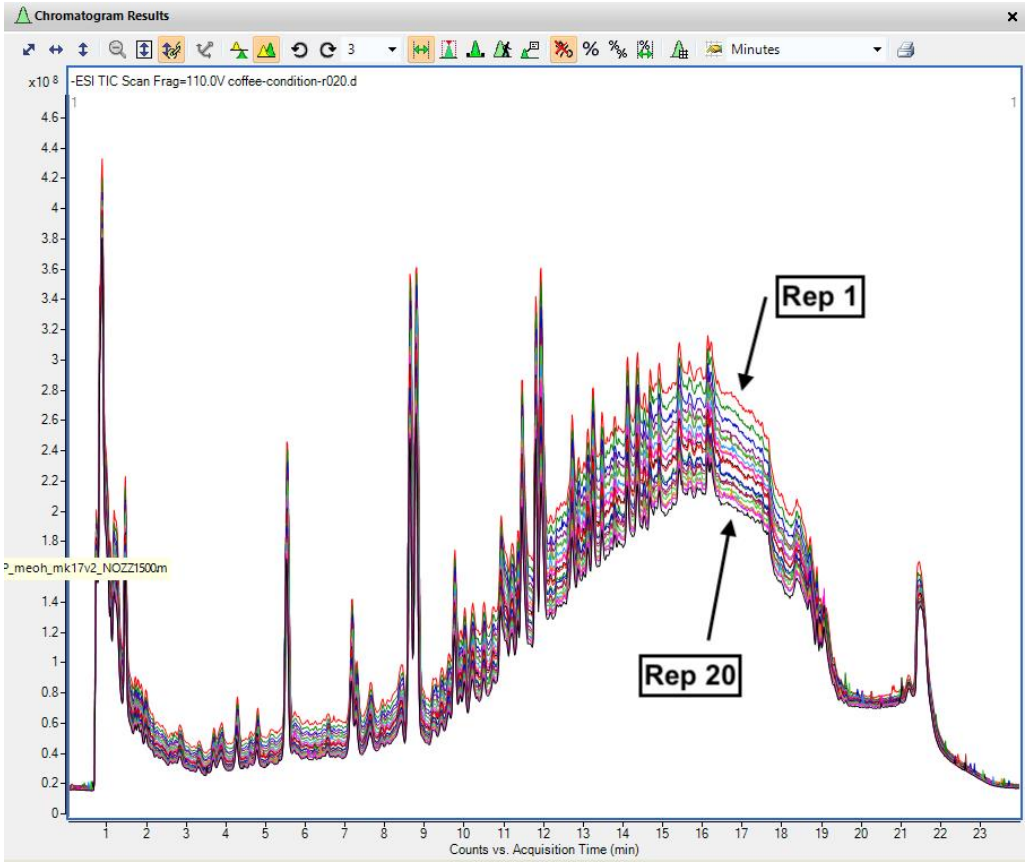



Figure 4-8 Twenty injections of QC in Polyscreen mk5.

It is evident that the response of total ion chromatograph decreased as the number of injections increased. It was most important to focus on the response of the

mass spectrometer between 2 and 17 minutes as this was the retention time range of targets in the PCDL (Table 4.10).

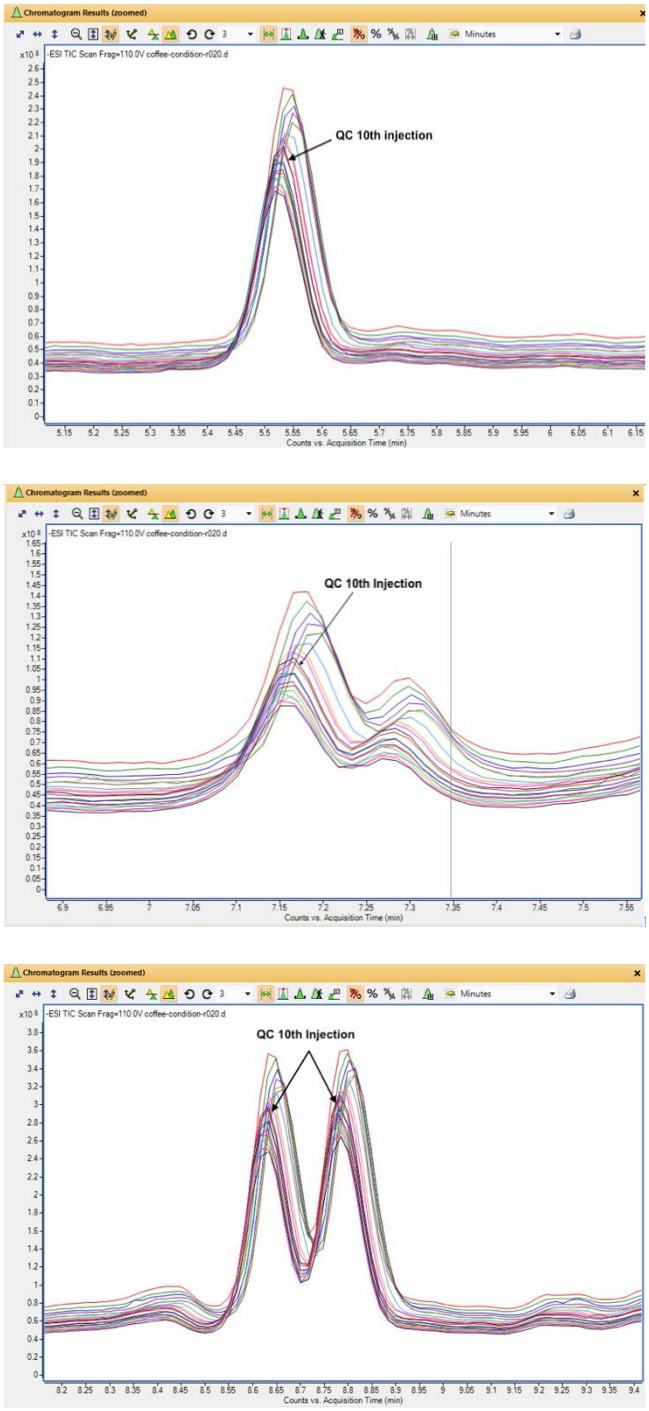



Figure 4-9 Magnified peaks of total ion chromatographs between 5 and 9 minutes.

Magnified peaks from total ion chromatographs are presented in Figure 4-9. It was observed that for the first 8 first injections of QC the peaks were – as expected – larger and shifted to the right. The remaining peaks were more

centralised grouped together. For this reason, the number of QC conditioning injections prior to every analysis was set to 10.

**Internal standard**

For targeted chemical analysis purposes, it was essential to choose a chemical reference standard as internal standard to normalise the abundance of chemical targets of interest with the aim to eliminate any variances caused by the mass spectrometer. A chemical compound can be used as chemical reference standard:

a. if its structure is similar to the chemical targets of interest
b. if it is not native in the sample to be analysed

A compound that fulfilled both requirements was Sinapic acid. Sinapic acid is classified as a phenolic compound (Figure 4-10). In addition, whilst several compounds detected in control coffee shared the same empirical formula as Sinapic acid, none had the same retention time as a reference standard for this material (Figure 4-11).

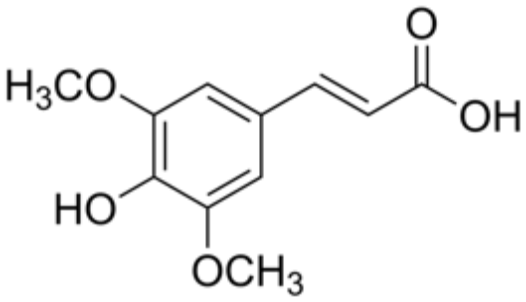



Figure 4-10 Chemical structure of Sinapic acid

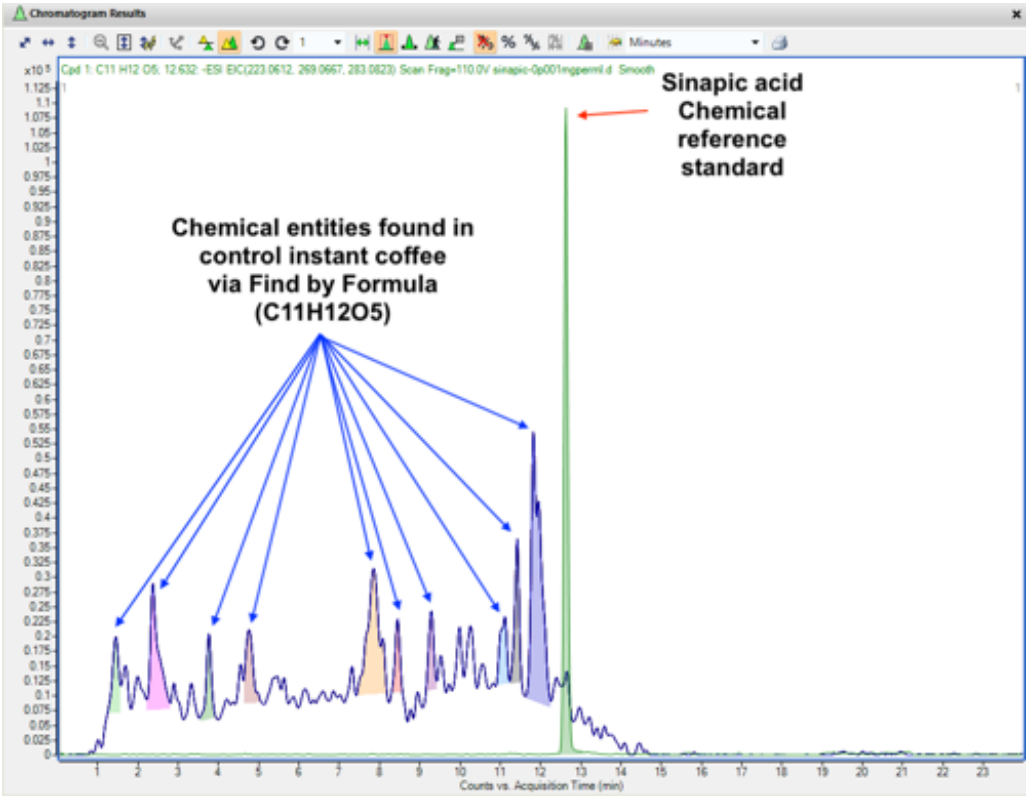



Figure 4-11 Chromatograph of a control instant coffee along with a chromatograph of Sinapic acid, used as a chemical reference standard. The red arrow indicates the peak of the Sinapic acid. The blue arrows indicate the chemical entities that were found by searching the empirical formula C11H12O5 with the "Find by Formula" tool

### 4.3.2 Results of targeted chemical analysis

The normalized abundance values (i.e. abundance of x compound divided by abundance of Sinapic acid) of 38 phenolic compounds throughout the 22 instant coffees samples are presented in Figure 4-12. It is evident that chemical compounds such as mono and di-caffeoylquinic acids, feruloylquinic acids and their lactones along with quinic acid had the highest abundance compared to the rest of the phenolic compounds.

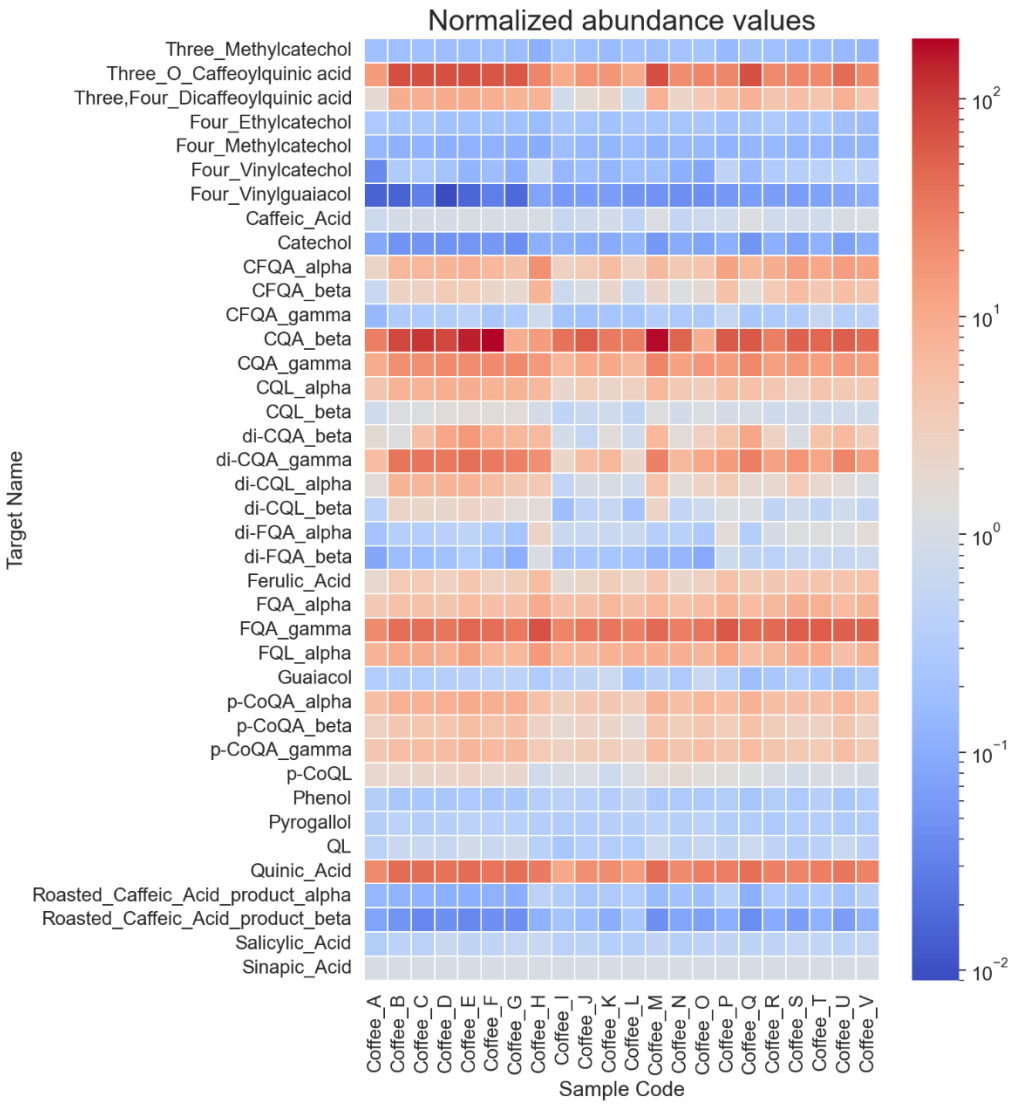



Figure 4-12 Heatmap of normalised abundance values of 38 phenolic compounds throughout the 22 instant coffee samples of Table 4.1(number of replicates = 5). Reference coffee: Control – Coffee_V.

The phenolic profile of instant coffees has already been reported in the literature. To the best of the authors' knowledge only two published papers have reported the levels of 3-Caffeoylquinic acid and 3,4-di-Caffeoylquinic acid in commercial instant coffees (Mills *et al.*, 2013; Rodrigues and Bragagnolo, 2013) including for Nescafe Gold Blend and Nescafe Gold Blend decaf, which are Coffee J and Coffee K respectively in the present chapter (Mills *et al.*, 2013). Based on the data acquired by the targeted chemical analysis, it was feasible to compare the ratio of 3-Caffeoylquinic acid to 3,4-di-Caffeoylquinic acid.

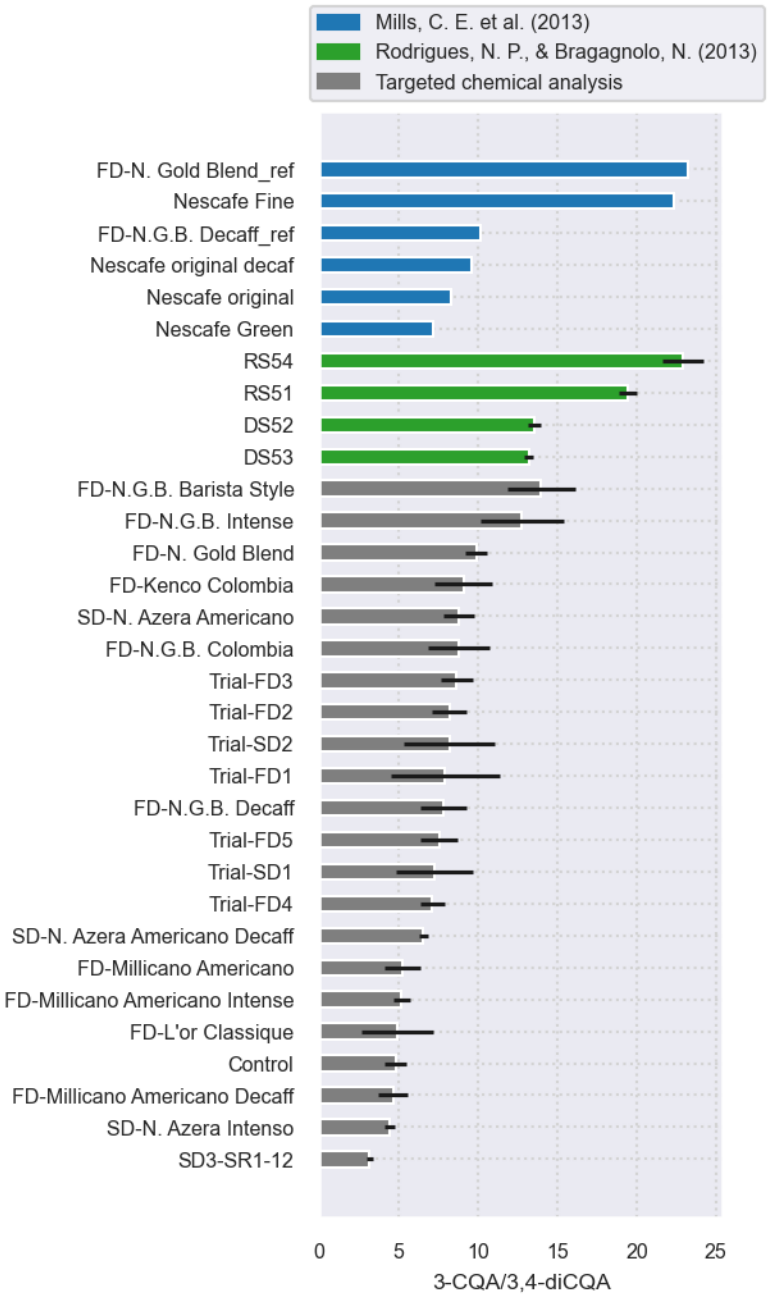



Figure 4-13 Ratio of 3-Caffeoylquinic acid per 3,4-di-Caffeoylquinic acid for commercial instant coffees. Data retrieved by Mills et al., 2013 and Rodrigues and Bragagnolo, 2013 (blue and green bars respectively).

The range of 3-CQA/3,4-diCQA ratio for samples analysed in this chapter was 3.16-13.9, while the range reported by Mills et al., 2013 and Rodrigues and Bragagnolo, 2013 was 7.16-23.25 and 13.20-22.91 respectively. It is important to highlight that differences in variety, origin, and instant coffee process

parameters can affect this analysis. Direct comparison was achieved for Nescafe Gold Blend and Nescafe Gold Blend decaf coffee samples (Figure 4-14).

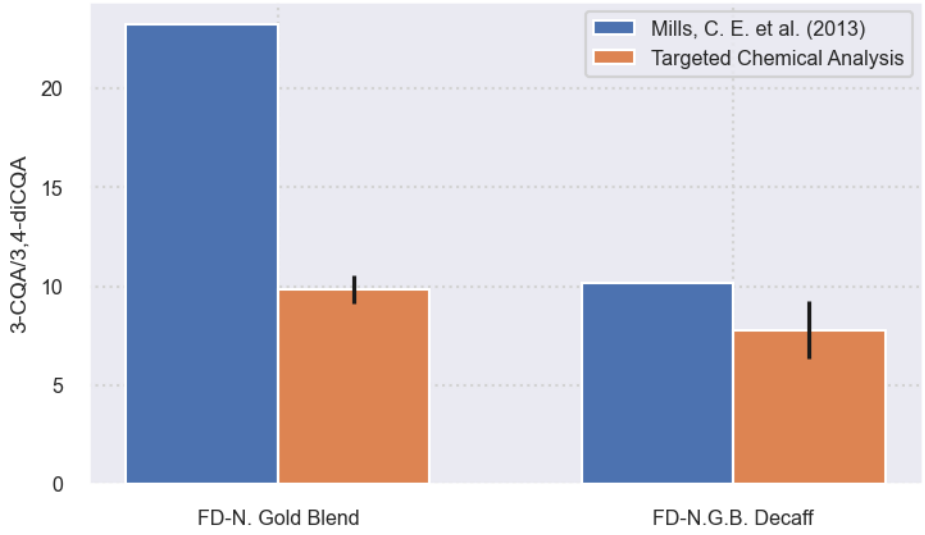



Figure 4-14 Ratio of 3-Caffeoylquinic acid per 3,4-di-Caffeoylquinic acid for Nescafe gold beld and Nescafe gold blend Decaff. Direct comparison of data from targeted chemical analysis and data from Mills et al., 2013.

The ratio of 3-CQA/3,4-diCQA for Nescafe Gold blend Decaff was similar between the results from targeted chemical analysis and (Mills *et al.*, 2013). However, the ratio reported by the cited paper for Nescafe Gold Blend was double the ratio identified from this chapter. It is important to highlight that there were differences in the sample preparation of coffee samples. In the cited paper, coffee samples were treated with Carrez I (1M crystallised zinc acetate, acidified with glacial acetic acid) and Carrez II solutions (250 mM potassium ferrocyanide trihydrate) along with 0.8 mL 100% ethanol, aiming to clarify the solutions by precipitating colloidal material (Clifford *et al.*, 2003; Mills *et al.*, 2013). It can be hypothesised that clarification step, which altered the matrix of samples, may enhanced the ionisation degree of 3-Caffeoylquinic acid resulted in higher signal from mass spectrometer.

At this point of analysis, it was important to understand which chemical compounds of the targeted chemical analysis were associated with foam quality

performance. For this reason, Pearson correlation analysis was performed between the normalised abundance (i.e. relative to Sinapic acid abundance) of each chemical compound against each Foam quality parameter (i.e. Foam Ability, Drainage Rate, and Disproportionation/Coalescence rate). It was found that 26 chemical compounds were significantly correlated ($p<0.05$) with at least one of the foam quality parameters (i.e. Foam Ability, Drainage Rate, and Disproportionation/Coalescence rate) (Figure 4-15)

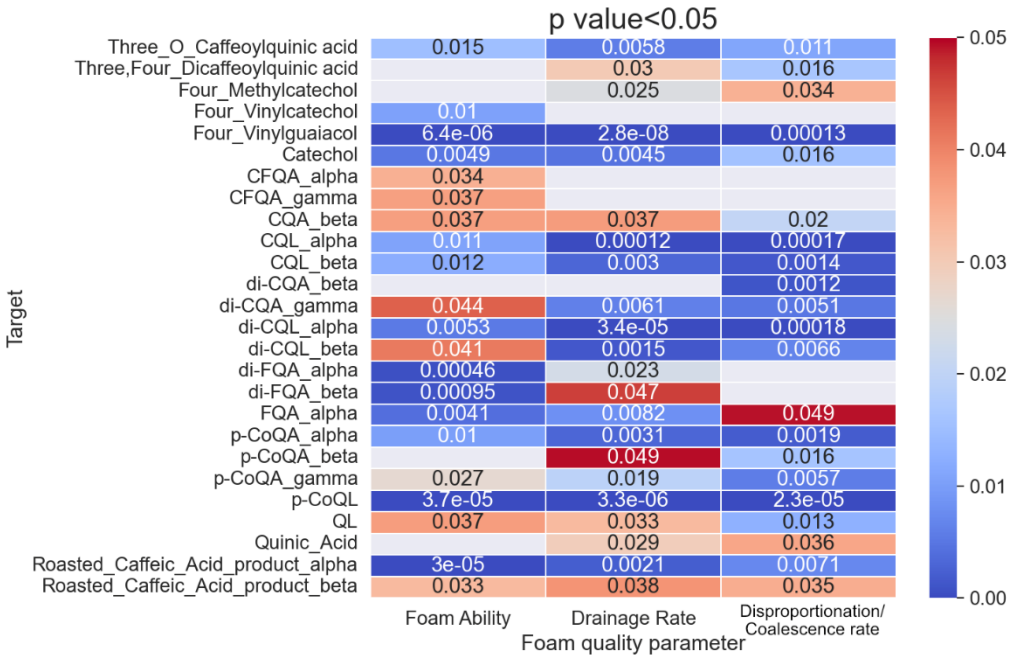



Figure 4-15 Heatmap of p values for compounds which are significantly correlated ($p<0.05$) with at least one of the foam quality parameters. Grey tiles without annotated value mean that the given Foam quality parameter is not correlated significantly ($p>0.05$) with the given chemical compound.

The correlation analysis showed that both the MS2 annotated Roasted Caffeic acid products (i.e. 4-vinylcatechol oligomers) were significantly correlated with all the foam quality parameters. Since these compounds were reported that influence foam quality, a significant correlation with at least a foam quality parameter was expected. The calculated $R^2$ from Pearson correlation analysis is presented in Figure 4-16.

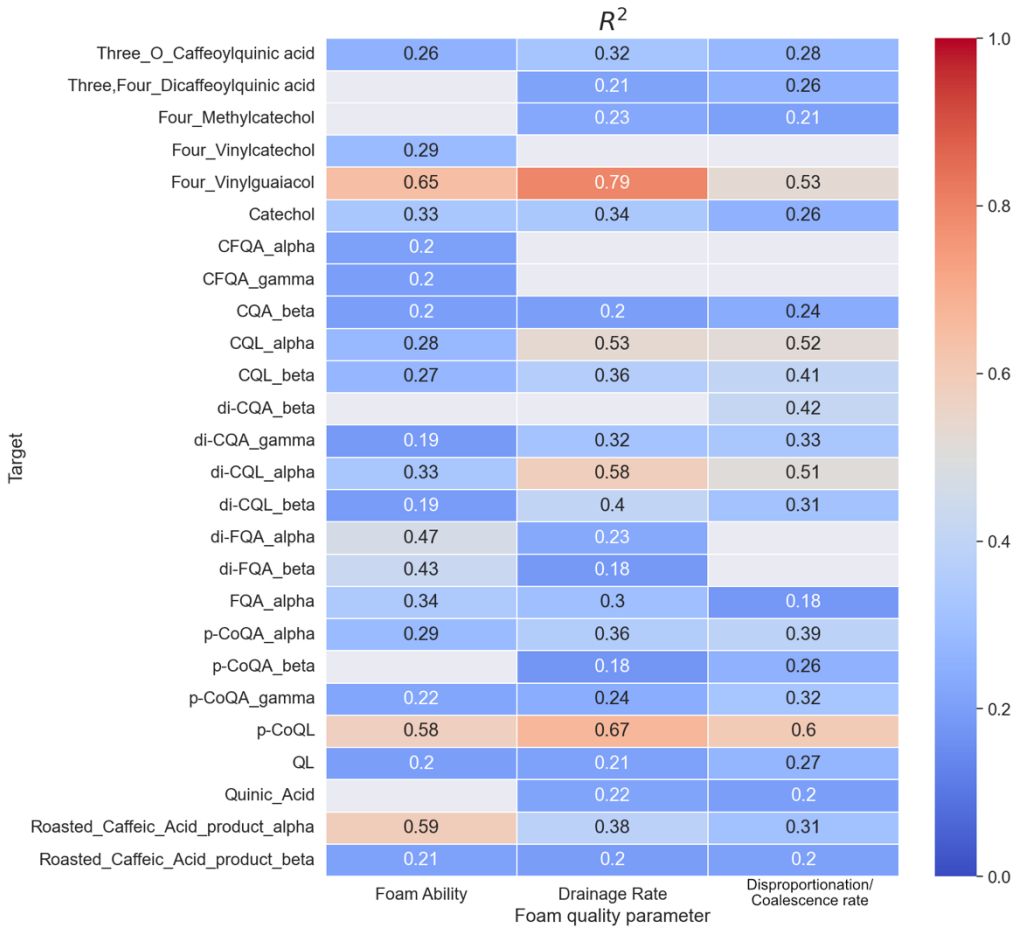



Figure 4-16 $R^2$ value of chemical compounds which are significantly correlated ($p<0.05$) with at least one of the foam quality parameters. Grey tiles without annotated value mean that the given chemical compound is not correlated significantly ($p>0.05$) with the given Foam quality parameter.

It can be concluded from Figure 4-16 that there was a mild correlation between the normalised abundance of each chemical compound with the foam quality parameters. The $R^2$ values for each of the foam quality parameters were plotted in a histogram (Figure 4-17) to observe and evaluate the results of correlation analysis. The range of $R^2$ calculated from correlation analysis was 0.0022-0.790. With the aim of focusing on the chemical compounds that are mostly correlated with the foam quality performance, the results were refined by looking at the top 15% of the 0.0022-0.790 range. Therefore, a threshold of $R^2$=0.67 was placed. The square root of $R^2$ is the r of Pearson correlation. The $|r| = \sqrt[2]{0.67} = 0.818$

and this means that a chemical compound with an absolute value of r≥ 0.818 could indicate a moderate correlation.

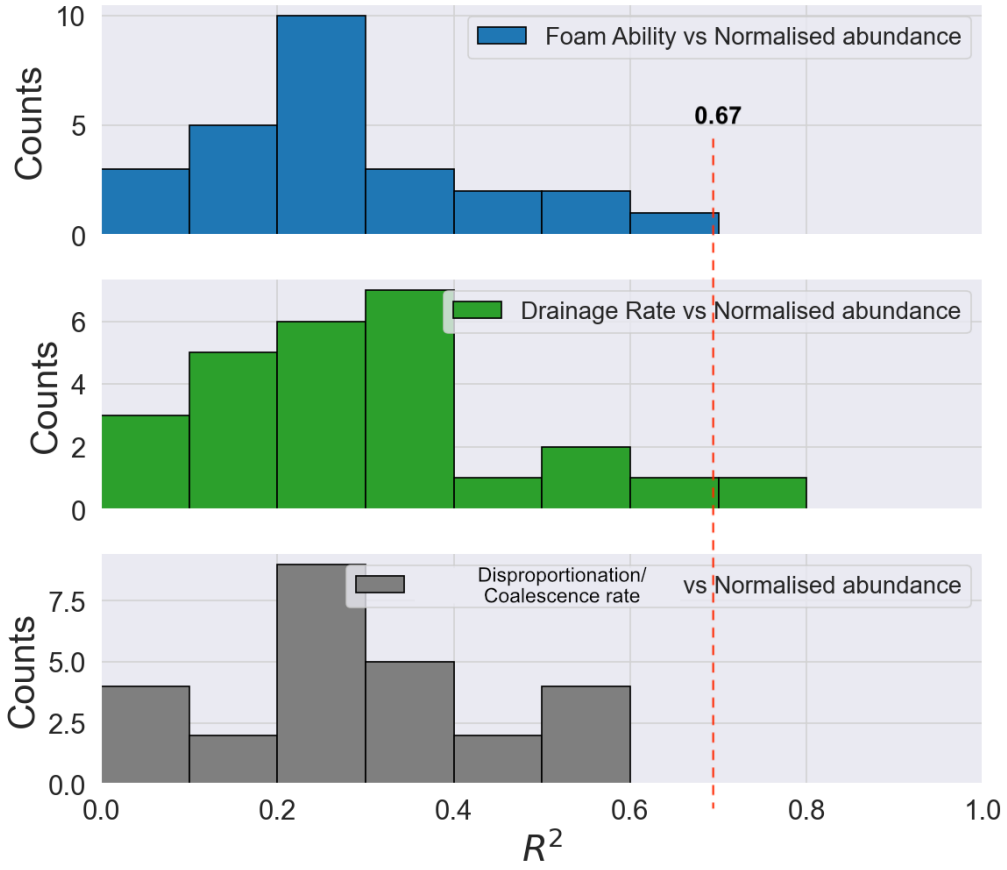



Figure 4-17 Histogram of $R^2$ of Normalised abundance vs foam quality parameters.

Only 2 out of 26 chemical compounds had $R^2$>=0.67. These compounds were 4-vinylguaiacol (Figure 4-18) and p-Coumaroylquinic acid lactone (Figure 4-19). Both compounds were correlated with the drainage rate. 4-vinylguaicol correlated with the drainage rate negatively, thus acting as a foam promoter. p-Coumaroyl-quinolactone correlated positively with the drainage rate, thus acting as an antifoam compound.

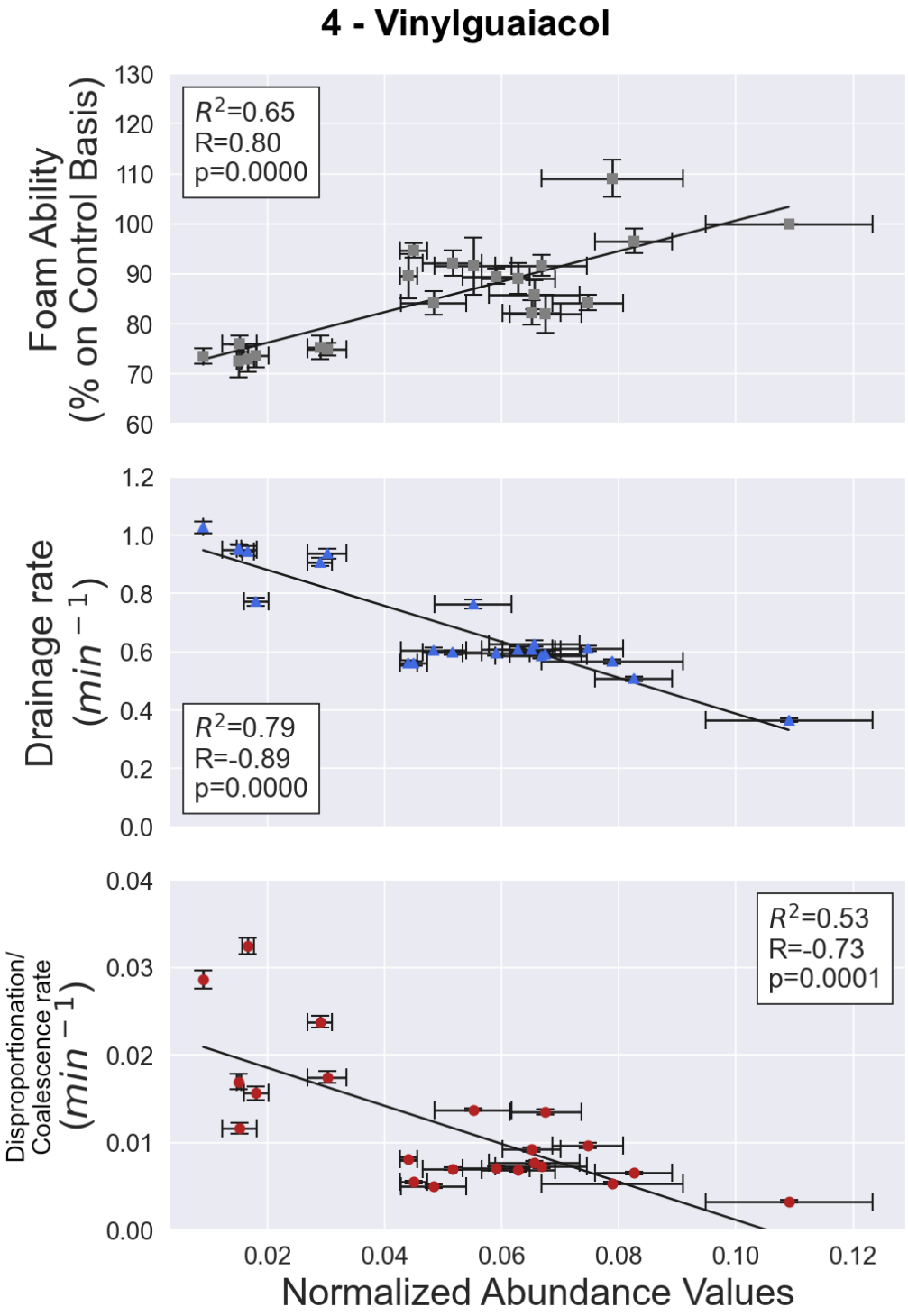



Figure 4-18 Pearson correlation analysis between the normalised abundance of 4-vinylguaiacol and each of the foam quality parameters.

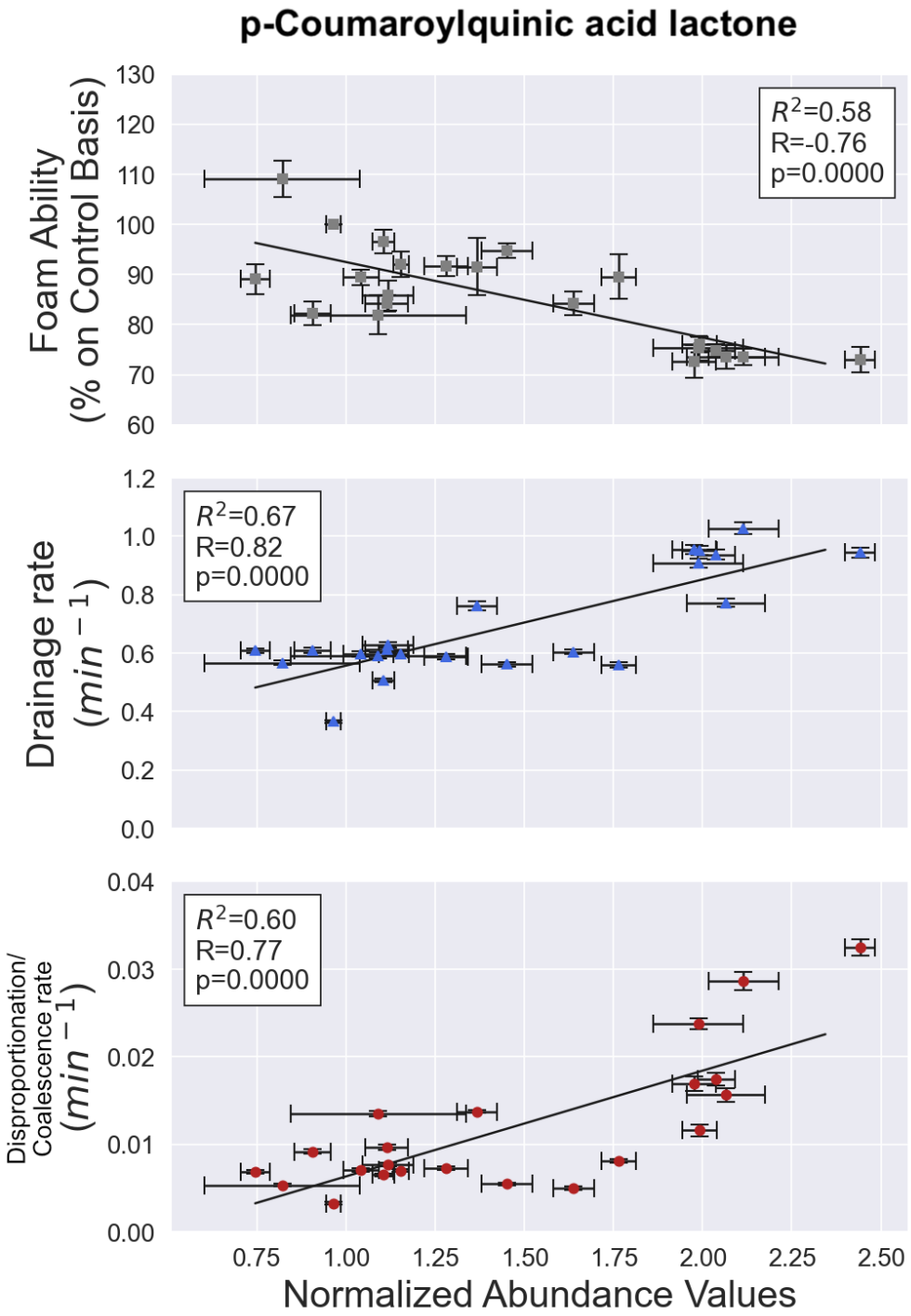



Figure 4-19 Pearson correlation analysis between the normalised abundance of p-Coumaroylquinic acid lactone and each of the foam quality parameters.

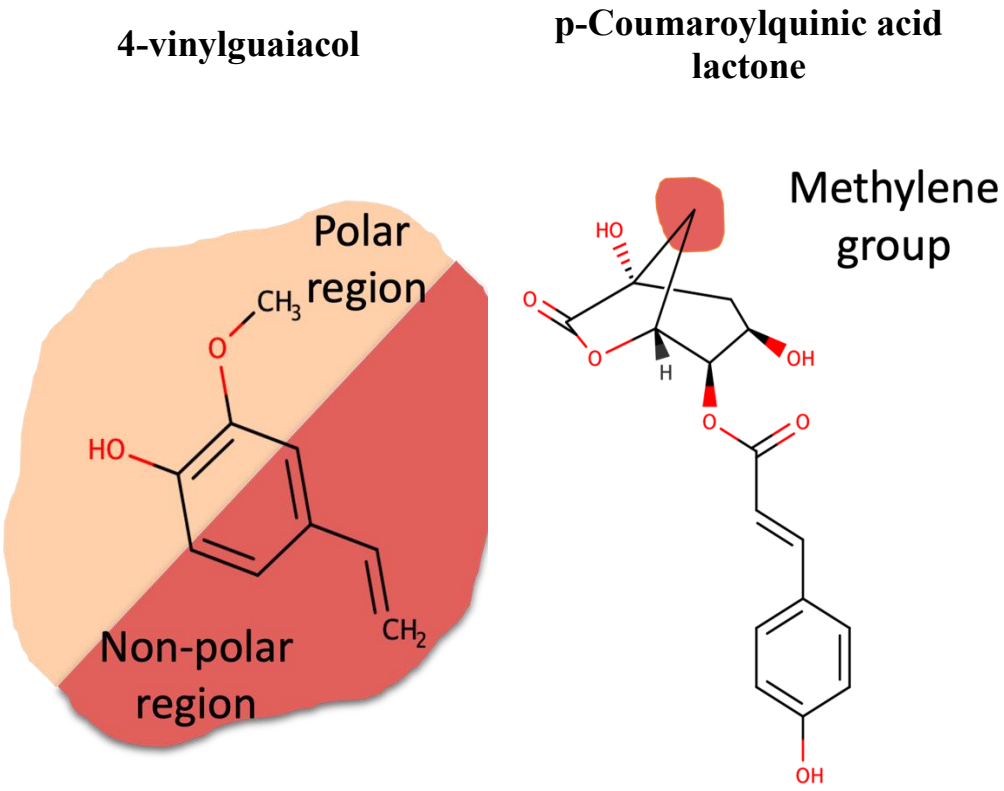



Figure 4-20 Chemical structures of 4-vinylguaiacol and p-Coumaroylquinic acid lactone

The potential foam-promoting nature of 4-vinylguaiacol may be attributed to its apparent amphiphilic nature, comprising a methyl group non-polar region, and an opposing polar region due to the hydroxyl group (Figure 4-20). The concentration of 4-vinylguaicol in green beans ranges from 0.23-1.1 μm/g of dry green bean (Scheidig, Czerny and Schieberle, 2007). To the best of the authors' knowledge, the change in concentration of 4-vinylguaiacol from green to roasted bean has not been reported. However, the influence of different roasting degrees (i.e. light, medium and dark roast) on concentration of 4-vinylguaicol been reported (Yu *et al.*, 2021). The abundance of 4-vinylguaicol at medium roasted coffee increased to 110-123% comparing to the light roasted, before it decreased to 50% at longer roasting times.

In the case of p-Coumaroyl-quinolactone, the lactonization of quinic acid (Figure 4-21) creates a methylene group (Figure 4-20) which may significantly increase the non-polar surface area of the compound.

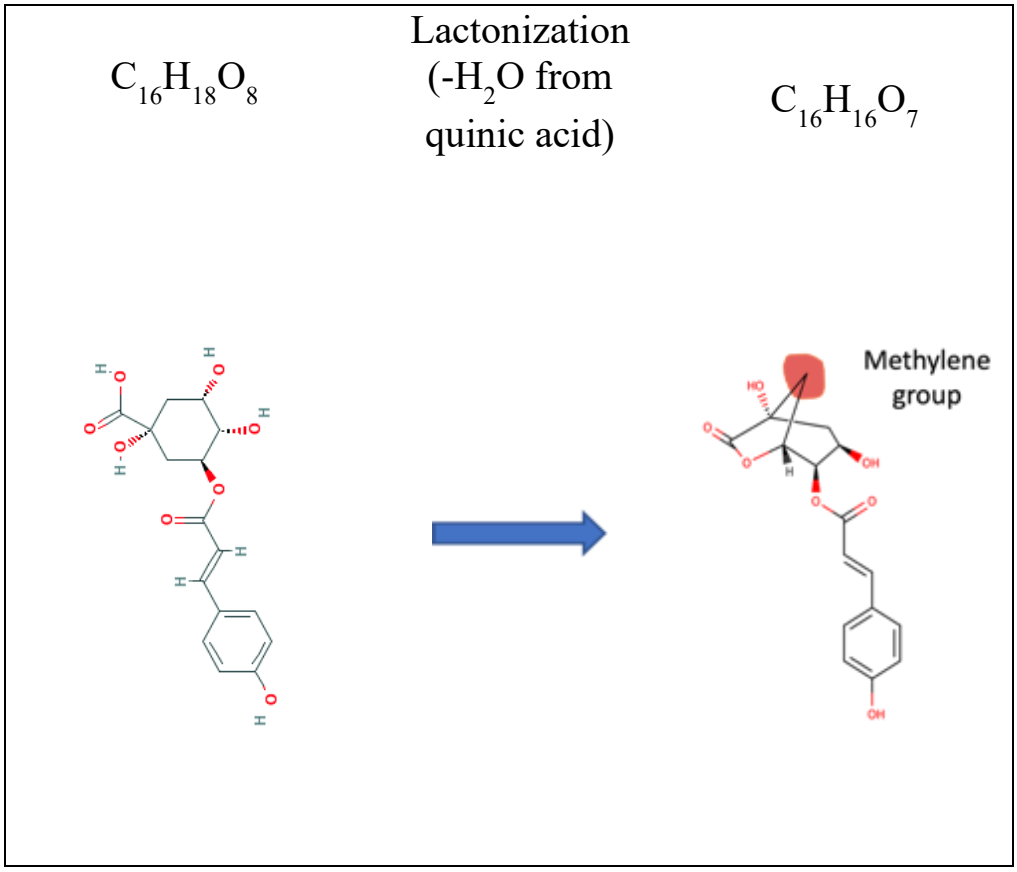



Figure 4-21 Lactonization of p-Coumaroylquinic acid

3-p- and 4-p-Coumaroylquinic acid lactones, which have been reported only in roasted coffee beans, are lactonization products of p-Coumaroylquinic acids. Depending on coffee variety (i.e. Arabica or Robusta), the concentration of p-Coumaroylquinic acid in green beans ranges from 52.4-68.9 mg/100 g dry green coffee (Perrone *et al.*, 2008). 3- and 4-p-Coumaroylquinic acids are formed at early stages of roasting degree with concentration 1.6-2.4 mg/100 g of coffee dry weight. At medium roasted coffee, the concentration of p-Coumaroylquinic acid lactones peaks at 4.5-7.5 mg/100 g dry coffee weight. Finally, in darker roasted coffees the concentration decreases and reaches the levels of the light roasted coffee (Farah *et al.*, 2005; Perrone *et al.*, 2008).

## 4.4 Conclusions

In this chapter, it was hypothesised that phenolic compounds in coffee influence foam quality. Therefore, a chromatographic method was developed in order to identify and semi-quantify phenolic compounds that have already been reported in coffee. It is acknowledged that the lack of fine quantification of MSI Level 1 identified compounds was a limitation. However, the normalised abundances of chemical compounds of interest were sufficient to perform the correlation analysis and address the primary aim of this chapter. The correlation analysis between the normalised abundance of phenolic compounds vs each foam quality parameter, identified two phenolic compounds - 4-vinylguaiacol and p-Coumaroylquinic acid lactone – that were moderately correlated with drainage rate. These compounds were annotated at MSI Level 2, and it was important to validate their ID via acquiring and analysing the equivalent chemical reference standards in the same chromatography method, which we do in section 5.3.3. In the pursuit of finding stronger association between the abundance of chemical compounds and foam quality performance, it was important to follow an untargeted metabolomics approach.

# Chapter 5: Untargeted chemical analysis of coffee samples of differing foam quality

## 5.1 Introduction

Following the targeted chemical analysis, an untargeted chemical analysis workflow was applied to the same 21 instant coffee samples, previously identified as significantly different from control in terms of foam ability. In the same manner as targeted chemical analysis, correlation analysis was performed to identify which chemical compounds were associated with foam quality performance. Compounds of interest from the correlation analysis were putatively annotated to MSI level 2 (i.e. similarity of MS2 spectra of a given compound with public metabolomics databases) (Sumner *et al.*, 2007). Finally, a MSI level 1 validation of identities (i.e. through chemical reference standards) was performed for compounds that were most strongly correlated with foam quality performance, using reference standards.

## 5.2 Materials and Methods

### 5.2.1 Chemicals

3-Indoleacrylic acid, Cyclo(-Leu-Phe),Cyclo(-Phe-Pro), D,L,-Leucyl-D,L-Leucine, Sinapic acid, Sorbic acid, trans-3-Indoleacrylic acid and Dimethyl sulfoxide were acquired from Merck life sciences Ltd (Gillingham, UK). Cyclo(L-Phe-L-Val) and Cyclo(L-Pro-L-Val) were acquired from Cambridge Biosciences Ltd (Cambridge, UK). 4-(Methylamino)butan-1-ol was acquired from ABCR Ltd (Manchester, UK). Cyclo(-Phe-Phe) was acquired from Generon LtD (Slough, UK). Cyclo(L-Phe-D-Pro) was acquired from Insight Biotechnology Ltd (Wembley, UK). Mannotetraose was acquired from Megazyme (Wicklow, Ireland). Myristic acid, n-Pentadecanoic acid, trans-Cinnamic Acid and Formic acid were acquired from Fisher Scientific (Loughborough, UK). Purine and Hexakis(1H, 1H, 3H-

tetrafluoropropoxy)phosphazine were acquired from Agilent Technologies (Cheadle, UK). Acetonitrile HPLC grade, ethanol absolute >99.7% and Methanol HPLC grade were acquired from VWR International Ltd (Lutterworth, UK). All reference standards were of high purity (>95%).

### 5.2.2 Instant coffees

The instant coffee samples that were analysed in this chapter are same samples that were analysed in Chapter 4: (i.e. Table 4.1).

### 5.2.3 Instant coffee sample preparation for chemical analysis

The sample preparation methodology that was used is described in 4.2.3.

### 5.2.4 Chemical analysis with high-resolution liquid chromatography-mass spectrometry method.

Mobile solvents for chemical analysis and Reference mass solution for chemical analysis subsections of section 4.2.5 were employed in this chapter.

Chemical analysis method

The chemical analysis method, that was employed in this chapter, was based on the one that is described in 4.2.5 with some adjustments. The key differences were as follows. The experiments were performed both in negative and positive polarity mode. The ionisation parameters for negative and positive polarity mode were the same for both polarity modes and are described in 4.2.5. The enabled ionisation adducts for compounds extracted in positive polarity mode are presented in Table 5.1.

Table 5.1 Positive polarity mode adducts. M: the neutral mass of the chemical compound of interest

| Positive polarity adducts | Comment |
|---|---|
| [M+H] | Proton added to neutral chemical compound |
| [M+$NH_4$] | Ammonium adduct |
| [M+Na] | Sodium adduct |
| [M+K] | Potassium adduct |

5.2.5 Data analysis

**Recursive extraction of features with Mass Profinder and Mass Profinder Professional**

In the untargeted chemical analysis workflow, the aim was to discover unknown chemical entities across the sample set of instant coffees that were pertinent to coffee foam quality. The first step was to perform a recursive extraction of features with MassHunter Profinder Software (Agilent Technologies, Santa Clara, CA, USA) from all coffee samples along with 5 QC samples from the beginning, end, middle and first and last 5ths of the worklist. The central QC of the worklist was used as a reference for time alignment of the chromatographs of the run. After the alignment, the recursive feature extraction commences with the parameters in Table 5.2.

Table 5.2 Recursive extraction feature parameters

| | |
|---|---|
| General parameters | |
| Restrict retention time to | 0-22 min |
| Use peaks with height | >=4000 counts |
| Compounds ion count threshold | Two or more ions |
| Alignments parameters | |
| RT tolerance | ±(0% + 0.3 min) |
| Mass tolerance | ±(10 ppm + 2 mDa) |
| Score (MFE) | >= 70.00 |
| A compound must satisfy the checked MFE filter conditions in at least | 4 files in at least one sample group |
| Match tolerance | |
| Masses | ±10 ppm |
| Retention times | ± 0.3 minutes |
| Filter on Peak height with Absolute height filter | >= 1000 counts |
| Allowed ion species | Positive ions: [+H], [+Na],[+K],[+NH4] Negative ions: [-H], [+HCOO],[+CH3COO] |
| Isotope grouping model | Common organic (no halogens) |

Detailed screenshots of Recursive Feature Extraction parameters can be found in Appendix H. The results of recursive extraction of features were exported in a MassHunter Profinder Archive (.PFA) file. The .PFA file was imported to MassHunter Profinder Professional software (Agilent Technologies, Santa Clara, CA, USA) to check the quality of data by performing Principal component analysis and to export the abundance of each chemical entity along the sample set. The abundances were baselined via Pareto method to reduce the relative importance of compounds with large intensities. The final abundances of chemical entities were Log2 normalised. Detailed screenshots of Mass Profinder Professional can be found in Appendix I.

**Correlation analysis**

Correlation analysis of two independent variables were performed via python packages and is presented in section 3.2.14.

**Level 2 identification of chemical compounds via MS2 analysis**

Level 2 identification methodology was performed to annotate the ID of chemical species of interest. The methodology can be found in section 4.2.7.

## 5.3 Results and discussion

### 5.3.1 Correlation analysis

As described in Chemical analysis method subsection of 4.2.5 section, every worklist commenced with 10 runs of QC to condition the ionisation source to avoid large variance of signal across the runs. Also, QC runs were injected every five sample injections to monitor the variability across the injection of the worklist. Principal components analysis plots visualise the variance of replicates for each coffee sample (Figure 5-1). It is evident that results from negative polarity had better repeatability than positive polarity mode. The variances of some samples in positive polarity mode were mostly controlled by 2 axes rather than 3 axes. As it was expected, QC samples were in the middle of the 3D plot because these samples were comprised of equal parts of each coffee sample.

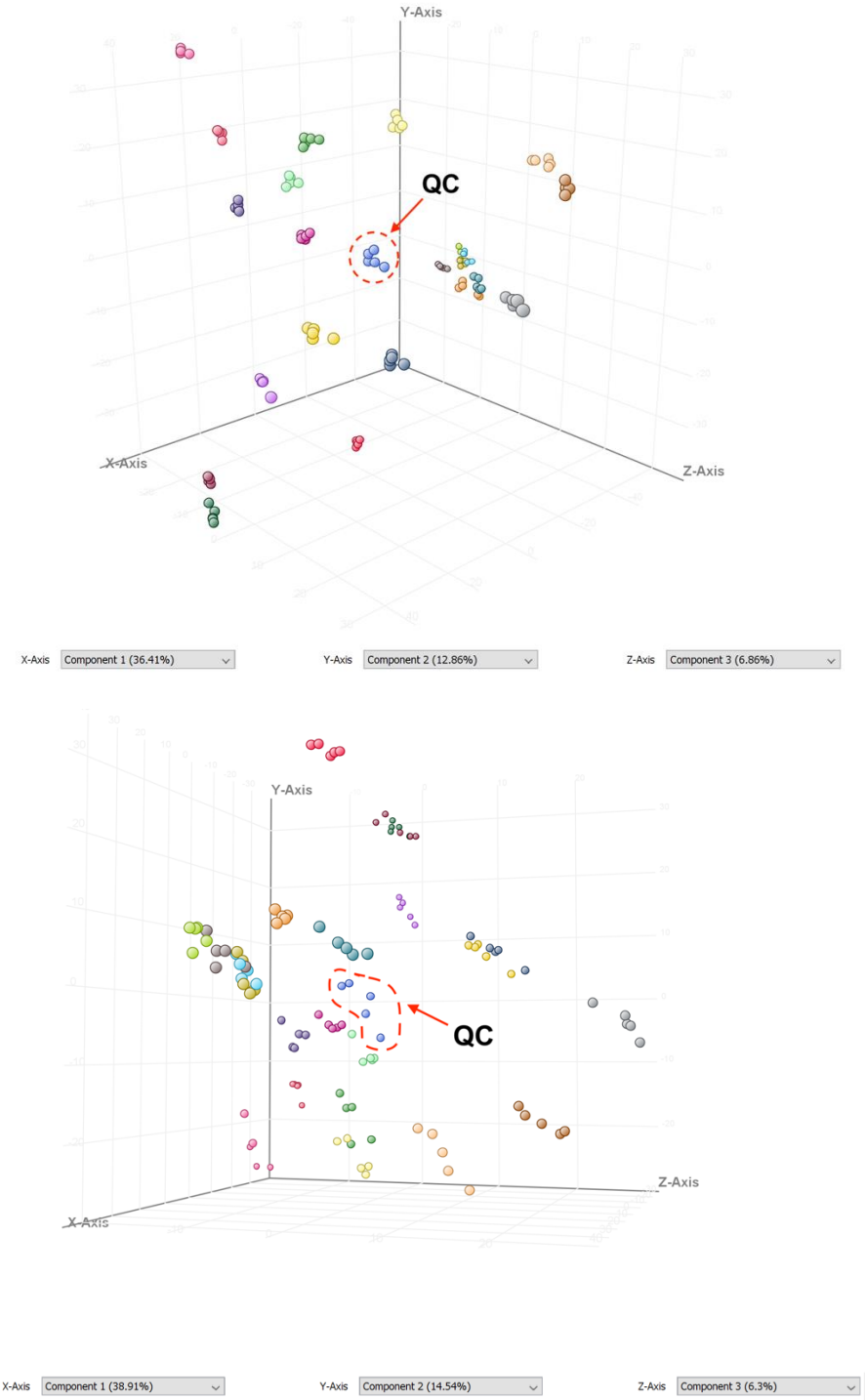



Figure 5-1 PCA plots of Total Ion Chromatographs for Negative (TOP) and Positive (BOTTOM) polarity mode.

The recursive feature extraction process extracted 1716 and 1793 chemical entities from negative and positive polarity mode respectively.

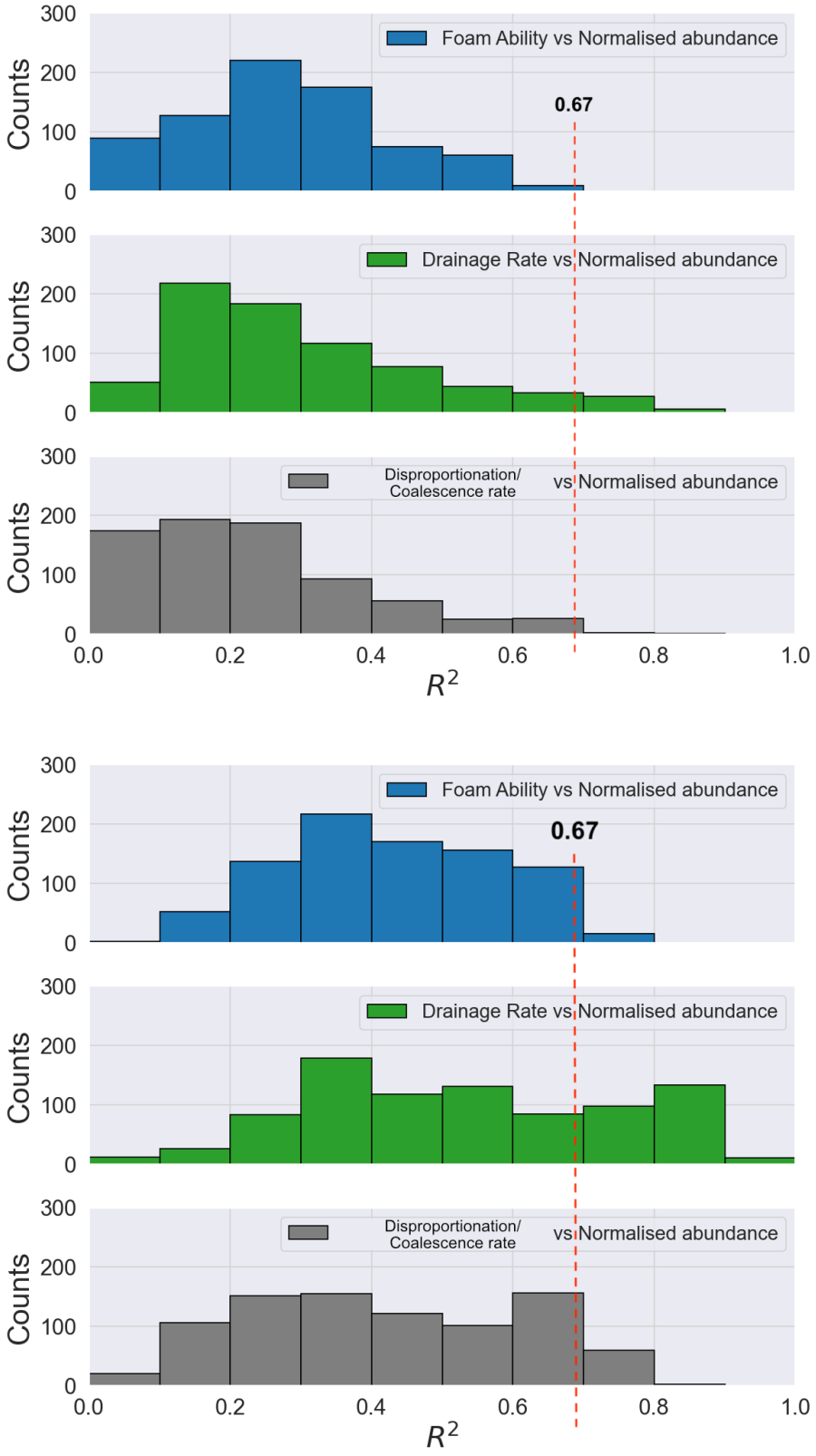



Figure 5-2 Histogram of $R^2$ of Normalised abundance vs foam quality parameters. TOP: Negative polarity mode. BOTTOM: Positive polarity mode

Pearson's correlation analysis was performed between the Log2 normalised abundance of chemical entities, identified from both polarity modes, vs each

foam quality parameter. The $R^2$ of correlation analysis from both polarity modes are presented in Figure 5-2. The same threshold of $R^2$; 0.67, as in Chapter 4: was applied here. It was found that 44 and 278 chemical entities from negative and positive polarity mode respectively were correlated with at least one foam quality parameter at level $R^2$>=0.67 (Figure 5-3, Figure 5-4).

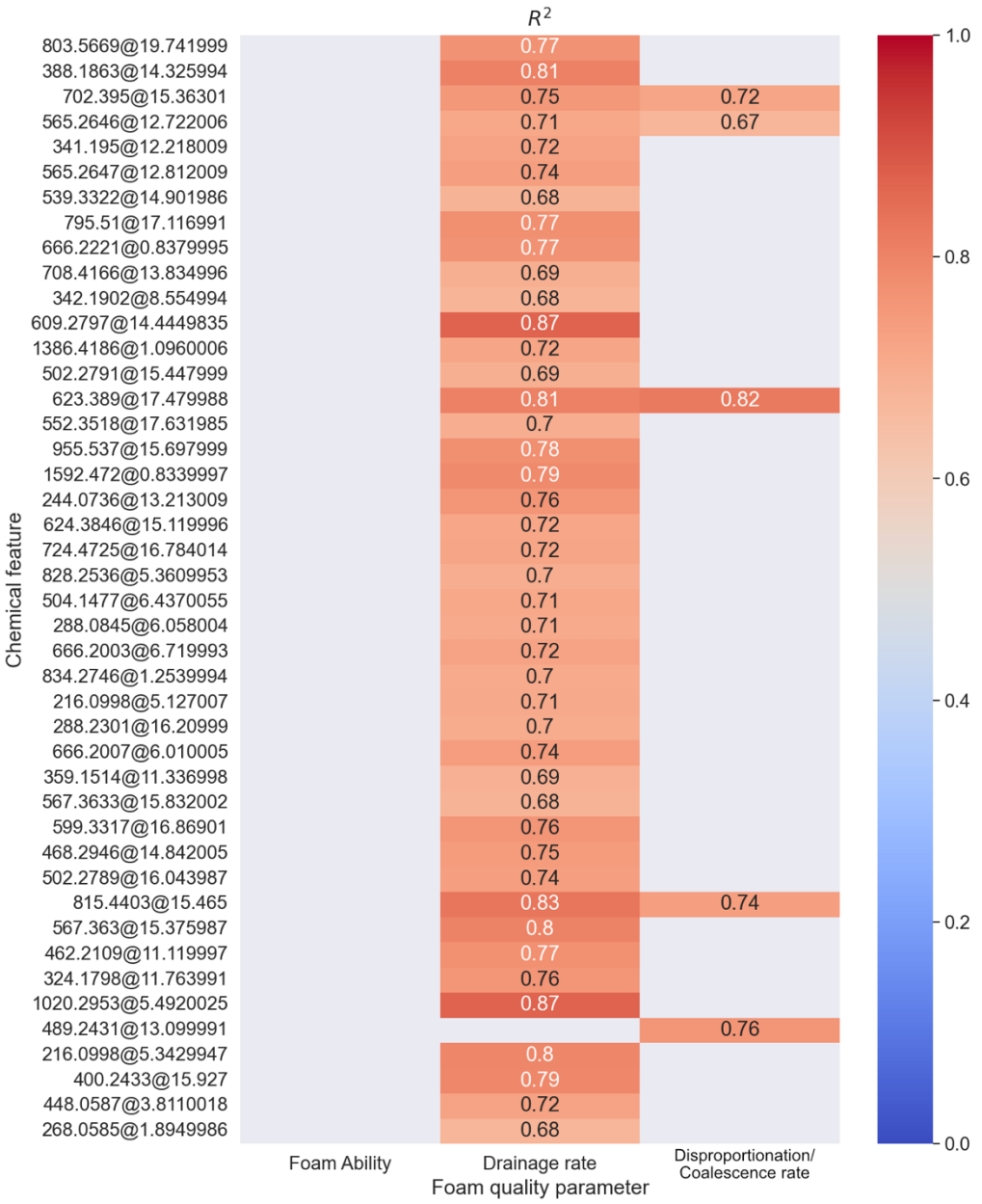



Figure 5-3 $R^2$ as calculated by Pearson correlation analysis for the 44 chemical entities found by the untargeted chemical analysis in negative polarity mode. Grey tiles indicate that the specific chemical entity acquired $R^2$<0.67 with the given foam quality parameter.

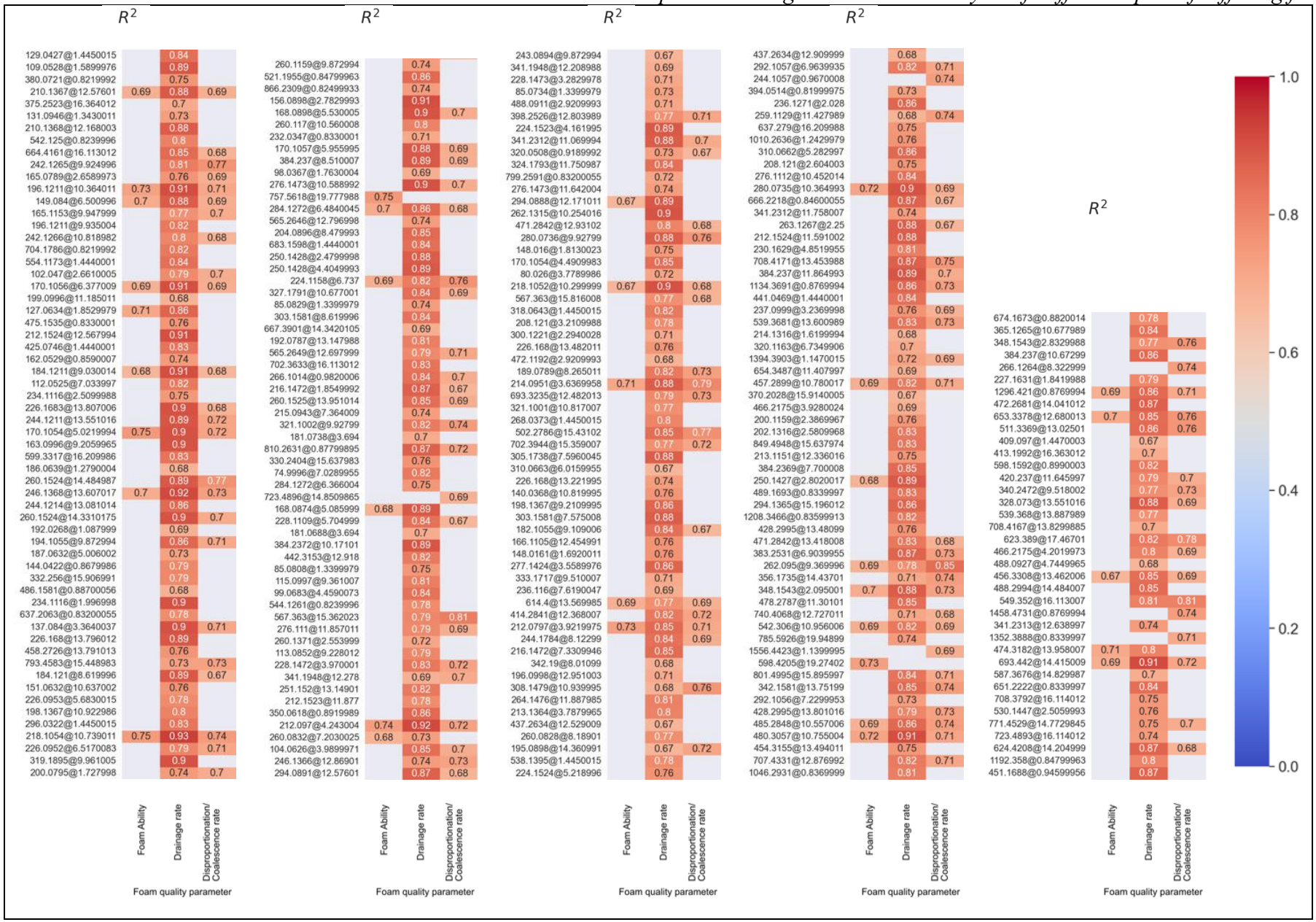



Figure 5-4 $R^2$ as calculated by Pearson correlation analysis for the 278 chemical entities found by the untargeted chemical analysis in positive polarity mode. Grey tiles indicate that the specific chemical entity had a correlation parameter $R^2$<0.67 with the given foam quality parameter.

### 5.3.2 MSI Level 2 identification of chemical compounds via MS2 analysis

To pursue putative identities of the above compounds, their MS2 spectra were acquired, and each ID was annotated using the SIRIUS software. The inclusion list for MS2 analysis of compounds identified from negative polarity mode generated 51 chemical spectra. As this originates from an initial list of 44 entities, it suggests that several chemical entities were ionised in multiple forms – i.e. not only by removing a proton from the chemical structure but also, they were ionised by having an ionised adduct attached to the neutral chemical structure. For example, the chemical entity 666.2221@0.8379995 was typically ionised in two ways:

1. by removing a proton (i.e. $H^+$) with m/z 665.2151
2. because an ionized adduct of formate ($HCOO^-$) (m/z 44.9978) was attached to the neutral mass of 666.2221 and resulted in an ion with an overall m/z 711.2199.

In the case of positive polarity mode, the inclusion list for MS2 generated 407 spectra from the original 228 chemical entities. Another example from positive mode is the chemical entity 341.1948@12.278 that was typically ionised in two ways:

1. by adding a proton (i.e. $H^+$) and the m/z was 342.2022
2. because an ionized adduct of Sodium (+Na) (m/z 22.9894) was attached to the neutral mass of 341.1948 and resulted in an ion with an overall m/z 364.1842.

The results from the MS2 annotation from both polarity modes are presented in Table 5.3. Detailed tables with the MS2 annotations can be found in the Appendix J.

Table 5.3 Summary results from MS2 annotation workflow

| Result | Negative polarity mode | Positive polarity mode |
|---|---|---|
| Annotated with high certainty | 12 | 197 |
| Annotated with low certainty | 11 | 90 |
| MS2 spectra not found to the online chemical species databases | 28 | 120 |
| Total | 51 | 407 |

**Negative polarity mode-Chemical entities annotated with high certainty.**

The chemical entities which were annotated with high certainty are presented in Table 5.4. These entities could be classified into 4 different families of compounds. The first family is oligosaccharides. All compounds consist of oligomers of mannose or glucopyranose. Oligomers and polymers which contain mannose and glucose have been reported in coffee (Flament, 2002; Bee *et al.*, 2005; Poisson *et al.*, 2017). The second family is oligosaccharides with attached phenolic groups. The monomers that exist in these chemical species have already been reported in coffee (Flament, 2002; Bee *et al.*, 2005; Poisson *et al.*, 2017). However, these specific compounds have not been identified in coffee. It has been reported that dietary fibres with bound antioxidant compounds are present in coffee (Vázquez-Sánchez *et al.*, 2018). It is important to highlight that the roasting process degrades the larger polymers in coffee and creates smaller fragments (Redgwell, Trovato, *et al.*, 2002; Redgwell and Fischer, 2006). Therefore, these oligomers with attached phenolic groups might be parts of larger dietary fibres and might be products of the roasting process. The third family is fatty acid and amphiphilic compounds. These chemical entities have not been reported in coffee apart from myristic acid (Koshima *et al.*, 2020). The fourth family is oligopeptides. These specific oligopeptides have not been

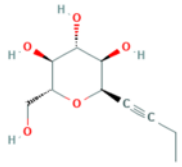
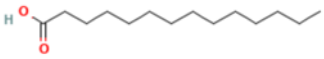
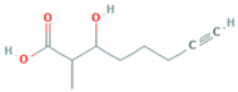
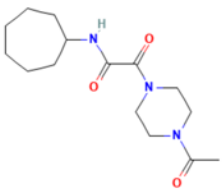
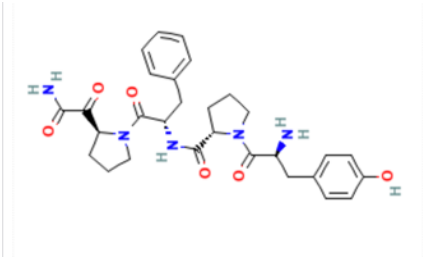
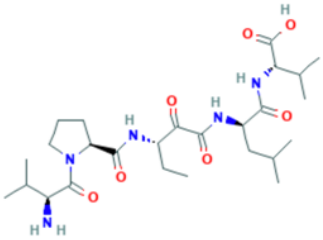
reported in coffee. However, the amino acids that comprise these chemical entities are present in coffee (Pokorný *et al.*, 1974, 1975; Tressl, Holzer and Kamperschoer, 1982; Macrae, 1985; Flament, 2001; Viani, Rinantonio; Petracco, 2012).

Table 5.4 Chemical entities annotated with high certainty in negative mode polarity

| Name | Empirical Formula | Family of compound |
|---|---|---|
| Mannotetraose | C24H42O21 | Oligosaccharides |
| 2-O-(2,3,4-Tri-O-acetyl-6-deoxy-alpha-L-mannopyranosyl)-D-glucose tetraacetate | C26H36O17 | |
| 6-Deoxy-4-O-alpha-D-glucopyranosyl-beta-D-glucopyranose heptaacetate | C26H36O17 | |
| 2-O-beta-D-Glucopyranosyl-6-O-(3,4-dihydroxy-trans-cinnamoyl)-alpha-D-glucopyranose | C21H28O14 | Oligosaccharides + Phenolic compound |
| beta-D-Glucopyranosiduronic acid, 3-hydroxyphenyl | C12H14O8 | |
| 1-alpha-D-Glucopyranosyl -1-butyne | C10H16O5 | Fatty acids and amphiphilic compounds |
| 4-[(E)-2-(2,4-dihydroxyphenyl) ethenyl] benzene-1,3-diol | C14H12O4 | |
| Myristic acid | C14H28O2 | |
| 3-Hydroxy-2-methyl-7-octynoic acid | C9H14O3 | |
| 2-(4-acetylpiperazin-1-yl)-N-cycloheptyl-2-oxoacetamide | C15H25N3O3 | Oligopeptides |
| NH2-Tyr-Pro-Phe-Pro-CONH2 | C29H35N5O6 | |
| N-[(S)-3-[(L-Val-L-Pro-)Amino]-1,2-dioxopentyl]-D-Leu-L-Val-OH | C26H45N5O7 | |

These compounds were found to be correlated with the drainage rate and the r of correlation was negative for all compounds. This indicates that these compounds are acting as foam promoters as their presence in a coffee system could indicate a low drainage rate. In principle, it is expected that foam-promoting compounds are amphiphilic compounds. This is true for the compounds in Table 5.5. The rest of the compounds appear to be mostly hydrophilic and are expected to be completely solubilised in the continuous liquid phase.

Table 5.5 Compounds which appear amphiphilic in structure

| Name | Structure | Comment |
|---|---|---|
| 1-alpha-D-Glucopyranosyl -1-butyne |  | The butyne moiety creates a non-polar area on this compound |
| Myristic acid |  | Myristic acid has a hydrophilic head and a hydrophobic tail, like a true surface-active compound |
| 3-Hydroxy-2-methyl-7-octynoic acid |  | The short aliphatic chain with the butyne moiety creates an amphiphilic compound. |
| 2-(4-acetylpiperazin -1-yl)-N-cycloheptyl-2-oxoacetamide |  | The 7-carbon ring could be the non-polar area while on the other end of the compound the hydroxyl group creates the polar area |
| NH2-Tyr-Pro-Phe-Pro-CONH2 |  | Both ends of the chemical compound are polar. The benzene ring in the middle of the compound creates a non-polar area. |
| N-[(S)-3-[(L-Val-L-Pro-)Amino]-1,2-dioxopentyl]-D-Leu-L-Val-OH |  | This compound consists of both hydrophobic short tails and hydrophilic carboxyl groups. The structure of this compound is not like a true surface-active compound. However, some of the non-polar groups could be adsorbed by the air/beverage interface. |

**Positive polarity mode-Chemical entities annotated with high certainty.**

The detailed table of 197 chemical entities that were annotated with high certainty can be found in Appendix J. At this point of analysis, the next step was to validate the ID of the 197 chemical entities. This could be achieved by acquiring the equivalent chemical reference standard. However, 197 chemical entities was a large number, and the validation of ID experiments would require substantial time and cost. For this reason, a methodology was developed to refine the 197 chemical entities and focus on the most important. There was no need to employ this methodology to targets from negative polarity mode as only 12 compounds were annotated with high certainty. The methodology was as follows.

Each chemical entity was assigned with 3 scores:

1. The r of correlation for at least one of the foam quality parameters (i.e. r of Foam ability, r of Drainage rate, r of Disproportionation/Coalescence rate). The r of correlation can take any value in the range of [-1,1]
2. The SIRIUS score, which can take any value in the range of [0,100]
3. The CSI score, which can take any negative value up to 0.

The most important chemical entities are those with the highest CSI score, highest SIRIUS score and highest absolute value of r of correlation. The visualisation of these scores is depicted in Figure 5-5, Figure 5-6 and Figure 5-7.

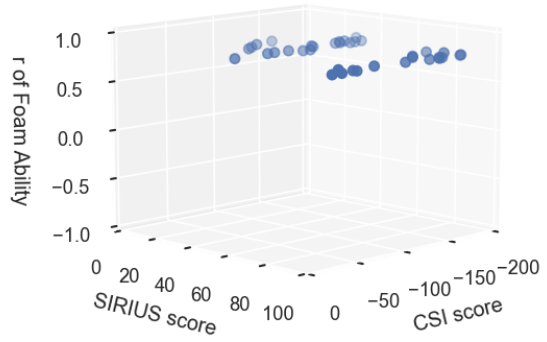



Figure 5-5 r of Foam Ability vs SIRIUS score vs CSI score for chemical entities from positive polarity mode which were annotated with high certainty.

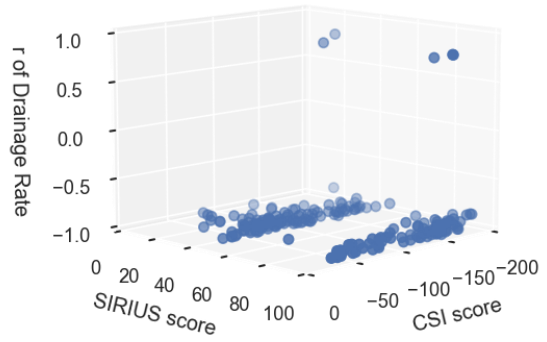



Figure 5-6 r of Drainage rate vs SIRIUS score vs CSI score for chemical entities from positive polarity mode which were annotated with high certainty.

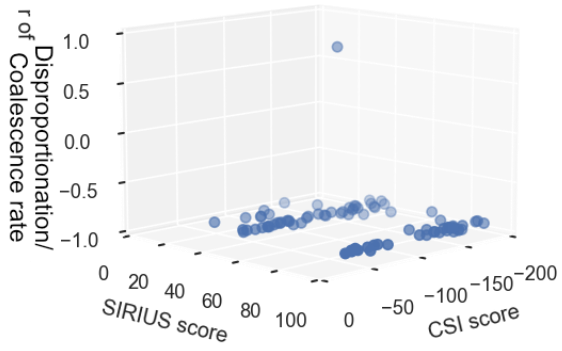



Figure 5-7 r of Disproportionation/Coalescence rate vs SIRIUS score vs CSI score for chemical entities from positive polarity mode which were annotated with high certainty.

The SIRIUS score represents the molecular formula identification, and this score is a combination of isotope pattern analysis on the MS1 data and the fragmentation

tree computation of MS2 data. An investigation on the mathematical formula that calculates the SIRIUS score might reveal the clustering effect of the results.

Let Score A be a variable with the following properties. Score A depicts:

a. the strength of the correlation between the normalised abundance of a given metabolite against the foam ability parameter
b. SIRIUS score
c. CSI score

Score A can take any value in the range of [0,1].

The construction of Score A was achieved by normalizing the r of correlation, the SIRIUS score, and the CSI score to take values in the range of [0,1]. The following mathematical expression calculated the Score A:

Equation 5.1Mathematical equation which calculates the Score A

$$\text{Score A} = \frac{1}{3} * |\text{r of Foam ability}| + \frac{1}{3} * \frac{\text{SIRIUS score}}{100} + \frac{1}{3} * \frac{\text{CSI score} + 180}{180}$$

Where:

- $\mathbf{|r\ of\ Foam\ ability|}$, is the absolute value of the r of correlation for foam ability. This specific parameter can take any value between the range of [0,1].
- $\mathbf{\frac{SIRIUS\ score}{100}}$, is the normalized SIRIUS score. This specific parameter can take any value between the range of [0,1].
- $\mathbf{\frac{CSI\ score+180}{180}}$, is the normalized CSI score. This parameter can take any value between the range [0,1] only if the CSI score take any value between [-180,0] – which was true as CSI score threshold was -180.

Score A depicts equally the strength of correlation, SIRIUS score and CSI score because each of the normalized parameters were multiplied with coefficient 1/3. The equal weight in three scores was assigned as it was important to determine chemical compounds which were highly correlated with the foam quality trait, while they were assigned with high certainty of annotation.

In the same manner, Score B and Score C depict the r of correlation for Drainage rate and disproportionation/coalescence rate respectively – along with the certainty of annotation.

Equation 5.2 Mathematical equation which calculates the Score B

$$\text{Score B} = \frac{1}{3} * |\text{r of Drainage rate}| + \frac{1}{3} * \frac{\text{SIRIUS score}}{100} + \frac{1}{3} * \frac{\text{CSI score} + 180}{180}$$

Equation 5.3 Mathematical equation which calculates the Score C

$$\text{Score C} = \frac{1}{3} * \left|\text{r of} \frac{\text{Disproportionation}}{\text{Coalescence}} \text{rate}\right| + \frac{1}{3} * \frac{\text{SIRIUS score}}{100} + \frac{1}{3} * \frac{\text{CSI score} + 180}{180}$$

Score A, B and C were calculated for the 197 chemical entities and were plotted in a histogram (Figure 5-8). Chemical entities that acquired Score A, Score B or Score C higher than 0.8 were considered the most important to focus on. After applying this methodology, out of the 197 chemical entities which were annotated with high certainty, 16 chemical entities were deemed

(by this rather arbitrary measure) most important to focus on, and qualified for the validation of ID experiments (Table 5.6).

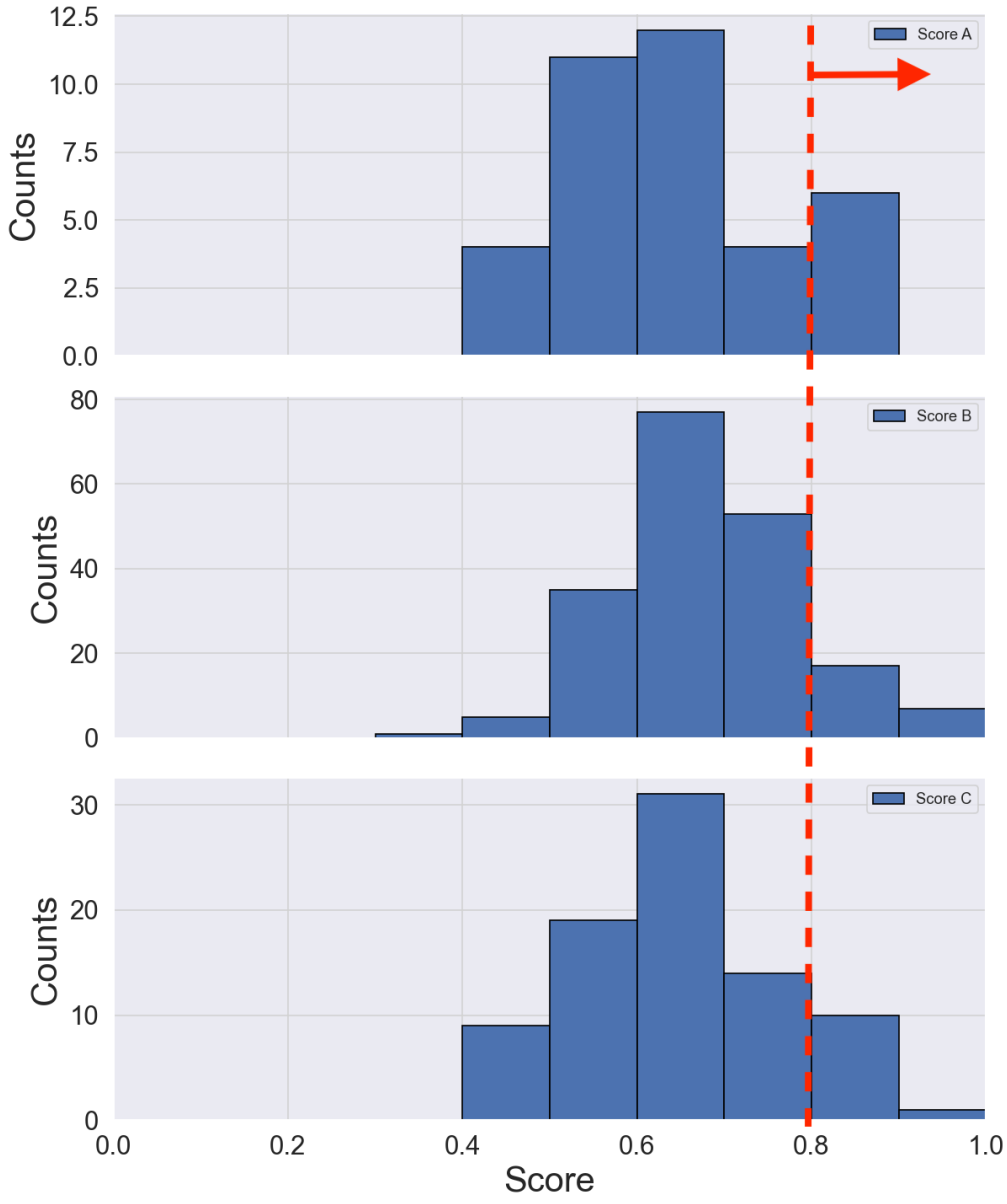



Figure 5-8 Histogram of Score A, Score B and Score C. Each score depicts the strength of correlation for each chemical entity with each of the foam quality parameters, along with the certainty of annotation. Score A is associated with Foam ability, Score B is associated with Drainage rate and Score C is associated with Disproportionation rate. Red dashed line and red arrow indicate that chemical compounds with Score A or Score B or Score C higher than were considered as most important.

Table 5.6 Chemical entities which acquired Score A, Score B or Score C higher than 0.8

| Name | PubChem CID | Prec. m/z | Ret. time (min) | Score A | Score B | Score C |
|---|---|---|---|---|---|---|
| 4-(Methylamino)butan-1-ol | 12545025 | 86.0963 | 1.34 | | 0.82 | |
| Cinnamic acid | 444539 | 166.0862 | 2.66 | | 0.86 | 0.84 |
| Indoleacrylic acid | 5355219 | 205.0971 | 5.01 | | 0.81 | |
| | 5355219 | 188.0705 | 5.01 | | 0.87 | |
| DL-pyroglutamyl-DL-tyrosine | 23422547 | 293.113 | 6.96 | | 0.90 | 0.88 |
| Sorbic acid | 643460 | 113.0597 | 7.03 | | 0.91 | |
| Pyroglutamylmethionine | 24695092 | 261.0902 | 7.20 | 0.86 | 0.87 | |
| cyclo(D)-Pro-(D)-Val | 6545869 | 197.1284 | 10.36 | 0.89 | 0.93 | 0.89 |
| DL-pyroglutamyl-DL-phenylalanine | 13961383 | 277.1181 | 11.86 | | 0.90 | 0.89 |
| Cyclo(Ile-Val) | 10443165 | 213.1597 | 12.57 | | 0.84 | |
| (2E,4E,6E,8E)-10-oxoundeca-2,4,6,8-tetraenoic acid | 134974073 | 193.0858 | 13.15 | | 0.82 | |
| Cyclo(D-Pro-L-Phe-) | 6992198 | 245.1284 | 13.55 | 0.89 | 0.93 | 0.90 |
| Cyclo(Phe-Val) | 139766 | 247.144 | 13.61 | 0.82 | 0.86 | 0.82 |
| L-leucyl-L-leucine | 76807 | 227.1754 | 13.80 | | 0.93 | |
| | 76807 | 227.1754 | 13.81 | 0.87 | 0.92 | 0.88 |
| Cyclo(Phe-Leu) | 562691 | 261.1597 | 13.95 | | 0.87 | 0.84 |
| | 562691 | 261.1597 | 14.33 | | 0.89 | 0.86 |
| | 562691 | 261.1598 | 14.48 | 0.85 | 0.89 | 0.86 |
| Cyclo(D-Phe-L-Phe-) | 1477298 | 295.1441 | 15.20 | | 0.84 | |
| 11,12,13-Trihydroxyoctadecanoic acid | 129854424 | 333.263 | 15.91 | | 0.90 | |

In overall 28 chemical entities both from negative and positive polarity mode were short listed as the most important compounds for further study.

### 5.3.3 Validation of key foam target identities

At this point of analysis, the next step was to validate the ID of 28 chemical entities by acquiring the equivalent chemical reference standard from the market. The chemical entities that were available in the market and acquired are listed in Table 5.7. Along with chemical entities from untargeted chemical analysis, 4-vinylguaicol, from targeted chemical analysis was appended in the validation list as this chemical was identified via MS2. The other compound that was identified

in targeted chemical analysis (i.e. p-Coumaroylquinic acid lactone) was not available in the market so it was excluded from the validation list.

Table 5.7 Chemical entities that were available in the market

| Type of analysis | Name | Solvent | Concentration |
|---|---|---|---|
| Untargeted in negative polarity | Myristic Acid | 100% EtOH | 0.01 mg/mL |
| | Mannotetraose | $H_2O$ | 0.01 mg/mL |
| Untargeted in positive polarity | 4-(Methylamino) butan-1-ol | | 0.01 mg/mL |
| | Cinnamic acid | 100% EtOH | 0.01 mg/mL |
| | Cyclo(D-Phe-L-Phe-) | 1% DMSO – 99% EtOH | 0.01 mg/mL |
| | Cyclo(D-Pro-L-Phe-) | 100% EtOH | 0.01 mg/mL |
| | cyclo(D)-Pro-(D)-Val | 100% EtOH | 0.01 mg/mL |
| | Cyclo(Phe-Leu) | 100% EtOH | 0.01 mg/mL |
| | Cyclo(Phe-Val) | 100% EtOH | 0.01 mg/mL |
| | Indoleacrylic acid | 100% EtOH | 0.01 mg/mL |
| | L-leucyl-L-leucine | 100% EtOH | 0.01 mg/mL |
| | Sorbic acid | 100% EtOH | 0.01 mg/mL |
| Targeted in negative polarity mode | 2-methoxy-4-vinylphenol (4-vinylguaicol) | 100% EtOH | 0.01 mg/mL |

A solution for each chemical entity was prepared at a concentration of 0.1 mg/mL and each solution was analysed in negative or positive polarity mode via Polyscreen mk5 (4.2.5). If there was a match of retention time and the mass-to-charge ratio between the MS2 annotated compound and the equivalent chemical reference standard, then the ID of the MS2 annotated compound was considered to be validated. As a second layer of validation, the MS2 spectra of chemical reference standards were compared with the MS2 spectra of the MS2 annotated compounds. The detailed MS1 and MS2 spectra are presented in Appendix K. Finally, 6 chemical compounds were validated in instant coffee; one carbohydrate (i.e. Mannotetraose) and 5 cyclo dipeptides (i.e. Cyclo(Phe-Pro),

Cyclo(Phe-Val), Cyclo(Pro-Val), Cyclo(Leu-Phe) and Cyclo(Phe-Phe) (Table 5.8).

Table 5.8 Summary of compounds that were positively or negatively ID validated

| Chemical compound | ID validated? | Retention time (min) |
|---|---|---|
| Mannotetraose | Yes | 0.83 |
| Cyclo(-Pro-Phe) alpha | Yes | 10.08 |
| Cyclo(D)-Pro-(D)-Val | Yes | 10.342 |
| Cyclo(-Pro-Phe) beta | Yes | 13.55 |
| Cyclo(Phe-Val) | Yes | 13.61 |
| Cyclo(Phe-Leu) | Yes | 14.294 |
| Cyclo(D-Phe-L-Phe) | Yes | 15.16 |
| 4-(Methylamino) butan-1-ol | No | |
| Myristic acid | No | |
| Cinnamic acid | No | |
| Indoleacrylic acid | No | |
| L-leucyl-L-leucine | No | |
| Sorbic acid | No | |
| 4-vinylguaiacol | No | |

According to Table 5.7, there was only one Cyclo(-Phe-Pro) but apparently an additional isomer of Cyclo(-Phe-Pro) was identified in coffee samples. The 244.1211@13.551016 had retention time and m/z 13.55 min and 245.1284 respectively. The chemical standard of Cyclo(L-Phe-L-Pro) from Merck was analysed and two peaks were detected (Figure 5-9). One peak had a retention time of 13.083 min with m/z 245.1289 and the other peak had a retention time of 13.566 min with m/z 245.1287. The correlation analysis indicated that the chemical entity of interest was the peak at 13.566 min as it matches with the MS1 spectrum of the compound of interest (Figure 5-10).

However, two peaks were identified in the chemical reference standard. It was hypothesised that the chemical standard of Cyclo(L-Phe-L-Pro) which had a purity of >95% may have also had some isomers of the dipeptide with variations of D and L amino acids. This hypothesis was addressed to Merck Life Science and the response was the following:

"*QC confirmed they do believe there is a variation of D and L peptides present. The specification is to report >95% chemical purity, so we do not concentrate on the other peaks during release. The recent LCMS analysis reveals the other minor peak corresponds to other possible isomers of Cyclo(Phe-Pro) (~4%) which might have been formed during cyclisation of L-Phe-L-Pro dipeptide by minor racemization*."

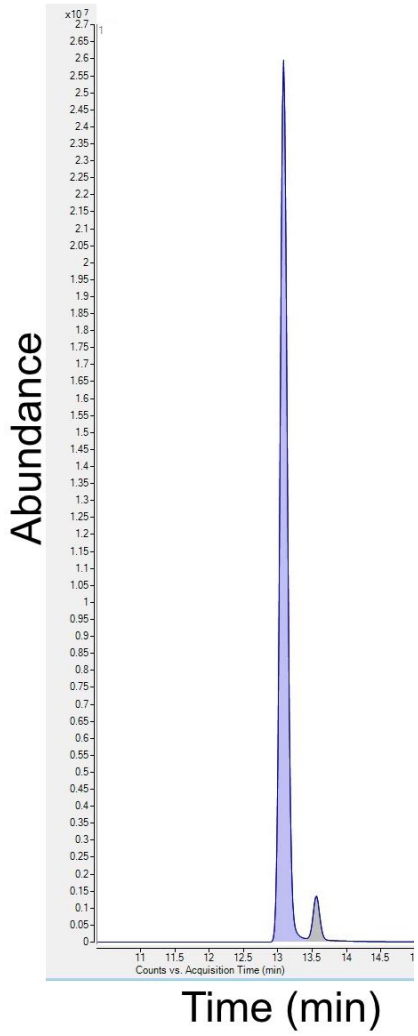



Figure 5-9 Two peaks detected for Cyclo(-Phe-Pro) chemical reference standard provided from Merck Life Science.

Taking this into account, the highest peak of Merck's standard is the Cyclo(L-Phe-L-Pro) and the smaller one is a Cyclo(-Phe-Pro) with at least one D form of

peptide. Since it is suggested by SIRIUS software that 244.1211@13.551016 was a Cyclo(L-Phe-D-Pro), the exact chemical reference standard was acquired from Santa Cruz Biotechnology Inc.(TX, USA).

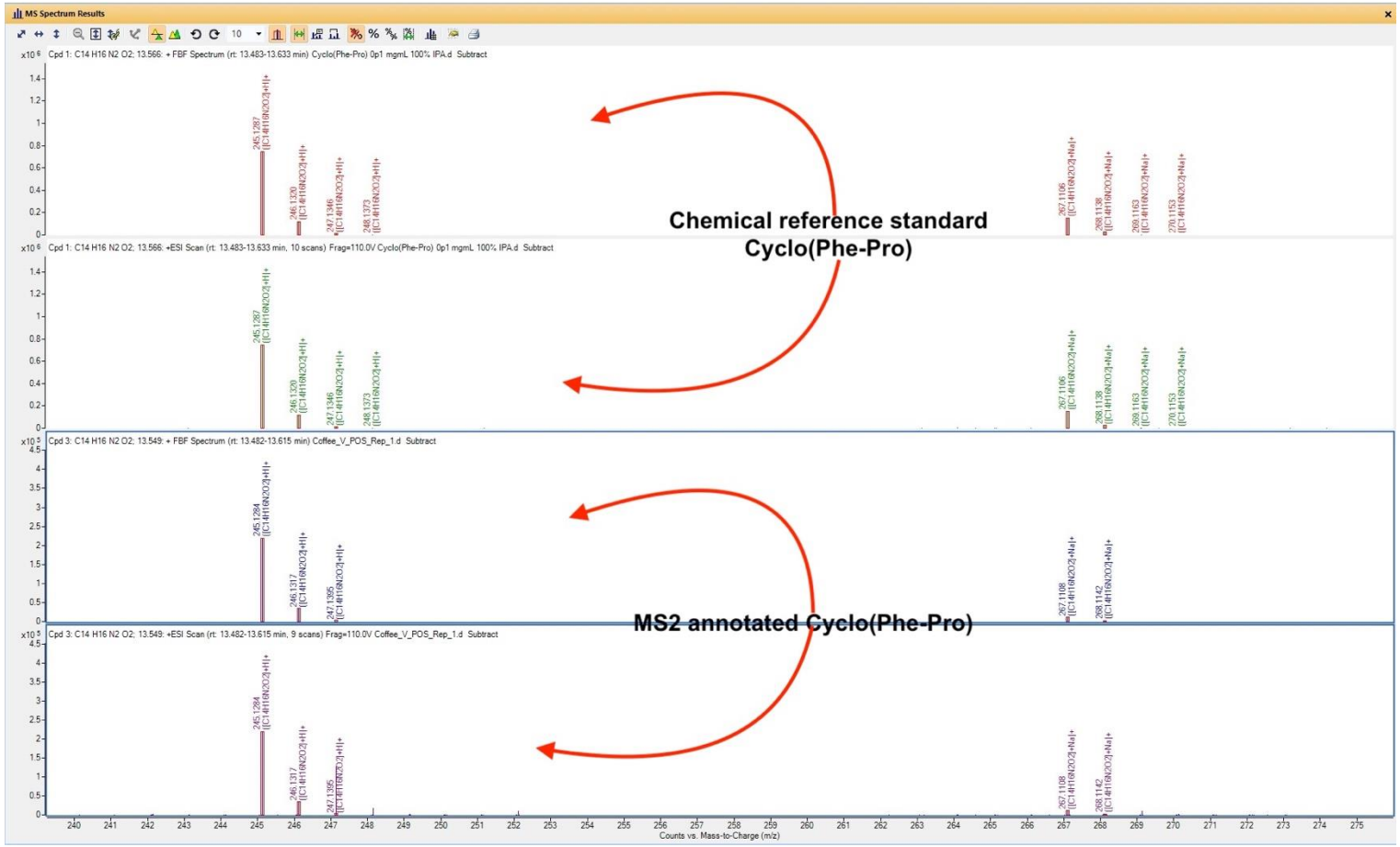



Figure 5-10 Top: MS1 spectra of chemical reference standard of Cyclo(-Phe-Pro). Bottom: MS1 spectra of MS2 annotated Cyclo(-Phe-Pro)

Cyclo(L-Phe-D-Pro) was analysed with the Polyscreen mk5 method and two peaks were identified at the same retention time as the Cyclo(L-Phe-L-Pro) from Merck. The retention time and m/z of Cyclo(L-Phe-D-Pro) peaks were 13.046 min and 13.512 min and 267.1107 and 267.1104 respectively.

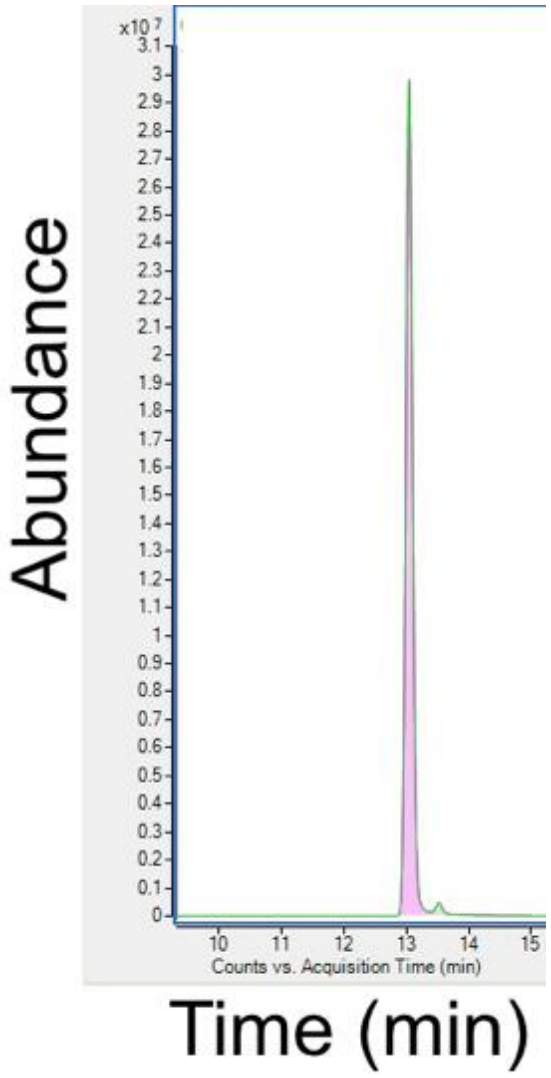



Figure 5-11 Two peaks detected for Cyclo(L-Phe-D-Pro) chemical reference standard provided by Santa Cruz Biotechnology Inc.

Since 244.1211@13.551016 is present in coffee and there is evidence that this compound is a Cyclo(-Phe-Pro), it was hypothesised that a variation of Cyclo(-Phe-Pro) that elutes at 13.08 min may be present in coffee samples. There is a compound 244.1214@13.081014 which is MS2 annotated as Cyclo(L-Phe-D-Pro) with SIRIUS score=50%, CSI SCORE=-26.861 and it is also highly

correlated with Drainage rate with Pearson's correlation r=-0.96 and Score B (which combines the CSI score, SIRIUS score and Pearson's correlation coefficient) = 0.7587. The threshold set for refining these targets was 0.8. So, despite the fact that 244.1214@13.081014 is highly correlated with the Drainage rate it did not end up in the final list of "most important" targets because of the value of Score B. The retention time and m/z of 244.1214@13.081014 matched with the retention time and m/z of chemical standards from both Merck Life Science and Santa Cruz Biotechnology. This indicated that D and L variations of Cyclo(-Phe-Pro) are not yet known for both 244.1214@13.081014 and 244.1211@13.551016. What has been proven though is that both compounds are highly correlated with at least one of the foam quality parameters and are identified as Cyclo(-Phe-Pro).

## 5.4 Conclusions

In this chapter, untargeted chemical analysis via liquid chromatography-mass spectrometry was performed in order to analyse the 21 instant coffee samples that were significantly different from the control coffee in terms of foam ability, with the aim to establish chemical differences. After performing the correlation analysis between the relative abundance of each chemical entity, which was identified in the sample set versus each of the foam quality parameters (i.e. Foam ability, Drainage rate, Disproportionation rate) 322 chemical entities were found to be highly correlated with foam quality performance. MS2 annotation was performed and 209 of these were annotated with high certainty. 16 of them were deemed the most important in terms of strength of correlation and certainty of annotation (i.e. Score A, Score B, Score C). Finally, 6 of them were successfully identified in coffee. Mannotetraose, cyclo(-pro-val), cyclo(phe-pro), cyclo(phe-

val) and cyclo(leu-phe) have already been reported in coffee (Ginz and Engelhardt, 2000, 2001; Flament, 2002; Bee et al., 2005; Poisson et al., 2017)(Ginz and Engelhardt, 2000, 2001; Flament, 2002; Bee et al., 2005; Poisson et al., 2017). Cyclo(phe-phe) is reported in coffee for the first time. As presented in Chapter 2:Literature Review, AGP isolated from green bean were reported to create foam. Roasting process and Instant coffee manufacture affects the native structure of AGP, by breaking down the large molecular weight chains to smaller oligosaccharides. It is hypothesised that the instant coffee samples that were used for the untargeted chemical analysis would contain mostly products of AGP. It has not been investigated if the roasting products of AGP are associated with foam. However, such compounds were not found by performing the untargeted chemical analysis.

The validation of identification through reference standards bears the limitation of availability of chemical reference standards in the market. Another possible route towards successful identification is their isolation via liquid chromatography of chemical compounds of interest and identification through NMR techniques.

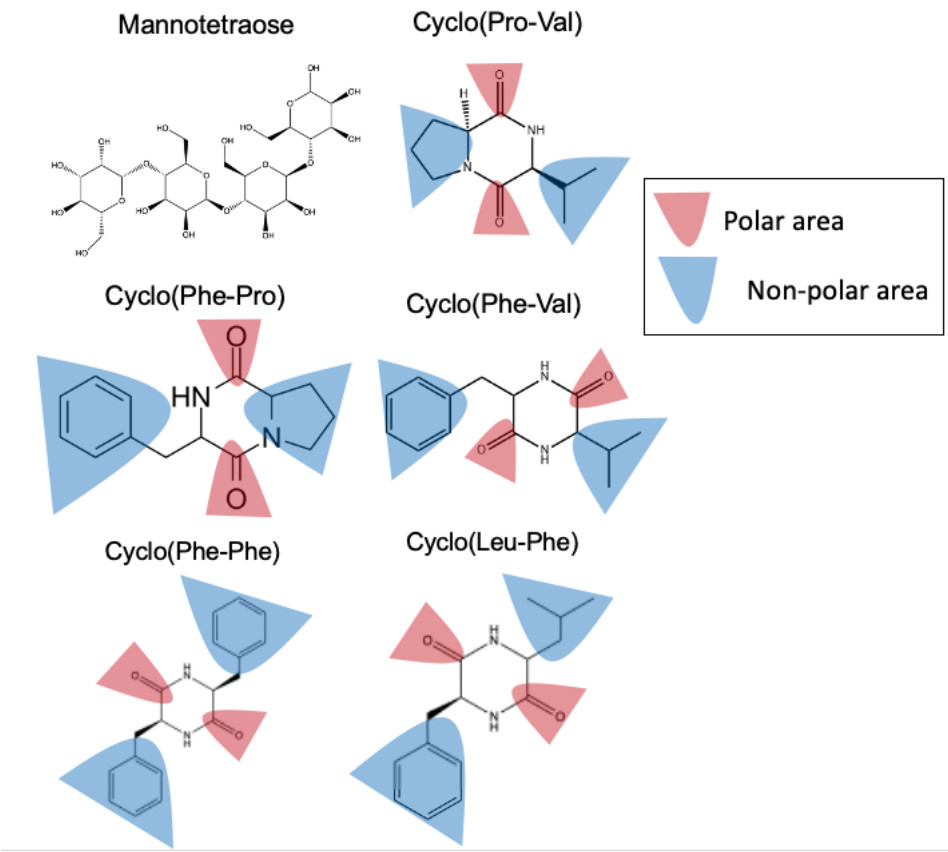



Figure 5-12 6 key foam identified in instant coffee

The 6 targets, that were identified in coffee, can be used as foam quality markers because their presence in an instant coffee system could indicate good foam quality. These foam targets can either be associated with good foam quality or can actively drive the foam quality performance of coffee and play an important role in foam ability or foam stability mechanisms. In principle, a surface-active chemical compound should consist of a polar area and a non-polar area. In the case of 6 key foam targets, mannotetraose does not have any non-polar area and is highly soluble in water. On the other hand, the rest, which are 5 cyclo-dipeptides, have similar structures. The two opposing non-polar areas and two opposing polar areas make these compounds highly symmetric. To examine the direct effect of certain compounds on foam quality, low foam quality coffee must be spiked with each foam target followed by a foam quality assessment.

# Chapter 6: Influence of key foam compounds on foam quality

## 6.1 Introduction

In the previous chapter, six chemical entities in coffee - correlated with at least one of the foam quality parameters (i.e. Foam Ability, Drainage Rate, Disproportionation Rate) - were identified at MSI Level 1 (Sumner *et al.*, 2007) via LCMS. The aim of this chapter was to investigate if these entities were merely associated with or were driving the observed foam quality phenomena. This was achieved by first establishing the precise levels of these compounds in coffees, and then artificially increasing the concentration of a given metabolite in a coffee system and assessing the foam quality.

## 6.2 Materials and Methods

### 6.2.1 Chemicals

Cyclo(-Leu-Phe), Cyclo(-Phe-Pro), Sinapic acid and Dimethyl sulfoxide were acquired from Merck life sciences Ltd (Gillingham, UK). Cyclo(L-Phe-L-Val) and Cyclo(L-Pro-L-Val) were acquired from Cambridge Biosciences Ltd (Cambridge, UK). Cyclo(-Phe-Phe) was acquired from Generon LtD (Slough, UK). Mannotetraose was acquired from Megazyme (Wicklow, Ireland). Formic acid were acquired from Fisher Scientific (Loughborough, UK). Purine and Hexakis(1H, 1H, 3H-tetrafluoropropoxy)phosphazine were acquired from Agilent Technologies (Cheadle, UK). Ethanol absolute >99.7% and Methanol HPLC grade were acquired from VWR International Ltd (Lutterworth, UK). All reference standards were of high purity (>95%).

### 6.2.2 Instant coffee

The instant coffees, that were analysed in this chapter, were introduced in Chapter 3:.

Table 6.1 Instant coffee samples that were used for the present chapter. SD3-SR1/12 and Trial-FD5 has the maximum and minimum foam ability, respectively.

| Instant coffee samples |
|---|
| Control |
| Trial-FD5 |
| SD 3-SR1/12 |

### 6.2.3 Fine quantitation of candidate molecules in coffee samples via high-resolution liquid chromatography-mass spectrometry

The instant coffee samples of Table 6.1 were prepared as described in section 4.2.3 and analysed in triplicates as per section 4.2.5. Sinapic acid was used as internal standard at a final concentration of 3 ug/mL. Mannotetraose was quantified in negative polarity while the cyclo-dipeptides were quantified in positive polarity mode. For fine quantification purposes, standard curves of key chemical compounds were created in absolute ethanol. The range of each standard curve is presented in Table 6.2.

Table 6.2 Standard curve ranges of key foam compounds

| Compound | Range of concentration (mg/mL) |
|---|---|
| Mannotetraose | 0.0001-0.005 |
| Cyclo(Phe-Val) | 0.00002-0.001 |
| Cyclo(Phe-Pro) alpha | 0.001-0.06 |
| Cyclo(Phe-Pro) beta | 0.00004-0.002 |
| Cyclo(Pro-Val) | 0.0001-0.005 |
| Cyclo(Phe-Phe) | 0.000004-0.0002 |
| Cyclo(Leu-Phe) | 0.00007-0.0035 |

### 6.2.4 Instant coffee sample preparation for surface tension measurement and foam analysis via KRÜSS Dynamic foam analyser 100

Instant coffee samples were prepared as per section 3.2.5. A 50 mL aliquot of instant coffee solution was decanted in 50mL Falcon centrifuge tubes (Corning Science, USA). The aliquot was centrifuged in a GT 4R Centrifuge (Fisherbrand, Loughborough, UK) at 3739 g, for 10 minutes at 20˚C. The pellet was discarded, and the supernatant was held for analysis. The final solution had a concentration of 1.5% w/w in coffee solids, and 1 mL of chemical reference standard solution

was combined with 169 mL of instant coffee sample in order to increase the concentration of key foam targets by 2.5, 5 and 7.5 times the initial concentration.

### 6.2.5 Density measurement of instant coffee solution

A 2mL aliquot of instant coffee solution was injected in DMA 5000 Density meter (Anton Paar, Graz, Austria) and the density was measured at 20˚C (number of replicates= 3). Before and after each measurement the U-tube of the density meter was flushed with 2 ml each of neutracon, followed by acetic acid, ultra-pure water, and absolute ethanol. The tube was flushed for 30 seconds with air.

### 6.2.6 Surface Tension measurement

Dynamic surface tension was measured by the technique of Profile Analysis Tensiometry (PAT) (Loglio *et al.*, 2011) via the pendant drop method, using a Drop and Bubble Shape Tensiometer PAT-1 (SINTERFACE Technologies, Germany). The studied system was the air/beverage interface, so a drop of liquid sample ($V_{drop}$= 21 $mm^3$) was formed in the air-filled cuvette. The measurement of surface tension started right after the formation of a fresh drop of sample. The dynamic surface tension was measured for 40000 seconds (approx. 11.11 hours) at 20˚C and the number of measurements was two (n=2). The acquired data were fitted to the Young-Laplace equation *via* SINTERFACE PAT1D ver. 8.01.23 software (SINTERFACE Technologies, Germany). The surface tension of ultrapure water at 20˚C was determined for 30 minutes prior each sample to verify that the tensiometer was calibrated and clean from impurities.

### 6.2.7 Foam quality assessment via KRÜSS Dynamic Foam Analyser 100

The foam height vs time and bubble structure of instant coffee samples was assessed via Dynamic Foam Analyser 100 for 30 minutes (KRÜSS GmbH,

Hamburg, Germany) (n=3). A 55 mL aliquot of instant coffee sample was decanted in a 40mm diameter prism column. Foam generation was achieved *via* the stirring method. The foaming and data acquisition parameters are presented in Table 6.3.

Table 6.3 Foaming and data acquisition parameters

| | Parameter | Value |
|---|---|---|
| Instrument setup | Column | CY4572 - 40 mm prism |
| | Stirrer | SR4501 |
| | Height illumination | Infrared - λ = 850 nm at 5% |
| | Speed | 8000 rpm |
| | Foaming time | 30 seconds |
| | Oscillation period | 0 seconds |
| Data sampling | Height Foaming | 5 fps |
| | Height Decay | 10 fps |
| | Structure Foaming | 2 fps |
| | Structure Decay | 2 fpd |
| | Camera height | 55 mm |
| | Camera position | 3 |

### 6.2.8 Data analysis

Raw data from surface tension measurement and foam quality assessment were fitted by mathematical equations. For this purpose, a script in Python 3 was developed utilising the scipy.optimize.curve_fit package (Virtanen *et al.*, 2020). Details of this method are presented in section 3.2.12.

### 6.2.9 Statistical analysis

One-way ANOVA was performed through Python 3 scripts by using the package scipy.stats.f_oneway (Virtanen *et al.*, 2020). The level of significance was set at $p = 0.05$.

## 6.3 Results and Discussion

### 6.3.1 Quantification of candidate compounds in coffee samples with standard addition method

The instant coffees that were selected for the spiking experiment were the control instant coffee, SD3-SR1/12 (sample with maximum foam ability) and Trial-FD5 (sample minimum foam ability). Before spiking the instant coffees with a known concentration of each key foam compound, it was important to determine the concentration of these metabolites in the samples of interest. Therefore, chemical analysis via LC-MS was employed.

As the internal standard (in the present case; Sinapic acid) was used to normalise the signal of compounds of interest to eliminate the variance induced by the instrument, the integrated peak area of Sinapic acid must be the same throughout the sample set and standard curve. However, even though the same amount of internal standard was injected in both samples and standard curves, the signal was observed to be different (Figure 6-1).

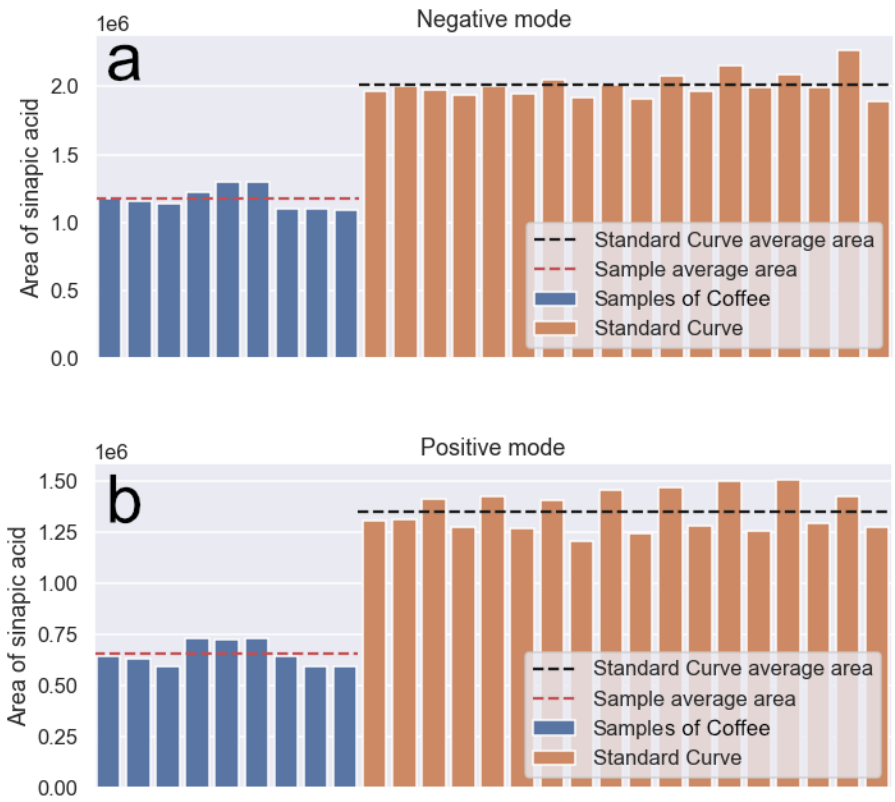



Figure 6-1 Area of sinapic acid as detected in instant coffee samples and standard curves in (a) Negative polarity mode and (b) Positive polarity mode

According to Figure 6-1a in negative polarity mode, the average area of Sinapic acid in standard curves was 2.02±0.1 * $10^6$ while in coffee samples it was 1.18±0.08 * $10^6$. The statistical analysis showed that there was a significant difference ($p<0.05$) between these values. The equivalent data in positive polarity mode (Figure 6-1b) was 1.35±0.09 * $10^6$ and 0.65±0.06 * $10^6$ and it was found that these values were significantly different ($p<0.05$). There was therefore a suppression of the Sinapic acid signal in coffee samples compared to the standard curve. It is important to highlight that the standard curve solutions were prepared in 100% ethanol, while the coffee samples were prepared with 70% aqueous coffee solution and 30% ethanol. Hence, it was hypothesised that the signal suppression could either be attributed to different diluents between standard curve (100% ethanol) and coffee sample (70/30 water/ethanol) or that

the chemical compounds that comprise the coffee sample were inducing a so-called matrix effect.

For this reason, three samples were prepared with the same concentration of Sinapic acid (i.e. C=0.003 mg/mL). The first sample was comprised of Sinapic acid dissolved in 100% ethanol, the second sample was comprised of Sinapic acid dissolved in 70/30 water/ethanol, and the third sample was a control coffee sample prepared with 70/30 water/ethanol diluent. The samples were analysed in triplicate and the area of Sinapic acid is presented in Figure 6-2.

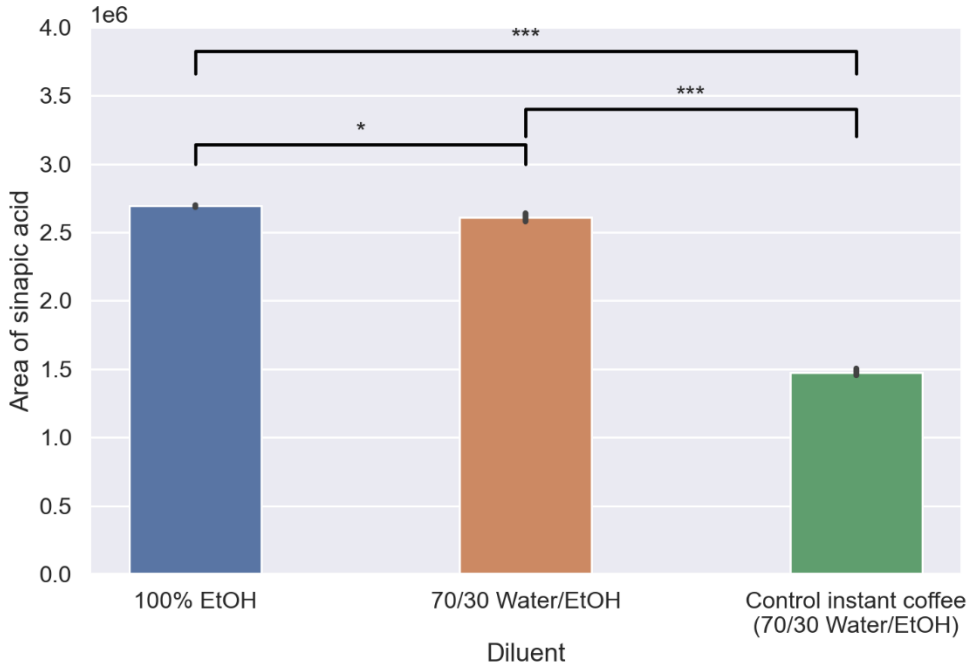



Figure 6-2 Area of Sinapic acid in three different samples (n=3). Significant difference: * $p<0.05$, ** $p<0.01$, *** $p<0.001$

The maximum signal of sinapic acid was detected for the 100% ethanol sample. Whilst changing the diluent from 100% ethanol to 70/30 water/ethanol, the signal was reduced ($p<0.05$) but the effect was negligible (3.08±1.09% loss). However, when using dissolved instant coffee in 70/30 water/ethanol, the IS signal was decreased by 45.3±1% ($p<0.001$). From these results, it can be concluded the sinapic acid signal was partially suppressed by the instant coffee

matrix. However, it was observed that whilst the abundance of internal standard between coffee samples and standard curve was different, the abundance of internal standard between different coffee samples was similar. Hypothetically, if a suitable internal standard shares sufficient structural similarity with target analytes, the ionisation of both targets and IS would be affected to the same degree. Alternatively, where an IS cannot control for a matrix effect, standard addition might prove a suitable alternative method to accurately quantify the candidate molecules in coffee.

In standard addition, the approach was to prepare the standard curves in a standardised coffee matrix rather than a plain diluent. In this case the coffee matrix was formed by mixing equal aliquots of the coffee samples to be analysed. Standard curves were comprised of the coffee matrix, 0.003 mg/mL of Sinapic acid and spiked with chemical reference standards of key foam compounds. The range of standard curves is presented in Table 6.2. In addition, a blank coffee matrix sample was analysed, and the standard curve of a given compound (e.g. compound x, Figure 6-3) was calculated by subtracting the intensity of blank from the rest of the curve samples.

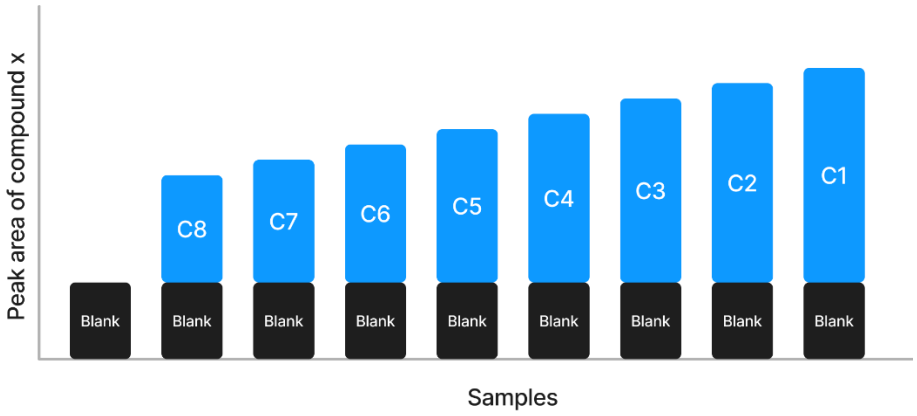



Figure 6-3 Theoretical bar plot which presents the peak area of compound x as identified in different samples. The intensity of each bar consists of the intensity of compound x that is native in the blank sample and the intensity of compound x that was spiked. C1 to C8 are theoretical concentrations of compound x.

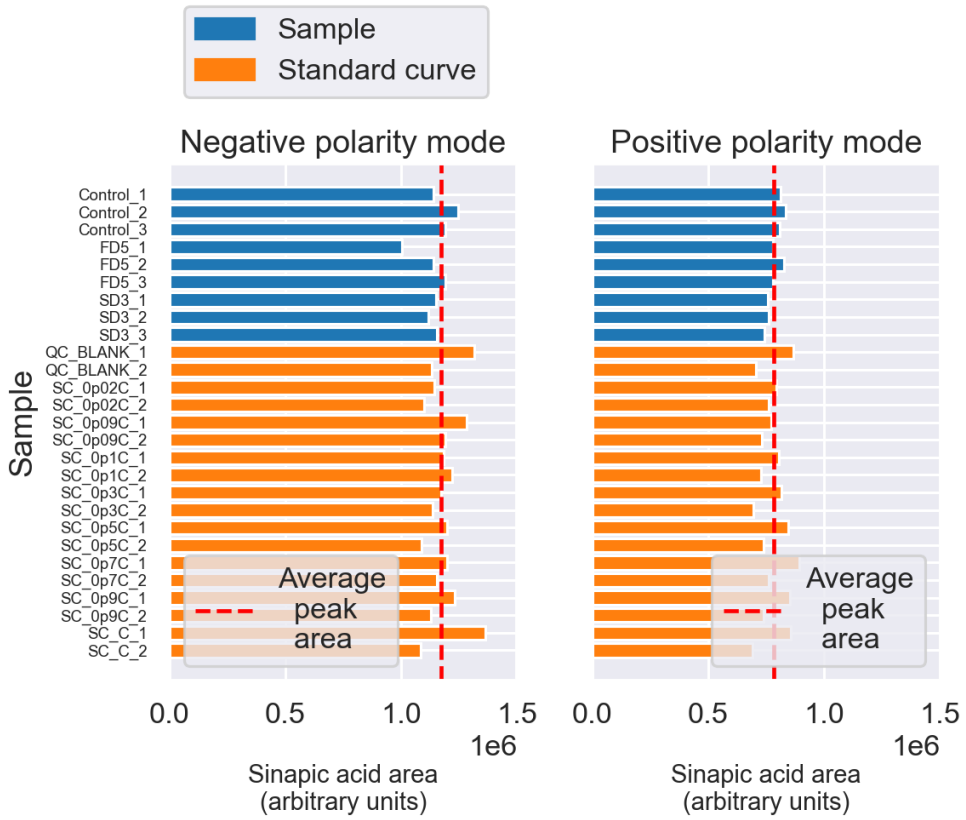



Figure 6-4 Area of sinapic acid as identified in negative and positive polarity mode for coffee samples and standard curve which were prepared via standard addition method (SAM).

The area of sinapic acid for negative and positive polarity mode was 1.2±0.07 x $10^6$ (RSD=6.31%) and 7.8±0.5 x $10^5$ (RSD=6.69%) respectively. This result confirms that with standard addition method, the signal of sinapic acid was stabilised around a specific value regardless of the nature of the sample (i.e. coffee sample or standard curve point).

Using standard addition, it was feasible to produce a standard curve for every chemical compound. An example of standard addition is presented in Figure 6-5, the rest of the standard curves can be found in the Appendix L.

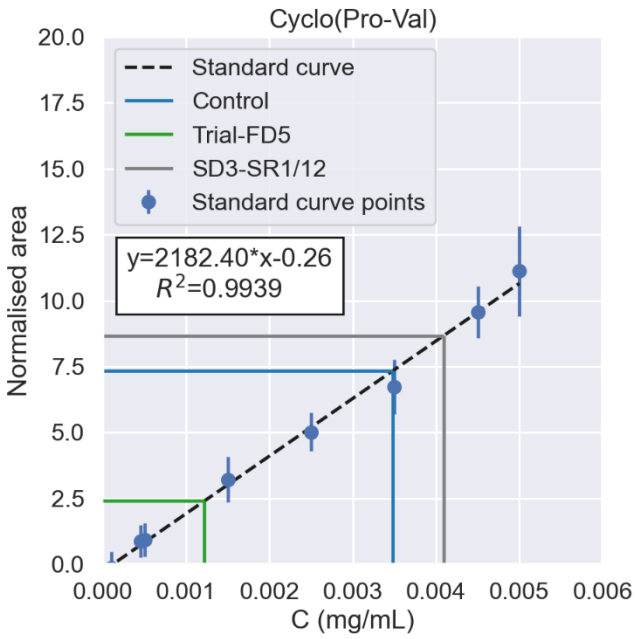



Figure 6-5 Standard curve of Cyclo(Pro-Val) prepared with Standard addition method (SAM)

The standard curve data points for Mannotetraose are presented in Figure 6-6. Despite spiking the blank solution with various amounts of Mannotetraose, it was not feasible to export a standard curve. According to the literature, a low molecular weight fraction (<12kDa) of instant coffee contains 6.1 g mannose/100 g coffee on a dry basis (Lopes et al., 2021). Mannose is not present in coffee in the form of monomers but there is a distribution of mannose oligomers. Data that were kindly provided by JDE indicate that Mannotetraose constitutes between 5% and 15% of the total mannose content.

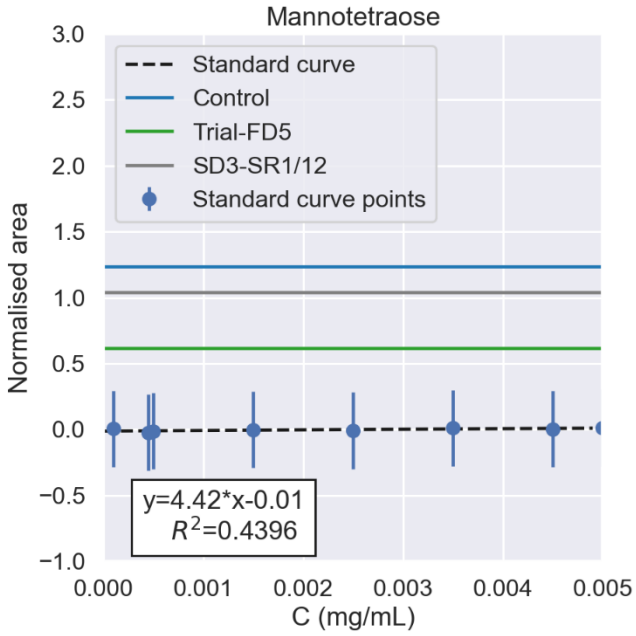



Figure 6-6 Standard curve points for Mannotetraose. Standard curve was prepared with standard addition method.

By combining the Mannotetraose content with information from Lopes et al. (2021) and assuming that the distribution of degree of polymerisation was for control coffee sample, then the concentration of Mannotetraose was ([5% to 15%]*6.1 g mannose/100 g coffee on a dry basis = ) 0.31 to 0.92 g/100 g coffee on a dry basis. The concentration of Mannotetraose in 1.5% w/w coffee solution was:

$$\frac{(0.31 \text{ to } 0.92)\ \text{g Mannotetraose} * \frac{1.5\ \text{g dry coffee}}{100\ \text{g coffee solution}}}{100\ \text{g dry coffee}} = 0.00465 \text{ to } 0.0138\ \text{g}\frac{\text{Mannotetraose}}{100\ \text{g solution}}$$

Or

$$C_{\text{Mannotetraose}} = 0.047 \text{ to } 0.14\,\frac{\text{mg}}{\text{mL}}$$

If it was assumed that the density of 1.5% coffee solution was ρ=1 g/mL. Based on these calculations and the normalised peak area of the detected Mannotetraose in Control, SD3-SR1/12 and Trial-FD5 (1.23±0.09, 1.04±0.01, 0.59±0.05 respectively) (Figure 6-6), the concentration of Mannotetraose in Blank solution (Figure 6-3) was

$$C = \frac{(0.047 \text{ to } 0.14)\ \frac{mg}{mL} + \frac{1.04 * (0.047 \text{ to } 0.14)}{1.23}\frac{mg}{mL} + \frac{0.59 * (0.047 \text{ to } 0.14)}{1.23}\frac{mg}{mL}}{3} = 0.036 \text{ to } 0.11 \text{ mg/mL}$$

The highest concentration of the Mannotetraose that was spiked into the standard curve was 0.005 mg/mL; equivalent to 4.5 to 13% of native concentration. Therefore, such small spiking might not be sufficient to increase the signal of Mannotetraose. Another hypothesis may be that Mannotetraose could not be completely solubilised with the rest of the cyclo-dipeptides in the first standard curve sample (i.e. C1).

The slope and intercept of standard curves prepared with Standard Addition Method (SAM) are presented in Table 6.4.

Table 6.4 Linear regression results for cyclo-dipeptides as analysed via standard addition method.

| Compound | Slope | Intercept | $R^2$ | Log-Log scale? |
|---|---|---|---|---|
| Cyclo(Leu-Phe) | 2535.55 | -0.3 | 0.9885 | No |
| Cyclo(Phe-Phe) | 1291.87 | 0.01 | 0.9647 | No |
| Cyclo(Phe-Pro) alpha | 1 | 3.25 | 0.9980 | Yes |
| Cyclo(Phe-Pro) beta | 1414.02 | -0.04 | 0.9835 | No |
| Cyclo(Phe-Val) | 1715.45 | 0.04 | 0.9734 | No |
| Cyclo(Pro-Val) | 2182.40 | -0.26 | 0.9939 | No |

It is important to highlight that standard curve for both forms of Cyclo(-Phe-Pro) compound (i.e alpha and beta) were calculated, under the assumption that the chemical reference standard that was used consisted of two forms of Cyclo(-Phe-Pro) with 96/4 (=24) ratio (see section 5.3.3). This ratio was confirmed by analyzing the Cyclo(-Phe-Pro) reference standard (26.82±3.12 n=18).

For fine quantification purposes via standard curve, is important to highlight that the normalized peak of a given compound in a given sample must be between the upper and lower standard point curve. In the case that a normalized peak area

is outside of the boundaries of standard curve then the quantification can be performed via extrapolation of the standard curve. However, such a technique gives only an approximation and assumes that the slope and intercept of the standard curve equations do not change by appending more standard curve data points. In addition, the extrapolation of standard curve lower than the lowest standard curve point might result in calculating negative concentration values which is impossible. Such a case appeared for Cyclo(Phe-Pro) alpha. An approach of estimating the said concentration is to plot the normalised area vs concentration in log-log scale and perform linear regression. Based on the above statements and assumptions, the concentration of cyclo-dipeptides as calculated via standard curves of Table 6.4 are presented in Figure 6-7.

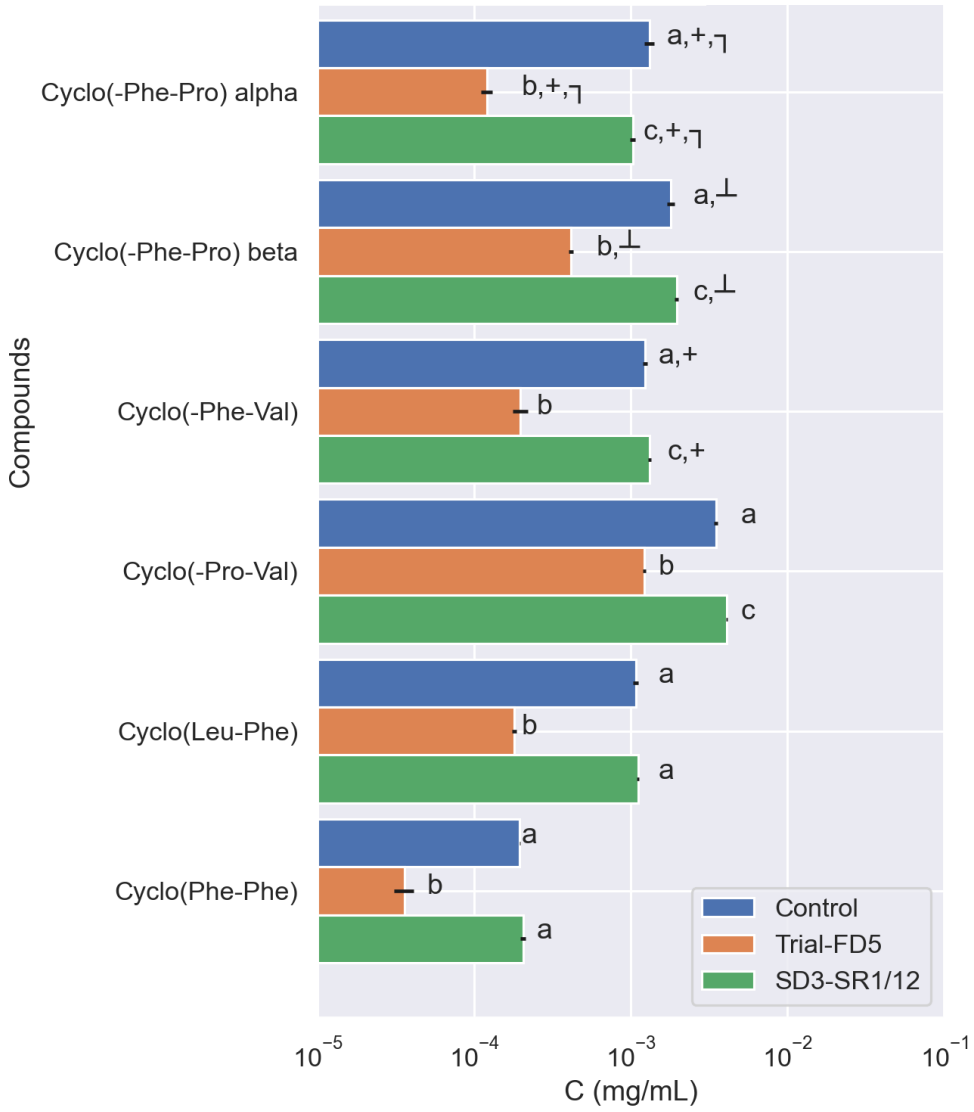



Figure 6-7 Concentration of Cyclo(-Phe-Pro) alpha and beta, Cyclo(-Phe-Val), Cyclo(-Pro-Val), Cyclo(Leu-Phe) and Cyclo(Phe-Phe) for Control, Trial-FD5 and SD3-SR1/12 instant coffee (n=3). Statistical test was performed for each chemical entity separately throughout the coffee samples. Different letters indicate significant difference at p=0.05. + **symbol**: The concentration was calculated by extrapolation of standard curve. ┐ **symbol**: Concentration was calculated via linear regression in log-log scale plots. ⊥ **symbol**: Concentration calculated under the assumption that Cyclo(-Phe-Pro) alpha/beta ratio was 96/4.

Statistical analysis showed that Cyclo(Phe-Pro) alpha, Cyclo(Phe-Pro) beta, Cyclo(Phe-Val) and Cyclo(Pro-Val) were significantly higher in SD3-SR1/12 than Control and Trial-FD5. As expected, the concentration of all cyclo dipeptides was significantly lower in Trial-FD5 (a poor foaming coffee) than the rest of the coffee samples.

### 6.3.2 What is the effect of coffee matrix on ionisation of cyclo dipeptides?

To evaluate if the coffee matrix influences the ionisation degree of metabolites, the concentration of key foam targets was compared as determined with or without standard addition method. An example of a standard curve prepared without standard addition method is presented in Figure 6-8. The rest of the standards curves which were prepared in the same way are presented in Appendix M.

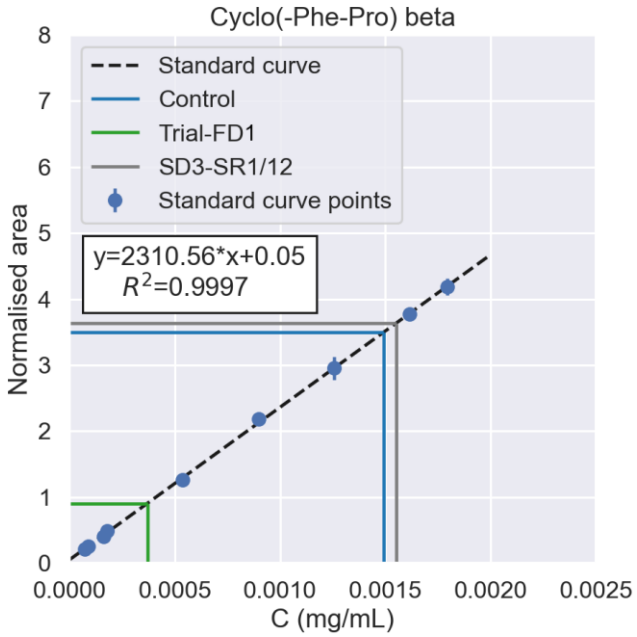



Figure 6-8 Standard curve of Cyclo(Phe-Pro) beta prepared without Standard addition method (SAM). Concentration of x-axis were calculated under the assumption that Cyclo(-Phe-Pro) alpha/beta ratio was 96/4.

Only the concentration of Cyclo(Phe-Pro) beta was directly comparable between the two methods for the control and SD3-SR1/12 sample. These concentrations are presented in Figure 6-9.

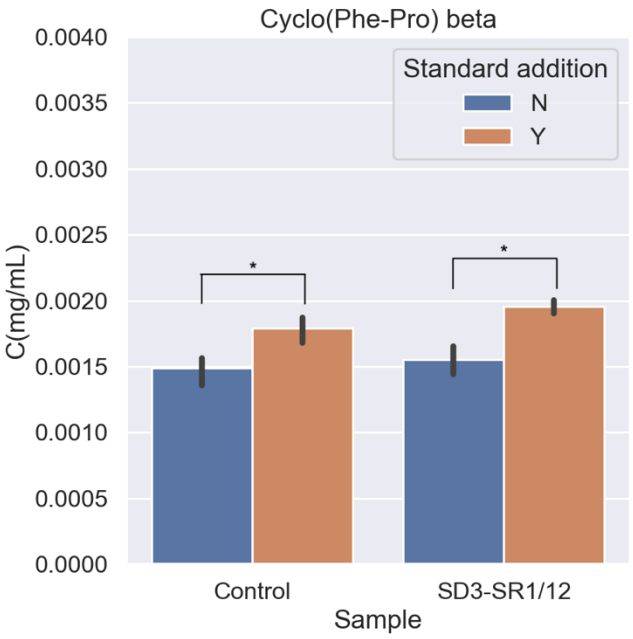



Figure 6-9 Cyclo(Phe-Pro) beta determined in Control and SD3-SR1/12 with or without Standard Addition Method. (n=3). Statistical analysis was performed at each sample between two different conditions. Significant difference: * $p<0.05$

The concentration of Cyclo(Phe-Pro) beta was higher when determined via standard addition method both in Control and SD3-SR1/12 coffee samples. The statistical analysis showed that whilst there was a significant difference ($p<0.05$) in the calculated concentration of Cyclo(Phe-Pro) beta, the range of the values was at the same order of magnitude (0.0015-0.0020 mg/mL). Considering that the determined concentration would be the baseline to spike and double or triple the amount of the given compound in a coffee solution, such a difference was considered small.

In principle, the ionisation of a given metabolite depends on the chemical structure. The closer the structure of the internal standard to the structure of the metabolites of interest then the more similar the ionisation degree in the electrospray ionisation step. Comparing the chemical structures of compounds of interest and internal standard it can be seen that sinapic acid shares a benzene

ring with all the metabolites of interest apart from cyclo(Pro-Val) and Mannotetraose (Figure 6-10). Sinapic acid was initially selected as internal standard for quantifying polyphenols (i.e. metabolites with benzene rings) but this selection was also indicated as suitable for the quantification of the cyclo-dipeptides, with or without a standard addition approach.

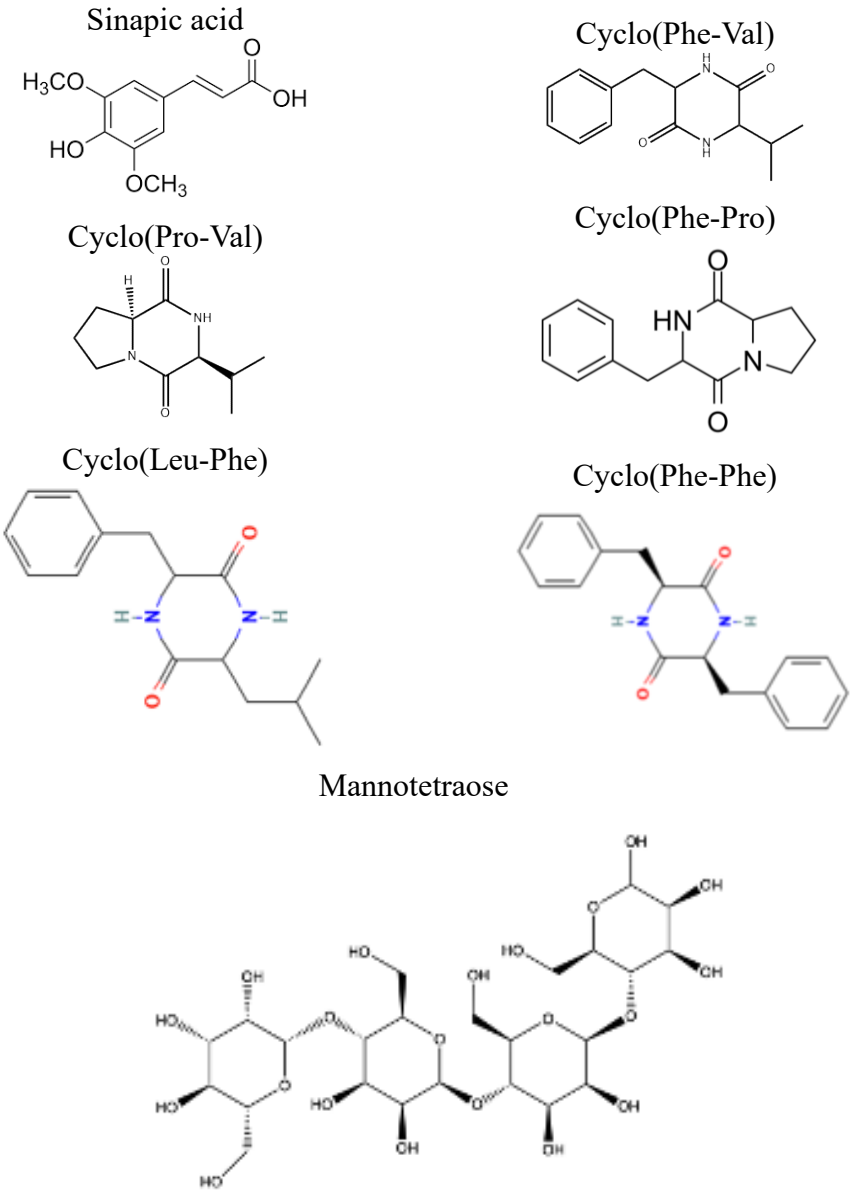



Figure 6-10 Chemical structure of key foam targets and internal standard

### 6.3.3 Estimating the concentration of Mannotetraose

According to the present data, it was not possible to quantify Mannotetraose in coffee via standard addition method. However, an estimation of concentration was vital for the spiking and foaming experiment.

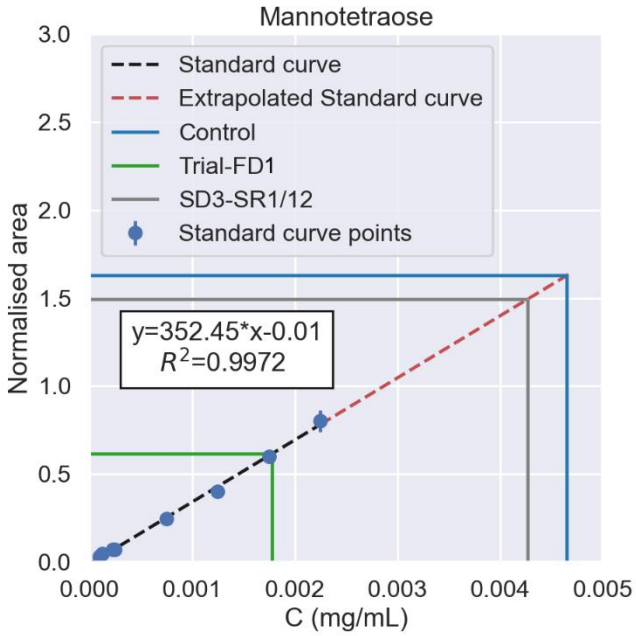



Figure 6-11 Standard curve for Mannotetraose. Standard curve was prepared without standard addition method.

The Mannotetraose content in control coffee without standard addition was calculated by extrapolation and its value was 0.0047±0.0002 mg/mL (Figure 6-11). Mannotetraose content of the same sample using the data provided by JDE and (Lopes *et al.*, 2021) was calculated in section 6.3.1 as 0.047 to 0.14 mg/mL. Even though one value was calculated by extrapolating the standard curve, which by itself leads to unreliability, the two calculated values are very different. Especially, the value estimated from bibliography was 10 to 29.8 times higher than the value from the standard curve without standard addition.

The explanation for this big difference may lie to the fact that distribution of degree of polymerisation includes only the free mannose oligomers that are products of degradation of chains with higher molecular weight. On the other hand, the cited authors (Lopes *et al.*, 2021) have performed hydrolysis of the instant coffee and measured the total mannose monomers. According to the literature (Viani, Rinantonio; Petracco, 2012), during the roasting process, monosaccharides are coupled with amino acids or chlorogenic acids for the creation of melanoidins or humic acid respectively. Also, high molecular weight polysaccharides are forming amino acid-polysaccharide complexes. During coffee extraction in the instant coffee process, the secondary and tertiary extraction steps are performed at high temperatures (T>180˚C). The application of such high temperature could break down the high molecular and insoluble polymers and thus increases the yield of the extraction (Vltzthum and Koch, 1995). In the end, instant coffee contains low molecular weight carbohydrate-amino acid-chlorogenic acid complexes. Therefore, if an instant coffee sample undergoes acid hydrolysis, the mannose content that would be determined would originate from the native mannose oligomers and the carbohydrate-amino acid-chlorogenic acid complexes. For this reason, it was suggested that the mannose content in instant coffee that corresponds to the native mannose oligomers was lower than the percentage reported by Lopes et al. (2021)(i.e. 6.1% w/w on dry instant coffee basis).

Estimating the Mannotetraose concentration through literature requires a series of assumptions which may result in unreliable results. However, determining the concentration via extrapolating the standard curve without standard addition

seems a more reliable way. In that case, it is assumed that a) the slope and intercept remain the same regardless of appending more standard curve points and b) the matrix effect does not influence the ionisation of Mannotetraose.

It is important to highlight that the chemical analysis without standard addition method was performed on Trial-FD1. Although, the amount of Trial-FD1 freeze-dried coffee was enough to perform the chemical analysis with standard addition method, it was not enough for the spiking and foaming experiments which is acknowledged as a limitation. Therefore, another instant coffee sample which had low foam quality performance had to be used and that was Trial-FD5 coffee sample.

The concentration of Mannotetraose in Control and SD3-SR1/12 was calculated via extrapolation (see Figure 6-11). The concentration of Trial-FD5 was estimated to be the same as Trial-FD1, as the normalised area of Mannotetraose for both coffee samples (i.e. Trial-FD5 and Trial-FD1) was very similar (0.59±0.05 and 0.61±0.03) and not significantly different ($p>0.05$). The estimated concentration of Mannotetraose in Control, SD3-SR1/12 and Trial-FD5 samples is presented in Table 6.5.

Table 6.5 Estimated concentration of Mannotetraose in Control, SD3-SR1/12 and Trial-FD5

| Sample | Estimated concentration (mg/mL) |
|---|---|
| Control | 0.0047±0.0002 |
| SD3-SR1/12 | 0.0043±0.0003 |
| Trial-FD5 | 0.0018±0.0001 |

### 6.3.4 Assessing the foam quality of spiked instant coffees with key foam metabolites.

**Optimising foaming parameters**

This set of experiments was performed by employing the Dynamic Foam Analyser, DFA 100 instead of using the foam quality assessment method that was developed in Chapter 3: because it could perform not only foam height measurements but also foam structure measurements. The aeration step was performed by a stirring method and a trial experiment was performed in order to optimise the aeration time. The sample that was used for this experiment was a Control instant coffee (1.5% w/w). The working volume of experiments was 55 mL as the minimum suggested amount by the manufacturer was 50 mL. The stirring speed was at its maximum level of 8000 rpm. The statistical analysis showed that the foam height significantly increased after 10 seconds of aeration and then reached a plateau which continued up until 60 seconds of aeration. Therefore, the aeration time that was used for the spiking experiments was 30 seconds.

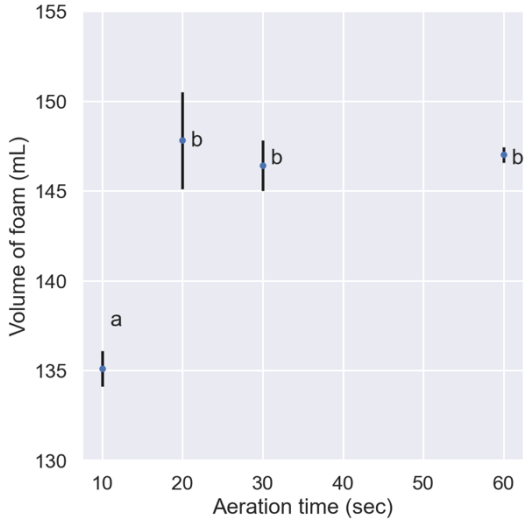



Figure 6-12 Control's coffee foam aerated at different aeration times. n=3. Different letters indicate a significant difference between samples at $p<0.05$.

The initial aeration and data acquisition parameters that were used are presented in Table 6.6.

Table 6.6 Initial foaming and data acquisition parameters

| | Parameter | Value |
|---|---|---|
| Instrument setup | Column | CY4572 - 40 mm prism |
| | Stirrer | SR4501 |
| | Height illumination | Infrared - λ = 850 nm at 15% |
| | Speed | 8000 rpm |
| | Foaming time | 30 seconds |
| | Oscillation period | 0 seconds |
| Data sampling | Height Foaming | 5 fps |
| | Height Decay | 10 fps |
| | Structure Foaming | 2 fps |
| | Structure Decay | 2 fpd |
| | Camera height | 55 mm |
| | Camera position | 3 |

**Spiking experiments**

Trial-FD5 was selected for spiking experiments as the initial concentration of key metabolites was at the lowest level compared to other coffees. This meant that fewer grams of expensive chemical reference standards were used for spiking compared to using Control coffee or SD3-SR1/12. Additionally, Trial-FD5 was a sample with poor foaming quality, so increasing the concentration of chemical compounds that were associated with good foam quality could potentially enhance the coffee's foam performance. The native concentration of candidate molecules in Trial-FD5 coffee is presented in Figure 6-13.

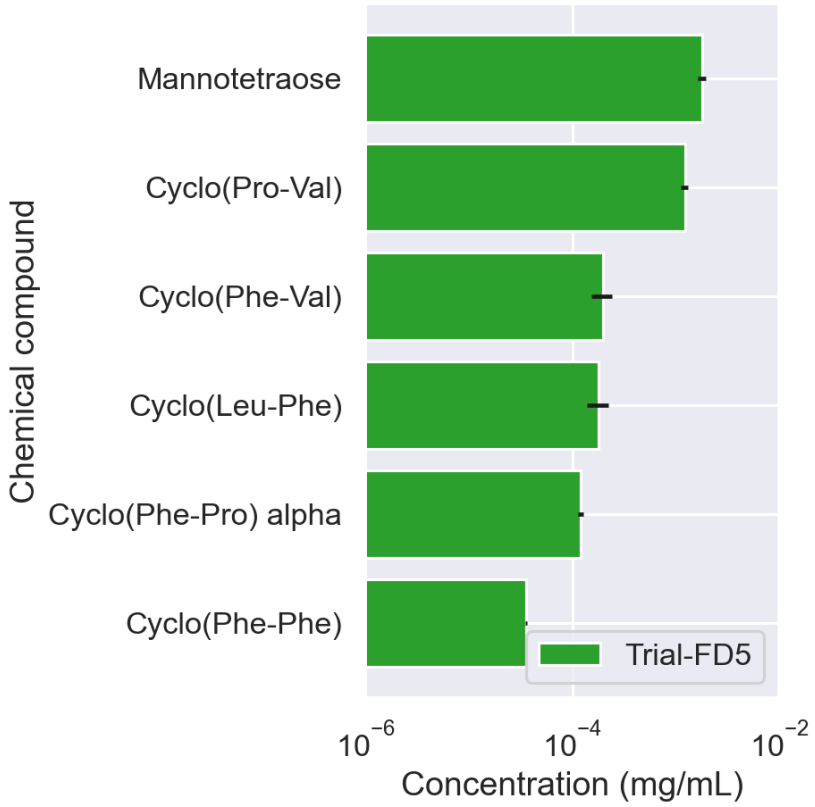



Figure 6-13 Baseline concentration for Trial-FD5.

Only Mannotetraose was solubilised in water. The rest, all cyclo dipeptides, were solubilised in either absolute ethanol or DMSO (Table 6.7). Therefore, by mixing an aliquot of 1 mL of spiking solution with 169 mL of coffee solution, it would result in spiked coffee solution where diluent would be 99.41% ultra-pure water and 0.59% ethanol or DMSO. For this reason, it was important to assess the foam quality of three blanks of Trial-FD5 coffee. The first blank consisted of 1.5% w/w coffee solids in 100% ultra-pure water. The other two blank samples were of the same concentration in solids, but the diluent was 99.41%-0.59% ultra-pure water – ethanol or ultra-pure water – DMSO.

Table 6.7 Key foam compounds and preferred solvent

| Compound | Dissolves In |
|---|---|
| Mannotetraose | Water |
| Cyclo(Pro-Val)<br>Cyclo(Phe-Val)<br>Cyclo(Leu-Phe) | EtOH |
| Cyclo(Phe-Phe)<br>Cyclo(Phe-Pro) | DMSO |

**Foam quality measurements**

The volume of foam vs time measurement for blank Trial-FD5 samples is presented in Figure 6-14. It is observed that addition of 0.59% EtOH or 0.59 % DMSO increased the foam stability. It is hypothesised that amphiphilic and antifoaming compounds were selectively solubilised in either solvent thus these were not present on the air/beverage interface and therefore did not destabilise the created foam.

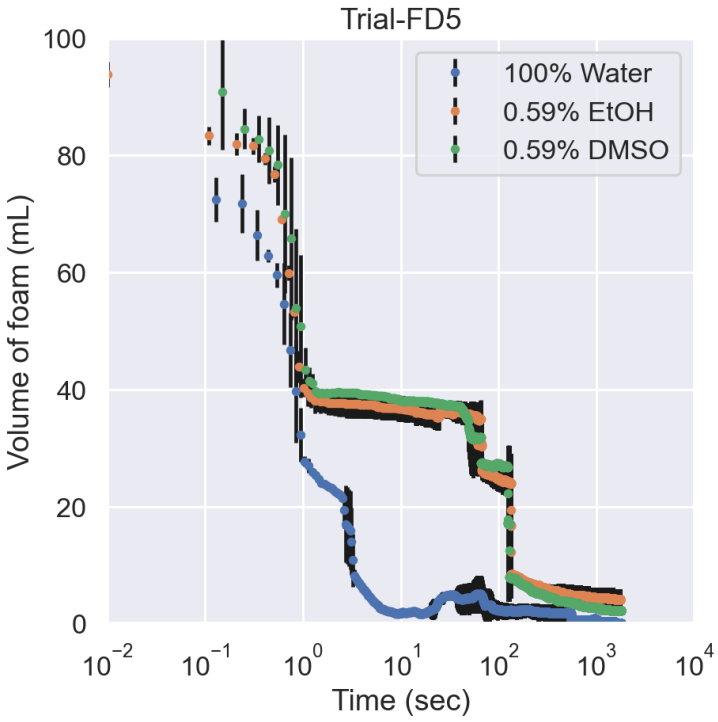



Figure 6-14 Volume of foam vs time plot for Trial-FD5 blanks.

Since the addition of such a small percentage of ethanol or DMSO affected the volume of foam curve, it was attempted to solubilise the candidate molecules in water. With a partition coefficient of -8, Mannotetraose was easily solubilised in water. Despite the positive LogP values of Cyclo(Pro-Val) and Cyclo(Phe-Pro), these chemical standards were also solubilised in ultra-pure water

Table 6.8 Partition coefficient values for key foam targets. Values of LogP were retrieved by https://pubchem.ncbi.nlm.nih.gov/

| Chemical compound | LogP | Dissolved in water? |
|---|---|---|
| Mannotetraose | -8 | Yes |
| Cyclo(Pro-Val) | 0.8 | Yes |
| Cyclo(Phe-Pro) | 1.4 | Yes |
| Cyclo(Phe-Val) | 2 | No |
| Cyclo(Leu-Phe) | 2.4 | No |
| Cyclo(Phe-Phe) | 2.7 | No |

The volume of foam vs time plots for Trial-FD5 spiked with different concentrations(i.e. $C_o$*2.5, $C_o$*5, $C_o$*7.5) of Mannotetraose and Cyclo(Pro-Val) are presented in Figure 6-15 and Figure 6-16. In the Mannotetraose plot (Figure 6-15), it is observed that by increasing the concentration of the key chemical compound this tends to stabilise the foam height. However, there are some inconsistencies among the replicates. In the case of Cyclo(Pro-Val) (Figure 6-16), inconsistencies between the replicates were present. Despite attempting to increase the number of replicates from three to six in order to tackle the inconsistency this was not achieved. Instead, the variation was even larger.

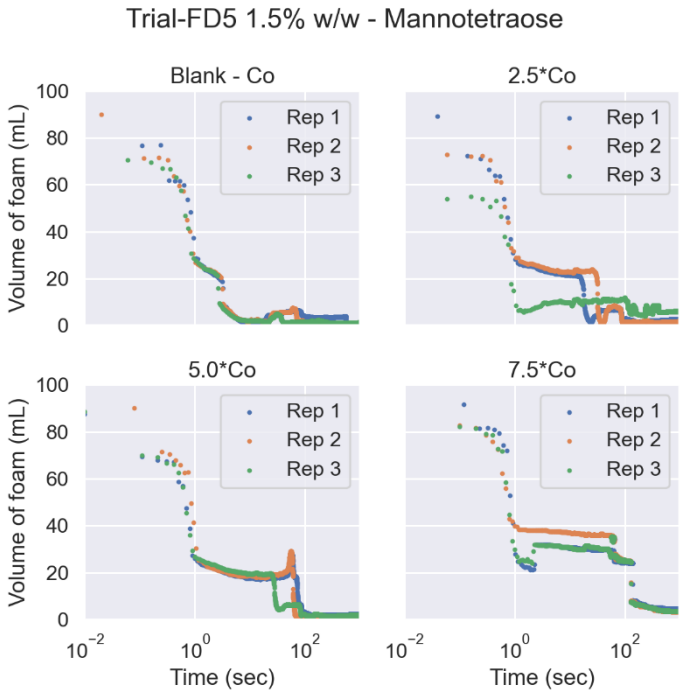



Figure 6-15 Volume of foam vs time plots for Trial-FD5 spiked with Mannotetraose at different concentrations. Top left: Blank - Co, Top right: Spiked x2.5, Bottom left: Spiked x5, Bottom right: Spiked x7.5.

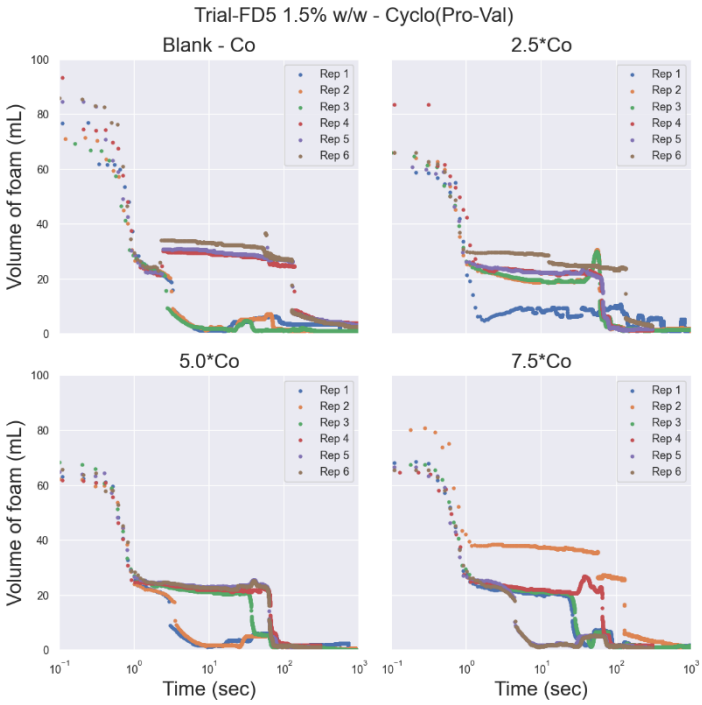



Figure 6-16 Volume of foam vs time plots for Trial-FD5 spiked with Cyclo(Pro-Val) at different concentrations. Top left: Blank - Co, Top right: Spiked x2.5, Bottom left: Spiked x5, Bottom right: Spiked x7.5.

In order to tackle this effect, the foam height generated curve was compared with snapshots captured during the measurement (Figure 6-17). The approach was to

compare what the DFA100 sensors perceive as foam height and what was observed by the snapshots. At the first moments of measurement (Figure 6-17a), the coffee sample reaches its maximum height. At this point, the aeration step was completed, and the coffee sample had its maximum kinetic energy provided by the stirrer. Between 0.1 and 1 sec of measurement (Figure 6-17b) the height collapsed instantly. It is observed that the sample is divided into two regions. On the top of the vessel, a foam structure has been created and below that, there was mixture of bubbles and liquid. As the time of measurement increased (Figure 6-17 c,d) the foam head became larger while the colour of liquid below was darker. This was observed because the bubbles that were created during aeration were rising and accumulated to the top. It is concluded that the installed sensors of DFA 100 were not able to determine the line between the foam structure and the liquid.

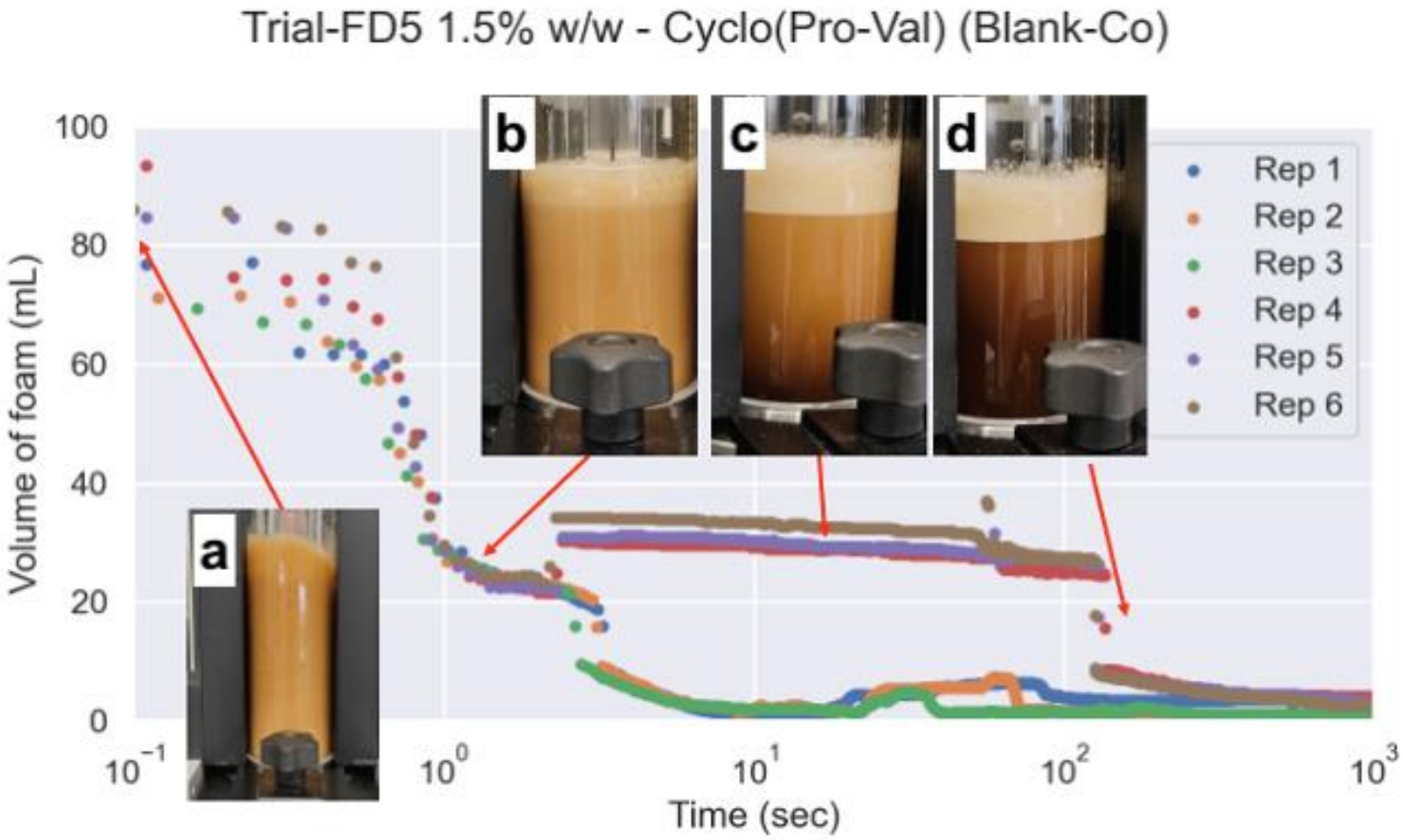



Figure 6-17 Volume of foam vs time for Blank Trial-FD5

The inability of the sensors to accurately identify the foam height relied on a specific parameter of the instrument. The principle of foam height detection is presented in Figure 6-18. A LED panel on one side of the column emits light while on the other end of the column, a photo detector is placed. At the areas where the light is scattered due to the presence of bubbles, the instrument determines this area as foam. The foam/liquid border is directly associated with the illumination degree of LED panel.

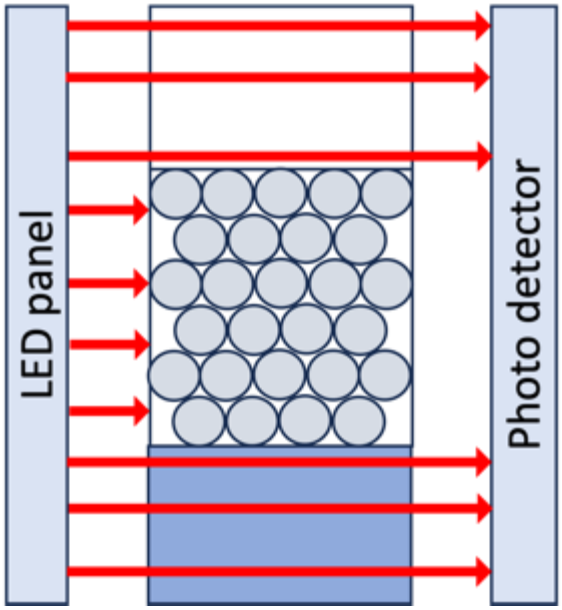



Figure 6-18 Principle of foam height detection for Dynamic Foam Analyser. Schematic adapted by Shankaran and Chinnaswamy (2019).

The inconsistency of foam height measurements was attributed to the fact that with illumination value at 15%, the instrument was unable to precisely identify the foam/liquid border. However, this was achieved successfully with illumination value at 5% (Figure 6-19).

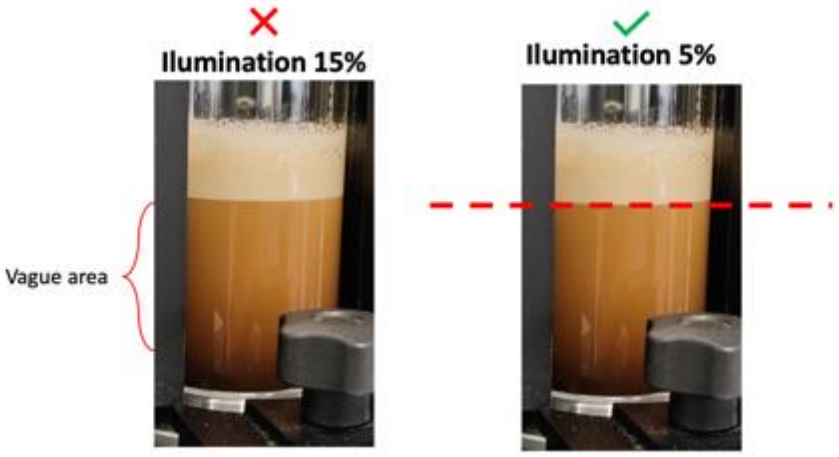



Figure 6-19 Effect of illumination value for identifying the foam height level.

**Foam quality measurements with optimised data acquisition parameters**

The experiment was repeated by setting the LED panel illumination at 5%. Mannotetraose, Cyclo(Phe-Pro) and Cyclo(Pro-Val) were spiked x2.5, x5.0 and x7.5 the initial concentration in Trial-FD5 and the volume of foam vs time and bubble count per $mm^2$ vs time plots are presented in Figure 6-20, Figure 6-21, Figure 6-22, Figure 6-23, Figure 6-24 and Figure 6-25. It is observed in the volume of foam vs time plots that during the first 10s there is initially a decrease in foam height and then (from about 2 until 10 seconds) the foam height increases (Figure 6-20, Figure 6-22, Figure 6-24). This is explained by the rising bubbles that accumulated at the foam on top of the liquid as described in (Figure 6-17b,c).

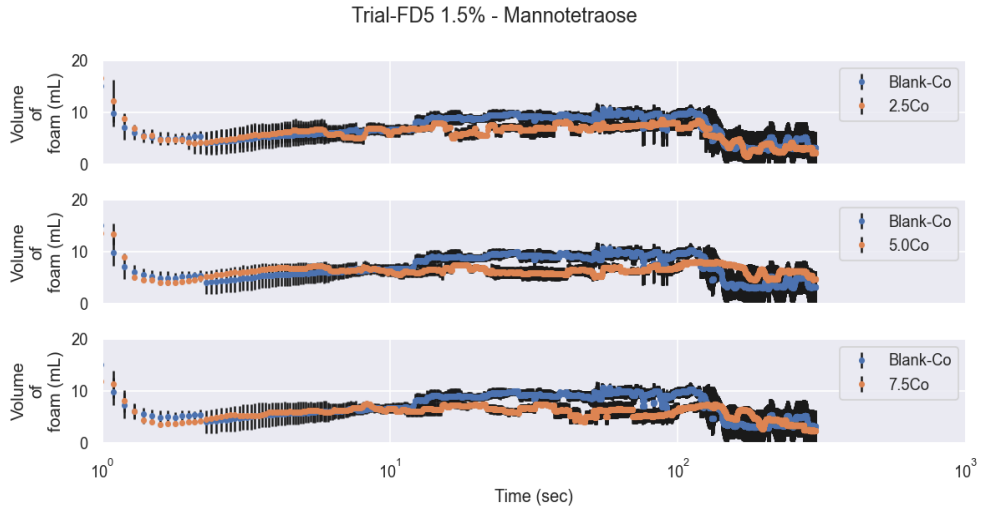



Figure 6-20 Volume of foam vs time plot for Trial-FD5 spiked with Mannotetraose x2.5, x5 and x7.5 (n=3). Error bars estimated by the device shown in black.

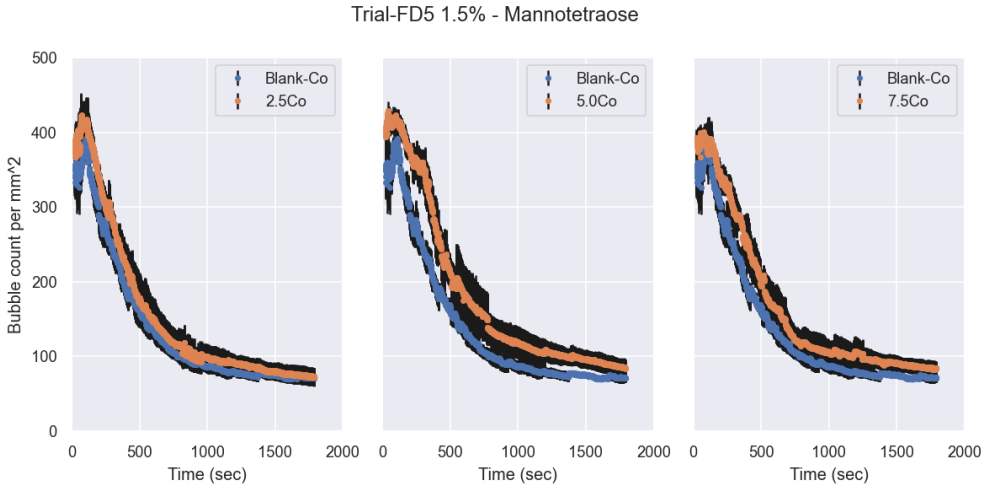



Figure 6-21 Bubble count per mm^2 vs time for Trial-FD5 instant coffee spiked x2.5 x5, x7.5 the initial concentration with Mannotetraose (n=3). Error bars estimated by the device shown in black.

In the case of Mannotetraose (Figure 6-20, Figure 6-21), the increase of its concentration did not affect either the volume of foam nor the bubble count per $mm^2$ when compared with the blank sample. This result could be expected as the Mannotetraose is a highly hydrophilic compound, and it is not expected to be adsorbed at the air/beverage interface.

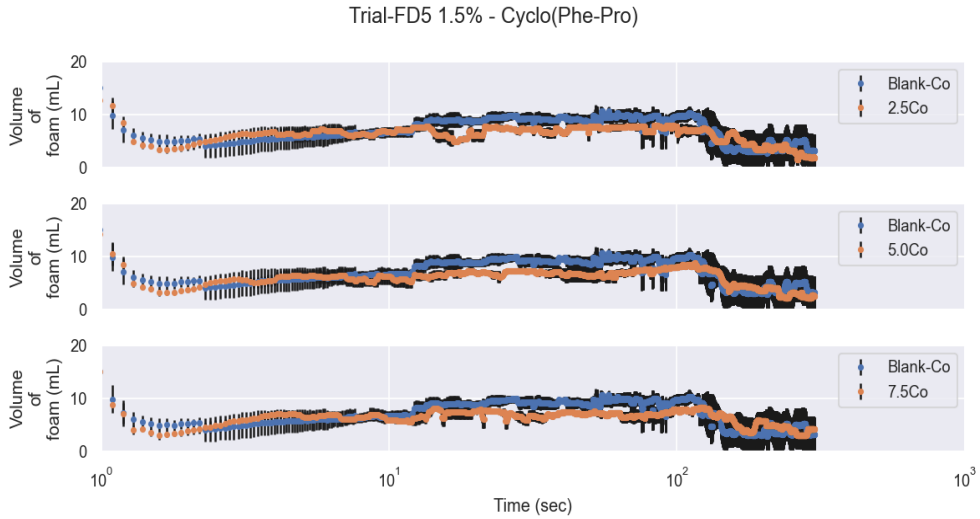



Figure 6-22 Volume of foam vs time plot for Trial-FD5 spiked with Cyclo(Phe-Pro) x2.5, x5 and x7.5.

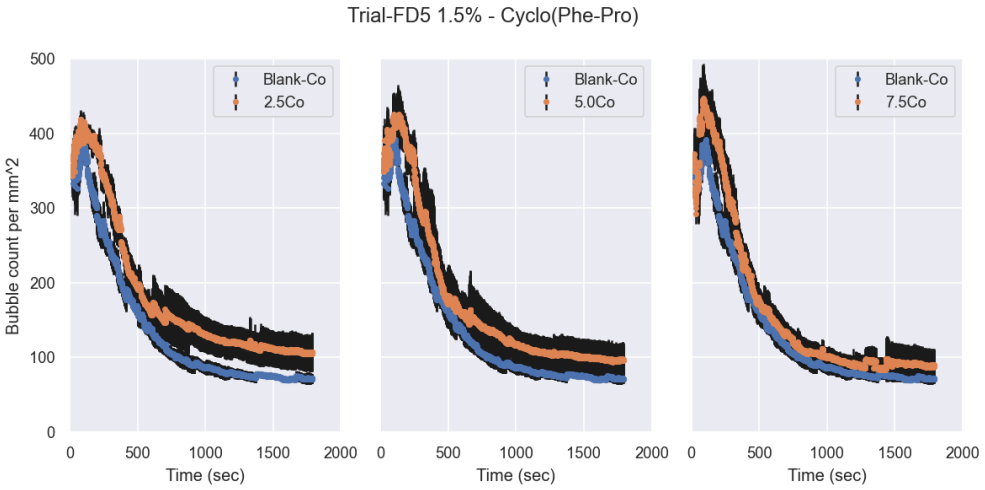



Figure 6-23 Bubble count per mm^2 vs time for Trial-FD5 instant coffee spiked x2.5 x5, x7.5 the initial concentration with Cyclo(Phe-Pro) (n=3).

As with Mannotetraose, no effect on volume of foam or bubble count was observed when the concentration of Cyclo(Phe-Pro) was increased in Trial-FD5 coffee (Figure 6-22, Figure 6-23).

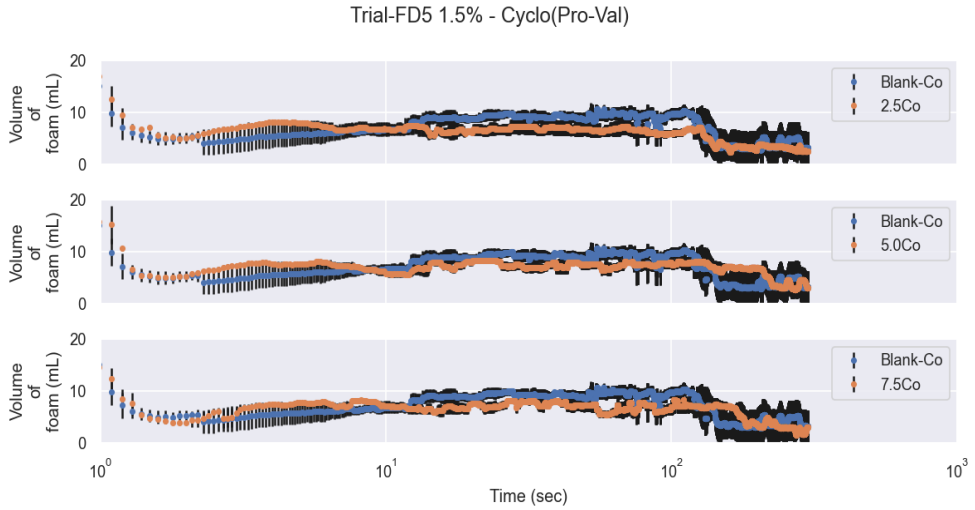



Figure 6-24 Volume of foam vs time plot for Trial-FD5 spiked with Cyclo(Pro-Val) x2.5, x5 and x7.5.

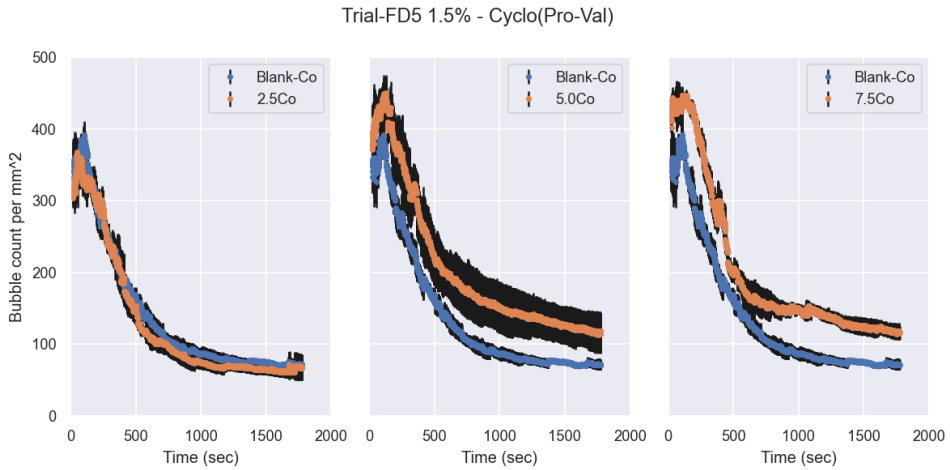



Figure 6-25 Bubble count per mm^2 vs time for Trial-FD5 instant coffee spiked x2.5 x5, x7.5 the initial concentration with Cyclo(Pro-Val (n=3).

In the case of Cyclo(Pro-Val), the increase of its concentration affected only the bubble count per $mm^2$ (Figure 6-25). It was observed that by increasing the concentration the spiked curves were above the blank curve which means that more bubbles were in the system at a given time. Therefore, the Cyclo(Pro-Val) may contribute to the creation of more bubbles per $mm^2$ after the aeration. This would mean that the presence of Cyclo(Pro-Val) may contribute in decreasing the coalescence rate of bubbles during the aeration step. Another hypothesis is

that Cyclo(Pro-Val) may contribute on lowering the foam disproportionation rate.

Given the difference in results using 5% illumination, the previous conclusions on the effect of 0.59% ethanol or DMSO on the foam height curves were reconsidered. As all Trial-FD5 coffee had been exhausted by the above experiments, the effects of 0.59% ethanol or DMSO on foam height and bubble structure was re-tested using a control instant coffee sample (Figure 6-26, Figure 6-27).

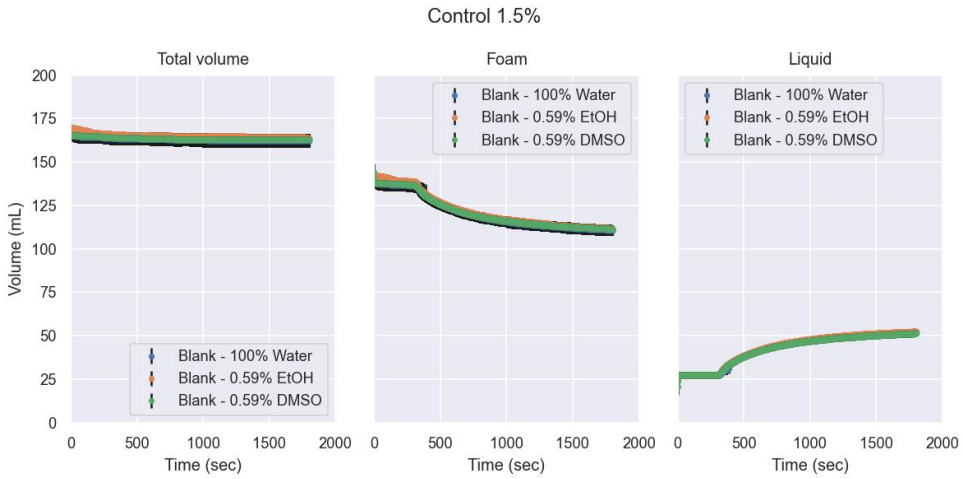



Figure 6-26 Effect of 0.59% EtOH or 0.59% DMSO in foam quality of control instant coffee (n=3).

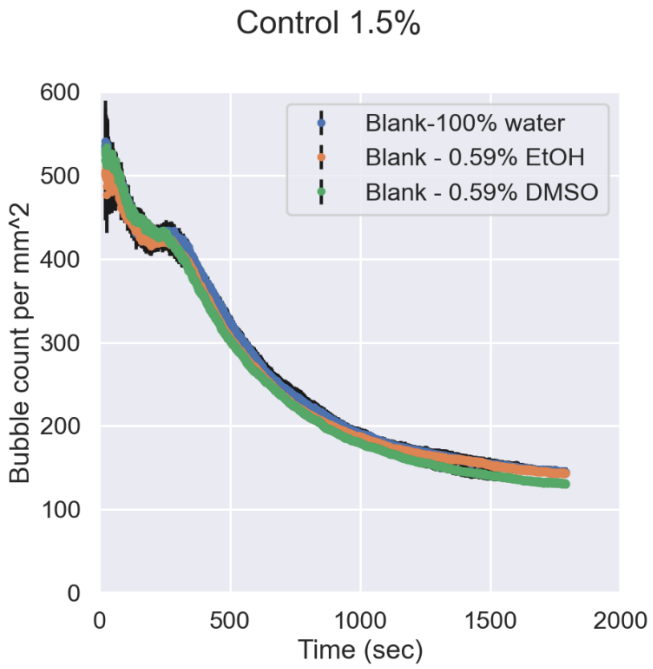



Figure 6-27 Effect of 0.59% EtOH or 0.59% DMSO in bubble count per mm^2 of control instant coffee (n=3).

It is observed that neither 0.59% ethanol nor DMSO had an effect on foam quality of control instant coffee, as there was no difference between the volume of foam and bubble count per $mm^2$ curves. At this point it is important to highlight a limitation of the Dynamic Foam Analyser. In Figure 6-26 of Liquid curve between t=0 and t<500 sec, the sensor detected a volume of liquid which was approximately 25 mL. This value did not correspond to reality because at the aeration step the liquid was transformed to 100% foam and no liquid remained accumulated at the bottom of the vessel. Essentially, the instrument was calibrated to detect the foam/liquid boundary when the liquid exceeded a certain limit. When time exceeded approximately 450 seconds, the sensor detected the actual boundary between foam and liquid.

Since there was not any effect of ethanol or DMSO on the foam height or bubble count per $mm^2$ for control coffee the chemical compounds that were not solubilised in water (i.e. Cyclo(Leu-Phe, Cyclo(Phe-Val), Cyclo(Phe-Phe)) were

spiked and the foam quality was assessed. The concentration of Cyclo(Leu-Phe) and Cyclo(Phe-Phe) in the spiked samples was ten times (x10) higher than the initial concentration of control. Also, all available grams of Cyclo(Phe-Val) were used therefore the final concentration of this compound was 5.9 times the initial concentration. The foam and bubble count per $mm^2$ curves are presented in Figure 6-28 to Figure 6-33. It was observed that none of the tested cyclo dipeptides affected the foam quality performance.

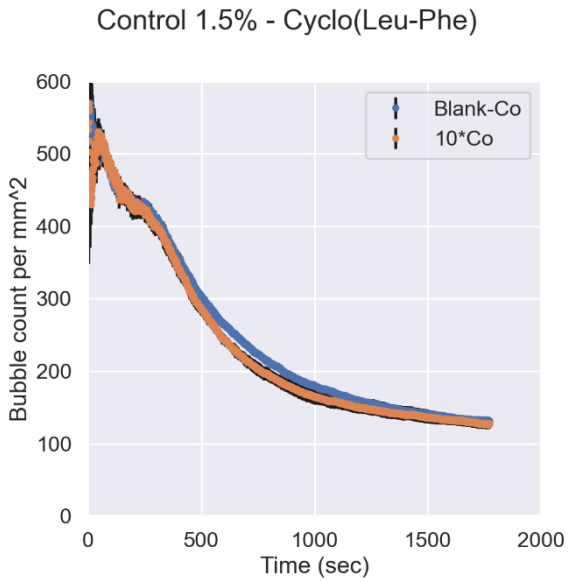



Figure 6-28 Bubble count per mm^2 vs time for Control instant coffee spiked x10 the initial concentration with Cyclo(Leu-Phe) (n=3).

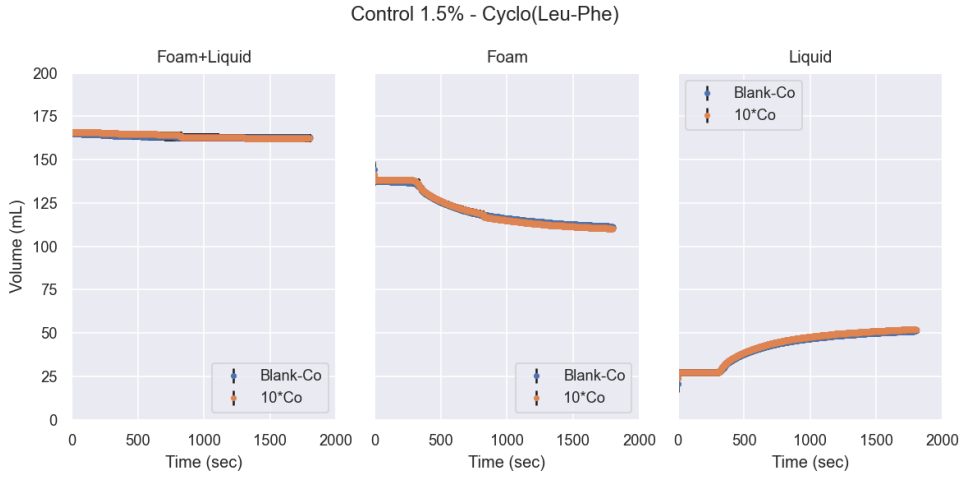



Figure 6-29 Foam quality vs time for Control instant coffee spiked x10 the initial concentration with Cyclo(Leu-Phe) (n=3).

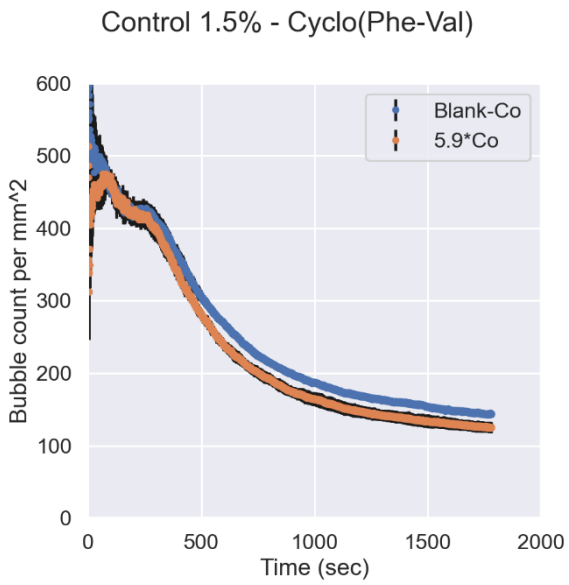



Figure 6-30 Bubble count per mm^2 vs time for Control instant coffee spiked x5.9 the initial concentration with Cyclo(Phe-Val) (n=3).

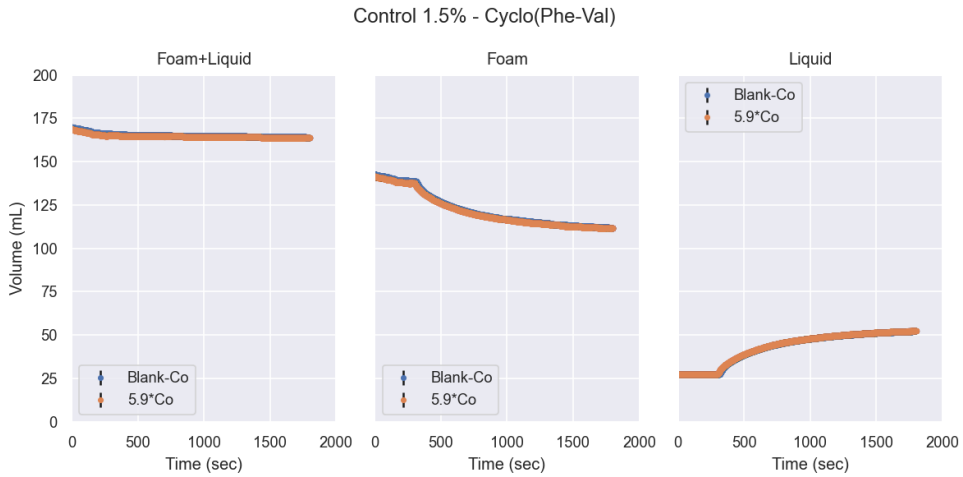



Figure 6-31 Foam quality vs time for Control instant coffee spiked x5.9 the initial concentration with Cyclo(Phe-Val) (n=3).

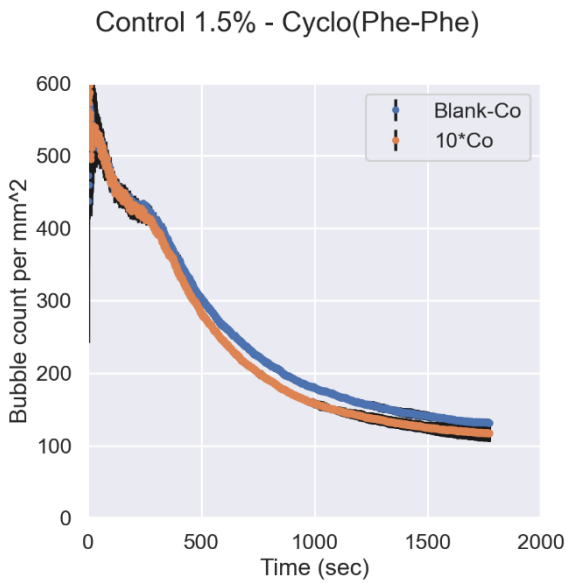



Figure 6-32 Bubble count per mm^2 vs time for Control instant coffee spiked x10 the initial concentration with Cyclo(Phe-Phe) (n=3).

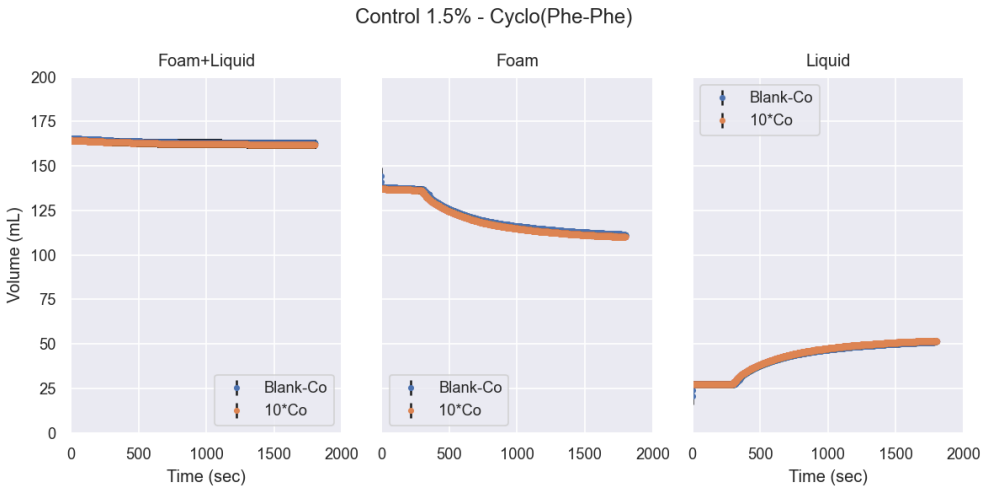



Figure 6-33 Foam quality vs time for Control instant coffee spiked x10 the initial concentration with Cyclo(Phe-Phel) (n=3).

**Role of Cyclo(Pro-Val) on foam quality**

Out of six key foam targets only Cyclo(Pro-Val) actively influenced foam quality performance in coffee. Apart from Mannotetraose, Cyclo(Pro-Val) was the least expected molecule to interact at the air/beverage interface because it has very small non polar areas compared to the rest of the cyclo-dipeptides (Figure 5-12).

In order to investigate the role of Cyclo(Pro-Val) on foam quality performance it was important to determine the dynamic surface tension of a pure solution and ultra-pure water at 20˚C. The surface tension of ultra-pure water was determined at 20˚C; 72.29±0.05 mN mN/m (Figure 6-34).

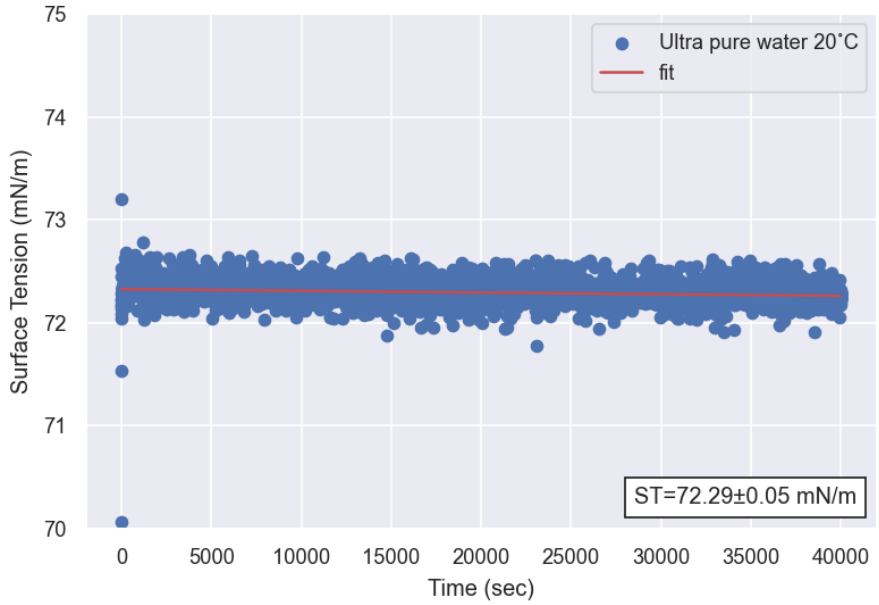



Figure 6-34 Surface tension of ultra-pure water at 20˚C

Cyclo(Pro-Val) was dissolved in ultra-pure water (C=0.0091 mg/mL) and the dynamic surface tension was measured (Figure 6-35). The concentration of Cyclo(Pro-Val) in pure solution was the same as Cyclo(Pro-Val) Trial-FD5 (x7.5*$C_o$) concentration of Figure 6-25. If Cyclo(Pro-Val) was a natural surface

active compound then a drop in surface tension would be observed. However, the surface tension of Cyclo(Pro-Val) was similar to ultra-pure water (Cyclo(Pro-Val): 72.47±0.04 mN/m; Ultra-pure water:72.78±0.03 mN/m). This result indicates that Cyclo(Pro-Val) may not adsorbed at the air/beverage interface (unless this happens in combination with other components).

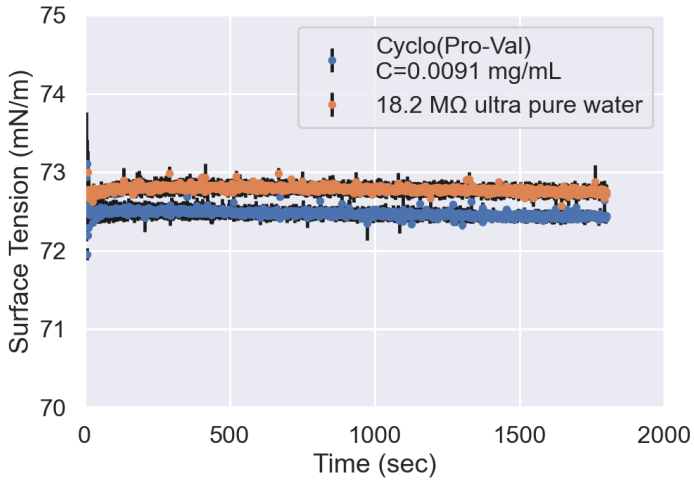



Figure 6-35 Dynamic surface tension of Cyclo(Pro-Val) and ultra-pure water at 20˚C (n=2).

It could be hypothesised that in a coffee foam system, Cyclo(Pro-Val) may be found in the lamellae between bubbles and would interact with other compounds. The oxygen atoms may interact with other polar areas of compounds, while the small aliphatic chain or the heterocyclic furan group may interact with non-polar areas of other compounds. Finally, these results may be the first indication of a synergistic effect on enhancing foam quality performance between Cyclo(Pro-Val) and other, yet unknown, compounds.

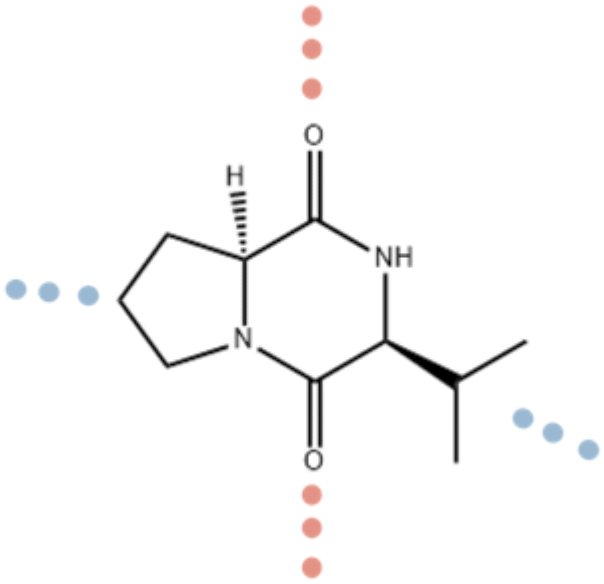



Figure 6-36 Schematic of Cyclo(Pro-Val). Red dots indicate polar-polar or charge-polar interaction. Blue indicates nonpolar interactions.

### 6.3.5 Dynamic surface tension of instant coffee

The aim of this experiment was to measure the dynamic surface tension of instant coffee and then artificially increase the concentration of key foam chemical compounds. It was hypothesised that by increasing the concentration of key metabolites, this would affect the dynamic surface tension curve. As described in the previous section, only Cyclo(Pro-Val) influenced the bubble count vs time plot, but it was proved that this compound was not surface active in pure water. Therefore, no spiking experiment was performed for Cyclo(Pro-Val). However, the dynamic surface tension at 20˚C for Control, SD3-SR1/12 and Trial-FD5 instant coffee was determined (Figure 6-37).

Foam quality assessment from Chapter 3:, showed that SD3-SR1/12 had the highest foam ability, followed by control while Trial-FD5 had the lowest foam ability. Therefore, it was expected at the first data point of measurement, the surface tension of Trial-FD5 would have the maximum value followed by Control and then SD3-SR1/12. However, this was not true as the first data points

for all samples were similar (see nested plot of Figure 6-37). It is important to highlight that the initial values of surface tension for all samples differ from the surface tension of ultra-pure water (72.29±0.05mN/m) which means that from the first moments of drop creation, surface active compounds were rapidly diffused and adsorbed on the air/beverage interface and decreased the surface tension.

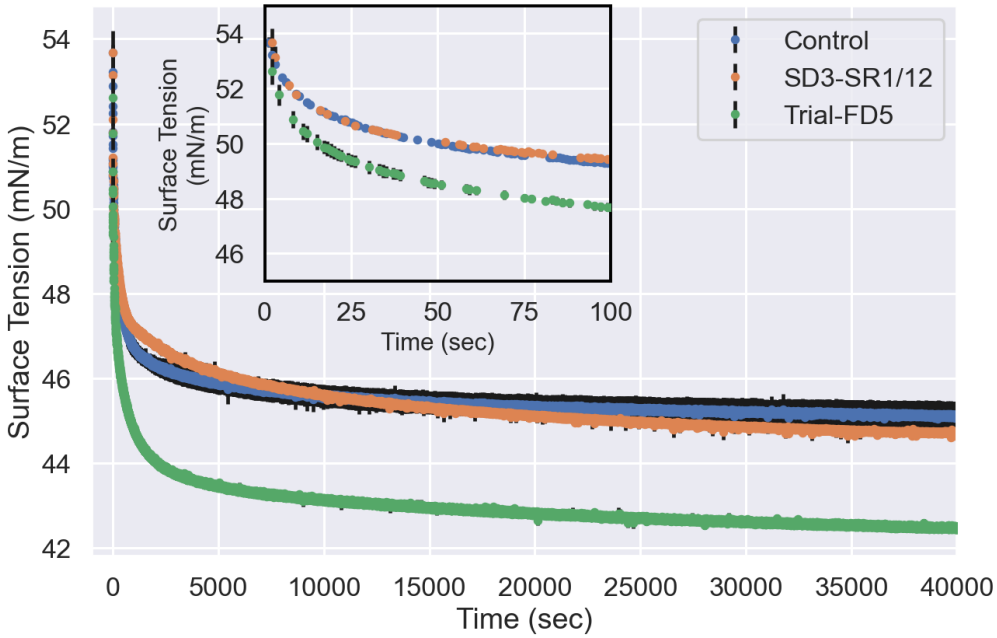



Figure 6-37 Dynamic surface tension for Control, SD3-SR1/12 and Trial-FD5 (n=2).

As the time of measurement increased, surface active compounds continued to be diffused and adsorbed on the interface which led to a further decrease of surface tension. At long times (i.e. time>10000 seconds), surface tension tends to reach an equilibrium, which shapes the dynamic surface tension of each coffee sample. It was observed that dynamic surface tension curves of Control and SD3-SR1/12 were similar, but the curve of Trial-FD5 reduced the surface tension more than the rest of the tested samples. This observation was not expected, because Trial-FD5 had very poor foam ability compared to Control and SD3-SR1/12.

In order to quantify the observed differences, surface tension vs time data has to be fitted in a relevant equation to estimate the diffusion coefficient. Ward and Tordai (1946) have proposed an equation which described the time dependent and diffusion-controlled adsorption of surface-active compounds (Equation 6.1).

Equation 6.1 Time dependent surface tension

$$\sigma(t) = \sigma_o - 2k_B T \frac{n}{V} * \left(k_d * \frac{t}{\pi}\right)^{\frac{1}{2}} \qquad \text{(Equation 6.1)}$$

Where:

| | | Units |
|---|---|---|
| t | Time | sec |
| $\sigma(t)$ | Surface tension | mN/m |
| $\sigma_o$ | Surface tension when t->0 | mN/m |
| $k_B$ | Boltzmann constant | J/K |
| T | Temperature | K |
| $n$ | Moles of Surfactant | mol |
| V | Droplet volume | $m^3$ |
| $k_d$ | diffusion coefficient | $m^2 * s^{-1} * mol^{-2}$ |

It is important to highlight that Equation 6.1 describes the surface tension of only one surface active compound, which is determined by its bulk concentration (ie. C=n/V) and by its diffusion coefficient ($k_d$). In the case of coffee, it is hypothesised that several surface-active compounds were present in the system and each compound's bulk concentration was not known. Therefore, by fitting the surface tension data it was possible to estimate the diffusivity of all surface-active compounds in coffee. Diffusivity was determined as:

$$\text{Diff} = n * \sqrt{k_d}$$

Therefore, Equation 6.2 was written as:

Equation 6.2 Time depended surface tension equation, adapted for coffee samples.

$$\sigma(t) = \sigma_o - \frac{2k_B T}{V} \text{Diff} * \left(\frac{t}{\pi}\right)^{\frac{1}{2}} \qquad \text{(Equation 6.2)}$$

Equation 6.2 is essentially a linear equation in the square root of time, where $\sigma_o$ is the intercept and $\frac{2k_B TDiff}{V\sqrt{\pi}}$ is the slope.

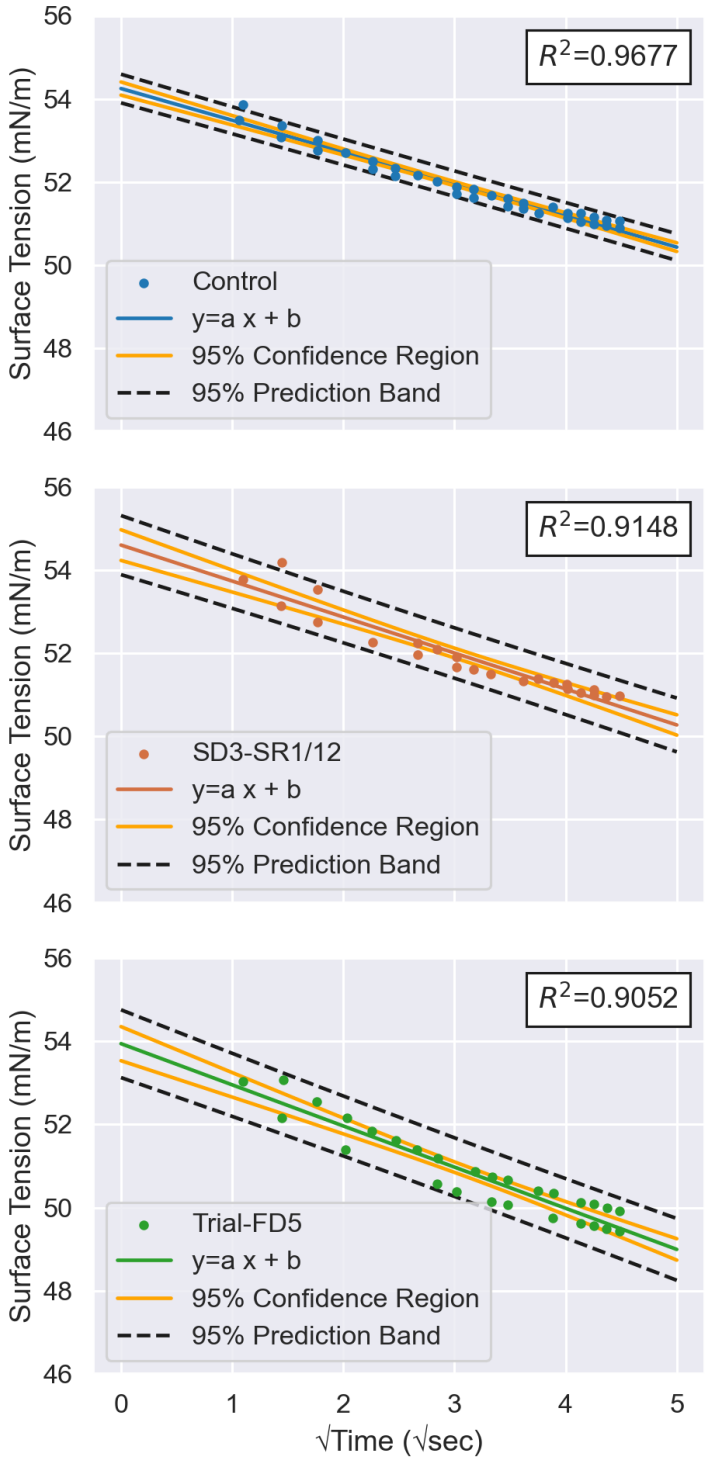



Figure 6-38 Fitted data of surface tension vs$\sqrt{time}$ for Control, SD3-SR1/12 and Trial-FD5

The fitted equation for the coffee samples is presented in Figure 6-38. As described in Chapter 3:, along with each fitted curve, a 95% confidence band and a 95% prediction band are displayed in the plot. The confidence band is the confidence region for the fitted equation. The prediction band is the region that contains approximately 95% of the measurements. The value of $n * \sqrt{k_d}$ was calculated by solving (Equation 6.3), and $\sigma_o$ was determined by extrapolating the linear equation to t=0. The data are presented in Figure 6-39.

Equation 6.3 Slope of Equation 6.2

$$\frac{2k_B Tn * \sqrt{k_d}}{V\sqrt{\pi}} = -\text{slope} \qquad \text{(Equation 6.3)}$$

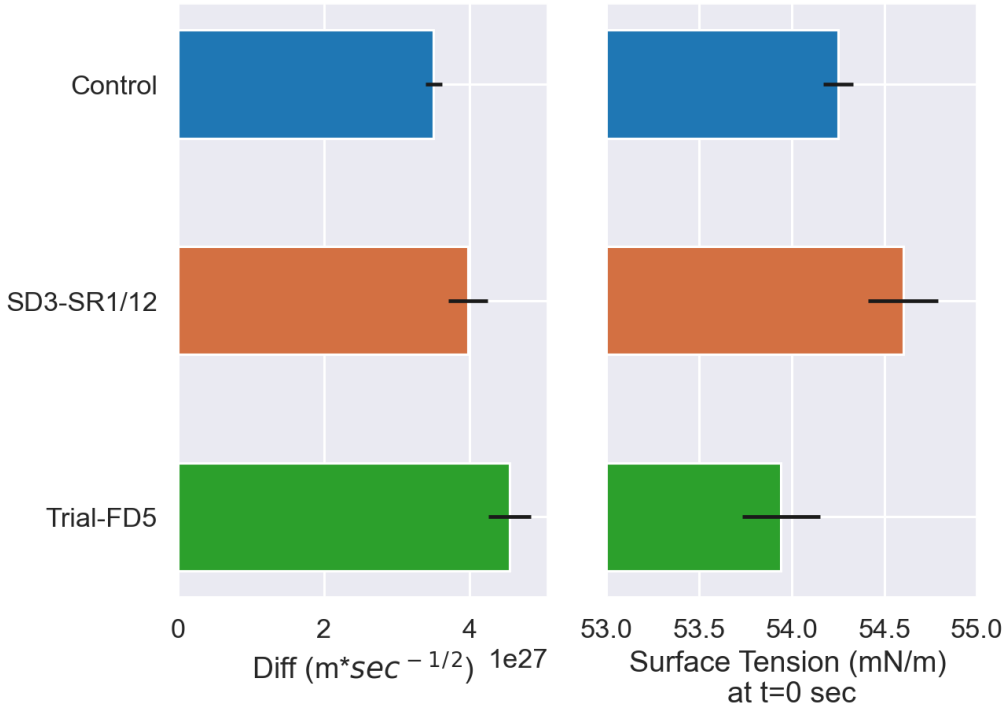



Figure 6-39 Diff and Surface tension at t=0 sec as calculated for Control, SD3-SR1/12 and Trial-FD5.

As these data were estimated by fitting the raw data points to a linear equation, as per foam quality parameters, the standard errors were estimated by covariance (pcov) square matrix of optimal parameters (popt). Therefore, one-way ANOVA was not possible to be performed. However, the diffusivity of Trial-FD5 had the

highest value compared to SD3-SR1/12 and Control, without any standard error bar of a given sample overlapping any other sample. Also, SD3-SR1/12 had the highest surface tension at t=0 without overlapping with the rest of coffee samples. These results describe indeed Trial-FD5 had the lowest surface tension at t=0 with the highest diffusivity.

This model described in a sufficient degree the time-dependent surface tension of coffee samples for the first moments of measurement. However, there was a scope for higher calculated $R^2$ values. This may be attributed to the fact that Equation 6.1 describes the dynamic surface tension of only one surface active compound. This means that a given surface-active compound is the only chemical compound solubilised in a given diluent (Figure 6-40a). On the other hand, the soluble solids which comprise the coffee matrix are divided in surface-active compounds and non-surface-active compounds (Figure 6-40b). This means that a given surface-active compound while diffusing towards the air/liquid interface would interact not only with water molecules but also with other solubilised compounds and therefore could meet a specific resistance if the two interacted. The intermolecular interactions of solubilised compounds are not considered in Ward and Tordai equation.

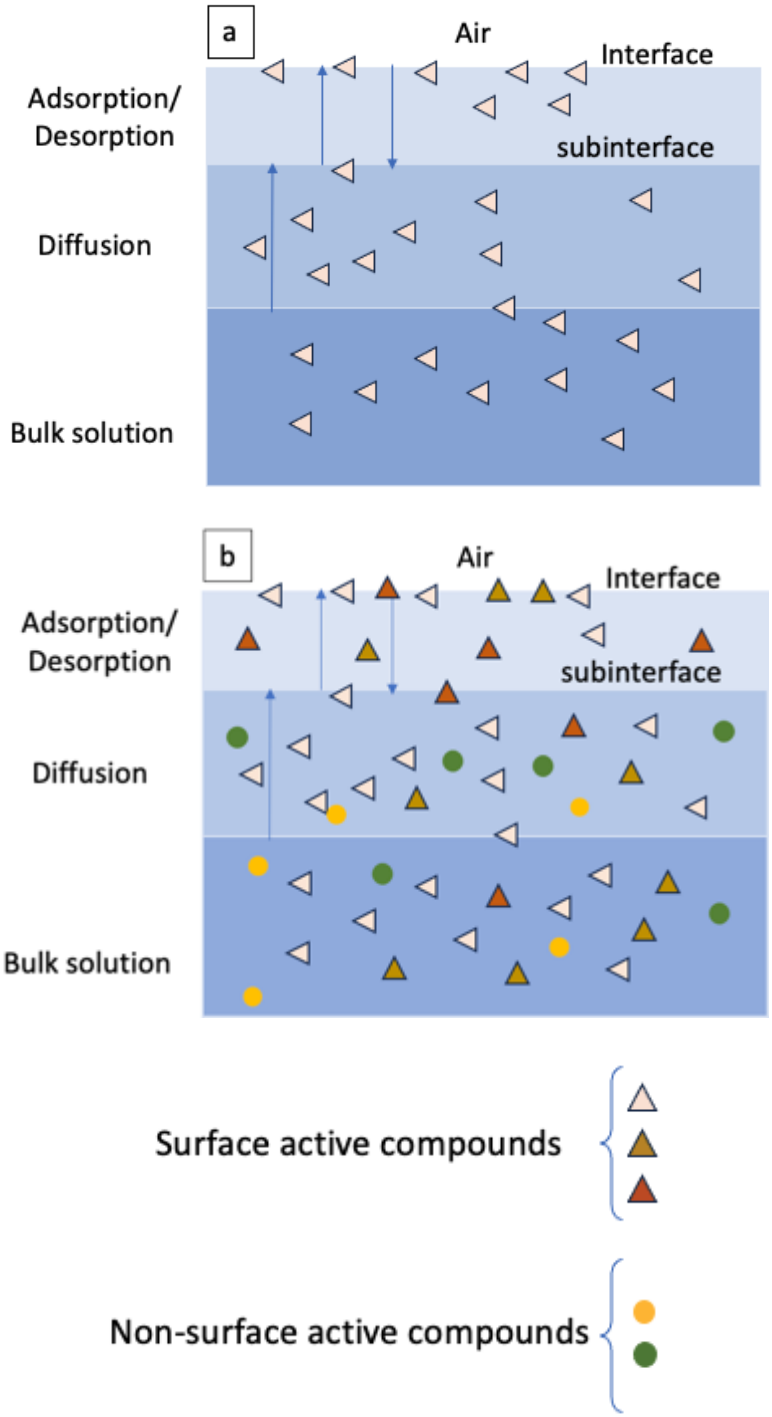



Figure 6-40 Schematic representation of diffusion-controlled adsorption of surface-active compounds as introduced by Ward and Tordai (1946).Ward and Tordai (1946). Figure (a) and (b) represents a pure surfactant solution and coffee solution respectively. Between interface and subinterface, only adsorption/desorption of surface-active compounds occurs. The thickness between interface and subinterface is a few molecular diameters. Just below subinterface, diffusion of soluble compounds occurs towards the interface. Image adapted by Chang and Franses (1995).

The fast diffusivity of surface-active compounds of Trial-FD5 compared to the rest of the sample set, still does not describe totally why the surface tension of the same sample had lower values to a greater extent than Control and SD3-SR1/12. It is important to highlight that the preparation of coffee solutions for surface tension experiments included a centrifugation step in order to remove insoluble particulates. This was mandatory because if insoluble particles were present in the formed drop, then these would accumulate at the bottom of the droplet which would eventually result in dragging it down and detaching it from the nozzle. On the other hand, centrifugation of the coffee samples was not included when prepared for foam quality assessment of Chapter 3:. It could be hypothesised that the lower values of surface tension for Trial-FD5 compared to Control might be attributed to the centrifugation step. For this reason, a Control and Trial-FD5 instant coffee were prepared as per section 3.2.5 (i.e. without centrifugation) and the surface tension was re-determined (Figure 6-41). It was observed that again, Trial-FD5 had lower surface tension values compared to Control, indicating that the centrifugation step had no effect.

These results suggest that Trial-FD5 coffee sample contains metabolites that decrease the surface-tension to a lower level than control coffee. However, the same metabolites fail to stabilise the generated interfaces during (and after) aeration. As described in Chapter 3:, the foam ability was assessed by creating a foam by disrupting the air/beverage interface and by entrapping air.

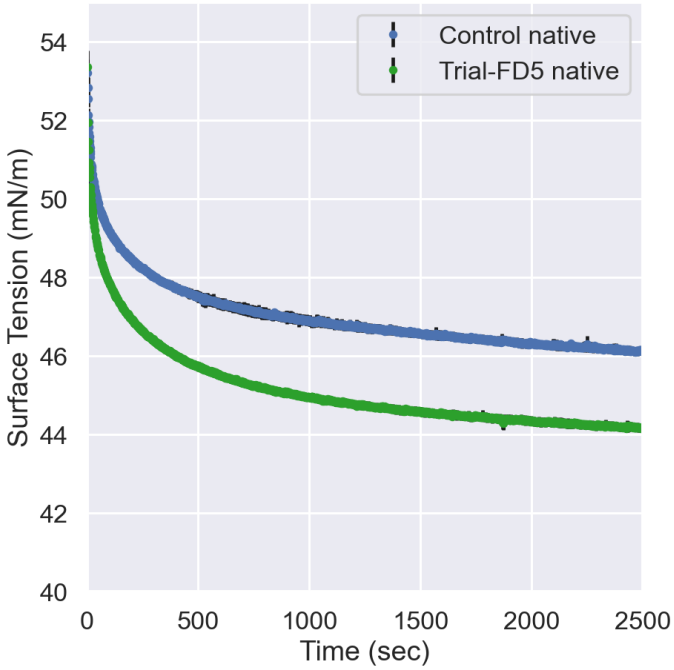



Figure 6-41 Surface tension of Control and Trial-FD5 for non-centrifuged samples (n=2)

The counter mechanism of air entrapment during the aeration step is bubble coalescence (Karakashev, 2017). Therefore, it could be hypothesised that the bubbles created by the surface-active compounds of Trial-FD5 were less able to inhibit bubble coalescence compared to the better-foaming samples, which resulted in lesser foam volume at the end of the aeration step.

## 6.4 Conclusions

In this chapter, the concentration of key foam metabolites was determined for Control, Trial-FD5 and SD3-SR1/12 instant coffee. It was found that the presence of coffee matrix affected the ionisation degree of the internal standard (i.e. Sinapic Acid), however the calculated concentration of Cyclo(Phe-Pro) was similar when using a traditional versus standard addition methodology. The spiking and foam assessment experiments showed that only Cyclo(Pro-Val) influenced the bubble count per $mm^2$ of coffee. It was found that Cyclo(Pro-Val) is not a surface active compound, but it may interact with other polar or non-

polar groups of other compounds and thus influence the foam quality of coffee. By fitting a diffusion-controlled model to dynamic surface tension data, it was found that the diffusivity of Trial-FD5 was higher than the rest of the sample set. Because Trial-FD5 actually has lower foam performance than the other samples, it was hypothesised that the group of compounds in Trial-FD5, which were associated with the lowering of dynamic surface tension were not able to prevent the coalescence rate during the aeration step. However, the same group of compounds were able to achieve lower surface tension values than the coffees with good foam quality (i.e. Control and SD3-SR1/12). In Chapter 3:, it was found that foam quality performance is highly dependent on roasting degree. Since Cyclo(Pro-Val) is a compound which is associated with foam quality, it is very important to consider if this compound is generated during coffee roasting.

# Chapter 7: Comparing the chemical profile of aqueous coffee brews across the roasting process and instant coffee manufacture

## 7.1 Introduction

In the previous chapter, it was established that key foam compound Cyclo(Pro-Val) actively influenced the foam structure of coffee. Chapter 3: illustrated that coffee foam quality is influenced by roasting degree. Since Cyclo(Pro-Val) influences foam quality it was important investigate if this compound is generated during roasting. This chapter aims to monitor the transformation of the chemical profile of coffee during the instant coffee manufacturing process (i.e. green bean, roasted bean, instant coffee). A targeted chemical analysis was employed to fine quantitate/screen polyphenols and key foam compounds. In addition, an untargeted chemical analysis was employed to shed light on chemical changes that occur during the coffee process. Finally, a correlation analysis between the whole bean colour and abundance of chemical entities was conducted in order to investigate which chemical compounds are associated with colour formation.

## 7.2 Materials and Methods

### 7.2.1 Chemicals

Reference standards (>95% pure) of 3-methylcatechol, 4-methylcatechol, Caffeic acid, Sinapic acid, Cyclo(-Leu-Phe), Cyclo(-Phe-Pro) and Dimethyl sulfoxide were acquired from Merck life sciences Ltd (Gillingham, UK). 3-O-Caffeoylquinic acid, 5-O-Caffeoylquinic acid, 3,4-Dicaffeoylquinic acid, 3,5-Dicaffeoylquinic acid, Cyclo(L-Phe-L-Val) and Cyclo(L-Pro-L-Val) were acquired from Cambridge Biosciences Ltd (Cambridge, UK). Cyclo(-Phe-Phe) was acquired from Generon LtD (Slough, UK). Mannotetraose was acquired from Megazyme (Wicklow, Ireland). Formic acid was acquired from Fisher Scientific (Loughborough, UK). Purine and Hexakis(1H, 1H, 3H-

tetrafluoropropoxy)phosphazine were acquired from Agilent Technologies (Cheadle, UK). HPLC grade methanol was acquired from VWR International Ltd (Lutterworth, UK).

### 7.2.2 Coffee samples

The coffee samples that were used in the present chapter, were introduced in Chapter 3:(Table 7.1, Table 7.2)In each case, samples represent a homogenous batch of single origin beans, taken through a variety of roasting or instant coffee manufacture processes.

Table 7.1 Green bean, roasted bean and instant coffee series

| Green Bean | Roasted bean | Instant coffee | Variety | Origin |
|---|---|---|---|---|
| T4 | TD4 | FD4 | 100% Arabica | Ethiopia Sidamo |
| T6 | TD6 | FD6 | 100% Robusta | Vietnam |

Table 7.2 Green and roasted whole beans

| Origin | Variety | Process | Roasting time (min) | | | |
|---|---|---|---|---|---|---|
| Nicaragua | 100% Arabica | Washed | 0 | 2 | 4 | 6 |
| Brazil | 100% Arabica | Unwashed | | | | |
| Vietnam | 100% Robusta | Unwashed | | | | |

### 7.2.3 Sample preparation for chemical analysis via high-resolution liquid chromatography-mass spectrometry

Green and roasted whole bean extracts were prepared as per sections 3.2.7 and 3.2.8 in Chapter 3:. Green bean, roasted bean and instant coffee solutions were prepared as per section 4.2.3 of Chapter 4:. The concentration of all samples was 0.15% w/w in solids and spiked with sinapic acid as internal standard at a final concentration of 0.007 mg/mL.

### 7.2.4 Fine quantitation and screening of polyphenols and key foam compounds in coffee samples via high-resolution liquid chromatography-mass spectrometry

The coffee samples of Table 7.1 and Table 7.2 were analysed in five replicates as per section 4.2.5 of Chapter 4:. Sinapic acid was used as internal standard at a final concentration of 0.007 mg/mL. 3-O-Caffeoylquinic acid, 5-O-Caffeoylquinic acid, 3,4-Dicaffeoylquinic acid, 3,5-Dicaffeoylquinic acid, 4,5-Dicaffeoylquinic acid and Mannotetraose were quantified in negative polarity while the cyclo-dipeptides were quantified in positive polarity mode. For fine quantification purposes, standard curves of key chemical compounds were created in absolute ethanol, ranging 1 ng/ml to 10 μg/ml. The abundance of polyphenols that were previously annotated via MS2 (as per subsection "MSI Level 1 and Level 2 identification of chemical entities" of section 4.3.1) was determined for all coffee samples (Table 7.1 and Table 7.2), as normalised to the internal standard.

### 7.2.5 Untargeted chemical analysis of coffee samples via high-resolution liquid chromatography-mass spectrometry

In parallel with chemical analysis for fine quantitation of candidate molecules, the same coffee samples were used for untargeted chemical analysis purposes. The methods of pre-conditioning, injection randomization, creation of QCs, acquisition, feature extraction and data analysis used were as described in section 5.2.4 and 5.2.5 of Chapter 5:.

### 7.2.6 Statistical analysis

One-way ANOVA was performed to investigate the effect of roasting degree (i.e. Roasting time 0 min; 2 min; 4 min; 6 min) and the effect of coffee process (i.e.

Green bean; Roasted bean; Instant coffee) on the abundance chemical entities extracted through the untargeted chemical analysis. This statistical tests were performed via Python 3 scripts by using the package scipy.stats.f_oneway (Virtanen *et al.*, 2020). The level of significance was set at p = 0.05 for the statistical test.

### 7.2.7 Correlation analysis

Correlation analysis of two independent variables were performed via python packages and is presented in section 3.2.14.

## 7.3 Results and discussion

### 7.3.1 Fine quantitation and screening of polyphenols and key foam compounds in coffee samples via high-resolution liquid chromatography-mass spectrometry

In the pursuit of quantifying the abundant major polyphenols (especially in green bean) (Farah and Donangelo, 2006; Perrone *et al.*, 2008) and key chemical compounds in coffee, the coffee solutions were 1/10 diluted to final concentration of 0.15% w/w while the range of standard curves was broad enough in order to avoid quantification by extrapolation. Also, by diluting the coffee solution the matrix effect at the ionisation, which was described in Chapter 6, was avoided as the response of Sinapic acid between the coffee samples ($4.69\pm0.2 *10^6$) and standard curve ($4.92\pm0.4*10^6$) was not significantly different ($p>0.05$).

**Polyphenols**

It has been reported that mono-caffeoylquinic acids comprise 80-84% and 67-76% of total chlorogenic acids in arabica and robusta green beans, respectively

(Ky *et al.*, 2001; Perrone *et al.*, 2008), while di-caffeoylquinic acids comprise 11-15% of chlorogenic acids in green arabica and robusta beans (Perrone *et al.*, 2008). Therefore, the abundance of such major chlorogenic acids in coffee was determined. The concentration of 3-O-Caffeoylquinic acid, 5-O-Caffeoylquinic acid, 3,4-Dicaffeoylquinic acid, 3,5-Dicaffeoylquinic acid and 4,5-Dicaffeoylquinic acid of samples in Table 7.1 and Table 7.2 are presented in Table 7.3 and Table 7.4. The standard curves that were used for the quantification of major polyphenols are presented in Appendix O.

3-O-Caffeoylquinic acid was more abundant in arabica green bean extracts, and it was degraded continuously during roasting. In the case of robusta extract, the concentration of 3-O-Caffeoylquinic acid peaked at 2 minutes roasted and then degraded to lower levels than in the green bean. The statistical analysis showed that Arabica washed green bean extract was significantly ($p<0.05$) more abundant in 3-O-Caffeoylquinic acid than the equivalent Arabica unwashed and Robusta unwashed extract. At 6 minutes of roasting the Robusta unwashed was significantly more abundant in 3-O-Caffeoylquinic acid (Table 7.3). The instant coffee manufacture increased the concentration of 3-O-Caffeoylquinic acid compared to the roasted bean extracts (Table 7.4). However, the levels of concentration for 3-CQA were lower than green coffee extract.

Table 7.3 Concentration (mg/100 mL coffee solution) for major chlorogenic acids in Arabica Washed, Arabica Unwashed and Robusta Unwashed coffee beans roasted at 0, 2, 4 and 6 minutes. CQA: Caffeoylquinic acid, diCQA: Dicaffeoylquinic acid. Each solution was normalised in 1.5% w/w soluble solids. One-way ANOVA was performed for each column. Different letters indicate significant differences at level p=0.05. + symbol: The concentration was calculated by extrapolation of standard curve.

| Chemical compound | Coffee | Roasting time (min) | | | |
|---|---|---|---|---|---|
| | | 0 | 2 | 4 | 6 |
| 3-O-CQA | Arabica Washed | 46.7±1.6$^{a,+}$ | 36.7±0.9$^{a,+}$ | 21.7±0.6$^{a,+}$ | 7.6±0.1$^{a}$ |
| | Arabica Unwashed | 44.2±1.1$^{b,+}$ | 34.7±0.7$^{b,+}$ | 21.3±0.7$^{a,+}$ | 6.8±0.1$^{b}$ |
| | Robusta Unwashed | 35.5±0.8$^{c,+}$ | 42.4±1.4$^{c,+}$ | 28.6±0.8$^{b,+}$ | 12.3±0.4$^{c,+}$ |
| 5-O-CQA | Arabica Washed | 12.7±0.5$^{d,+}$ | 16.9±0.4$^{d,+}$ | 12.0±0.3$^{c,+}$ | 4.1±0.1$^{d}$ |
| | Arabica Unwashed | 10.0±0.2$^{e}$ | 16.8±0.4$^{d,+}$ | 12.0±0.5$^{c,+}$ | 3.8±0.1$^{d}$ |
| | Robusta Unwashed | 9.2±0.2$^{f}$ | 20.0±0.8$^{e,+}$ | 18.7±1.3$^{d,+}$ | 7.1±0.2$^{e}$ |
| 3,4-diCQA | Arabica Washed | 3.0±0.1$^{f}$ | 2.3±0.0$^{f,h}$ | 1.1±0.0$^{e}$ | 0.5±0.0$^{f,h,+}$ |
| | Arabica Unwashed | 2.4±0.0$^{g}$ | 2.3±0.0$^{f,h}$ | 1.1±0.0$^{e}$ | 0.5±0.0$^{f,+}$ |
| | Robusta Unwashed | 4.3±0.1$^{f,h}$ | 6.1±0.1$^{g}$ | 2.8±0.5$^{f}$ | 1.1±0.0$^{g,h}$ |
| 3,5-diCQA | Arabica Washed | 2.8±0.0$^{f,h}$ | 1.4±0.0$^{f,+}$ | 0.6±0.0$^{e,+}$ | 0.4±0.0$^{f,+}$ |
| | Arabica Unwashed | 3.0±0.0$^{f,h}$ | 1.4±0.0$^{f,+}$ | 0.6±0.0$^{e,+}$ | 0.4±0.0$^{f,+}$ |
| | Robusta Unwashed | 2.6±0.1$^{f,h}$ | 2.9±0.0$^{h}$ | 1.2±0.3$^{e,+}$ | 0.6±0.0$^{f,h,+}$ |
| 4,5-diCQA | Arabica Washed | 3.2±0.0$^{f,g,h}$ | 2.6±0.0$^{h}$ | 0.9±0.0$^{e}$ | 0.4±0.0$^{f,+}$ |
| | Arabica Unwashed | 2.1±0.1$^{f,h}$ | 2.7±0.0$^{h}$ | 0.9±0.0$^{e}$ | 0.4±0.0$^{f,+}$ |
| | Robusta Unwashed | 4.3±0.0$^{g}$ | 6.3±0.1$^{g}$ | 2.8±0.0$^{f}$ | 0.8±0.0$^{h}$ |

The concentration of 5-O-Caffeoylquinic acid peaked at 2 minutes of roasting and then decreased at longer times of roasting. The abundance of this compound was lower in coffee extracts roasted for 6 minutes than the green bean extracts. It was found that 5-O-Caffeoylquinic acid was significantly ($p<0.05$) more abundant in green Arabica washed than the rest of the tested green bean coffees (Table 7.3). As with 3-O-Caffeoylquinic acid, the instant coffee process

increased the concentration of 5-O-Caffeoylquinic acid compared to the roasted bean extracts. In the case of Robusta, the levels of 5-O-Caffeoylquinic acid were lower in instant coffee than green bean. However, in the case of Arabica this compound reached higher levels than green and roasted coffee (Table 7.4).

3,4-, 3,5- and 4,5- Dicaffeoylquinic acids in Arabica coffees decreased continuously during roasting but for Robusta coffee peaked at 2 minutes of roasting and the decreased at lower levels than green bean extract. It was found that 3,4- and 4,5-Dicaffeoylquinic acid was significantly ($p<0.05$) more abundant in Robusta green bean extract than the equivalent Arabica extracts, but the opposite occurred for 3,5-Dicaffeoylquinic acid (Table 7.3). The instant coffee process slightly enhanced the concentration of 3,4-, 3,5- and 4,5-Dicaffeoylquinic acids compared to roasted bean extracts, but the levels were still lower than green bean extracts (Table 7.4). As a general comment, it was observed that both mono- and di-Caffeoylquinic acids of Robusta coffee were increased at the first moments of roasting reached a peak and then decreased.

Table 7.4 Concentration (mg/100 mL coffee solution) for major chlorogenic acids in Robusta and Arabica green bean, roasted bean and instant coffee extracts. CQA: Caffeoylquinic acid, diCQA: Dicaffeoylquinic acid. Each solution was normalised in 1.5% w/w soluble solids. One-way ANOVA was performed for each column. Different letters indicate significant differences at level p=0.05. + symbol: The concentration was calculated by extrapolation of standard curve The roasting time for each coffee was not provided.

| Chemical compound | Coffee | Green bean | Roasted bean | Instant coffee |
|---|---|---|---|---|
| 3-O-CQA | Robusta | $49.8\pm1.3^{a,+}$ | $2.3\pm0.1^{a}$ | $8.2\pm0.4^{a}$ |
| | Arabica | $52.1\pm1.9^{b,+}$ | $13.1\pm0.3^{b,+}$ | $23.1\pm0.6^{b,+}$ |
| 5-O-CQA | Robusta | $13.5\pm0.4^{c,+}$ | $1.5\pm0.0^{c}$ | $6.5\pm0.2^{c}$ |
| | Arabica | $7.0\pm0.1^{d}$ | $6.2\pm0.3^{d}$ | $15.9\pm0.5^{d,+}$ |
| 3,4-diCQA | Robusta | $6.2\pm0.1^{d}$ | $0.4\pm0.0^{f,g,+}$ | $0.8\pm0.0^{e,f}$ |
| | Arabica | $1.7\pm0.0^{e}$ | $0.6\pm0.0^{f,+}$ | $1.3\pm0.0^{e}$ |
| 3,5-diCQA | Robusta | $3.8\pm0.0^{f}$ | $0.4\pm0.0^{f,g,+}$ | $0.5\pm0.0^{f,+}$ |
| | Arabica | $3.2\pm0.0^{f}$ | $0.4\pm0.0^{f,g,+}$ | $0.6\pm0.0^{f,+}$ |
| 4,5-diCQA | Robusta | $6.2\pm0.1^{d}$ | $0.3\pm0.0^{g,+}$ | $0.6\pm0.0^{f,+}$ |
| | Arabica | $2.3\pm0.0^{e,f}$ | $0.5\pm0.0^{f,g,+}$ | $1.0\pm0.0^{e,f}$ |

Comparison of the levels of major chlorogenic acids have been reported in the literature for green, roasted and instant coffee solutions (Table 7.5), and these can be compared against the levels reported in this chapter. It is important to highlight that the concentration levels reported in the literature has been normalised in 1.5% w/w coffee solution knowing the total solid content of the initial brew (Table 7.6). In addition, it is important to highlight that only the diluent reported by Perrone, Farah and Donangelo (2012b) was 100% water. The other cited authors used 11.8% Ethanol/Water (Mills *et al.*, 2013) or 15.8% Acetonitrile /Water (Lin *et al.*, 2022). The levels of 3-O-Caffeoylquinic acid from commercial roasted and instant coffee brews ranges from 0.35-16.21 and 5.39-15.3 mg/100 mL of coffee solution, respectively. This range falls in the range of 3-O-Caffeoylquinic acid that is reported in the present work. The range of 5-O-Caffeoylquinic acid that has been reported in the literature for green bean extracts (133.28-224.31 mg/100 mL) (Table 7.5) was higher than the levels of equivalent compound reported in the present study (7.0-12.7 mg/100 mL) (Table 7.3 and Table 7.4). However, the levels of the same compound for roasted beans at various degrees in the literature (0.37-59.15 mg/100 mL) falls in the range of 5-O-Caffeoylquinic acid in equivalent coffee samples of the present work (3.8-20 mg/100 mL). The levels of 5-O-Caffeoylquinic acid in instant coffee from literature (7.88-60 mg/100 mL) are in the range of the same compound for instant coffees of this chapter (6.5-15.9 mg/100 mL)

The ranges of 3,4-,3,5- and 4,5-Dicaffeoylquinic acid in roasted bean samples of the literature (0-0.04 mg/100 mL) agree with the range of the same compound in equivalent samples – especially the coffee samples roasted at 6 minutes (0.4-

1.1 mg/100 mL). In the case of instant coffees for the same compound, the range form the literature (0-8.1 mg/100 mL) overlaps the range of diCaffeoylquinic acid in the present work (0.5-1.3 mg/100 mL).

Table 7.5 Reported values of 3-O-Caffeoylquinic acid (3-CQA), 5-O-Caffeoylquinic acid, 3,4-Dicaffeoylquinic acid (3,4-DiCQA), 3,5-Dicaffeoylquinic acid (3,5-DiCQA), 4,5-Dicaffeoylquinic acid (4,5-DiCQA) in green bean, roasted bean at various degrees of roasting and, instant coffee solutions. The concentration is expressed as mg/100 mL coffee solution of 1.5% w/w coffee solution. **i**- Coffee samples were clarified with Carrez's I & II solutions. **ii**- Polyphenols were extracted via Solid Phase Extraction (SPE). **a**-Diluent 100% water, **b**- Diluent 11.8% Ethanol/Water, **c**-Diluent - 15.8% Acetonitrile/Water

| Chemical Compound | Coffee | Green bean | Roasted bean | Instant coffee | Reference |
|---|---|---|---|---|---|
| 3-CQA | Arabica and Robusta in various blends | - | 0.35-0.81[i,b] | - | (Mills *et al.*, 2013) |
| | - | - | - | 5.39-13.55[i,b] | |
| | Arabica and Robusta coffees | - | 16.21[ii,c] | - | (Lin *et al.*, 2022) |
| | - | - | - | 15.3 | (Renouf *et al.*, 2010) |
| 5-CQA | C. Arabica cv. Mundo Novo | 139.18[i,a] | 0.89-35.50[i,a] | - | (Perrone, Farah and Donangelo, 2012b) |
| | C. Arabica cv. Red Catuai | 199.89[i,a] | 0.97-49.04[i,a] | - | |
| | C. Arabica cv. Yellow Bourbon | 133.28[i,a] | 0.37-45.44[i,a] | - | |
| | C. canephora cv. Conillon | 224.31[i,a] | 0.45-59.15[i,a] | - | |
| | Arabica and Robusta in various blends | - | 0.56-1.62[i,b] | - | (Mills *et al.*, 2013) |
| | - | - | - | 7.88-34.21[i,b] | |
| | Arabica and Robusta coffees | - | 19.48[ii,c] | - | (Lin *et al.*, 2022) |
| | - | - | - | 60 | (Renouf *et al.*, 2010) |
| 3,4-diCQA | Arabica and Robusta in various blends | - | 0-0.03[i,b] | - | (Mills *et al.*, 2013) |
| | - | - | - | 0.3-1.89[i,b] | |
| | - | - | - | 7.5 | (Renouf *et al.*, 2010) |
| 3,5-diCQA | Arabica and Robusta in various blends | - | 0-0.02[i,b] | - | (Mills *et al.*, 2013) |
| | - | - | - | 0.23-1.73[i,b] | |
| 4,5-diCQA | Arabica and Robusta in various blends | - | 0-0.04[i,b] | - | Mills *et al.*, 2013) |
| | - | - | - | 0-1.02[i,b] | |
| | - | - | - | 8.1 | (Renouf *et al.*, 2010) |

Table 7.6 Total solid (%w/w) of coffee brews as reported in the literature

| Reference | Green bean | Roasted bean | Instant coffee |
|---|---|---|---|
| (Mills *et al.*, 2013) | - | 5.5 | 0.9 |
| (Lin *et al.*, 2022) | - | - | 1.6 |
| (Renouf *et al.*, 2010) | - | - | 1 |
| (Perrone, Farah and Donangelo, 2012b) | 2.4 | 2.4 | - |

It has been previously reported that 5-O-Caffeoylquinic acid was more abundant than 3-O-Caffeoylquinic acid in both Arabica and Robusta coffees (Farah *et al.*, 2005; Perrone *et al.*, 2008; Renouf *et al.*, 2010; Mills *et al.*, 2013; Park, 2013). However, the results of the present chapter showed the opposite. The identification of 3-O-Caffeoylquinic acid and 5-O-Caffeoylquinic acid conducted via comparing the m/z and retention time of chemical reference standards with peaks of interest. The only author that used chemical reference standards for both compounds was Park (2013).Park (2013). Farah et al., (2005) and Perrone et al (2008) acquired a chemical reference standard for 5-O-Caffeoylquinic acid and synthesised the 3-O-Caffeoylquinic acid *via* an isomerisation method as described in Trugo and Macrae (1984) and assigned by assumption the identity of 3-O-Caffeoylquinic acid based on the isomerisation rate. Mills et al. (2013) identified the 3-O-Caffeoylquinic acid via comparison of MS fragments with published data, while Renouf et al. (2010) did not report the identification steps for the caffeoylquinic acids of interest.

According to the literature, there is a contradiction regarding the name of 3-O-Caffeoylquinic acid and 5-O-Caffeoylquinic acid. The latter compound was reported to be isolated and identified in 1837 (Kremr *et al.*, 2016). From that time until 1976, 5-O-Caffeoylquinic acid was known as chlorogenic acid while the 3-O-Caffeoylquinic acid was known as isochlorogenic acid. In 1976, IUPAC

published new definition rules which affected the order of number of carbon atoms in quinic acid. In fact, the order of carbon atoms were reversed and the correct name of 5-O-Caffeoylquinic acid is 3-O-Caffeoylquinic acid, and vice versa. Therefore, according to the rules of 1976, 3-O-Caffeoylquinic acid is known as chlorogenic acid and 5-O-Caffeoylquinic acid is known as isochlorogenic acid. Despite the new IUPAC rules of definition, some chemical companies continued to use the old rules from before 1976, and this left confusion in the literature (Kremr *et al.*, 2016).

It is important to highlight that in the present work, it was found the 3-O-Caffeoyquinic acid in arabica coffees was continuously degraded during roasting. 5-O-Caffeoylquinic acid increased, reached a peak at 2 minutes of roasting and then decreased, which might be attributed to the isomerisation from 3-O-Caffeoylquinic acid. In opposition, it has been reported that 5-O-Caffeoylquinic acid decreased continuously and 3-O-Caffeoylquinic acid reached a peak and then decreased during roasting (Farah *et al.*, 2005; Perrone *et al.*, 2008). Therefore, it can be hypothesised that these authors might have been supplied chemical reference standards from companies that have not implemented the 1976 IUPAC rules of definition.

The effect of roasting degree on 33 polyphenols present in 0.15% w/w coffee solutions is presented in Figure 7-1.

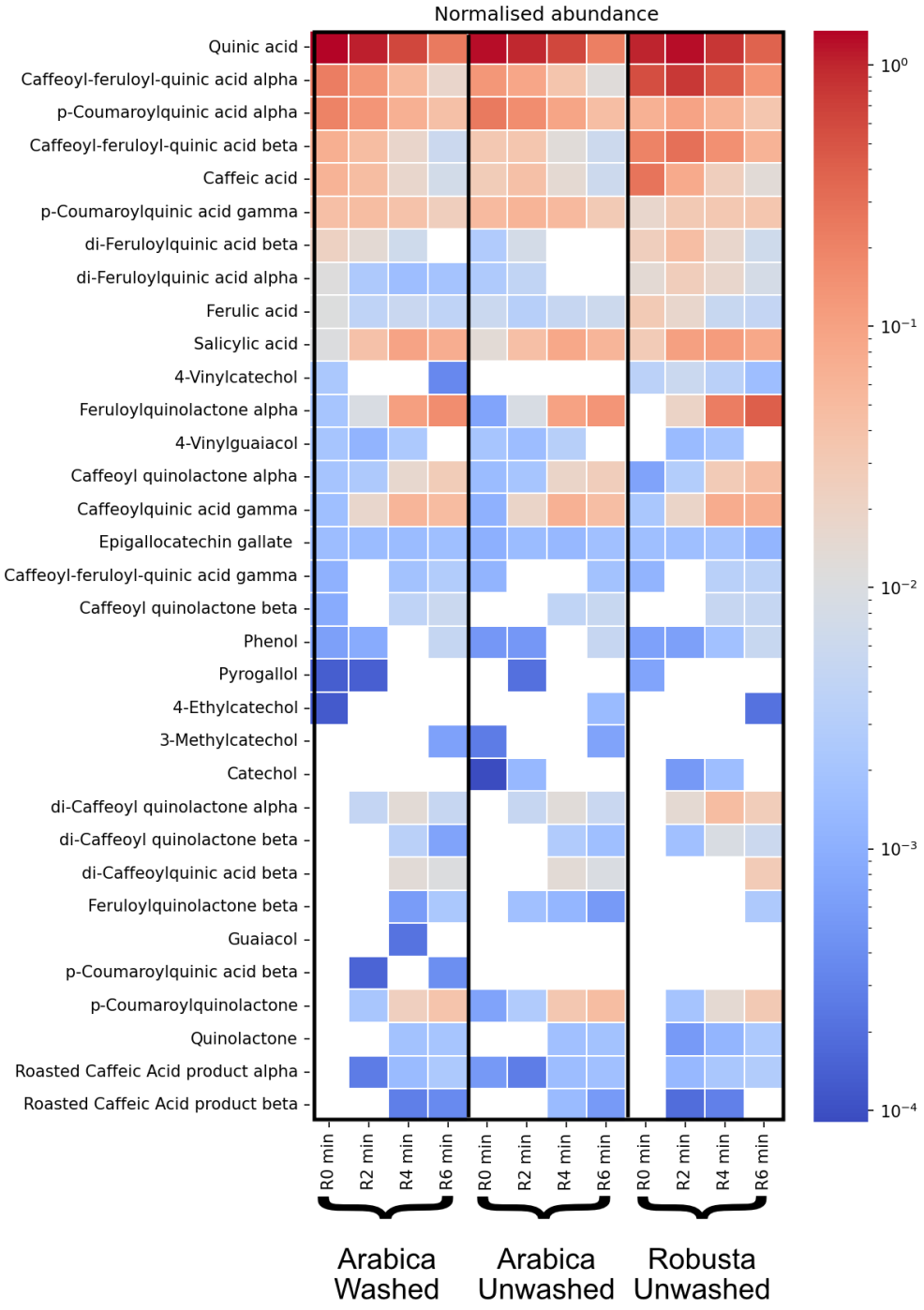



Figure 7-1 Normalised abundance of MS2 annotated polyphenols for Arabica washed, Arabica unwashed and Robusta unwashed coffee beans roasted for 0, 2, 4 and 6 minutes. White tiles indicate that the given compound was not detected at the given sample. The presented data were normalised to the abundance of the internal standard (i.e. Sinapic acid). Raw data are presented in Appendix P.

It is observed that quinic acid, caffeic acid, ferulic acid, caffeoyl-feruloylquinic acids, di-feruloylquinic acids, p-coumaroloylquinic acid and pyrogallol were degraded during roasting degree. The degradation of mono and di-caffeoyl,

feruloyl or p-Coumaroylquinic acid during roasting has been previously reported (Farah *et al.*, 2005; Perrone *et al.*, 2008; Wei *et al.*, 2012a; Król *et al.*, 2020). The degradation of quinic acid in favour of phenol has been previously reported by Leloup, Louvrier and Liardon (1995) and Frank et al (2007).

On the other hand, caffeoylquinic acid gamma, di-caffeoylquinic acid beta, caffeoyl-feruloylquinic acid gamma, phenol, salicylic acid, 4-vinylgaicol and lactones such as quinolactone, feruloylquinolactone, mono- and dicaffeoylquinolactone, p-coumaroylquinolactone and roasted caffeic acid products were generated during roasting. The increase in the concentration of phenol, salicylic acid and 4-vinylguaicol has been reported by Dorfner et al, (2003) and Król et al. (2020). Farah et al. (2005) has reported that di-Caffeoylquinolactones are generated during roasting, reach a peak and then decrease. The same response has been observed for di-Caffeoylquinolactones in the present work.

Heat has been shown to stimulate reactions that degrade caffeic acid in favour of 4-vinylcatechol as intermediate compound for creation of 4-vinylcatechol oligomers (i.e. Roasted caffeic acid products; Frank et al., 2007) (Figure 7-2). A more detailed review on the relative abundance of caffeic acid (Figure 7-3a), 4-vinylcatechol (Figure 7-3b) and roasted caffeic acids products alpha and beta (Figure 7-3c and Figure 7-3d) is shown below. This indicates that the caffeic acid was continuously degraded, and 4-vinylcatechol levels were initially increased and then decreased, while roasted caffeic acid products were more abundant in coffee roasted for longer times.

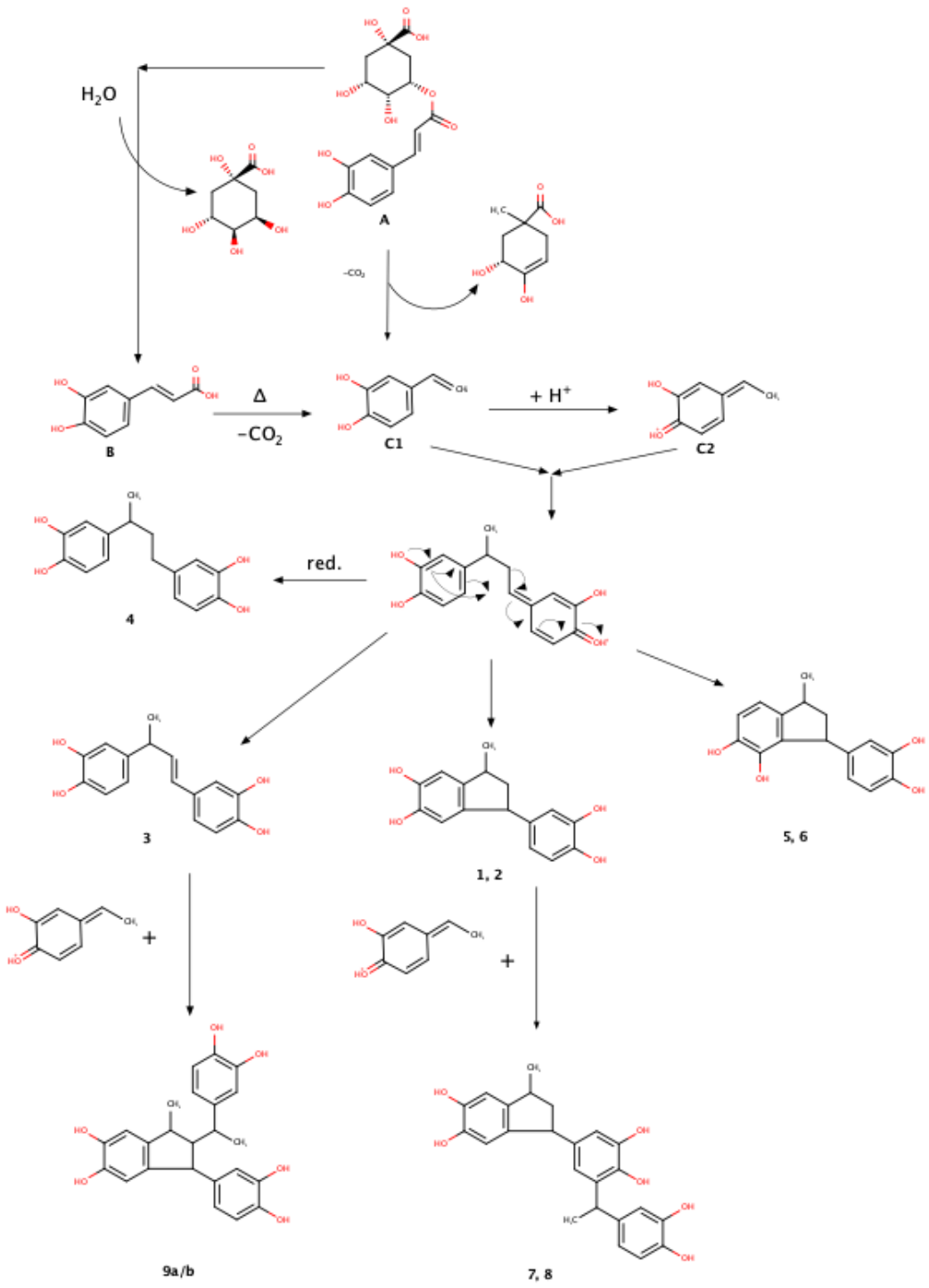



Figure 7-2 Proposed metabolic pathway of production of 4-vinylcatechol oligomers (1 to 9a/b) from 5-O-caffeoylquinic acid (A) and caffeic acid (B) via 4-vinylcatechol as an intermediate metabolite (C1). Image adapted from Frank et al., 2007.

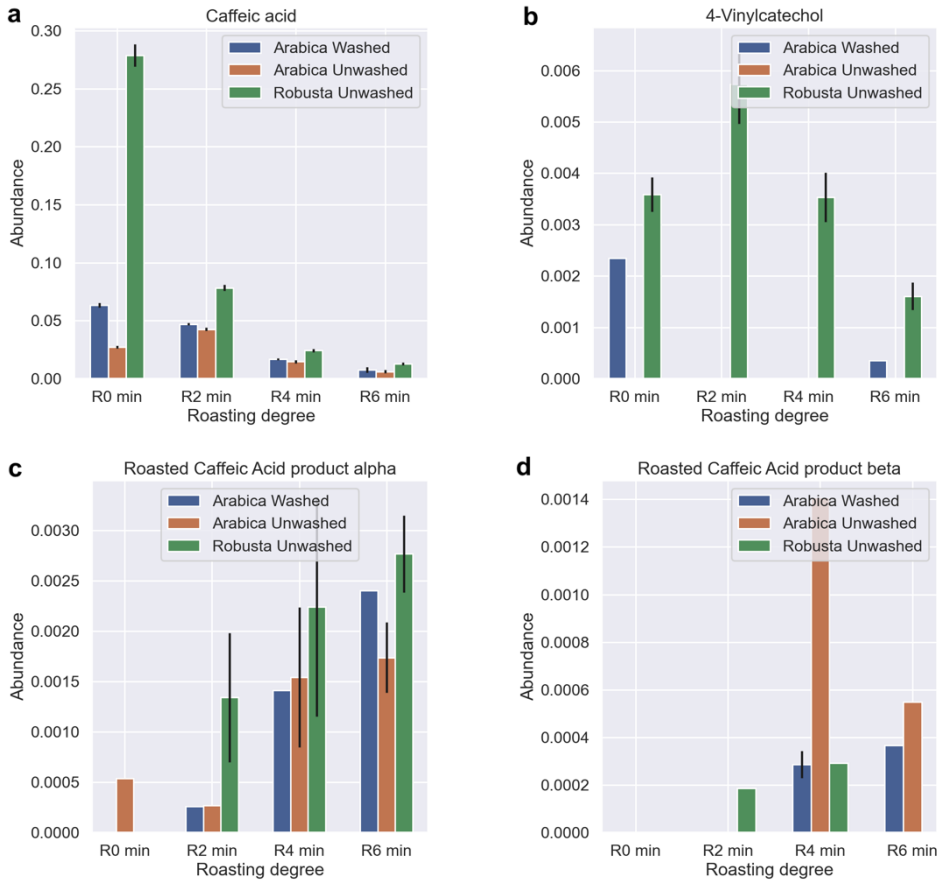



Figure 7-3 Normalised abundance of (a) caffeic acid, (b) 4-vinylcatechol and (c and d) )roasted caffeic acid product alpha and beta in coffee samples roasted at different roasting degree. The presented data were normalised to the abundance of the internal standard (i.e. Sinapic acid)

The effect of the instant coffee manufacturing process on 33 polyphenols is presented in Figure 7-4. It is observed that quinic acid, caffeic acid, p-Coumaroylquinic acid alpha, di-Feruloylquinic acid alpha and both caffeoyl-ferulloylquinic acid alpha and beta were degraded from green bean to roasted bean. These molecules were more abundant in instant coffee than roasted bean. The overall effect of the instant coffee manufacturing process was a decline in several individual polyphenols, with continuous degradation observed for di-Feruloylquinic acid beta, ferulic acid and 4-vinylcatechol. On the other hand, continuous increase in abundance was observed for p-Coumaroylquinic acid gamma, Caffeoylquinic acid gamma, di-Caffeoylquinic acid alpha, 3-methylcatechol, 4-ethylcatechol, pyrogallol and salicylic acid. Similar to the

effect of roasting degree, quinolactone, feruloylquinolactones, p-Coumaroylquinolactone and caffeoylquinolactones were continuously increased during the coffee process.

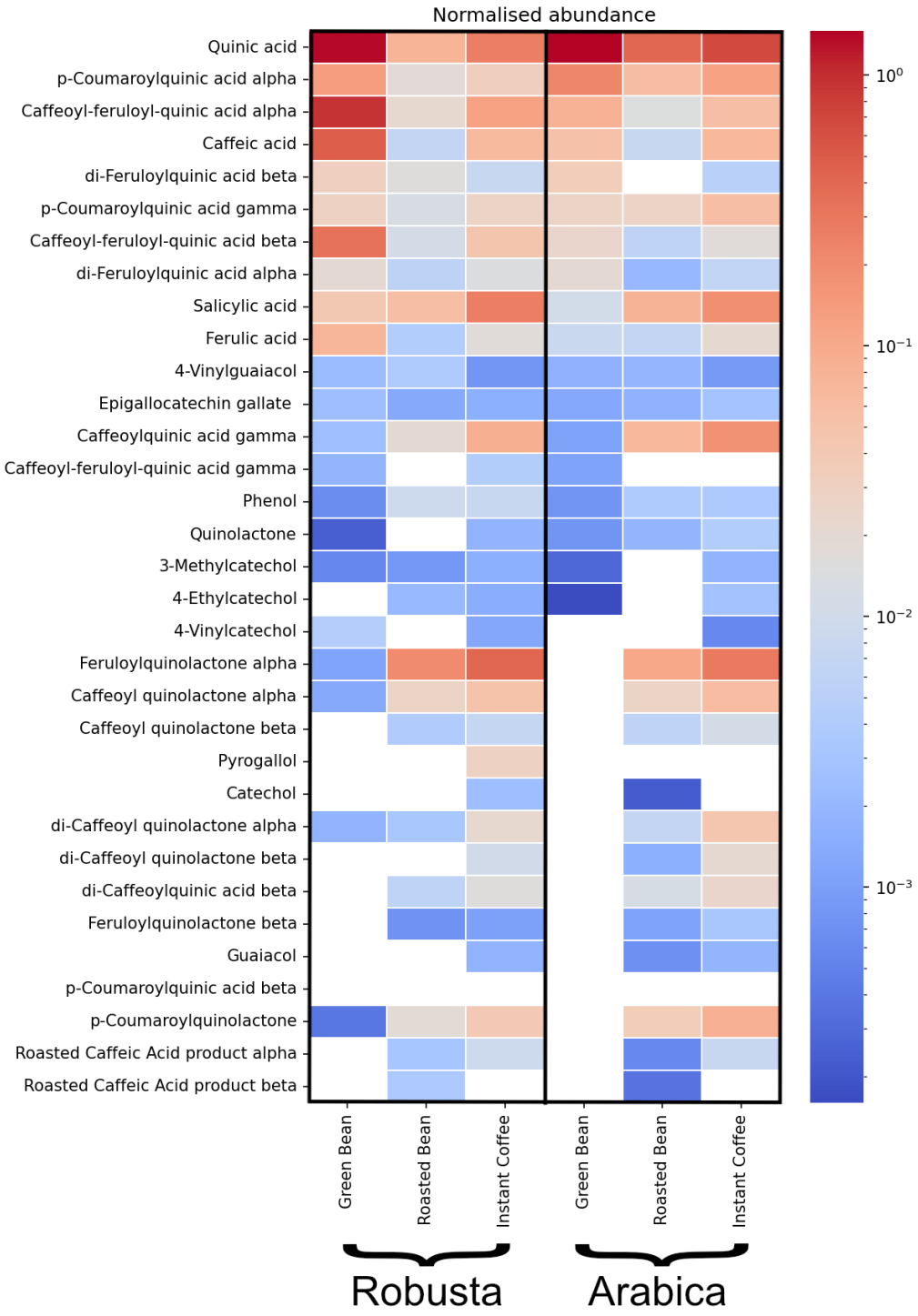



Figure 7-4 Normalised abundance of MS2 annotated polyphenols for Robusta and Arabica green bean, roasted and instant coffee. White tiles indicate that the given compound was not detected at the given sample. The presented data were normalised to the abundance of the internal standard (i.e. Sinapic acid). Raw data are presented in Appendix P.

**Key foam compounds**

In Chapter 3: it was found that the roasting process positively influences coffee foam formation (Figure 7-5). It was therefore hypothesised that roasting creates chemical compounds which are associated with good foam quality, and that these will be produced according to the degree of roasting.

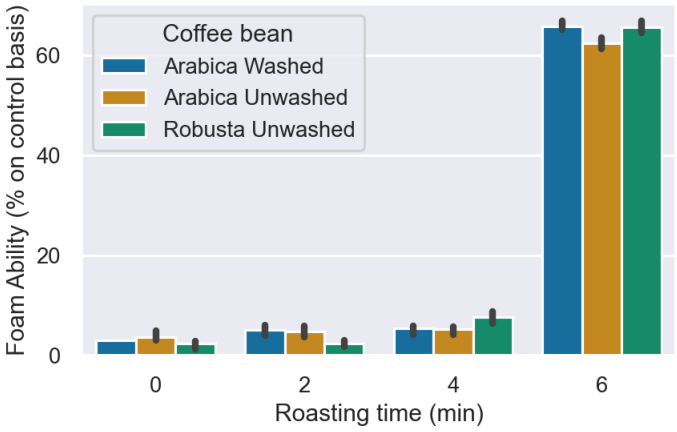



Figure 7-5 Foam Ability for Arabica Nicaragua Washed, Arabica Brazil Unwashed and Robusta Vietnam Unwashed green and roasted bean extracts.

As described in Chapter 5: and Chapter 6:, six chemical compounds (Cyclo(Phe-Pro), Cyclo(Phe-Val), Cyclo(Pro-Val), Cyclo(Leu-Phe), Cyclo(Phe-Phe) and Manntetraose) were associated with good foam quality, and one of the compounds (i.e. Cyclo(Pro-Val)) actively influences the bubble structure of the foam system. For this reason, it was important to determine the levels of abundance of such compounds for different degrees of roasting and through the coffee process (i.e. Green Bean, Roasted Bean, Instant Coffee).

The dilution of coffee samples for avoiding the matrix effect and assisting the fine quantitation of major polyphenols proved to have a limitation. The levels of abundance for key foam compounds throughout the sample set were very low and outside of the standard curves, therefore fine quantitation was not achieved.

For this reason, the normalised abundance of key foam compounds is presented in Figure 7-6a and Figure 7-6b.

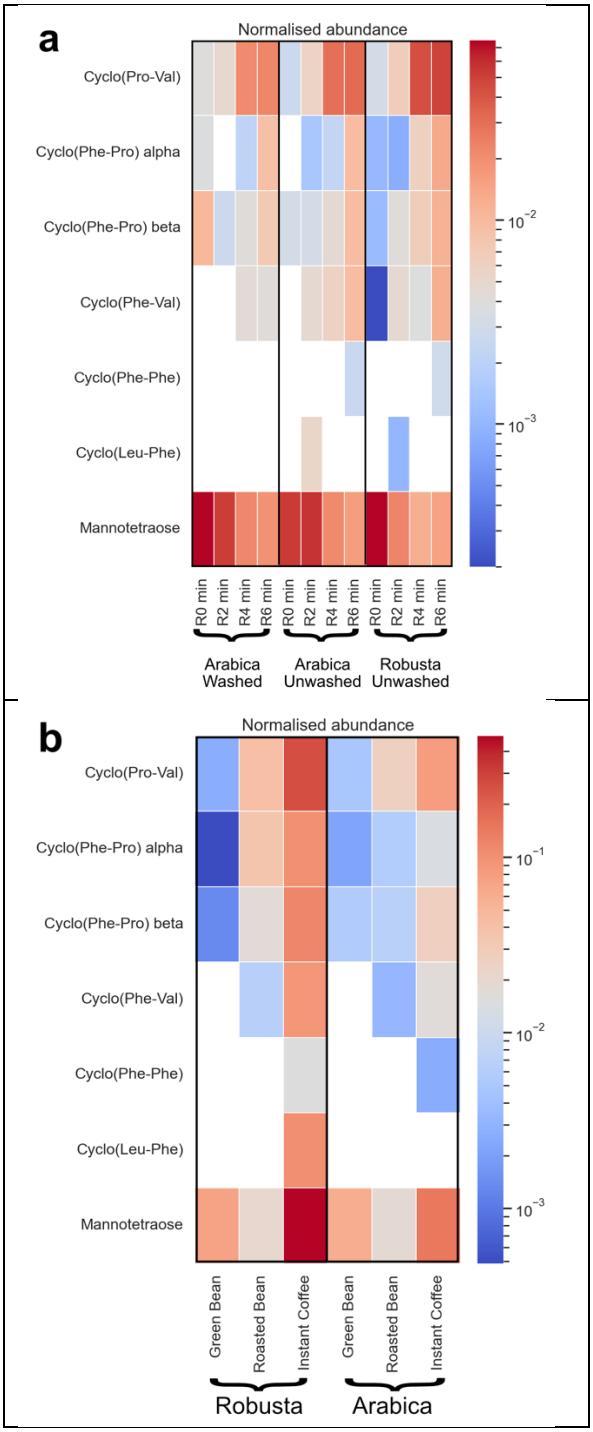



Figure 7-6 Effect of roasting degree (a) and effect of coffee process (b) on normalised abundance of key foam compounds. White tiles indicate that a given compound was not detected in a given sample.

It was observed in Figure 7-6a that roasting indeed increased the levels of cyclo-dipeptides and this might be explained by the decomposition of proteins during roasting as reported in the literature (Nunes and Coimbra, 2001; Viani, Rinantonio; Petracco, 2012). Cyclo(Pro-Val), Cyclo(Phe-Pro) alpha and beta were more abundant in coffee than Cyclo(Phe-Val), Cyclo(Pro-Val) and Cyclo(Leu-Phe). Contrary to the cyclo dipeptides, Mannotetraose levels were decreased during roasting. The degradation of low molecular weight carbohydrates during roasting has been reported in the literature (Bonnländer *et al.*, 2005b; Wei *et al.*, 2012a) .

By investigating the effect of the instant coffee manufacturing process (Figure 7-6b), it was found that instant coffee was more abundant in cyclo dipteptides than roasted bean and green bean. In the case of Mannotetraose, it was found that the levels of abundance were decreased during roasting but were subsequently increased in the instant coffee. This could be attributed to the degradation of high molecular weight carbohydrates upon the high temperature secondary (100-215˚C) and tertiary extraction (150˚-240˚C) steps that occurs during the instant coffee process (Vltzthum and Koch, 1995).

### 7.3.2 Untargeted chemical analysis of coffee samples via high-resolution liquid chromatography-mass spectrometry

**Influence of roasting degree and coffee process on the chemical profile of coffee**

Principal component analysis plots were used to visualise the variance of replicates for each coffee sample of Table 7.1 and Table 7.2 (Figure 7-7). The results from negative and positive polarity mode had good repeatability. It was observed that the majority of variance in positive polarity mode (Figure 7-7b)

was explained on two axis, rather than 3 (Figure 7-8). As was expected, QC samples were in the middle of the 3D plot because these samples were comprised of equal parts of each coffee sample.

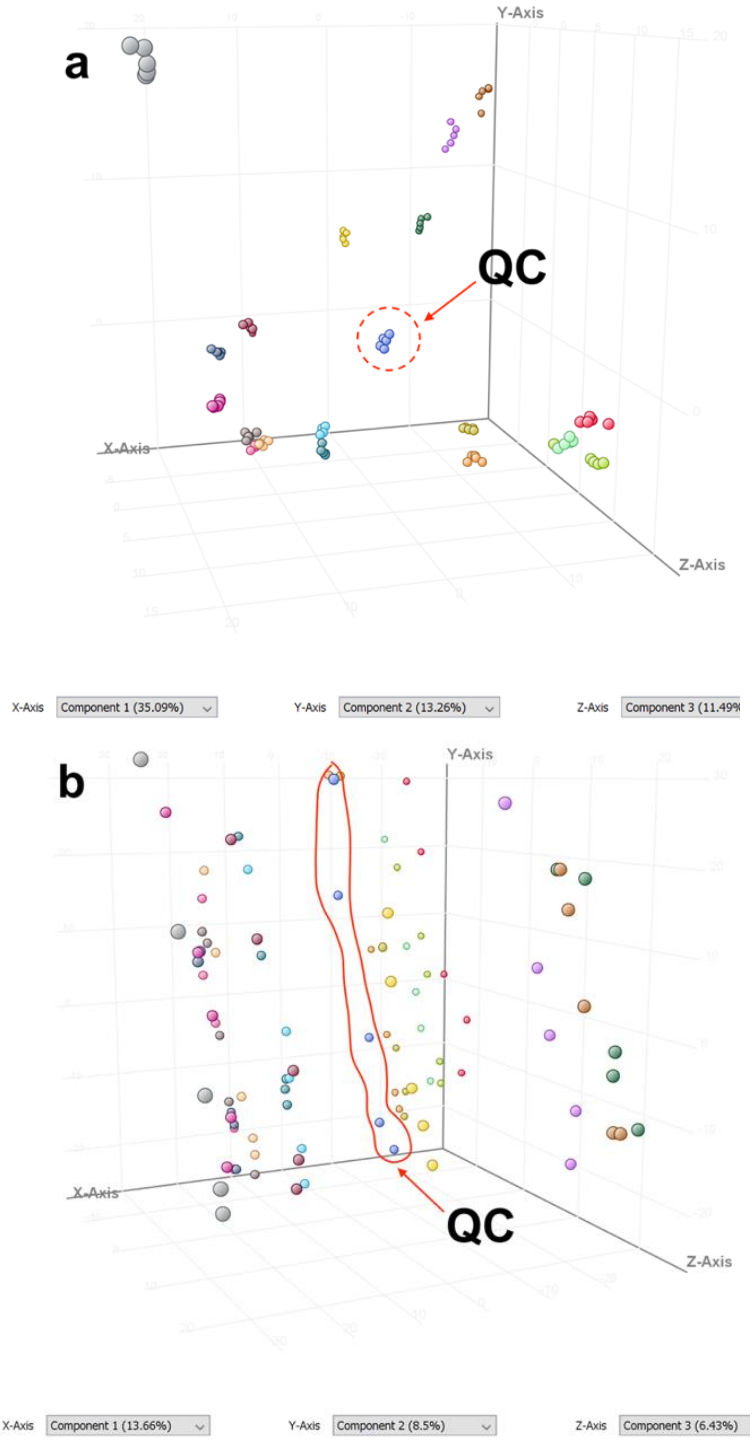



Figure 7-7 PCA plots of Total Ion Chromatographs for Negative (a) and Positive (b) polarity mode.

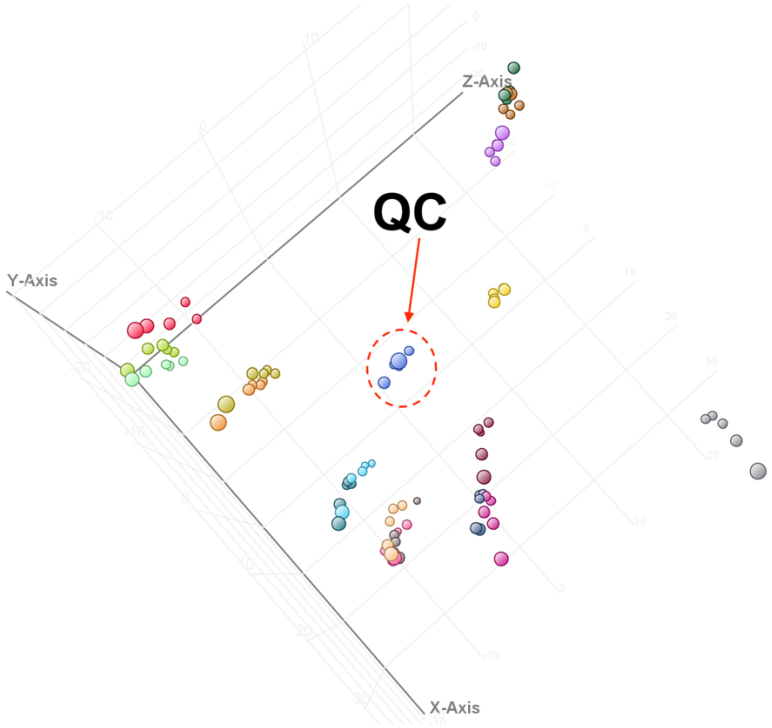



Figure 7-8 PCA plot of Total Ion Chromatograph for Positive polarity mode

The recursive feature extraction process extracted 488 and 2617 chemical entities from negative and positive polarity mode respectively, with total compounds 3105.

One-way ANOVA was performed for each chemical entity in order to investigate which chemical compounds were significantly affected by roasting degree (i.e. roasting at 0, 2, 4 and 6 minutes) and by coffee process (i.e. green bean, roasted bean, instant coffee). It was found that 724 chemical entities were significantly influenced ($p<0.05$) by roasting degree in all three coffees (i.e. Arabica washed, Arabica unwashed, Robusta unwashed), 267 compounds were up regulated during roasting and 457 compound were down regulated. The one-way ANOVA on the effect of coffee process revealed that 952 chemical entities were

significantly influenced ($p<0.05$) by the process. In more detail, 464 chemical entities where in maximum abundance in green bean, 44 were in maximum abundance in roasted bean and 444 were in maximum abundance in instant coffee. To reveal the identities of the combined 1676 compounds, their MS2 spectra were acquired, and their ID annotation was achieved by employing the SIRIUS software. The inclusion list that was formed to perform the MS2 analysis, generated 2335 chemical entities. As these compounds originate from the initial list of 1676 compounds, it is suggested that several compounds were ionised in multiple forms (e.g. Positive mode: [M+H],[M+K],[M+Na],[M+$NH_4$]; Negative mode: [M-H],[M+$HCOO^-$],[M+$C_2H_3O_2$-]). In order to eliminate any false identities, the compounds that were considered annotated with high certainty had SIRIUS score higher than 33.33% and CSI score higher than -150. Out of 2335 chemical entities, 419 were annotated with high certainty. Detailed tables including the match criteria for these compounds can be found in the Appendix O.

The normalized abundance of compounds that were up-regulated during roasting degree and were annotated (MSI Level 2 Molecular Identification (Sumner *et al.*, 2007)) with high certainty are presented in Figure 7-9. It was observed that the roasting process generated chemical compounds which belong to the following classes:

- Amino acids, peptides and analogues: Cyclo(Pro-Val) and Cyclo(Pro-Pro)
- Benzene and substituted derivatives: 2'-Hydroxy-4'-O-methylpyridoxine and 1-(4-Acetylphenyl)butane-1,3-dione

- Carbohydrate and carbohydrate conjugates: 2-O-alpha-L-Rhamnopyranosyl-D-glucopyranose, 4-O-(6-O-caffeylglucosyl) caffeic acid
- Cinnamic acid and derivatives: Caffeoylcholine and Caffeoylshikimic acid
- Pyrimidines and pyrimidine derivatives: 3-Hydroxy-2-methylpyridine and 2,6-Dimethyl-3-hydroxypyridine.

Along with the increase of key foam cyclo dipeptides, it was observed that the roasting process generates a group of cyclo dipeptides. Among the peptides one specific oligopeptide, which was annotated as N-[(R)-3-[(L-Val-L-Pro-)Amino]-1,2-dioxopentyl]-D-Leu-L-Val-OH, continuously increased during roasting. This compound, which contains the dipeptide Pro-Val, was found to be positively correlated with good foam stability (Pearson's r for drainage rate= -0.82, section 5.3.2). It can be hypothesized that this oligopeptide could be the precursor of the key foam compound cyclo(Pro-Val).

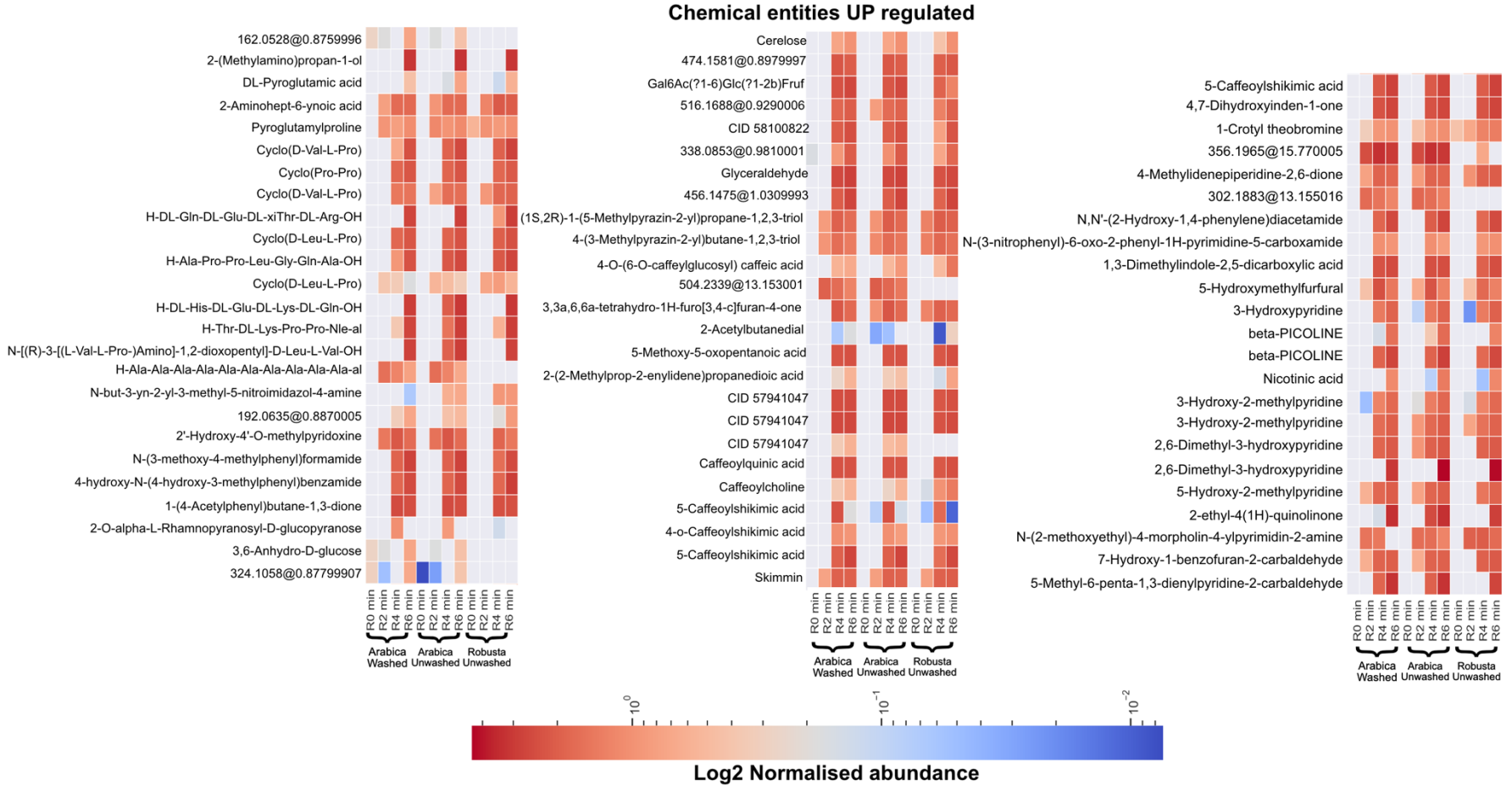



Figure 7-9 Chemical entities significantly up regulated during roasting. The full name of compounds presented as *Neutral mass x@Retention time y* can be found in the Appendix O.

The normalized abundance of compounds that were down-regulated during roasting degree and were annotated with high certainty are presented in Figure 7-10 and Figure 7-11. It was observed that the following chemical compounds were degraded during roasting:

- Amino acids, peptides and analogues: aspartic acid, DL-glutamic acid, DL-Valine
- Carbohydrate and carbohydrate conjugates: Maltotriose, Mannobiosylmannitol, Trehalose
- Cinnamic acid and derivatives: mono- and di-Caffeoylquinic acid and mono-and di-Feruloylquinic acids.

Phenolic acids combined with amino acids were identified in this set of analyses. It was observed that caffeoyltriptophan, p-Coumaroyl-L-tryptophan amd 4-carboxylphenylalalin were more abundant in green beans and degraded during roasting degree. The degradation of alpha amino acids, cinnamic acids and low molecular weight carbohydrates is in accordance with the literature (Macdonald and Macrae, 1985; Nunes and Coimbra, 2001; Bonnländer *et al.*, 2005b; Farah *et al.*, 2005; Perrone *et al.*, 2008; Wei *et al.*, 2012a)

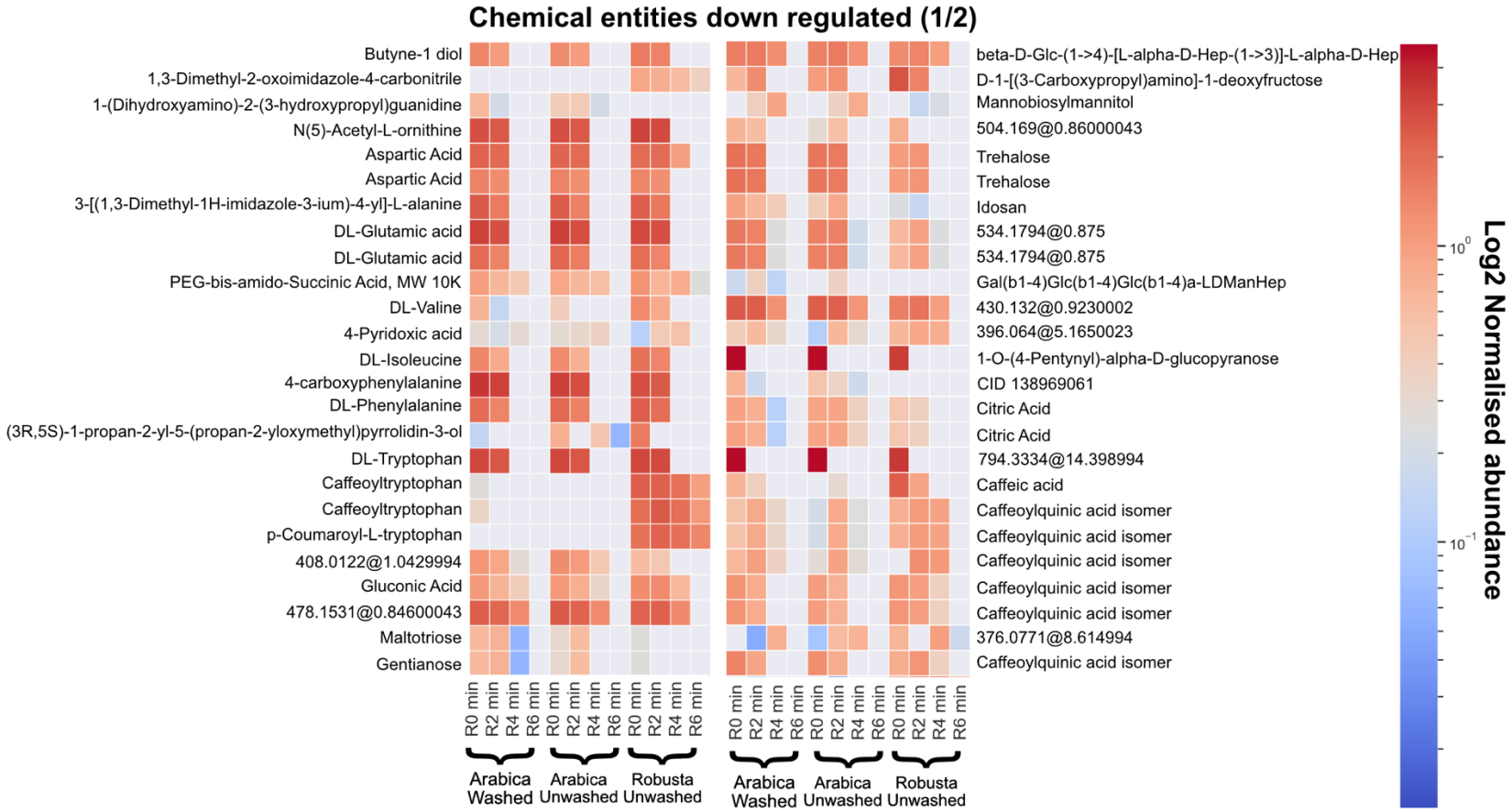



Figure 7-10 Chemical entities significantly down regulated during roasting (1 of 2). The full name of compounds presented as *Neutral mass x@Retention time y* can be found in Appendix O.

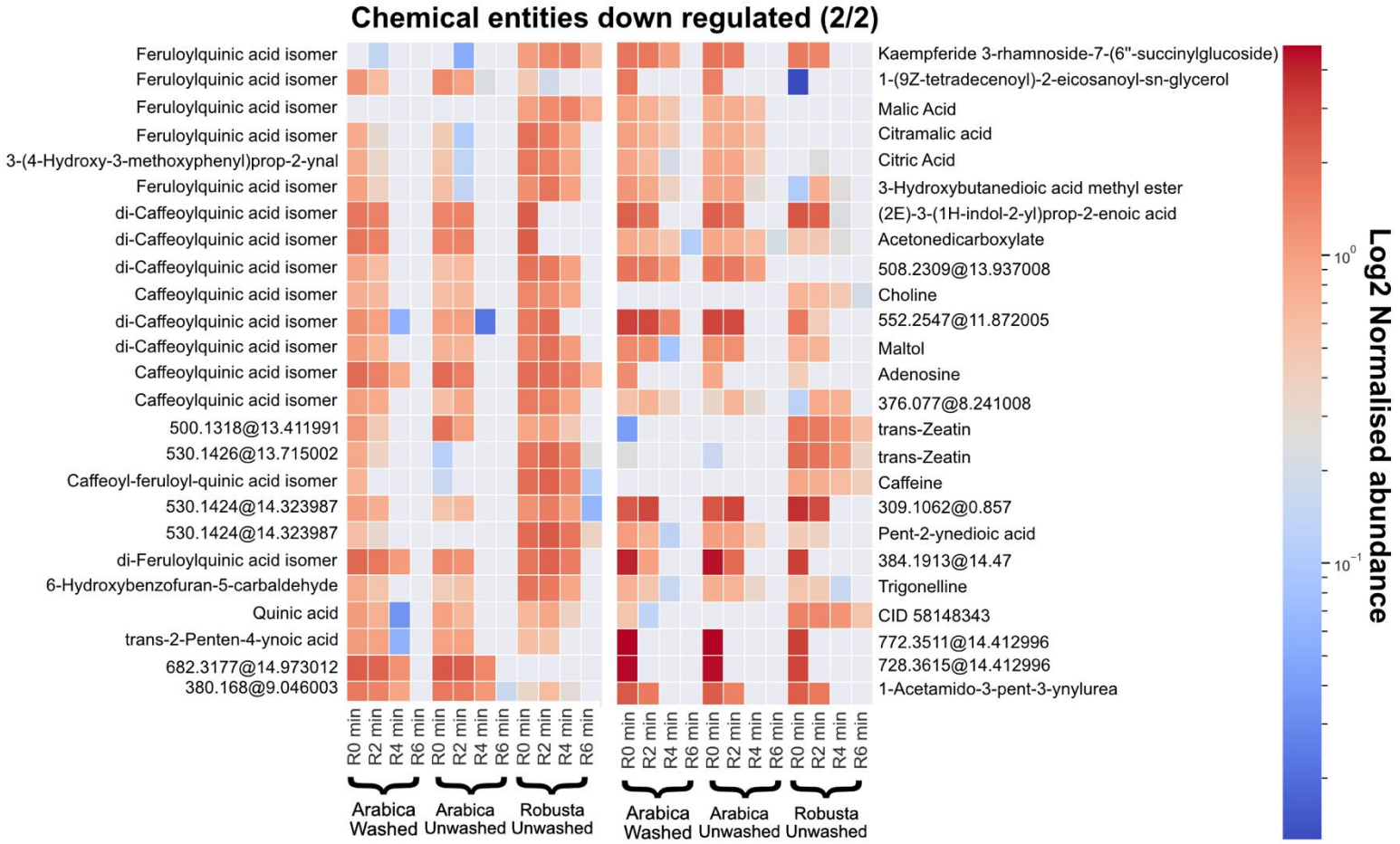



Figure 7-11 Chemical entities significantly down regulated during roasting (2 of 2). The full name of compounds presented as *Neutral mass x@Retention time y* can be found in Appendix O.

The majority of chemical compounds that were in maximum abundance in green beans were similar to the chemical entities that degraded during roasting (e.g. Amino acids such as DL-glutamic acid and DL-Tryptophan; Carbohydrates such as Mannitol and Trehalose and Cinnamic acids such as mono- and di-Caffeoylquinic acid and mono-and di-Feruloylquinic acids) (Figure 7-12, Figure 7-13)

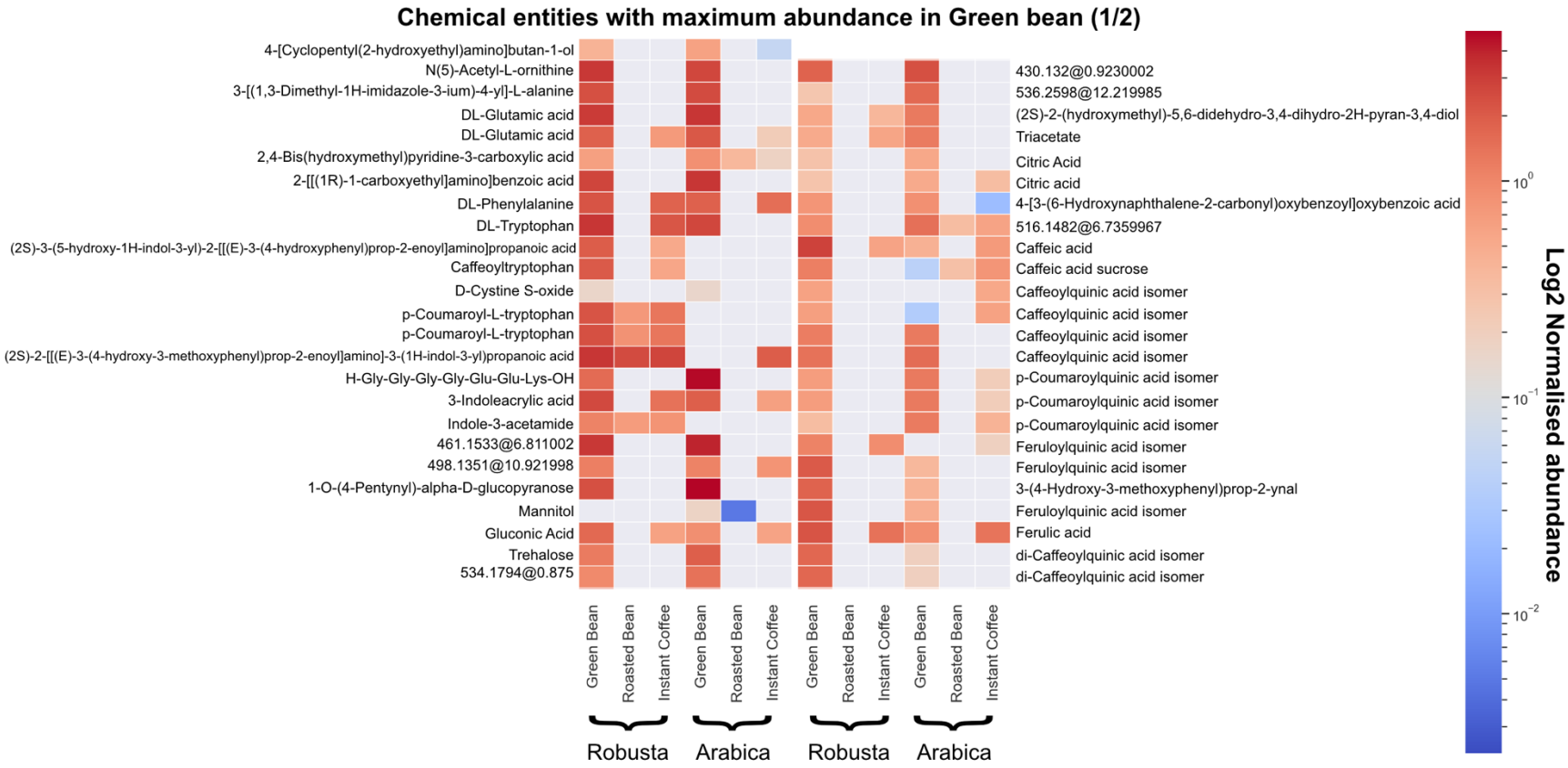



Figure 7-12 Chemical entities with maximum abundance in green bean (1 of 2). The full name of compounds presented as *Neutral mass x@Retention time y* can be found in Appendix O.

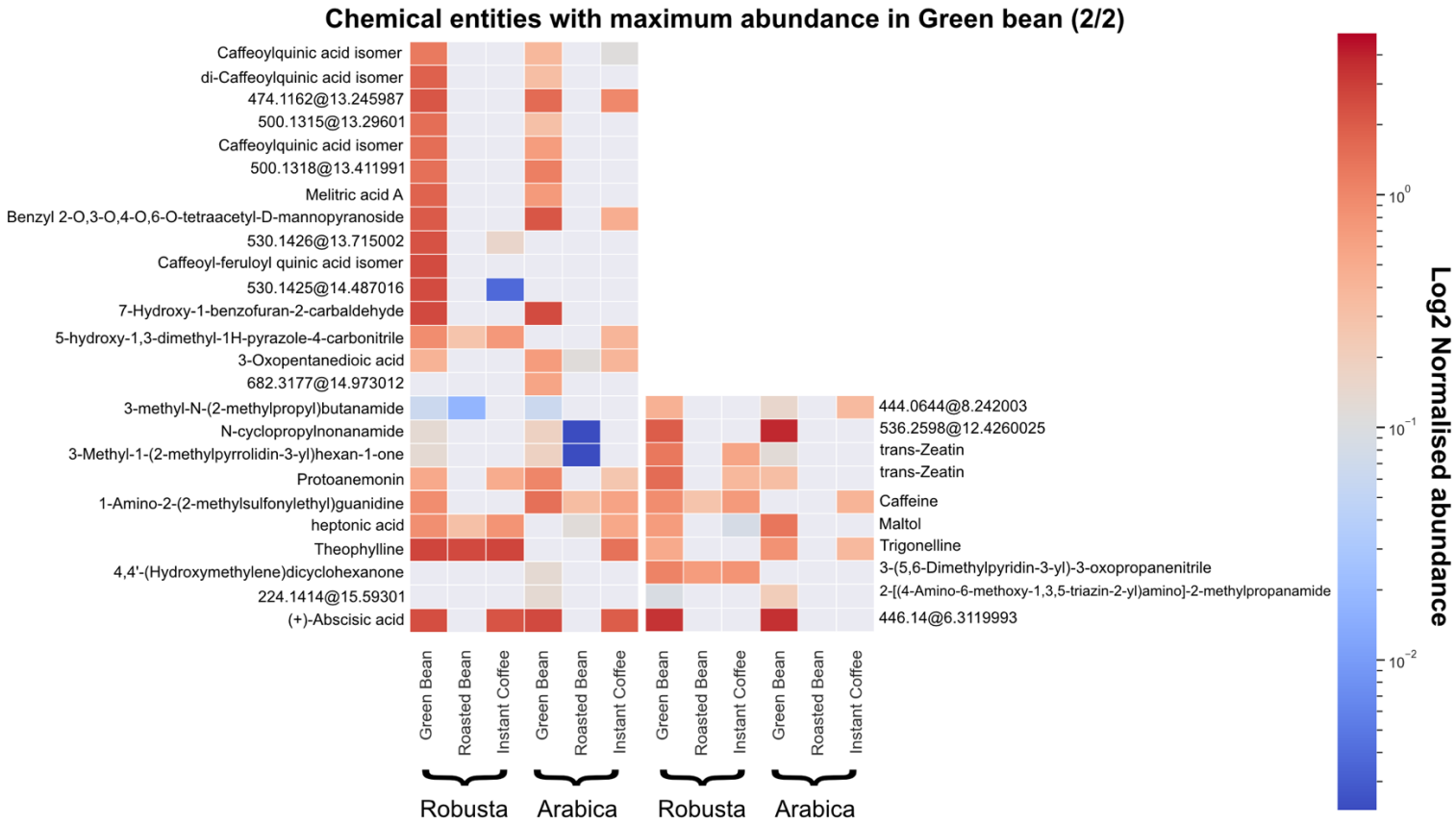



Figure 7-13 Chemical entities with maximum abundance in green bean (2 of 2). The full name of compounds presented as *Neutral mass x@Retention time y* can be found in Appendix O.

The statistical analysis showed that chemical entities with maximum abundance in roasted beans (Figure 7-14) were much fewer compared to those in green bean or instant coffee. The compounds that were in maximum abundance in roasted bean were amines such as 2-(Methylamino)propan-1-ol, Carbohydrate and carbohydrate conjugates such us Idosan, Carboxylic acids and derivatives such as (E)-2-methyl-4-methylidenepent-2-enedioic acid Cyclitols and derivatives such as L-Quebrachitol and Pyridines and derivatives such as beta-PICOLINE.

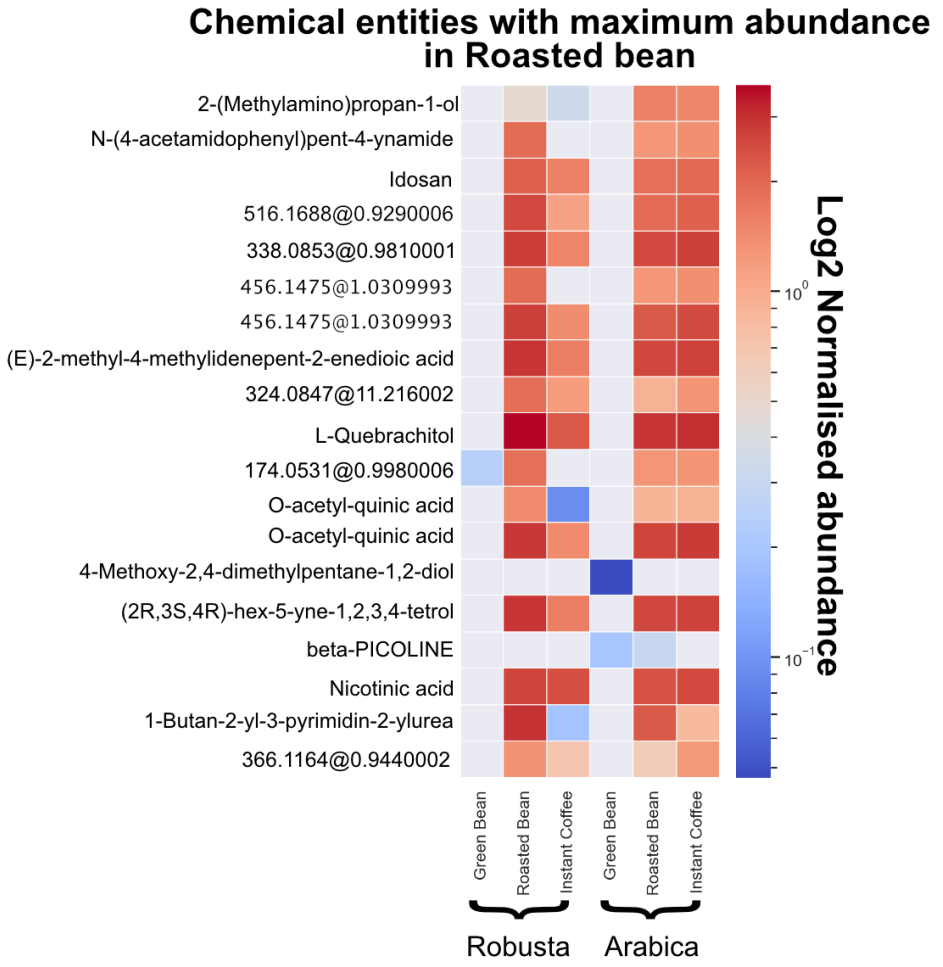



Figure 7-14 Chemical entities with maximum abundance in roasted beans. The full name of compounds presented as *Neutral mass x@Retention time y* can be found in Appendix O.

Finally, the compounds that were in maximum abundance in instant coffee (Figure 7-15, Figure 7-16) are similar to the compounds that were up regulated during the roasting process. The MS2 annotation revealed that cyclo dipeptides (e.g. Cyclo(His-Pro), Cyclo(Gly-Pro), Cyclo(Pro-Tyr), Cyclo(Ala-Phe) ) and peptides (e.g. H-DL-Leu-DL-xiThr-DL-Pro-DL-Pro-OH, H-DL-xiThr-DL-Pro-DL-Pro-DL-Leu-OH and H-Pro-Leu-Leu-Asp-Lys-OH) were in high abundance in instant coffee. In addition, many carbohydrate and carbohydrate conjugates were increased in instant coffee (e.g. D-Glucose, Cartose, Erythrulose, 2-Dehydro-D-galactonate,) and this could be attributed to the breakdown of carbohydrates due to increased temperature of the secondary and tertiary hydrolysis steps of the instant coffee process (Vltzthum and Koch, 1995).

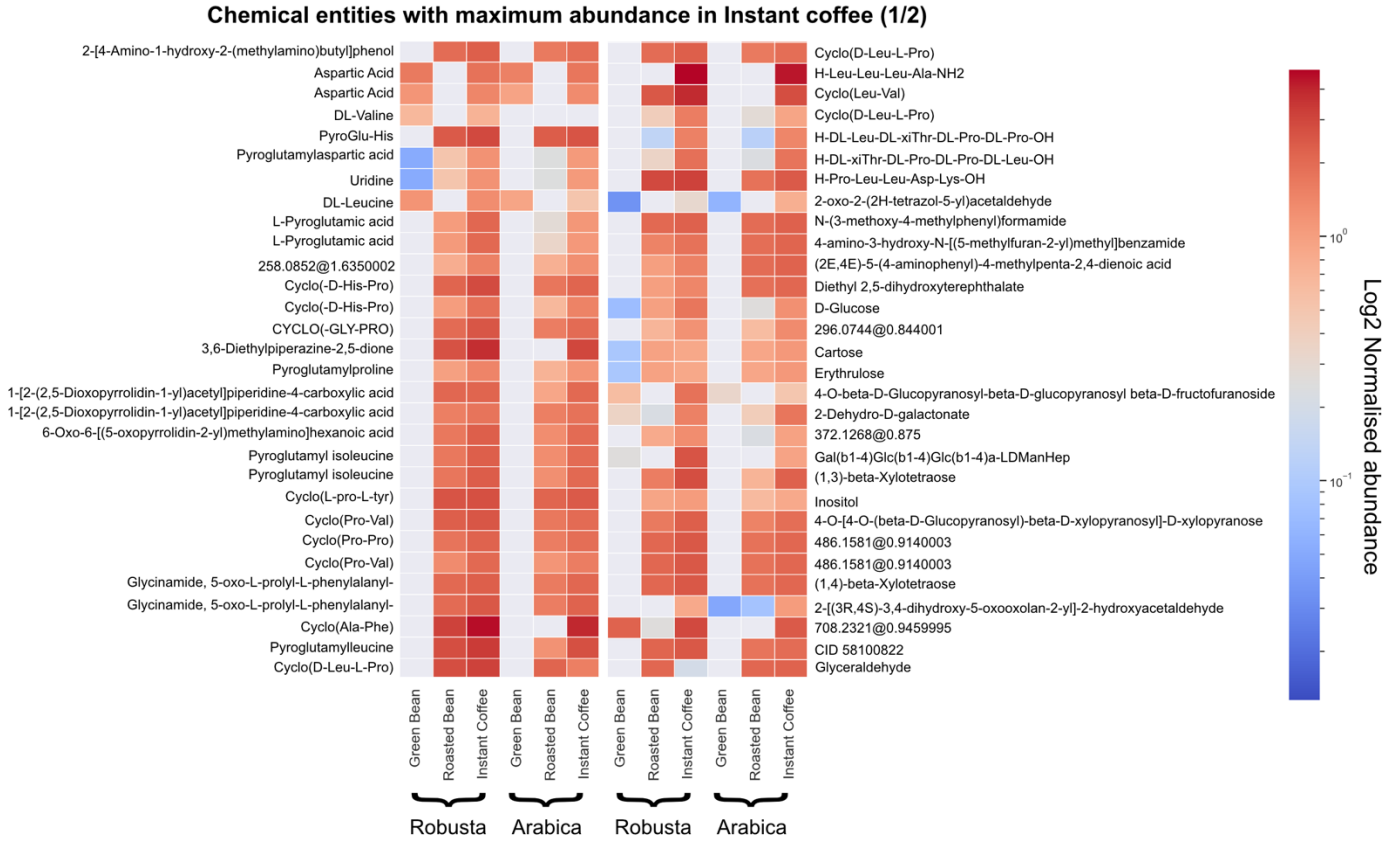



Figure 7-15 Chemical entities with maximum abundance in instant coffee (1/2). The full name of compounds presented as *Neutral mass x@Retention time y* can be found in Appendix O.

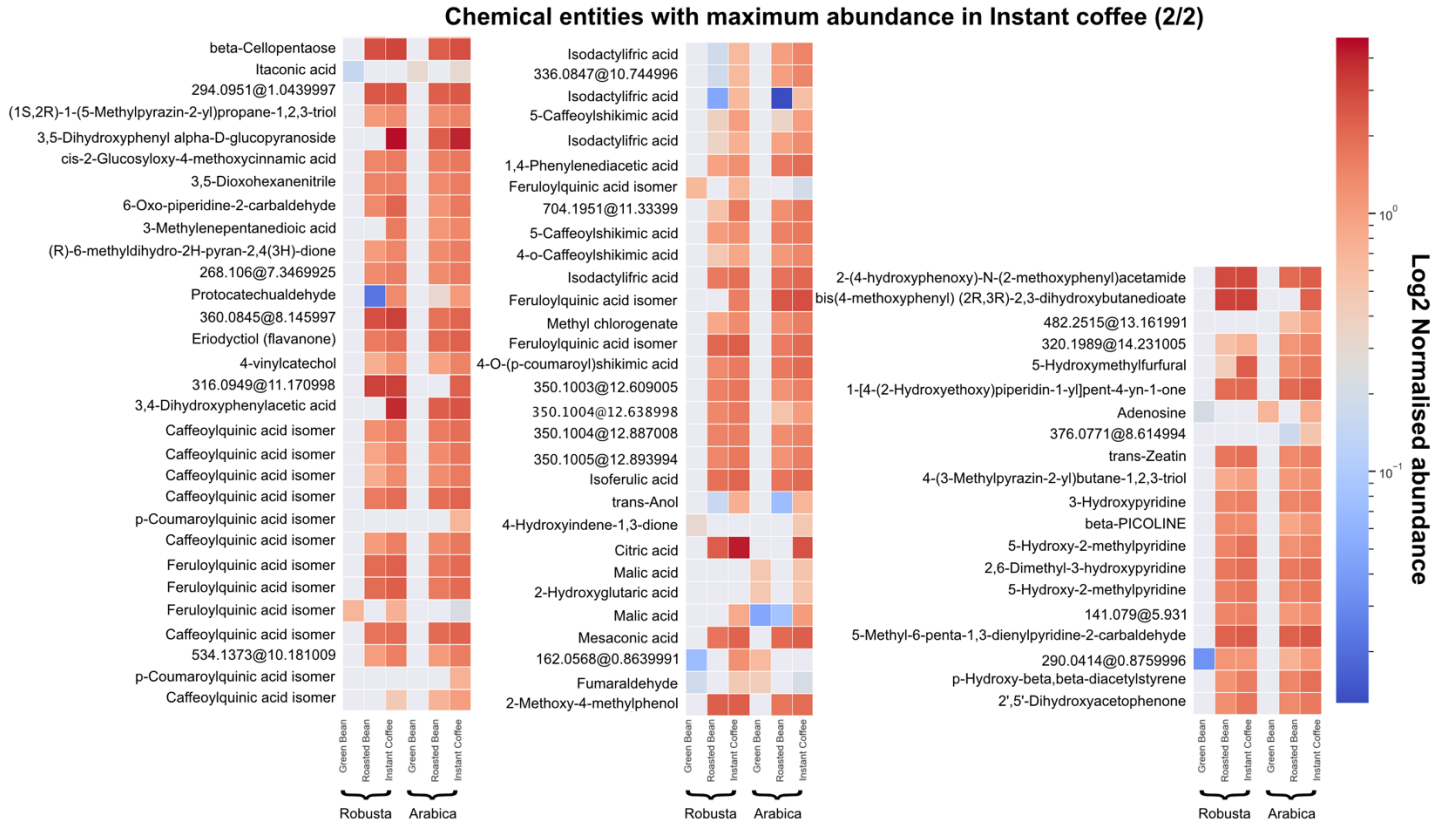



Figure 7-16 Chemical entities with maximum abundance in instant coffee (2/2). The full name of compounds presented as *Neutral mass x@Retention time y* can be found in Appendix O.

Cinnamic acids and derivatives were reported to be in maximum abundance in instant coffee (e.g. caffeoylquinic acid). This finding contradicts the previous findings on fine quantification and screening of polyphenols. A comparison of Log2 Normalised abundance between the MSI Level 1 identified 5-O-Caffeoylquinic acid and the MSI Level 2 annotated Caffeoylquinic acids (Figure 7-17) shows that the former compound was in higher abundance in green bean than the MS2 annotated chemical compounds. During roasting, 5-O-Caffeoylquinic acid was degraded while the rest MS2 annotated compounds were generated. Therefore, these compounds could not be major isomers of Caffeoylquinic acid. The second-best suggestions for these compounds from SIRIUS software were 1-O-Caffeoylquinic acid or phenolic isomers (Figure 7-18). The compound in Figure 7-18c, consists of a moiety of quinic acid and a moiety of caffeic acid isomer. The only difference with caffeic acid is the position of the hydroxyl groups. The "correct" position of the hydroxyl group to consider this moiety as caffeic acid is shown in Figure 7-18c. The compound of Figure 7-18d, consists of a p-Coumaric acid moiety and a quinic acid moiety with one more hydroxyl group. The "correct" position of hydroxyl group to consider this compound as Caffeoylquinic acid is shown in Figure 7-18d.

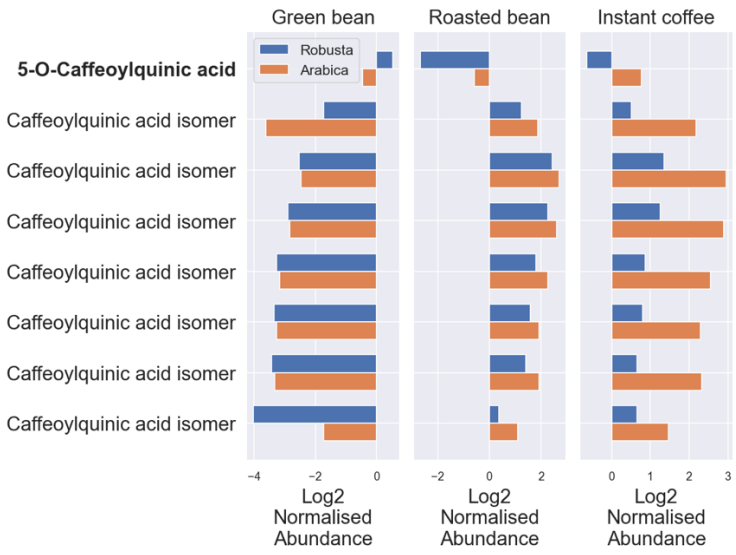



Figure 7-17 Log2 Normalised abundance of 5-O-Caffeylquinic acid ((MSI Level 1 Identification) and several MSI Level 2 annotated caffeoylquinic, Feruloylquinic and p-Coumaroylquinic acids. The MSI Level 2 compounds were in maximum abundance in instant coffee.

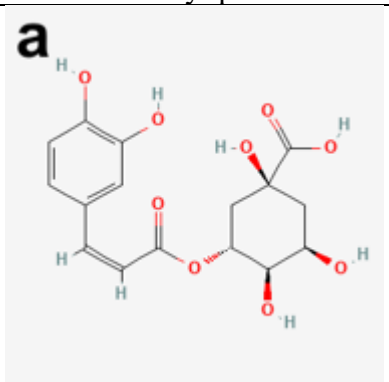
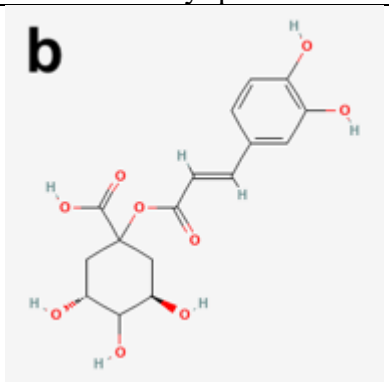
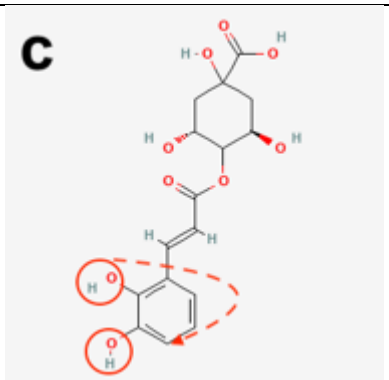
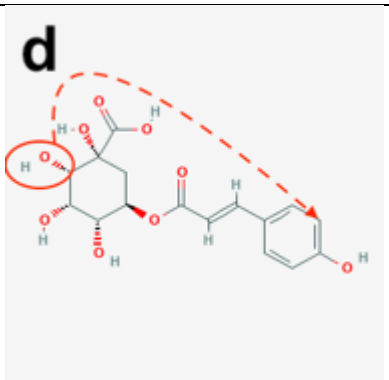
| 5-O-Caffeoylquinic acid | 1-O-Caffeoylquinic acid |
|---|---|
|  |  |
| (3R,5R)-4-[(E)-3-(2,3-dihydroxyphenyl)prop-2-enoyl]oxy-1,3,5-trihydroxycyclohexane-1-carboxylic acid | (1R,2S,3S,4R,5R)-1,2,3,4-tetrahydroxy-5-[(E)-3-(4-hydroxyphenyl)prop-2-enoyl]oxycyclohexane-1-carboxylic acid |
|  |  |

Figure 7-18 Chemical structure of 5-O-Caffeoylquinic acid (a) and MS2 annotated isomers (b,c,d).

**Correlation of whole bean colour with relative abundance of coffee chemical entities**

It is a common practice in the coffee industry to roast green coffee beans up to a given colour and not based on roasting time. Roasting based on colour standardizes the process and is a very useful parameter to consider when process scale-up is developed. Another parameter that could be used as a roasting marker is the abundance of compounds that are associated with whole bean colour. Therefore, whole bean colour was determined for the above coffee samples. And Pearson's correlation analysis was performed between the Log2 normalised abundance of chemical entities, which were identified in positive and negative polarity mode, vs the whole bean colour of samples.

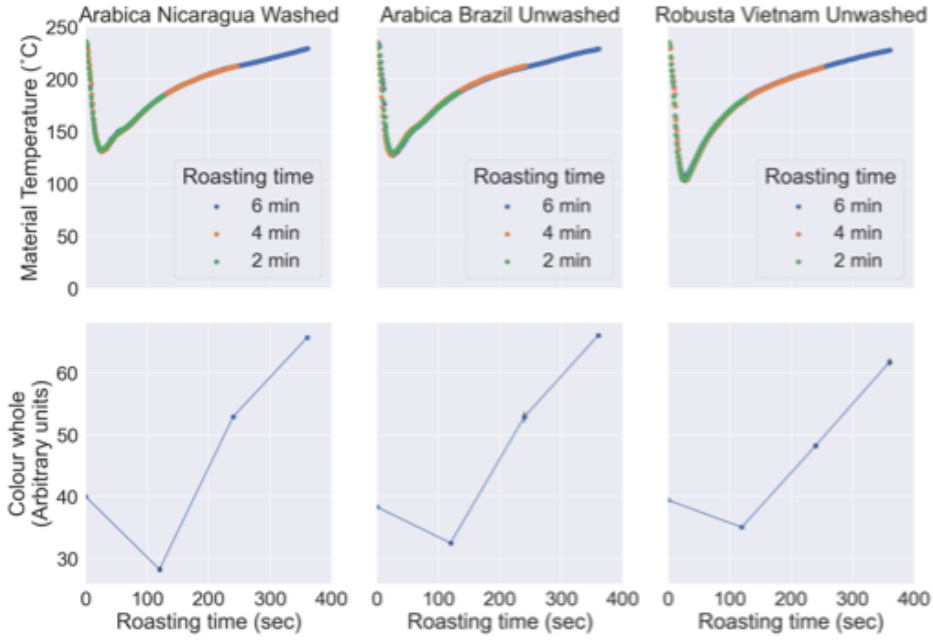



Figure 7-19 Roasting profile and whole bean colour for Arabica Nicaragua Washed, Arabica Brazil Unwashed and Robusta Vietnam Unwashed

The $R^2$ of correlation analysis from both polarity modes are presented in Figure 7-20. As per previous chapters (Chapter 4:, Chapter 5:) the threshold for good correlation was $R^2>0.67$. It was found that 220 chemical entities were

significantly correlated ($p<0.05$) while the $R^2$ was higher than 0.67 indicating a good correlation.

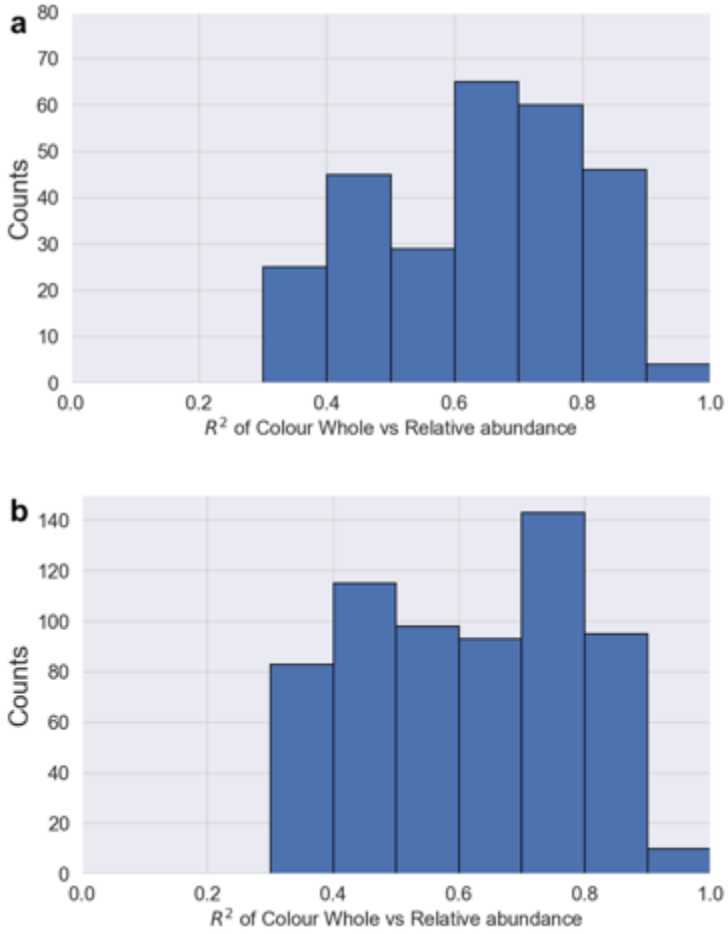



Figure 7-20 Histogram of $R^2$ of Normalised abundance vs whole bean colour.(a) Negative polarity mode. (b) Positive polarity mode

The aim was to annotate the identities of the 220 chemical entities, therefore their MS2 data were acquired, and the SIRIUS software was employed. An inclusion list of 280 chemical compounds was generated in order to acquire the MS2 data, which indicates that several compounds from the initial list of 220 were ionised in more than one form. Out of 280 chemical compounds, only 7 were annotated with high certainty and their details are presented in Table 7.7

Table 7.7 Chemical entities correlated with whole bean colour

| Compound | Prec. m/z | Retention time (min) | Pearson's r | SIRIUS NAME | Pubchem ID | SIRIUS score | CSI score | Class |
|---|---|---|---|---|---|---|---|---|
| 147.0532@0.83100057 | 148.0604 | 0.83100057 | -0.9074 | DL-Glutamic acid | 611 | 100 | -4.081 | Alpha amino acids and derivatives |
| 144.047@0.8619996 | 145.0496 | 0.8619996 | -0.9393 | Triacetate | 5459844 | 100 | -54.714 | Fatty acyls |
| 126.0317@0.8659997 | 127.039 | 0.8659997 | -0.9374 | Maltol | 8369 | 100 | -66.945 | Pyrans |
| 534.1794@0.875 | 533.1725 | 0.875 | -0.9376 | (2R,3S,4R,5S,6S)-2-[(2R,3S,4R,5R,6S)-5-hydroxy-2-(hydroxymethoxy)-6-(hydroxymethyl)-3-[(2S,3R,4S,5R,6R)-3,4,5-trihydroxy-6-(hydroxymethyl)oxan-2-yl]oxyoxan-4-yl]oxy-6-(hydroxymethyl)oxane-3,4,5-triol | 44429606 | 42.892 | -102.267 | Carbohydrates and carbohydrate conjugates |
| 137.0479@1.0439992 | 138.0552 | 1.0439992 | -0.8985 | Trigonelline | 5570 | 100 | -13.205 | Pyridines and derivatives |
| 230.1057@1.0469995 | 231.1129 | 1.0469995 | 0.9642 | 4-[(1-Methylpyrrol-3-yl)methylamino]benzoic acid | 66397664 | 78.258 | -85.363 | Amino acids and peptides and analogues |
| 162.0317@8.609005 | 163.039 | 8.609005 | -0.9244 | Umbelliferone | 5281426 | 33.818 | -62.345 | Benzopyrans |

DL-Glutamic acid, maltol and trigonelline have already been reported in coffee (Macrae, 1985; Yanagimoto et al., 2004; Konstantinidis et al., 2023) whereas the rest of the compounds have not been reported in coffee. It is observed that DL-Glutamic acid, maltol, Trigonelline and the Pubchem CID 44429606 carbohydrate were negatively correlated with whole bean colour. This means that the darker the colour of the bean, the lower the abundance of such compounds in coffee. It is important to highlight that all these compounds (i.e amino acids, carbohydrate, pyrans) take part in Mailliard reactions which leads to the colour formation. Therefore, their association with the colour formation was expected.

## 7.4 Conclusions

The present chapter investigated the effect of roasting degree and coffee process on the chemical profile of coffee beans. Fine quantitation and screening of polyphenols in coffee confirmed the previously reported findings that mono- and di- hydroxycinnamic acids (i.e. Caffeoyl-, Feruloyl-, p-Coumaroyl-) are degraded during roasting. It was confirmed that the degradation of caffeic acid during roasting favoured the generation of 4-vinylcatechol, which acts as intermediate for the bitter 4-vinylcatechol oligomers. In the case of key foam compounds, it was found that indeed roasting increases the concentration of cyclo-dipeptides which are associated with good foam quality. On the other hand, the roasting process degraded Mannotetraose.

The untargeted chemical analysis revealed the chemical transformation of coffee during roasting and through the subsequent instant coffee process. As stated in the literature, it was found that major hydroxycinnamic acids along with carbohydrates and amino acids were degraded during roasting. Along with traditional hydroxycinnamic acids and amino acids, it was found that phenolic

acid-amino acid molecules (e.g. Caffeoyltryptophan, p-Coumaroyl-L-tryptophan) were more abundant in green bean than its roasted versions.

It was found that the roasting process favours the generation of a range of dipeptides (e.g. Cyclo(His-Pro), Cyclo(Gly-Pro), Cyclo(Pro-Tyr), Cyclo(Ala-Phe) ) along with the generation of oligopeptides (e.g. H-DL-Leu-DL-xiThr-DL-Pro-DL-Pro-OH, H-DL-xiThr-DL-Pro-DL-Pro-DL-Leu-OH and H-Pro-Leu-Leu-Asp-Lys-OH). An important oligopeptide that was found to be generated during roasting is N-[(R)-3-[(L-Val-L-Pro-)Amino]-1,2-dioxopentyl]-D-Leu-L-Val-OH and it was hypothesised that this oligopeptide is the precursor of the key foam compound Cyclo(Pro-Val). Finally, the correlation analysis between the whole bean colour and normalized abundance, revealed that carbohydrates, pyrans and amino acids, which are involved in Maillard reactions, are associated with whole bean colour.

# Chapter 8: Conclusions and Future Work

## 8.1 General conclusions

An important characteristic that determines the sensory profile and visual appearance of coffee in the cup is the formation of Crema, a layer of light-coloured foam deposited at the top of the coffee cup. Understanding the physical-chemical phenomena that occur during the formation of the foam may contribute towards increasing quality of coffee and enhancing the associated consumer experience during coffee consumption. Therefore, this research aimed to elucidate which chemical compounds in coffee influence coffee foam quality.

The approach was to acquire a group 41 instant coffee samples launched in the UK market both from JDE and competitors, assess the foam quality performance and then classify the coffees in products with good or poor foaming behaviour. For this reason, a foam quality assessment method was developed and proved sufficient to distinguish optimal from poor foaming behaviour samples. The foam quality was comprised by three parameters: Foam Ability; Drainage rate; Disproportionation/Coalescence rate. It was found that 21 instant coffee samples were significantly different ($p<0.05$) in terms of foam ability from a control coffee sample. Correlation analysis between the lipid content of samples and foam quality performance showed that lipid content can be associated with foam quality, but the chemical profile of lipid content has to be considered as foaming mechanisms are driven by the chemical compounds. It was found the roasting degree plays a significant role on the formation of coffee foam. So, it was hypothesised that during roasting, foam promoting compounds are generated. It is already reported in the literature that foam promoting compounds, which originate from caffeic acid, were generated during roasting. Therefore, these

results strongly indicated the importance of the phenolic profile in the pursuit of understanding the foaming mechanisms. For this reason, a chemical screening of 38 phenolic compounds (MSI level 1 or level 2 identification) was performed via LCMS for the instant coffee samples of interest. The normalised abundance of each chemical entity was correlated with each foam quality parameter (i.e. Foam Ability, Drainage Rate, Disproportionation Rate). It was found that two chemical compounds were moderately correlated with Drainage rate. 4-vinylguaiacol appeared to have a foam promoting nature (Pearson's r= -0.89), whereas p-Coumaroylquinic acid lactone appeared to have antifoaming activity (Drainage rate; Pearson's r=0.82).

As the association between most of the selected polyphenols and foam quality was not as hypothesised, there was a need to employ untargeted metabolomic techniques to investigate which chemical compounds were strongly associated with foam quality performance. It was found that 322 chemical entities were significantly correlated ($p<0.05$, $R^2>0.67$) with at least one foam quality parameter and 209 chemical entities out of the initial 322 were annotated with high certainty (CSI score>-150). Subsequently, 16 compounds were most important in terms of strength of correlation and certainty of annotation. Finally, 6 chemical compounds were successfully identified (MSI level 1). These compounds were 5 cyclo dipeptides (Cyclo(-Pro-Val), Cyclo(Phe-Pro), Cyclo(Phe-Val) and Cyclo(Leu-Phe) and Cyclo(Phe-Phe)) and Mannotetraose. All compounds were previously reported in coffee, with the exception of Cyclo(Phe-Phe) which is reported in instant coffee for the first time here.

It was found that these chemical compounds can act as foam quality markers, because their presence in a given coffee system indicates good foam quality. At this point it was considered whether such compounds were only good foam quality indicators or actively influence foam quality. For this reason, the key foam targets were spiked in a poor foam quality coffee and the foam quality of the spiked solution was assessed. An automated foam analyser was employed for this set of experiments and the assessment comprised by the Foam height vs time and Bubble structure per $mm^2$ vs time. Although bubble structure was not used as a parameter to identify the foam associated compounds, it was found that by increasing the concentration of Cyclo(Pro-Val) 7.5 times the initial concentration, more bubbles were created per $mm^2$ compared to control unspiked sample. Based on these results, it was important to understand how Cyclo(Pro-Val) interacts with the rest of the molecules in the foam structure. A dynamic surface tension experiment using Cyclo(Pro-Val) solubilised in ultra-pure water showed that the surface tension did not decrease but it stayed constant and close to the surface tension of ultra-pure water at 20˚C (i.e. 72.8 mN/m). Thus, it was hypothesised that Cyclo(Pro-Val) may be found in the lamellae between bubbles and interact with other surface active compounds. Its structure may indicate the oxygen atoms interact with polar areas of other compounds while the small aliphatic chain or the heterocyclic furan group interact with non-polar areas of other compounds.

Dynamic surface tension experiments were performed for the control sample and two samples (SD3-SR1/12 and Trial-FD5) with the highest and lowest foam ability, respectively. Since Trial-FD5 has the lowest foam quality it was expected

that its surface tension would be higher than control and SD3-SR1/12. However, the opposite was observed. A diffusion-controlled model was fitted to the dynamic surface tension and sufficiently described ($R^2$ >0.91) the diffusion phenomena that occurred during the first moments of droplet creation. It was found that the poor foam coffee (i.e. Trial-FD5) had higher values of diffusivity towards the air/beverage interface than the rest of the sample set. It was observed that there was a scope for higher $R^2$ and this could potentially be achieved by developing a diffusion-controlled model where the intermolecular interactions between surface active and other soluble molecules is considered. It was hypothesised that the chemical compounds which were present in Trial-FD5 and were associated with foam quality, were not able to assist on the creation of stable foam, but these compounds were able to decrease the surface tension to lower levels than good foam quality samples, such as Control and SD3-SR1/12.

At this point, it was important to investigate whether the foam promoting Cyclo(Pro-Val) is a product of the roasting process. For this reason, in the final chapter of this thesis, LCMS was employed in order to monitor the chemical transformation of coffee during roasting and during the different stages of process (i.e. from green bean to roasted bean to instant coffee). It was found that indeed Cyclo(Pro-Val) along with the other previously identified foam-associated cyclo dipeptides were generated during roasting. The associated untargeted chemical analysis revealed that the N-[(R)-3-[(**L-Val-L-Pro-**)Amino]-1,2-dioxopentyl]-D-Leu-L-Val-OH peptide, which was correlated with Drainage Rate, is also generated during roasting. Thus, it is can be hypothesised that this oligopeptide could be the precursor of foam promoting Cyclo(Pro-Val).

The chemical analysis on samples showed that hydroxycinnamic acids, amino acids and carbohydrates are degraded in roasting degree, which findings are in accordance with literature. It was also found that many hydroxycinnamic acid were more abundant in instant coffee than in green bean and it could be hypothesised these polyphenolic acids were once bound in arabinogalactan structures and were released during the hydrolysis step of the instant coffee process.

Overall, the precise compounds which directly affect the foam ability and drainage rate were not identified by the spiking experiment. However, it was found that Cyclo(Pro-Val) may have an effect on bubble coalescence during aeration step. Taking into account the example of Cyclo(Pro-Val) and its potentially foam-associated precursor (i.e. N-[(R)-3-[(L-Val-L-Pro-)Amino]-1,2-dioxopentyl]-D-Leu-L-Val-OH peptide), it can be hypothesized that the other 5 key foam compounds, which were previously reported in Chapter 6, may be related, through chemical pathways, to some of rest 201 highly foam associated compounds which were presented in Chapter 5. An important example of this hypothesis is the foam associated oligopeptide NH2-Tyr-Pro-**Phe-Pro**-CONH2 (reported in Chapter 5) and the key foam compound Cyclo(Phe-Pro).

## 8.2 Future work

Further understanding of the foam formation mechanisms and the role of key foam compounds would require further experiments. Immediate action points for future work would include:

- **Improving the identification techniques for key foam compounds**: In the present thesis it was found that 211 chemical entities were strongly correlated with foam quality. However, only 6 chemical entities were unambiguously identified at MSI level 1. The list of key foam candidates was shortened to such an extent because many of the MS2 annotated compounds were not commercially available. Therefore, employing other identification techniques such as NMR, coupled to a preparative LCMS workflow, would assist in identifying any chemical compound that is isolated from the coffee matrix.
- **Understanding the intermolecular interactions of key foam compounds**: The literature review on beer foam showed that the optimum foam quality is achieved by synergistic effects of beer protein with iso-a-acids. In this thesis, it was found Cyclo(Pro-Val) actively influences foam structure and there was an indication that it interacts with other chemical compounds. If another compound is found to actively influence foam quality, it is very important to understand the intermolecular interactions of key foam compounds. The nature of interactions could be investigated by running molecular dynamic simulations of a mixture of key foam compounds dissolved in water.
- **Role of N-[(R)-3-[(L-Val-L-Pro-)Amino]-1,2-dioxopentyl]-D-Leu-L-Val-OH peptide on foam quality:** This compound was found to be correlated with good foam quality and it was also found to be generated during roasting. Therefore, there is strong evidence that this compound actively influences foam quality. Isolation of this compound and spiking

experiment with subsequent foam quality assessment would reveal if this compound enhanced foam quality of coffee.

- **Viscosity determination of instant coffee samples:** Since the gravitational drainage is highly dependent by the viscosity of instant coffee samples, its determination and correlation analysis with drainage rate will reveal the characteristics of sample set. Such measurements can be utilized in order to understand the effect of key foaming compounds to foaming quality

The work presented in this thesis has shown the potential of correlating data from metabolomic analysis with foam quality performance to investigate chemical compounds that influence foam. On a wider spectrum, the same methodology can be used to investigate chemical compounds that drive any physico-chemical trait of interest in a given system (e.g. coffee aroma, whole bean colour etc.).

In terms of industrial applications, the key foam targets that were validated via MSI level 1, can be considered as foam quality markers because their presence in an instant coffee system could indicate good foam quality. Since it was found that these compounds were mostly generated during roasting, it is very important to perform optimisation experiments on roasting profiles of different coffee blends in order to acquire more foam promoting compounds in the final coffee product. Finally, the establishment of foam quality markers throughout the instant coffee process can assist in manufacturing products with desirable physico-chemical traits.

# Reference


Acuña, R., Bassüner, R., Beilinson, V., Cortina, H., Cadena-Gómez, G., Montes, V. and Nielsen, N.C. (1999) 'Coffee seeds contain 11S storage proteins', *Physiologia Plantarum*, 105(1), pp. 122–131. Available at: https://doi.org/10.1034/j.1399-3054.1999.105119.x.

Adams, A., De Kimpe, N. and Van Boekel, M.A.J.S. (2008) 'Modification of casein by the lipid oxidation product malondialdehyde', *Journal of Agricultural and Food Chemistry*, 56(5), pp. 1713–1719. Available at: https://doi.org/10.1021/jf072385b.

Ali, M., Homann, T., Kreisel, J., Khalil, M., Puhlmann, R., Kruse, H.P. and Rawel, H. (2012) 'Characterization and modeling of the interactions between coffee storage proteins and phenolic compounds', *Journal of Agricultural and Food Chemistry*, 60(46), pp. 11601–11608. Available at: https://doi.org/10.1021/jf303372a.

Al-Shemmeri, M., Windows-Yule, K., Lopez-Quiroga, E. and Fryer, P.J. (2021) 'Coffee bean particle motion in a spouted bed measured using Positron Emission Particle Tracking (PEPT)', *Journal of Food Engineering*, 311, p. 110709. Available at: https://doi.org/https://doi.org/10.1016/j.jfoodeng.2021.110709.

Alves, R.C., Rodrigues, F., Nunes, M.A., Vinha, A.F. and Oliveira, M.B.P.P. (2017) 'State of the art in coffee processing by-products', in *Handbook of Coffee Processing By-Products*. Elsevier, pp. 1–26.

Andres-Lacueva, C., Monagas, M., Khan, N., Izquterdo-Pulido, M., Urpi-Sarda, M., Permanyer, J. and Lamuela-Raventós, R.M. (2008) 'Flavanol and flavonol contents of cocoa powder products: Influence of the manufacturing process', *Journal of Agricultural and Food Chemistry*, 56(9), pp. 3111–3117. Available at: https://doi.org/10.1021/JF0728754/ASSET/IMAGES/LARGE/JF-2007-028754_0002.JPEG.

Anzueto, F., Baumann, T.W., Graziosi, G., Piccin, C.R. and van der Vossen, H.A.M. (2005) 'The plant', *Espresso Coffee. The Science of Quality*, pp. 21–86.

Asano, K. and Hashimoto, N. (1980) 'Isolation and Characterization of Foaming Proteins of Beer', *Journal of the American Society of Brewing Chemists*, 38(4), pp. 129–137. Available at: https://doi.org/10.1094/ASBCJ-38-0129.

Baeza, G., Sarriá, B., Bravo, L. and Mateos, R. (2016) 'Exhaustive Qualitative LC-DAD-MSn Analysis of Arabica Green Coffee Beans: Cinnamoyl-glycosides and Cinnamoylshikimic Acids as New Polyphenols in Green Coffee', *Journal of Agricultural and Food Chemistry*, 64(51), pp. 9663–9674. Available at: https://doi.org/10.1021/acs.jafc.6b04022.

Ballesteros, L.F., Teixeira, J.A. and Mussatto, S.I. (2014) 'Chemical, Functional, and Structural Properties of Spent Coffee Grounds and Coffee Silverskin', *Food and Bioprocess Technology*, 7(12), pp. 3493–3503. Available at: https://doi.org/10.1007/s11947-014-1349-z.

Bee, S., Brando, C.H.J., Brumen, G., Carvalhaes, N., Kölling-Speer, I., Speer, K., Suggi Liverani, F., Teixeira, A.A., Teixeira, R., Thomaziello, R.A., Viani, R. and Vitzthum, O.G. (2005) *The raw bean*, *Espresso Coffee*. Available at: https://doi.org/10.1016/b978-012370371-2/50004-4.

Bekedam, E.K. (2008) ‘Coffee brew melanoidins’, *Structural and Functional Properties of Brown-Colored Coffee Compounds*, pp. 2–15. Available at: http://library.wur.nl/WebQuery/wda/1883928.

Bekedam, E.K., De Laat, M.P.F.C., Schols, H.A., Van Boekel, M.A.J.S. and Smit, G. (2007) ‘Arabinogalactan proteins are incorporated in negatively charged coffee brew melanoidins’, *Journal of Agricultural and Food Chemistry*, 55(3), pp. 761–768. Available at: https://doi.org/10.1021/jf063010d.

Bekedam, E.K., Loots, M.J., Schols, H.A., Van Boekel, M.A.J.S. and Smit, G. (2008) ‘Roasting effects on formation mechanisms of coffee brew melanoidins’, *Journal of Agricultural and Food Chemistry*, 56(16), pp. 7138–7145. Available at: https://doi.org/10.1021/jf800999a.

Bekedam, E.K., Roos, E., Schols, H.A., Van Boekel, M.A.J.S. and Smit, G. (2008) ‘Low molecular weight melanoidins in coffee brew’, *Journal of Agricultural and Food Chemistry*, 56(11), pp. 4060–4067. Available at: https://doi.org/10.1021/jf8001894.

Bekedam, E.K., Schols, H.A., Van Boekel, M.A.J.S. and Smit, G. (2006) ‘High molecular weight melanoidins from coffee brew’, *Journal of Agricultural and Food Chemistry*, 54(20), pp. 7658–7666. Available at: https://doi.org/10.1021/jf0615449.

Bekedam, E.K., Schols, H.A., Van Boekel, M.A.J.S. and Smit, G. (2008) ‘Incorporation of chlorogenic acids in coffee brew melanoidins’, *Journal of Agricultural and Food Chemistry*, 56(6), pp. 2055–2063. Available at: https://doi.org/10.1021/jf073157k.

Belay, A., Ture, K., Redi, M. and Asfaw, A. (2008) ‘Measurement of caffeine in coffee beans with UV/vis spectrometer’, *Food Chemistry*, 108(1), pp. 310–315. Available at: https://doi.org/10.1016/j.foodchem.2007.10.024.

Belitz, H.-D., Grosch, W. and Schieberle, P. (eds) (2009) ‘Coffee, Tea, Cocoa BT - Food Chemistry’, in. Berlin, Heidelberg: Springer Berlin Heidelberg, pp. 938–970. Available at: https://doi.org/10.1007/978-3-540-69934-7_22.

Bikerman, J.J. (1973) *Foams*. Berlin, Heidelberg: Springer Berlin Heidelberg. Available at: https://doi.org/10.1007/978-3-642-86734-7.

Bonnländer, B., Eggers, R., Engelhardt, U.H. and Maier, H.G. (2005a) ‘Roasting’, *Espresso coffee: the science of quality*, 398.

Bonnländer, B., Eggers, R., Engelhardt, U.H. and Maier, H.G. (2005b) ‘Roasting’, *Espresso coffee: the science of quality*, 398.

Borrelli, R.C., Visconti, A., Mennella, C., Anese, M. and Fogliano, V. (2002) ‘Chemical characterization and antioxidant properties of coffee melanoidins’, *Journal of Agricultural and Food Chemistry*, 50(22), pp. 6527–6533. Available at: https://doi.org/10.1021/jf025686o.

Bradbury, A.G.W. and Halliday, D.J. (1987) ‘Polysaccharides in green coffee beans’, in *COLLOQUE Scientifique International sur le Café, 12. Montreux (Suiza), Juin 29-Juillet 3, 1987.*.

Bradbury, A.G.W. and Halliday, D.J. (1990) ‘Chemical Structures of Green Coffee Bean Polysaccharides’, *Journal of Agricultural and Food Chemistry*, 38(2), pp. 389–392. Available at: https://doi.org/10.1021/jf00092a010.

British Coffee Association (2018) ‘The UK coffee market and its impact on the economy. A report for the British Coffee Association’, *Business in Confidence*, (April), pp. 1–30. Available at: https://www.britishcoffeeassociation.org/assets/files/uploads/BCA CEBR - The economic value of coffee in the UK 20 April_FINAL.pdf.

‘BS 5752-6:1983, ISO 3726-1993 - Methods of test for coffee and coffee products. Instant coffee. Determination of loss in mass at 70°C under reduced pressure’ (1993) *Spelt Trade Publication Pvt. Lim-ited*. BSI, pp. 1–14.

Caldero N, A.I., Wright, B.J., Hurst, W.J. and van Breemen, R.B. (2009) ‘Screening Antioxidants Using LC-MS: Case Study with Cocoa’, *J. Agric. Food Chem*, 57, p. 5693. Available at: https://doi.org/10.1021/jf9014203.

Cämmerer, B., Jalyschko, W. and Kroh, L.W. (2002) ‘Intact carbohydrate structures as part of the melanoidin skeleton’, *Journal of Agricultural and Food Chemistry*, 50(7), pp. 2083–2087. Available at: https://doi.org/10.1021/jf011106w.

Cämmerer, B. and Kroh, L.W. (1995) ‘Investigation of the influence of reaction conditions on the elementary composition of melanoidins’, *Food Chemistry*, 53(1), pp. 55–59. Available at: https://doi.org/10.1016/0308-8146(95)95786-6.

Capek, P., Matulová, M., Navarini, L. and Suggi-Liverani, F. (2010) ‘Structural features of an arabinogalactan-protein isolated from instant coffee powder of Coffea arabica beans’, *Carbohydrate Polymers*, 80(1), pp. 180–185. Available at: https://doi.org/10.1016/j.carbpol.2009.11.016.

Caprioli, G., Fiorini, D., Maggi, F., Nicoletti, M., Ricciutelli, M., Toniolo, C., Prosper, B., Vittori, S. and Sagratini, G. (2016) ‘Nutritional composition, bioactive compounds and volatile profile of cocoa beans from different regions of Cameroon’, *https://doi.org/10.3109/09637486.2016.1170769*, 67(4), pp. 422–430. Available at: https://doi.org/10.3109/09637486.2016.1170769.

Castaño-Castrillón, J.J., Quintero, G.P. and León Vargas, R. (2000) ‘Characterization of yield extraction and content of soluble solids in the coffee drink’, *Cenicafé*, 51(3), pp. 185–195.

Chang, C.H. and Franses, E.I. (1995) ‘Adsorption dynamics of surfactants at the air/water interface: a critical review of mathematical models, data, and mechanisms’, *Colloids and Surfaces A: Physicochemical and Engineering Aspects*, 100(C), pp. 1–45. Available at: https://doi.org/10.1016/0927-7757(94)03061-4.

Christopher M. Bishop (2006) *Pattern Recognition and Machine Learning*. Springer.

Clarke, R. and Vitzthum, O.G. (2008) *Coffee: recent developments*. John Wiley & Sons.

Clarke, R.J. (2001) ‘Technology III: instant coffee’, *Coffee: Recent Developments*, pp. 125–139.

Clarke, R.J. and Macrae, R. (1985) *Volume 1: Chemistry*.

Clifford, M.N. (1985) ‘Chemical and Physical Aspects of Green Coffee and Coffee Products’, in *Coffee*. Springer US, pp. 305–374. Available at: https://doi.org/10.1007/978-1-4615-6657-1_13.

Clifford, M.N., Johnston, K.L., Knight, S. and Kuhnert, N. (2003) ‘Hierarchical scheme for LC-MSn identification of chlorogenic acids’, *Journal of Agricultural and Food Chemistry*, 51(10), pp. 2900–2911. Available at: https://doi.org/10.1021/JF026187Q/ASSET/IMAGES/LARGE/JF026187QF00011.JPEG.

Cordoba, N., Fernandez-Alduenda, M., Moreno, F.L. and Ruiz, Y. (2020) ‘Coffee extraction: A review of parameters and their influence on the physicochemical characteristics and flavour of coffee brews’, *Trends in Food Science and Technology*, 96(November 2019), pp. 45–60. Available at: https://doi.org/10.1016/j.tifs.2019.12.004.

D’Agostina, A., Boschin, G., Bacchini, F. and Arnoldi, A. (2004) ‘Investigations on the high molecular weight foaming fractions of espresso coffee’, *Journal of*

*Agricultural and Food Chemistry*, 52(23), pp. 7118–7125. Available at: https://doi.org/10.1021/jf049013c.

Deotale, S.M., Dutta, S., Moses, J.A. and Anandharamakrishnan, C. (2019) 'Coffee oil as a natural surfactant', *Food Chemistry*, 295(January), pp. 180–188. Available at: https://doi.org/10.1016/j.foodchem.2019.05.090.

Djoumbou Feunang, Y., Eisner, R., Knox, C., Chepelev, L., Hastings, J., Owen, G., Fahy, E., Steinbeck, C., Subramanian, S., Bolton, E., Greiner, R. and Wishart, D.S. (2016) 'ClassyFire: automated chemical classification with a comprehensive, computable taxonomy', *Journal of Cheminformatics*, 8(1), pp. 1–20. Available at: https://doi.org/10.1186/s13321-016-0174-y.

Dorfner, R., Ferge, T., Kettrup, A., Zimmermann, R. and Yeretzian, C. (2003) 'Real-time monitoring of 4-vinylguaiacol, guaiacol, and phenol during coffee roasting by resonant laser ionization time-of-flight mass spectrometry', *Journal of Agricultural and Food Chemistry*, 51(19), pp. 5768–5773. Available at: https://doi.org/10.1021/jf0341767.

Drenckhan, W. and Saint-Jalmes, A. (2015) 'The science of foaming', *Advances in Colloid and Interface Science*, 222, pp. 228–259. Available at: https://doi.org/10.1016/j.cis.2015.04.001.

Dührkop, K., Fleischauer, M., Ludwig, M., Aksenov, A.A., Melnik, A. V., Meusel, M., Dorrestein, P.C., Rousu, J. and Böcker, S. (2019) 'SIRIUS 4: a rapid tool for turning tandem mass spectra into metabolite structure information', *Nature Methods 2019 16:4*, 16(4), pp. 299–302. Available at: https://doi.org/10.1038/S41592-019-0344-8.

Dührkop, K., Nothias, L.F., Fleischauer, M., Reher, R., Ludwig, M., Hoffmann, M.A., Petras, D., Gerwick, W.H., Rousu, J., Dorrestein, P.C. and Böcker, S. (2020) 'Systematic classification of unknown metabolites using high-resolution fragmentation mass spectra', *Nature Biotechnology 2020 39:4*, 39(4), pp. 462–471. Available at: https://doi.org/10.1038/S41587-020-0740-8.

Dührkop, K., Shen, H., Meusel, M., Rousu, J. and Böcker, S. (2015) 'Searching molecular structure databases with tandem mass spectra using CSI:FingerID', *Proceedings of the National Academy of Sciences of the United States of America*, 112(41), pp. 12580–12585. Available at: https://doi.org/10.1073/PNAS.1509788112/SUPPL_FILE/PNAS.201509788SI.PDF.

Eugénie, S. de P., Fabrice, D., Gérard, C. and Samir, M. (2014) 'Effect of bulk viscosity and surface tension kinetics on structure offoam generated at the pilot scale', *Food Hydrocolloids*, 34, pp. 104–111. Available at: https://doi.org/10.1016/j.foodhyd.2012.12.001.

Euston, S.R., Hughes, P., Naser, M.A. and Westacott, R.E. (2008) 'Molecular dynamics simulation of the cooperative adsorption of barley lipid transfer protein and cis-isocohumulone at the vacuum-water interface', *Biomacromolecules*, 9(11), pp. 3024–3032. Available at: https://doi.org/10.1021/bm8004325.

Evans, D.E. and Bamforth, C.W. (2009) 'Beer foam: Achieving a suitable head', *Beer*, pp. 1–60. Available at: https://doi.org/10.1016/B978-0-12-669201-3.00001-4.

Evans, D.E. and Sheehan, M.C. (2002) 'Don't be fobbed off: The substance of beer foam - A review', *Journal of the American Society of Brewing Chemists*, 60(2), pp. 47–57. Available at: https://doi.org/10.1094/asbcj-60-0047.

Farah, A. and Donangelo, C.M. (2006) 'Phenolic compounds in coffee', *Brazilian Journal of Plant Physiology*, 18(1), pp. 23–36. Available at: https://doi.org/10.1590/S1677-04202006000100003.

Farah, A., De Paulis, T., Trugo, L.C. and Martin, P.R. (2005) 'Effect of roasting on the formation of chlorogenic acid lactones in coffee', *Journal of Agricultural and Food Chemistry*, 53(5), pp. 1505–1513. Available at: https://doi.org/10.1021/jf048701t.

Ferrari, M., Ravera, F., De Angelis, E., Liverani, F.S. and Navarini, L. (2010) 'Interfacial properties of coffee oils', *Colloids and Surfaces A: Physicochemical and Engineering Aspects*, 365(1–3), pp. 79–82. Available at: https://doi.org/10.1016/j.colsurfa.2010.02.002.

Fincher, G.B., Stone, B.A. and Clarke, A.E. (1983) 'Arabinogalactan-proteins: structure, biosynthesis, and function', *Annual Review of Plant Physiology*, 34(1), pp. 47–70.

Fischer, M., Reimann, S., Trovato, V. and Redgwell, R.J. (2001) 'Polysaccharides of green Arabica and Robusta coffee beans', *Carbohydrate Research*, 330(1), pp. 93–101. Available at: https://doi.org/10.1016/S0008-6215(00)00272-X.

Flament, I. (2001) *Coffee flavor chemistry*. John Wiley & Sons.

Flament, I. (2002) 'Coffee Flavor Chemistry', p. 424.

Folmer, B., Blank, I. and Hofmann, T. (2017) *Crema-Formation, Stabilization, and Sensation*, *The Craft and Science of Coffee*. Elsevier Inc. Available at: https://doi.org/10.1016/B978-0-12-803520-7.00017-7.

Folstar, P. (1985) 'Lipids. Coffee Chemistry, Vol. I'. Elsevier Applied Science, London.

Folstar, P., Pilnik, W., HEUS, J. and PLAS, H. (1975) 'The composition of the fatty acids in coffee oil and coffee wax..', in *COLLOQUE Scientifique International sur le Café, 7. Hamburgo (Alemania), Juin 9-14, 1975.*.

Frank, O., Blumberg, S., Kunert, C., Zehentbauer, G. and Hofmann, T. (2007a) 'Structure determination and sensory analysis of bitter-tasting 4-vinylcatechol oligomers and their identification in roasted coffee by means of LC-MS/MS', *Journal of Agricultural and Food Chemistry*, 55(5), pp. 1945–1954. Available at: https://doi.org/10.1021/jf0632280.

Frank, O., Blumberg, S., Kunert, C., Zehentbauer, G. and Hofmann, T. (2007b) 'Structure determination and sensory analysis of bitter-tasting 4-vinylcatechol oligomers and their identification in roasted coffee by means of LC-MS/MS', *Journal of Agricultural and Food Chemistry*, 55(5), pp. 1945–1954. Available at: https://doi.org/10.1021/jf0632280.

Friedman, M. (1996) 'Food browning and its prevention: An overview', *Journal of Agricultural and Food Chemistry*, 44(3). Available at: https://doi.org/10.1021/jf950394r.

Ginz, M. and Engelhardt, U.H. (2000) 'Identification of proline-based diketopiperazines in roasted coffee', *Journal of Agricultural and Food Chemistry*, 48(8), pp. 3528–3532. Available at: https://doi.org/10.1021/jf991256v.

Ginz, M. and Engelhardt, U.H. (2001) 'Identification of new diketopiperazines in roasted coffee', *European Food Research and Technology*, 213(1), pp. 8–11. Available at: https://doi.org/10.1007/s002170100322.

Gmoser, R., Bordes, R., Nilsson, G., Altskär, A., Stading, M., Lorén, N. and Berta, M. (2017) 'Effect of dispersed particles on instant coffee foam stability and

rheological properties', *European Food Research and Technology*, 243(1), pp. 115–121. Available at: https://doi.org/10.1007/s00217-016-2728-7.
Gniechwitz, D., Reichardt, N., Meiss, E., Ralph, J., Steinhart, H., Blaut, M. and Bunzel, M. (2008) 'Characterization and fermentability of an ethanol soluble high molecular weight coffee fraction', *Journal of Agricultural and Food Chemistry*, 56(14), pp. 5960–5969. Available at: https://doi.org/10.1021/jf800231q.
Hayase, F., Usui, T. and Watanabe, H. (2006) 'Chemistry and some biological effects of model melanoidins and pigments as Maillard intermediates', *Molecular Nutrition and Food Research*, 50(12), pp. 1171–1179. Available at: https://doi.org/10.1002/mnfr.200600078.
Hernández, J.A., Heyd, B. and Trystram, G. (2008a) 'On-line assessment of brightness and surface kinetics during coffee roasting', *Journal of Food Engineering*, 87(3), pp. 314–322. Available at: https://doi.org/10.1016/j.jfoodeng.2007.12.009.
Hernández, J.A., Heyd, B. and Trystram, G. (2008b) 'Prediction of brightness and surface area kinetics during coffee roasting', *Journal of Food Engineering*, 89(2), pp. 156–163. Available at: https://doi.org/10.1016/j.jfoodeng.2008.04.026.
Hoffmann, M.A., Nothias, L.-F., Ludwig, M., Fleischauer, M., Gentry, E.C., Witting, M., Dorrestein, P.C., Dührkop, K. and Böcker, S. (2021) 'Assigning confidence to structural annotations from mass spectra with COSMIC', *bioRxiv*, p. 2021.03.18.435634. Available at: https://doi.org/10.1101/2021.03.18.435634.
Hofmann, T. (1998a) 'Studies on melanoidin-type colorants generated from the Maillard reaction of protein-bound lysine and furan-2-carboxaldehyde - Chemical characterisation of a red coloured domaine', *Zeitschrift fur Lebensmittel -Untersuchung und -Forschung*, 206(4), pp. 251–258. Available at: https://doi.org/10.1007/s002170050253.
Hofmann, T. (1998b) 'Studies on the Relationship between Molecular Weight and the Color Potency of Fractions Obtained by Thermal Treatment of Glucose/Amino Acid and Glucose/Protein Solutions by Using Ultracentrifugation and Color Dilution Techniques', *Journal of Agricultural and Food Chemistry*, 46(10), pp. 3891–3895. Available at: https://doi.org/10.1021/jf980397e.
Hofmann, T., Bors, W. and Stettmaier, K. (1999a) 'Radical-assisted melanoidin formation during thermal processing of foods as well as under physiological conditions', *Journal of Agricultural and Food Chemistry*, 47(2), pp. 391–396. Available at: https://doi.org/10.1021/jf980627p.
Hofmann, T., Bors, W. and Stettmaier, K. (1999b) 'Studies on radical intermediates in the early stage of the nonenzymatic browning reaction of carbohydrates and amino acids', *Journal of Agricultural and Food Chemistry*, 47(2), pp. 379–390. Available at: https://doi.org/10.1021/jf980626x.
Hofmann, T. and Schieberle, P. (2002) 'Chemical interactions between odor-active thiols and melanoidins involved in the aroma staling of coffee beverages', *Journal of Agricultural and Food Chemistry*, 50(2), pp. 319–326. Available at: https://doi.org/10.1021/jf010823n.
Homma, S. (2001) 'Chemistry II: Non-Volatile Compounds, Part II', *Coffee: recent developments*, pp. 50–67.
Hudson, J.R. (1968) 'Measurement of head-retention in bottled beer', *Journal of Institute of Brewing*, 74(3), pp. 275-.
Hwang, C.F., Chen, C.C. and Ho, C.T. (2012) 'Contribution of coffee proteins to roasted coffee volatiles in a model system', *International Journal of Food*

*Science and Technology*, 47(10), pp. 2117–2126. Available at: https://doi.org/10.1111/j.1365-2621.2012.03078.x.

Iaccheri, E., Ragni, L., Cevoli, C., Romani, S., Dalla Rosa, M. and Rocculi, P. (2019) 'Glass transition of green and roasted coffee investigated by calorimetric and dielectric techniques'. Available at: https://doi.org/10.1016/j.foodchem.2019.125187.

Illy, E. and Navarini, L. (2011) 'Neglected Food Bubbles: The Espresso Coffee Foam', *Food Biophysics*, 6(3), pp. 335–348. Available at: https://doi.org/10.1007/s11483-011-9220-5.

International Coffee Organization, I. (2023) *International Coffee Organization - Trade Statistics Table*. Available at: http://www.ico.org/trade_statistics.asp?section=Statistics (Accessed: 2 June 2020).

Jaiswal, R., Matei, M.F., Golon, A., Witt, M. and Kuhnert, N. (2012) 'Understanding the fate of chlorogenic acids in coffee roasting using mass spectrometry based targeted and non-targeted analytical strategies', *Food and Function*, 3(9), pp. 976–984. Available at: https://doi.org/10.1039/c2fo10260a.

Kaersoaard, B.P. and Hejgaard, J. (1979) 'Antigenic beer macromolecules an experimental survey of purification methods', *J.Inst. Brew.*, 85, pp. 103–111.

Kampmann, B. and Maier, H.G. (1982) 'Säuren des Kaffees', *Zeitschrift für Lebensmittel-Untersuchung und Forschung*, 175(5), pp. 333–336.

Karakashev, S.I. (2017) *Hydrodynamics of foams*, *Experiments in Fluids*. Springer Berlin Heidelberg. Available at: https://doi.org/10.1007/s00348-017-2332-z.

Kaufman, L. (1990) *Finding groups in data : an introduction to cluster analysis*. Edited by P.J. Rousseeuw. New York: Wiley (Wiley series in probability and mathematical statistics. Applied probability and statistics).

Van Kempen, S.E.H.J., Schols, H.A., Van Der Linden, E. and Sagis, L.M.C. (2014) 'Molecular assembly, interfacial rheology and foaming properties of oligofructose fatty acid esters', *Food and Function*, 5(1), pp. 111–122. Available at: https://doi.org/10.1039/c3fo60324e.

Kim, H.W., Wang, M., Leber, C.A., Nothias, L.F., Reher, R., Kang, K. Bin, Van Der Hooft, J.J.J., Dorrestein, P.C., Gerwick, W.H. and Cottrell, G.W. (2021) 'NPClassifier: A Deep Neural Network-Based Structural Classification Tool for Natural Products', *Journal of Natural Products*, 84(11), pp. 2795–2807. Available at: https://doi.org/10.1021/ACS.JNATPROD.1C00399/SUPPL_FILE/NP1C00399_SI_002.XLSX.

Kitts, D.D., Wu, C.H., Kopec, A. and Nagasawa, T. (2006) 'Chemistry and genotoxicity of caramelized sucrose', *Molecular Nutrition and Food Research*, 50(12), pp. 1180–1190. Available at: https://doi.org/10.1002/mnfr.200600181.

Kobayashi, N., Segawa, S., Umemoto, S., Kuroda, H., Kaneda, H., Mitani, Y., Watari, J. and Takashio, M. (2002) 'A new method for evaluating foam-damaging effect by free fatty acids', *Journal of the American Society of Brewing Chemists*, 60(1), pp. 37–41. Available at: https://doi.org/10.1094/asbcj-60-0037.

Kölling-Speer, I., Kurt, A. and Speer, K. (1997) 'Cafestol an dehydrocafestol in roasted coffee', in *COLLOQUE SCIENTIFIQUE INTERNATIONAL SUR LE CAFE*. ASIC ASSOCIATION SCIENTIFIQUE INTERNATIONALE, pp. 201–204.

Kölling-Speer, I. and Speer, K. (2001) '16-O-methylkahweol in Robusta coffee', in *19th International Colloquium on the Chemistry of Coffee. Paris: ASIC*.

Konstantinidis, N., Franke, H., Schwarz, S. and Lachenmeier, D.W. (2023) 'Risk Assessment of Trigonelline in Coffee and Coffee By-Products', *Molecules*. MDPI. Available at: https://doi.org/10.3390/molecules28083460.

Koshima, Y., Kitamura, Y., Islam, M.Z. and Kokawa, M. (2020) 'Quantitative and qualitative evaluation of fatty acids in coffee oil and coffee residue', *Food Science and Technology Research*, 26(4), pp. 545–552. Available at: https://doi.org/10.3136/FSTR.26.545.

Kremr, D., Bajer, T., Bajerová, P., Surmová, S. and Ventura, K. (2016) 'Unremitting problems with chlorogenic acid nomenclature: A review', *Quimica Nova*. Sociedade Brasileira de Quimica, pp. 530–533. Available at: https://doi.org/10.5935/0100-4042.20160063.

Król, K., Gantner, M., Tatarak, A. and Hallmann, E. (2020) 'The content of polyphenols in coffee beans as roasting, origin and storage effect', *European Food Research and Technology*, 246(1), pp. 33–39. Available at: https://doi.org/10.1007/s00217-019-03388-9.

Ky, C.L., Louarn, J., Dussert, S., Guyot, B., Hamon, S. and Noirot, M. (2001) 'Caffeine, trigonelline, chlorogenic acids and sucrose diversity in wild Coffea arabica L. and C. canephora P. accessions', *Food Chemistry*, 75(2), pp. 223–230. Available at: https://doi.org/10.1016/S0308-8146(01)00204-7.

Lang, R., Mueller, C. and Hofmann, T. (2006) 'Development of a stable isotope dilution analysis with liquid chromatography-tandem mass spectrometry detection for the quantitative analysis of di- and trihydroxybenzenes in foods and model systems', *Journal of Agricultural and Food Chemistry*, 54(16), pp. 5755–5762. Available at: https://doi.org/10.1021/JF061118N/ASSET/IMAGES/LARGE/JF061118NF00005.JPEG.

Leloup, V., Louvrier, A. and Liardon, R. (1995) 'Degradation mechanisms of chlorogenic acids during roasting', in *16th International Scientific Colloquium on Coffee*. International Scientific Association on Coffee Paris.

LELOUP, Valérie Martine, Jeanine (CH), C.-1350 O., MORA, Federico (CH), C.-1110 M., DOSSIN, Eric (FR), F.-25370 J. and MONTAVON, Philippe (CH), C.-1112 E. (2019) 'PROCESS OF PREPARING A FOAMING AID, THE FOAMING AID AND USES'.

Lewis, M.J. and Lewis, A.S. (2003) 'Correlation of beer foam with other beer properties', *Technical quarterly-Master Brewers Association of the Americas*, 40(2), pp. 114–124.

Lin, H., Tello, E., Simons, C.T. and Peterson, D.G. (2022) 'Identification of Non-Volatile Compounds Generated during Storage That Impact Flavor Stability of Ready-to-Drink Coffee', *Molecules*, 27(7), p. 2120. Available at: https://doi.org/https://doi.org/10.3390/molecules27072120.

Loglio, G., Pandolfini, P., Liggieri, L., Makievski, A. V. and Ravera, F. (2011) 'Determination of interfacial properties by the pendant drop tensiometry: Optimisation of experimental and calculation procedures', *Bubble and Drop Interfaces*, pp. 7–38.

Lopes, G.R., Passos, C.P., Petronilho, S., Rodrigues, C., Teixeira, J.A. and Coimbra, M.A. (2021) 'Carbohydrates as targeting compounds to produce infusions resembling espresso coffee brews using quality by design approach', *Food Chemistry*, 344, p. 128613. Available at: https://doi.org/10.1016/j.foodchem.2020.128613.

Lu, Y., Bergenståhl, B. and Nilsson, L. (2020) 'Interfacial properties and interaction between beer wort protein fractions and iso-humulone', *Food Hydrocolloids*, 103(December 2019). Available at: https://doi.org/10.1016/j.foodhyd.2020.105648.

Ludwig, E., Raczek, N.N. and Kurrock, T. (1995) 'Contribution to composition and reactivity of coffee protein', in *XVI International Scientific Colloquium on Coffee*.

Lusk, L.T., Goldstein, H. and Ryder, D. (1995) 'Independent Role of Beer Proteins, Melanoidins and Polysaccharides in Foam Formation', *Journal of the American Society of Brewing Chemists*, 53(3), pp. 93–103. Available at: https://doi.org/10.1094/ASBCJ-53-0093.

Macdonald, I.A. and Macrae, R. (1985) 'The determination of amino acids in coffee products..', in *COLLOQUE Scientifique International sur le Café, 11. Lomé (Togo), Fevrier 11-15, 1985.*.

MacLeod, C.S., McKittrick, J.A., Hindmarsh, J.P., Johns, M.L. and Wilson, D.I. (2006) 'Fundamentals of spray freezing of instant coffee', *Journal of Food Engineering*, 74(4), pp. 451–461. Available at: https://doi.org/10.1016/j.jfoodeng.2005.03.034.

Macrae, R. (1985) 'Nitrogenous components', in *Coffee*. Springer, pp. 115–152.

Mariani, C. and Fedeli, E. (1991) 'Sterols of coffee grain of Arabica and Robusta species', *La Riv. It. Sost. Grasse*, 68, pp. 111–115.

Matulová, M., Capek, P., Kaneko, S., Navarini, L. and Suggi, F. (2011) 'Structure of arabinogalactan oligosaccharides derived from arabinogalactan-protein of Coffea arabica instant coffee powder', 346, pp. 1029–1036. Available at: https://doi.org/10.1016/j.carres.2011.03.016.

Mills, C.E., Oruna-Concha, M.J., Mottram, D.S., Gibson, G.R. and Spencer, J.P.E. (2013) 'The effect of processing on chlorogenic acid content of commercially available coffee', *Food Chemistry*, 141(4), pp. 3335–3340. Available at: https://doi.org/10.1016/j.foodchem.2013.06.014.

Moreira, A.S.P., Nunes, F.M., Domingues, M.R. and Coimbra, M.A. (2012) 'Coffee melanoidins: Structures, mechanisms of formation and potential health impacts', *Food and Function*, 3(9), pp. 903–915. Available at: https://doi.org/10.1039/c2fo30048f.

Müller, C. and Hofmann, T. (2005) 'Screening of raw coffee for thiol binding site precursors using "in bean" model roasting experiments', *Journal of Agricultural and Food Chemistry*, 53(7), pp. 2623–2629. Available at: https://doi.org/10.1021/jf048027f.

Murthy, P.S. and Madhava Naidu, M. (2012) 'Sustainable management of coffee industry by-products and value addition - A review', *Resources, Conservation and Recycling*, 66, pp. 45–58. Available at: https://doi.org/10.1016/j.resconrec.2012.06.005.

Nunes, F.M. and Coimbra, M.A. (2001) 'Chemical characterization of the high molecular weight material extracted with hot water from green and roasted arabica coffee', *Journal of Agricultural and Food Chemistry*, 49(4), pp. 1773–1782. Available at: https://doi.org/10.1021/jf0012953.

Nunes, F.M. and Coimbra, M.A. (2002a) 'Chemical characterization of galactomannans and arabinogalactans from two arabica coffee infusions as affected by the degree of roast', *Journal of Agricultural and Food Chemistry*, 50(6), pp. 1429–1434. Available at: https://doi.org/10.1021/jf0109625.

Nunes, F.M. and Coimbra, M.A. (2002b) 'Chemical characterization of the high-molecular-weight material extracted with hot water from green and roasted robusta coffees as affected by the degree of roast', *Journal of Agricultural and Food Chemistry*, 50(24), pp. 7046–7052. Available at: https://doi.org/10.1021/jf020534e.

Nunes, F.M. and Coimbra, M.A. (2007) 'Melanoidins from coffee infusions. Fractionation, chemical characterization, and effect of the degree of roast', *Journal of Agricultural and Food Chemistry*, 55(10), pp. 3967–3977. Available at: https://doi.org/10.1021/jf063735h.

Nunes, F.M. and Coimbra, M.A. (2010) 'Role of hydroxycinnamates in coffee melanoidin formation', *Phytochemistry Reviews*, 9(1), pp. 171–185. Available at: https://doi.org/10.1007/s11101-009-9151-7.

Nunes, F.M., Coimbra, M.A., Duarte, A.C. and Delgadillo, I. (1997) 'Foamability, Foam Stability, and Chemical Composition of Espresso Coffee As Affected by the Degree of Roast', *Journal of Agricultural and Food Chemistry*, 45(8), pp. 3238–3243. Available at: https://doi.org/10.1021/jf970009t.

Nunes, F.M., Cruz, A.C.S. and Coimbra, M.A. (2012) 'Insight into the mechanism of coffee melanoidin formation using modified "in Bean" models', *Journal of Agricultural and Food Chemistry*, 60(35), pp. 8710–8719. Available at: https://doi.org/10.1021/jf301527e.

Nunes, F.M., Domingues, M.R. and Coimbra, M.A. (2005) 'Arabinosyl and glucosyl residues as structural features of acetylated galactomannans from green and roasted coffee infusions', *Carbohydrate Research* [Preprint]. Available at: https://doi.org/10.1016/j.carres.2005.05.002.

Nunes, F.M., Reis, A., Silva, A.M.S., Domingues, M.R.M. and Coimbra, M.A. (2008) 'Rhamnoarabinosyl and rhamnoarabinoarabinosyl side chains as structural features of coffee arabinogalactans', *Phytochemistry*, 69(7), pp. 1573–1585. Available at: https://doi.org/10.1016/j.phytochem.2008.01.021.

Onishi, A. and Proudlove, M.O. (1994) 'Isolation of beer foam polypeptides by hydrophobic interaction chromatography and their partial characterisation', *Journal of the Science of Food and Agriculture*, 65(2), pp. 233–240. Available at: https://doi.org/10.1002/jsfa.2740650218.

Oosterveld, A., Coenen, G.J., Vermeiden, N.C.B., Voragen, A.G.J. and Schols, H.A. (2004) 'Structural features of acetylated galactomannans from green Coffea arabica beans', *Carbohydrate Polymers* [Preprint]. Available at: https://doi.org/10.1016/j.carbpol.2004.08.009.

Oosterveld, A., Harmsen, J.S., Voragen, A.G.J. and Schols, H.A. (2003) 'Extraction and characterization of polysaccharides from green and roasted Coffea arabica beans', *Carbohydrate Polymers*, 52(3), pp. 285–296. Available at: https://doi.org/10.1016/S0144-8617(02)00296-5.

Oracz, J., Zyzelewicz, D. and Nebesny, E. (2015) 'The Content of Polyphenolic Compounds in Cocoa Beans (Theobroma cacao L.), Depending on Variety, Growing Region, and Processing Operations: A Review', *https://doi-org.nottingham.idm.oclc.org/10.1080/10408398.2012.686934*, 55(9), pp. 1176–1192. Available at: https://doi.org/10.1080/10408398.2012.686934.

Padma Ishwarya, S. and Nisha, P. (2021) 'Foaming agents from spent coffee grounds: A mechanistic understanding of the modes of foaming and the role of coffee oil as antifoam', *Food Hydrocolloids*, 112(April 2020), p. 106354. Available at: https://doi.org/10.1016/j.foodhyd.2020.106354.

Park, J.B. (2013) ‘Isolation and quantification of major chlorogenic acids in three major instant coffee brands and their potential effects on H2O 2-induced mitochondrial membrane depolarization and apoptosis in PC-12 cells’, *Food and Function*, 4(11), pp. 1632–1638. Available at: https://doi.org/10.1039/c3fo60138b.

Perrone, D., Farah, A. and Donangelo, C.M. (2012a) ‘Influence of coffee roasting on the incorporation of phenolic compounds into melanoidins and their relationship with antioxidant activity of the brew’, *Journal of Agricultural and Food Chemistry*, 60(17), pp. 4265–4275. Available at: https://doi.org/10.1021/jf205388x.

Perrone, D., Farah, A. and Donangelo, C.M. (2012b) ‘Influence of coffee roasting on the incorporation of phenolic compounds into melanoidins and their relationship with antioxidant activity of the brew’, *Journal of Agricultural and Food Chemistry*, 60(17), pp. 4265–4275. Available at: https://doi.org/10.1021/jf205388x.

Perrone, D., Farah, A., Donangelo, C.M., de Paulis, T. and Martin, P.R. (2008) ‘Comprehensive analysis of major and minor chlorogenic acids and lactones in economically relevant Brazilian coffee cultivars’, *Food Chemistry*, 106(2), pp. 859–867. Available at: https://doi.org/10.1016/j.foodchem.2007.06.053.

Perry, R.H. and Green, D.W. (1997) *Chemical Engineers’ Hanbook*. New York: McGraw-Hill.

Petracco, M. (2005) ‘The cup’, *Espresso coffee: The science of quality*, pp. 290–315.

Phongkanpai, V., Benjakul, S. and Tanaka, M. (2006) ‘Effect of pH on antioxidative activity and other characteristics of caramelization products’, *Journal of Food Biochemistry*, 30(2), pp. 174–186. Available at: https://doi.org/10.1111/j.1745-4514.2006.00053.x.

Piazza, L., Gigli, J. and Bulbarello, A. (2008) ‘Interfacial rheology study of espresso coffee foam structure and properties’, *Journal of Food Engineering*, 84(3), pp. 420–429. Available at: https://doi.org/10.1016/j.jfoodeng.2007.06.001.

Picard, H., Guyot, B. and Vincent, J.-C. (1984) ‘Étude des composés stéroliques de l’huile de café coffea canephora’, *Café, Cacao, Thé (Francia) v. 28 (1) p. 47-62* [Preprint].

Poisson, L., Blank, I., Dunkel, A. and Hofmann, T. (2017) *The Chemistry of Roasting-Decoding Flavor Formation*, *The Craft and Science of Coffee*. Elsevier Inc. Available at: https://doi.org/10.1016/B978-0-12-803520-7.00012-8.

Pokorný, J., Côń, N. huy, Šmidrkalová, E. and Janíček, G. (1974) ‘Veranderungen von Aminosauren und reduzierenden Zuckern wahrend des Rostens von Kaffeel’, 18(8), pp. 799–805.

Pokorný, J., Côń, N. huy, Šmidrkalová, E. and Janíček, G. (1975) ‘Nonenzymic browning. XII. Maillard reactions in green coffee beans on storage’, *Zeitschrift für Lebensmittel-Untersuchung und -Forschung*, 158(2), pp. 87–92. Available at: https://doi.org/10.1007/BF01460026.

Pugh, Robert J (2016) ‘Particle-stabilized foams’, *BUBBLE AND FOAM CHEMISTRY*, pp. 269–306.

Pugh, Robert J. (2016) ‘The stability/instability of bubbles and foams’, in R.J. Pugh (ed.) *Bubble and Foam Chemistry*. Cambridge: Cambridge University Press, pp. 220–268. Available at: https://doi.org/DOI: 10.1017/CBO9781316106938.008.

Raju, R., Balachandar, S., Hill, D.F. and Adrian, R.J. (2005) ‘Reynolds number scaling of flow in a stirred tank with Rushton turbine. Part II - Eigen decomposition of

fluctuation', *Chemical Engineering Science*, 60(12), pp. 3185–3198. Available at: https://doi.org/10.1016/j.ces.2004.12.040.

Rawel, H.M., Rohn, S. and Kroll, J. (2005) 'Characterisation of 11S protein fractions and phenolic compounds from green coffee beans under special consideration of their interactions-A review'.

Redgwell, R. and Fischer, M. (2006) 'Coffee carbohydrates', *Brazilian Journal of Plant Physiology*, 18(1), pp. 165–174. Available at: https://doi.org/10.1590/S1677-04202006000100012.

Redgwell, R.J., Curti, D., Fischer, M., Nicolas, P. and Fay, L.B. (2002) 'Coffee bean arabinogalactans: Acidic polymers covalently linked to protein', *Carbohydrate Research*, 337(3), pp. 239–253. Available at: https://doi.org/10.1016/S0008-6215(01)00316-0.

Redgwell, R.J., Curti, D., Rogers, J., Nicolas, P. and Fischer, M. (2003) 'Changes to the galactose/mannose ratio in galactomannans during coffee bean (Coffea arabica L.) development: Implications for in vivo modification of galactomannan synthesis', *Planta*, 217(2), pp. 316–326. Available at: https://doi.org/10.1007/s00425-003-1003-x.

Redgwell, R.J., Schmitt, C., Beaulieu, M. and Curti, D. (2005) 'Hydrocolloids from coffee: Physicochemical and functional properties of an arabinogalactan-protein fraction from green beans', *Food Hydrocolloids*, 19(6), pp. 1005–1015. Available at: https://doi.org/10.1016/j.foodhyd.2004.12.010.

Redgwell, R.J., Trovato, V., Curti, D. and Fischer, M. (2002) 'Effect of roasting on degradation and structural features of polysaccharides in Arabica coffee beans', *Carbohydrate Research* [Preprint]. Available at: https://doi.org/10.1016/S0008-6215(02)00010-1.

Renouf, M., Guy, P.A., Marmet, C., Fraering, A.L., Longet, K., Moulin, J., Enslen, M., Barron, D., Dionisi, F., Cavin, C., Williamson, G. and Steiling, H. (2010) 'Measurement of caffeic and ferulic acid equivalents in plasma after coffee consumption: Small intestine and colon are key sites for coffee metabolism', *MOLECULAR NUTRITION & FOOD RESEARCH*, 54(6), pp. 760–766. Available at: https://doi.org/10.1002/mnfr.200900056.

Ripper, B., Kaiser, C.R. and Perrone, D. (2020) 'Use of NMR techniques to investigate the changes on the chemical composition of coffee melanoidins', *Journal of Food Composition and Analysis*, 87(August 2019), p. 103399. Available at: https://doi.org/10.1016/j.jfca.2019.103399.

Rodrigues, N.P. and Bragagnolo, N. (2013) 'Identification and quantification of bioactive compounds in coffee brews by HPLC-DAD-MSn', *Journal of Food Composition and Analysis*, 32(2), pp. 105–115. Available at: https://doi.org/10.1016/j.jfca.2013.09.002.

Rogers, W.J., Bézard, G., Deshayes, A., Meyer, I., Pétiard, V. and Marraccini, P. (1999) 'Biochemical and molecular characterization and expression of the 11S-type storage protein from Coffea arabica endosperm', *Plant Physiology and Biochemistry*, 37(4), pp. 261–272. Available at: https://doi.org/10.1016/S0981-9428(99)80024-2.

Rufián-Henares, J.A. and Pastoriza, S. (2015) *Melanoidins in Coffee*, *Coffee in Health and Disease Prevention*. Elsevier Inc. Available at: https://doi.org/10.1016/B978-0-12-409517-5.00020-6.

Rusconi, M. and Conti, A. (2010) 'Theobroma cacao L., the Food of the Gods: A scientific approach beyond myths and claims', *Pharmacological Research*, 61(1), pp. 5–13. Available at: https://doi.org/10.1016/J.PHRS.2009.08.008.

S, P.I. and Nisha, P. (2020) ‘Unraveling the science of coffee foam – a comprehensive review’, *Critical Reviews in Food Science and Nutrition*, 0(0), pp. 1–21. Available at: https://doi.org/10.1080/10408398.2020.1765136.

Sarker, D.K., Wilde, P.J. and Clark, D.C. (1998) ‘Enhancement of protein foam stability by formation of wheat arabinoxylan-protein crosslinks’, *Cereal Chemistry*, 75(4), pp. 493–499. Available at: https://doi.org/10.1094/CCHEM.1998.75.4.493.

Scheidig, C., Czerny, M. and Schieberle, P. (2007) ‘Changes in key odorants of raw coffee beans during storage under defined conditions’, *Journal of Agricultural and Food Chemistry*, 55(14), pp. 5768–5775. Available at: https://doi.org/10.1021/jf070488o.

Scholze, A. and Maier, H.G. (1983) ‘Die sauren des kaffees. 7. Ameisen-, apfel-, citronen-und essigsaure..’, *Kaffee & Tee Markt (Alemania)*, 33(22), pp. 3–6.

Scholze, A. and Maier, H.G. (1984) ‘The acids of coffee. 8. Glycolic and phosphoric acid.’, *Zeitschrift fuer Lebensmittel Untersuchung und Forschung* [Preprint].

Sehat, N., Montag, A. and Speer, K. (1993) ‘Lipids in the coffee brew’, in *15th International Colloquium on the Chemistry of Coffee, ASIC, Paris*.

Serra Bonvehí, J. and Ventura Coll, F. (1998) ‘Evaluation of Smoky Taste in Cocoa Powder’, *Journal of Agricultural and Food Chemistry*, 46(2), pp. 620–624. Available at: https://doi.org/10.1021/JF9705429/ASSET/IMAGES/LARGE/JF9705429F00002.JPEG.

Shankaran, P.I. and Chinnaswamy, A. (2019) ‘Instant coffee foam: An investigation on factors controlling foamability, foam drainage, coalescence, and disproportionation’, *Journal of Food Process Engineering*, 42(6), pp. 1–12. Available at: https://doi.org/10.1111/jfpe.13173.

Siebert, K.J. (2014) ‘Recent Discoveries in Beer Foam’, 72(2), pp. 79–87.

Simpson, W.J. and Hughes, P.S. (1994) ‘Stabilization of foams by hop-derived bitter acids. Chemical interactions in beer foam’, *Cerevisia and Biotechnology (Belgium)* [Preprint].

Slack, P.T. and Bamforth, C.W. (1983) ‘The fractionation of polyptides from barley and beer by hydrophobic interaction chromatography: The influence of their hydrophobicity on foam stability’, 89, pp. 397–401.

Speer, K., Tewis, R. and Montag, A. (1991) ‘A new roasting component in coffee’, in *International Colloquium on the Chemistry of Coffee*.

Sumner, L.W., Amberg, A., Barrett, D., Beale, M.H., Beger, R., Daykin, C.A., Fan, T.W.M., Fiehn, O., Goodacre, R., Griffin, J.L., Hankemeier, T., Hardy, N., Harnly, J., Higashi, R., Kopka, J., Lane, A.N., Lindon, J.C., Marriott, P., Nicholls, A.W., Reily, M.D., Thaden, J.J. and Viant, M.R. (2007) ‘Proposed minimum reporting standards for chemical analysis Chemical Analysis Working Group (CAWG) Metabolomics Standards Initiative (MSI)’, *Metabolomics : Official journal of the Metabolomic Society*, 3(3), p. 211. Available at: https://doi.org/10.1007/S11306-007-0082-2.

Tewis, R., Montag, A. and Speer, K. (1993) ‘Dehydrocafestol and dehydrokahweol: two new roasting components in coffee’, in *Colloq. Sci. Int. Cafe*.

ThermoFisher Scientific (2021) *MSDS; CAS: 64742-49-0*.

Tressl, R., Holzer, M. and Kamperschoer, H. (1982) ‘Bildung von Aromastoffen in Röstkaffee in Abhängigkeit vom Gehalt an freien Aminosäuren und reduzierenden Zuckern’, in *ASIC, 10C Colloque*.

Tressl, R., Wondark, G.T., Krüger, R.P. and Rewicki, D. (1998) 'New Melanoidin-like Maillard Polymers from 2-Deoxypentoses', *Journal of Agricultural and Food Chemistry*, 46(1), pp. 104–110. Available at: https://doi.org/10.1021/jf970657c.

Tressl, R., Wondrak, G.T., Garbe, L.A., Krüger, R.P. and Rewicki, D. (1998) 'Pentoses and Hexoses as Sources of New Melanoidin-like Maillard Polymers', *Journal of Agricultural and Food Chemistry*, 46(5), pp. 1765–1776. Available at: https://doi.org/10.1021/jf970973r.

Trugo, L.C. and Macrae, R. (1984) 'A study of the effect of roasting on the chlorogenic acid composition of coffee using HPLC', *Food Chemistry* [Preprint]. Available at: https://doi.org/10.1016/0308-8146(84)90006-2.

Vázquez-Sánchez, K., Martinez-Saez, N., Rebollo-Hernanz, M., del Castillo, M.D., Gaytán-Martínez, M. and Campos-Vega, R. (2018) 'In vitro health promoting properties of antioxidant dietary fiber extracted from spent coffee (Coffee arabica L.) grounds', *Food Chemistry*, 261, pp. 253–259. Available at: https://doi.org/10.1016/J.FOODCHEM.2018.04.064.

Viani, Rinantonio; Petracco, M. (2012) 'Coffee', *Ullmann's Encyclopedia of Industrial Chemistry*, pp. 467–498. Available at: https://doi.org/10.1002/14356007.a07.

Virtanen, P., Gommers, R., Oliphant, T.E., Haberland, M., Reddy, T., Cournapeau, D., Burovski, E., Peterson, P., Weckesser, W., Bright, J., van der Walt, S.J., Brett, M., Wilson, J., Millman, K.J., Mayorov, N., Nelson, A.R.J., Jones, E., Kern, R., Larson, E., Carey, C.J., Polat, İ., Feng, Y., Moore, E.W., VanderPlas, J., Laxalde, D., Perktold, J., Cimrman, R., Henriksen, I., Quintero, E.A., Harris, C.R., Archibald, A.M., Ribeiro, A.H., Pedregosa, F., van Mulbregt, P. and Contributors, S. 1. 0 (2020) 'SciPy 1.0: fundamental algorithms for scientific computing in Python', *Nat. Methods*, 17(3), pp. 261–272. Available at: https://doi.org/10.1038/s41592-019-0686-2.

Vltzthum, O. and Koch, K. (1995) 'Process for the preparation of soluble coffee.' Available at: https://patents.google.com/patent/EP0489401B1.

Ward, A.F.H. and Tordai, L. (1946) 'Time-dependence of boundary tensions of solutions I. The role of diffusion in time-effects', *The Journal of Chemical Physics*, 14(7), pp. 453–461. Available at: https://doi.org/10.1063/1.1724167.

Wei, F., Furihata, K., Hu, F., Miyakawa, T. and Tanokura, M. (2010) 'Complex mixture analysis of organic compounds in green coffee bean extract by two-dimensional NMR spectroscopy', *Magnetic Resonance in Chemistry*, 48(11), pp. 857–865. Available at: https://doi.org/10.1002/mrc.2678.

Wei, F., Furihata, K., Koda, M., Hu, F., Miyakawa, T. and Tanokura, M. (2012a) 'Roasting process of coffee beans as studied by nuclear magnetic resonance: Time course of changes in composition', *Journal of Agricultural and Food Chemistry*, 60(4), pp. 1005–1012. Available at: https://doi.org/10.1021/jf205315r.

Wei, F., Furihata, K., Koda, M., Hu, F., Miyakawa, T. and Tanokura, M. (2012b) 'Roasting process of coffee beans as studied by nuclear magnetic resonance: Time course of changes in composition', *Journal of Agricultural and Food Chemistry*, 60(4), pp. 1005–1012. Available at: https://doi.org/10.1021/jf205315r.

Wei, F. and Tanokura, M. (2015) *Organic Compounds in Green Coffee Beans*, *Coffee in Health and Disease Prevention*. Elsevier Inc. Available at: https://doi.org/10.1016/B978-0-12-409517-5.00017-6.

*Whatman Grade 114 Qualitative Filter Papers* (2022) *https://www.cytivalifesciences.com/en/us/shop/whatman-laboratory-*

*filtration/cellulose-filter-papers/wet-strengthened-filter-paper/grade-114-qualitative-filter-papers-p-00213*.

Wolfrom, M.L., Laver, M.L. and Patin, D.L. (1961) 'Carbohydrates of the Coffee Bean. II. Isolation and Characterization of a Mannan1', *The Journal of Organic Chemistry*, 26(11), pp. 4533–4535.

Yanagimoto, K., Ochi, H., Lee, K.G. and Shibamoto, T. (2004) 'Antioxidative Activities of Fractions Obtained from Brewed Coffee', *Journal of Agricultural and Food Chemistry*, 52(3), pp. 592–596. Available at: https://doi.org/10.1021/jf030317t.

Yu, J.M., Chu, M., Park, H., Park, J. and Lee, K.G. (2021) 'Analysis of volatile compounds in coffee prepared by various brewing and roasting methods', *Foods*, 10(6). Available at: https://doi.org/10.3390/foods10061347.

Zamora, R. and Hidalgo, F.J. (2005) 'Coordinate contribution of lipid oxidation and Maillard reaction to the nonenzymatic food browning', *Critical Reviews in Food Science and Nutrition*, 45(1), pp. 49–59. Available at: https://doi.org/10.1080/10408690590900117.

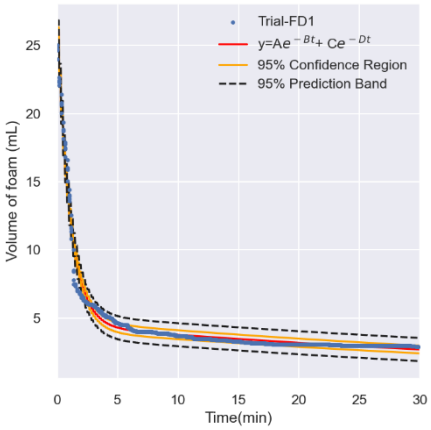
# Appendix A: Foam height curves fit

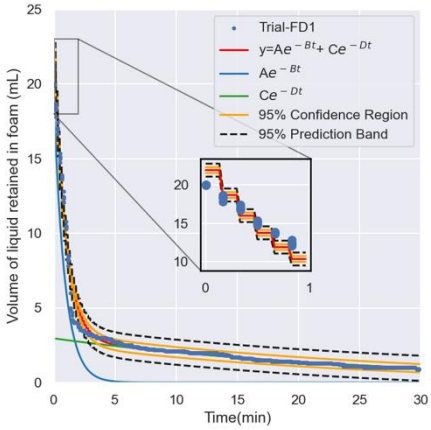
The fitted curves on foam data are presented below.

| # | Sample Name | # | Sample Name |
|---|---|---|---|
| 1 | Trial-FD1 | 22 | SD-Mellow Birds |
| 2 | Trial-FD2 | 23 | SD-Maxwell House mild (LRIC) |
| 3 | Trial-FD3 | 24 | SD3-SR1/12 |
| 4 | Trial-FD4 | 25 | SD4-SR10 |
| 5 | Trial-FD5 | 26 | SD5-SR11B |
| 6 | Trial-SD1 | 27 | SD6-BIC |
| 7 | Trial-SD2 | 28 | SD7-SR16 |
| 8 | FD-Kenco Smooth (KRS) | 29 | ASD-N. Original |
| 9 | FD-Kenco Rich (KRR) | 30 | ASD-N. Original Decaff |
| 10 | FD-Kenco Decaff | 31 | FD-N. Gold Blend |
| 11 | FD-Kenco Colombia | 32 | FD-N.G.B. Decaff |
| 12 | FD-Millicano Americano | 33 | SD-N.G.B. Espresso |
| 13 | FD-Millicano Americano Decaff | 34 | SD-N.G.B. Smooth |
| 14 | FD-Millicano Americano Intense | 35 | FD-N.G.B. Intense |
| 15 | FD-Douwe Egberts Gold (3070) | 36 | FD-N.G.B. Barista Style |
| 16 | FD-Douwe Egbers Decaff | 37 | FD-N.G.B.Colombia |
| 17 | FD-Douwe Egberts Pure Indulgence | 38 | FD-N.G.B.Indonesia |
| 18 | FD-L'or Classique | 39 | SD-N.Azera Americano |
| 19 | FD-L'or Decaff | 40 | SD-N. Azera Americano Decaff |
| 20 | FD-L'or Intense | 41 | SD-N. Azera Intenso |
| 21 | FD-BQI | 42 | SD-N. Azera Espresso |

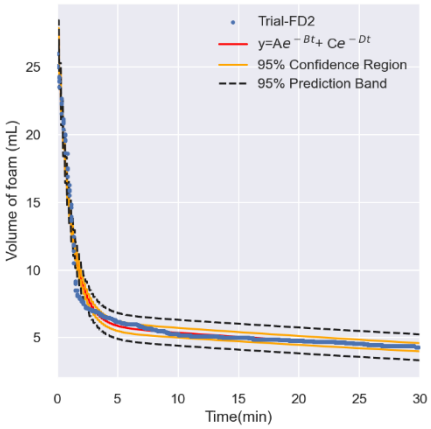
Foam Height | Liquid retained in foam structure

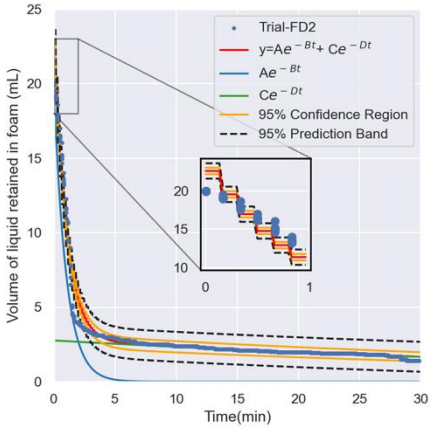
#1



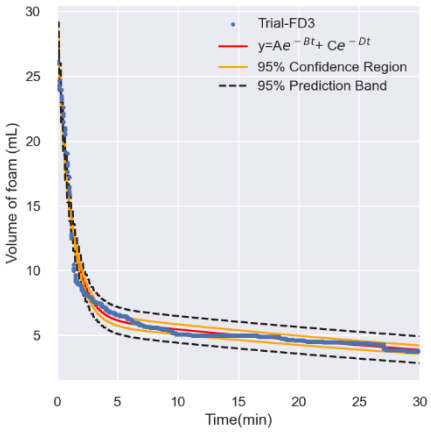



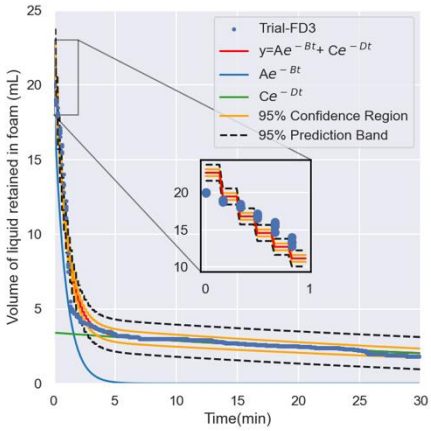

#2



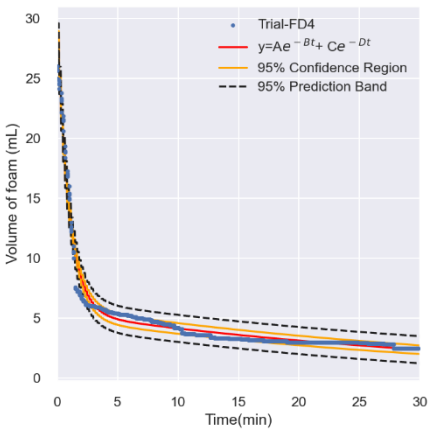



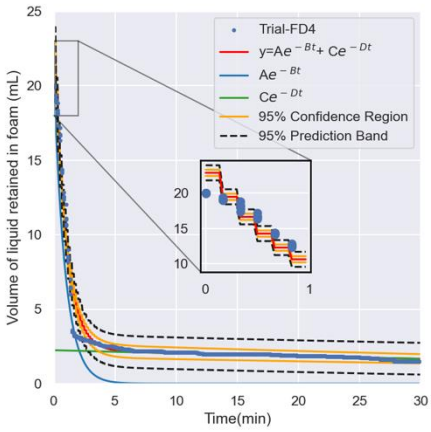

#3



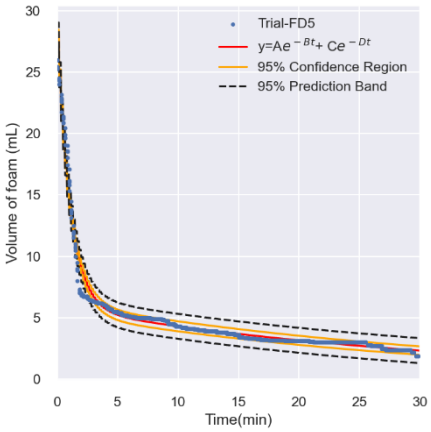



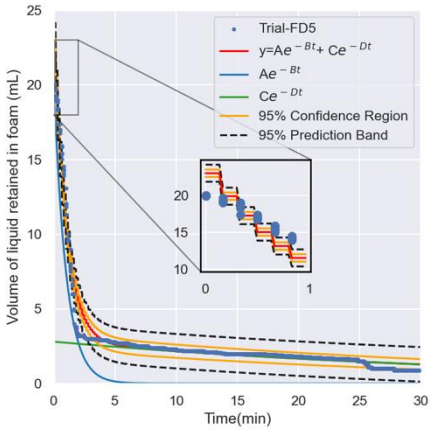
#4


Trial-FD4
y=Ae^−Bt+ Ce^−Dt
95% Confidence Region
95% Prediction Band
Volume of foam (mL)
Time(min)

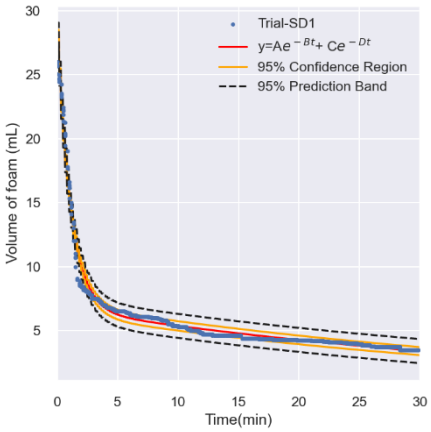

Trial-FD4
y=Ae^−Bt+ Ce^−Dt
Ae^−Bt
Ce^−Dt
95% Confidence Region
95% Prediction Band
Volume of liquid retained in foam (mL)
Time(min)

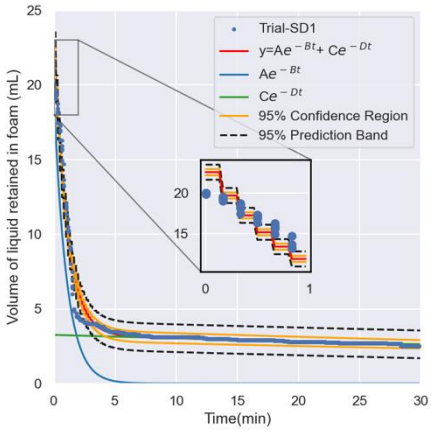
#5


Trial-FD5
y=Ae^−Bt+ Ce^−Dt
95% Confidence Region
95% Prediction Band
Volume of foam (mL)
Time(min)

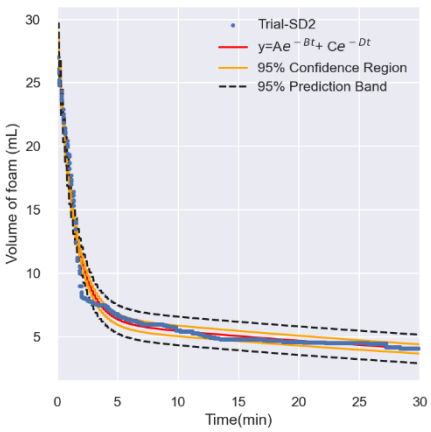

Trial-FD5
y=Ae^−Bt+ Ce^−Dt
Ae^−Bt
Ce^−Dt
95% Confidence Region
95% Prediction Band
Volume of liquid retained in foam (mL)
Time(min)

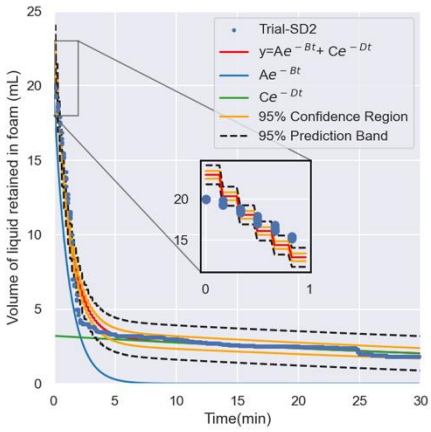
#6


Trial-SD1
y=Ae^−Bt+ Ce^−Dt
95% Confidence Region
95% Prediction Band
Volume of foam (mL)
Time(min)

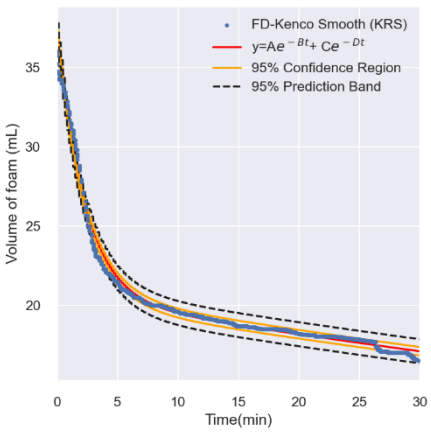

Trial-SD1
y=Ae^−Bt+ Ce^−Dt
Ae^−Bt
Ce^−Dt
95% Confidence Region
95% Prediction Band
Volume of liquid retained in foam (mL)
Time(min)

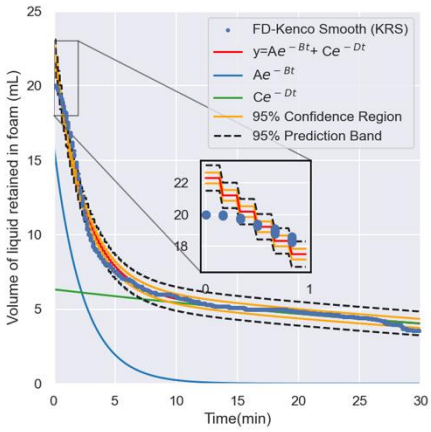
#7


Trial-SD2
y=Ae^−Bt+ Ce^−Dt
95% Confidence Region
95% Prediction Band
Volume of foam (mL)
Time(min)

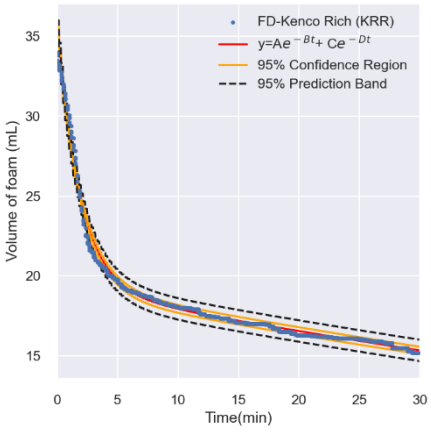

Trial-SD2
y=Ae^−Bt+ Ce^−Dt
Ae^−Bt
Ce^−Dt
95% Confidence Region
95% Prediction Band
Volume of liquid retained in foam (mL)
Time(min)

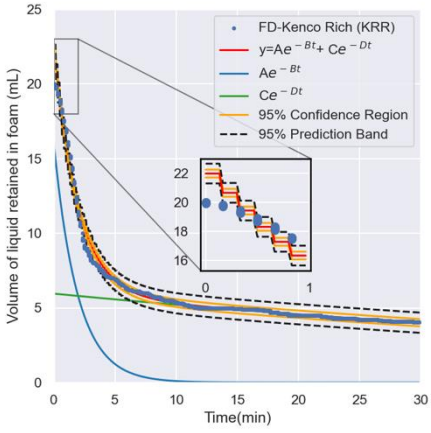
#8


FD-Kenco Smooth (KRS)
y=Ae^−Bt+ Ce^−Dt
95% Confidence Region
95% Prediction Band
Volume of foam (mL)
Time(min)

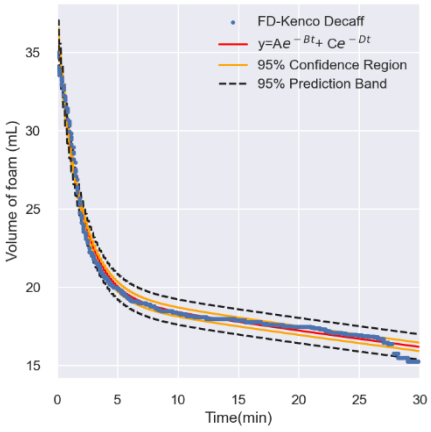

FD-Kenco Smooth (KRS)
y=Ae^−Bt+ Ce^−Dt
Ae^−Bt
Ce^−Dt
95% Confidence Region
95% Prediction Band
Volume of liquid retained in foam (mL)
Time(min)

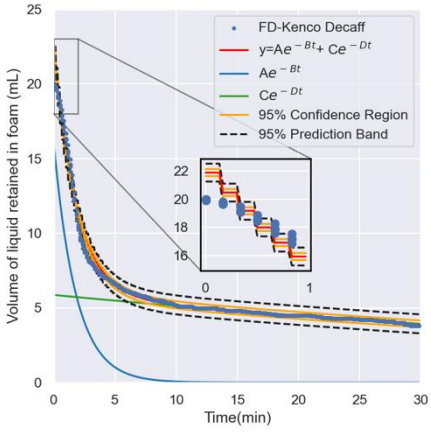
#9


FD-Kenco Rich (KRR)
y=Ae^−Bt+ Ce^−Dt
95% Confidence Region
95% Prediction Band
Volume of foam (mL)
Time(min)

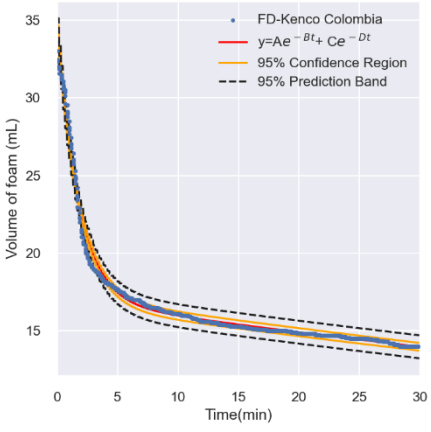

FD-Kenco Rich (KRR)
y=Ae^−Bt+ Ce^−Dt
Ae^−Bt
Ce^−Dt
95% Confidence Region
95% Prediction Band
Volume of liquid retained in foam (mL)
Time(min)

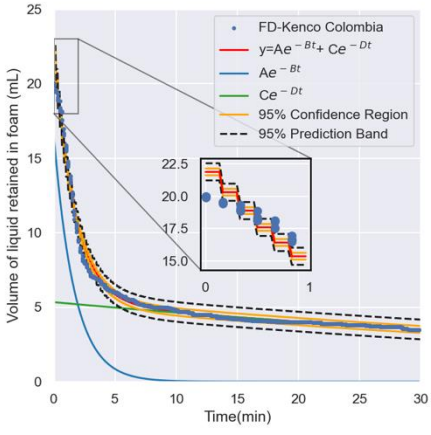
#10


FD-Kenco Decaff
y=Ae^−Bt+ Ce^−Dt
95% Confidence Region
95% Prediction Band
Volume of foam (mL)
Time(min)

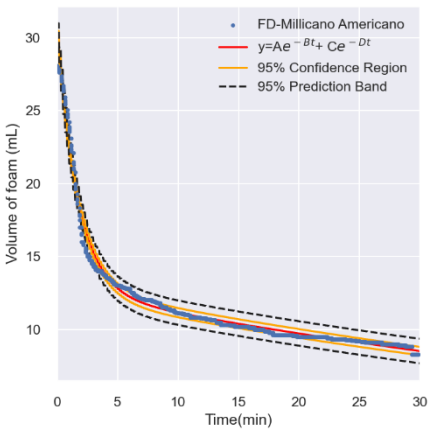

FD-Kenco Decaff
y=Ae^−Bt+ Ce^−Dt
Ae^−Bt
Ce^−Dt
95% Confidence Region
95% Prediction Band
Volume of liquid retained in foam (mL)
Time(min)

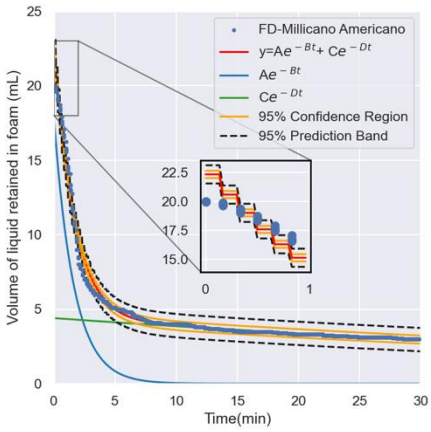
#11


FD-Kenco Colombia
y=Ae^−Bt+ Ce^−Dt
95% Confidence Region
95% Prediction Band
Volume of foam (mL)
Time(min)

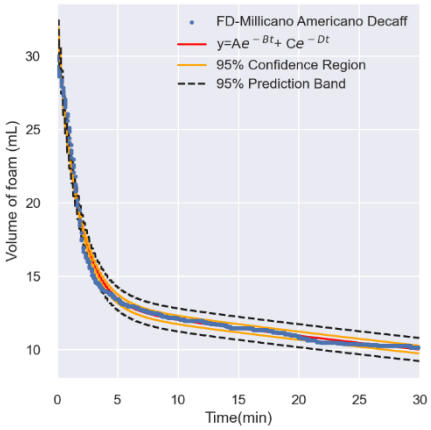

FD-Kenco Colombia
y=Ae^−Bt+ Ce^−Dt
Ae^−Bt
Ce^−Dt
95% Confidence Region
95% Prediction Band
Volume of liquid retained in foam (mL)
Time(min)

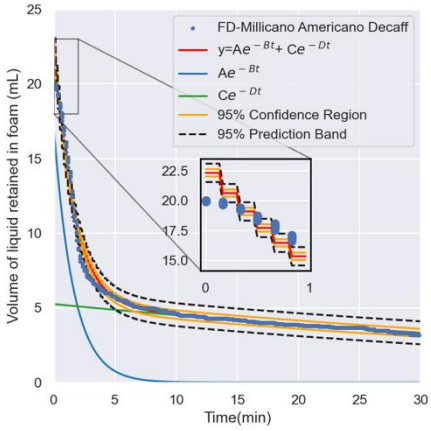
#12


FD-Millicano Americano
y=Ae^-Bt+ Ce^-Dt
95% Confidence Region
95% Prediction Band
Volume of foam (mL)
Time(min)

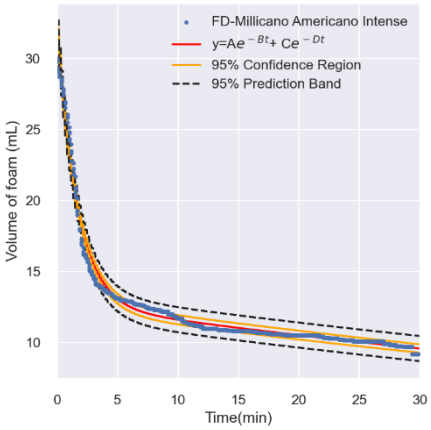

FD-Millicano Americano
y=Ae^-Bt+ Ce^-Dt
Ae^-Bt
Ce^-Dt
95% Confidence Region
95% Prediction Band
Volume of liquid retained in foam (mL)
Time(min)

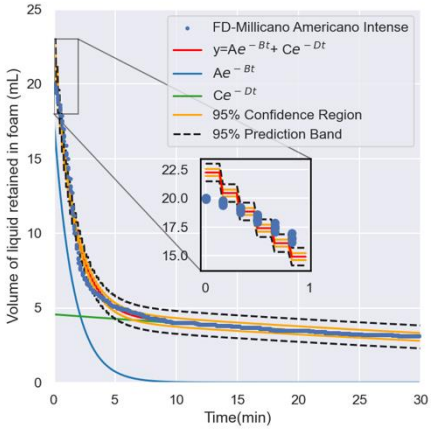
#13


FD-Millicano Americano Decaff
y=Ae^-Bt+ Ce^-Dt
95% Confidence Region
95% Prediction Band
Volume of foam (mL)
Time(min)

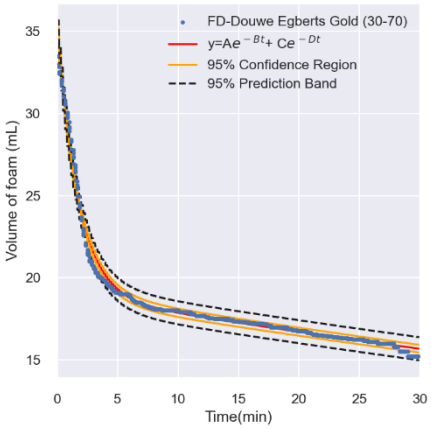

FD-Millicano Americano Decaff
y=Ae^-Bt+ Ce^-Dt
Ae^-Bt
Ce^-Dt
95% Confidence Region
95% Prediction Band
Volume of liquid retained in foam (mL)
Time(min)

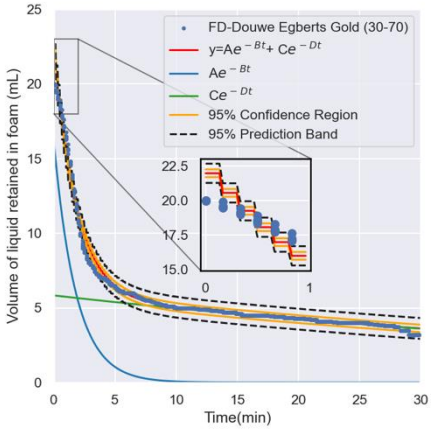
#14


FD-Millicano Americano Intense
y=Ae^-Bt+ Ce^-Dt
95% Confidence Region
95% Prediction Band
Volume of foam (mL)
Time(min)

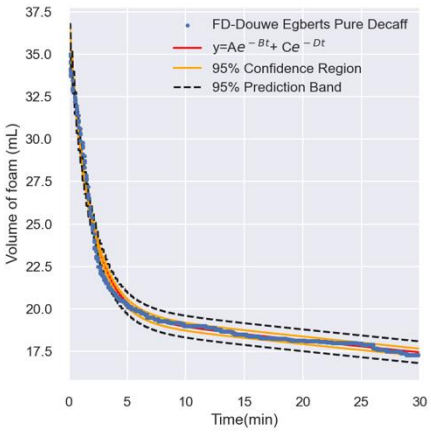

FD-Millicano Americano Intense
y=Ae^-Bt+ Ce^-Dt
Ae^-Bt
Ce^-Dt
95% Confidence Region
95% Prediction Band
Volume of liquid retained in foam (mL)
Time(min)

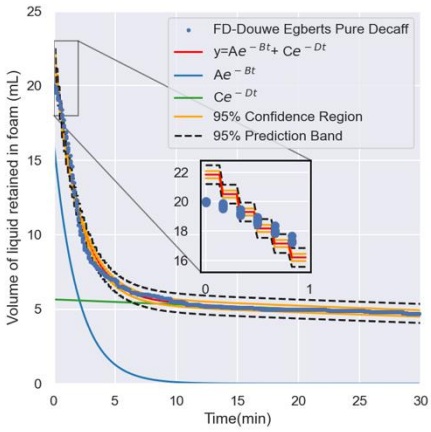
#15


FD-Douwe Egberts Gold (30-70)
y=Ae^-Bt+ Ce^-Dt
95% Confidence Region
95% Prediction Band
Volume of foam (mL)
Time(min)

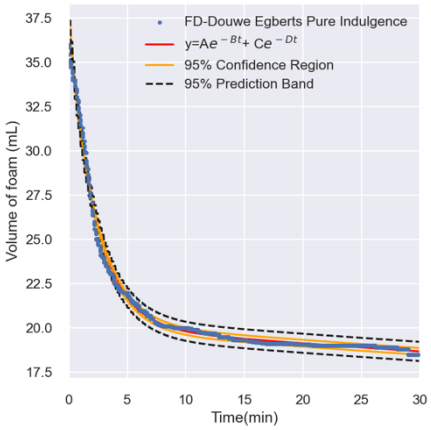

FD-Douwe Egberts Gold (30-70)
y=Ae^-Bt+ Ce^-Dt
Ae^-Bt
Ce^-Dt
95% Confidence Region
95% Prediction Band
Volume of liquid retained in foam (mL)
Time(min)

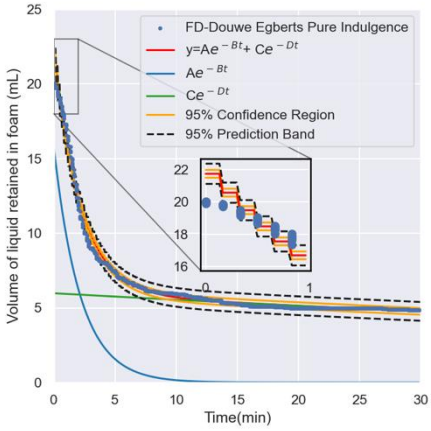
#16


FD-Douwe Egberts Pure Decaff
y=Ae^−Bt+ Ce^−Dt
95% Confidence Region
95% Prediction Band
Volume of foam (mL)
Time(min)

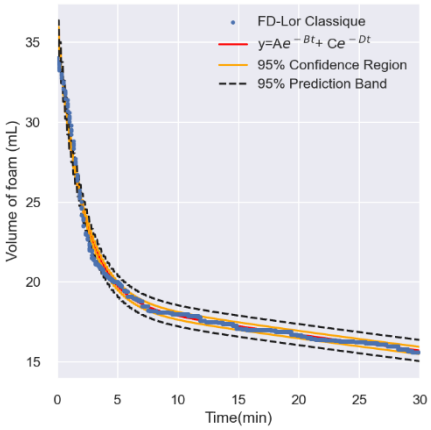

FD-Douwe Egberts Pure Decaff
y=Ae^−Bt+ Ce^−Dt
Ae^−Bt
Ce^−Dt
95% Confidence Region
95% Prediction Band
Volume of liquid retained in foam (mL)
Time(min)

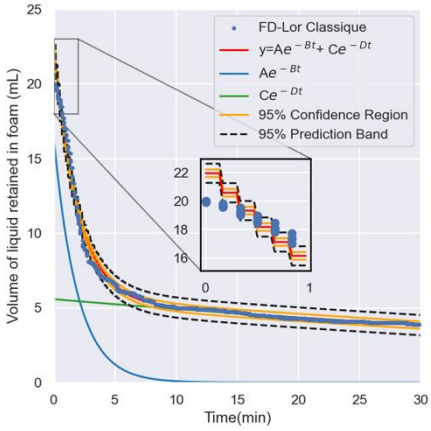
#17


FD-Douwe Egberts Pure Indulgence
y=Ae^−Bt+ Ce^−Dt
95% Confidence Region
95% Prediction Band
Volume of foam (mL)
Time(min)

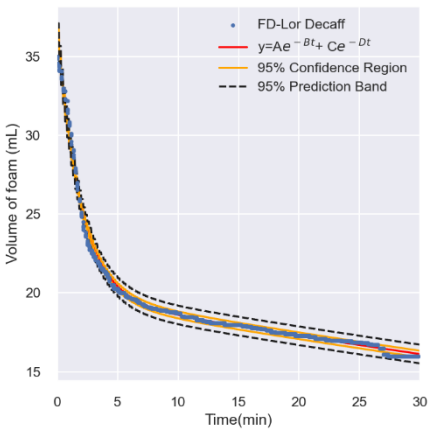

FD-Douwe Egberts Pure Indulgence
y=Ae^−Bt+ Ce^−Dt
Ae^−Bt
Ce^−Dt
95% Confidence Region
95% Prediction Band
Volume of liquid retained in foam (mL)
Time(min)

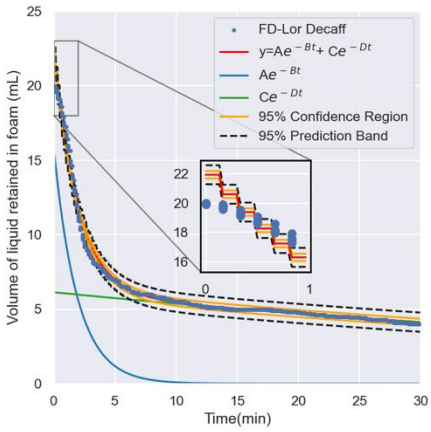
#18


FD-Lor Classique
y=Ae^−Bt+ Ce^−Dt
95% Confidence Region
95% Prediction Band
Volume of foam (mL)
Time(min)

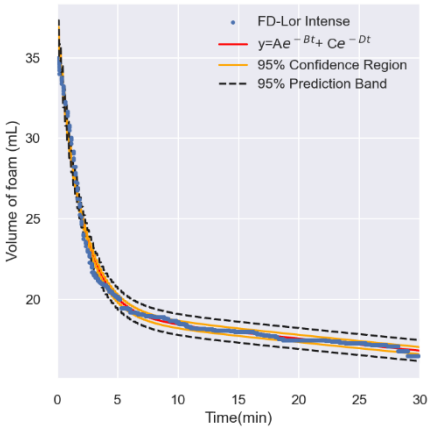

FD-Lor Classique
y=Ae^−Bt+ Ce^−Dt
Ae^−Bt
Ce^−Dt
95% Confidence Region
95% Prediction Band
Volume of liquid retained in foam (mL)
Time(min)

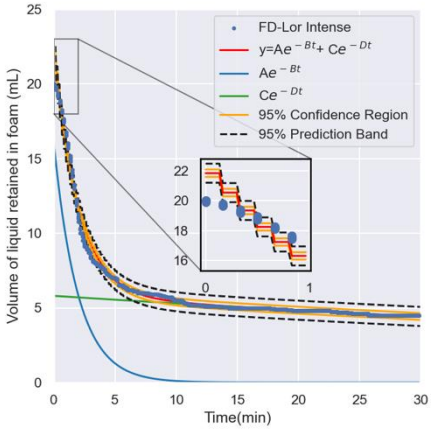
#19


FD-Lor Decaff
y=Ae^−Bt+ Ce^−Dt
95% Confidence Region
95% Prediction Band
Volume of foam (mL)
Time(min)

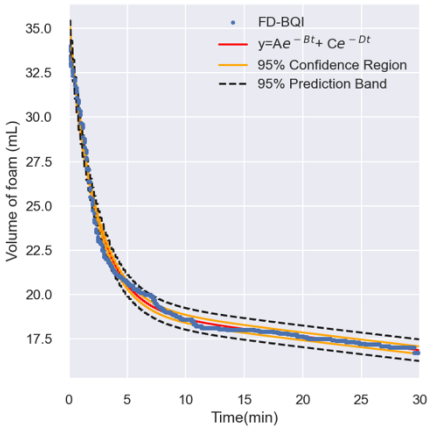

FD-Lor Decaff
y=Ae^−Bt+ Ce^−Dt
Ae^−Bt
Ce^−Dt
95% Confidence Region
95% Prediction Band
Volume of liquid retained in foam (mL)
Time(min)

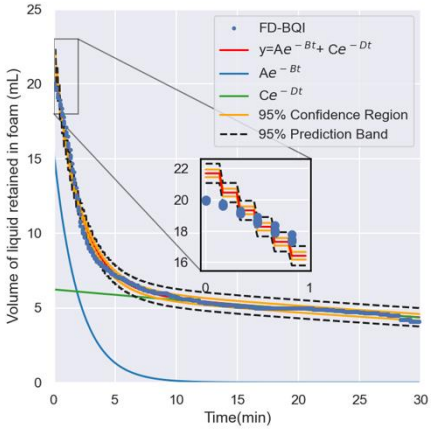
#20


FD-Lor Intense
y=Ae^−Bt+ Ce^−Dt
95% Confidence Region
95% Prediction Band
Volume of foam (mL)
Time(min)

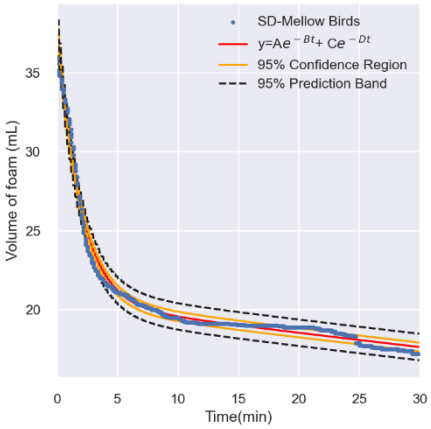

FD-Lor Intense
y=Ae^−Bt+ Ce^−Dt
Ae^−Bt
Ce^−Dt
95% Confidence Region
95% Prediction Band
Volume of liquid retained in foam (mL)
Time(min)

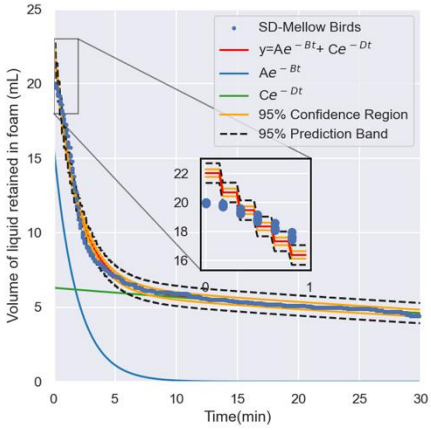
#21


FD-BQI
y=Ae^−Bt+ Ce^−Dt
95% Confidence Region
95% Prediction Band
Volume of foam (mL)
Time(min)

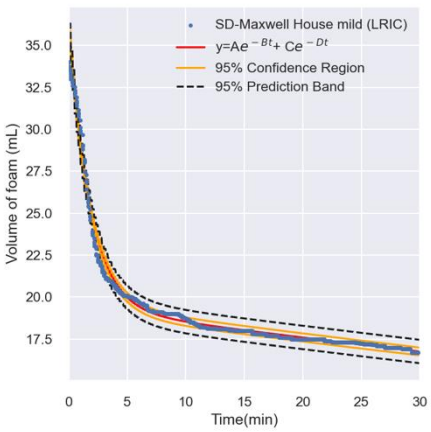

FD-BQI
y=Ae^−Bt+ Ce^−Dt
Ae^−Bt
Ce^−Dt
95% Confidence Region
95% Prediction Band
Volume of liquid retained in foam (mL)
Time(min)

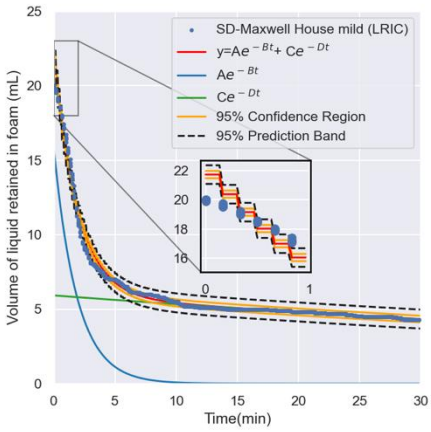
#22


SD-Mellow Birds
y=Ae^−Bt+ Ce^−Dt
95% Confidence Region
95% Prediction Band
Volume of foam (mL)
Time(min)

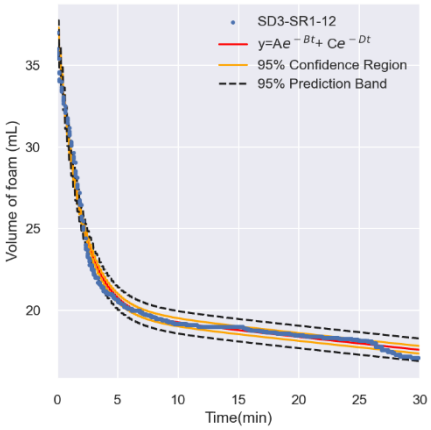

SD-Mellow Birds
y=Ae^−Bt+ Ce^−Dt
Ae^−Bt
Ce^−Dt
95% Confidence Region
95% Prediction Band
Volume of liquid retained in foam (mL)
Time(min)

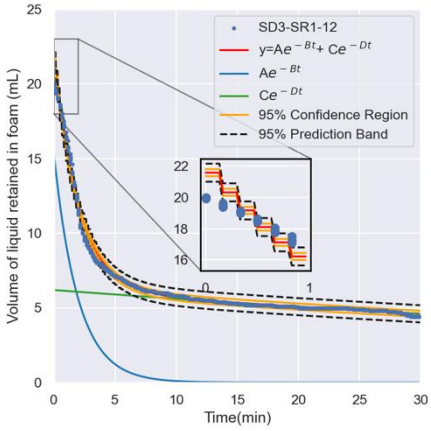
#23


SD-Maxwell House mild (LRIC)
y=Ae^-Bt+ Ce^-Dt
95% Confidence Region
95% Prediction Band
Volume of foam (mL)
Time(min)

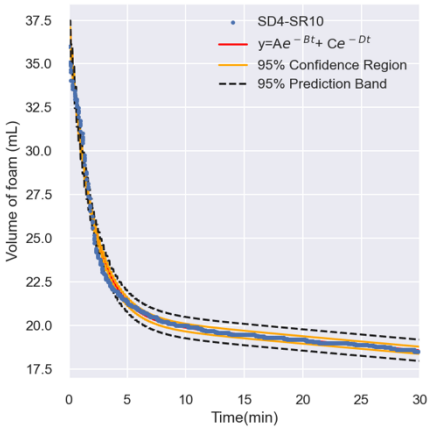

SD-Maxwell House mild (LRIC)
y=Ae^-Bt+ Ce^-Dt
Ae^-Bt
Ce^-Dt
95% Confidence Region
95% Prediction Band
Volume of liquid retained in foam (mL)
Time(min)

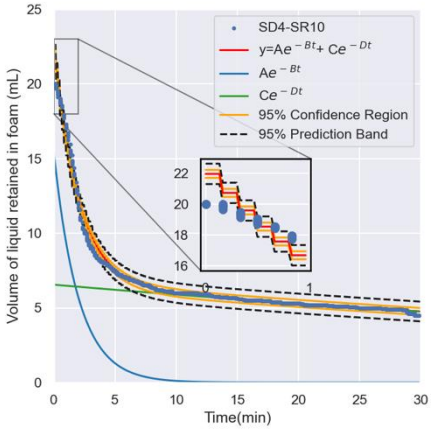
#24


SD3-SR1-12
y=Ae^-Bt+ Ce^-Dt
95% Confidence Region
95% Prediction Band
Volume of foam (mL)
Time(min)

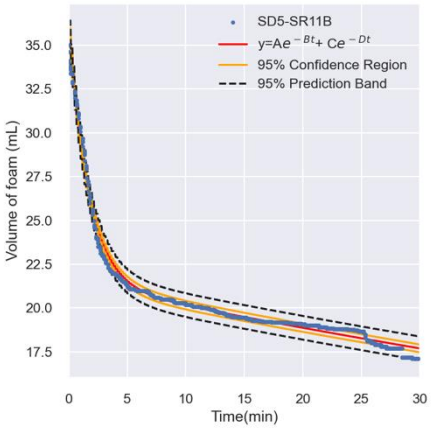

SD3-SR1-12
y=Ae^-Bt+ Ce^-Dt
Ae^-Bt
Ce^-Dt
95% Confidence Region
95% Prediction Band
Volume of liquid retained in foam (mL)
Time(min)

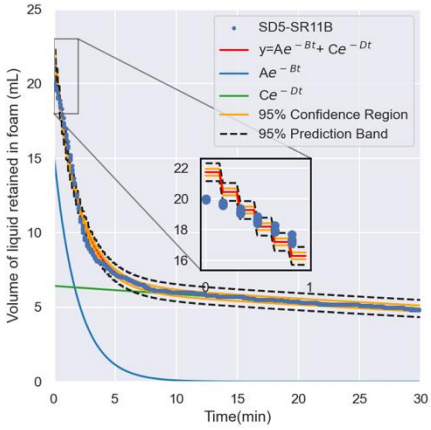
#25


SD4-SR10
y=Ae^-Bt+ Ce^-Dt
95% Confidence Region
95% Prediction Band
Volume of foam (mL)
Time(min)

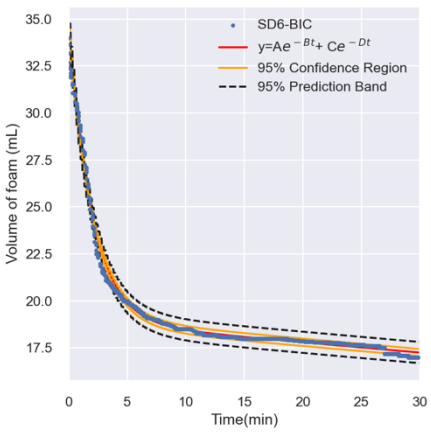

SD4-SR10
y=Ae^-Bt+ Ce^-Dt
Ae^-Bt
Ce^-Dt
95% Confidence Region
95% Prediction Band
Volume of liquid retained in foam (mL)
Time(min)

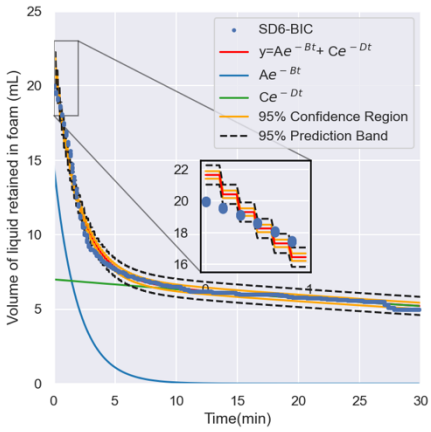
#26


SD5-SR11B
y=Ae^-Bt+ Ce^-Dt
95% Confidence Region
95% Prediction Band
Volume of foam (mL)
Time(min)

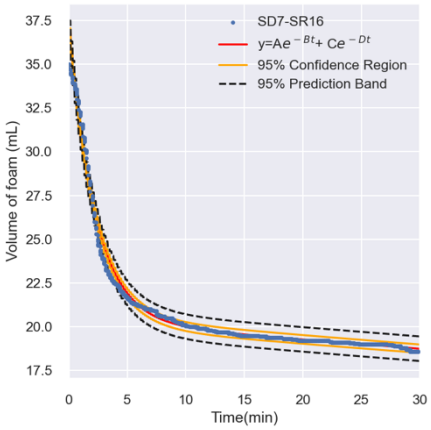

SD5-SR11B
y=Ae^-Bt+ Ce^-Dt
Ae^-Bt
Ce^-Dt
95% Confidence Region
95% Prediction Band
Volume of liquid retained in foam (mL)
Time(min)

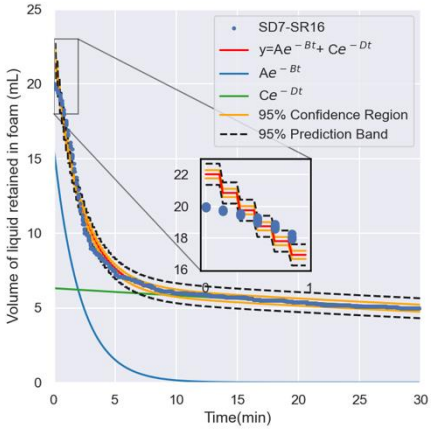
#27


SD6-BIC
y=Ae^−Bt+ Ce^−Dt
95% Confidence Region
95% Prediction Band
Volume of foam (mL)
Time(min)

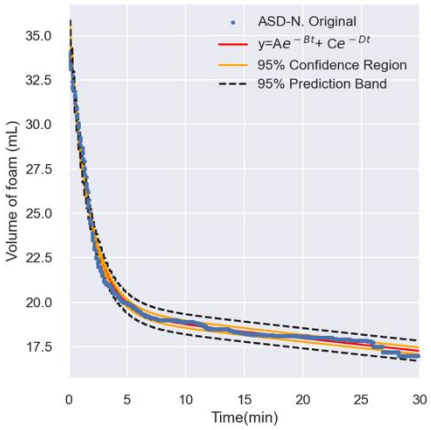

SD6-BIC
y=Ae^−Bt+ Ce^−Dt
Ae^−Bt
Ce^−Dt
95% Confidence Region
95% Prediction Band
Volume of liquid retained in foam (mL)
Time(min)

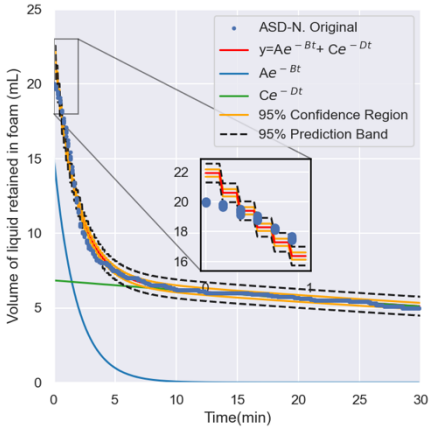
#28


SD7-SR16
y=Ae^−Bt+ Ce^−Dt
95% Confidence Region
95% Prediction Band
Volume of foam (mL)
Time(min)

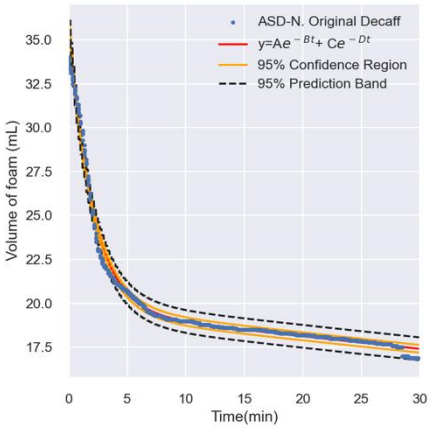

SD7-SR16
y=Ae^−Bt+ Ce^−Dt
Ae^−Bt
Ce^−Dt
95% Confidence Region
95% Prediction Band
Volume of liquid retained in foam (mL)
Time(min)

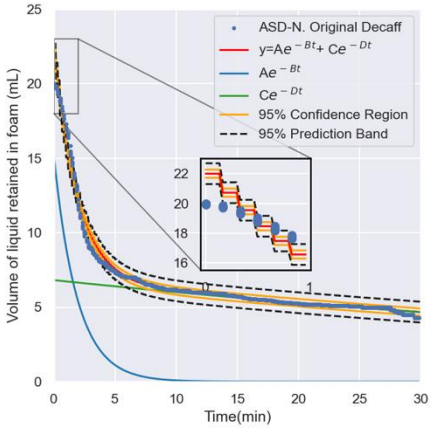
#29


ASD-N. Original
y=Ae^−Bt+ Ce^−Dt
95% Confidence Region
95% Prediction Band
Volume of foam (mL)
Time(min)

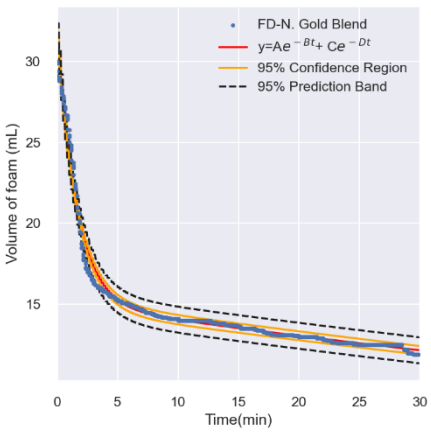

ASD-N. Original
y=Ae^−Bt+ Ce^−Dt
Ae^−Bt
Ce^−Dt
95% Confidence Region
95% Prediction Band
Volume of liquid retained in foam (mL)
Time(min)

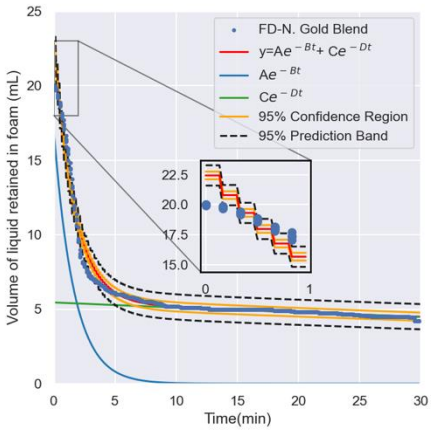
#30


ASD-N. Original Decaff
y=Ae^−Bt+ Ce^−Dt
95% Confidence Region
95% Prediction Band
Volume of foam (mL)
Time(min)

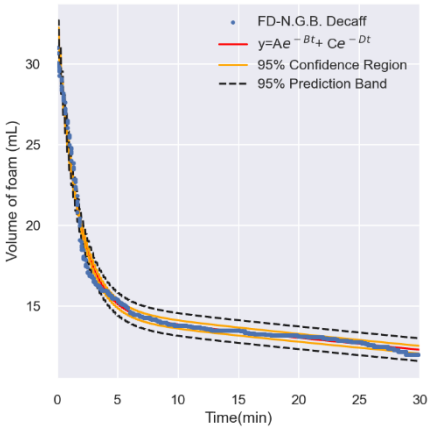

ASD-N. Original Decaff
y=Ae^−Bt+ Ce^−Dt
Ae^−Bt
Ce^−Dt
95% Confidence Region
95% Prediction Band
Volume of liquid retained in foam (mL)
Time(min)

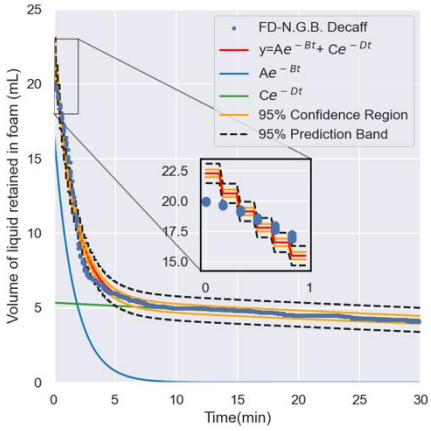
#31


FD-N. Gold Blend
y=Ae$^{-Bt}$+ Ce$^{-Dt}$
95% Confidence Region
95% Prediction Band
Volume of foam (mL)
Time(min)

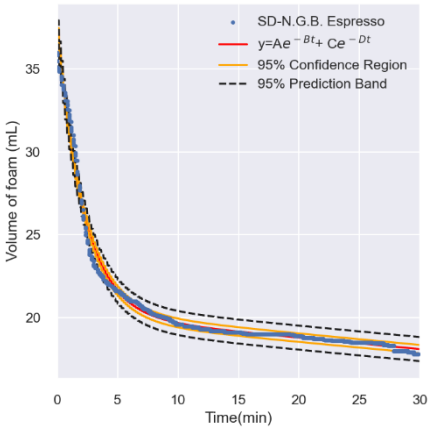

FD-N. Gold Blend
y=Ae$^{-Bt}$+ Ce$^{-Dt}$
Ae$^{-Bt}$
Ce$^{-Dt}$
95% Confidence Region
95% Prediction Band
Volume of liquid retained in foam (mL)
Time(min)

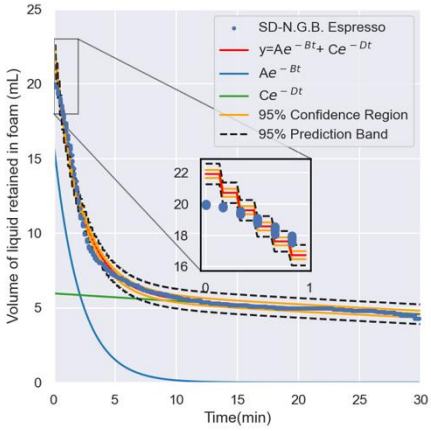
#32


FD-N.G.B. Decaff
y=Ae$^{-Bt}$+ Ce$^{-Dt}$
95% Confidence Region
95% Prediction Band
Volume of foam (mL)
Time(min)

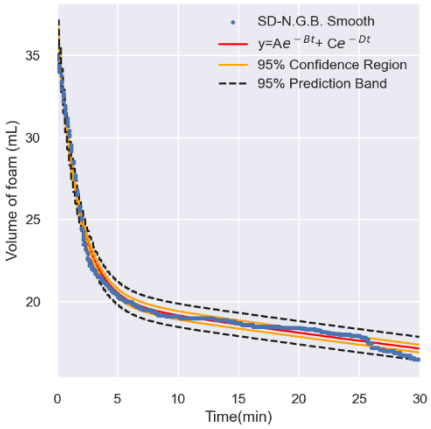

FD-N.G.B. Decaff
y=Ae$^{-Bt}$+ Ce$^{-Dt}$
Ae$^{-Bt}$
Ce$^{-Dt}$
95% Confidence Region
95% Prediction Band
Volume of liquid retained in foam (mL)
Time(min)

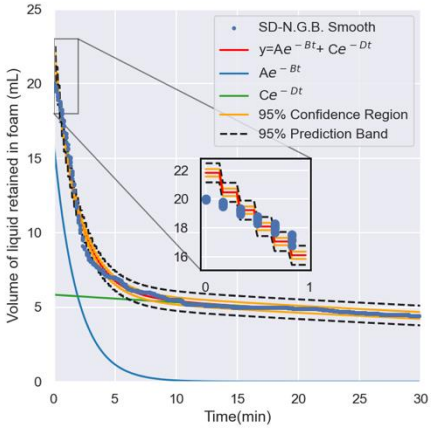
#33


SD-N.G.B. Espresso
y=Ae$^{-Bt}$+ Ce$^{-Dt}$
95% Confidence Region
95% Prediction Band
Volume of foam (mL)
Time(min)

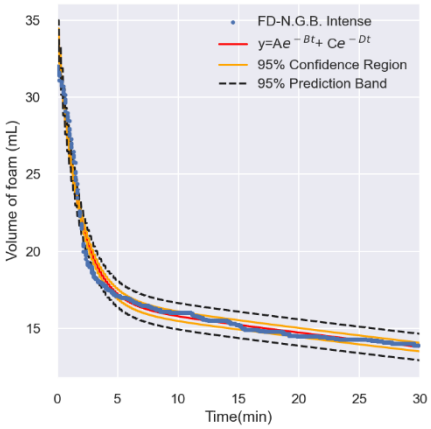

SD-N.G.B. Espresso
y=Ae$^{-Bt}$+ Ce$^{-Dt}$
Ae$^{-Bt}$
Ce$^{-Dt}$
95% Confidence Region
95% Prediction Band
Volume of liquid retained in foam (mL)
Time(min)

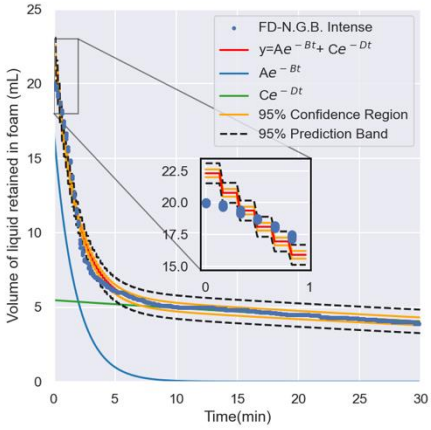
#34


SD-N.G.B. Smooth
y=Ae$^{-Bt}$+ Ce$^{-Dt}$
95% Confidence Region
95% Prediction Band
Volume of foam (mL)
Time(min)

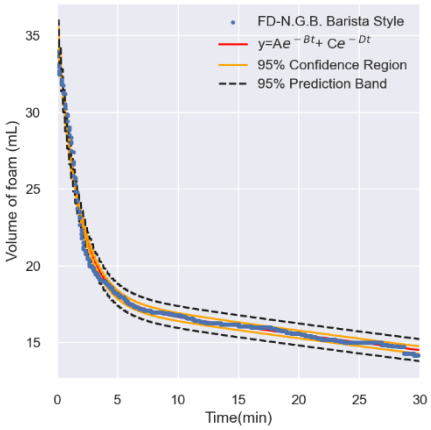

SD-N.G.B. Smooth
y=Ae$^{-Bt}$+ Ce$^{-Dt}$
Ae$^{-Bt}$
Ce$^{-Dt}$
95% Confidence Region
95% Prediction Band
Volume of liquid retained in foam (mL)
Time(min)

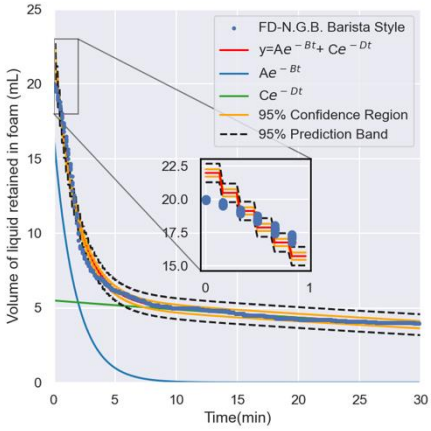
#35


FD-N.G.B. Intense
y=Ae^-Bt+ Ce^-Dt
95% Confidence Region
95% Prediction Band
Volume of foam (mL)
Time(min)

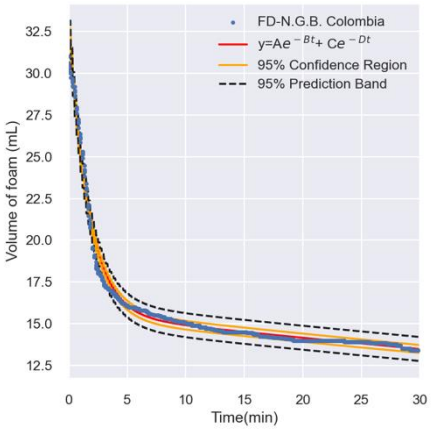

FD-N.G.B. Intense
y=Ae^-Bt+ Ce^-Dt
Ae^-Bt
Ce^-Dt
95% Confidence Region
95% Prediction Band
Volume of liquid retained in foam (mL)
Time(min)

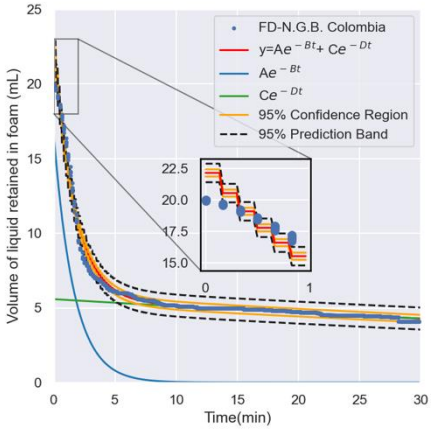
#36


FD-N.G.B. Barista Style
y=Ae^-Bt+ Ce^-Dt
95% Confidence Region
95% Prediction Band
Volume of foam (mL)
Time(min)

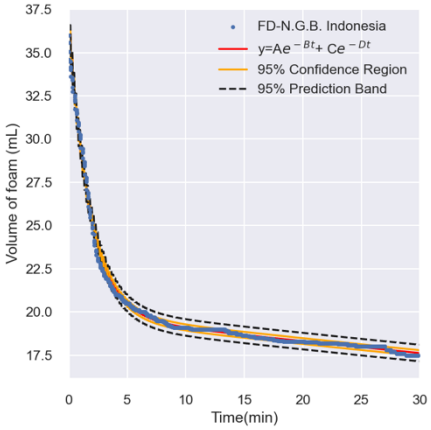

FD-N.G.B. Barista Style
y=Ae^-Bt+ Ce^-Dt
Ae^-Bt
Ce^-Dt
95% Confidence Region
95% Prediction Band
Volume of liquid retained in foam (mL)
Time(min)

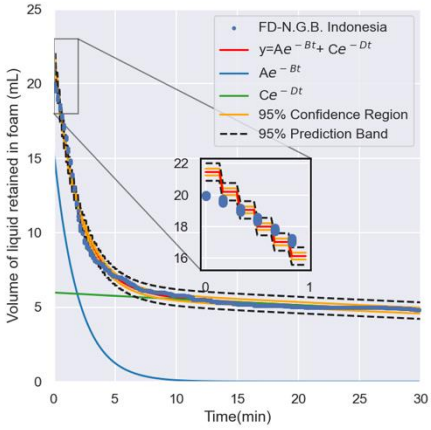
#37


FD-N.G.B. Colombia
y=Ae^-Bt+ Ce^-Dt
95% Confidence Region
95% Prediction Band
Volume of foam (mL)
Time(min)

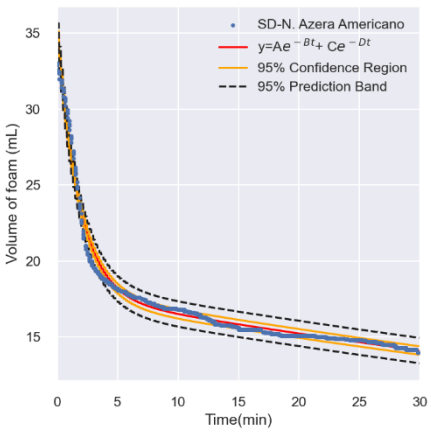

FD-N.G.B. Colombia
y=Ae^-Bt+ Ce^-Dt
Ae^-Bt
Ce^-Dt
95% Confidence Region
95% Prediction Band
Volume of liquid retained in foam (mL)
Time(min)

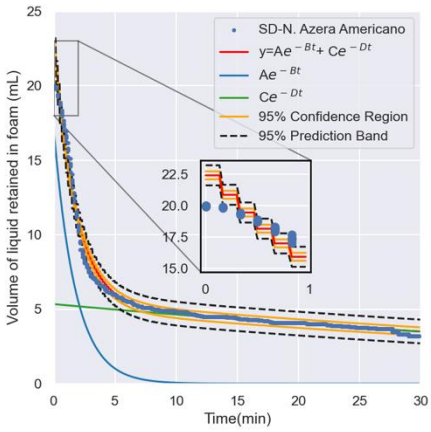
#38


FD-N.G.B. Indonesia
y=Ae^-Bt+ Ce^-Dt
95% Confidence Region
95% Prediction Band
Volume of foam (mL)
Time(min)

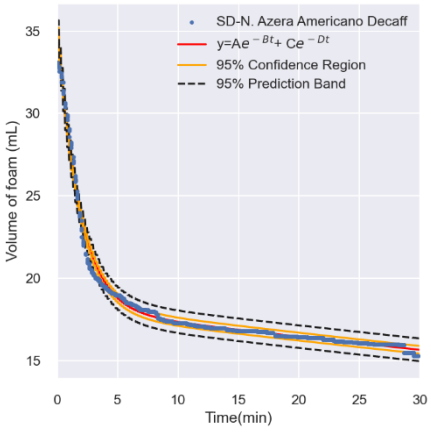

FD-N.G.B. Indonesia
y=Ae^-Bt+ Ce^-Dt
Ae^-Bt
Ce^-Dt
95% Confidence Region
95% Prediction Band
Volume of liquid retained in foam (mL)
Time(min)

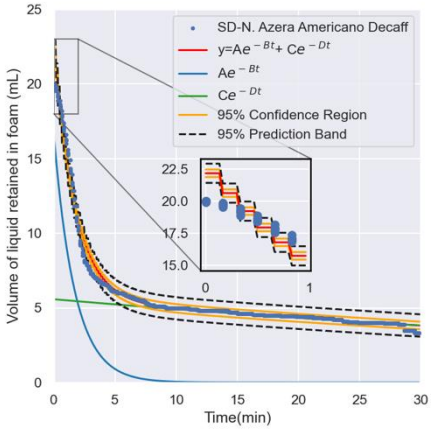
#39


SD-N. Azera Americano
y=Ae$^{-Bt}$+ Ce$^{-Dt}$
95% Confidence Region
95% Prediction Band
Volume of foam (mL)
Time(min)

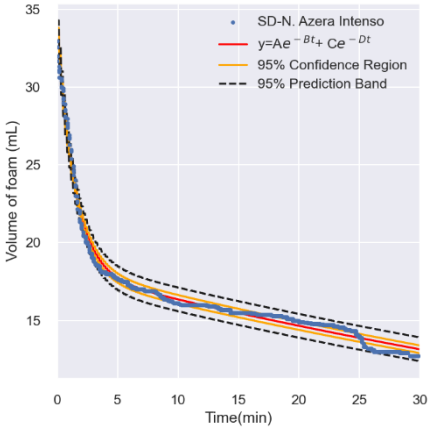

SD-N. Azera Americano
y=Ae$^{-Bt}$+ Ce$^{-Dt}$
Ae$^{-Bt}$
Ce$^{-Dt}$
95% Confidence Region
95% Prediction Band
Volume of liquid retained in foam (mL)
Time(min)

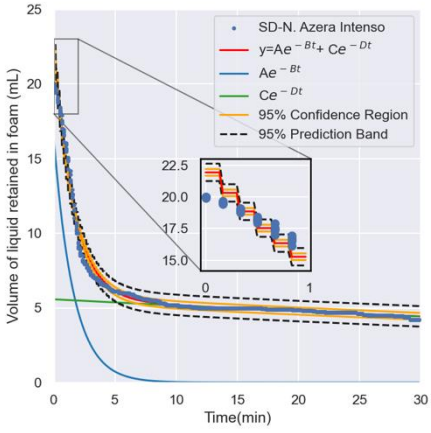
#40


SD-N. Azera Americano Decaff
y=Ae$^{-Bt}$+ Ce$^{-Dt}$
95% Confidence Region
95% Prediction Band
Volume of foam (mL)
Time(min)

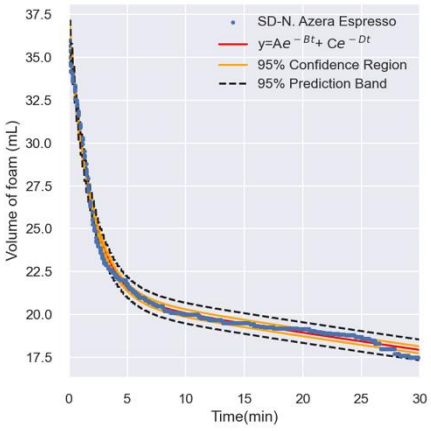

SD-N. Azera Americano Decaff
y=Ae$^{-Bt}$+ Ce$^{-Dt}$
Ae$^{-Bt}$
Ce$^{-Dt}$
95% Confidence Region
95% Prediction Band
Volume of liquid retained in foam (mL)
Time(min)

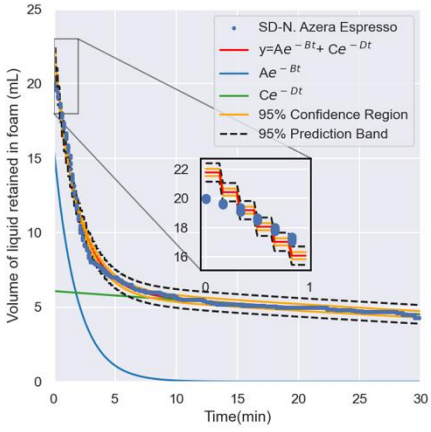
#41


SD-N. Azera Intenso
y=Ae$^{-Bt}$+ Ce$^{-Dt}$
95% Confidence Region
95% Prediction Band
Volume of foam (mL)
Time(min)


SD-N. Azera Intenso
y=Ae$^{-Bt}$+ Ce$^{-Dt}$
Ae$^{-Bt}$
Ce$^{-Dt}$
95% Confidence Region
95% Prediction Band
Volume of liquid retained in foam (mL)
Time(min)

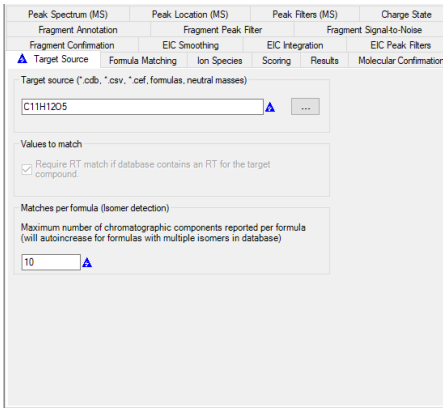
#42

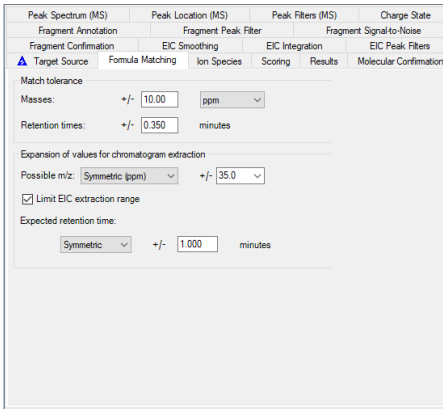

SD-N. Azera Espresso
y=Ae$^{-Bt}$+ Ce$^{-Dt}$
95% Confidence Region
95% Prediction Band
Volume of foam (mL)
Time(min)

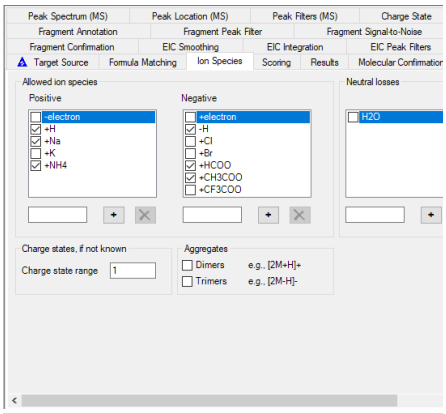

SD-N. Azera Espresso
y=Ae$^{-Bt}$+ Ce$^{-Dt}$
Ae$^{-Bt}$
Ce$^{-Dt}$
95% Confidence Region
95% Prediction Band
Volume of liquid retained in foam (mL)
Time(min)

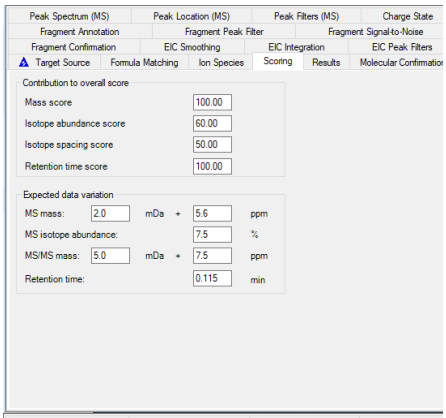
# Appendix B: Find by Formula Parameters

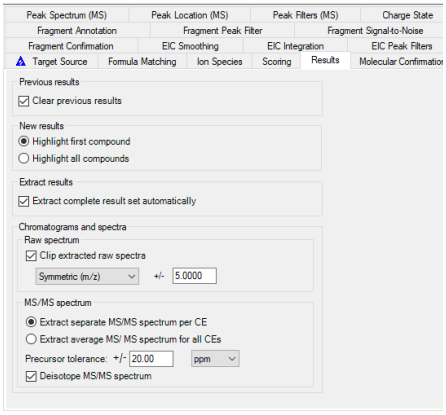
Detailed screen shots of Find by Formula parameters from MassHunter Qualitative analysis software are presented below.

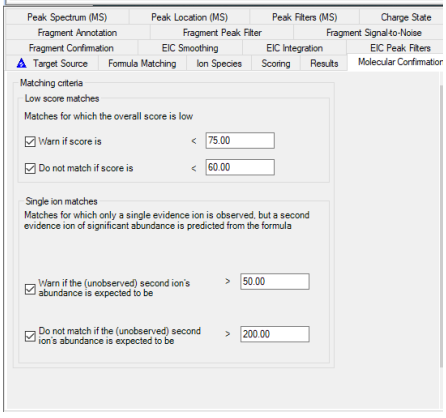


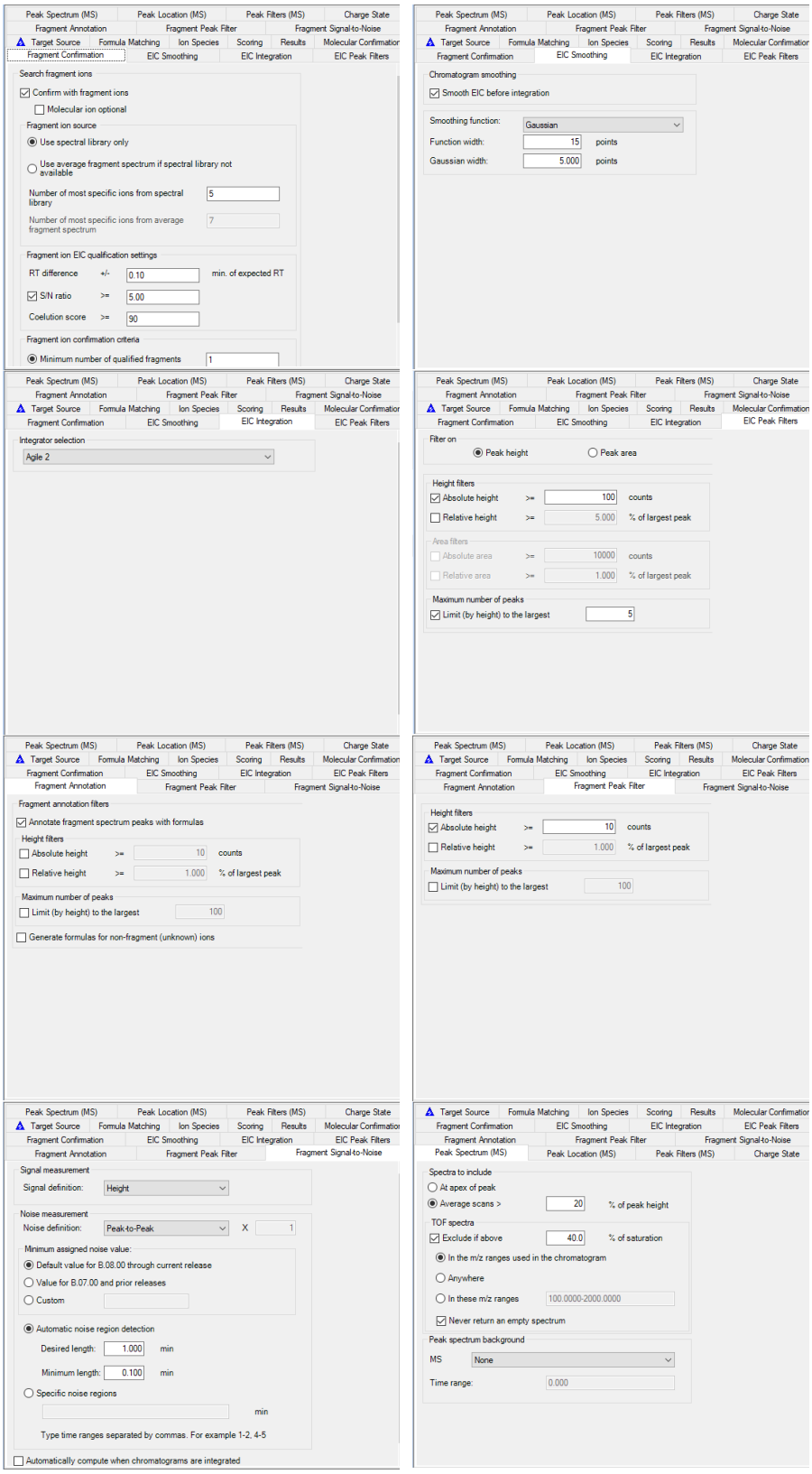



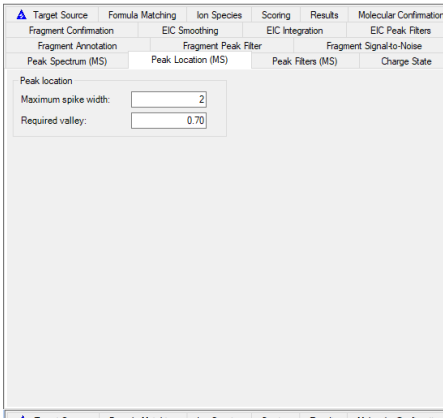



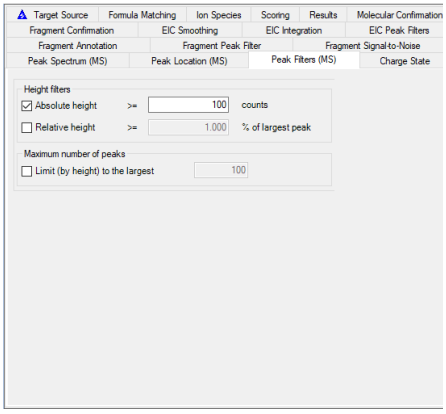



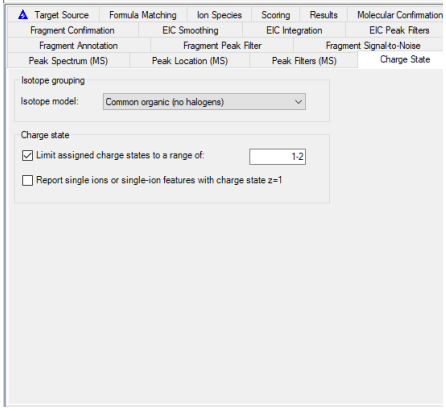




Peak Spectrum (MS)
Peak Location (MS)
Peak Filters (MS)
Charge State
Fragment Annotation
Fragment Peak Filter
Fragment Signal-to-Noise
Target Source
Formula Matching
Ion Species
Scoring
Results
Molecular Confirmation
Fragment Confirmation
EIC Smoothing
EIC Integration
EIC Peak Filters
Search fragment ions
Confirm with fragment ions
Molecular ion optional
Fragment ion source
Use spectral library only
Use average fragment spectrum if spectral library not available
Number of most specific ions from spectral library
Number of most specific ions from average fragment spectrum
Fragment ion EIC qualification settings
RT difference
min. of expected RT
S/N ratio
Coelution score
Fragment ion confirmation criteria
Minimum number of qualified fragments
Chromatogram smoothing
Smooth EIC before integration
Smoothing function:
Gaussian
Function width:
points
Gaussian width:
Integrator selection
Agile 2
Filter on
Peak height
Peak area
Height filters
Absolute height
Relative height
counts
% of largest peak
Area filters
Absolute area
Relative area
Maximum number of peaks
Limit (by height) to the largest
Fragment annotation filters
Annotate fragment spectrum peaks with formulas
Generate formulas for non-fragment (unknown) ions
Signal measurement
Signal definition:
Height
Noise measurement
Noise definition:
Peak-to-Peak
Minimum assigned noise value:
Default value for B.08.00 through current release
Value for B.07.00 and prior releases
Custom
Automatic noise region detection
Desired length:
Minimum length:
min
Specific noise regions
Type time ranges separated by commas. For example 1-2, 4-5
Automatically compute when chromatograms are integrated
Spectra to include
At apex of peak
Average scans >
% of peak height
TOF spectra
Exclude if above
% of saturation
In the m/z ranges used in the chromatogram
Anywhere
In these m/z ranges
Never return an empty spectrum
Peak spectrum background
MS
None
Time range:


Target Source
Formula Matching
Ion Species
Scoring
Results
Molecular Confirmation
Fragment Confirmation
EIC Smoothing
EIC Integration
EIC Peak Filters
Fragment Annotation
Fragment Peak Filter
Fragment Signal-to-Noise
Peak Spectrum (MS)
Peak Location (MS)
Peak Filters (MS)
Charge State
Peak location
Maximum spike width:
2
Required valley:
0.70


Target Source
Formula Matching
Ion Species
Scoring
Results
Molecular Confirmation
Fragment Confirmation
EIC Smoothing
EIC Integration
EIC Peak Filters
Fragment Annotation
Fragment Peak Filter
Fragment Signal-to-Noise
Peak Spectrum (MS)
Peak Location (MS)
Peak Filters (MS)
Charge State
Height filters
Absolute height
>=
100
counts
Relative height
>=
1.000
% of largest peak
Maximum number of peaks
Limit (by height) to the largest
100


Target Source
Formula Matching
Ion Species
Scoring
Results
Molecular Confirmation
Fragment Confirmation
EIC Smoothing
EIC Integration
EIC Peak Filters
Fragment Annotation
Fragment Peak Filter
Fragment Signal-to-Noise
Peak Spectrum (MS)
Peak Location (MS)
Peak Filters (MS)
Charge State
Isotope grouping
Isotope model:
Common organic (no halogens)
Charge state
Limit assigned charge states to a range of:
1-2
Report single ions or single-ion features with charge state z=1

# Appendix C: Chromatography column vs non-polar mobile phase system.

Table C.1 Extracted ion chromatographs of chemical entities by using two mobile phases (Acetonitrile vs Methanol) vs two chromatography columns (C18 vs Biphenyl)

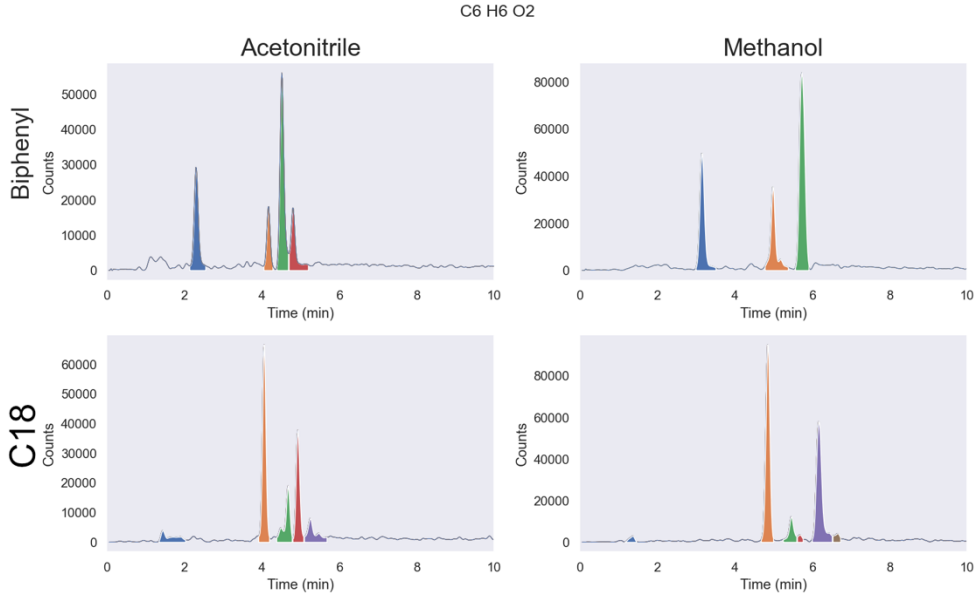
| Extracted ion chromatographs | Optimal separation | Comment |
|---|---|---|
|  | Methanol-Biphenyl | More dispersed and sharp peaks |

Table C.1 cont.

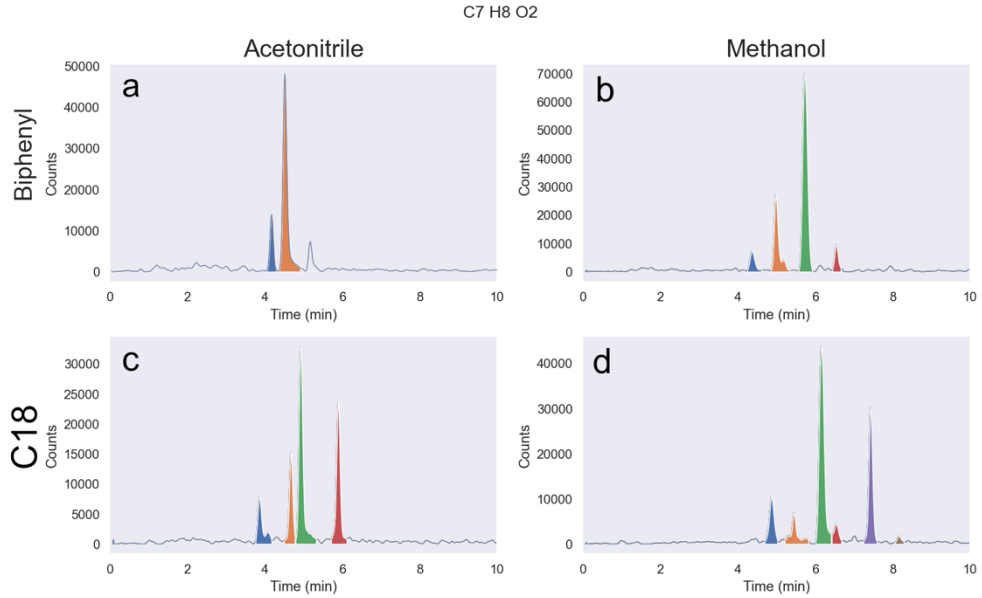
| | Extracted ion chromatographs | Optimal separation | Comment |
|---|---|---|---|
| |  | Methanol-Biphenyl | More dispersed and sharp peaks |

Table C.1 cont.

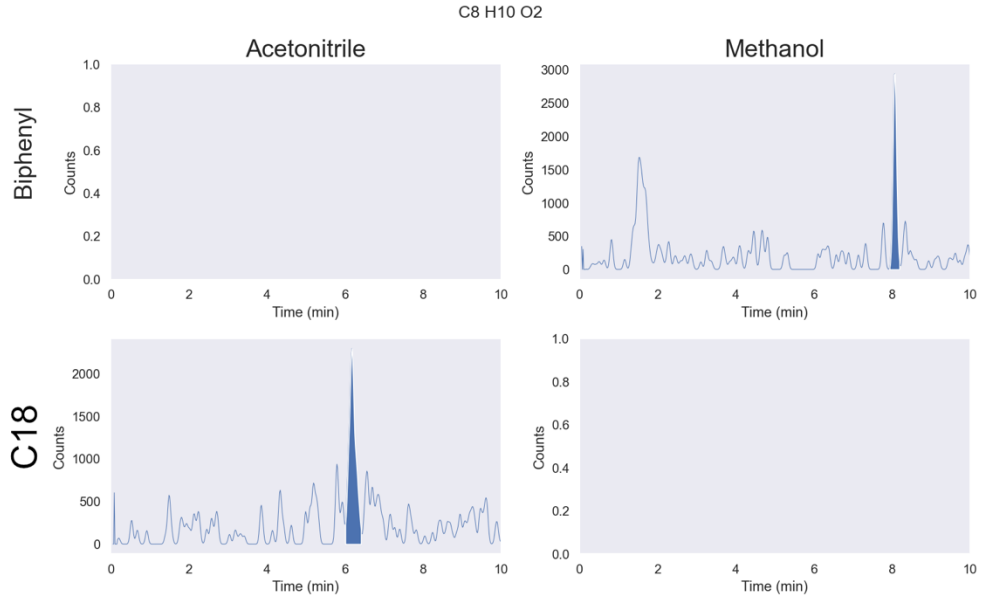
| | Extracted ion chromatographs | Optimal separation | Comment |
|---|---|---|---|
| |  | N/A | It is very likely that C8H10O2 is not present in the tested sample because the signal is very low. |

Table C.1 cont.

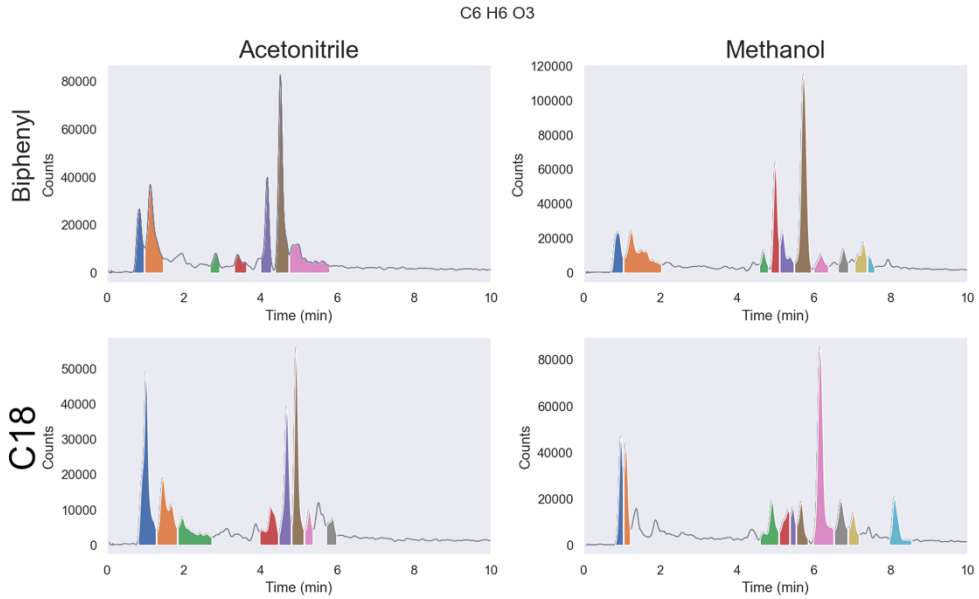
| | Extracted ion chromatographs | Optimal separation | Comment |
|---|---|---|---|
| |  | All | All system meet the criteria of good native separation |

Table C.1 cont.

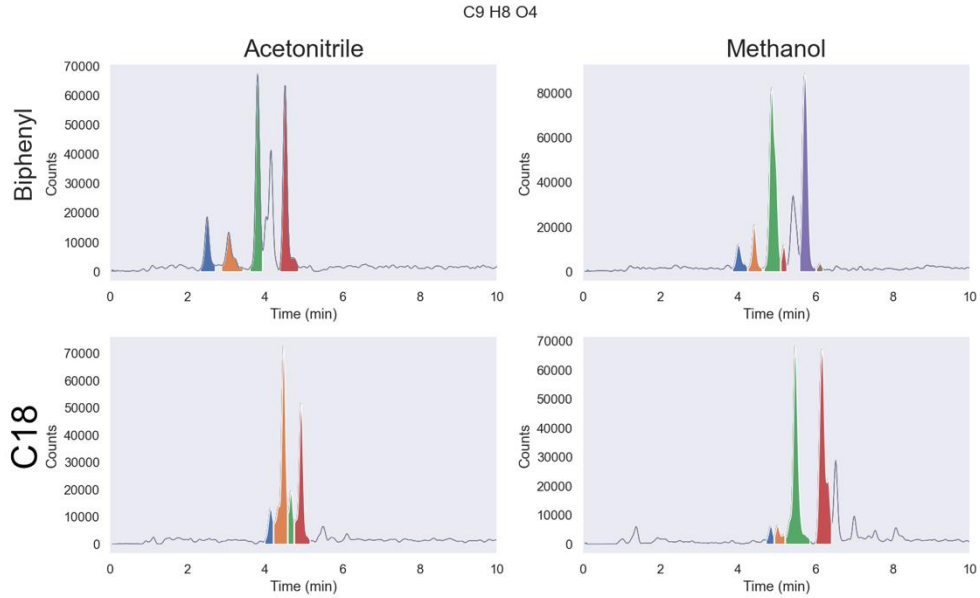
| | Extracted ion chromatographs | Optimal separation | Comment |
|---|---|---|---|
| |  | Methanol-Biphenyl | Biphenyl column gives better separability of caffeic acid compared to waters column. Methanol gives more sharp peaks and better separate ability from acetonitrile. |

Table C.1 cont.

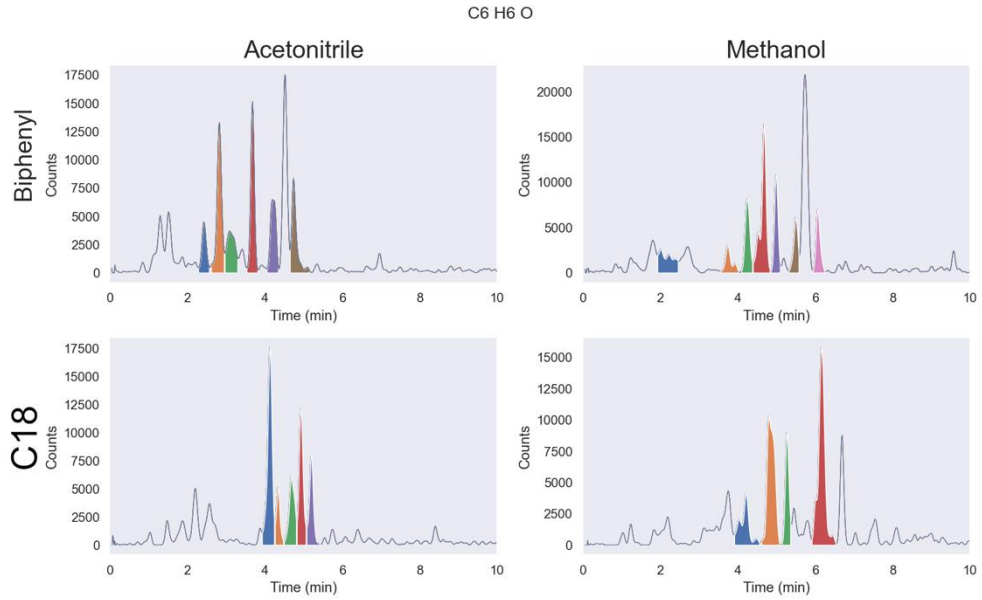
| | Extracted ion chromatographs | Optimal separation | Comment |
|---|---|---|---|
| |  | Acetonitrile-Biphenyl or Methanol-Biphenyl | Biphenyl gives better separateability from waters. Acetonitrile and MeOH are more or less the same. |

Table C.1 cont.

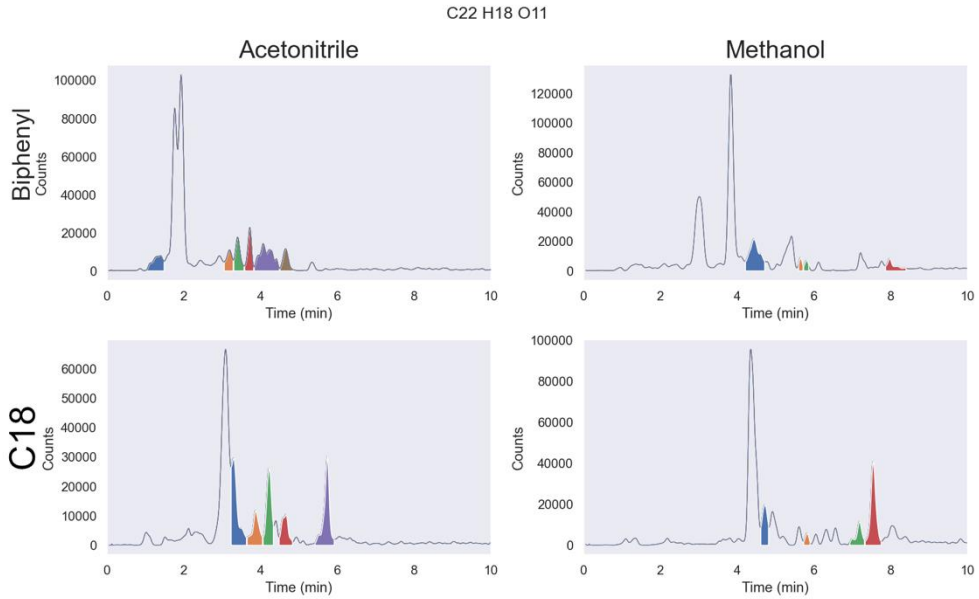
| | Extracted ion chromatographs | Optimal separation | Comment |
|---|---|---|---|
| |  | Waters-Acetonitrile | Same separateability for all comparisons. Best peaks for waters-acetonitrile |

Table C.1 cont.

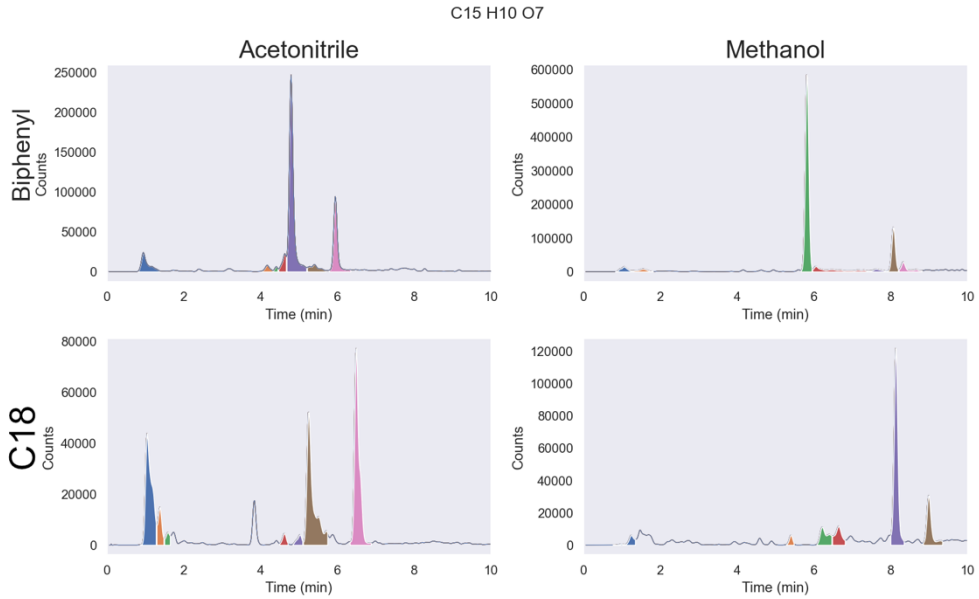
| | Extracted ion chromatographs | Optimal separation | Comment |
|---|---|---|---|
| |  | Methanol-Biphenyl | Methanol biphenyl gives the sharpest peaks along with methanol waters. |

Table C.1 cont.

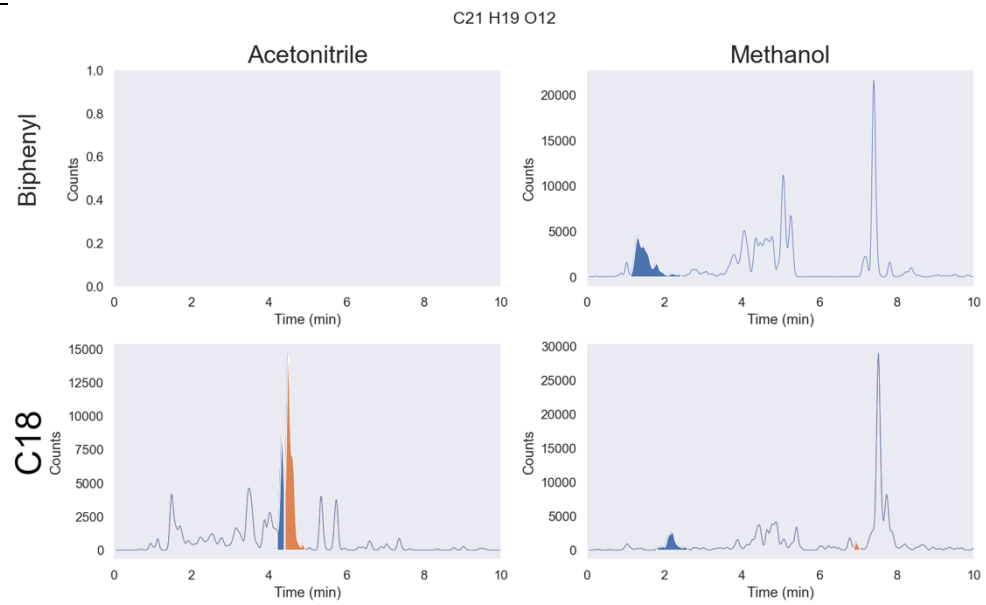
| | Extracted ion chromatographs | Optimal separation | Comment |
|---|---|---|---|
| |  | N/A | Not enough data from combinations so unable to judge which system provided an optimum separation |

Table C.1 cont.

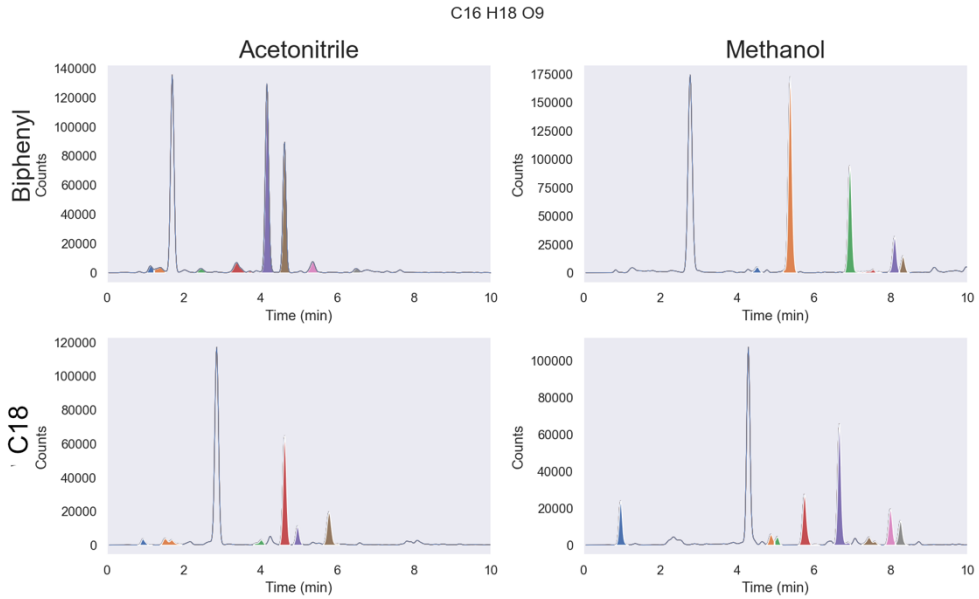
| | Extracted ion chromatographs | Optimal separation | Comment |
|---|---|---|---|
| |  | Biphenyl-methanol | Sharpest and more spread peaks. |

Table C.1 cont.

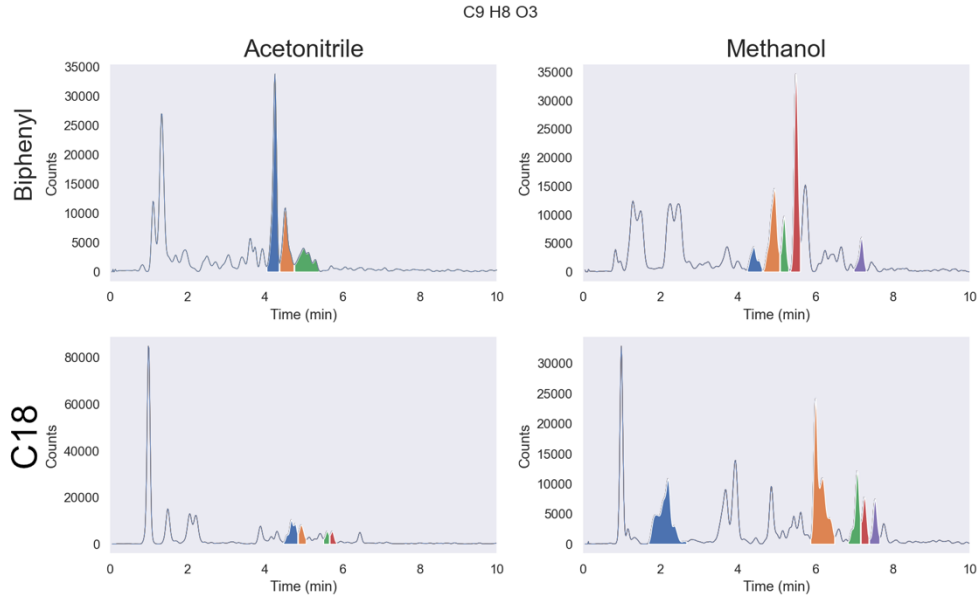
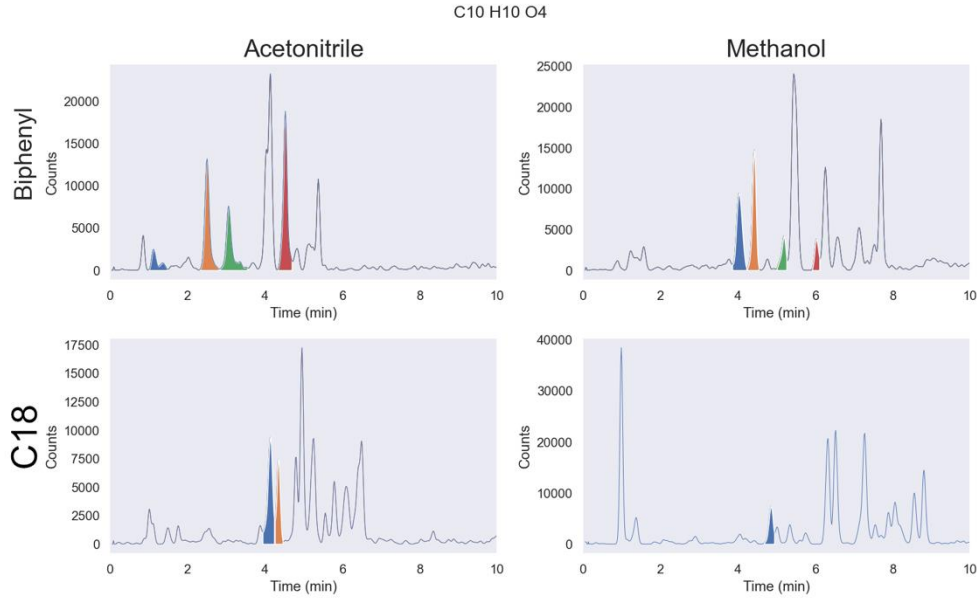
| | Extracted ion chromatographs | Optimal separation | Comment |
|---|---|---|---|
| |  | Biphenyl-methanol | Sharpest and more spread peaks. |

Table C.1 cont.

| | Extracted ion chromatographs | Optimal separation | Comment |
|---|---|---|---|
| |  | Biphenyl-methanol or Biphenyl-acetonitrile | Both nonpolar mobile phases along with biphenyl column provide sharp peaks with base-to-base separation |

# Appendix D: Initial list of polyphenols reported in coffee.

Table D.1 Phenolic compounds reported in coffee

| Number of chemical compound | Name | Abbreviation | Empirical Formula | Number of Empirical Formula |
|---|---|---|---|---|
| 1 | Ferulic acid | FA | C10H10O4 | 1 |
| 2 | 3,5-Dihydroxy-4-methoxycinnamic acid | Dihydroxy-meth-cinA | C10H10O5 | 2 |
| 3 | 2,4,5-Trimethoxycinnamic acid | TrimethcinA | C10H14O5 | 3 |
| 4 | 3,4 - Dimethoxycinnamic acid : 3,5-Dimethoxycinnamic | di-MethCinA | C11H12O4 | 4 |
| 5 | Sinapic acid | SA | C11H12O5 | 5 |
| 6 | Kaempferol | Kaemp | C15H10O6 | 6 |
| 7 | Quercetin | Querc | C15H10O7 | 7 |
| 8 | trans-5,6-Dihydroxy-1-methyl-3-(3’-4’-dihydroxyphenyl) indane (compound 1) | Compound 01 | C16H16O4 | 8 |
| 9 | cis-5,6-dihydroxy-1-methyl-3-(3',4'-dihydroxyphenyl) indane (compound 2) | Compound 02 | | |
| 10 | trans-1,3-bis(3’-4’-dihydroxyphenyl)butene (compound 3) | Compound 03 | | |
| 11 | trans - 4,5-dihydroxy-1-methyl-3-(3’,4’-dihydroxyphenyl) indane (compound 5) | Compound 05 | | |
| 12 | cis-4,5-dihydroxy-1-methyl-3-(3’,4’-dihydroxyphenyl) indane (compound 6) | Compound 06 | | |
| 13 | 3-O-p-Coumaroylquinic acid lactone | 3-pCoQL | C16H16O7 | 9 |
| 14 | 4-O-p-Coumaroylquinic acid lactone | 4-pCoQL | | |
| 15 | 5-O-p-Coumaroylquinic acid lactone | 5-pCoQL | | |
| 16 | 3-O-Caffeoylquinic acid lactone | 3-CQL | C16H16O8 | 10 |
| 17 | 4-O-Caffeoylquinic acid lactone | 4-CQL | | |
| 18 | 5-O-Caffeoylquinic acid lactone | 5-CQL | | |
| 19 | 1,3-Bis(3,4-dihydroxyphenyl)butane (compound 4) | Compound 04 | C16H18O4 | 11 |

Table D.1 cont.

| Number of chemical compound | Name | Abbreviation | Empirical Formula | Number of Empirical Formula |
|---|---|---|---|---|
| 20 | 3-O-p-Coumaroylquinic acid | 3-pCoQA | C16H18O8 | 12 |
| 21 | 4-O-p-Coumaroylquinic acid | 4-pCoQA | | |
| 22 | 5-O-p-Coumaroylquinic acid | 5-pCoQA | | |
| 23 | 3-O-Caffeoylquinic acid | 3-CQA | C16H18O9 | 13 |
| 24 | 4-O-Caffeoylquinic acid | 4-CQA | | |
| 25 | 5-O-Caffeoylquinic acid | 5-CQA | | |
| 26 | 5,6-Dihydroxy-2-carboxy-1-methyl-3-(3'-4'-dihydroxyphenyl) indane | Compound 10 | C17H16O6 | 14 |
| 27 | 3-O-Feruloylquinic acid lactone | 3-FQL | C17H18O8 | 15 |
| 28 | 4-O-Feruloylquinic acid lactone | 4-FQL | | |
| 29 | 5-O-Feruloylquinic acid lactone | 5-FQL | | |
| 30 | 3-O-Feruloylquinic acid | 3-FQA | C17H20O9 | 16 |
| 31 | 4-O-Feruloylquinic acid | 4-FQA | | |
| 32 | 5-O-Feruloylquinic acid | 5-FQA | | |
| 33 | 3-O-Sinapoylquinic acid lactone | 3-SiQL | C18H20O9 | 17 |
| 34 | 4-O-Sinapoylquinic acid lactone | 4-SiQL | | |
| 35 | 5-O-Sinapoylquinic acid lactone | 5-SiQL | | |
| 36 | 3-O-Dimethoxycinnamoylquinic acid lactone | 3-DQL | C18H21O8 | 18 |
| 37 | 4-O-Dimethoxycinnamoylquinic acid lactone | 4-DQL | | |
| 38 | 5-O-Dimethoxycinnamoylquinic acid lactone | 5-DQL | | |
| 39 | 3-O-Sinapoylquinic acid | 3-SiQA | C18H22O10 | 19 |
| 40 | 4-O-Sinapoylquinic acid | 4-SiQA | | |
| 41 | 5-O-Sinapoylquinic acid | 5-SiQA | | |
| 42 | 3-O-Dimethoxycinnamoylquinic acid | 3-DQA | C18H23O9 | 20 |
| 43 | 4-O-Dimethoxycinnamoylquinic acid | 4-DQA | | |
| 44 | 5-O-Dimethoxycinnamoylquinic acid | 5-DQA | | |
| 45 | Quercetin-3-glucoside | Querc-3-Glu | C21H19O12 | 21 |

Table D.1 cont.

| Number of chemical compound | Name | Abbreviation | Empirical Formula | Number of Empirical Formula |
|---|---|---|---|---|
| 46 | Kaempferol-3-glucoside | Kemp-3-Glu | C21H20O11 | 22 |
| 47 | Epigallocatechin gallate | EG | C22H18O11 | 23 |
| 48 | 3-O-p-Coumaroyl-4-O-caffeoylquinic acid lactone | 3pCo-4CQL | C24H22O10 | 24 |
| 49 | 3-O-Caffeoyl-4-O-p-coumaroylquinic acid lactone | 3C-4pCoQL | | |
| 50 | 3-O-p-Coumaroyl-5-O-caffeoylquinic acid lactone | 3pCo-5CQL | | |
| 51 | 3-O-Caffeoyl-5-O-p-coumaroylquinic acid lactone | 3C-5pCoQL | | |
| 52 | 4-O-Caffeoyl-5-O-p-coumaroylquinic acid lactone | 4C-5pCoQL | | |
| 53 | 4-O-p-Coumaroyl-5-O-caffeoylquinic acid lactone | 4pCo-5CQL | | |
| 54 | trans-5,6-dihydroxy-1-methyl-3-[3’,4’-dihydroxy-5’-(1-(3",4"-dihydroxyphenyl)-1-ethyl)phenyl] indane (compound 7) | Compound 07 | C24H24O6 | 25 |
| 55 | cis-5,6-dihydroxy-1-methyl-3-[3’,4’-dihydroxy-5’-(1-(3",4"-dihydroxyphenyl)-1-ethyl)phenyl] indane (compounfd 8) | Compound 08 | | |
| 56 | 5,6-dihydroxy-1-methyl-2-[1-(3’,4’-dihydroxyphenyl)-1-ethyl]-3-(3",4"-dihydroxyphenyl) indane (compound 9a,9b) | Compound 09a,09b | | |
| 57 | 3,4-Di-O-caffeoylquinic acid lactone | 3,4-diCQL | C25H22O11 | 26 |
| 58 | 3,5-Di-O-caffeoylquinic acid lactone | 3,5-diCQL | | |
| 59 | 4,5-Di-O-caffeoylquinic acid lactone | 4,5-diCQL | | |
| 60 | 3,4-Di-O-p-coumaroylquinic acid lactone | 3,4-dipCoQL | C25H22O9 | 27 |
| 61 | 3,5-Di-O-p-coumaroylquinic acid lactone | 3,5-dipCoQL | | |
| 62 | 4,5-Di-O-p-coumaroylquinic acid lactone | 4,5-dipCoQL | | |
| 63 | 3,4-Di-O-p-coumaroylquinic acid | 3,4-dipCoQA | C25H24O10 | 28 |
| 64 | 3,5-Di-O-p-coumaroylquinic acid | 3,5-dipCoQA | | |

Table D.1 cont.

| Number of chemical compound | Name | Abbreviation | Empirical Formula | Number of Empirical Formula |
|---|---|---|---|---|
| 65 | 4,5-Di-O-p-coumaroylquinic acid | 4,5-dipCoQA | | |
| 66 | 3-O-p-Coumaroyl-4-O-caffeoylquinic acid | 3pCo-4CQA | C25H24O11 | 29 |
| 67 | 3-O-Caffeoyl-4-O-p-coumaroylquinic acid | 3C-4pCoQA | | |
| 68 | 3-O-p-Coumaroyl-5-O-caffeoylquinic acid | 3pCo-5CQA | | |
| 69 | 3-O-Caffeoyl-5-O-p-coumaroylquinic acid | 3C-5pCoQA | | |
| 70 | 4-O-Caffeoyl-5-O-p-coumaroylquinic acid | 4C-5pCoQA | | |
| 71 | 4-O-p-Coumaroyl-5-O-caffeoylquinic acid | 4pCo-5CQA | | |
| 72 | 3,4-Di-O-caffeoylquinic acid | 3,4-diCQA | C25H24O12 | 30 |
| 73 | 3,5-Di-O-caffeoylquinic acid | 3,5-diCQA | | |
| 74 | 4,5-Di-O-caffeoylquinic acid | 4,5-diCQA | | |
| 75 | 3-O-p-Coumaroyl-4-O-feruloylquinic acid lactone | 3pCo-4FQL | C26H24O10 | 31 |
| 76 | 3-O-p-Coumaroyl-5-O-feruloylquinic acid lactone | 3pCo-5FQL | | |
| 77 | 4-O-p-Coumaroyl-5-O-feruloylquinic acid lactone | 4pCo-5FQL | | |
| 78 | 3-O-Feruloyl-4-O-caffeoylquinic acid lactone | 3F-4CQL | C26H24O11 | 32 |
| 79 | 3-O-Caffeoyl-4-O-feruloylquinic acid lactone | 3C-4FQL | | |
| 80 | 3-O-Feruloyl-5-O-caffeoylquinic acid lactone | 3F-5CQL | | |
| 81 | 3-O-Caffeoyl-5-O-feruloylquinic acid lactone | 3C-5FQL | | |
| 82 | 4-O-Feruloyl-5-O-caffeoylquinic acid lactone | 4F-5CQL | | |
| 83 | 4-O-Caffeoyl-5-O-feruloylquinic acid lactone | 4C-5FQL | | |
| 84 | 3-O-p-Coumaroyl-4-O-feruloylquinic acid | 3pCo-4FQA | C26H26O11 | 33 |
| 85 | 3-O-p-Coumaroyl-5-O-feruloylquinic acid | 3pCo-5FQA | | |
| 86 | 4-O-p-Coumaroyl-5-O-feruloylquinic acid | 4pCo-5FQA | | |
| 87 | 3-O-Feruloyl-4-O-caffeoylquinic acid | 3F-4CQA | C26H26O12 | 34 |
| 88 | 3-O-Caffeoyl-4-O-feruloylquinic acid | 3C-4FQA | | |
| 89 | 3-O-Feruloyl-5-O-caffeoylquinic acid | 3F-5CQA | | |
| 90 | 3-O-Caffeoyl-5-O-feruloylquinic acid | 3C-5FQA | | |

Table D.1 cont.

| Number of chemical compound | Name | Abbreviation | Empirical Formula | Number of Empirical Formula |
|---|---|---|---|---|
| 91 | 4-O-Feruloyl-5-O-caffeoylquinic acid | 4F-5CQA | | |
| 92 | 4-O-Caffeoyl-5-O-feruloylquinic acid | 4C-5FQA | | |
| 93 | 4-O-Dimethoxycinnamoyl-5-O-p- coumaroylquinic acid lactone | 4D-5PCOQL | | |
| 94 | 3-O-p-Coumaroyl-4-O-dimethoxycinnamoylquinic acid lactone | 3pCo-4DQL | C27H26O10 | 35 |
| 95 | 3-O-p-Coumaroyl-5-O-dimethoxycinnamoylquinic acid lactone | 3pCo-5DQL | | |
| 96 | 3,4-Di-O-feruloylquinic acid lactone | 3,4-diFQL | | |
| 97 | 3,5-Di-O-feruloylquinic acid lactone | 3,5-diFQL | | |
| 98 | 4,5-Di-O-feruloylquinic acid lactone | 4,5-diFQL | | |
| 99 | 3-O-Dimethoxycinnamoyl-4-O-caffeoylquinic acid lactone | 3D-4CQL | C27H26O11 | 36 |
| 100 | 3-O-Dimethoxycinnamoyl-5-O-caffeoylquinic acid lactone | 3D-5CQL | | |
| 101 | 4-O-Dimethoxycinnamoyl-5-O-caffeoylquinic acid lactone | 4D-5CQL | | |
| 102 | 3-O-Sinapoyl-5-O-caffeoylquinic acid lactone | 3Si-5CQL | | |
| 103 | 3-O-Sinapoyl-4-O-caffeoylquinic acid lactone | 3Si-4CQL | | |
| 104 | 3-O-(3,5-Dihydroxy-4-methoxy) cinnamoyl-4-O-feruloylquinic acid lactone | 3DM-4FQL | C27H26O12 | 37 |
| 105 | 4-O-Sinapoyl-3-O-caffeoylquinic acid lactone | 4Si-3CQL | | |
| 106 | 4-O-Dimethoxycinnamoyl-5-O-p- coumaroylquinic acid | 4D-5PCOQA | | |
| 107 | 3-O-p-Coumaroyl-4-O-dimethoxycinnamoylquinic acid | 3pCo-4DQA | C27H28O11 | 38 |
| 108 | 3-O-p-Coumaroyl-5-O-dimethoxycinnamoylquinic acid | 3pCo-5DQA | | |
| 109 | 3,4-Di-O-feruloylquinic acid | 3,4-diFQA | | |
| 110 | 3,5-Di-O-feruloylquinic acid | 3,5-diFQA | C27H28O12 | 39 |
| 111 | 4,5-Di-O-feruloylquinic acid | 4,5-diFQA | | |

Table D.1 cont.

| Number of chemical compound | Name | Abbreviation | Empirical Formula | Number of Empirical Formula |
|---|---|---|---|---|
| 112 | 3-O-Dimethoxycinnamoyl-4-O-caffeoylquinic acid | 3D-4CQA | | |
| 113 | 3-O-Dimethoxycinnamoyl-5-O-caffeoylquinic acid | 3D-5CQA | | |
| 114 | 4-O-Dimethoxycinnamoyl-5-O-caffeoylquinic acid | 4D-5CQA | | |
| 115 | 3-O-Sinapoyl-5-O-caffeoylquinic acid | 3Si-5CQA | | |
| 116 | 3-O-Sinapoyl-4-O-caffeoylquinic acid | 3Si-4CQA | | |
| 117 | 3-O-(3,5-Dihydroxy-4-methoxy) cinnamoyl-4-O-feruloylquinic acid | 3DM-4FQA | C27H28O13 | 40 |
| 118 | 4-O-Sinapoyl-3-O-caffeoylquinic acid | 4Si-3CQA | | |
| 119 | Quercetin-3-rutinoside | Querc-3-Rut | C27H30O16 | 41 |
| 120 | 3-O-Dimethoxycinnamoyl-4-O-feruloylquinic acid lactone | 3D-4FQL | | |
| 121 | 3-O-Dimethoxycinnamoyl-5-O-feruloylquinic acid lactone | 3D-5FQL | C28H28O11 | 42 |
| 122 | 4-O-Dimethoxycinnamoyl-5-O-feruloylquinic acid lactone | 4D-5FQL | | |
| 123 | 3-O-Sinapoyl-5-O-feruloylquinic acid lactone | 3Si-5FQL | | |
| 124 | 4-O-Sinapoyl-5-O-feruloylquinic acid lactone | 4Si-5FQL | | |
| 125 | 4-O-Sinapoyl-3-O-feruloylquinic acid lactone | 4Si-3FQL | C28H28O12 | 43 |
| 126 | 4-O-Trimethoxycinnamoyl-5-O- caffeoylquinic acid lactone | 4T-5CQL | | |
| 127 | 3-O-Trimethoxycinnamoyl-5-O- caffeoylquinic acid lactone | 3T-5CQL | | |
| 128 | 3-O-Dimethoxycinnamoyl-4-O-feruloylquinic acid | 3D-4FQA | | |
| 129 | 3-O-Dimethoxycinnamoyl-5-O-feruloylquinic acid | 3D-5FQA | C28H30O12 | 44 |
| 130 | 4-O-Dimethoxycinnamoyl-5-O-feruloylquinic acid | 4D-5FQA | | |
| 131 | 3-O-Sinapoyl-5-O-feruloylquinic acid | 3Si-5FQA | | |
| 132 | 4-O-Sinapoyl-5-O-feruloylquinic acid | 4Si-5FQA | | |
| 133 | 4-O-Sinapoyl-3-O-feruloylquinic acid | 4Si-3FQA | C28H30O13 | 45 |
| 134 | 4-O-Trimethoxycinnamoyl-5-O- caffeoylquinic acid | 4T-5CQA | | |
| 135 | 3-O-Trimethoxycinnamoyl-5-O- caffeoylquinic acid | 3T-5CQA | | |

Table D.1 cont.

| Number of chemical compound | Name | Abbreviation | Empirical Formula | Number of Empirical Formula |
|---|---|---|---|---|
| 136 | 3-O-Trimethoxycinnamoyl-5-O- feruloylquinic acid lactone | 3T-5FQL | C29H30O12 | 46 |
| 137 | 3-O-Trimethoxycinnamoyl-4-O-feruloylquinic acid lactone | 3T-4FQL | | |
| 138 | 4-O-Trimethoxycinnamoyl-5-O-feruloylquinic acid lactone | 4T-5FQL | | |
| 139 | 3-O-Trimethoxycinnamoyl-5-O- feruloylquinic acid | 3T-5FQA | C29H32O13 | 47 |
| 140 | 3-O-Trimethoxycinnamoyl-4-O-feruloylquinic acid | 3T-4FQA | | |
| 141 | 4-O-Trimethoxycinnamoyl-5-O-feruloylquinic acid | 4T-5FQA | | |
| 142 | 3,4,5-Tri-O-caffeoylquinic acid lactone | 3,4,5-triCQL | C34H28O14 | 48 |
| 143 | 3,4,5-Tri-O-caffeoylquinic acid | 3,4,5-triCQA | C34H30O15 | 49 |
| 144 | 3,5-Di-O-caffeoyl-4-O-feruloylquinic acid lactone | 3,5-diC-4FQL | C35H30O14 | 50 |
| 145 | 3-O-Feruloyl-4,5-di-O-caffeoylquinic acid lactone | 3F-4,5-DICQL | | |
| 146 | 3,4-Di-O-caffeoyl-5-O-feruloylquinic acid lactone | 3,4-diC-5FQL | | |
| 147 | 3,5-Di-O-caffeoyl-4-O-feruloylquinic acid | 3,5-diC-4FQA | C35H32O15 | 51 |
| 148 | 3-O-Feruloyl-4,5-di-O-caffeoylquinic acid | 3F-4,5-DICQA | | |
| 149 | 3,4-Di-O-caffeoyl-5-O-feruloylquinic acid | 3,4-diC-5FQA | | |
| 150 | 3-O-Dimethoxycinnamoyl-4-O-feruloyl-5-O-caffeoylquinic acid lactone | 3D-4f-5CQL | C36H32O12 | 52 |
| 151 | 3-O-Caffeoyl-4,5-di-O-feruloylquinic acid lactone | 3C-4,5-diFQL | C36H32O14 | 53 |
| 152 | 3,4-Di-O-feruloyl-5-O-caffeoylquinic acid lactone | 3,4-diF-5CQL | | |
| 153 | 3,4-Di-O-caffeoyl-5-O-sinapoylquinic acid lactone | 3,4-diC-5SiQL | C36H32O15 | 54 |
| 154 | 3-O-Sinapoyl-4,5-di-O-caffeoylquinic acid lactone | 3Si-4,5-DICQL | | |
| 155 | 3-O-Dimethoxycinnamoyl-4-O-feruloyl-5-O-caffeoylquinic acid | 3D-4f-5CQA | C36H34O13 | 55 |
| 156 | 3-O-Caffeoyl-4,5-di-O-feruloylquinic acid | 3C-4,5-diFQA | C36H34O15 | 56 |
| 157 | 3,4-Di-O-feruloyl-5-O-caffeoylquinic acid | 3,4-diF-5CQA | | |
| 158 | 3,4-Di-O-caffeoyl-5-O-sinapoylquinic acid | 3,4-diC-5SiQA | C36H34O16 | 57 |
| 159 | 3-O-Sinapoyl-4,5-di-O-caffeoylquinic acid | 3Si-4,5-DICQA | | |

Table D.1 cont.

| Number of chemical compound | Name | Abbreviation | Empirical Formula | Number of Empirical Formula |
|---|---|---|---|---|
| 160 | Phenol | Ph | C6H6O | 58 |
| 161 | Catechol | Cat | C6H6O2 | 59 |
| 162 | Pyrogallol | Pyr | C6H6O3 | 60 |
| 163 | Quinic acid lactone | QL | C7H10O5 | 61 |
| 164 | Quinic acid | QA | C7H12O6 | 62 |
| 165 | Salicylic acid | SA | C7H6O3 | 63 |
| 166 | Gallic acid | GA | C7H6O5 | 64 |
| 167 | 3-methylcatechol | 3-MethCat | C7H8O2 | 65 |
| 168 | 4-methylcatechol | 4-MethCat | | |
| 169 | Guaiacol | Gua | | |
| 170 | 4-ethylcatechol | 4-EthCat | C8H10O2 | 66 |
| 171 | 4-vinylcatechol | 4-VC | C8H8O2 | 67 |
| 172 | 4-vinylguaiacol | 4-VinG | C9H10O2 | 68 |
| 173 | 4-ethylguaicol | 4-EthG | C9H12O2 | 69 |
| 174 | p-Coumaric acid | p-CoA | C9H8O3 | 70 |
| 175 | Caffeic acid | CA | C9H8O4 | 71 |

# Appendix E: List of phenolic compounds found by Find by Formula function in control instant coffee.

Table E.1 Chemical entities found in control instant coffee

| Number of chemical compound | Name | Abbreviation | Empirical formula | Number of empirical formulas |
|---|---|---|---|---|
| 1 | Ferulic acid | FA | C10H10O4 | 1 |
| 2 | 3,4 - Dimethoxycinnamic acid : 3,5-Dimethoxycinnamic | di-MethCinA | C11H12O4 | 2 |
| 3 | trans-5,6-Dihydroxy-1-methyl-3-(3’-4’-dihydroxyphenyl) indane (compound 1) | Compound 01 | C16H16O4 | 3 |
| 4 | cis-5,6-dihydroxy-1-methyl-3-(3',4'-dihydroxyphenyl) indane (compound 2) | Compound 02 | | |

Table E.1 cont.

| Number of chemical compound | Name | Abbreviation | Empirical formula | Number of empirical formulas |
|---|---|---|---|---|
| 5 | trans-1,3-bis(3'-4'-dihydroxyphenyl)butene (compound 3) | Compound 03 | | |
| 6 | trans - 4,5-dihydroxy-1-methyl-3-(3',4'-dihydroxyphenyl) indane (compound 5) | Compound 05 | | |
| 7 | cis-4,5-dihydroxy-1-methyl-3-(3',4'-dihydroxyphenyl) indane (compound 6) | Compound 06 | | |
| 8 | 3-O-p-Coumaroylquinic acid lactone | 3-pCoQL | | |
| 9 | 4-O-p-Coumaroylquinic acid lactone | 4-pCoQL | C16H16O7 | 4 |
| 10 | 5-O-p-Coumaroylquinic acid lactone | 5-pCoQL | | |
| 11 | 3-O-Caffeoylquinic acid lactone | 3-CQL | | |
| 12 | 4-O-Caffeoylquinic acid lactone | 4-CQL | C16H16O8 | 5 |
| 13 | 5-O-Caffeoylquinic acid lactone | 5-CQL | | |
| 14 | 1,3-Bis(3,4-dihydroxyphenyl)butane (compound 4) | Compound 04 | C16H18O4 | 6 |
| 15 | 3-O-p-Coumaroylquinic acid | 3-pCoQA | | |
| 16 | 4-O-p-Coumaroylquinic acid | 4-pCoQA | C16H18O8 | 7 |
| 17 | 5-O-p-Coumaroylquinic acid | 5-pCoQA | | |
| 18 | 3-O-Caffeoylquinic acid | 3-CQA | | |
| 19 | 4-O-Caffeoylquinic acid | 4-CQA | C16H18O9 | 8 |
| 20 | 5-O-Caffeoylquinic acid | 5-CQA | | |
| 21 | 5,6-Dihydroxy-2-carboxy-1-methyl-3-(3'-4'-dihydroxyphenyl) indane | Compound 10 | C17H16O6 | 9 |
| 22 | 3-O-Feruloylquinic acid lactone | 3-FQL | | |
| 23 | 4-O-Feruloylquinic acid lactone | 4-FQL | C17H18O8 | 10 |
| 24 | 5-O-Feruloylquinic acid lactone | 5-FQL | | |
| 25 | 3-O-Feruloylquinic acid | 3-FQA | | |
| 26 | 4-O-Feruloylquinic acid | 4-FQA | C17H20O9 | 11 |
| 27 | 5-O-Feruloylquinic acid | 5-FQA | | |
| 28 | Phenol | Ph | C6H6O | 12 |
| 29 | Catechol | Cat | C6H6O2 | 13 |
| 30 | Pyrogallol | Pyr | C6H6O3 | 14 |
| 31 | Quinic acid lactone | QL | C7H10O5 | 15 |
| 32 | Quinic acid | QA | C7H12O6 | 16 |
| 33 | Salicylic acid | SA | C7H6O3 | 17 |

Table E.1 cont.

| Number of chemical compound | Name | Abbreviation | Empirical formula | Number of empirical formulas |
|---|---|---|---|---|
| 34 | 3-methylcatechol | 3-MethCat | C7H8O2 | 18 |
| 35 | 4-methylcatechol | 4-MethCat | | |
| 36 | Guaiacol | Gua | | |
| 37 | 4-ethylcatechol | 4-EthCat | C8H10O2 | 19 |
| 38 | 4-vinylcatechol | 4-VC | C8H8O2 | 20 |
| 39 | 4-vinylguaiacol | 4-VinG | C9H10O2 | 21 |
| 40 | p-Coumaric acid | p-CoA | C9H8O3 | 22 |
| 41 | Caffeic acid | CA | C9H8O4 | 23 |
| 42 | 3,4-Di-O-caffeoylquinic acid lactone | 3,4-diCQL | C25H22O11 | 24 |
| 43 | 3,5-Di-O-caffeoylquinic acid lactone | 3,5-diCQL | | |
| 44 | 4,5-Di-O-caffeoylquinic acid lactone | 4,5-diCQL | | |
| 45 | 3,4-Di-O-p-coumaroylquinic acid | 3,4-dipCoQA | C25H24O10 | 25 |
| 46 | 3,5-Di-O-p-coumaroylquinic acid | 3,5-dipCoQA | | |
| 47 | 4,5-Di-O-p-coumaroylquinic acid | 4,5-dipCoQA | | |
| 48 | 3,4-Di-O-caffeoylquinic acid | 3,4-diCQA | C25H24O12 | 26 |
| 49 | 3,5-Di-O-caffeoylquinic acid | 3,5-diCQA | | |
| 50 | 4,5-Di-O-caffeoylquinic acid | 4,5-diCQA | | |
| 51 | 3-O-Feruloyl-4-O-caffeoylquinic acid | 3F-4CQA | C26H26O12 | 27 |
| 52 | 3-O-Caffeoyl-4-O-feruloylquinic acid | 3C-4FQA | | |
| 53 | 3-O-Feruloyl-5-O-caffeoylquinic acid | 3F-5CQA | | |
| 54 | 3-O-Caffeoyl-5-O-feruloylquinic acid | 3C-5FQA | | |
| 55 | 4-O-Feruloyl-5-O-caffeoylquinic acid | 4F-5CQA | | |
| 56 | 4-O-Caffeoyl-5-O-feruloylquinic acid | 4C-5FQA | | |
| 57 | 3-O-Sinapoyl-5-O-caffeoylquinic acid lactone | 3Si-5CQL | C27H26O12 | 28 |
| 58 | 3-O-Sinapoyl-4-O-caffeoylquinic acid lactone | 3Si-4CQL | | |
| 59 | 3-O-(3,5-Dihydroxy-4-methoxy) cinnamoyl-4-O-feruloylquinic acid lactone | 3DM-4FQL | | |
| 60 | 4-O-Sinapoyl-3-O-caffeoylquinic acid lactone | 4Si-3CQL | | |
| 61 | 3,4-Di-O-feruloylquinic acid | 3,4-diFQA | C27H28O12 | 29 |
| 62 | 3,5-Di-O-feruloylquinic acid | 3,5-diFQA | | |

Table E.1 cont.

| Number of chemical compound | Name | Abbreviation | Empirical formula | Number of empirical formulas |
|---|---|---|---|---|
| 63 | 4,5-Di-O-feruloylquinic acid | 4,5-diFQA | | |
| 64 | 3-O-Dimethoxycinnamoyl-4-O-caffeoylquinic acid | 3D-4CQA | | |
| 65 | 3-O-Dimethoxycinnamoyl-5-O-caffeoylquinic acid | 3D-5CQA | | |
| 66 | 4-O-Dimethoxycinnamoyl-5-O-caffeoylquinic acid | 4D-5CQA | | |

# Appendix F: Extracted ion chromatographs from Polyscreen mk1 to mk6.

Table F.1 Extracted ion chromatographs for targets analysed via Polyscreen mk1 to m6

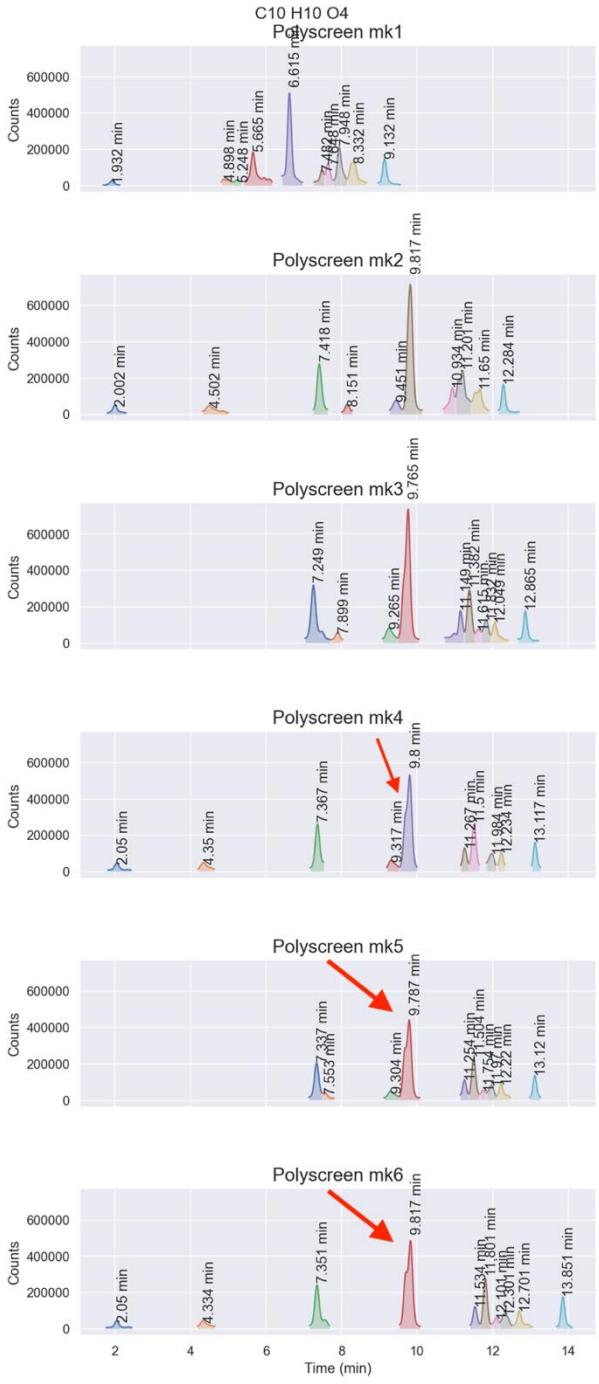
| Extracted ion chromatograph | Comment |
|---|---|
|  | Sharp peaks and base-to-base separation were achieved from Polyscreen mk1 to mk4. The peaks at:<br>• MK4 at 9.8 min<br>• Mk5 at 9.797 min<br>• Mk6 at 9.817 min<br><br>Shoulder effect (red arrow) appeared on Polyscreen mk5 and mk6. |

Table F.1 cont.

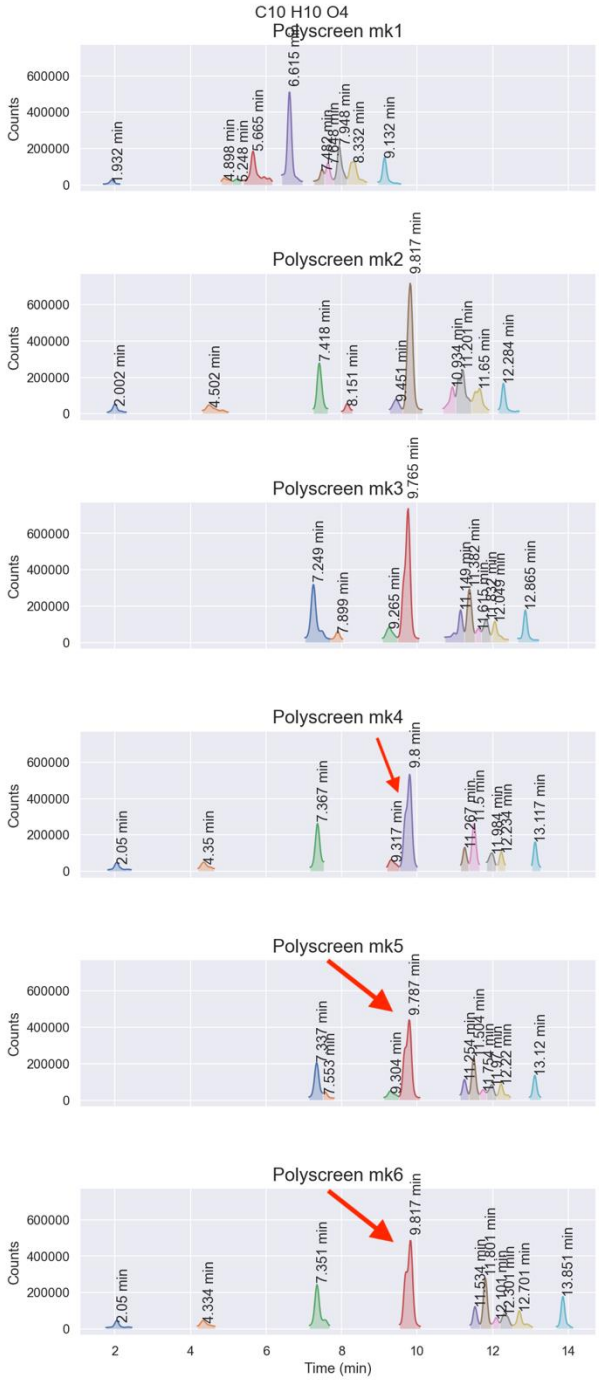
| Extracted ion chromatograph | Comment |
|---|---|
|  | Sharp peaks and base-to-base separation were achieved from Polyscreen mk1 to mk4. The peaks at:<br>• MK4 at 9.8 min<br>• Mk5 at 9.797 min<br>• Mk6 at 9.817 min<br><br>Shoulder effect (red arrow) appeared on Polyscreen mk5 and mk6. |

Table F.1 cont.

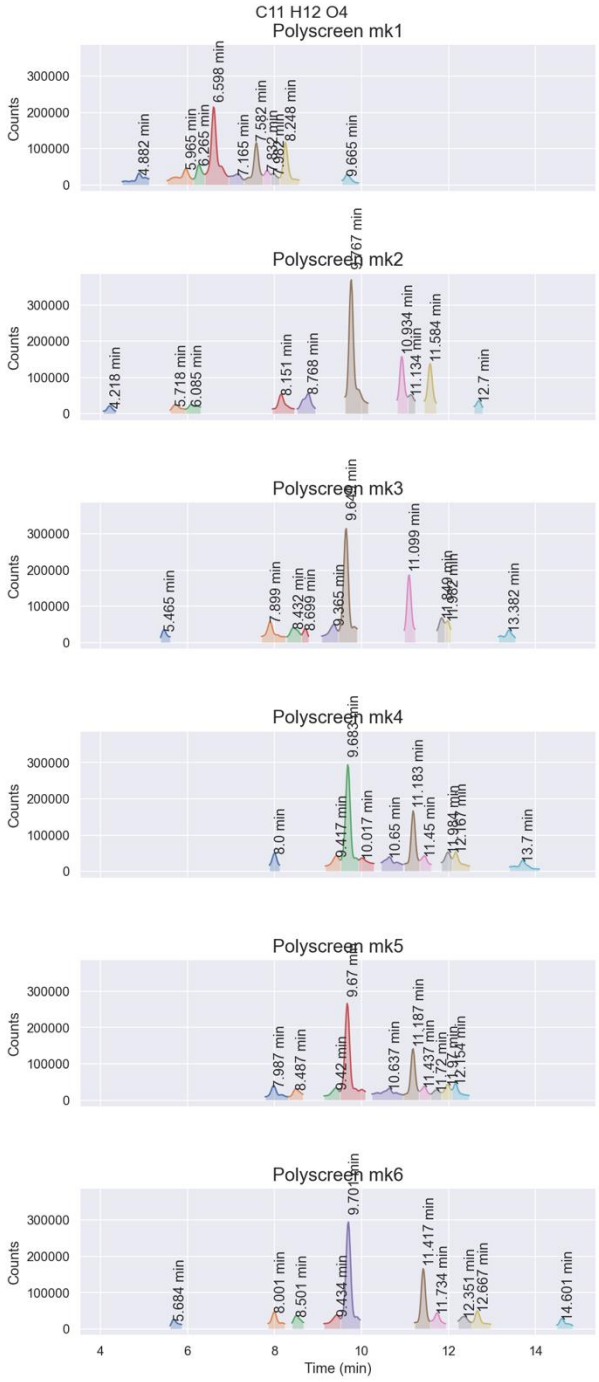
| Extracted ion chromatograph | Comment |
|---|---|
|  | Sharp peaks and base-to-base separation were achieved from Polyscreen mk2 to mk6. |

Table F.1 cont.

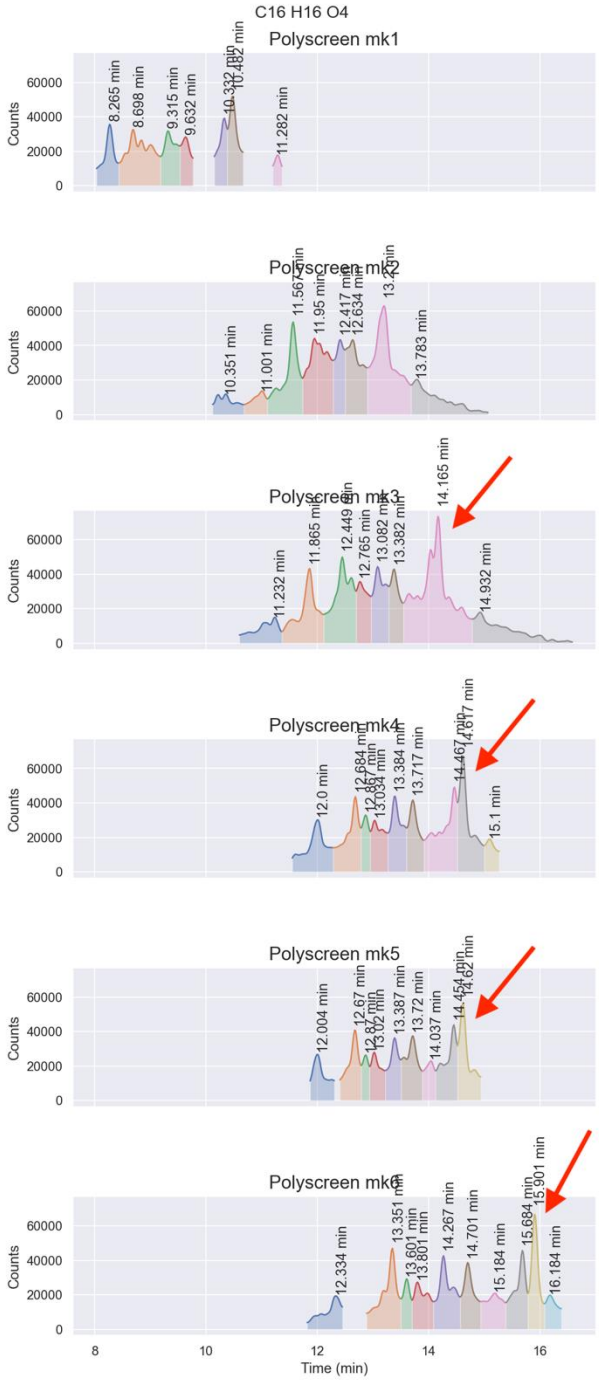
| Extracted ion chromatograph | Comment |
|---|---|
|  | Abundance was low so base to base separation was not achieved. However, the peaks pointed with red arrow were separated from Polyscreen mk4 to Polyscreen mk6. |

Table F.1 cont.

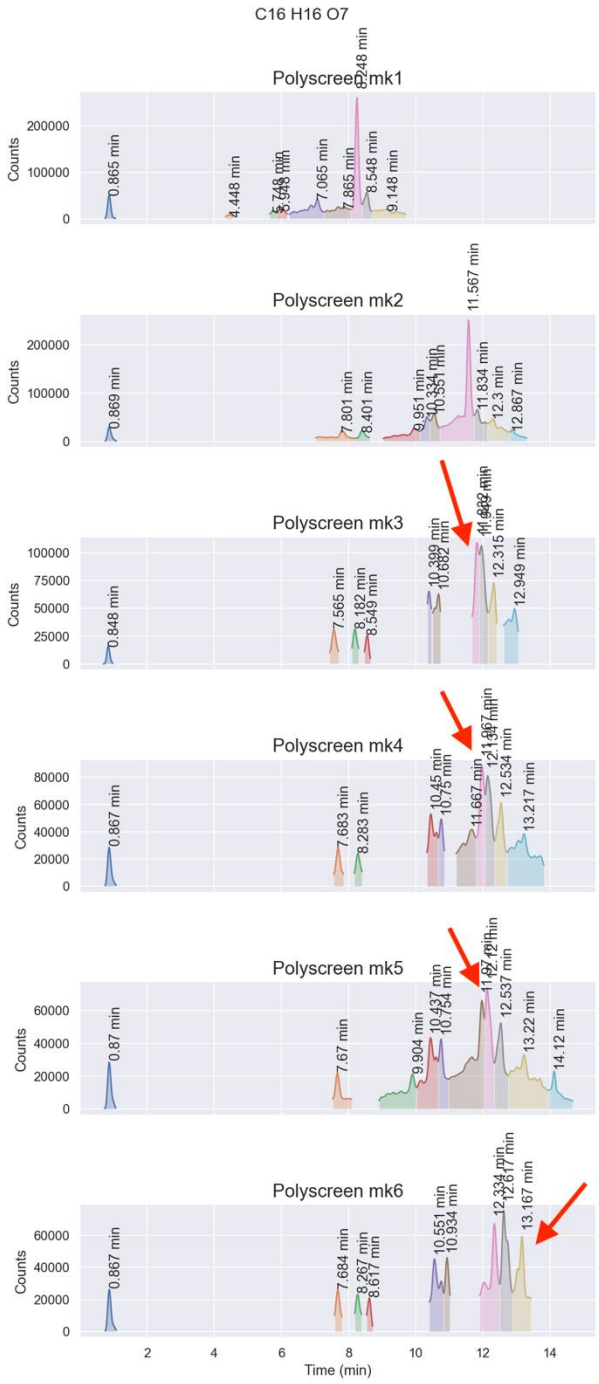
| Extracted ion chromatograph | Comment |
|---|---|
|  | Abundance was low so base to base separation was not achieved. The peak pointed with a red arrow is gradually separated from Polyscreen mk4 to mk5. In Polyscreen mk6, shoulder effect appeared due to over-smoothing of gradient. |

Table F.1 cont.

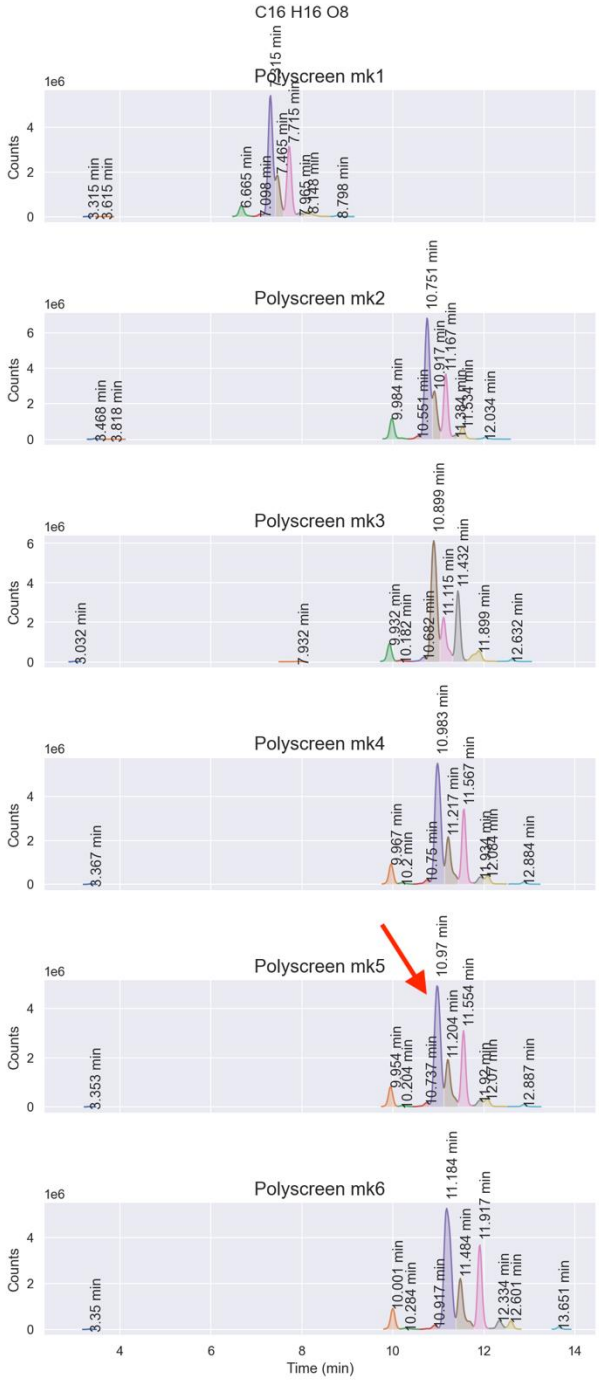
| Extracted ion chromatograph | Comment |
|---|---|
|  | Base to base separation and pointy peaks were achieved for all peaks only on Polyscreen mk5 and Polyscreen mk6. |

Table F.1 cont.

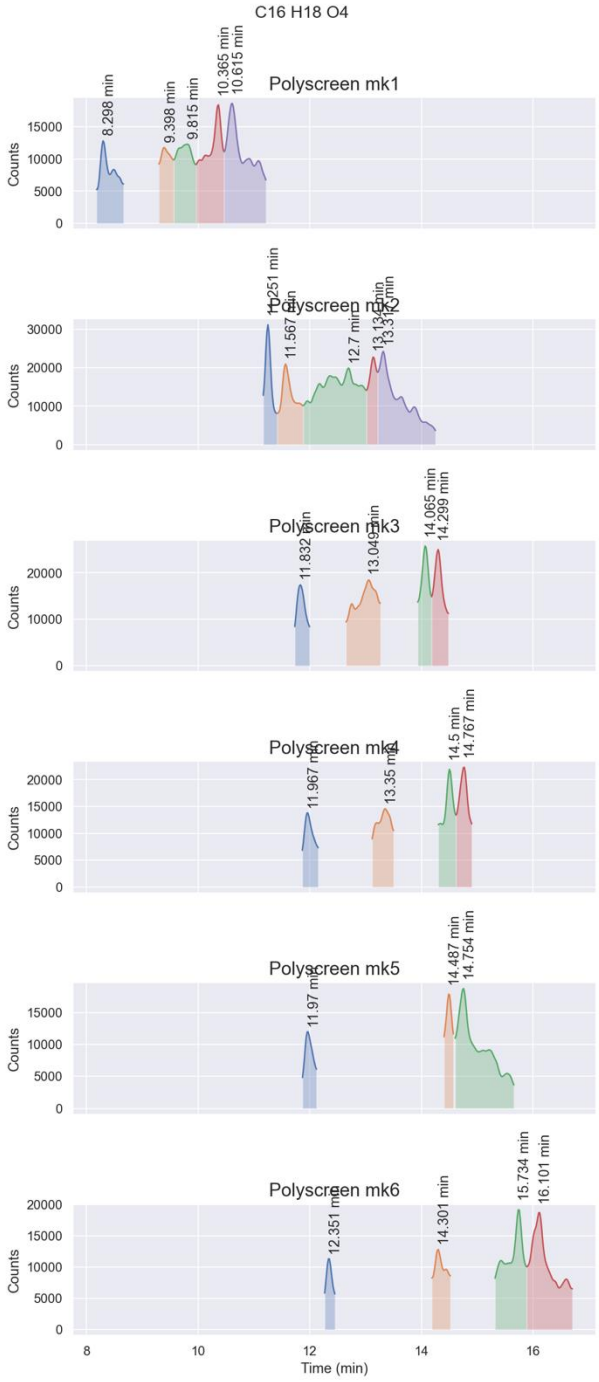
| Extracted ion chromatograph | Comment |
|---|---|
|  | Abundance was low so base to base separation was not achieved. Sharp peaks were achieved only at Polyscreen mk3 and Polyscreen mk4. |

Table F.1 cont.

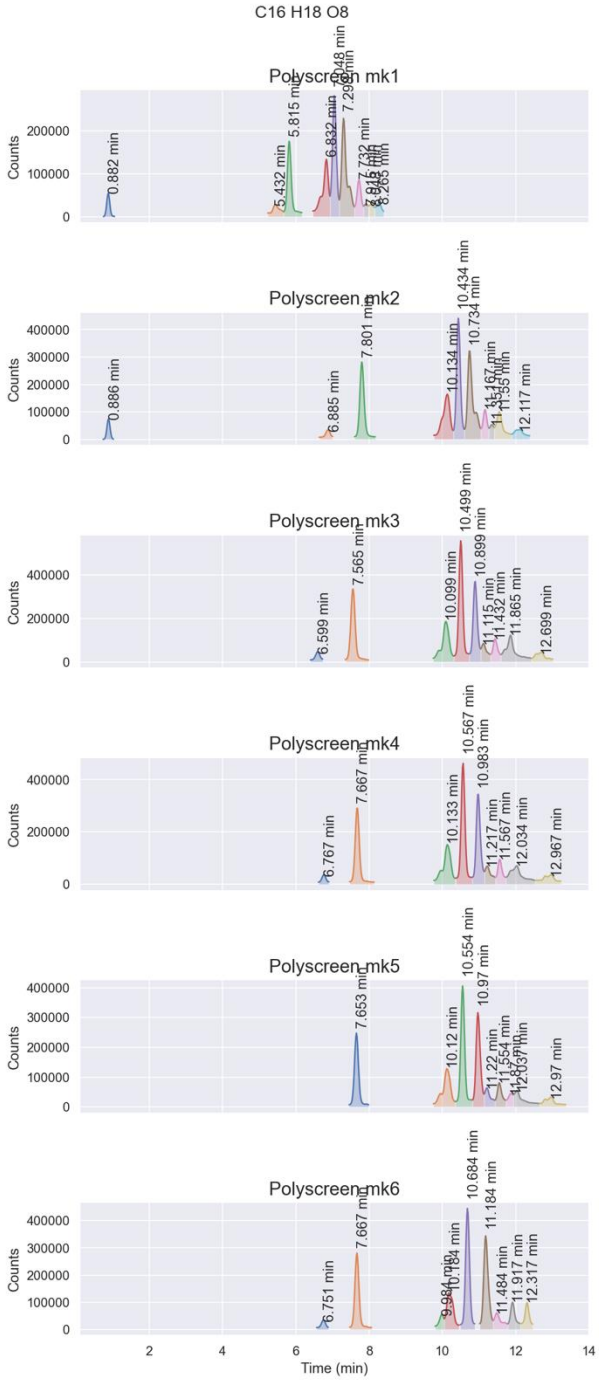
| Extracted ion chromatograph | Comment |
|---|---|
|  | Sharp peaks and base-to-base separation were achieved only after Polyscreen mk3. |

Table F.1 cont.

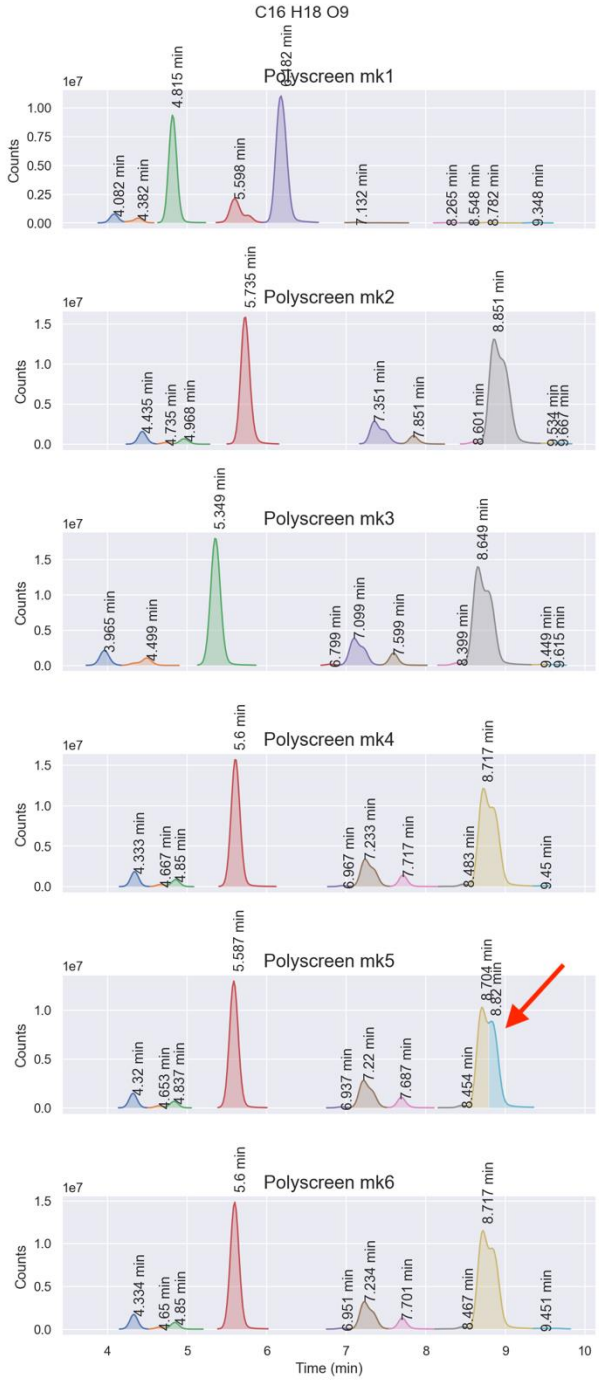
| Extracted ion chromatograph | Comment |
|---|---|
|  | Sharp peaks and base-to-base separation were achieved in every Polyscreen method. However, the peak which is pointed with a red arrow comprises chemical entities eluting at a similar retention time – hence the shouldering of the peak. The two chemical entities are identified only at Polyscreen mk5. |

Table F.1 cont.

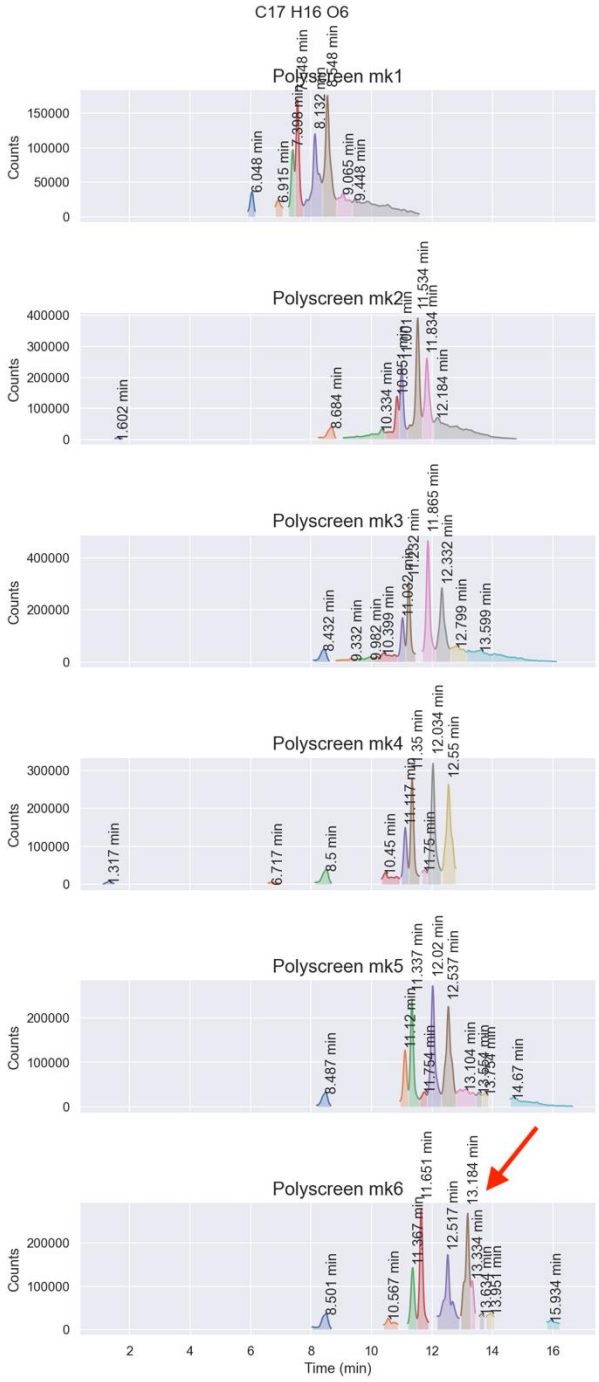
| Extracted ion chromatograph | Comment |
|---|---|
|  | Sharp peaks and base to base to separation were achieved for all peaks only on Polyscreen mk4 and Polyscreen mk5. Shoulder effect on peaks appeared on Polyscreen mk6 (red arrow). |

Table F.1 cont.

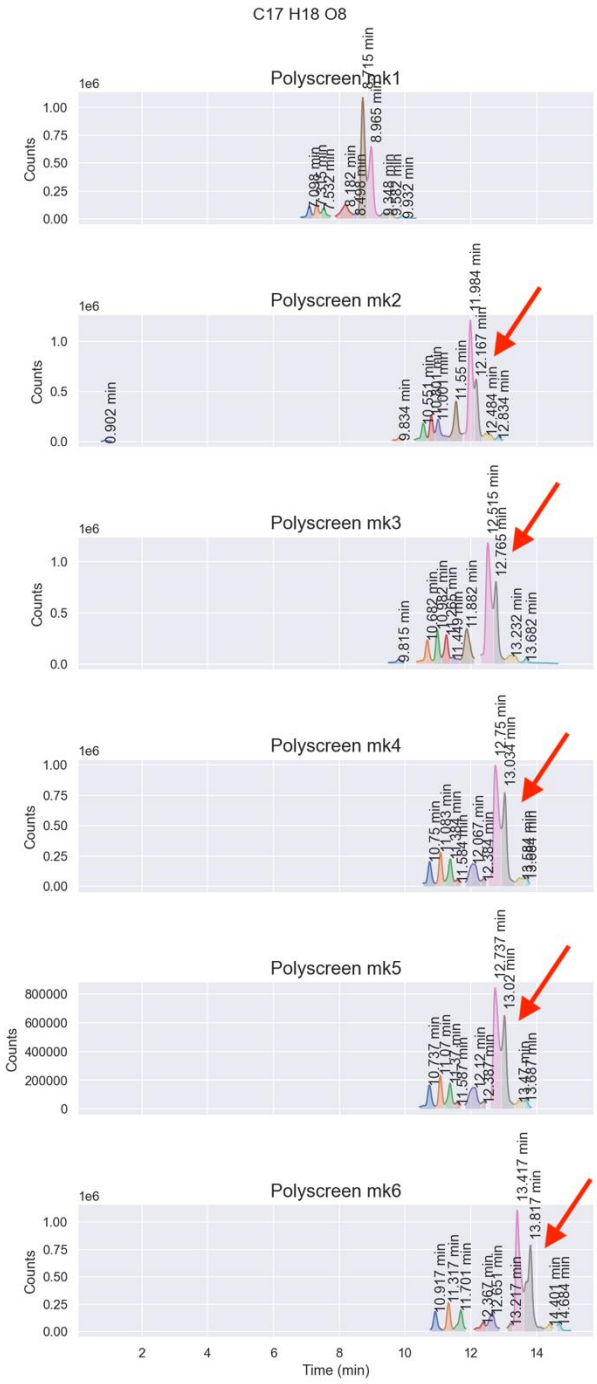
| Extracted ion chromatograph | Comment |
|---|---|
|  | Sharp peaks were achieved on all applied gradients. Base-to-base separation was achieved on all peaks apart from the two peaks that are pointed with a red arrow. The optimal separation without the shouldering effect was achieved on Polyscreen mk4 and Polyscreen mk5. |

Table F.1 cont.

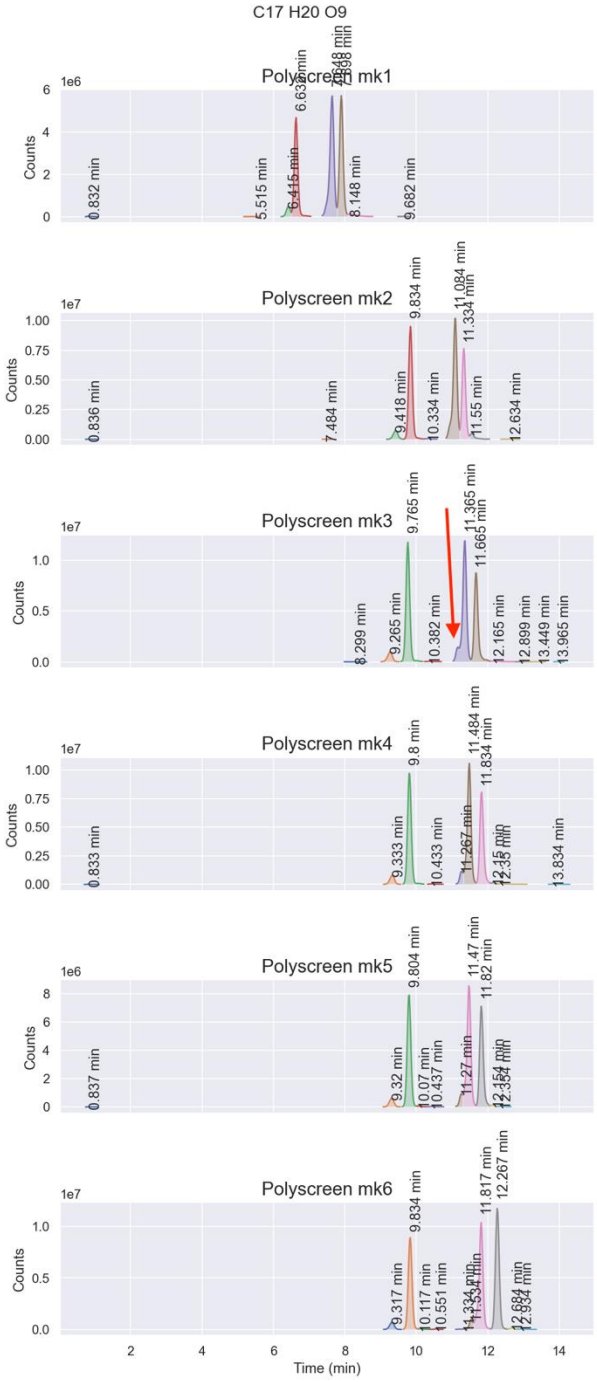
| Extracted ion chromatograph | Comment |
|---|---|
|  | Sharp peaks were achieved on all applied gradients. The shouldering effect appeared at a peak at 11.365 min at Polyscreen mk3 (red arrow). The shouldering effect was resolved only after Polyscreen mk4. |

Table F.1 cont.

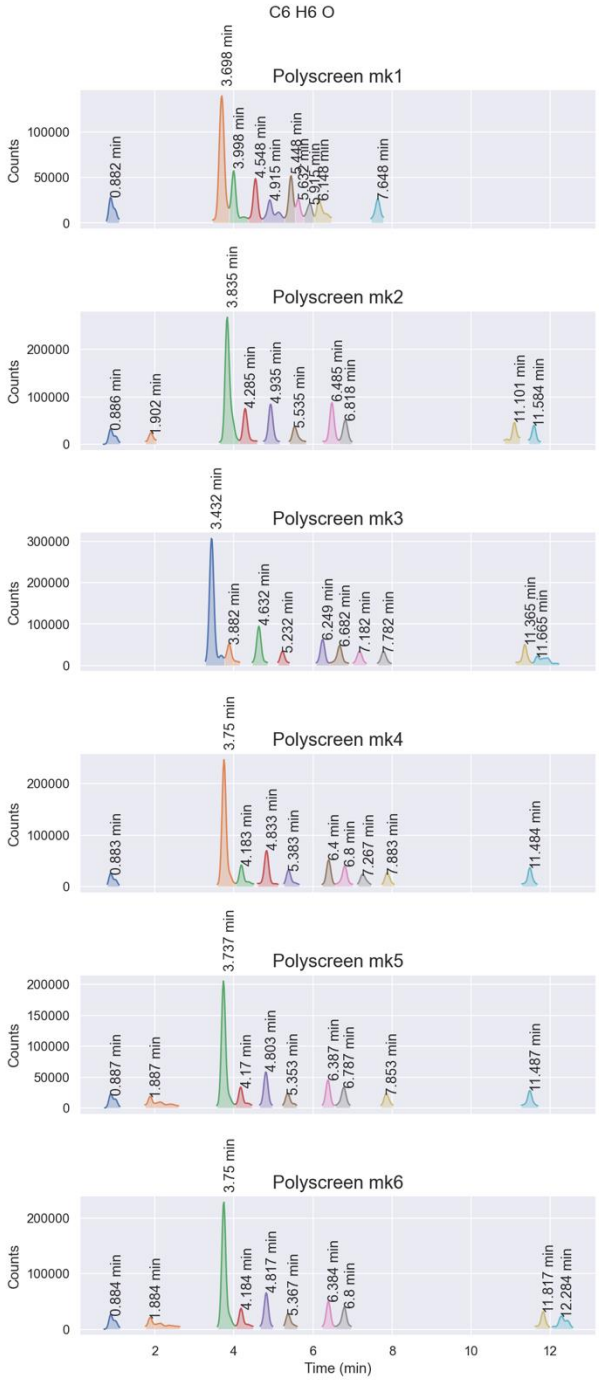
| Extracted ion chromatograph | Comment |
|---|---|
|  | Sharp peaks and base-to-base separation were achieved on all applied gradients. |

Table F.1 cont.

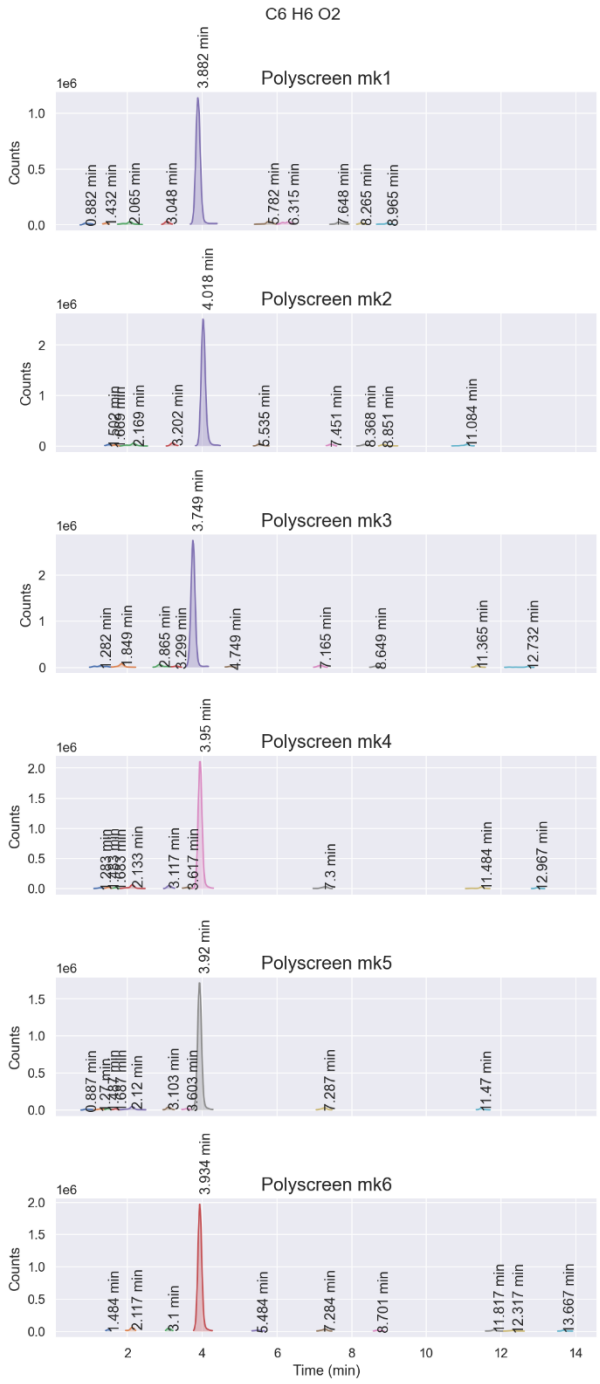
| Extracted ion chromatograph | Comment |
|---|---|
|  | Sharp peak and base-to-base separation were achieved on all applied gradients |

Table F.1 cont.

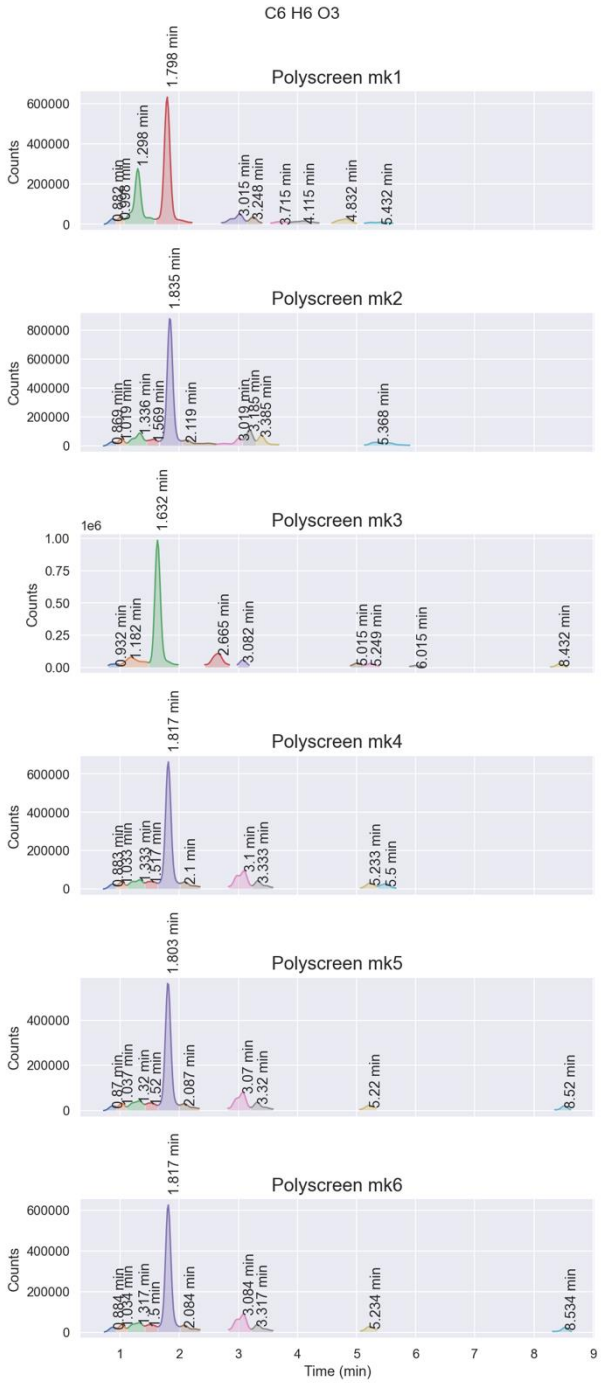
| Extracted ion chromatograph | Comment |
|---|---|
|  | Sharp peak and base-to-base separation were achieved on all applied gradients. |

Table F.1 cont.

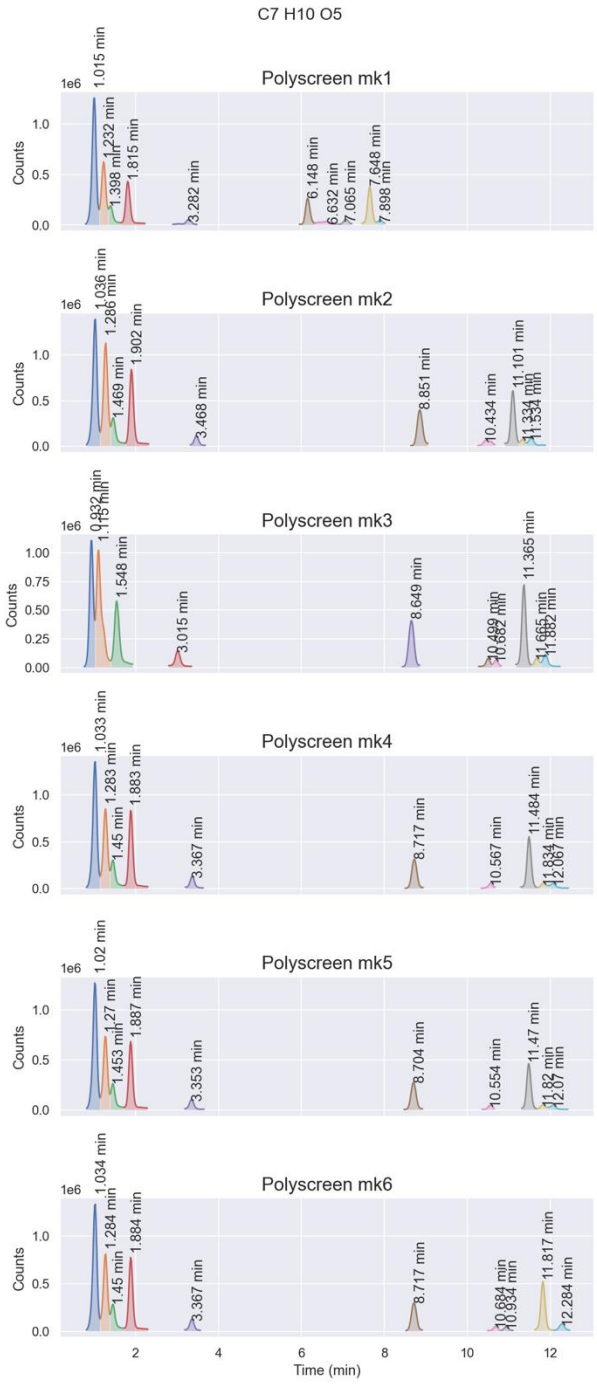
| Extracted ion chromatograph | Comment |
|---|---|
|  | Base-to-base separation and sharp peaks were achieved on all applied gradients. |

Table F.1 cont.

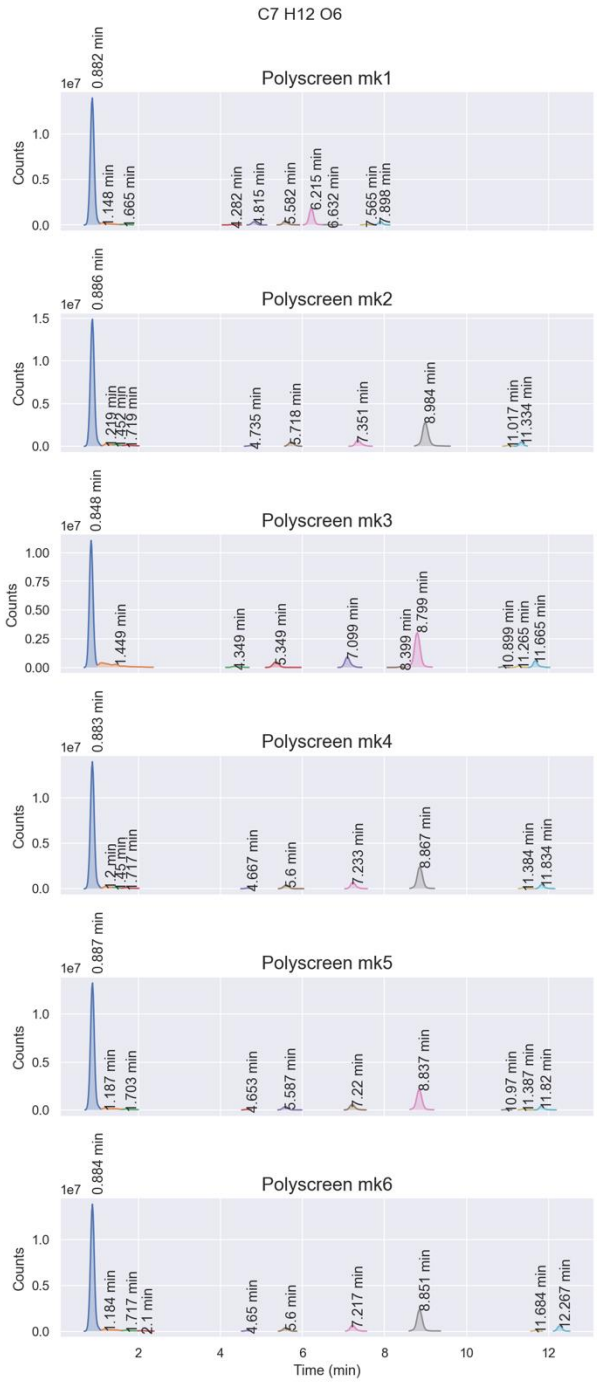
| Extracted ion chromatograph | Comment |
|---|---|
|  | Base-to-base separation and sharp peaks were achieved on all applied gradients. |

Table F.1 cont.

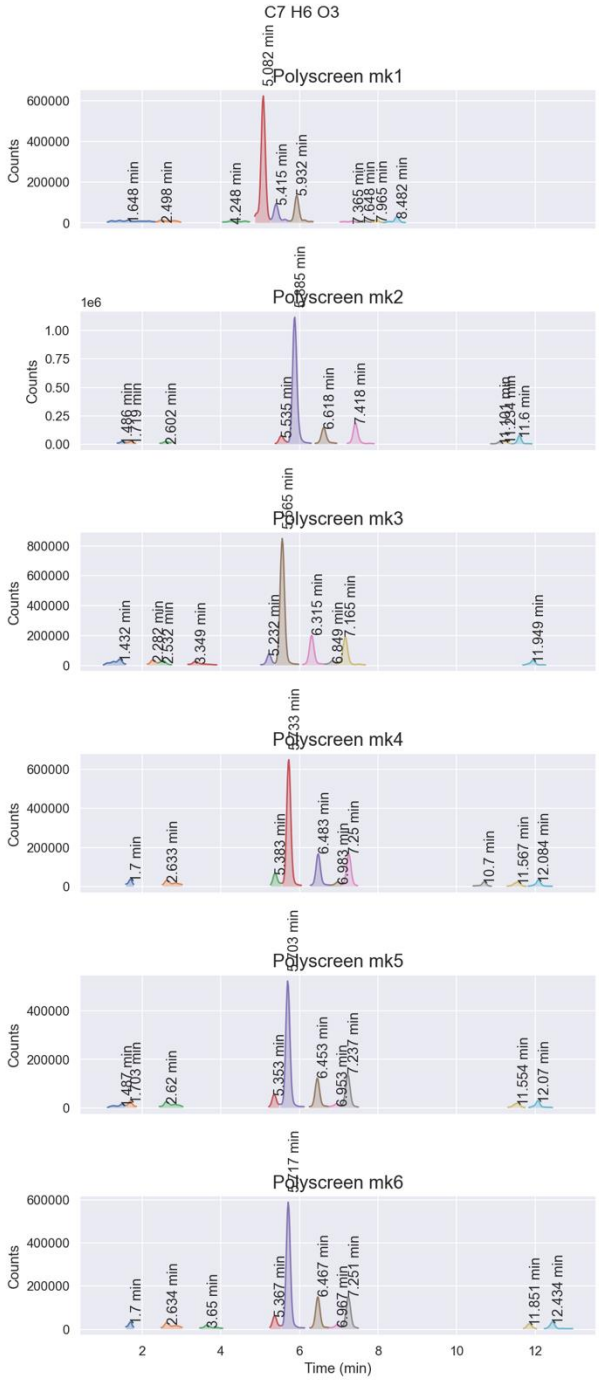
| Extracted ion chromatograph | Comment |
|---|---|
|  | Base-to-base separation and sharp peaks were achieved on all applied gradients. |

Table F.1 cont.

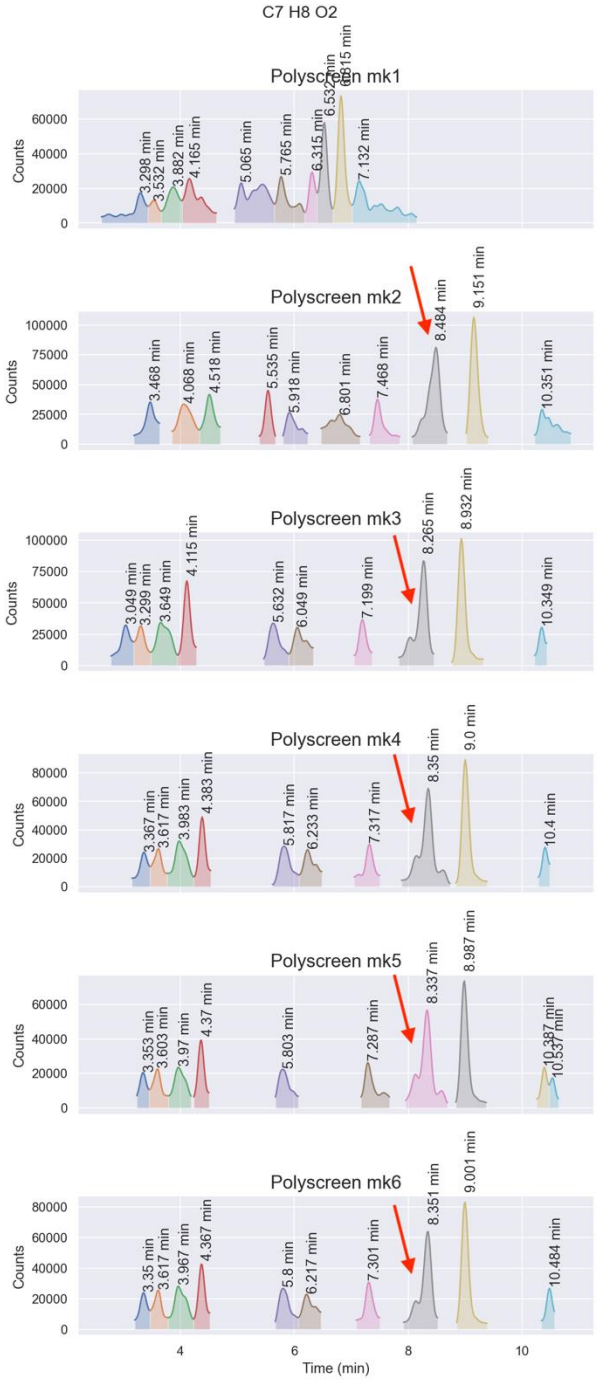
| Extracted ion chromatograph | Comment |
|---|---|
|  | Sharp peaks and base-to-base separation were achieved on all applied gradients apart from Polyscreen mk1. The peak which is pointed with a red arrow appeared the shouldering effect from Polyscreen mk2 to mk6. |

Table F.1 cont.

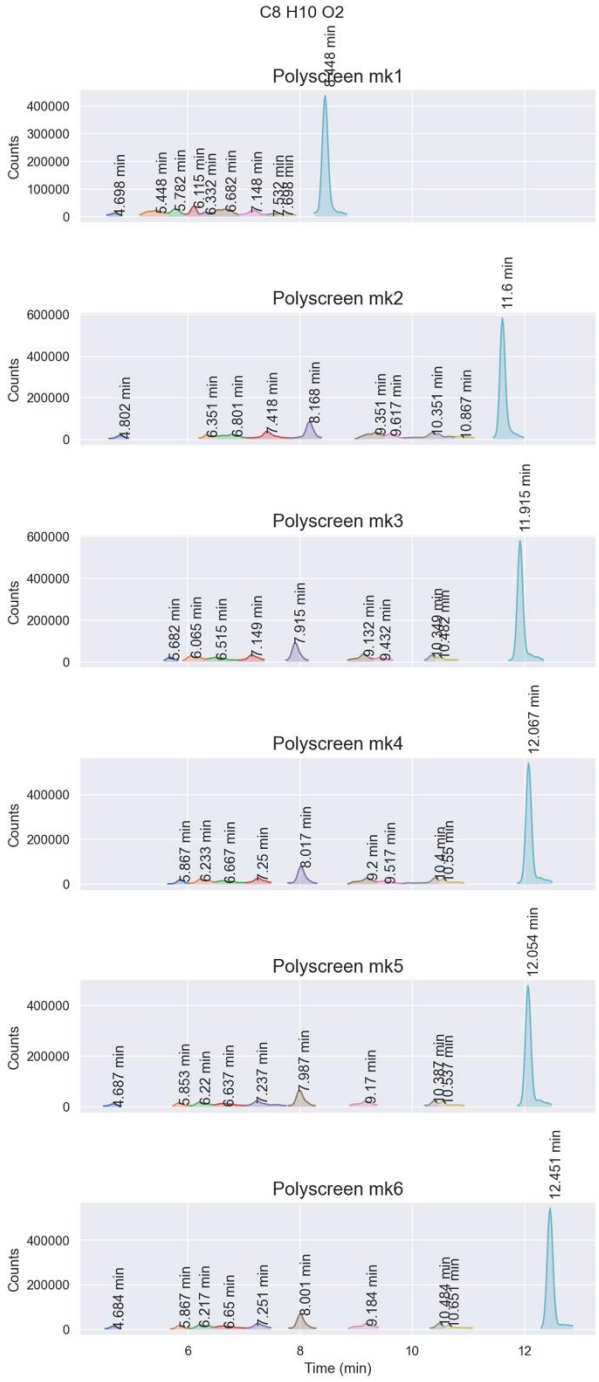
| Extracted ion chromatograph | Comment |
|---|---|
|  | Base-to-base separation and sharp peaks were achieved on all applied gradients. |

Table F.1 cont.

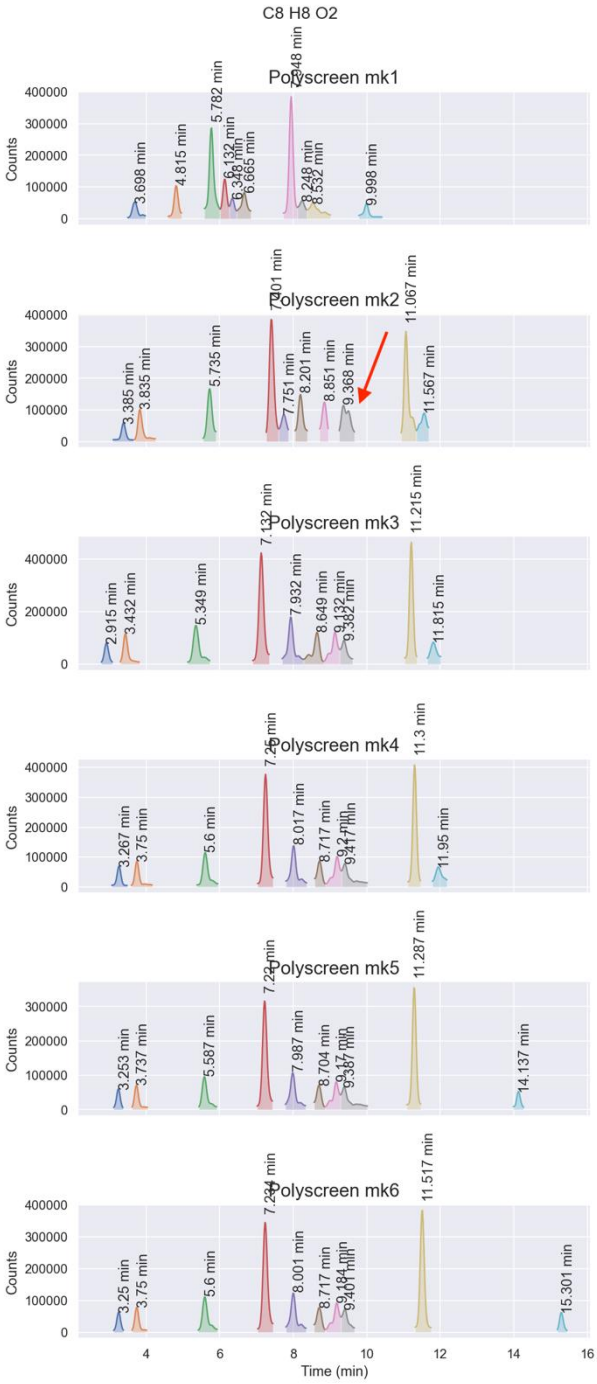
| Extracted ion chromatograph | Comment |
|---|---|
|  | Sharp peaks and base-to-base separation were achieved only after Polyscreen mk3. The peak at 9.368 min at Polyscreen mk2 appeared to consist of two chemical entities with similar retention times. These peaks were separated only after Polyscreen mk3. |

Table F.1 cont.

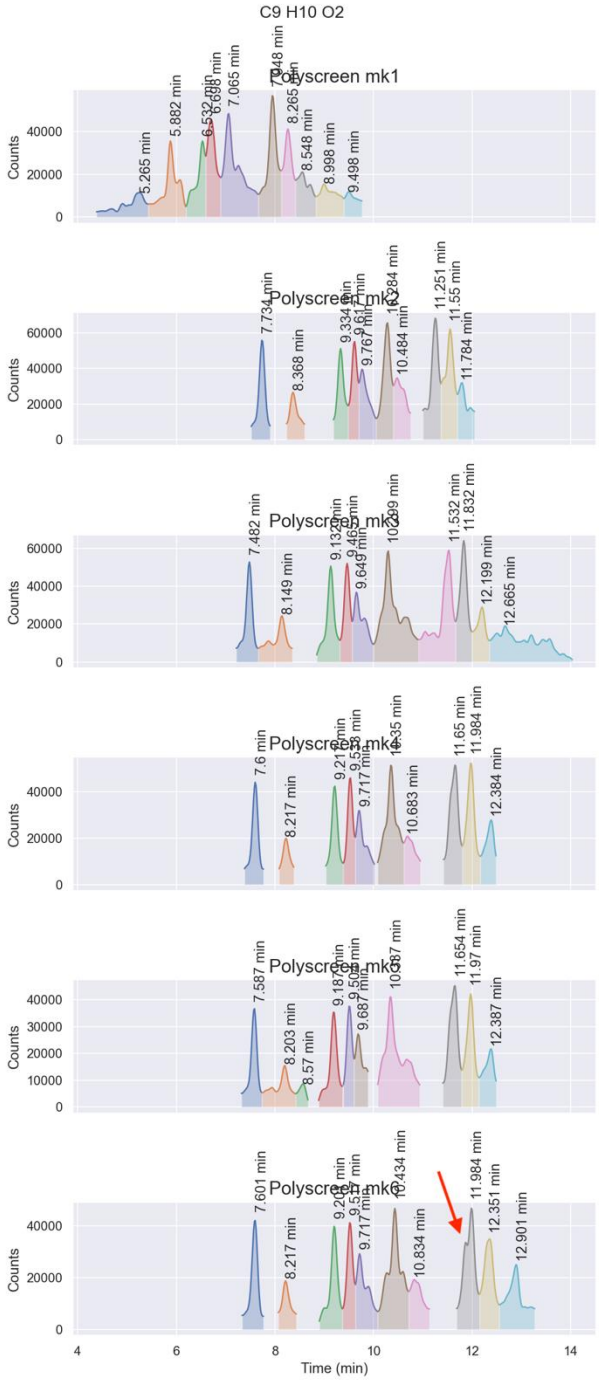
| Extracted ion chromatograph | Comment |
|---|---|
|  | Abundance was low so base to base separation was not achieved. Sharp peaks were achieved only at Polyscreen mk4 and Polyscreen mk5. Shoulder effect appeared at peaks on Polyscreen mk6 (red arrow). |

Table F.1 cont.

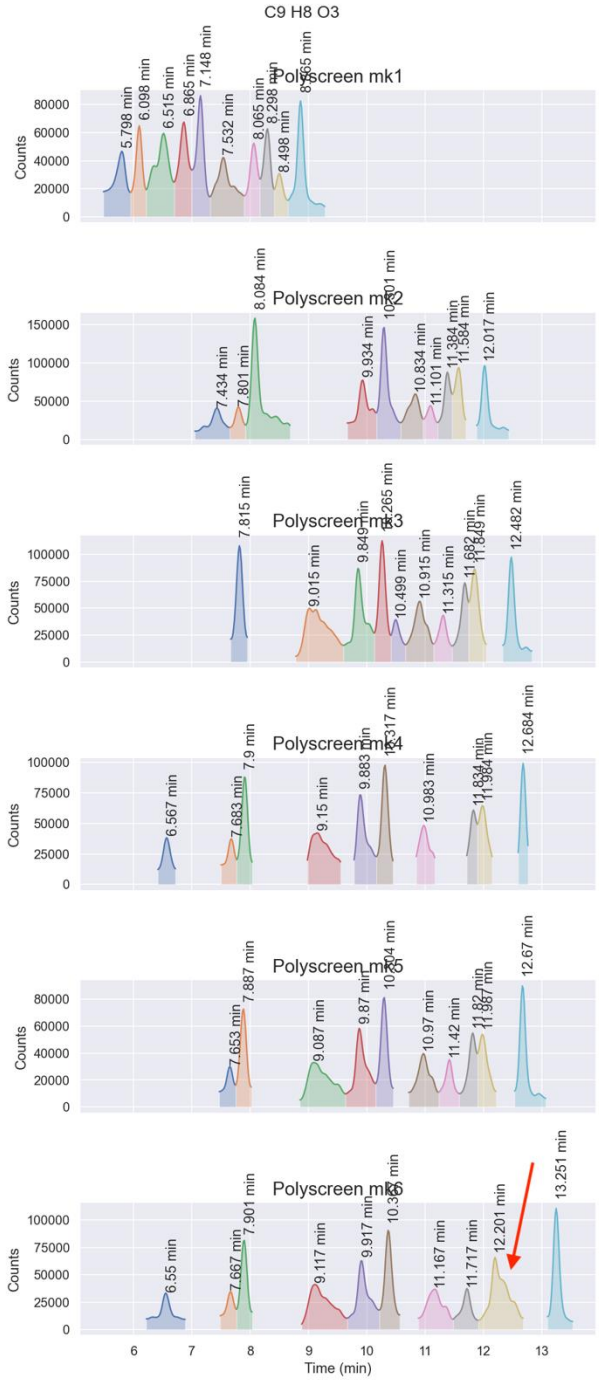
| Extracted ion chromatograph | Comment |
|---|---|
|  | Abundance was low so base to base separation was not achieved. Sharp peaks were achieved only at Polyscreen mk4 and Polyscreen mk5. Shoulder effect appeared at peaks on Polyscreen mk6 (red arrow). |

Table F.1 cont.

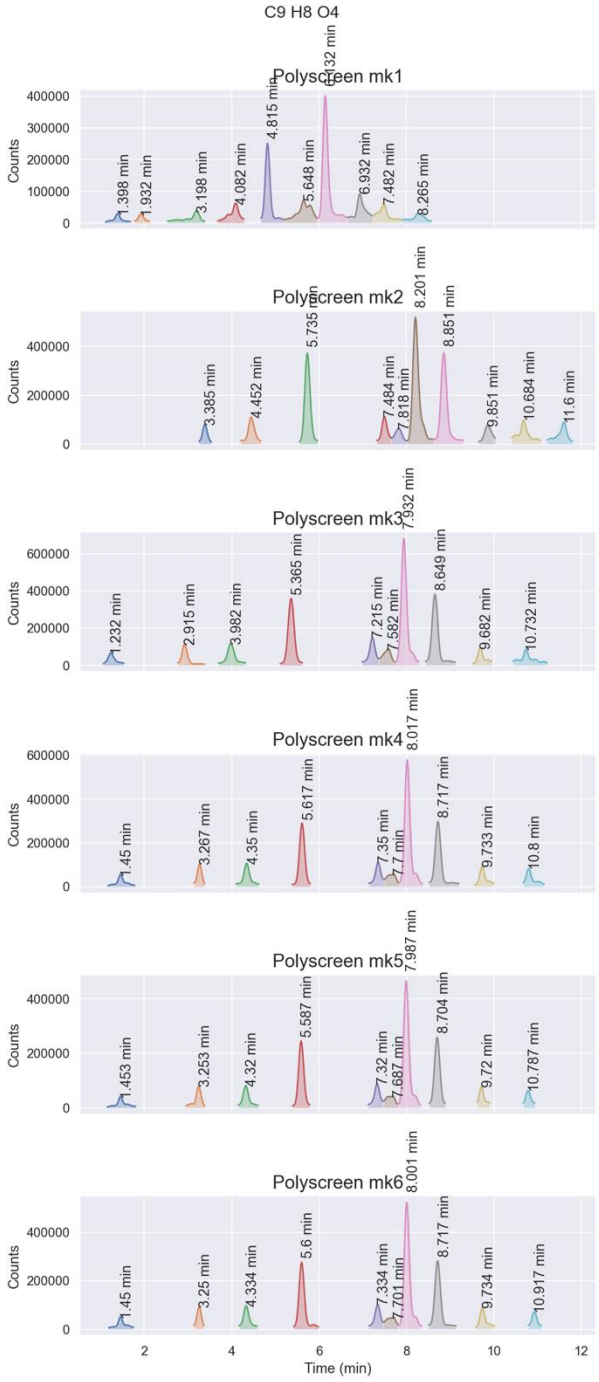
| Extracted ion chromatograph | Comment |
|---|---|
|  | Sharp peaks and base-to-base separation were achieved only after Polyscreen mk2. |

Table F.1 cont.

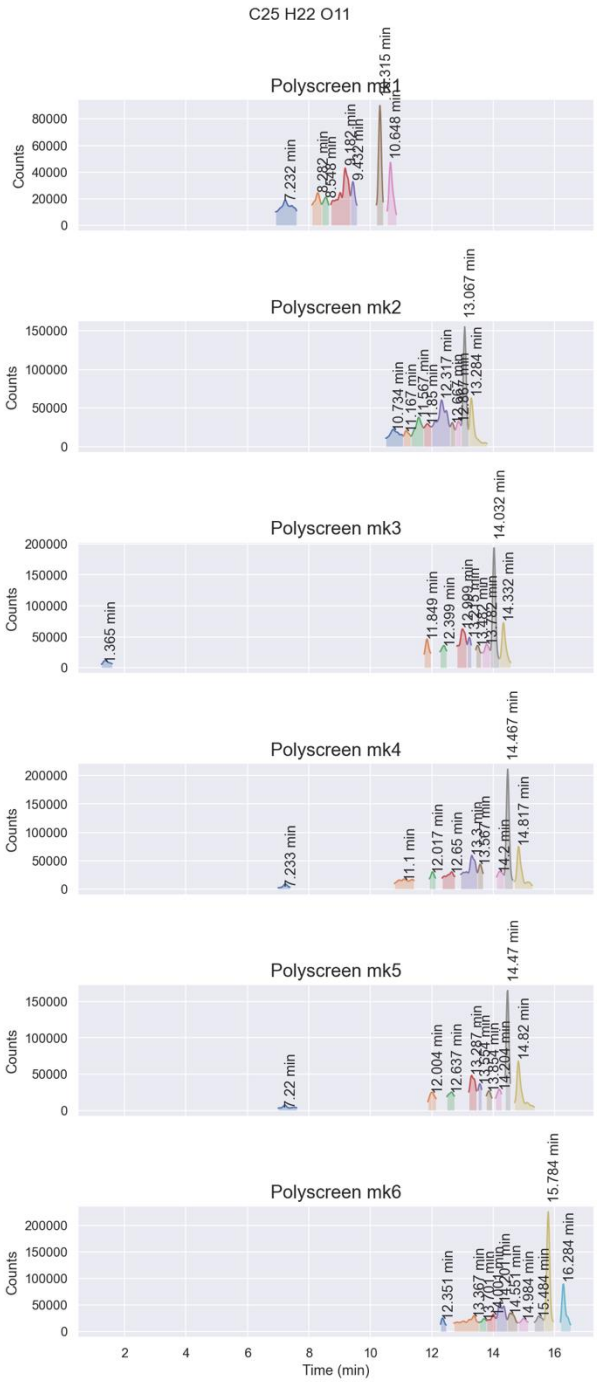
| Extracted ion chromatograph | Comment |
|---|---|
|  | Sharp peaks and base-to-base separation were achieved only after Polyscreen mk3. |

Table F.1 cont.

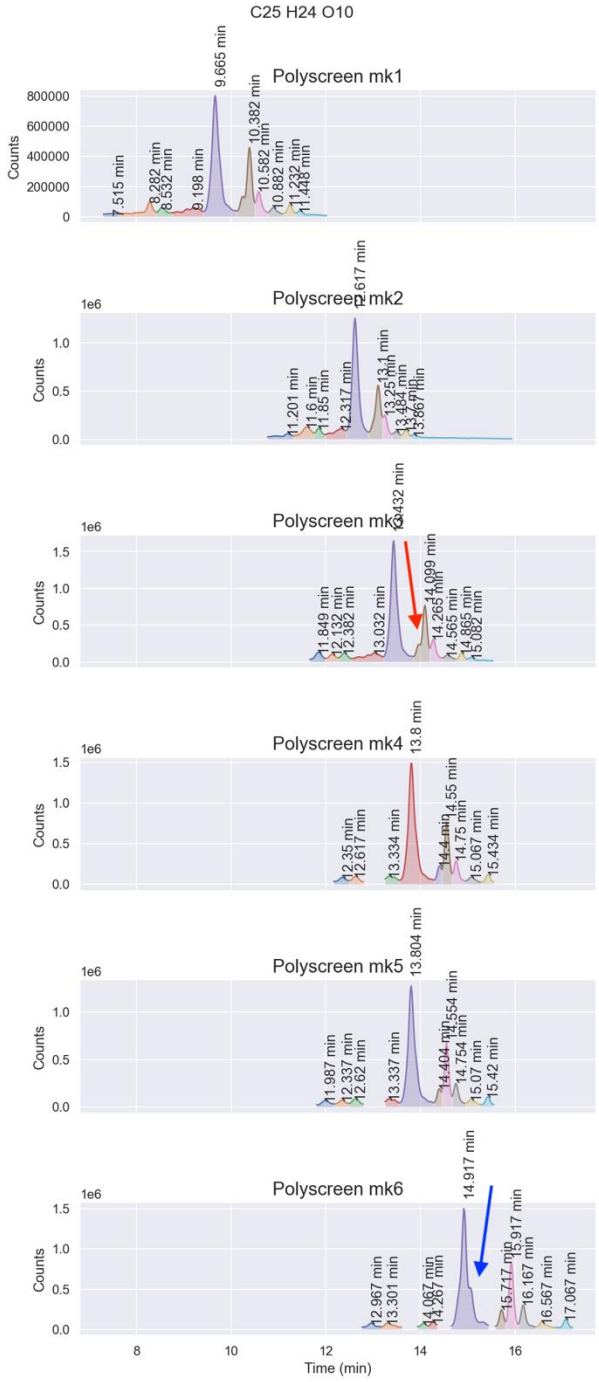
| Extracted ion chromatograph | Comment |
|---|---|
|  | Sharp peaks and base-to-base separation were achieved on all applied gradients.<br><br>Shoulder effect appeared on Polyscreen mk3 (red arrow) but it was resolved at Polyscreen mk4, mk5 and mk6.<br><br>Shoulder effect appeared on Polyscreen mk6 (blue arrow) due to the smoothing of the gradient. |

Table F.1 cont.

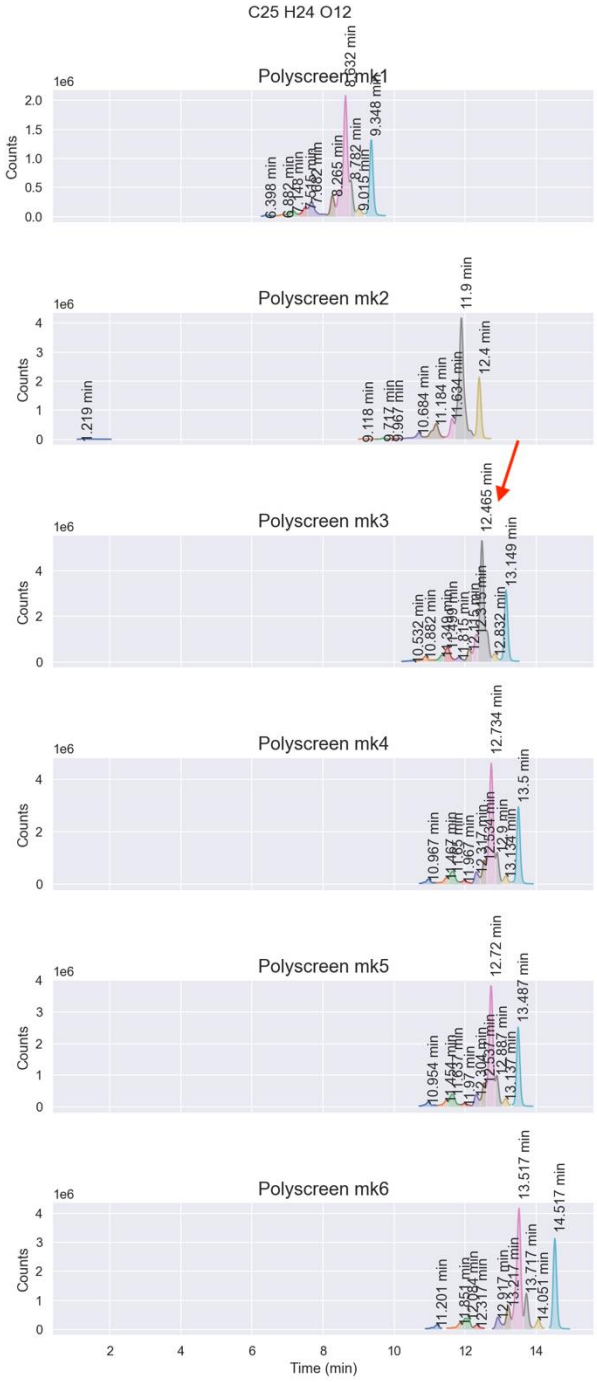
| Extracted ion chromatograph | Comment |
|---|---|
|  | Optimum base-to-base was achieved only after Polyscreen mk4.<br><br>Shoulder effect appeared on Polyscreen mk3, but it was resolved by smoothing the gradient at Polyscreen mk4, mk5 and mk6. |

Table F.1 cont.

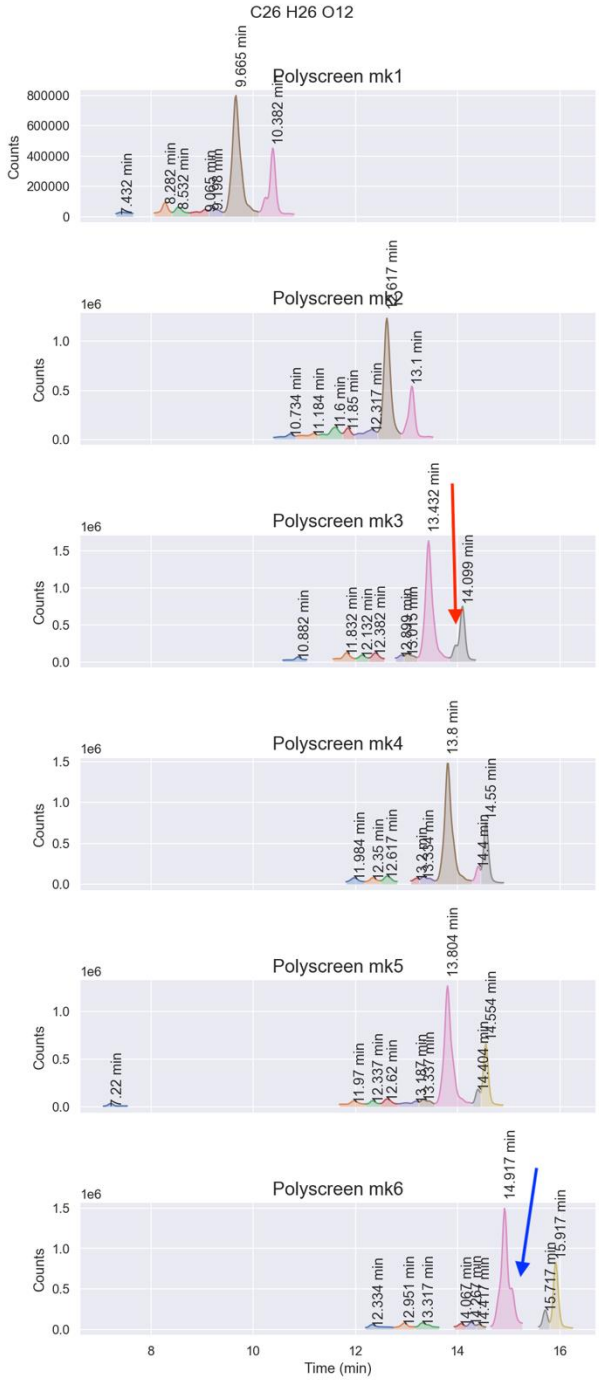
| Extracted ion chromatograph | Comment |
|---|---|
|  | Sharp peaks and base-to-base separation were achieved on all applied gradients.<br><br>Shoulder effect appeared on Polyscreen mk3 (red arrow) but it was resolved at Polyscreen mk4, mk5 and mk6.<br><br>Shoulder effect appeared on Polyscreen mk6 (blue arrow) due to the smoothing of the gradient. |

Table F.1 cont.

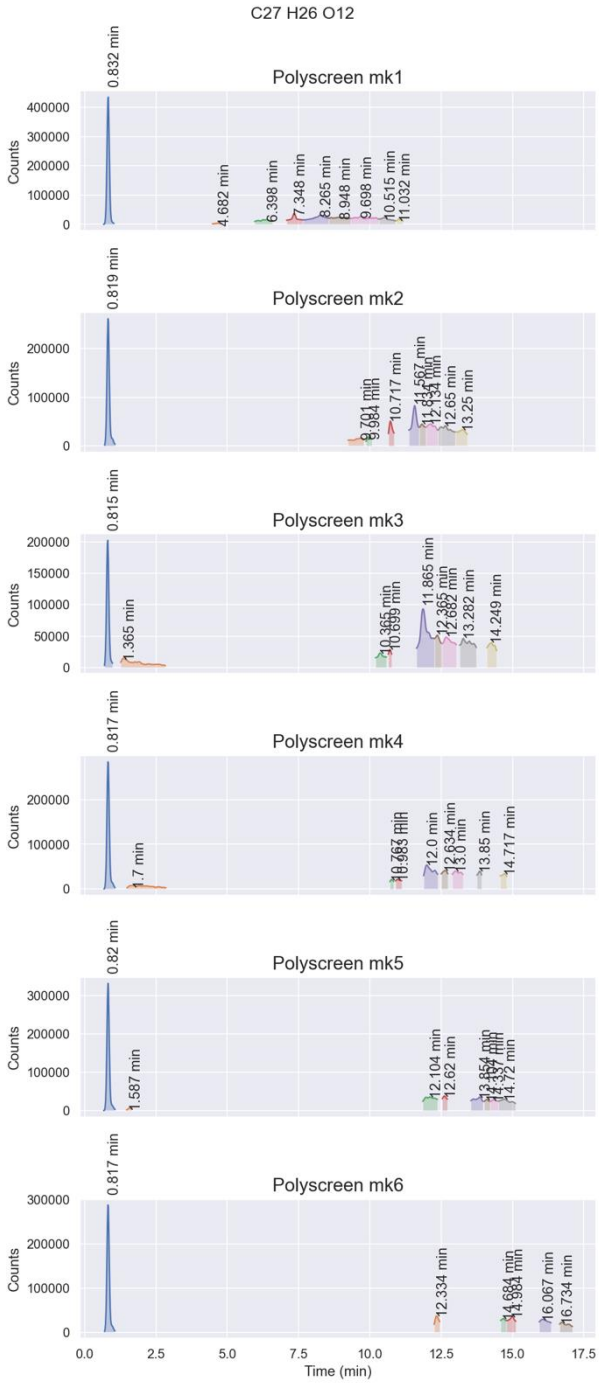
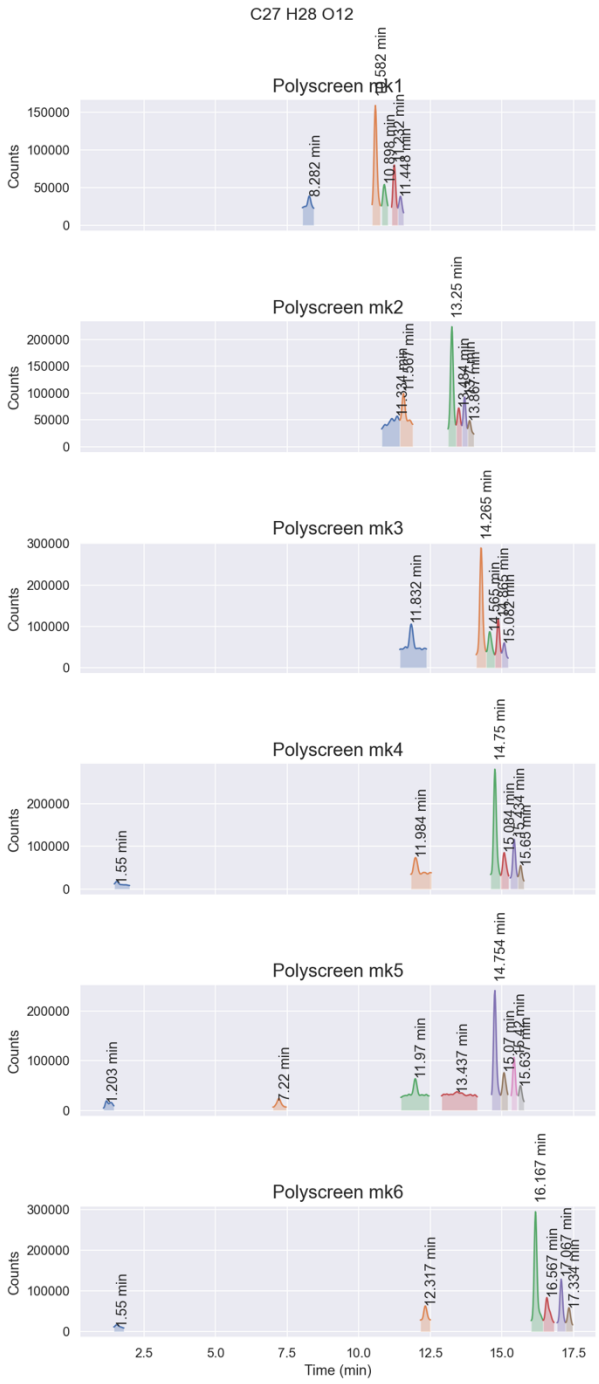
| Extracted ion chromatograph | Comment |
|---|---|
|  | Sharp peaks and base-to-base separation were achieved on all applied gradients. |

Table F.1 cont.

| Extracted ion chromatograph | Comment |
|---|---|
|  | Sharp peaks and base-to-base separation were achieved on all applied gradients. |

# Appendix G: MS2 annotation results of polyphenols

Number of chemical compound and number of chemical formula in each table correspond to numbers in table of Appendix A:.

Table G.1 Ferulic acid - MS2 Results

| Number of chemical compound | Empirical formula | Number of empirical formula | Precursor m/z | Retention time (min) | Annotated name | CSI SCORE | SIRIUS SCORE | Comment |
|---|---|---|---|---|---|---|---|---|
| 1 | C10H10O4 | 1 | 193.050689 | 12.21785 | Ferulate | -196.406 | 33.33 | 100th suggestion |
| | | | 193.0506664 | 11.50117 | Ferulate | -185.646 | 33.33 | 75th suggestion |
| | | | 193.0506956 | 13.11787 | Ferulate | -179.346 | 33.33 | 45th suggestion |
| | | | 193.0507359 | 9.80113 | Ferulate | -121.8 | 33.33 | 7th suggestion |

The peak 193.0507359@9.80113 min with the highest CSI SCORE (-121.8) and the highest SIRIUS SCORE (33.33) was annotated as Ferulic acid. 193.0507359@9.80113 min was in the 7th position at the exported annotated list from SIRIUS software.

Table G.2 ,4 - Dimethoxycinnamic acid : 3,5- Dimethoxycinnamic - MS2 Results

| Number of chemical compound | Empirical formula | Number of empirical formula | Precursor m/z | Retention time (min) | Annotated name | CSI SCORE | SIRIUS SCORE | Comment |
|---|---|---|---|---|---|---|---|---|
| 2 | C11H12O4 | 2 | 207.0663143 | 11.1845 | 2,4-dimethoxycinnamic acid | -227.849 | 33.33 | 79th suggestion |
| | | | 207.0662719 | 8.48443 | N/A | N/A | N/A | |
| | | | 207.0662943 | 9.41778 | N/A | N/A | N/A | No spectra |
| | | | 207.0662681 | 9.66778 | N/A | N/A | N/A | found with |
| | | | 253.0717139 | 10.63448 | N/A | N/A | N/A | MS2 analysis |
| | | | 253.0718695 | 11.4345 | N/A | N/A | N/A | |
| Out of 6 chemical entities, it was feasible to collect only the MS2 spectra of 207.0663143@11.1845. This peak has very low CSI score and it was the 79th suggestion at the exported annotated list from SIRIUS software. This compound was not annotated with high certainty and was not included to the final list of targets. | | | | | | | | |

Table G.3 Roasted caffeic acid products - MS2 Results

| Number of chemical compound | Empirical formula | Number of empirical formula | Precursor m/z | Retention time (min) | Annotated name | CSI SCORE | SIRIUS SCORE | Comment |
|---|---|---|---|---|---|---|---|---|
| 3-7 | C16H16O4 | 3 | 317.1032279 | 12.86787 | 1-(2,3-dihydroxyphenyl)-3-methyl-2,3-dihydro-1H-indene-5,6-diol | -189.309 | 33.33 | 11th suggestion |
| | | | 271.097597 | 13.71788 | | -175.055 | 33.33 | 3rd suggestion |
| | | | 271.097653 | 14.45123 | | -171.882 | 33.33 | 2nd suggestion |

5 chemical entities had the same empirical formula (C16H16O4). It was feasible to collect the spectra of only 3 chemical entities. 2 chemical entities had the highest CSI score and were 2nd and 3rd suggestion of the exported annotated list from SIRIUS software. Therefore the 271.097653@14.45123 was annotated as Roasted Caffeic Acid product alpha and the 217.097597@13.71788 was annotated as Roasted Caffeic Acid product beta.

Table G.4 p-Coumaroylquinic acid lactone - MS2 Results

| Number of chemical compound | Empirical formula | Number of empirical formula | Precursor m/z | Retention time (min) | Annotated name | CSI SCORE | SIRIUS SCORE | Comment |
|---|---|---|---|---|---|---|---|---|
| | | | 379.1057478 | 0.86763 | [(1R,3S,4S,5S)-3,4-dihydroxy-7-oxo-6-oxabicyclo[3.2.1]octan-1-yl] (E)-3-(4-hydroxyphenyl)prop-2-enoate | -310.519 | 49.9 | 85th suggestion |
| 8-10 | C16H16O7 | 4 | 379.1034597 | 10.75115 | 4-p-Coumaroyl-1,5-quinolactone | -236.445 | 49.9 | 3rd suggestion |
| | | | 319.082296 | 12.53452 | 4-p-Coumaroyl-1,5-quinolactone | -220.521 | 50.1 | 3rd suggestion |
| | | | 319.0823479 | 12.13452 | 4-p-Coumaroyl-1,5-quinolactone | -212.587 | 50.1 | 4th suggestion |
| | | | 319.08 | 12.09 | 4-p-Coumaroyl-1,5-quinolactone | -199.891 | 50.1 | 4th suggestion |

319.08@12.09 had the highest CSI score and it was the 4th suggestion at the exported annotated list from SIRIUS software. Therefore, it was annotated as p-Coumaroylquinic acid lactone. The rest compounds were not annotated as the score of annotation was low.

Table G.5 Caffeoyl quinic acid lactone - MS2 results

| Number of chemical compound | Empirical formula | Number of empirical formula | Precursor m/z | Retention time (min) | Annotated name | CSI SCORE | SIRIUS SCORE | Comment |
|---|---|---|---|---|---|---|---|---|
| 11-13 | C16H16O8 | 5 | 395.0983638 | 10.73448 | 3-O-caffeoyl-epi-delta-quinide | -235.833 | 13.7 | 9th suggestion |
| | | | 395.0981924 | 12.88453 | 4-Caffeoylquinolactone | -173.855 | 65.3 | 5th suggestion |
| | | | 335.0774447 | 11.55117 | 3-O-caffeoyl-epi-delta-quinide | -170.751 | 65.3 | 8th suggestion |
| | | | 335.0774586 | 10.98171 | 3-O-caffeoyl-epi-delta-quinide | -182.862 | 13.7 | 9th suggestion |
| | | | 335.0773002 | 11.91783 | 3-O-caffeoyl-epi-delta-quinide | -124.493 | 65.3 | 1st suggestion |

335.0773002@11.91783 and 395.0981926@12.88453 had the highest CSI SCORE and SIRIUS score, while their position on the exported list from SIRIUS was 5th and 1st. So, these chemical entities were annotated as CQL alpha and CQL beta respectively. The rest compounds were not annotated as the score of annotation was low.

Table G.6 p-Coumaroylquinic acid - MS2 Results

| Number of chemical compound | Empirical formula | Number of empirical formula | Precursor m/z | Retention time (min) | Annotated name | CSI SCORE | SIRIUS SCORE | Comment |
|---|---|---|---|---|---|---|---|---|
| 15-17 | C16H18O8 | 7 | 337.092807 | 12.96787 | 4-p-coumaroylquinic acid | -263.947 | 50 | 39th suggestion |
| | | | 337.0929508 | 7.65108 | 2-p-CoQA | -96.822 | 50 | 1st suggestion |
| | | | 337.09294 | 10.55115 | 4-p-CoQA | -85.57 | 50 | 1st suggestion |
| | | | 337.0918588 | 10.96783 | 2-p-CoQA | -72.996 | 50 | 1st suggestion |

The aim was to annotate 3 p-Coumaroylquinic acids. The MS2 spectra of 4 chemical entities were collected through MS2 analysis. 3 chemical entities were annotated as p-Coumaroylquinic acid with high CSI and SIRIUS score while these were the top suggestion of exported list from SIRIUS. Therefore the 337.091858@10.96783 , 337.0929508@7.65108 and 337.09294@10.55115 were annotated as p-Coumaroylquinic acid alpha, beta and gamma respectively.

Table G.7 Caffeoylquinic acid - MS2 Results

| Number of chemical compound | Empirical formula | Number of empirical formula | Precursor m/z | Retention time (min) | Annotated name | CSI SCORE | SIRIUS SCORE | Comment |
|---|---|---|---|---|---|---|---|---|
| 18-20 | C16H18O9 | 8 | 353.087846 | 4.65103 | 3-CQA | -79.217 | 100 | 1st suggestion |
| | | | 353.0882135 | 5.58438 | 3-CQA | -69.152 | 100 | 1st suggestion |
| | | | 353.0878652 | 4.83437 | 4-CQA | -62.652 | 100 | 1st suggestion |
| | | | 353.0879161 | 7.21775 | 3-CQA | -57.08 | 100 | 1st suggestion |
| | | | 353.0879971 | 4.3177 | 4-CQA | -53.431 | 100 | 1st suggestion |
| | | | 353.0881851 | 8.81778 | 3-CQA | -50.774 | 100 | 3-CQA identified with Chemical Reference Standard |
| | | | 353.0878764 | 8.45112 | 4-CQA | -46.79 | 100 | 1st suggestion |

The aim was to annotate 3 Caffeoylquinic acids.The MS2 spectra of 7 chemical entities were collected through MS2 analysis. 353.0881851@8.81778 was identified as the 3-Caffeoylquinic acid with a chemical reference standard. The rest 2 chemical entities which had the highest CSI and SIRIUS score were annotated as Caffeoylquinic acids. Therefore, 353.0878764@8.45112 and 353.0879971@4.3177 were annotated as Caffeoylquinic acid beta and gamma respectively.

Table G.8 Roasted caffeic acid product - MS2 Results

| Number of chemical compound | Empirical formula | Number of empirical formula | Precursor m/z | Retention time (min) | Annotated name | CSI SCORE | SIRIUS SCORE | Comment |
|---|---|---|---|---|---|---|---|---|
| 21 | C17H16O6 | 9 | 315.0875144 | 12.03452 | 1-(3,4-dihydroxyphenyl)-5,6-dihydroxy-3-methyl-2,3-dihydro-1H-indene-2-carboxylic acid | -255.406 | 0.01 | 19th suggestion |
| | | | 315.0873887 | 11.11783 | 1-(3,4-dihydroxyphenyl)-5,6-dihydroxy-3-methyl-2,3-dihydro-1H-indene-2-carboxylic acid | -212.817 | 0.01 | 6th suggestion |
| None of compounds were annotated with high certainty as ,6-Dihydroxy-2-carboxy-1-methyl-3-(3'-4'-dihydroxyphenyl) indane. Therefore, none of these was included at the final list of targets. | | | | | | | | |

Table G.9 Feruloylquinic acid lactone - MS2 Results

| Number of chemical compound | Empirical formula | Number of empirical formula | Precursor m/z | Retention time (min) | Annotated name | CSI SCORE | SIRIUS SCORE | Comment |
|---|---|---|---|---|---|---|---|---|
| 22-24 | C17H18O8 | 10 | 349.0928886 | 13.68455 | 3beta,4beta,5alpha-Trihydroxy-1-[[3-(3-methoxy-4-hydroxyphenyl)acryloyl]oxy]cyclohexane-1alpha-carboxylic acid 1,4-lactone | -227.877 | 0 | 4th suggestion |
| | | | 349.0927144 | 13.46787 | 4-Feruloyl-1,5-quinolactone | -225.855 | 23 | 4th suggestion |
| | | | 349.0929566 | 12.73452 | 3beta,4beta,5alpha-Trihydroxy-1-[[3-(3-methoxy-4-hydroxyphenyl)acryloyl]oxy]cyclohexane-1alpha-carboxylic acid 1,4-lactone | -178.782 | 91 | 3rd suggestion |
| | | | 273.1130764 | 14.48455 | 4-Feruloyl-1,5-quinolactone | -193.583 | 90 | 9th suggestion |

The aim was to annotate 3 Feruloylquinic acid lactones. The MS2 spectra of 4 chemical entities were collected through MS2 analysis. 349.0929566@12.73452 acquired the highest score of annotation. Therefore, this compound was annotated as Feruloylquinic acid lactone alpha. The rest chemical entities acquired low score, thus were not included at the final list of targets.

Table G.10 Feruloylquinic acid - MS2 Results

| Number of chemical compound | Empirical formula | Number of empirical formula | Precursor m/z | Retention time (min) | Annotated name | CSI SCORE | SIRIUS SCORE | Comment |
|---|---|---|---|---|---|---|---|---|
| 25-27 | C17H20O9 | 11 | 367.1054879 | 0.83428 | 3-FQA | -178.346 | 0 | 3rd suggestion |
| | | | 367.1031981 | 10.43448 | 3-FQA | -171.361 | 0 | 7th suggestion |
| | | | 367.1033796 | 12.35118 | 3FQA | -131.08 | 90 | 5th suggestion |
| | | | 367.1033704 | 12.15118 | 3-FQA | -121.755 | 80 | 7th suggestion |
| | | | 367.1039208 | 11.81783 | 3-FQA | -79.632 | 85 | 4th suggestion |
| | | | 367.1037512 | 11.4845 | 3-FQA | -76.59 | 99 | 3rd suggestion |
| | | | 367.1035811 | 11.26783 | 3-FQA | -173.518 | 0 | 9th suggestion |
| | | | 367.1035922 | 9.31778 | 3-FQA | -67.093 | 99 | 1st suggestion |

The aim was to annotate 3 Feruloylquinic acids. The MS2 spectra of 8 chemical entities were collected through MS2 analysis. 367.1035922@9.31778 and 367.1037512@11.4845 acquired the highest score of annotation. Therefore, these compounds were annotated as Feruloylquinic acids alpha and beta respectively. The rest chemical entities acquired low score, thus were not included at the final list of targets.

Table G.11 Phenol - MS2 Results

| Number of chemical compound | Empirical formula | Number of empirical formula | Precursor m/z | Retention time (min) | Annotated name | CSI SCORE | SIRIUS SCORE | Comment |
|---|---|---|---|---|---|---|---|---|
| 28 | C6H6O | 12 | 139.0401014 | 6.78442 | phenol | -36.153 | 100 | 1st suggestion |
| | | | 139.0401132 | 6.3844 | benzenod | -35.441 | 100 | 1st suggestion |
| | | | 153.0558182 | 4.16768 | phenol | -34.356 | 100 | 1st suggestion |
| | | | 139.0401652 | 7.8511 | phenol | -33.986 | 100 | 1st suggestion |
| | | | 139.0400804 | 4.8177 | benzenod | -26.033 | 100 | 1st suggestion |
| | | | 93.0345145 | 11.4845 | benzenod | -20.774 | 100 | 1st suggestion |
| | | | 93.034948 | 0.8843 | benzenod | -19.951 | 100 | 1st suggestion |

The aim was to annotate the phenol. MS2 spectra of 7 chemical entities were acquired and all of them were annotated as Phenol. The highest score of annotation was acquired by the 93.034948@0.8843.

Table G.12 Catechol - MS2 Results

| Number of chemical compound | Empirical formula | Number of empirical formula | Precursor m/z | Retention time (min) | Annotated name | CSI SCORE | SIRIUS SCORE | Comment |
|---|---|---|---|---|---|---|---|---|
| 29 | C6H6O2 | 13 | 155.0349837 | 1.68432 | catechol | -107.049 | 100 | 4th suggestion |
| | | | 169.0507231 | 3.60102 | catechol | -87.781 | 100 | 1st suggestion |
| | | | 109.0294999 | 3.10102 | catechol | -30.325 | 100 | 1st suggestion |
| | | | 109.0294667 | 12.96787 | catechol | -25.576 | 100 | 1st suggestion |

The aim was to annotate the catechol. MS2 spectra of 4 chemical entities were acquired and all of them were annotated as catechol. The highest score of annotation was acquired by the 109.0294667@12.96787.

Table G.13 Pyrogallol - MS2 Results

| Number of chemical compound | Empirical formula | Number of empirical formula | Precursor m/z | Retention time (min) | Annotated name | CSI SCORE | SIRIUS SCORE | Comment |
|---|---|---|---|---|---|---|---|---|
| 30 | C6H6O3 | 14 | 125.0244432 | 8.51778 | pyrogallol | -155.087 | 95 | 42nd suggestion |
| | | | 185.0456104 | 5.21772 | pyrogallol | -151.141 | 95 | 43rd suggestion |
| | | | 125.0244411 | 3.31767 | pyrogallol | -112.843 | 100 | 5th suggestion |

The aim was to annotate the pyrogallol. MS2 spectra of 3 chemical entities were acquired and all of them were annotated as pyrogallol. The highest score of annotation was acquired by the 125.024441@3.31767.

Table G.14 Quinic acid lactone - MS2 Results

| Number of chemical compound | Empirical formula | Number of empirical formula | Precursor m/z | Retention time (min) | Annotated name | CSI SCORE | SIRIUS SCORE | Comment |
|---|---|---|---|---|---|---|---|---|
| 31 | C7H10O5 | 15 | 173.0455006 | 11.4845 | Quinide | -153.1 | 45 | 23rd suggestion |
| | | | 173.0456816 | 10.55115 | 2,3,4-Trihydroxy-6-oxabicyclo[3.2.1]octan-7-one | -146.181 | 33.33 | 10th suggestion |

The aim was to annotate the quinic acid lactone. MS2 spectra of 2 chemical entities were acquired and all of them were annotated as quinic acid lactone. The highest score of annotation was acquired by the 173.0456816@10.55115.

Table G.15 Quinic acid - MS2 Results

| Number of chemical compound | Empirical formula | Number of empirical formula | Precursor m/z | Retention time (min) | Annotated name | CSI SCORE | SIRIUS SCORE | Comment |
|---|---|---|---|---|---|---|---|---|
| 32 | C7H12O6 | 16 | 191.0562036 | 4.65103 | L-quinate | -109.543 | 95 | 1st suggestion |
| | | | 191.0562332 | 1.71765 | L-quinate | -86.109 | 95 | 2nd suggestion |
| | | | 191.0557679 | 1.1843 | L-Quinate | -79.318 | 100 | 2nd suggestion |
| | | | 191.0561656 | 11.3845 | l-quinate | -73.211 | 95 | 1st suggestion |
| | | | 191.0561642 | 10.96783 | L-Quinate | -72.381 | 95 | 2nd suggestion |
| | | | 191.0561975 | 5.58438 | L-Quinate | -68.979 | 78 | 1st suggestion |
| | | | 191.056151 | 7.21775 | L-Quinate | -68.708 | 65.6 | 1st suggestion |
| | | | 191.0561344 | 11.81783 | l-quinate | -66.753 | 100 | 1st suggestion |
| | | | 191.0562748 | 8.85112 | l-quinate | -59.593 | 100 | 1st suggestion |

The aim was to annotate the quinic acid. MS2 spectra of 9 chemical entities were acquired and all of them were annotated as quinic acid. The highest score of annotation was acquired by the 191.0562748@8.85112

Table G.16 Salicylic acid - MS2 Results

| Number of chemical compound | Empirical formula | Number of empirical formula | Precursor m/z | Retention time (min) | Annotated name | CSI SCORE | SIRIUS SCORE | Comment |
|---|---|---|---|---|---|---|---|---|
| 33 | C7H6O3 | 17 | 183.0297003 | 2.61767 | Salicylic acid | -148.699 | 0.15 | 32nd suggestion |
| | | | 197.0455996 | 6.45107 | Salicylic acid | -83.864 | 55 | 6th suggestion |
| | | | 183.0299102 | 1.70098 | Salicylic acid | -71.68 | 55 | 2nd suggestion |
| | | | 137.060801 | 7.23442 | Salicylic acid | -67.419 | 67.3 | 2nd suggestion |
| | | | 137.0244766 | 5.36772 | Salicylic acid | -51.298 | 100 | 1st suggestion |
| The aim was to annotate the salicylic acid. MS2 spectra of 5 chemical entities were acquired and all of them were annotated as salicylic acid. The highest score of annotation was acquired by the 137.0244766@5.36772. | | | | | | | | |

Table G.17 Guaiacol - MS2 Results

| Number of chemical compound | Empirical formula | Number of empirical formula | Precursor m/z | Retention time (min) | Annotated name | CSI SCORE | SIRIUS SCORE | Comment |
|---|---|---|---|---|---|---|---|---|
| 34-36 | C7H8O2 | 18 | 169.0509178 | 3.95103 | guaiacol | -120.639 | 0.015 | 18th suggestion |
| | | | 123.0451994 | 5.7844 | 3-methylcatechol | -176.653 | 0.015 | 23rd suggestion |
| | | | 123.0452373 | 4.35103 | guaiacol | -63.974 | 60 | 2nd suggestion |
| | | | 123.0451666 | 8.33443 | 3-methylcatechol | -48.156 | 65 | 4-Methylcatechol - Chemical Reference Standard |
| | | | 123.045184 | 8.98445 | 4-methylcatechol | -40.985 | 100 | 3-Methylcatechol - Chemical Reference Standard |
| The 3-methylcatechol, 4-methylcatechol and the guaiacol share the same empirical formula (C7H8O2). The 3-methylcatechol and 4-methylcatechol were identified through chemical reference standards. The highest score of annotation for guaiacol was acquired by 123.0452373@4.350103. | | | | | | | | |

Table G.18 4-ethylcatechol - MS2 Results

| Number of chemical compound | Empirical formula | Number of empirical formula | Precursor m/z | Retention time (min) | Annotated name | CSI SCORE | SIRIUS SCORE | Comment |
|---|---|---|---|---|---|---|---|---|
| 37 | C8H10O2 | 19 | 137.0608513 | 12.05118 | 4-ethylcatechol | -111.86 | 20 | 14th suggestion |
| | | | 137.060845 | 7.98443 | 4-ethylcatechol | -102.104 | 30 | 8th suggestion |
| | | | 135.0452114 | 9.16778 | 4-ethylcatechol | -86.773 | 89 | 1st suggestion |
| The aim was to annotate the 4-ethylcatechol. MS2 spectra of 3 chemical entities were acquired and all of them were annotated as 4-ethylcatechol. The highest score of annotation was acquired by the 135.0452114@9.16778 | | | | | | | | |

Table G.19 4-vinylcatechol - MS2 Results

| Number of chemical compound | Empirical formula | Number of empirical formula | Precursor m/z | Retention time (min) | Annotated name | CSI SCORE | SIRIUS SCORE | Comment |
|---|---|---|---|---|---|---|---|---|
| 38 | C8H8O2 | 20 | 135.0451999 | 8.70112 | 4-vinylcatechol | -78.863 | 100 | 4th suggestion |
| | | | 135.0451894 | 7.98443 | 4-vinylcatechol | -70.071 | 100 | 1st suggestion |
| | | | 135.0452074 | 11.2845 | 4-vinylcatechol | -60.217 | 100 | 1st suggestion |
| | | | 135.0451822 | 14.13455 | 4-vinylcatechol | -50.818 | 100 | 1st suggestion |
| The aim was to annotate the 4-vinylcatechol. MS2 spectra of 4 chemical entities were acquired and all of them were annotated as 4-vinylcatechol. The highest score of annotation was acquired by the 135.0451822@14.13455 | | | | | | | | |

Table G.20 4-vinylguaiacol - MS2 Results

| Number of chemical compound | Empirical formula | Number of empirical formula | Precursor m/z | Retention time (min) | Annotated name | CSI SCORE | SIRIUS SCORE | Comment |
|---|---|---|---|---|---|---|---|---|
| 39 | C9H10O2 | 21 | 149.0608088 | 12.38452 | 4-vinylguaiacol | -108.128 | 50 | 5th suggestion |
| | | | 195.0663442 | 7.58442 | N/A | N/A | N/A | N/A |
| | | | 195.0664088 | 8.2011 | N/A | N/A | N/A | N/A |
| | | | 195.0663144 | 10.35115 | N/A | N/A | N/A | N/A |
| | | | 195.0663188 | 11.65117 | N/A | N/A | N/A | N/A |
| | | | 195.0662663 | 11.96783 | N/A | N/A | N/A | N/A |
| 6 chemical entities were found with the empirical formula C9H10O2. 1 entity was annotated as 4-vinylguaicol (149.0608088@12.38452). The MS2 spectra of the rest chemical entities were not found through the MS2 analysis, therefore the annotation was not feasible. | | | | | | | | |

Table G.21 p-Coumaric acid - MS2 Results

| Number of chemical compound | Empirical formula | Number of empirical formula | Precursor m/z | Retention time (min) | Annotated name | CSI SCORE | SIRIUS SCORE | Comment |
|---|---|---|---|---|---|---|---|---|
| 40 | C9H8O3 | 22 | 163.040156 | 7.88443 | p-Coumaric acid | -200 | 0 | 57th suggestion |
| | | | 163.0401219 | 12.66785 | p-Coumaric acid | -187.504 | 0 | 39th suggestion |
| | | | 163.0400856 | 7.65108 | p-Coumaric acid | -174.857 | 0 | 42nd suggestion |
| | | | 209.0455927 | 9.08445 | N/A | N/A | N/A | N/A |
| | | | 163.0400937 | 10.30113 | N/A | N/A | N/A | N/A |
| | | | 209.0455724 | 10.96783 | N/A | N/A | N/A | N/A |
| | | | 223.0611542 | 11.41783 | N/A | N/A | N/A | N/A |
| 7 chemical entities were found with the empirical formula C9H8O3. 3 chemical entities were annotated as p-Coumaric acid but the annotation score was very poor. The MS2 spectra of the rest chemical entities were not found through the MS2 analysis, therefore the annotation was not feasible. | | | | | | | | |

Table G.22 Caffeic acid - MS2 Results

| Number of chemical compound | Empirical formula | Number of empirical formula | Precursor m/z | Retention time (min) | Annotated name | CSI SCORE | SIRIUS SCORE | Comment |
|---|---|---|---|---|---|---|---|---|
| 41 | C9H8O4 | 23 | 225.0405026 | 1.45098 | Caffeic acid | -173.405 | 0 | 79th suggestion |
| | | | 179.0350346 | 7.93442 | Caffeic acid | -142.508 | 0 | 6th suggestion |
| | | | 179.035051 | 5.58438 | Caffeic acid | -124.391 | 100 | 5th suggestion |
| 179.0350345@7.93422 was identified as caffeic acid with a chemical reference standard. | | | | | | | | |

Table G.23 di-Caffeoylquinic acid lactone - MS2 Results

| Number of chemical compound | Empirical formula | Number of empirical formula | Precursor m/z | Retention time (min) | Annotated name | CSI SCORE | SIRIUS SCORE | Comment |
|---|---|---|---|---|---|---|---|---|
| 42-44 | C25H22O11 | 24 | 497.1087909 | 14.46788 | 3,4-Dicaffeoylquinolactone | -232.082 | 10 | 2nd suggestion |
| | | | 497.1094674 | 14.8179 | 3,4-Dicaffeoylquinolactone | -230.772 | 10 | 2nd suggestion |
| The aim was to annotate 3 di-Caffeoylquinic acid lactones. 2 chemical entities were found with empirical formula C25H22O11. Both chemical entities were annotated as 3,4-Dicaffeoylquinic acid lactone (497.1087909@14.46788 and 497.1094674@14.8179) . The CSI and Sirius score are not high enough compared to other annotations, but it was 2nd on the exported list of suggestions. Therefore the two entities were annotated as di-Caffeoylquinic acid lactone alpha and beta. | | | | | | | | |

Table G.24 di-Caffeoylquinic acid - MS2 Results

| Number of chemical compound | Empirical formula | Number of empirical formula | Precursor m/z | Retention time (min) | Annotated name | CSI SCORE | SIRIUS SCORE | Comment |
|---|---|---|---|---|---|---|---|---|
| 48-50 | C25H24O12 | 26 | 515.1193151 | 11.46783 | 4,5-dicaffeoyl quinic acid | -241.018 | 33.33 | 1st suggestion |
| | | | 515.119588 | 11.6345 | isochlorogenic acid c | -215.925 | 33.33 | 1st suggestion |
| | | | 515.1194066 | 10.95117 | isochlorogenic acid c | -198.57 | 0 | 1st suggestion |
| | | | 515.1195395 | 11.96783 | 4,5-dicaffeoyl quinic acid | -197.574 | 33.33 | 1st suggestion |
| | | | 515.1196857 | 12.73452 | 3,4-di-Caffeoylquinic acid | -112.225 | 50 | Identified with chemical reference standard |
| | | | 515.1194101 | 12.30118 | isochlorogenic acid c | -109.081 | 100 | 1st suggestion |
| | | | 515.1198204 | 12.88453 | 4,5-dicaffeoyl quinic acid | -97.343 | 100 | 1st suggestion |
| | | | 515.119453 | 13.13453 | 4,5-dicaffeoyl quinic acid | -73.859 | 100 | 1st suggestion |
| | | | 515.1196198 | 13.48453 | isochlorogenic acid c | -72.82 | 100 | 1st suggestion |

The aim was to annotate 3 di-Caffeoylquinic acids. The MS2 spectra of 9 chemical entities were collected through MS2 analysis. 515.1196857@12.73452 was identified as the 3,4-di-Caffeoylquinic acid with a chemical reference standard. The rest 2 chemical entities which had the highest CSI and SIRIUS score were annotated as di-caffeoylquinic acids. Therefore, 515.119453@13.13453 and 515.1196198@13.48453 were annotated as di-caffeoylquinic acid beta and gamma respectively.

Table G.25 Caffeoyl-Feruloylquinic acid - MS2 Results

| Number of chemical compound | Empirical formula | Number of empirical formula | Precursor m/z | Retention time (min) | Annotated name | CSI SCORE | SIRIUS SCORE | Comment |
|---|---|---|---|---|---|---|---|---|
| 51-56 | C26H26O12 | 27 | 529.1352824 | 12.62 | 3-Caffeoyl-4-feruloylquinic acid | -278.08 | 0 | 1st suggestion |
| | | | 529.1355243 | 13.80122 | 3-Caffeoyl-4-feruloylquinic acid | -101.072 | 33.33 | 2nd suggestion |
| | | | 529.1350466 | 13.33 | 4-O-Caffeoyl-3-O-feruloylquinic acid | -181.159 | 33.33 | 1st suggestion |
| | | | 529.1352123 | 14.55 | (1R,3R,4S,5R)-3-[(E)-3-(3,4-dihydroxyphenyl)prop-2-enoyl]oxy-1,5-dihydroxy-4-[(E)-3-(3-hydroxy-4-methoxyphenyl)prop-2-enoyl]oxycyclohexane-1-carboxylic acid | -105.744 | 50 | 1st suggestion |
| | | | 529.1355601 | 13.80122 | (1R,3R,4S,5R)-4-[(E)-3-(3,4-dihydroxyphenyl)prop-2-enoyl]oxy-1,3-dihydroxy-5-[(E)-3-(3-hydroxy-4-methoxyphenyl)prop-2-enoyl]oxycyclohexane-1-carboxylic acid | -194.188 | 0 | 19th suggestion |

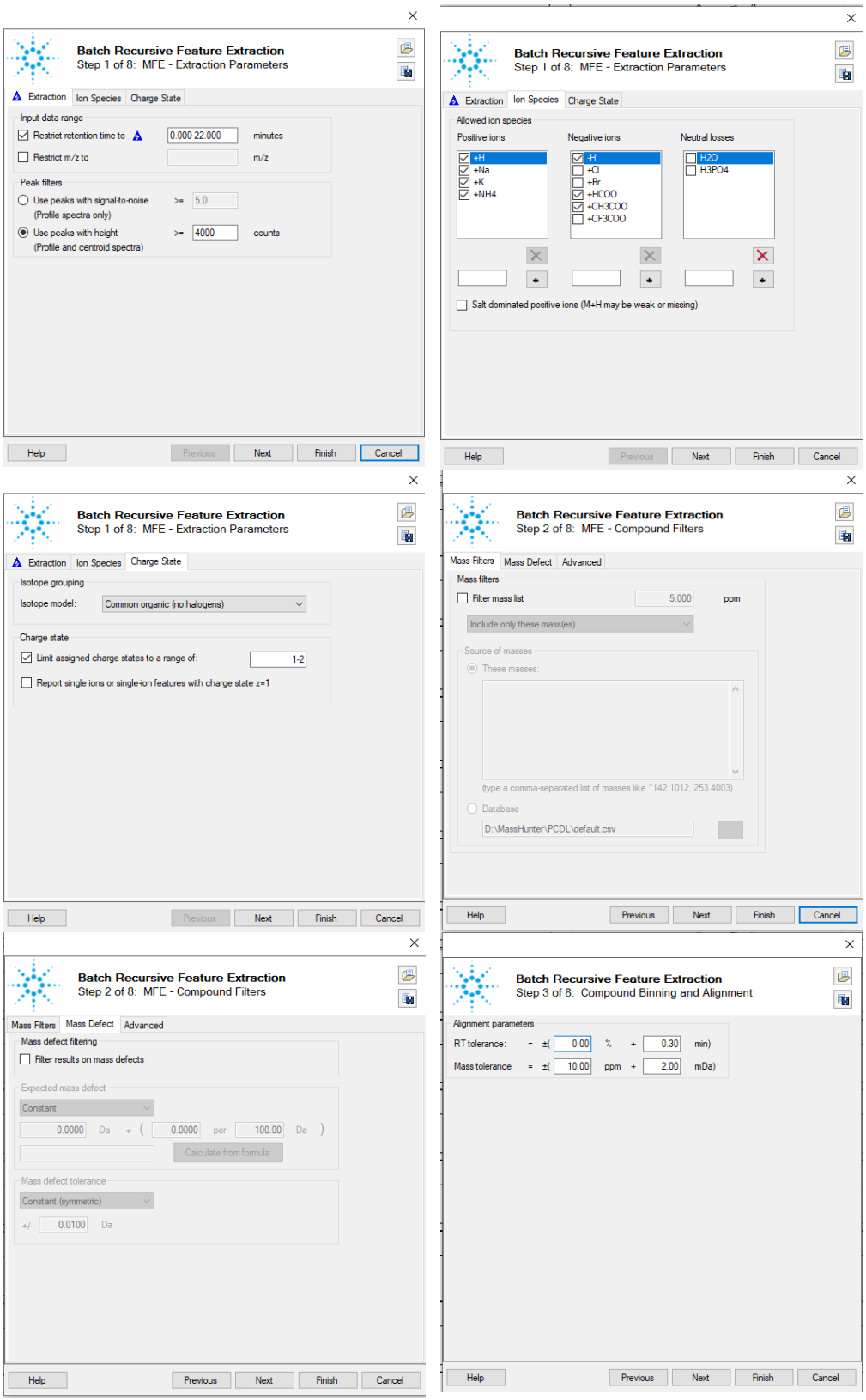
The aim was to annotate 6 Caffeoyl-Feruloyl-quinic acids. The MS2 spectra of 6 chemical entities were collected through MS2 analysis. 4 chemical entities which had the highest CSI and SIRIUS score were annotated as Caffeoyl-Feruloyl-quinic acids. Therefore, 529.1355243@13.80122, 529.1352123@14.55 and 529.1350466@13.33 were annotated as Caffeoyl-Feruloyl-quinic acid alpha, beta and gamma respectively.

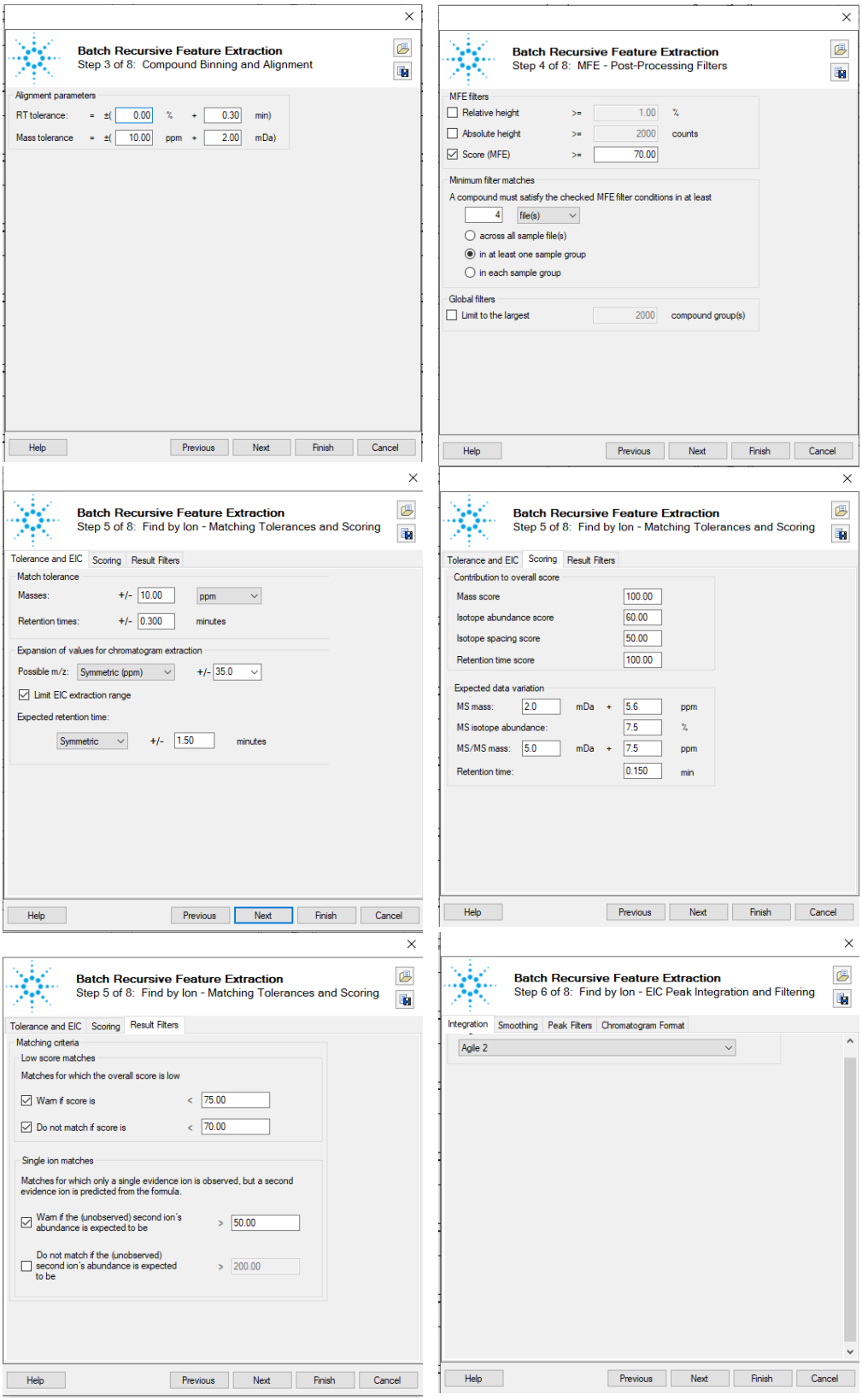
Table G.26 di-Feruloylquinic acid - MS2 results

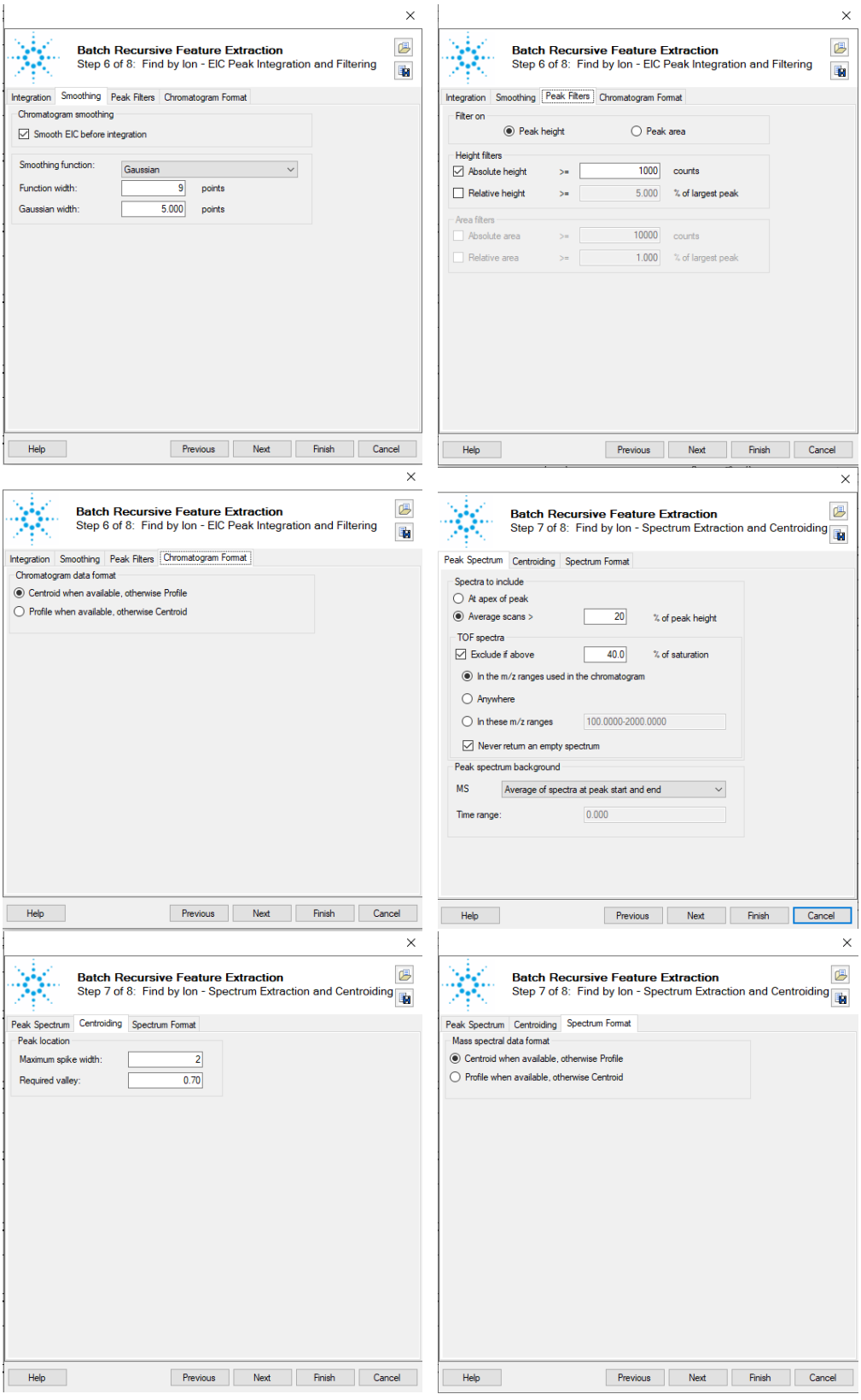
| Number of chemical compound | Empirical formula | Number of empirical formula | Precursor m/z | Retention time (min) | Annotated name | CSI SCORE | SIRIUS SCORE | Comment |
|---|---|---|---|---|---|---|---|---|
| 61-66 | C27H28O12 | 29 | 543.1508028 | 15.0679 | 4,5-Diferuloylquinic acid | -244.675 | 0 | 7th suggestion |
| | | | 543.1505511 | 15.4179 | 4,5-Diferuloylquinic acid | -162.594 | 33.33 | 1st suggestion |
| | | | 543.1507265 | 14.75122 | 4,5-Diferuloylquinic acid | -128.67 | 33.33 | 1st suggestion |

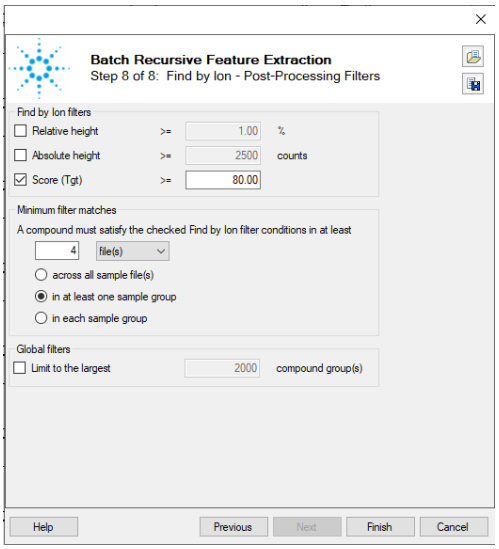
The aim was to annotate di-feruloylquinic acid and dimethoxycinnamoyl-caffeoylquinic acid because these chemical entities have the same empirical formula (C27H28O12). 3 chemical entities were annotated as di-Feruloylquinic acids and 2 of these had high score of annotation. Therefore, 543.1507265@14.75122 and 543.1505511@15.4179 were annotated as di-Feruloylquinic acids alpha and beta respectively.

# Appendix H: Recursive extraction parameters

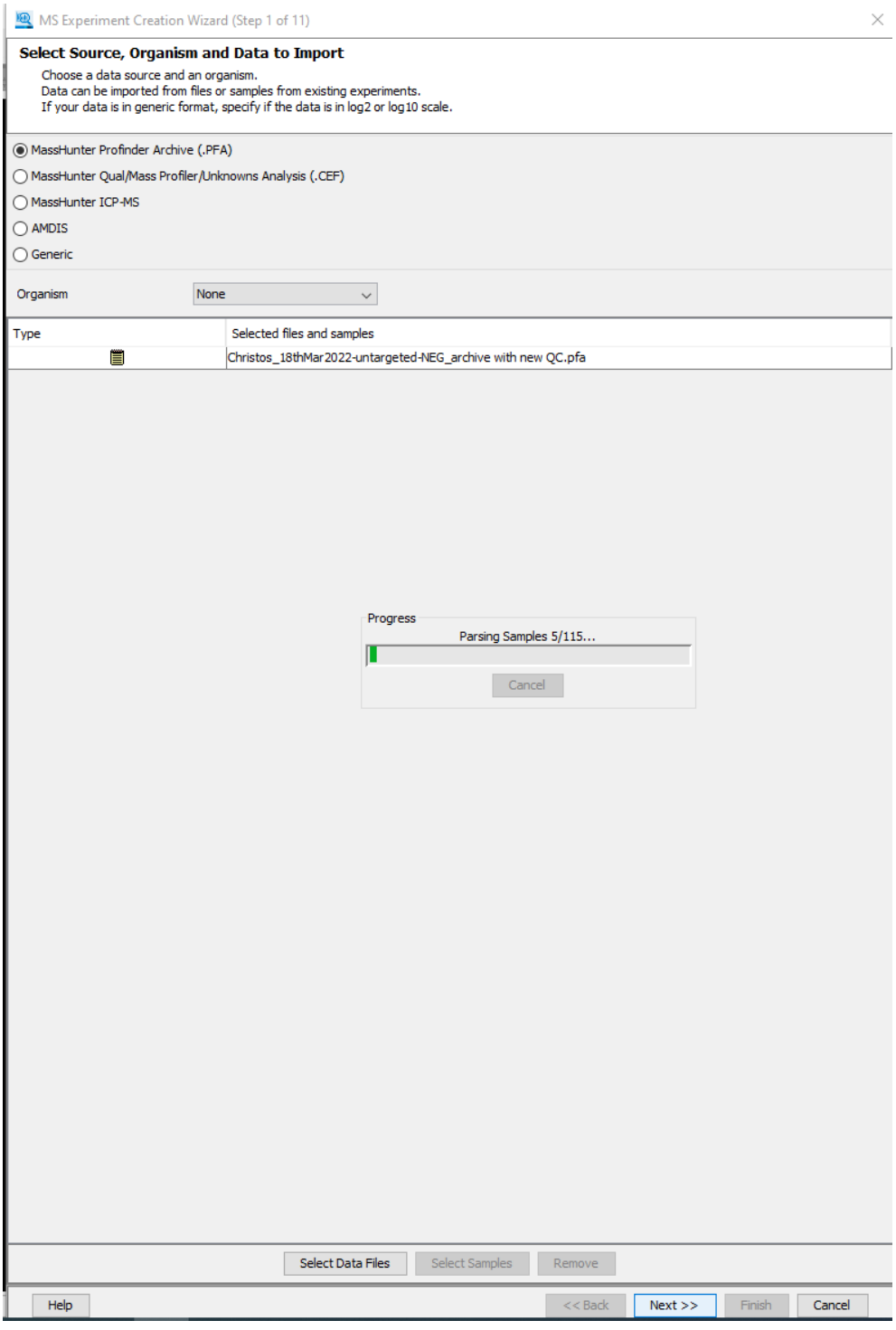


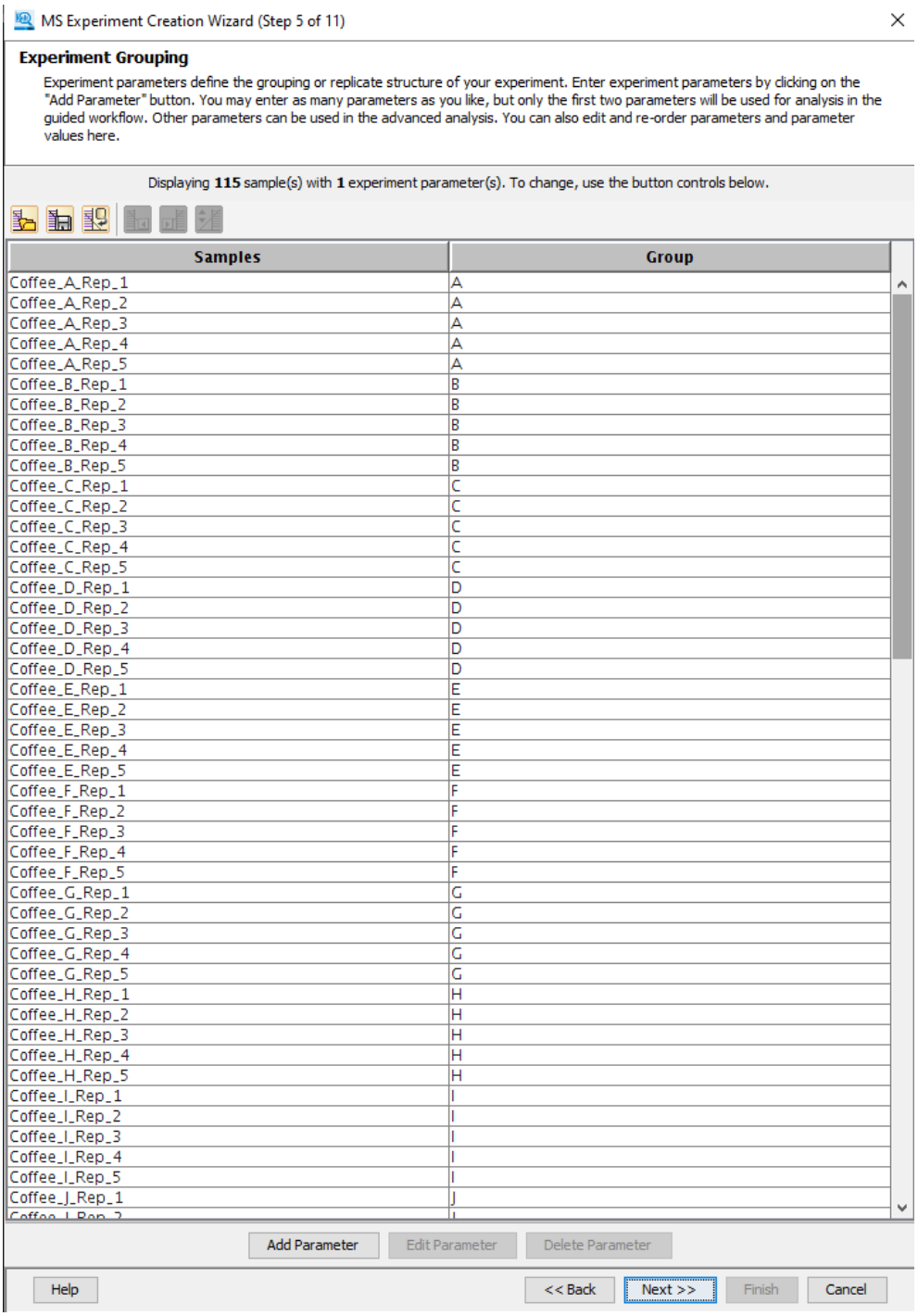

Batch Recursive Feature Extraction
Step 3 of 8: Compound Binning and Alignment
Alignment parameters
RT tolerance: = ±( 0.00 % + 0.30 min)
Mass tolerance = ±( 10.00 ppm + 2.00 mDa)
Help Previous Next Finish Cancel
Batch Recursive Feature Extraction
Step 4 of 8: MFE - Post-Processing Filters
MFE filters
Relative height >= 1.00 %
Absolute height >= 2000 counts
Score (MFE) >= 70.00
Minimum filter matches
A compound must satisfy the checked MFE filter conditions in at least
4 file(s)
across all sample file(s)
in at least one sample group
in each sample group
Global filters
Limit to the largest 2000 compound group(s)
Help Previous Next Finish Cancel
Batch Recursive Feature Extraction
Step 5 of 8: Find by Ion - Matching Tolerances and Scoring
Tolerance and EIC Scoring Result Filters
Match tolerance
Masses: +/- 10.00 ppm
Retention times: +/- 0.300 minutes
Expansion of values for chromatogram extraction
Possible m/z: Symmetric (ppm) +/- 35.0
Limit EIC extraction range
Expected retention time:
Symmetric +/- 1.50 minutes
Help Previous Next Finish Cancel
Batch Recursive Feature Extraction
Step 5 of 8: Find by Ion - Matching Tolerances and Scoring
Tolerance and EIC Scoring Result Filters
Contribution to overall score
Mass score 100.00
Isotope abundance score 60.00
Isotope spacing score 50.00
Retention time score 100.00
Expected data variation
MS mass: 2.0 mDa + 5.6 ppm
MS isotope abundance: 7.5 %
MS/MS mass: 5.0 mDa + 7.5 ppm
Retention time: 0.150 min
Help Previous Next Finish Cancel
Batch Recursive Feature Extraction
Step 5 of 8: Find by Ion - Matching Tolerances and Scoring
Tolerance and EIC Scoring Result Filters
Matching criteria
Low score matches
Matches for which the overall score is low
Warn if score is < 75.00
Do not match if score is < 70.00
Single ion matches
Matches for which only a single evidence ion is observed, but a second evidence ion is predicted from the formula.
Warn if the (unobserved) second ion's abundance is expected to be > 50.00
Do not match if the (unobserved) second ion's abundance is expected to be > 200.00
Help Previous Next Finish Cancel
Batch Recursive Feature Extraction
Step 6 of 8: Find by Ion - EIC Peak Integration and Filtering
Integration Smoothing Peak Filters Chromatogram Format
Agile 2
Help Previous Next Finish Cancel


Batch Recursive Feature Extraction
Step 6 of 8: Find by Ion - EIC Peak Integration and Filtering
Integration
Smoothing
Peak Filters
Chromatogram Format
Chromatogram smoothing
Smooth EIC before integration
Smoothing function:
Gaussian
Function width:
9
points
Gaussian width:
5.000
points
Help
Previous
Next
Finish
Cancel
Batch Recursive Feature Extraction
Step 6 of 8: Find by Ion - EIC Peak Integration and Filtering
Integration
Smoothing
Peak Filters
Chromatogram Format
Filter on
Peak height
Peak area
Height filters
Absolute height
>=
1000
counts
Relative height
>=
5.000
% of largest peak
Area filters
Absolute area
>=
10000
counts
Relative area
>=
1.000
% of largest peak
Help
Previous
Next
Finish
Cancel
Batch Recursive Feature Extraction
Step 6 of 8: Find by Ion - EIC Peak Integration and Filtering
Integration
Smoothing
Peak Filters
Chromatogram Format
Chromatogram data format
Centroid when available, otherwise Profile
Profile when available, otherwise Centroid
Help
Previous
Next
Finish
Cancel
Batch Recursive Feature Extraction
Step 7 of 8: Find by Ion - Spectrum Extraction and Centroiding
Peak Spectrum
Centroiding
Spectrum Format
Spectra to include
At apex of peak
Average scans >
20
% of peak height
TOF spectra
Exclude if above
40.0
% of saturation
In the m/z ranges used in the chromatogram
Anywhere
In these m/z ranges
100.0000-2000.0000
Never return an empty spectrum
Peak spectrum background
MS
Average of spectra at peak start and end
Time range:
0.000
Help
Previous
Next
Finish
Cancel
Batch Recursive Feature Extraction
Step 7 of 8: Find by Ion - Spectrum Extraction and Centroiding
Peak Spectrum
Centroiding
Spectrum Format
Peak location
Maximum spike width:
2
Required valley:
0.70
Help
Previous
Next
Finish
Cancel
Batch Recursive Feature Extraction
Step 7 of 8: Find by Ion - Spectrum Extraction and Centroiding
Peak Spectrum
Centroiding
Spectrum Format
Mass spectral data format
Centroid when available, otherwise Profile
Profile when available, otherwise Centroid
Help
Previous
Next
Finish
Cancel


Batch Recursive Feature Extraction
Step 8 of 8: Find by Ion - Post-Processing Filters
Find by Ion filters
Relative height >= 1.00 %
Absolute height >= 2500 counts
Score (Tgt) >= 80.00
Minimum filter matches
A compound must satisfy the checked Find by Ion filter conditions in at least
4 file(s)
across all sample file(s)
in at least one sample group
in each sample group
Global filters
Limit to the largest 2000 compound group(s)
Help
Previous
Next
Finish
Cancel

# Appendix I: Mass Profiler Professional settings




MS Experiment Creation Wizard (Step 5 of 11)

**Experiment Grouping**

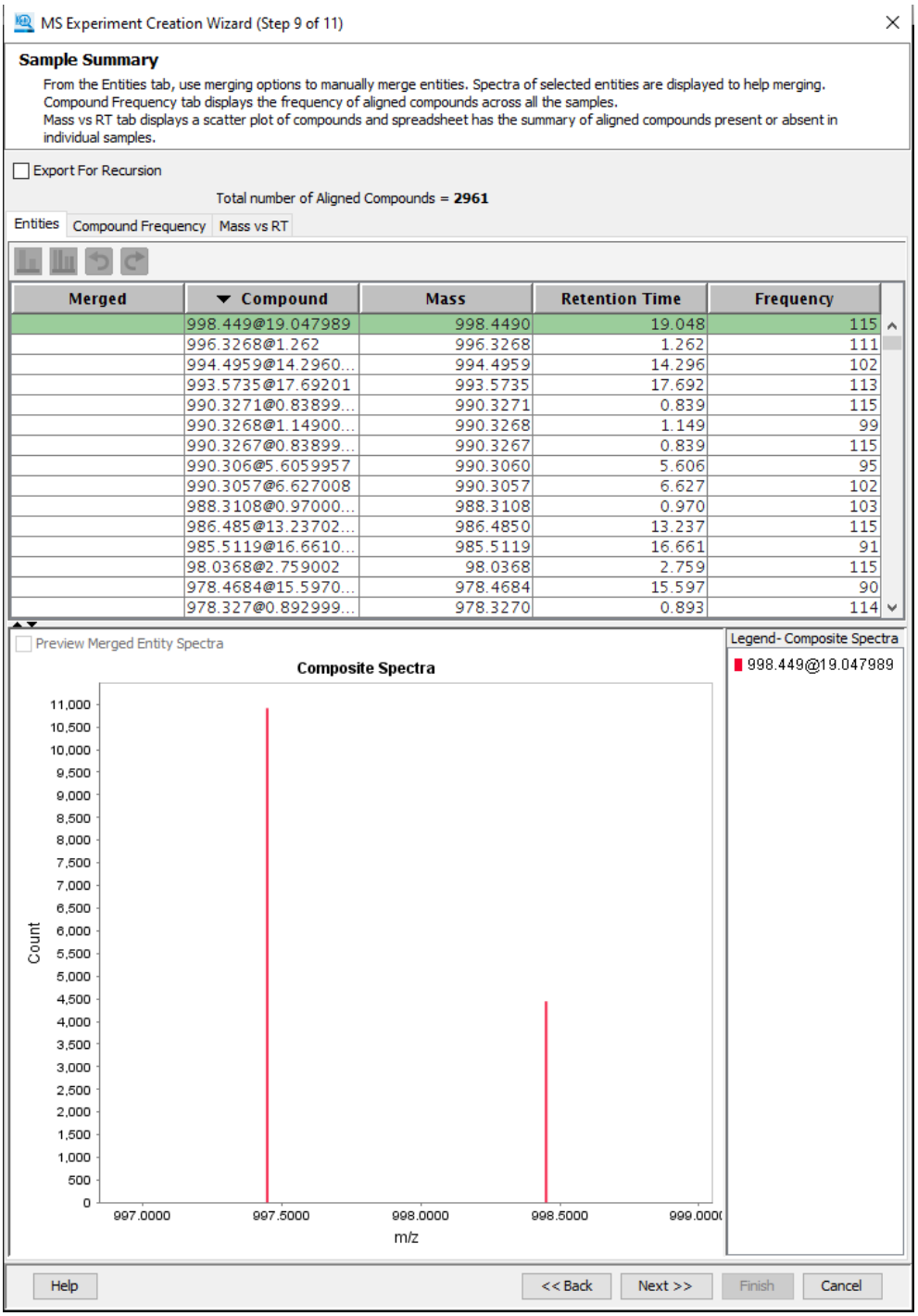
Experiment parameters define the grouping or replicate structure of your experiment. Enter experiment parameters by clicking on the "Add Parameter" button. You may enter as many parameters as you like, but only the first two parameters will be used for analysis in the guided workflow. Other parameters can be used in the advanced analysis. You can also edit and re-order parameters and parameter values here.

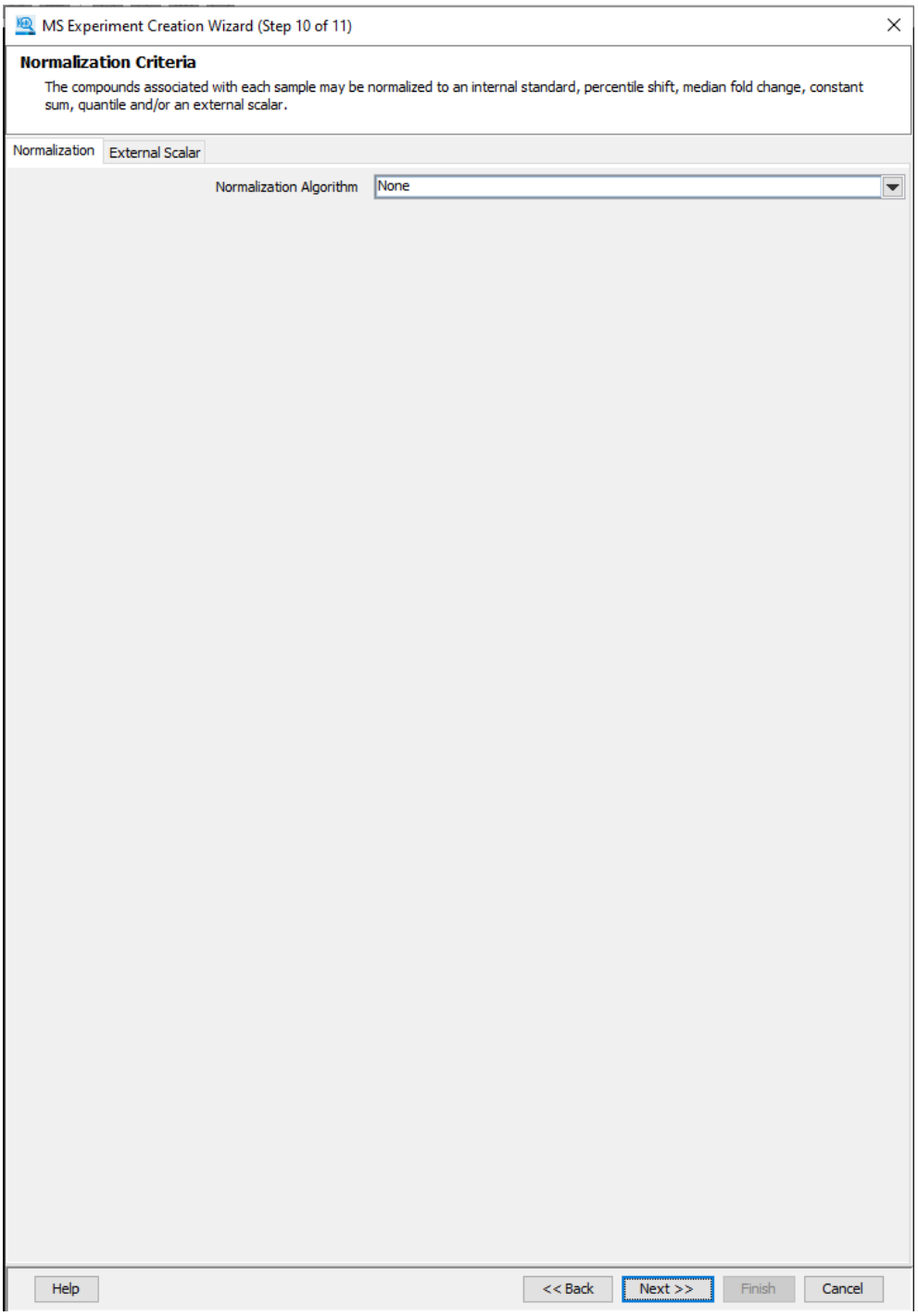
Displaying **115** sample(s) with **1** experiment parameter(s). To change, use the button controls below.

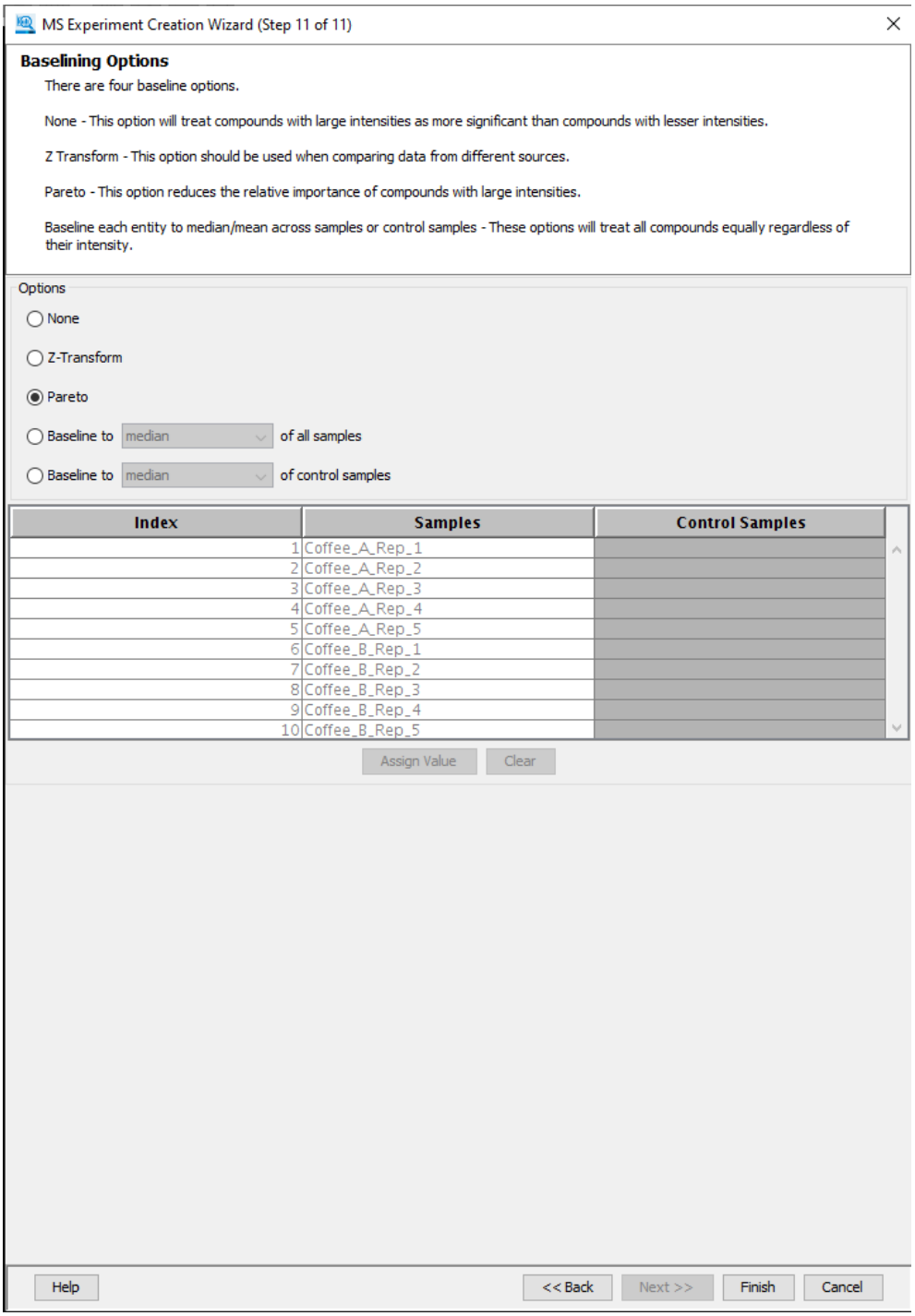
| Samples | Group |
|---|---|
| Coffee_A_Rep_1 | A |
| Coffee_A_Rep_2 | A |
| Coffee_A_Rep_3 | A |
| Coffee_A_Rep_4 | A |
| Coffee_A_Rep_5 | A |
| Coffee_B_Rep_1 | B |
| Coffee_B_Rep_2 | B |
| Coffee_B_Rep_3 | B |
| Coffee_B_Rep_4 | B |
| Coffee_B_Rep_5 | B |
| Coffee_C_Rep_1 | C |
| Coffee_C_Rep_2 | C |
| Coffee_C_Rep_3 | C |
| Coffee_C_Rep_4 | C |
| Coffee_C_Rep_5 | C |
| Coffee_D_Rep_1 | D |
| Coffee_D_Rep_2 | D |
| Coffee_D_Rep_3 | D |
| Coffee_D_Rep_4 | D |
| Coffee_D_Rep_5 | D |
| Coffee_E_Rep_1 | E |
| Coffee_E_Rep_2 | E |
| Coffee_E_Rep_3 | E |
| Coffee_E_Rep_4 | E |
| Coffee_E_Rep_5 | E |
| Coffee_F_Rep_1 | F |
| Coffee_F_Rep_2 | F |
| Coffee_F_Rep_3 | F |
| Coffee_F_Rep_4 | F |
| Coffee_F_Rep_5 | F |
| Coffee_G_Rep_1 | G |
| Coffee_G_Rep_2 | G |
| Coffee_G_Rep_3 | G |
| Coffee_G_Rep_4 | G |
| Coffee_G_Rep_5 | G |
| Coffee_H_Rep_1 | H |
| Coffee_H_Rep_2 | H |
| Coffee_H_Rep_3 | H |
| Coffee_H_Rep_4 | H |
| Coffee_H_Rep_5 | H |
| Coffee_I_Rep_1 | I |
| Coffee_I_Rep_2 | I |
| Coffee_I_Rep_3 | I |
| Coffee_I_Rep_4 | I |
| Coffee_I_Rep_5 | I |
| Coffee_J_Rep_1 | J |

Add Parameter | Edit Parameter | Delete Parameter

Help | << Back | Next >> | Finish | Cancel


MS Experiment Creation Wizard (Step 9 of 11)
Sample Summary
From the Entities tab, use merging options to manually merge entities. Spectra of selected entities are displayed to help merging.
Compound Frequency tab displays the frequency of aligned compounds across all the samples.
Mass vs RT tab displays a scatter plot of compounds and spreadsheet has the summary of aligned compounds present or absent in individual samples.
Export For Recursion
Total number of Aligned Compounds = 2961
Entities
Compound Frequency
Mass vs RT
Merged
Compound
Mass
Retention Time
Frequency
998.449@19.047989 998.4490 19.048 115
996.3268@1.262 996.3268 1.262 111
994.4959@14.2960... 994.4959 14.296 102
993.5735@17.69201 993.5735 17.692 113
990.3271@0.83899... 990.3271 0.839 115
990.3268@1.14900... 990.3268 1.149 99
990.3267@0.83899... 990.3267 0.839 115
990.306@5.6059957 990.3060 5.606 95
990.3057@6.627008 990.3057 6.627 102
988.3108@0.97000... 988.3108 0.970 103
986.485@13.23702... 986.4850 13.237 115
985.5119@16.6610... 985.5119 16.661 91
98.0368@2.759002 98.0368 2.759 115
978.4684@15.5970... 978.4684 15.597 90
978.327@0.892999... 978.3270 0.893 114
Preview Merged Entity Spectra
Composite Spectra
Count
m/z
Legend- Composite Spectra
998.449@19.047989
Help
<< Back
Next >>
Finish
Cancel


MS Experiment Creation Wizard (Step 10 of 11)
Normalization Criteria
The compounds associated with each sample may be normalized to an internal standard, percentile shift, median fold change, constant sum, quantile and/or an external scalar.
Normalization
External Scalar
Normalization Algorithm
None
Help
<< Back
Next >>
Finish
Cancel


MS Experiment Creation Wizard (Step 11 of 11)
Baselining Options
There are four baseline options.
None - This option will treat compounds with large intensities as more significant than compounds with lesser intensities.
Z Transform - This option should be used when comparing data from different sources.
Pareto - This option reduces the relative importance of compounds with large intensities.
Baseline each entity to median/mean across samples or control samples - These options will treat all compounds equally regardless of their intensity.
Options
None
Z-Transform
Pareto
Baseline to median of all samples
Baseline to median of control samples
Index
Samples
Control Samples
1 Coffee_A_Rep_1
2 Coffee_A_Rep_2
3 Coffee_A_Rep_3
4 Coffee_A_Rep_4
5 Coffee_A_Rep_5
6 Coffee_B_Rep_1
7 Coffee_B_Rep_2
8 Coffee_B_Rep_3
9 Coffee_B_Rep_4
10 Coffee_B_Rep_5
Assign Value
Clear
Help
<< Back
Next >>
Finish
Cancel

# Appendix J: MSI Level 2 annotation results of untargeted chemical analysis

Table J.1 Results from the annotation of ID of chemical entities found with negative polarity mode.

| Target | r of correlation for each foam quality parameter | | | MS2 details | | Certainty of annotation | | ID | | | Comment |
|---|---|---|---|---|---|---|---|---|---|---|---|
| | Foam Ability | Drainage rate | Disproportionation Rate | Prec. m/z | Ret. Time (min) | SIRIUS score | CSI score | Empirical Formula | Name | PubChem CID | |
| 666.2221@0.8379995 | | -0.88 | | 711.2199 | 0.84 | 33.278 | -110.5 | C24H42O21 | Mannotetraose | 53477669 | Good annotation |
| 268.0585@1.8949986 | | -0.82 | | 267.0511 | 1.89 | 99.99 | -180.305 | C12H14O8 | beta-D-Glucopyranosiduronic acid, 3-hydroxyphenyl | 178560 | Good annotation |
| 216.0998@5.127007 | | -0.84 | | 215.0926 | 5.13 | 33.33 | -95.024 | C9H14O3 | 3-Hydroxy-2-methyl-7-octynoic acid | 73102428 | Good annotation |
| 216.0998@5.3429947 | | -0.89 | | 215.0926 | 5.34 | 33.33 | -131.495 | C10H16O5 | 1-alpha-D-Glucopyranosyl-1-butyne | 102393544 | Good annotation |
| 666.2007@6.010005 | | -0.86 | | 665.1933 | 6.01 | 32.925 | -142.789 | C26H36O17 | 6-Deoxy-4-O-alpha-D-glucopyranosyl-beta-D-glucopyranose heptaacetate | 134159036 | Good annotation |
| 504.1477@6.4370055 | | -0.84 | | 503.1405 | 6.44 | 93.745 | -160.342 | C21H28O14 | 2-O-beta-D-Glucopyranosyl-6-O-(3,4-dihydroxy-trans-cinnamoyl)-alpha-D-glucopyranose | 11071183 | Good annotation |
| 666.2003@6.719993 | | -0.85 | | 665.1931 | 6.72 | 33.268 | -155.652 | C26H36O17 | 6-Deoxy-4-O-alpha-D-glucopyranosyl-beta-D-glucopyranose heptaacetate | 12775671 | Good annotation |
| 341.195@12.218009 | | -0.85 | | 340.1878 | 12.22 | 33.21 | -136.822 | C15H25N3O3 | 2-(4-acetylpiperazin-1-yl)-N-cycloheptyl-2-oxoacetamide | 108508438 | Good annotation |

Table J.1 cont.

| Target | r of correlation for each foam quality parameter | | | MS2 details | | Certainty of annotation | | ID | | | Comment |
|---|---|---|---|---|---|---|---|---|---|---|---|
| | Foam Ability | Drainage rate | Disproportionation Rate | Prec. m/z | Ret. Time (min) | SIRIUS score | CSI score | Empirical Formula | Name | PubChem CID | |
| 244.0736@13.213009 | | -0.87 | | 243.0664 | 13.21 | 33.33 | -70.325 | C14H12O4 | 4-[(E)-2-(2,4-dihydroxyphenyl)ethenyl]benzene-1,3-diol | 9881314 | Good annotation |
| 609.2797@14.4449835 | | -0.93 | | 608.2724 | 14.44 | 27.516 | -160.991 | C29H35N5O6 | NH2-Tyr-Pro-Phe-Pro-CONH2 | 134825944 | Good annotation |
| 539.3322@14.901986 | | -0.83 | | 538.3251 | 14.90 | 26.147 | -166.393 | C26H45N5O7 | N-[(S)-3-[(L-Val-L-Pro-)Amino]-1,2-dioxopentyl]-D-Leu-L-Val-OH | 102000539 | Good annotation |
| 288.2301@16.20999 | | -0.84 | | 287.2228 | 16.21 | 33.33 | -72.287 | C14H28O2 | Myristic Acid | 153693963 | Good annotation |
| 666.2221@0.8379995 | | -0.88 | | 665.2151 | 0.84 | 0.02 | -418.619 | C25H40N4O18 | 2-O-[1-[4-(alpha-D-Mannopyranosyl)-1H-1,2,3-triazole-1-yl]-1,3-dideoxy-beta-D-galactopyranose-3-yl]-N-acetyl-alpha-neuraminic acid | 102143402 | Poor annotation |
| 834.2746@1.2539994 | | -0.84 | | 833.2676 | 1.25 | 0.605 | -428.147 | C30H42N6O18 | 2,5,8,11,14,17-Hexaoxo-1,4,7,10,13,16-hexaazacyclooctadecane-1,4,7,10,13,16-hexapropanoic acid | 102501184 | Poor annotation |
| 448.0587@3.8110018 | | -0.85 | | 447.0512 | 3.81 | 0.022 | -153.763 | C16H20N2O9S2 | Glucobrassicin | 9601691 | Poor annotation |
| 216.0998@5.127007 | | -0.84 | | 261.0979 | 5.13 | 0.01 | -126.437 | C11H12N4O | 7-Amino-2-cyclopropyl-5-methylpyrazolo[1,5-a]pyrimidine-6-carbaldehyde | 58034557 | Poor annotation |
| 828.2536@5.3609953 | | -0.83 | | 827.2466 | 5.36 | 6.813 | -301.006 | C39H42O17 | Spinosin 6'''-(E)-ferulate | 44258336 | Poor annotation |

Table J.1 cont.

| Target | r of correlation for each foam quality parameter | | | MS2 details | | Certainty of annotation | | ID | | | Comment |
|---|---|---|---|---|---|---|---|---|---|---|---|
| | Foam Ability | Drainage rate | Disproportionation Rate | Prec. m/z | Ret. Time (min) | SIRIUS score | CSI score | Empirical Formula | Name | PubChem CID | |
| 288.0845@6.058004 | | -0.84 | | 333.0828 | 6.06 | 0.26 | -173.847 | C12H16O8 | 3,5-Dihydroxyphenyl alpha-D-glucopyranoside | 54455264 | Poor annotation |
| 288.0845@6.058004 | | -0.84 | | 287.0773 | 6.06 | 0.003 | -228.48 | C13H12N4O4 | 2-[(4-Methylpyridin-3-yl)methylamino]-5-nitropyridine-4-carboxylic acid | 105618466 | Poor annotation |
| 342.1902@8.554994 | | -0.82 | | 341.1832 | 8.55 | 0 | -110.873 | C13H28O7 | 2,3-Bis[2-(2-methoxyethoxy)ethoxy]-1-propanol | 12857522 | Poor annotation |
| 342.1902@8.554994 | | -0.82 | | 387.1885 | 8.55 | 0 | -162.217 | C15H20N8O | 2,3-Bis[2-(2-methoxyethoxy)ethoxy]-1-propanol | 16191089 | Poor annotation |
| 502.2791@15.447999 | | -0.83 | | 501.2717 | 15.45 | 2.14 | -143.023 | C20H36N6O6 | L-asparagyl-L-asparagyl-L-leucyl-L-leucinal | 123812059 | Poor annotation |
| 400.2433@15.927 | | -0.89 | | 399.2364 | 15.93 | 0.005 | -109.293 | C20H28N4O | 4-(1-piperidinylmethyl)-N-[(1-propyl-1H-imidazol-2-yl)methyl]benzamide | 72918706 | Poor annotation |

Table J.2 Results from the annotation of ID of chemical entities found with positive polarity mode

Table J.2 Cont.

| Target | r of correlation for each foam quality parameter | | | MS2 details | Certainty of annotation | | | ID | | | Comment | Score | | |
|---|---|---|---|---|---|---|---|---|---|---|---|---|---|---|
| | Foam Ability | Drainage Rate | Disproportionation rate | Prec. m/z | Ret. time (min) | SIRIUS score | CSI score | Empirical Formula | Name | PubChem CID | | A | B | C |
| 394.0514@0.81999975 | | 0.86 | | 395.06 | 0.82 | 31.25 | -169.90 | C11H15N4O10P | [(2R,5R)-5-[2-(dihydroxymethyl)-6-oxo-1H-purin-9-yl]-3,4-dihydroxyoxolan-2-yl]methyl dihydrogen phosphate | 135404920 | Good annotation | | 0.41 | |
| 380.0721@0.8219992 | | -0.87 | | 381.08 | 0.82 | 90.23 | -178.89 | C13H18N4O7 | 1,3-Dimethyl-8-methoxy-7-beta-D-ribofuranosylxanthine | 10042987 | Good annotation | | 0.59 | |
| 232.0347@0.8330001 | | 0.84 | | 233.04 | 0.83 | 100.00 | -154.74 | C8H10N4O2 | 5-Ethyl-1-(2-isocyanoethyl)-4-nitroimidazole | 88567108 | Good annotation | | 0.66 | |
| 162.0529@0.8590007 | | -0.86 | | 163.06 | 0.86 | 50.00 | -46.25 | C6H12O6 | FRUCTOSE, (D) | 3426 | Good annotation | | 0.70 | |
| 144.0422@0.8679986 | | -0.89 | | 145.05 | 0.87 | 33.33 | -40.51 | C6H12O6 | L-Glucose | 24749 | Good annotation | | 0.67 | |
| 486.1581@0.88700056 | | -0.83 | | 504.19 | 0.89 | 29.56 | -34.94 | C18H33NO15 | 4-O-(4-O-beta-D-Galactopyranosyl-beta-D-galactopyranosyl)-2-amino-2-deoxy-D-glucopyranose | 11329568 | Good annotation | | 0.64 | |
| 320.0508@0.9189992 | | 0.86 | 0.82 | 321.06 | 0.92 | 45.74 | -127.48 | C9H13N4O7P | 1-(5-O-Phosphono-beta-D-ribofuranosyl)-5-amino-1H-imidazole-4-carbonitrile | 101084767 | Good annotation | | 0.54 | 0.52 |

Table J.2 Cont.

| Target | r of correlation for each foam quality parameter | | | MS2 details | Certainty of annotation | | | ID | | | Comment | Score | | |
|---|---|---|---|---|---|---|---|---|---|---|---|---|---|---|
| | Foam Ability | Drainage Rate | Disproportionation rate | Prec. m/z | Ret. time (min) | SIRIUS score | CSI score | Empirical Formula | Name | PubChem CID | | A | B | C |
| 244.1057@0.9670008 | | | -0.86 | 245.11 | 0.97 | 50.00 | -122.99 | C10H16N2O5 | Prolylglutamic acid | 194260 | Good annotation | | | 0.56 |
| 266.1014@0.9820006 | | -0.92 | -0.83 | 267.11 | 0.98 | 49.99 | -52.72 | C11H14N4O4 | DL-pyroglutamyl-DL-histidine | 3839181 | Good annotation | | 0.71 | 0.68 |
| 186.0639@1.2790004 | | -0.82 | | 187.07 | 1.28 | 100.00 | -139.29 | C7H14N2O6 | 2,6-Bis(hydroxyamino)pimelic acid | 101993507 | Good annotation | | 0.68 | |
| 85.0808@1.3399979 | | -0.87 | | 86.10 | 1.34 | 100.00 | -75.45 | C5H13NO | 4-(Methylamino)butan-2-ol | 12545025 | Good annotation | | 0.82 | |
| 85.0829@1.3399979 | | -0.86 | | 86.10 | 1.34 | 100.00 | -83.44 | C5H13NO | N-(2-methylbutyl)hydroxylamine | 19073515 | Good annotation | | 0.80 | |
| 131.0946@1.3430011 | | -0.86 | | 132.10 | 1.34 | 50.00 | -34.48 | C6H13NO2 | l-Isoleucine | 6306 | Good annotation | | 0.72 | |
| 131.0946@1.3430012 | | -0.86 | | 154.09 | 1.34 | 50.00 | -78.94 | C8H8O2 | (E)-3-(furan-2-yl)but-2-enal | 12601620 | Good annotation | | 0.64 | |
| 129.0427@1.4450015 | | -0.92 | | 130.05 | 1.45 | 50.00 | -40.82 | C5H7NO3 | DL-Pyroglutamic acid | 499 | Good annotation | | 0.73 | |
| 129.0427@1.4450016 | | -0.92 | | 152.03 | 1.45 | 100.00 | -148.89 | C5H7NO3 | 2-Cyano-3-methoxypropanoic acid | 55303075 | Good annotation | | 0.70 | |
| 109.0528@1.5899976 | | -0.94 | | 110.06 | 1.59 | 50.00 | -21.71 | C6H7NO | 5-Hydroxy-2-methylpyridine | 14275 | Good annotation | | 0.77 | |
| 214.1316@1.6199994 | | -0.82 | | 215.14 | 1.62 | 50.00 | -68.24 | C10H18N2O3 | L-Prolyl-L-valine | 152307 | Good annotation | | 0.65 | |
| 200.0795@1.727998 | | -0.86 | -0.84 | 201.09 | 1.73 | 33.33 | -55.29 | C8H14N2O5 | d-Glutamyl-d-alanine | 129733605 | Good annotation | | 0.63 | 0.62 |
| 227.1631@1.8419988 | | -0.89 | | 228.17 | 1.84 | 50.00 | -124.51 | C11H21N3O2 | L-Leucinamide, L-prolyl- | 54413316 | Good annotation | | 0.57 | |

Table J.2 Cont.

| Target | r of correlation for each foam quality parameter | | | MS2 details | Certainty of annotation | | | ID | | | Comment | Score | | |
|---|---|---|---|---|---|---|---|---|---|---|---|---|---|---|
| | Foam Ability | Drainage Rate | Disproportionation rate | Prec. m/z | Ret. time (min) | SIRIUS score | CSI score | Empirical Formula | Name | PubChem CID | | A | B | C |
| 127.0634@1.85 29979 | 0.85 | -0.93 | | 128.07 | 1.85 | 50.00 | -107.07 | C6H11NO3 | Hexanoic acid, 5-amino-4-oxo-, (5S)- | 23656929 | Good annotation | 0.58 | 0.61 | |
| 216.1472@1.85 49992 | | -0.93 | -0.82 | 217.15 | 1.85 | 50.00 | -21.23 | C10H20N2O3 | L-Valyl-L-valine | 107475 | Good annotation | | 0.77 | 0.73 |
| 234.1116@1.99 6998 | | -0.95 | | 235.12 | 2.00 | 49.87 | -95.07 | C11H14N4O2 | Cyclo(his-pro) | 449094 | Good annotation | | 0.64 | |
| 236.1271@2.02 8 | | -0.93 | | 237.13 | 2.03 | 50.00 | -145.64 | C11H13N3O2 | CID 131574078 | 131574078 | Good annotation | | 0.54 | |
| 348.1543@2.09 5001 | 0.84 | -0.94 | -0.85 | 349.16 | 2.10 | 48.32 | -139.99 | C15H20N6O4 | (2S)-1-[(2S)-3-(1H-imidazol-5-yl)-2-[[(2S)-4-oxoazetidine-2-carbonyl]amino]propanoyl]pyrrolidine-2-carboxamide | 65841 | Good annotation | 0.52 | 0.55 | 0.52 |
| 263.1267@2.25 | | -0.94 | -0.82 | 264.13 | 2.25 | 50.00 | -167.53 | C13H17N3O3 | 1-[2-Acetyl-4-(4-methoxyphenyl)-1,2,4-triazolidin-1-yl]ethanone | 57115186 | Good annotation | | 0.50 | 0.46 |
| 300.1221@2.29 40028 | | -0.84 | | 301.13 | 2.29 | 49.97 | -108.86 | C15H16N4O3 | 3-[(4-hydroxyphenyl)methyl]-6-(1H-imidazol-5-ylmethyl)piperazine-2,5-dione | 14132662 | Good annotation | | 0.58 | |
| 200.1159@2.38 69967 | | -0.87 | | 201.12 | 2.39 | 33.33 | -95.20 | C9H18N2O4 | Threonyl-valine | 7020902 | Good annotation | | 0.56 | |
| 250.1428@2.47 99998 | 0.82 | -0.94 | | 251.15 | 2.48 | 50.00 | -96.36 | C12H18N4O2 | Cyclo(D-Leu-L-His-) | 101013136 | Good annotation | 0.59 | 0.63 | |
| 234.1116@2.50 99988 | | -0.87 | | 235.12 | 2.51 | 50.00 | -72.24 | C11H14N4O2 | Cyclo(his-pro) | 449094 | Good annotation | | 0.65 | |
| 260.1371@2.55 3999 | | -0.85 | | 261.14 | 2.55 | 100.00 | -154.03 | C11H17NO5 | 2-(2-Cyclopropylpropanoyl | 83146732 | Good annotation | | 0.66 | |

Table J.2 Cont.

| Target | r of correlation for each foam quality parameter | | | MS2 details | Certainty of annotation | | | ID | | | Comment | Score | | |
|---|---|---|---|---|---|---|---|---|---|---|---|---|---|---|
| | Foam Ability | Drainage Rate | Disproportionation rate | Prec. m/z | Ret. time (min) | SIRIUS score | CSI score | Empirical Formula | Name | PubChem CID | | A | B | C |
| | | | | | | | | | amino)pentanedioic acid | | | | | |
| 202.1316@2.58 09968 | | -0.91 | | 203.14 | 2.58 | 100.0 0 | -127.36 | C9H15NO3 | 2-Methyl-3-sec-butoxy-3-cyanopropionic acid | 23629620 | Good annotation | | 0.73 | |
| 208.121@2.604 003 | | -0.87 | | 226.15 | 2.60 | 50.00 | -92.09 | C11H19N3O2 | 1-(Piperidine-4-carbonyl)pyrrolidine-2-carboxamide | 43212185 | Good annotation | | 0.62 | |
| 165.0789@2.65 89973 | | -0.87 | -0.83 | 166.09 | 2.66 | 100.0 0 | -54.55 | C9H8O2 | Cinnamic acid | 444539 | Good annotation | | 0.86 | 0.84 |
| 156.0898@2.78 29993 | 0.82 | -0.95 | | 157.10 | 2.78 | 50.00 | -104.15 | C7H12N2O2 | (S)-3-Isopropyl-2,5-piperazinedione | 736942 | Good annotation | 0.58 | 0.63 | |
| 250.1427@2.80 20017 | 0.83 | -0.94 | | 251.15 | 2.80 | 48.13 | -157.03 | C12H15N3O2 | 4-[[2-(1H-imidazol-5-yl)ethylamino]methyl] benzene-1,3-diol | 65231973 | Good annotation | 0.48 | 0.52 | |
| 348.1543@2.83 29988 | | -0.88 | -0.87 | 349.16 | 2.83 | 42.40 | -153.38 | C15H20N6O4 | Azetirelin | 65841 | Good annotation | | 0.48 | 0.48 |
| 208.121@3.210 9988 | | -0.88 | | 226.15 | 3.21 | 100.0 0 | -87.84 | C11H16N2O2 | 2-but-3-enyl-6,7,8,8a-tetrahydro-3H-pyrrolo[1,2-a]pyrazine-1,4-dione | 116038128 | Good annotation | | 0.80 | |
| 237.0999@3.23 69998 | | -0.87 | -0.83 | 238.11 | 3.24 | 50.00 | -112.63 | C12H12O4 | 4-Hydroxy-3-methoxycinnamylideneacetic acid | 14053117 | Good annotation | | 0.58 | 0.57 |
| 137.084@3.364 0037 | | -0.95 | -0.84 | 138.09 | 3.36 | 50.00 | -47.91 | C8H9O+ | 4-Methoxybenzyl cation | 15178799 | Good annotation | | 0.73 | 0.69 |
| 277.1424@3.55 89976 | | -0.93 | | 278.15 | 3.56 | 50.00 | -154.62 | C14H19N3O3 | N-[(2-methoxyphenyl)methyl]-2-(3-oxopiperazin-1-yl)acetamide | 8962927 | Good annotation | | 0.52 | |

Table J.2 Cont.

| Target | r of correlation for each foam quality parameter | | | MS2 details | Certainty of annotation | | | ID | | | Comment | Score | | |
|---|---|---|---|---|---|---|---|---|---|---|---|---|---|---|
| | Foam Ability | Drainage Rate | Disproportionation rate | Prec. m/z | Ret. time (min) | SIRIUS score | CSI score | Empirical Formula | Name | PubChem CID | | A | B | C |
| 214.0951@3.6369958 | 0.85 | -0.94 | -0.89 | 215.10 | 3.64 | 50.00 | -131.25 | C9H14N2O4 | 2-(2-Aminopent-4-ynoylamino)-3-hydroxybutanoic acid | 81775612 | Good annotation | 0.54 | 0.57 | 0.55 |
| 181.0738@3.695 | | -0.84 | | 200.09 | 3.69 | 100.00 | -150.39 | C9H13NO4 | 2-(3-Cyano-3-methylbutyl)propanedioic acid | 87846186 | Good annotation | | 0.67 | |
| 181.0688@3.695 | | -0.84 | | 200.09 | 3.69 | 50.00 | -139.64 | C9H15NO5 | N-[(2R,3R,4R,5S,6R)-6-ethenyl-2,4,5-trihydroxyoxan-3-yl]acetamide | 21580055 | Good annotation | | 0.52 | |
| 181.0738@3.694 | | -0.84 | | 182.08 | 3.69 | 50.00 | -53.88 | C9H8O3 | p-coumaric acid | 637542 | Good annotation | | 0.68 | |
| 181.0688@3.694 | | -0.84 | | 182.08 | 3.69 | 50.00 | -59.62 | C9H8O3 | p-coumaric acid | 637542 | Good annotation | | 0.67 | |
| 80.026@3.7789986 | | -0.85 | | 81.03 | 3.78 | 100.00 | -68.33 | C5H5O+ | Pyrylium | 9548819 | Good annotation | | 0.82 | |
| 213.1364@3.7879965 | | -0.90 | | 231.17 | 3.79 | 50.00 | -74.16 | C11H22N2O3 | Leucylvaline | 352038 | Good annotation | | 0.66 | |
| 213.1364@3.7879966 | | -0.90 | | 214.14 | 3.79 | 50.00 | -86.09 | C11H21NO4 | 6-aminoundecanedioic Acid | 1801483 | Good annotation | | 0.64 | |
| 212.0797@3.9219975 | 0.86 | -0.92 | -0.84 | 213.09 | 3.92 | 50.00 | -141.35 | C9H9NO4 | 2-(Carboxymethyl)-1-ethenylpyrrole-3-carboxylic acid | 15718635 | Good annotation | 0.53 | 0.55 | 0.52 |
| 466.2175@3.9280024 | | -0.83 | | 467.22 | 3.93 | 46.43 | -83.93 | C20H30N6O7 | DL-alpha-aspartyl-DL-prolyl-DL-valyl-DL-histidine | 18252477 | Good annotation | | 0.61 | |
| 228.1472@3.9700001 | | -0.91 | -0.85 | 229.15 | 3.97 | 100.00 | -131.60 | C11H17NO3 | 2-Cyclopropyl-2-(3-cyclopropylpropanoylamino)acetic acid | 115730824 | Good annotation | | 0.73 | 0.71 |

Table J.2 Cont.

| Target | r of correlation for each foam quality parameter | | | MS2 details | Certainty of annotation | | | ID | | | Comment | Score | | |
|---|---|---|---|---|---|---|---|---|---|---|---|---|---|---|
| | Foam Ability | Drainage Rate | Disproportionation rate | Prec. m/z | Ret. time (min) | SIRIUS score | CSI score | Empirical Formula | Name | PubChem CID | | A | B | C |
| 104.0626@3.9899971 | | -0.92 | -0.83 | 105.07 | 3.99 | 100.00 | -35.50 | C8H9+ | 3-Methylbenzyl cation | 85865932 | Good annotation | | 0.91 | 0.88 |
| 224.1523@4.161995 | | -0.94 | | 242.19 | 4.16 | 50.00 | -90.18 | C12H20N2O2 | Cyclo-(D-Pipecolinyl-L-isoleucine) | 139586736 | Good annotation | | 0.65 | |
| 212.097@4.243005 | 0.86 | -0.96 | -0.85 | 235.11 | 4.24 | 33.33 | -79.66 | C12H14N2O3 | 3-[(4-Hydroxyphenyl)methyl]-6-methylpiperazine-2,5-dione | 571964 | Good annotation | 0.58 | 0.62 | 0.58 |
| 212.097@4.243004 | 0.86 | -0.96 | -0.85 | 213.09 | 4.24 | 50.00 | -135.69 | C9H14N2O5 | DL-alpha-aspartyl-DL-proline | 14647618 | Good annotation | 0.54 | 0.57 | 0.53 |
| 250.1428@4.4049993 | | -0.94 | | 251.15 | 4.40 | 50.00 | -102.00 | C12H18N4O2 | Cyclo(D-Leu-L-His-) | 101013136 | Good annotation | | 0.63 | |
| 99.0683@4.4590073 | | -0.91 | | 100.08 | 4.46 | 33.33 | -64.12 | C5H13NO3 | 1-Aminopentane-2,3,4-triol | 54394765 | Good annotation | | 0.63 | |
| 170.1054@4.4909983 | | -0.92 | | 171.11 | 4.49 | 100.00 | -116.31 | C8H11NO2 | N-(2-Methyl-1-oxoallyl)methacrylamide | 81837 | Good annotation | | 0.76 | |
| 230.1629@4.8519955 | | -0.90 | | 231.17 | 4.85 | 50.00 | -69.13 | C11H22N2O3 | Valylleucine | 6993118 | Good annotation | | 0.67 | |
| 187.0632@5.006003 | | -0.85 | | 188.07 | 5.01 | 100.00 | -43.41 | C11H9NO2 | Indoleacrylic acid | 5355219 | Good annotation | | 0.87 | |
| 187.0632@5.006002 | | -0.85 | | 205.10 | 5.01 | 100.00 | -77.44 | C11H9NO2 | Indoleacrylic acid | 5355219 | Good annotation | | 0.81 | |
| 170.1054@5.0219994 | 0.87 | -0.95 | -0.85 | 171.11 | 5.02 | 100.00 | -109.61 | C8H11NO2 | Pyrrolidin-2-one, N-crotonoyl- | 5365844 | Good annotation | 0.75 | 0.78 | 0.75 |
| 168.0874@5.085999 | 0.82 | -0.94 | | 169.10 | 5.09 | 100.00 | -142.24 | C8H9NO2 | 1-Prop-1-ynylpiperidine-2,6-dione | 66778840 | Good annotation | 0.68 | 0.72 | |
| 224.1524@5.218996 | | -0.87 | | 242.19 | 5.22 | 50.00 | -101.76 | C12H20N2O2 | Cyclo-(D-Pipecolinyl-L-isoleucine) | 139586736 | Good annotation | | 0.60 | |

Table J.2 Cont.

| Target | r of correlation for each foam quality parameter | | | MS2 details | Certainty of annotation | | | ID | | | Comment | Score | | |
|---|---|---|---|---|---|---|---|---|---|---|---|---|---|---|
| | Foam Ability | Drainage Rate | Disproportionation rate | Prec. m/z | Ret. time (min) | SIRIUS score | CSI score | Empirical Formula | Name | PubChem CID | | A | B | C |
| 310.0662@5.282997 | | -0.93 | | 311.07 | 5.28 | 99.50 | -163.26 | C13H12N4O4 | 4-(acetylamino)-N-(2,4-dioxo-1,2,3,4-tetrahydropyrimidin-5-yl)benzamide | 742581 | Good annotation | | 0.67 | |
| 168.0898@5.530005 | | -0.95 | -0.83 | 169.10 | 5.53 | 100.00 | -148.65 | C8H9NO2 | 1-Prop-1-ynylpiperidine-2,6-dione | 66778840 | Good annotation | | 0.71 | 0.67 |
| 226.0953@5.6830015 | | -0.89 | | 227.10 | 5.68 | 50.00 | -46.93 | C10H14N2O4 | 5-Oxo-L-prolyl-L-proline | 13306589 | Good annotation | | 0.71 | |
| 228.1109@5.705000 | | -0.91 | -0.82 | 251.10 | 5.70 | 99.99 | -138.24 | C12H11NO4 | 4-(4-Cyano-2-methoxyphenoxy)but-2-enoic acid | 76941101 | Good annotation | | 0.72 | 0.68 |
| 228.1109@5.704999 | | -0.91 | -0.82 | 229.12 | 5.70 | 33.33 | -23.79 | C10H16N2O4 | Pyroglutamylvaline | 152416 | Good annotation | | 0.71 | 0.67 |
| 170.1057@5.955995 | | -0.94 | -0.83 | 171.11 | 5.96 | 100.00 | -118.53 | C8H11NO2 | 1-Acetyl-3-ethylidenepyrrolidin-2-one | 131863766 | Good annotation | | 0.76 | 0.72 |
| 170.1057@5.955996 | | -0.94 | -0.83 | 193.10 | 5.96 | 50.00 | -86.55 | C10H12N2O2 | N,N'-Diacetyl-1,4-phenylenediamine | 67324 | Good annotation | | 0.65 | 0.62 |
| 170.1056@6.377009 | 0.83 | -0.95 | -0.83 | 171.11 | 6.38 | 100.00 | -102.01 | C8H11NO2 | 1-[(E)-but-1-enyl]pyrrolidine-2,5-dione | 21324946 | Good annotation | 0.76 | 0.79 | 0.76 |
| 284.1272@6.4840045 | 0.84 | -0.93 | -0.82 | 285.13 | 6.48 | 50.00 | -66.15 | C15H16N4O2 | Cyclo(-his-phe) | 7408279 | Good annotation | 0.66 | 0.69 | 0.65 |
| 149.084@6.500996 | 0.84 | -0.94 | -0.83 | 150.09 | 6.50 | 50.00 | -58.98 | C9H8O | 2-(4-Methylphenyl)ethen-1-one | 12787657 | Good annotation | 0.67 | 0.70 | 0.67 |
| 226.0952@6.5170083 | | -0.89 | -0.84 | 227.10 | 6.52 | 50.00 | -21.82 | C10H14N2O4 | L-pyroglutamyl-L-proline | 13306589 | Good annotation | | 0.76 | 0.74 |
| 224.1158@6.737 | 0.84 | -0.90 | -0.87 | 242.15 | 6.74 | 50.00 | -80.86 | C11H19N3O3 | (2S)-N-[(2S,3S)-1-amino-3-methyl-1- | 22799705 | Good annotation | 0.63 | 0.65 | 0.64 |

Table J.2 Cont.

| Target | r of correlation for each foam quality parameter | | | MS2 details | Certainty of annotation | | | ID | | | Comment | Score | | |
|---|---|---|---|---|---|---|---|---|---|---|---|---|---|---|
| | Foam Ability | Drainage Rate | Disproportionation rate | Prec. m/z | Ret. time (min) | SIRIUS score | CSI score | Empirical Formula | Name | PubChem CID | | A | B | C |
| 224.1158@6.738 | 0.84 | -0.90 | -0.87 | 225.12 | 6.74 | 49.99 | -160.29 | C11H13NO3 | oxopentan-2-yl]-5-oxopyrrolidine-2-carboxamide N-(2-oxopropyl)-2-phenoxyacetamide | 52145950 | Good annotation | 0.48 | 0.50 | 0.49 |
| 383.2531@6.9039956 | 0.82 | -0.93 | -0.86 | 384.26 | 6.90 | 85.72 | -156.28 | C18H33N5O4 | N-acetyl-D-lysyl-D-prolyl-D-valinamide | 9864830 | Good annotation | 0.60 | 0.64 | 0.61 |
| 292.1057@6.9639935 | | -0.91 | -0.84 | 293.11 | 6.96 | 100.00 | -38.12 | C14H16N2O5 | DL-pyroglutamyl-DL-tyrosine | 23422547 | Good annotation | | 0.90 | 0.88 |
| 112.0525@7.033997 | | -0.91 | | 113.06 | 7.03 | 100.00 | -31.73 | C6H8O2 | Sorbic acid | 643460 | Good annotation | | 0.91 | |
| 260.0832@7.2030026 | 0.83 | -0.86 | | 283.08 | 7.20 | 100.00 | -138.77 | C10H16N2O4S | 2-Acetamido-3-(4-cyanobutylsulfinyl)propanoic acid | 107768594 | Good annotation | 0.69 | 0.69 | |
| 260.0832@7.2030025 | 0.83 | -0.86 | | 261.09 | 7.20 | 100.00 | -46.78 | C10H16N2O4S | Pyroglutamylmethionine | 24695092 | Good annotation | 0.86 | 0.87 | |
| 292.1056@7.2299953 | | -0.86 | | 293.11 | 7.23 | 49.89 | -54.00 | C14H16N2O5 | Pyroglutamyltyrosine | 23422547 | Good annotation | | 0.69 | |
| 215.0943@7.364009 | | -0.86 | | 216.10 | 7.36 | 100.00 | -151.35 | C13H17NO4 | 4-[4-(2-Carboxyethyl)anilino]butanoic acid | 84012260 | Good annotation | | 0.67 | |
| 303.1581@7.575008 | | -0.94 | | 304.17 | 7.58 | 46.07 | -151.55 | C16H21N3O3 | N-acetyl-L-alanyl-L-proline anilide | 54044650 | Good annotation | | 0.52 | |
| 305.1738@7.5960045 | | -0.94 | | 306.18 | 7.60 | 47.70 | -138.43 | C16H20N2O3 | 4'-Methoxy-4-oxo-4-piperidinocrotonanilide | 5367887 | Good annotation | | 0.55 | |
| 236.116@7.6190047 | | -0.83 | | 237.12 | 7.62 | 100.00 | -157.84 | C12H13NO3 | CID 59890962 | 59890962 | Good annotation | | 0.65 | |
| 384.2369@7.700008 | | -0.92 | | 385.24 | 7.70 | 49.68 | -90.30 | C18H32N4O5 | DL-valyl-DL-prolyl-DL-valyl-DL-alanine | 20052804 | Good annotation | | 0.64 | |

Table J.2 Cont.

| Target | r of correlation for each foam quality parameter | | | MS2 details | Certainty of annotation | | | ID | | | Comment | Score | | |
|---|---|---|---|---|---|---|---|---|---|---|---|---|---|---|
| | Foam Ability | Drainage Rate | Disproportionation rate | Prec. m/z | Ret. time (min) | SIRIUS score | CSI score | Empirical Formula | Name | PubChem CID | | A | B | C |
| 342.19@8.01100 | | -0.83 | | 365.18 | 8.01 | 99.90 | -179.03 | C15H26N4O5 | L-asparagyl-L-prolyl-L-leucine | 145454240 | Good annotation | | 0.61 | |
| 342.19@8.01099 | | -0.83 | | 343.20 | 8.01 | 99.90 | -87.49 | C15H26N4O5 | L-asparagyl-L-leucyl-D-proline | 145454176 | Good annotation | | 0.78 | |
| 244.1784@8.12299 | | -0.91 | -0.83 | 245.19 | 8.12 | 50.00 | -68.40 | C12H24N2O3 | Leucylisoleucine | 435718 | Good annotation | | 0.68 | 0.65 |
| 260.0828@8.18901 | | -0.88 | | 261.09 | 8.19 | 50.00 | -61.26 | C10H16N2O4S | Pyroglutamylmethionine | 24695092 | Good annotation | | 0.68 | |
| 189.0789@8.265011 | | -0.91 | -0.85 | 190.09 | 8.27 | 33.33 | -131.03 | C11H13NO3 | 3-Hydroxy-4-(3-methoxyphenoxy)butanenitrile | 13010437 | Good annotation | | 0.50 | 0.49 |
| 266.1264@8.322999 | | | -0.86 | 267.13 | 8.32 | 50.00 | -170.84 | C13H15NO4 | 2-[4-[(2-Cyclopropylacetyl)amino]phenoxy]acetic acid | 63746061 | Good annotation | | | 0.47 |
| 204.0896@8.479993 | | -0.92 | | 205.10 | 8.48 | 50.00 | -115.90 | C11H12N2O2 | 3-Benzyl-piperazine-2,5-dione | 138409 | Good annotation | | 0.59 | |
| 384.237@8.510007 | | -0.94 | -0.83 | 385.24 | 8.51 | 49.07 | -69.42 | C18H32N4O5 | L-isoleucyl-L-prolyl-L-valyl-glycine | 10407686 | Good annotation | | 0.68 | 0.65 |
| 303.1581@8.619996 | | -0.91 | | 304.17 | 8.62 | 49.96 | -156.14 | C16H18N2O3 | 2-(2-oxo-3-phenylpropyl)-6,7,8,8a-tetrahydro-3H-pyrrolo[1,2-a]pyrazine-1,4-dione | 79927417 | Good annotation | | 0.52 | |
| 184.121@8.619996 | | -0.94 | -0.82 | 185.13 | 8.62 | 100.00 | -132.77 | C9H13NO2 | N-but-2-ynyl-4-oxopentanamide | 115866920 | Good annotation | | 0.74 | 0.69 |
| 184.1211@9.030014 | 0.82 | -0.95 | -0.82 | 185.13 | 9.03 | 100.00 | -128.20 | C9H20N2O4 | 2-amino-N-[1,3-dihydroxy-2-(hydroxymethyl)propan-2-yl]-2-methylbutanamide | 107852881 | Good annotation | 0.70 | 0.75 | 0.70 |

Table J.2 Cont.

| Target | r of correlation for each foam quality parameter | | | MS2 details | Certainty of annotation | | | ID | | | Comment | Score | | |
|---|---|---|---|---|---|---|---|---|---|---|---|---|---|---|
| | Foam Ability | Drainage Rate | Disproportionation rate | Prec. m/z | Ret. time (min) | SIRIUS score | CSI score | Empirical Formula | Name | PubChem CID | | A | B | C |
| 182.1055@9.109006 | | -0.92 | -0.82 | 183.11 | 9.11 | 50.00 | -98.84 | C9H14N2O2 | 3-Cyclopropyl-6-ethylpiperazine-2,5-dione | 22147538 | Good annotation | | 0.62 | 0.59 |
| 163.0996@9.2059965 | | -0.95 | | 164.11 | 9.21 | 100.00 | -120.38 | C10H15NO2 | 5-(1-Hydroxyethyl)-1,2,3-trimethylpyridin-4-one | 68223760 | Good annotation | | 0.76 | |
| 198.1367@9.2109995 | | -0.93 | | 199.14 | 9.21 | 100.00 | -144.28 | C10H15NO2 | 2-(Butylamino)benzene-1,4-diol | 67785668 | Good annotation | | 0.71 | |
| 113.0852@9.228012 | | -0.89 | | 136.08 | 9.23 | 50.00 | -50.87 | C8H6O | Phenyl ketene | 137963 | Good annotation | | 0.70 | |
| 113.0852@9.228013 | | -0.89 | | 114.09 | 9.23 | 100.00 | -64.92 | C6H11NO | CID 60038858 | 60038858 | Good annotation | | 0.84 | |
| 262.095@9.369996 | 0.84 | -0.88 | -0.92 | 263.10 | 9.37 | 50.00 | -147.76 | C13H14N2O4 | 2-(5-Benzyl-3,6-dioxopiperazin-2-yl)acetic acid | 119494 | Good annotation | 0.50 | 0.52 | 0.53 |
| 333.1717@9.510007 | | -0.84 | | 334.18 | 9.51 | 49.38 | -81.58 | C14H27N3O4S | L-Alanyl-L-methionyl-L-leucine | 145453639 | Good annotation | | 0.63 | |
| 340.2472@9.518002 | | -0.88 | -0.85 | 341.25 | 9.52 | 49.94 | -106.88 | C17H32N4O3 | (2S)-1-[(2S)-2-[(2S)-2-aminopropanamido]-3-methylbutanoyl]-N-(2-methylpropyl)pyrrolidine-2-carboxamide | 11450670 | Good annotation | | 0.60 | 0.59 |
| 243.0894@9.872995 | | -0.82 | | 244.10 | 9.87 | 99.98 | -117.85 | C14H13NO3 | 2-(4-Hydroxy-2-methylphenylamino)benzoic acid | 13371479 | Good annotation | | 0.72 | |
| 260.1159@9.872994 | | -0.86 | | 261.12 | 9.87 | 33.33 | -31.09 | C14H16N2O3 | Cyclo(L-pro-L-tyr) | 119404 | Good annotation | | 0.67 | |
| 243.0894@9.872994 | | -0.82 | | 261.12 | 9.87 | 33.33 | -31.94 | C14H16N2O3 | Cyclo(L-pro-L-tyr) | 119404 | Good annotation | | 0.66 | |

Table J.2 Cont.

| Target | r of correlation for each foam quality parameter | | | MS2 details | Certainty of annotation | | | ID | | | Comment | Score | | |
|---|---|---|---|---|---|---|---|---|---|---|---|---|---|---|
| | Foam Ability | Drainage Rate | Disproportionation rate | Prec. m/z | Ret. time (min) | SIRIUS score | CSI score | Empirical Formula | Name | PubChem CID | | A | B | C |
| 194.1055@9.872994 | | -0.93 | -0.84 | 195.11 | 9.87 | 50.00 | -46.19 | C10H14N2O2 | Cyclo(Pro-Pro) | 529063 | Good annotation | | 0.72 | 0.70 |
| 260.1159@9.872995 | | -0.86 | | 283.11 | 9.87 | 100.00 | -149.22 | C14H16N2O3 | N-[4-(3-Oxobutanamido)phenyl]cyclopropanecarboxamide | 18071598 | Good annotation | | 0.68 | |
| 242.1265@9.924997 | | -0.90 | -0.87 | 265.12 | 9.92 | 100.00 | -144.40 | C11H18N2O4 | 6-[2-Carboxyethyl(cyanomethyl)amino]hexanoic acid | 82328524 | Good annotation | | 0.70 | 0.69 |
| 242.1265@9.924996 | | -0.90 | -0.87 | 243.13 | 9.92 | 50.00 | -72.59 | C11H18N2O4 | (2S)-3,6-Dioxo-5beta-isobutylpiperazine-2beta-propanoic acid | 16098234 | Good annotation | | 0.67 | 0.66 |
| 196.1211@9.935004 | | -0.91 | | 197.13 | 9.94 | 50.00 | -33.89 | C10H16N2O2 | Pyrrolo(1,2-a)pyrazine-1,4-dione, hexahydro-3-(1-methylethyl)- | 98951 | Good annotation | | 0.74 | |
| 165.1153@9.947999 | | -0.88 | -0.84 | 166.12 | 9.95 | 100.00 | -137.78 | C10H19NO3 | 6-(2-Methylpropylamino)-6-oxohexanoic acid | 43529330 | Good annotation | | 0.70 | 0.69 |
| 384.2372@10.17101 | | -0.94 | | 385.24 | 10.17 | 49.78 | -50.39 | C18H32N4O5 | L-isoleucyl-L-prolyl-L-valyl-glycine | 10407686 | Good annotation | | 0.72 | |
| 262.1315@10.254016 | 0.82 | -0.95 | | 263.14 | 10.25 | 100.00 | -162.19 | C14H15NO3 | 2-[4-[[(2E,4E)-hexa-2,4-dienoyl]amino]phenyl]acetic acid | 24702717 | Good annotation | 0.64 | 0.68 | |
| 218.1052@10.299999 | 0.82 | -0.95 | -0.82 | 219.11 | 10.30 | 100.00 | -163.33 | C12H18N2O4 | 5-(Hex-1-yn-3-ylcarbamoylamino)-5-oxopentanoic acid | 106231113 | Good annotation | 0.64 | 0.68 | 0.64 |
| 196.1211@10.364011 | 0.86 | -0.95 | -0.84 | 197.13 | 10.36 | 100.00 | -31.88 | C10H16N2O2 | cyclo(D)-Pro-(D)-Val | 6545869 | Good annotation | 0.89 | 0.93 | 0.89 |

Table J.2 Cont.

| Target | r of correlation for each foam quality parameter | | | MS2 details | Certainty of annotation | | | ID | | | Comment | Score | | |
|---|---|---|---|---|---|---|---|---|---|---|---|---|---|---|
| | Foam Ability | Drainage Rate | Disproportionation rate | Prec. m/z | Ret. time (min) | SIRIUS score | CSI score | Empirical Formula | Name | PubChem CID | | A | B | C |
| 196.1211@10.364012 | 0.86 | -0.95 | -0.84 | 219.11 | 10.36 | 50.00 | -105.27 | C12H14N2O2 | 3-Benzyl-6-methyl-2,5-piperazinedione | 139767 | Good annotation | 0.59 | 0.62 | 0.59 |
| 276.1112@10.452014 | | -0.92 | | 277.12 | 10.45 | 50.00 | -76.19 | C14H16N2O4 | Pyroglutamylphenylalanine | 13961383 | Good annotation | | 0.67 | |
| 485.2848@10.557006 | 0.83 | -0.93 | -0.86 | 486.29 | 10.56 | 40.94 | -173.27 | C22H39N5O7 | 2-cyclohexyl-L-glycyl-L-glutaminyl-L-seryl-L-leucine | 101207480 | Good annotation | 0.43 | 0.46 | 0.43 |
| 260.117@10.560008 | | -0.89 | | 261.12 | 10.56 | 33.33 | -40.55 | C14H16N2O3 | Cyclo(L-pro-L-tyr) | 119404 | Good annotation | | 0.67 | |
| 276.1473@10.588992 | | -0.95 | -0.83 | 277.15 | 10.59 | 100.00 | -138.43 | C15H17NO3 | (E)-N-(but-3-yn-1-yl)-3-(3,4-dimethoxyphenyl)acrylamide | 90537886 | Good annotation | | 0.73 | 0.69 |
| 151.0632@10.637002 | | -0.87 | | 152.07 | 10.64 | 50.00 | -68.70 | C8H11NO3 | Pyridoxine | 1054 | Good annotation | | 0.66 | |
| 384.237@10.67299 | | -0.93 | | 385.24 | 10.67 | 48.40 | -61.65 | C18H32N4O5 | DL-leucyl-DL-prolyl-DL-valyl-glycine | 18300322 | Good annotation | | 0.69 | |
| 218.1054@10.739011 | 0.87 | -0.96 | -0.86 | 219.11 | 10.74 | 100.00 | -144.04 | C12H11NO2 | 1-(2-Vinylphenyl)pyrrolidine-2,5-dione | 85741816 | Good annotation | 0.69 | 0.72 | 0.69 |
| 457.2899@10.780017 | 0.84 | -0.91 | -0.84 | 458.30 | 10.78 | 35.17 | -67.72 | C21H39N5O6 | L-alanyl-L-leucyl-L-alanyl-L-leucyl-L-alanine | 16730298 | Good annotation | 0.60 | 0.63 | 0.61 |
| 242.1266@10.818982 | | -0.89 | -0.82 | 243.13 | 10.82 | 50.00 | -56.32 | C11H18N2O4 | Pyroglutamylisoleucine | 21405068 | Good annotation | | 0.69 | 0.67 |
| 242.1266@10.818983 | | -0.89 | -0.82 | 265.12 | 10.82 | 100.00 | -133.48 | C11H18N2O4 | N,N'-bis(2-oxopropyl)pentanediamide | 89037982 | Good annotation | | 0.72 | 0.69 |
| 198.1367@10.922986 | | -0.90 | | 199.14 | 10.92 | 100.00 | -158.39 | C10H15NO2 | 1,3-Di(propan-2-yl)pyrrole-2,5-dione | 58403106 | Good annotation | | 0.67 | |

Table J.2 Cont.

| Target | r of correlation for each foam quality parameter | | | MS2 details | Certainty of annotation | | | ID | | | Comment | Score | | |
|---|---|---|---|---|---|---|---|---|---|---|---|---|---|---|
| | Foam Ability | Drainage Rate | Disproportionation rate | Prec. m/z | Ret. time (min) | SIRIUS score | CSI score | Empirical Formula | Name | PubChem CID | | A | B | C |
| 341.2312@11.069994 | | -0.94 | -0.84 | 342.24 | 11.07 | 49.97 | -40.80 | C17H31N3O4 | L-isoleucyl-L-prolyl-L-leucine | 67308769 | Good annotation | | 0.74 | 0.70 |
| 199.0996@11.185011 | | -0.82 | | 200.11 | 11.19 | 50.00 | -59.82 | C13H10O | Benzophenone | 3102 | Good annotation | | 0.66 | |
| 478.2787@11.30101 | | -0.92 | | 479.29 | 11.30 | 42.33 | -62.98 | C24H38N4O6 | L-Tyrosyl-L-valyl-L-valyl-L-valine | 71428846 | Good annotation | | 0.66 | |
| 654.3487@11.407997 | | -0.83 | | 655.36 | 11.41 | 26.44 | -178.61 | C32H46N8O7 | L-tyrosyl-glycyl-L-arginyl-L-phenylalanyl-L-leucine | 71350048 | Good annotation | | 0.37 | |
| 259.1129@11.427989 | | -0.82 | -0.86 | 277.15 | 11.43 | 100.00 | -172.68 | C15H17NO3 | 5-[1-(4-Hydroxyphenyl)propan-2-ylamino]benzene-1,3-diol | 69942410 | Good annotation | | 0.62 | 0.63 |
| 212.1524@11.591002 | | -0.94 | | 213.16 | 11.59 | 100.00 | -150.68 | C11H17NO2 | N,N-bis(prop-1-ynoxy)pentan-1-amine | 89823519 | Good annotation | | 0.70 | |
| 276.1473@11.642004 | | -0.86 | | 277.15 | 11.64 | 50.00 | -94.87 | C15H20N2O3 | Cyclo(D-Tyr-L-Leu) | 124350923 | Good annotation | | 0.61 | |
| 420.237@11.645997 | | -0.89 | -0.84 | 421.24 | 11.65 | 48.55 | -62.47 | C21H32N4O5 | L-phenylalanyl-L-alanyl-L-leucyl-L-alanine | 10180448 | Good annotation | | 0.68 | 0.66 |
| 324.1793@11.750987 | | -0.92 | | 325.19 | 11.75 | 100.00 | -124.38 | C15H24N4O4 | 5-oxo-N-[5-[[(2S)-5-oxopyrrolidine-2-carbonyl]amino]pentyl]pyrrolidine-2-carboxamide | 54264135 | Good annotation | | 0.74 | |
| 341.2312@11.758007 | | -0.86 | | 342.24 | 11.76 | 48.15 | -64.58 | C17H31N3O4 | 2-{[1-(2-Amino-3-methyl-pentanoyl)-pyrrolidine-2-carbonyl]-amino}-3-methyl-pentanoic acid | 3107 | Good annotation | | 0.66 | |

Table J.2 Cont.

| Target | r of correlation for each foam quality parameter | | | MS2 details | Certainty of annotation | | | ID | | | Comment | Score | | |
|---|---|---|---|---|---|---|---|---|---|---|---|---|---|---|
| | Foam Ability | Drainage Rate | Disproportionation rate | Prec. m/z | Ret. time (min) | SIRIUS score | CSI score | Empirical Formula | Name | PubChem CID | | A | B | C |
| 276.111@11.857011 | | -0.89 | -0.83 | 277.12 | 11.86 | 100.00 | -31.41 | C14H16N2O4 | DL-pyroglutamyl-DL-phenylalanine | 13961383 | Good annotation | | 0.90 | 0.89 |
| 384.237@11.864993 | | -0.94 | -0.84 | 385.24 | 11.86 | 35.63 | -66.42 | C18H32N4O5 | L-isoleucyl-L-prolyl-L-valyl-glycine | 10407686 | Good annotation | | 0.64 | 0.61 |
| 264.1476@11.887985 | | -0.90 | | 265.15 | 11.89 | 49.99 | -50.87 | C14H20N2O3 | L-valyl-L-phenylalanine | 6993120 | Good annotation | | 0.71 | |
| 210.1368@12.168003 | | -0.94 | | 211.14 | 12.17 | 50.00 | -12.61 | C11H18N2O2 | Cyclo(d-leucyl-d-prolyl) | 129851101 | Good annotation | | 0.79 | |
| 341.1948@12.208988 | | -0.83 | | 364.18 | 12.21 | 63.60 | -165.16 | C16H28N3O5+ | [Bis(1,1,4-trimethyl-4-nitro-2-pentenyl)aminooxy]radical | 102095525 | Good annotation | | 0.52 | |
| 341.1948@12.208988 | | -0.83 | | 342.20 | 12.21 | 95.91 | -145.97 | C16H27N3O5 | (2S)-2-[[(2S)-2-[[(2S)-1-acetylpyrrolidine-2-carbonyl]amino]propanoyl]amino]-4-methylpentanoic acid | 53635786 | Good annotation | | 0.66 | |
| 341.1948@12.278 | | -0.83 | -0.84 | 364.18 | 12.28 | 48.27 | -159.72 | C16H27N3O5 | (2S)-2-[[(2S)-2-[[(2S)-1-acetylpyrrolidine-2-carbonyl]amino]propanoyl]amino]-4-methylpentanoic acid | 53635786 | Good annotation | | 0.47 | 0.48 |
| 341.1948@12.278 | | -0.83 | -0.84 | 342.20 | 12.28 | 99.73 | -117.99 | C16H27N3O5 | (2S)-2-[[(2S)-2-[[(2S)-1-acetylpyrrolidine-2-carbonyl]amino]propanoyl]amino]-4-methylpentanoic acid | 53635786 | Good annotation | | 0.72 | 0.73 |
| 213.1151@12.336016 | | -0.87 | | 214.12 | 12.34 | 100.00 | -142.49 | C14H19NO3 | 6-[(2-Phenylacetyl)amino]hexanoic acid | 1612319 | Good annotation | | 0.69 | |

Table J.2 Cont.

| Target | r of correlation for each foam quality parameter | | | MS2 details | Certainty of annotation | | | ID | | | Comment | Score | | |
|---|---|---|---|---|---|---|---|---|---|---|---|---|---|---|
| | Foam Ability | Drainage Rate | Disproportionation rate | Prec. m/z | Ret. time (min) | SIRIUS score | CSI score | Empirical Formula | Name | PubChem CID | | A | B | C |
| 414.2841@12.368007 | | -0.91 | -0.85 | 415.29 | 12.37 | 49.15 | -35.27 | C20H38N4O5 | DL-alanyl-DL-leucyl-DL-valyl-DL-leucine | 18236933 | Good annotation | | 0.73 | 0.71 |
| 437.2634@12.529009 | | -0.82 | | 438.27 | 12.53 | 93.09 | -119.58 | C21H35N5O5 | DL-prolyl-DL-lysyl-DL-prolyl-DL-proline | 20014119 | Good annotation | | 0.70 | |
| 437.2634@12.529009 | | -0.82 | | 460.25 | 12.53 | 99.96 | -176.86 | C21H35N5O5 | N-acryloyl-L-alanyl-L-prolyl-glycyl-L-leucine ethylamide | 122467380 | Good annotation | | 0.61 | |
| 212.1524@12.567994 | | -0.95 | | 213.16 | 12.57 | 100.00 | -75.33 | C11H20N2O2 | 2,5-Piperazinedione, 3-(1-methylethyl)-6-(1-methylpropyl)- | 10443165 | Good annotation | | 0.84 | |
| 210.1367@12.57601 | 0.84 | -0.94 | -0.83 | 211.14 | 12.58 | 50.00 | -25.38 | C11H18N2O2 | Cyclo(d-leucyl-d-prolyl) | 129851101 | Good annotation | 0.73 | 0.77 | 0.73 |
| 398.2526@12.803989 | | -0.88 | -0.85 | 399.26 | 12.80 | 49.10 | -48.12 | C19H34N4O5 | glycyl-DL-leucyl-DL-leucyl-DL-prolin | 18488888 | Good annotation | | 0.70 | 0.69 |
| 246.1366@12.86901 | | -0.86 | -0.85 | 247.14 | 12.87 | 100.00 | -123.63 | C14H18N2O2 | C21H35N5O5 | 139766 | Good annotation | | 0.72 | 0.72 |
| 442.3153@12.918 | | -0.90 | | 443.32 | 12.92 | 15.46 | -56.08 | C22H42N4O5 | DL-leucyl-DL-valyl-DL-valyl-DL-leucine | 18302316 | Good annotation | | 0.58 | |
| 471.2842@12.93102 | | -0.89 | -0.82 | 472.29 | 12.93 | 49.39 | -140.38 | C25H34N4O4 | Cyclo-[phenylalanyl-prolyl-leucyl-prolyl] | 24851291 | Good annotation | | 0.54 | 0.51 |
| 196.0998@12.951003 | | -0.84 | | 197.11 | 12.95 | 50.00 | -33.02 | C13H12N2 | 1,3-dimethyl-9H-pyrido[3,4-b]indole | 5342313 | Good annotation | | 0.72 | |
| 244.1214@13.081014 | | -0.93 | | 245.13 | 13.08 | 50.00 | -26.86 | C14H16N2O2 | Cyclo(D-Pro-L-Phe-) | 6992198 | Good annotation | | 0.76 | |
| 244.1214@13.081014 | | -0.93 | | 267.11 | 13.08 | 33.33 | -118.63 | C16H14N2O2 | 1-(10-Acetylphenazin-5-yl)ethanone | 345317 | Good annotation | | 0.53 | |
| 192.0787@13.147988 | | -0.90 | | 215.07 | 13.15 | 100.00 | -99.95 | C11H12O3 | 4-(2-Hydroxyphenyl)-2-methylidenebutanoic acid | 17917118 | Good annotation | | 0.78 | |

Table J.2 Cont.

| Target | r of correlation for each foam quality parameter | | | MS2 details | Certainty of annotation | | | ID | | | Comment | Score | | |
|---|---|---|---|---|---|---|---|---|---|---|---|---|---|---|
| | Foam Ability | Drainage Rate | Disproportionation rate | Prec. m/z | Ret. time (min) | SIRIUS score | CSI score | Empirical Formula | Name | PubChem CID | | A | B | C |
| 192.0787@13.147988 | | -0.90 | | 193.09 | 13.15 | 99.63 | -79.09 | C11H12O3 | (2E,4E,6E,8E)-10-oxoundeca-2,4,6,8-tetraenoic acid | 134974073 | Good annotation | | 0.82 | |
| 251.152@13.14901 | | -0.91 | | 252.16 | 13.15 | 49.99 | -85.73 | C14H18O3 | 7-Oxo-8-phenyloctanoic acid | 12431179 | Good annotation | | 0.64 | |
| 226.168@13.221995 | | -0.86 | | 227.18 | 13.22 | 50.00 | -61.59 | C12H22N2O2 | Cyclo(L-leucyl-L-leucyl) | 192731 | Good annotation | | 0.67 | |
| 471.2842@13.418008 | | -0.91 | -0.82 | 472.29 | 13.42 | 49.41 | -133.42 | C25H34N4O4 | Cyclo-[phenylalanyl-prolyl-leucyl-prolyl] | 24851291 | Good annotation | | 0.55 | 0.53 |
| 456.3308@13.462006 | 0.82 | -0.92 | -0.83 | 457.34 | 13.46 | 29.03 | -82.51 | C23H44N4O5 | DL-valyl-DL-isoleucyl-DL-isoleucyl-DL-leucine | 20050632 | Good annotation | 0.55 | 0.58 | 0.55 |
| 226.168@13.482011 | | -0.87 | | 227.18 | 13.48 | 50.00 | -41.56 | C12H24N2O3 | Leu-Leu | 76807 | Good annotation | | 0.71 | |
| 454.3155@13.494011 | | -0.87 | | 455.32 | 13.49 | 49.57 | -36.43 | C23H42N4O5 | DL-isoleucyl-DL-prolyl-DL-isoleucyl-DL-leucine | 18297187 | Good annotation | | 0.72 | |
| 244.1211@13.551016 | 0.82 | -0.95 | -0.85 | 245.13 | 13.55 | 100.00 | -25.51 | C14H16N2O2 | Cyclo(D-Pro-L-Phe-) | 6992198 | Good annotation | 0.89 | 0.93 | 0.90 |
| 244.1211@13.551016 | 0.82 | -0.95 | -0.85 | 267.11 | 13.55 | 22.22 | -117.28 | C16H16N2O3 | N-(4-methoxyphenyl)-N'-(2-methylphenyl)oxamide | 44995879 | Good annotation | 0.46 | 0.51 | 0.47 |
| 246.1368@13.607017 | 0.84 | -0.96 | -0.86 | 269.13 | 13.61 | 92.86 | -125.33 | C14H18N2O2 | 1,1'-(2,3-Dihydroquinoxaline-1,4-diyl)dipropan-1-one | 265693 | Good annotation | 0.69 | 0.73 | 0.70 |
| 246.1368@13.607017 | 0.84 | -0.96 | -0.86 | 247.14 | 13.61 | 100.00 | -68.83 | C14H18N2O2 | 3-Benzyl-6-isopropyl-2,5-piperazinedione | 139766 | Good annotation | 0.82 | 0.86 | 0.82 |
| 342.1581@13.75199 | | -0.92 | -0.86 | 343.17 | 13.75 | 49.79 | -159.70 | C19H19NO4 | 2-[3-(4-Methoxy-phenyl)- | 20199861 | Good annotation | | 0.51 | 0.49 |

Table J.2 Cont.

| Target | r of correlation for each foam quality parameter | | | MS2 details | Certainty of annotation | | | ID | | | Comment | Score | | |
|---|---|---|---|---|---|---|---|---|---|---|---|---|---|---|
| | Foam Ability | Drainage Rate | Disproportionation rate | Prec. m/z | Ret. time (min) | SIRIUS score | CSI score | Empirical Formula | Name | PubChem CID | | A | B | C |
| | | | | | | | | | acryloylamino]-3-phenyl-propionic acid | | | | | |
| 226.168@13.796012 | | -0.94 | | 227.18 | 13.80 | 100.00 | -26.04 | C12H24N2O3 | L-leucyl-L-leucine | 76807 | Good annotation | | 0.93 | |
| 428.2995@13.801016 | | -0.89 | -0.85 | 429.31 | 13.80 | 89.01 | -114.79 | C21H40N4O5 | DL-alanyl-DL-isoleucyl-DL-isoleucyl-DL-leucine | 18236344 | Good annotation | | 0.71 | 0.70 |
| 226.1683@13.807006 | 0.82 | -0.95 | -0.82 | 227.18 | 13.81 | 100.00 | -35.50 | C12H24N2O3 | L-leucyl-L-leucine | 76807 | Good annotation | 0.87 | 0.92 | 0.88 |
| 260.1525@13.951014 | | -0.92 | -0.83 | 261.16 | 13.95 | 100.00 | -58.32 | C15H20N2O2 | Cyclo(Phe-Leu) | 562691 | Good annotation | | 0.87 | 0.84 |
| 260.1525@13.951014 | | -0.92 | -0.83 | 283.14 | 13.95 | 75.83 | -168.41 | C15H20N2O2 | 4-[3-[2-(Hydroxymethyl)pyrrolidin-1-yl]propoxy]benzonitrile | 55137251 | Good annotation | | 0.58 | 0.55 |
| 260.1524@14.3310175 | | -0.95 | -0.84 | 261.16 | 14.33 | 100.00 | -48.00 | C15H20N2O2 | Cyclo(Phe-Leu) | 562691 | Good annotation | | 0.89 | 0.86 |
| 195.0898@14.360991 | | -0.82 | -0.85 | 196.10 | 14.36 | 50.00 | -125.14 | C10H15NO4 | 5-Cyanoazelaic acid | 122230606 | Good annotation | | 0.54 | 0.55 |
| 195.0898@14.360991 | | -0.82 | -0.85 | 218.08 | 14.36 | 46.75 | -94.52 | C12H8O3 | Dibenzofuran-3,7-diol | 654792 | Good annotation | | 0.59 | 0.60 |
| 488.2994@14.484007 | | -0.92 | | 489.31 | 14.48 | 15.72 | -109.70 | C26H40N4O5 | DL-leucyl-DL-phenylalanyl-DL-leucyl-DL-proline | 18299751 | Good annotation | | 0.49 | |
| 260.1524@14.484987 | 0.82 | -0.94 | -0.88 | 261.16 | 14.48 | 100.00 | -50.89 | C15H20N2O2 | Cyclo(Phe-Leu) | 562691 | Good annotation | 0.85 | 0.89 | 0.86 |
| 260.1524@14.484987 | 0.82 | -0.94 | -0.88 | 283.14 | 14.48 | 99.99 | -139.12 | C15H20N2O2 | N-[4-(2-methylpropanamido)phenyl]cyclobutanecarboxamide | 26679959 | Good annotation | 0.68 | 0.72 | 0.70 |

Table J.2 Cont.

| Target | r of correlation for each foam quality parameter | | | MS2 details | Certainty of annotation | | | ID | | | Comment | Score | | |
|---|---|---|---|---|---|---|---|---|---|---|---|---|---|---|
| | Foam Ability | Drainage Rate | Disproportionation rate | Prec. m/z | Ret. time (min) | SIRIUS score | CSI score | Empirical Formula | Name | PubChem CID | | A | B | C |
| 294.1365@15.196012 | | -0.93 | | 295.14 | 15.20 | 99.99 | -75.46 | C18H18N2O2 | Cyclo(D-Phe-L-Phe-) | 1477298 | Good annotation | | 0.84 | |
| 567.363@15.362023 | | -0.89 | -0.90 | 568.37 | 15.36 | 96.90 | -155.11 | C28H49N5O7 | Ac-Ser-Ala-Val-Leu-Cha-al | 56849696 | Good annotation | | 0.67 | 0.67 |
| 567.363@15.362023 | | -0.89 | -0.90 | 590.35 | 15.36 | 56.67 | -164.02 | C28H49N5O7 | Cyclo(L-Leu-L-Leu-L-Leu-L-Leu-L-betaAsp-) | 101448932 | Good annotation | | 0.51 | 0.52 |
| 330.2404@15.637983 | | -0.87 | | 331.25 | 15.64 | 75.87 | -30.10 | C18H34O5 | CID 153003 | 153003 | Good annotation | | 0.82 | |
| 567.363@15.816008 | | -0.88 | -0.83 | 590.35 | 15.82 | 99.63 | -166.34 | C28H49N5O7 | Nodupetide | 132494469 | Good annotation | | 0.65 | 0.63 |
| 332.256@15.906991 | | -0.89 | | 333.26 | 15.91 | 100.00 | -34.88 | C18H36O5 | 11,12,13-Trihydroxyoctadecanoic acid | 129854424 | Good annotation | | 0.90 | |
| 375.2523@16.364012 | | 0.84 | | 393.29 | 16.36 | 99.35 | -156.43 | C21H33N3O3 | N-butyl-1-[2-[(2-methoxyphenyl)methyl-methylamino]-2-oxoethyl]piperidine-4-carboxamide | 86984107 | Good annotation | | 0.65 | |
| 375.2523@16.364012 | | 0.84 | | 398.24 | 16.36 | 99.62 | -134.81 | C21H33N3O3 | N-[3,5-bis(pentanoylamino)phenyl]pentanamide | 58436291 | Good annotation | | 0.69 | |
| 375.2523@16.364012 | | 0.84 | | 376.26 | 16.36 | 99.93 | -155.70 | C21H33N3O3 | 1,3,5-Tris(2,2-dimethylpropionylamino)benzene | 53421640 | Good annotation | | 0.66 | |

# Appendix K: MS1 and MS2 spectra of key foam targets

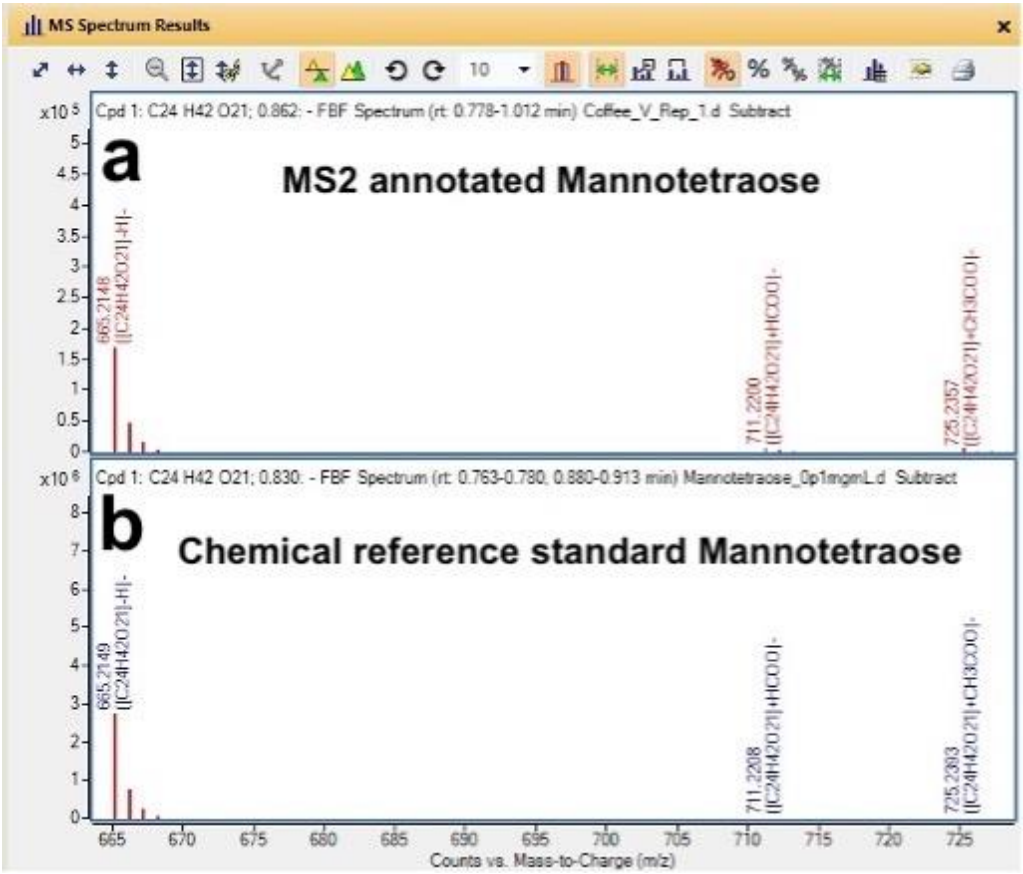



Figure K-1(a) MS1 spectra of MS2 annotated Mannotetraose.(b) MS1 spectra of chemical reference standard of Mannotetraose




Figure K-2 (a) and (b) MS1 spectra of chemical reference standard of Cyclo(-Phe-Phe). (c) and (d) MS1 spectra of MS2 annotated Cyclo(-Phe-Phe)

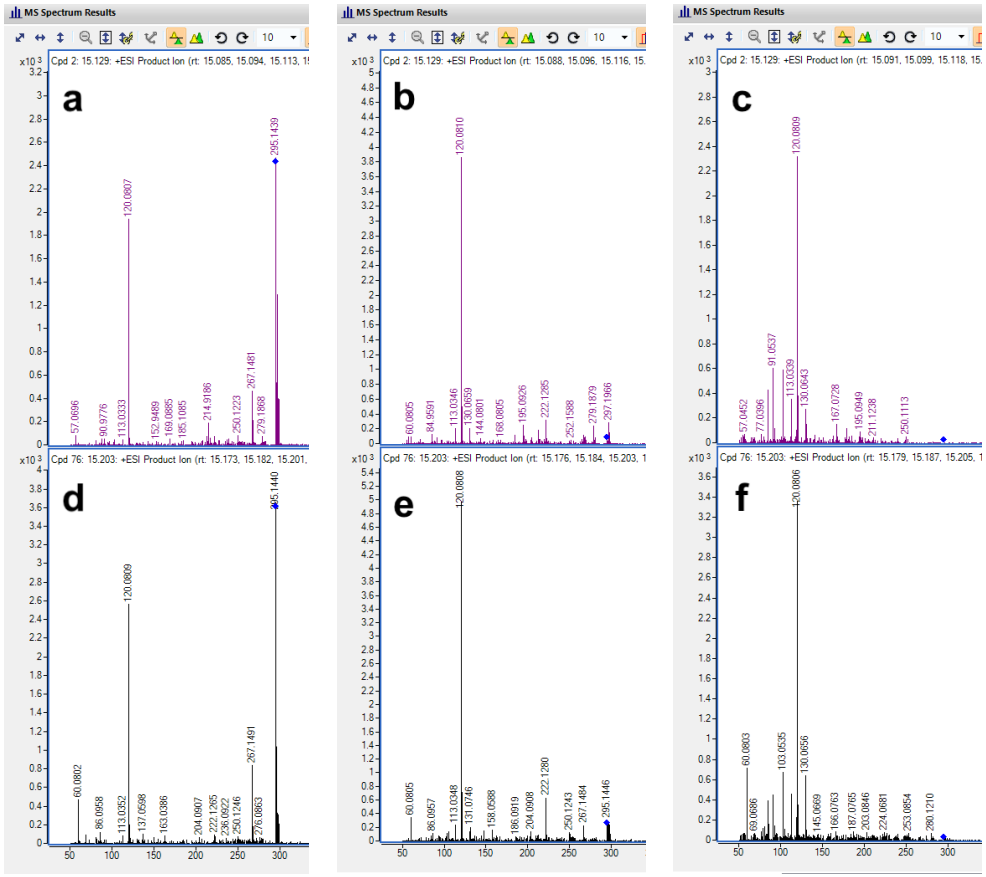



Figure K-3 (a,b,c) MS2 spectra of chemical reference standard of Cyclo(-Phe-Phe) at 10V,20V and 40V. (d,e,f) MS2 spectra of MS2 annotated Cyclo(-Phe-Phe) at at 10V,20V and 40V.

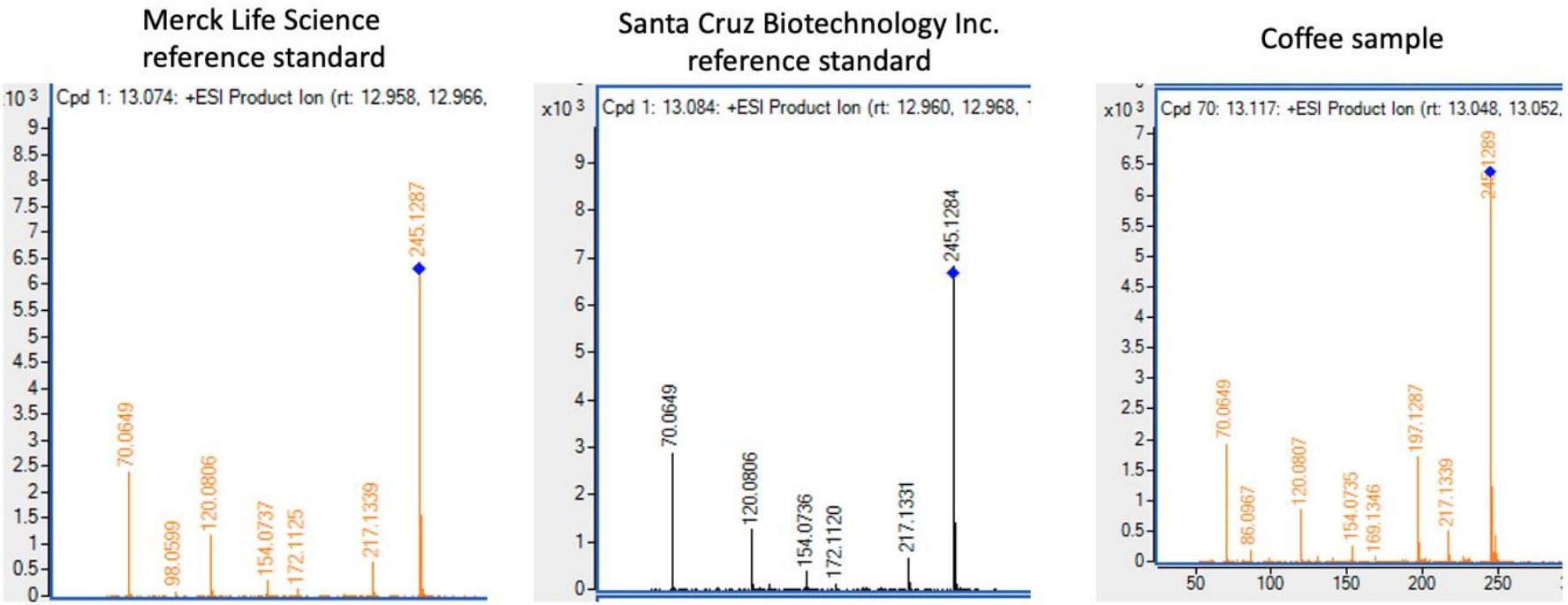



Figure K-4 Cyclo(-Phe-Pro) MS2 spectra @13.08 min @10V

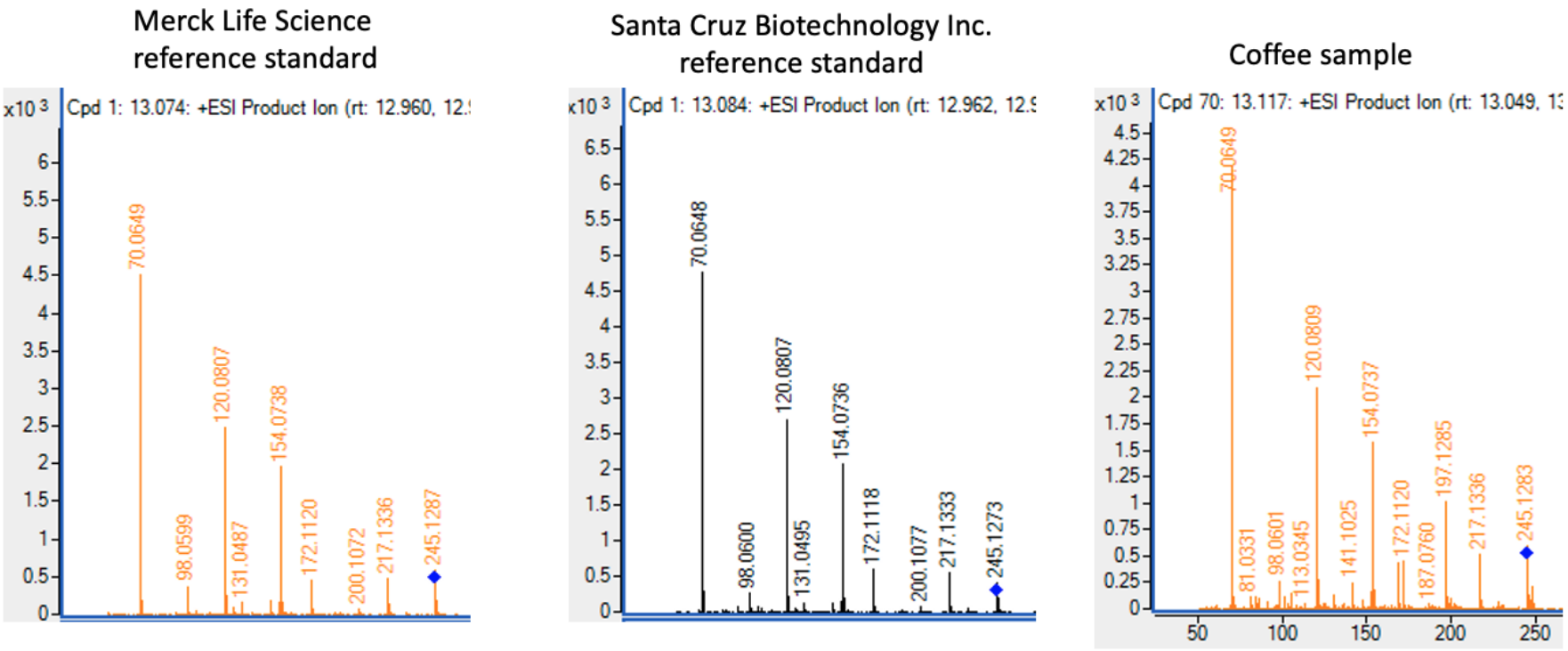



Figure K-5 Cyclo(-Phe-Pro) MS2 spectra @13.08 min @20V

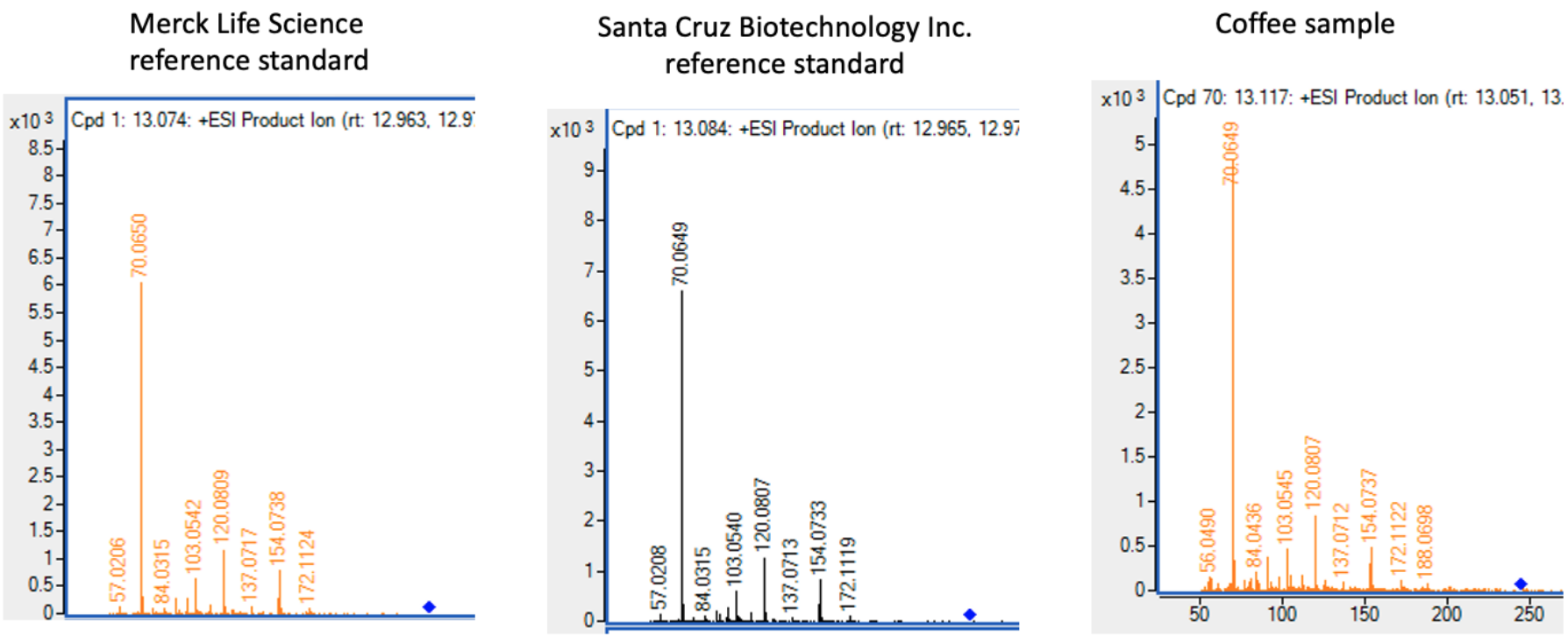



Figure K-6 Cyclo(-Phe-Pro) MS2 spectra @13.08 min @40V

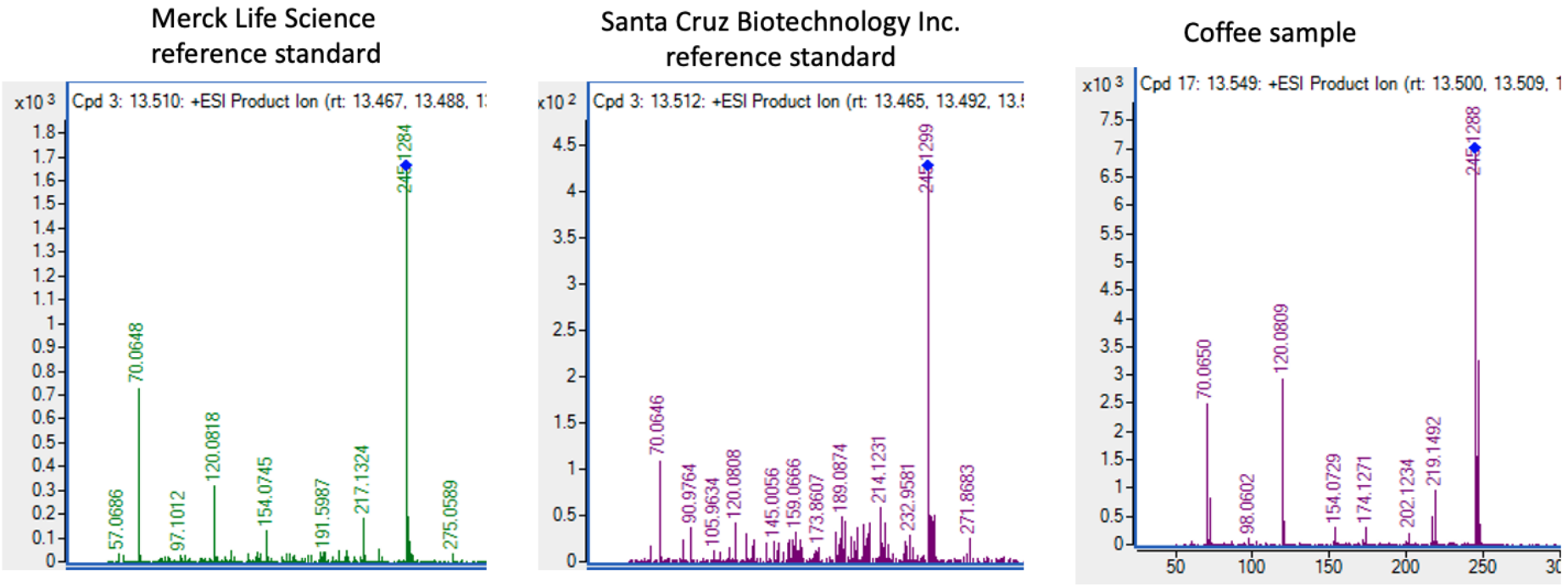



Figure K-7 Cyclo(-Phe-Pro) MS2 spectra @13.55 min @10V

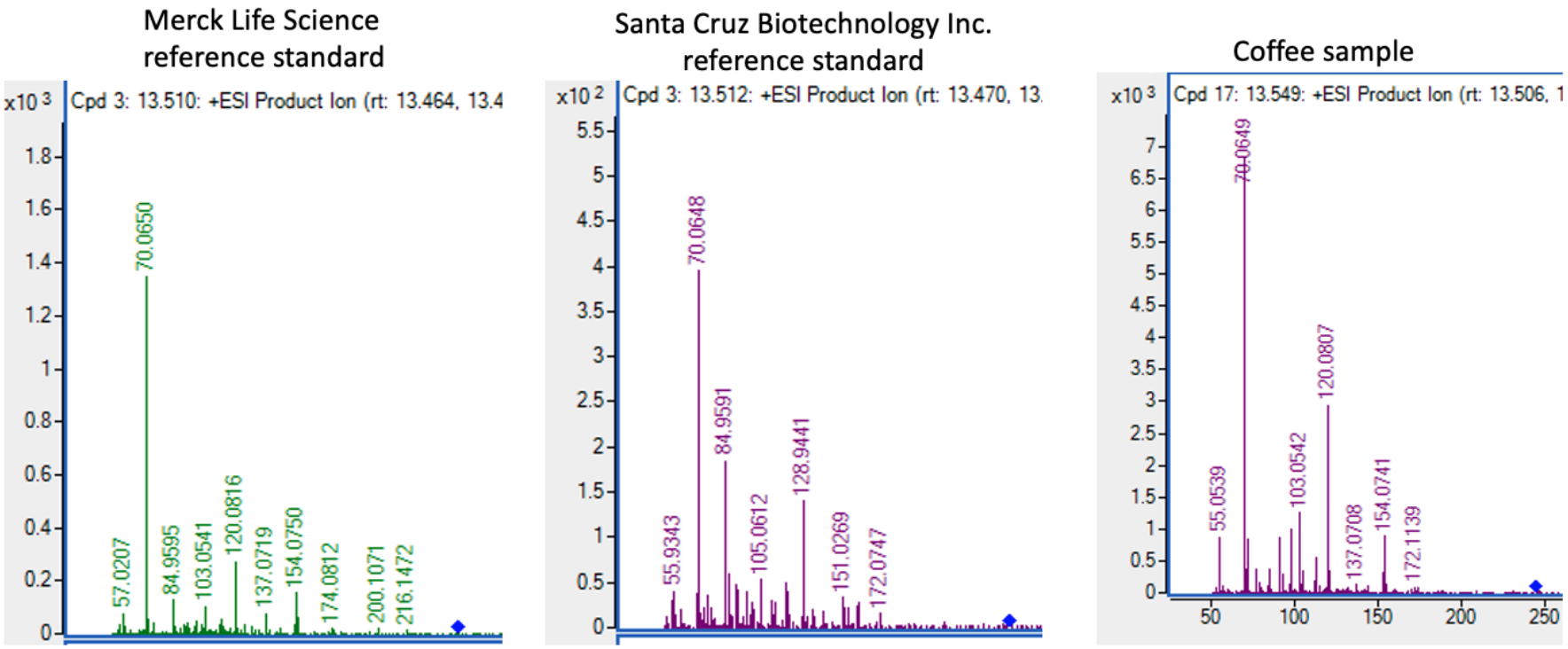



Figure K-8 Cyclo(-Phe-Pro) MS2 spectra @13.55 min @20V

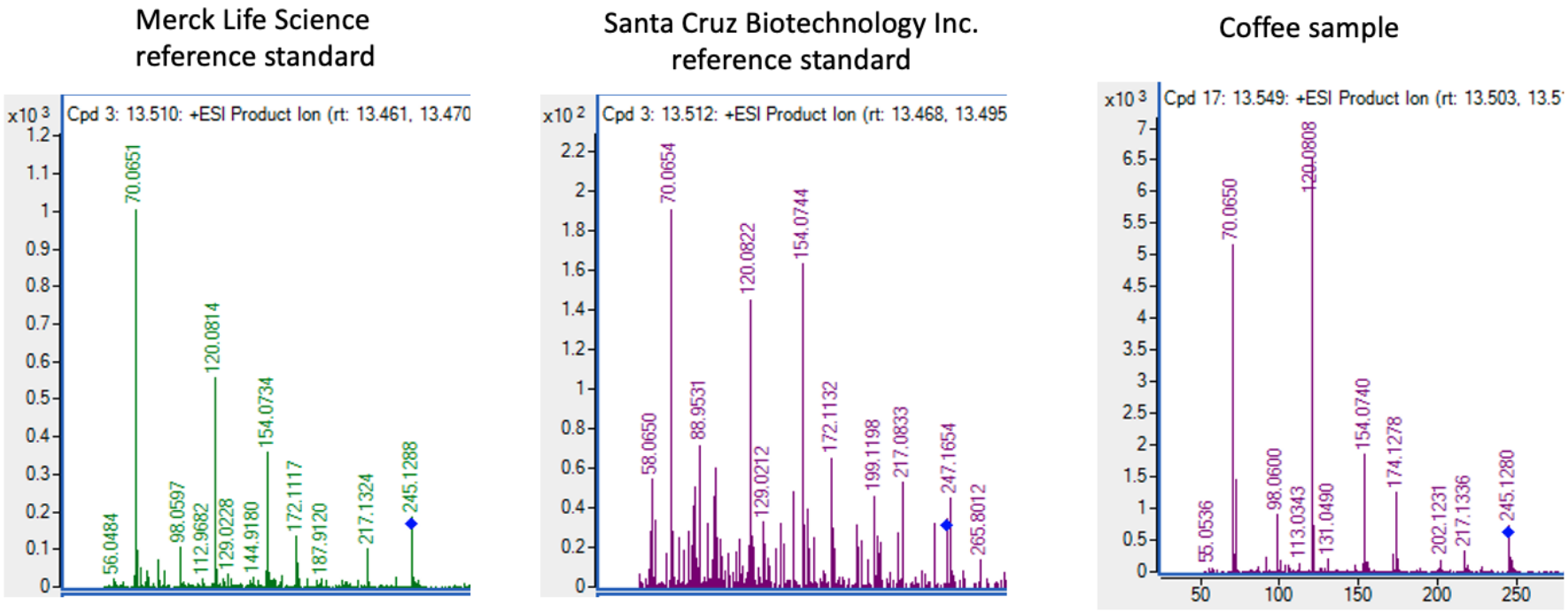



Figure K-9 Cyclo(-Phe-Pro) MS2 spectra @13.55 min @40

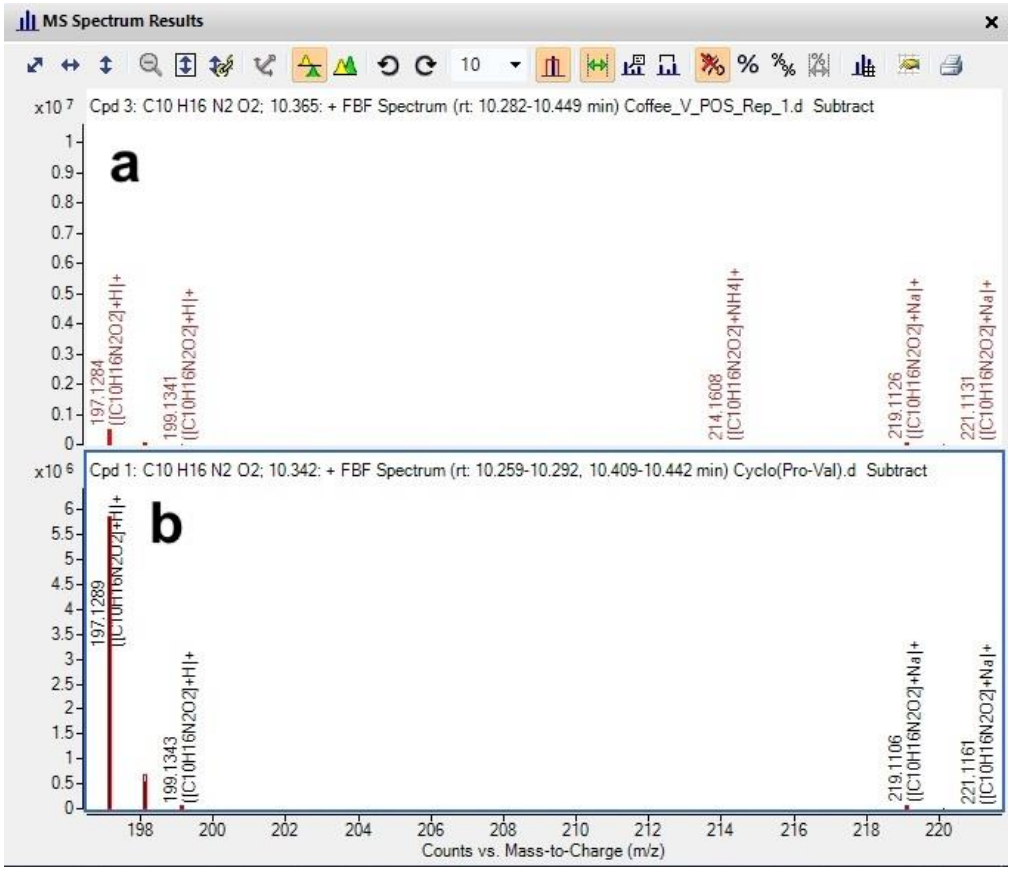



Figure K-10 (a) MS1 spectra of MS2 annotated Cyclo(-Pro-Val). (b) MS1 spectra chemical reference standard of Cyclo(-Pro-Val).

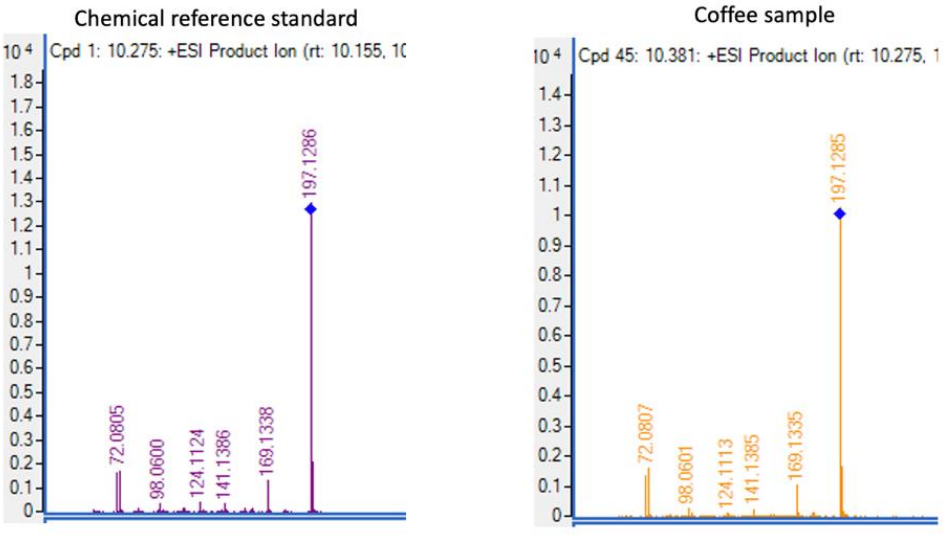



Figure K-11 Cyclo(-Pro-Val) MS2 spectra @10V

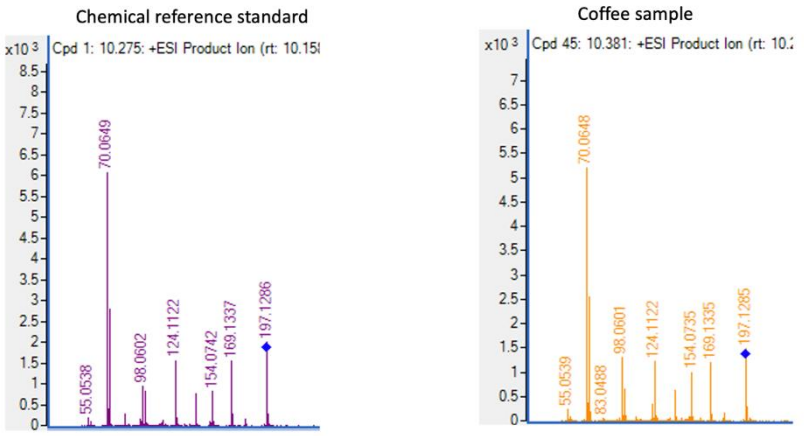



Figure K-12 Cyclo(-Pro-Val) MS2 spectra @20V

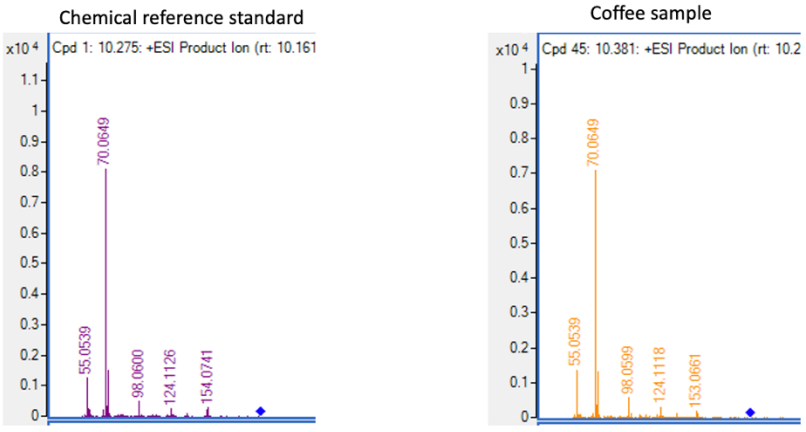



Figure K-13 Cyclo(-Pro-Val) MS2 spectra @40V

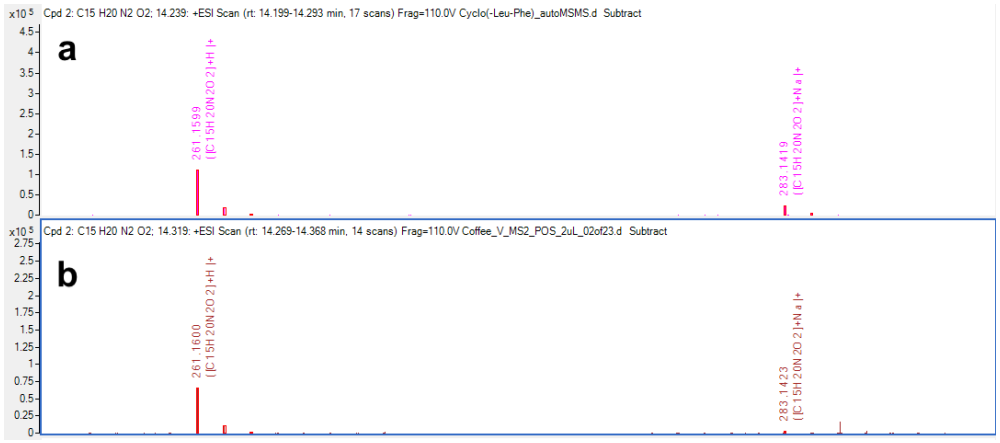



Figure K-14 (a) MS1 spectra of chemical reference standard of Cyclo(-Leu-Phe). (b) MS1 spectra of MS2 annotated Cyclo(-Leu-Phe).

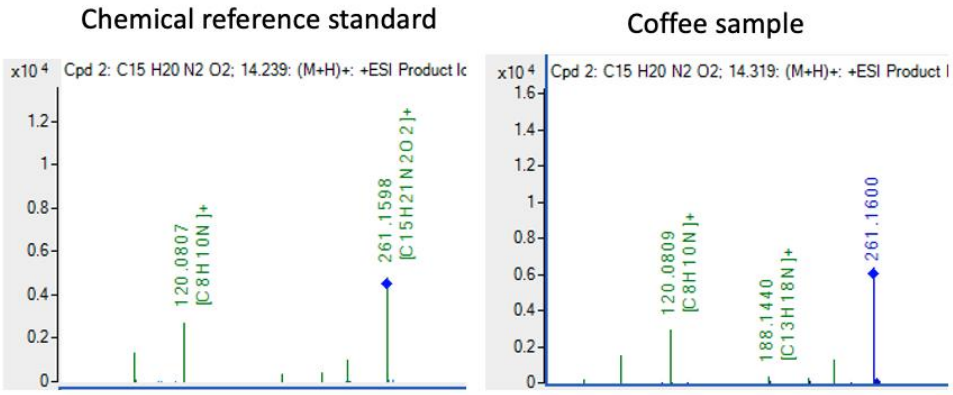



Figure K-15 Cyclo(-Leu-Phe) MS2 spectra @10V

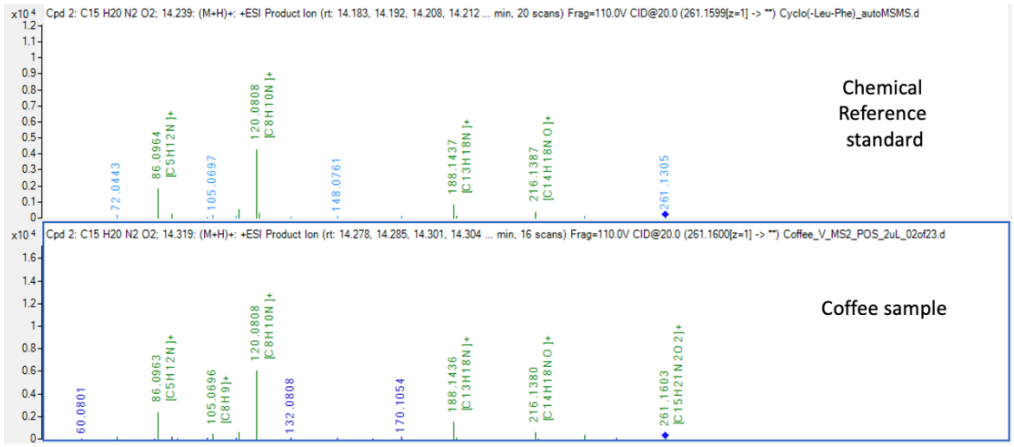



Figure K-16 Cyclo(-Leu-Phe) MS2 spectra @20V

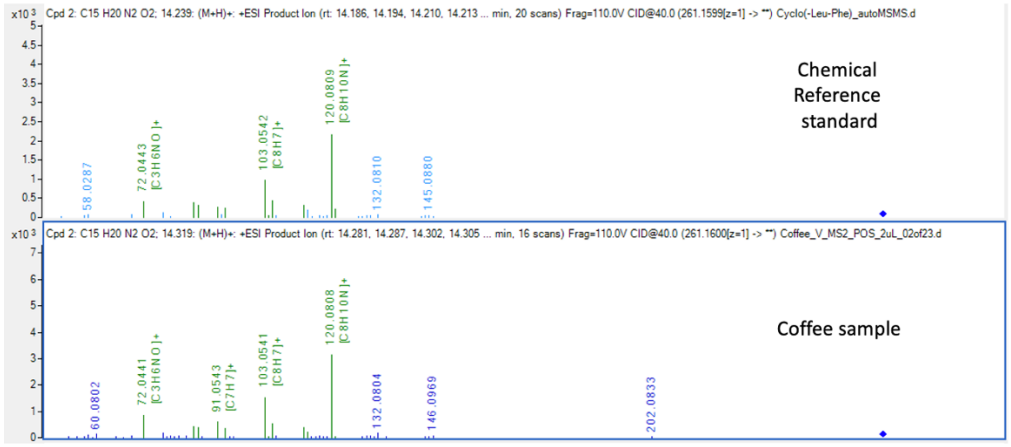



Figure K-17 Cyclo(-Leu-Phe) MS2 spectra @40V

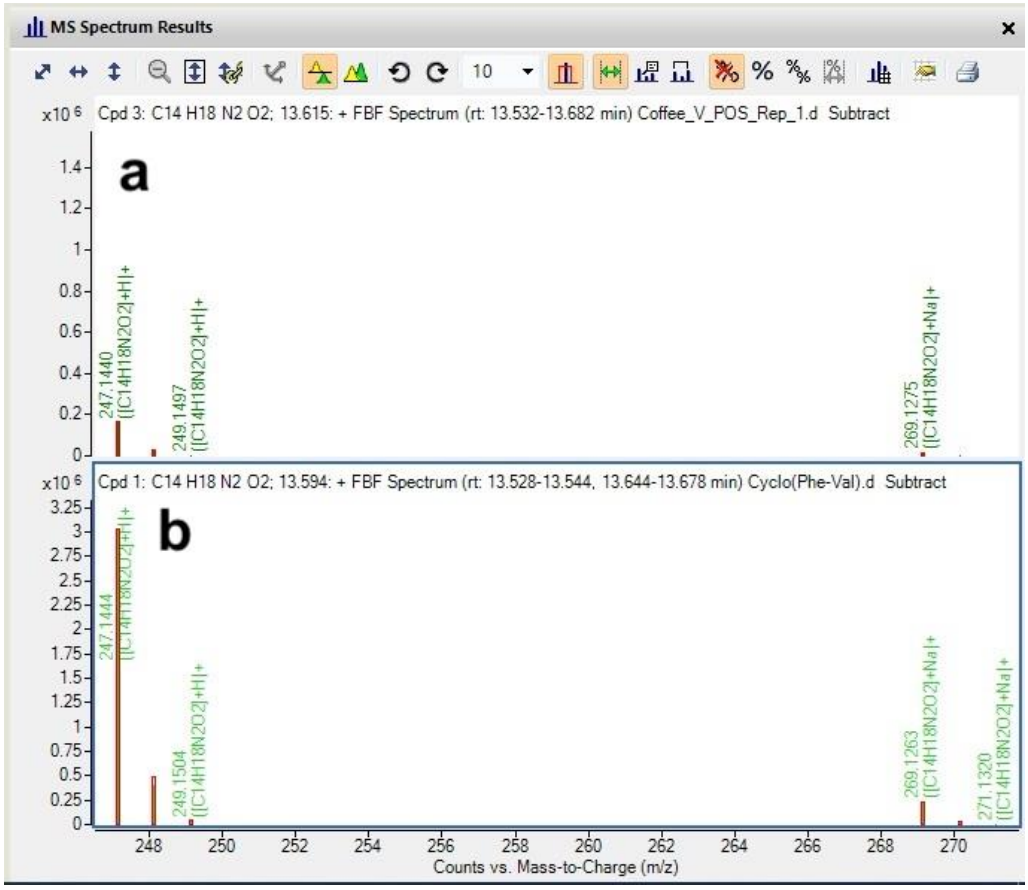



Figure K-18 (a) MS1 spectra of MS2 annotated Cyclo(-Phe-Val). (b) MS1 spectra of chemical reference standard of Cyclo(-Phe-Val)

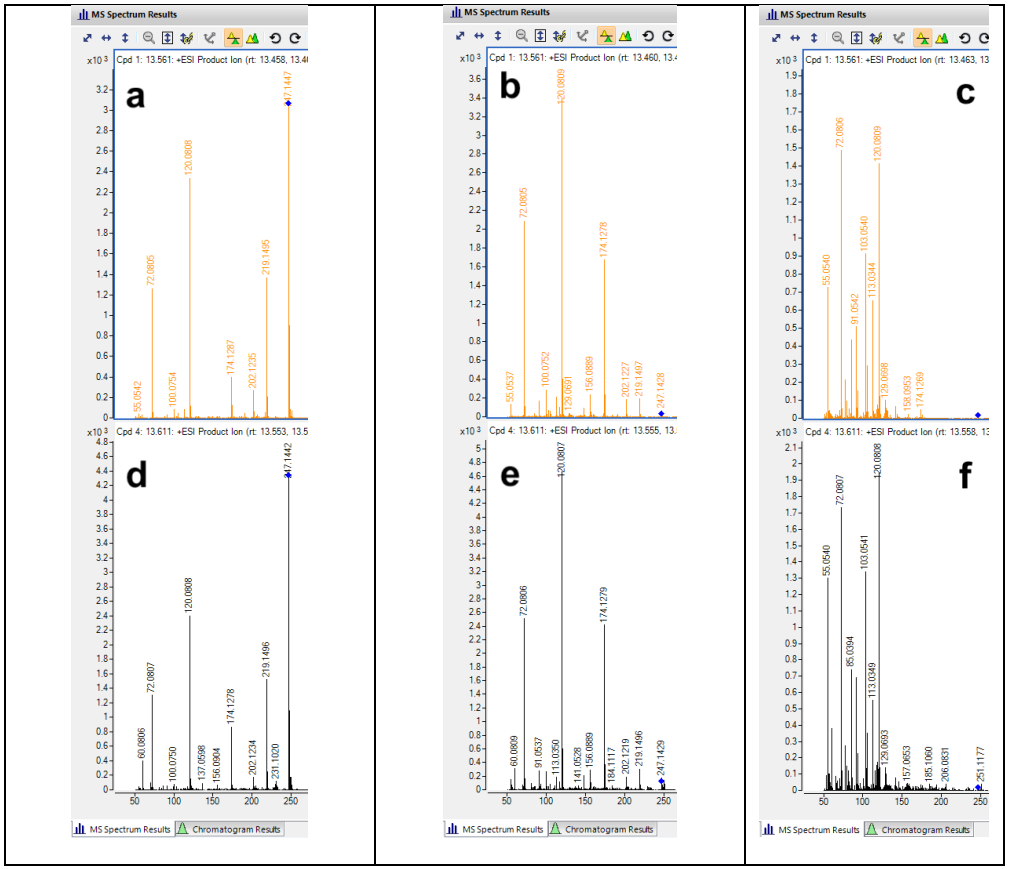



Figure K-19 Cyclo(-Phe-Val) MS2 spectra @10V, 20V and 40V. (a,b,c):Chemical reference standard,(d,e,f): MS2 annotated Cyclo(-Phe-Val)

# Appendix L: Standard curves of key foam compounds prepared with standard addition method

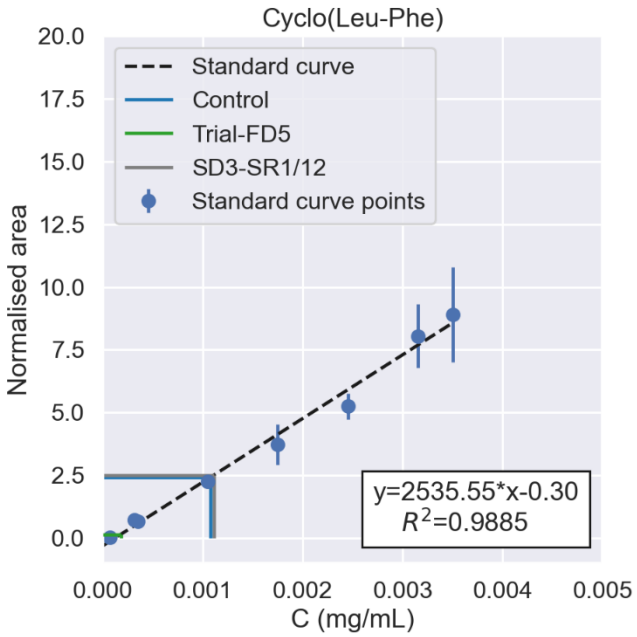



Figure L-1 Standard curve for Cyclo(Leu-Phe) prepared with standard addition method

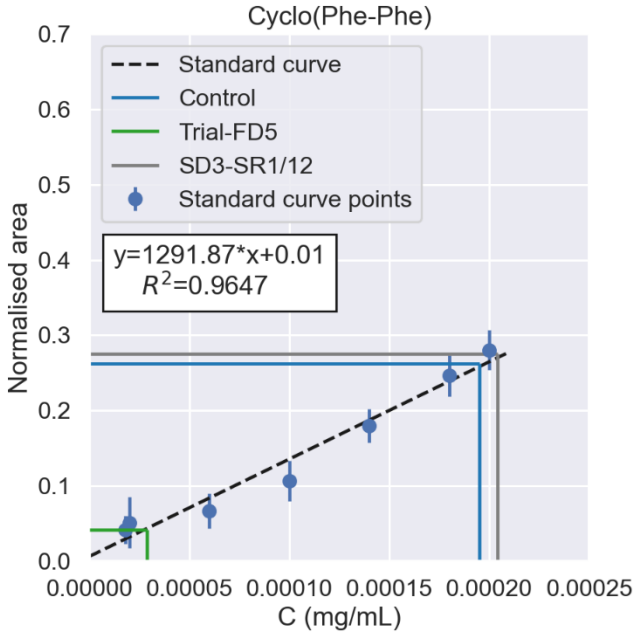



Figure L-2 Standard curve for Cyclo(Phe-Phe) prepared with standard addition method.

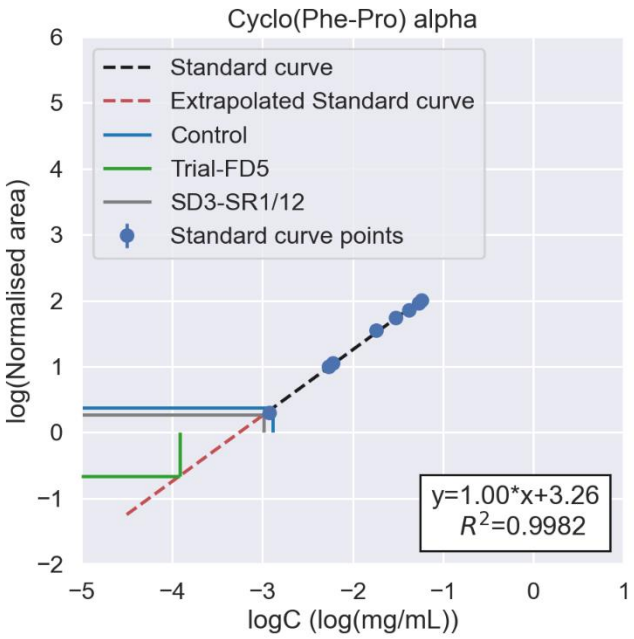



Figure L-3 Standard curve for Cyclo(Phe-Pro) alpha (log-log scale) prepared with standard addition method

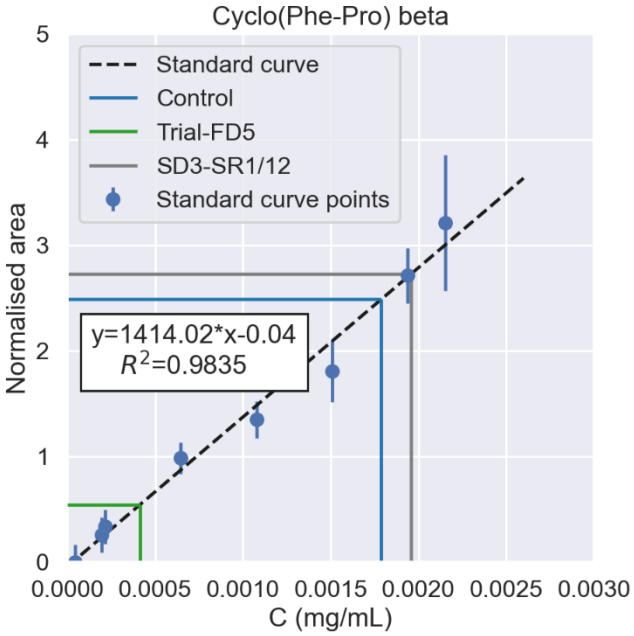



Figure L-4 Standard curve for Cyclo(Phe-Pro) beta prepared with standard addition method

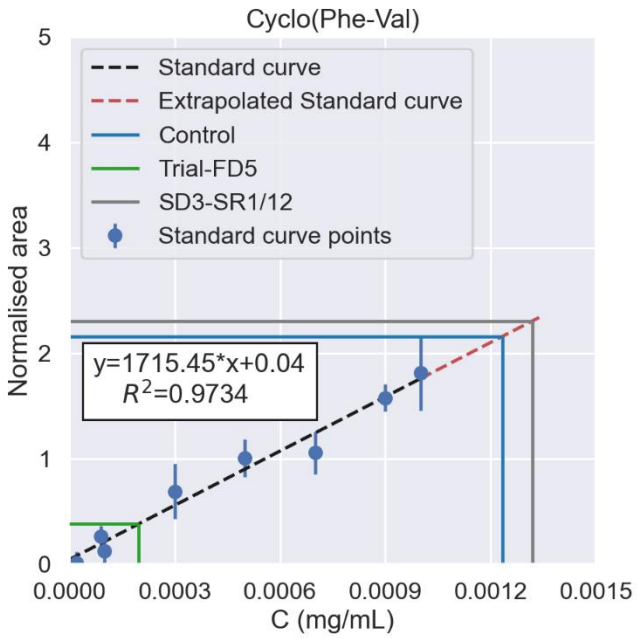



Figure L-5 Standard curve for Cyclo(Phe-Val) prepared with standard addition methods

# Appendix M: Standard curves of key foam compounds prepared without standard addition method

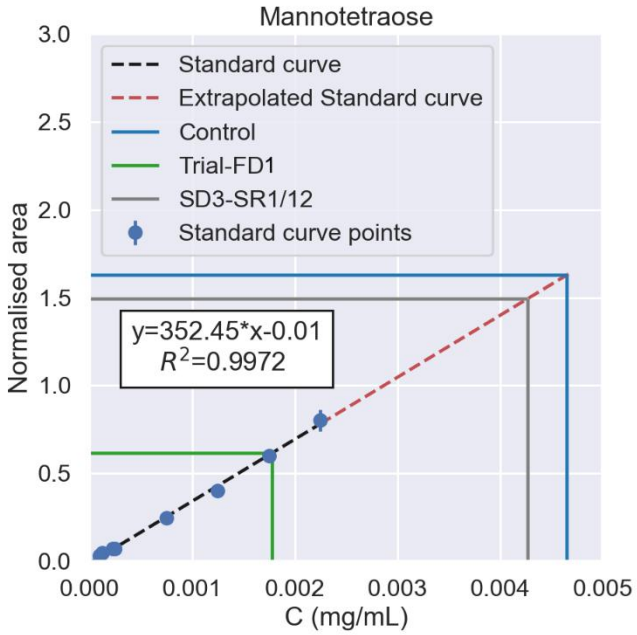



Figure M-1 Standard curve for Mannotetraose prepared without standard addition method

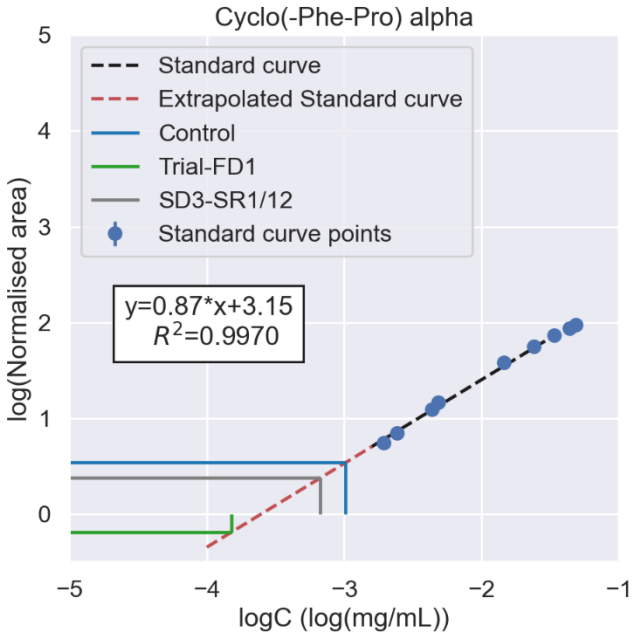



Figure M-2 Standard curve for Cyclo(Phe-Pro) alpha in log-log scale prepared without standard addition method

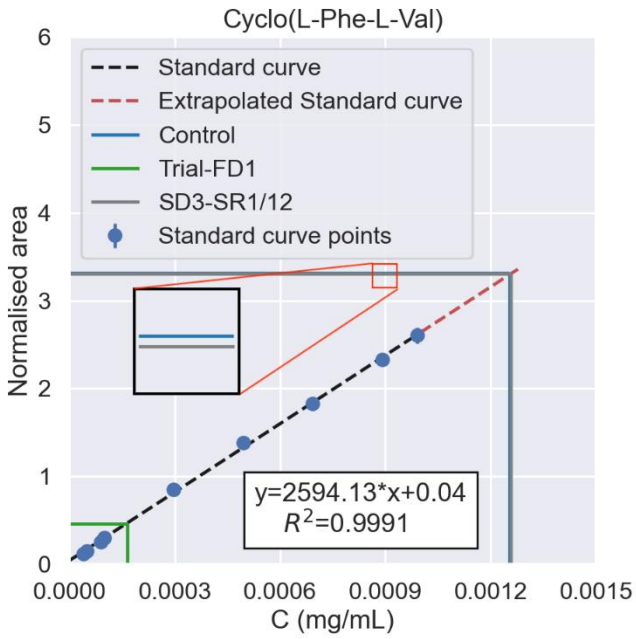



Figure M-3 Standard curve for Cyclo(Phe-Val) prepared without standard addition method

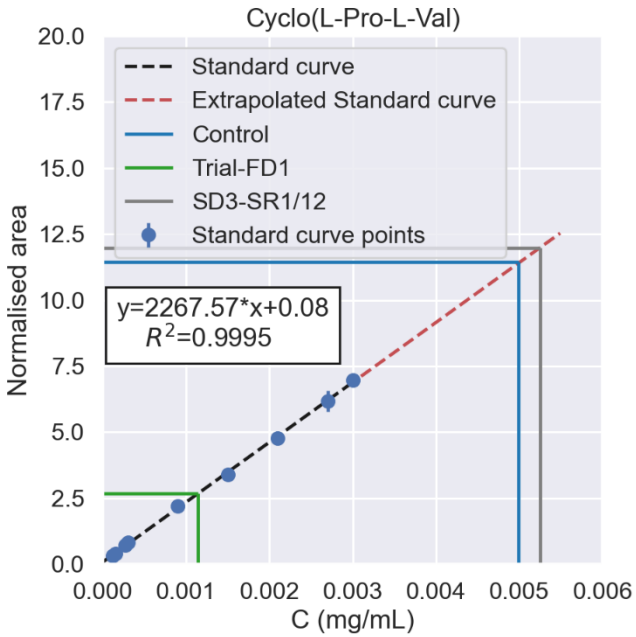



Figure M-4 Standard curve for Cyclo(Pro-Val) prepared without standard addition method

# Appendix N: Standard curves for major polyphenols in coffee samples.

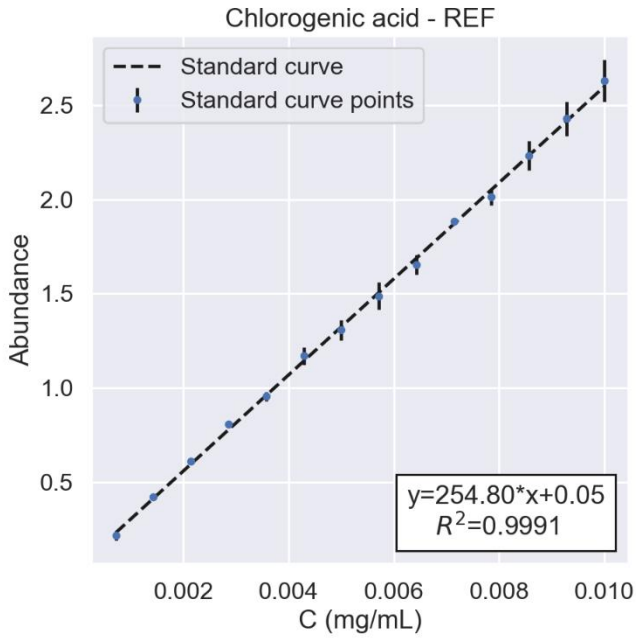



Figure N-1 Standard curve for 3-O-Caffeoylquinic acid prepared without standard addition method

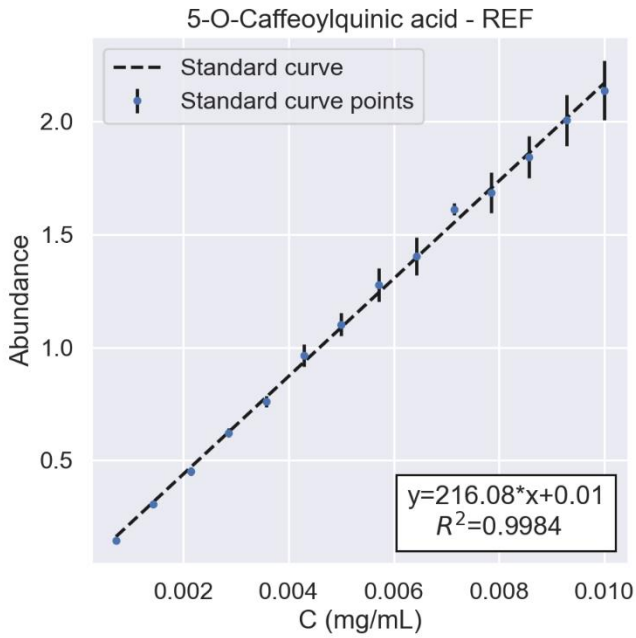



Figure N-2 Standard curve for 5-O-Caffeoylquinic acid prepared without standard addition method

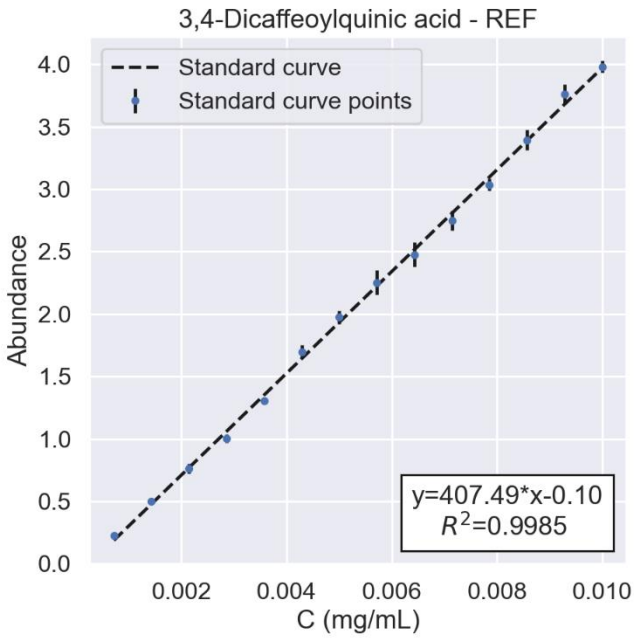



Figure N-3 Standard curve for 3,4-diCaffeoylquinic acid prepared without standard addition method

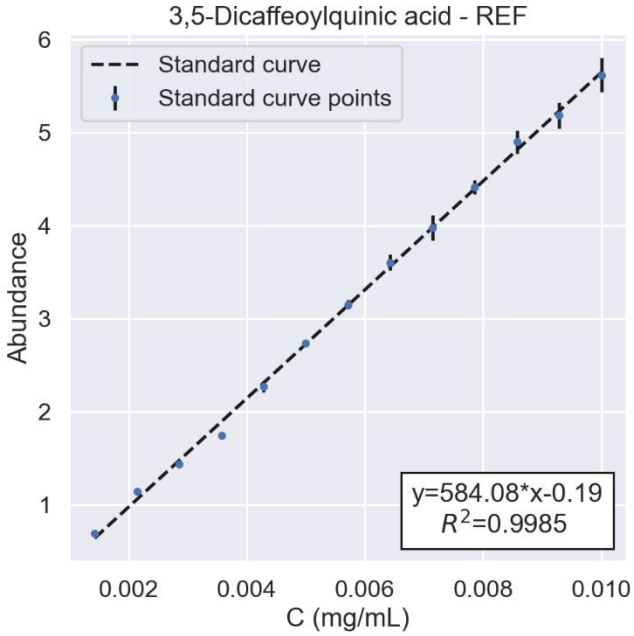



Figure N-4 Standard curve for 3,5-diCaffeoylquinic acid prepared without standard addition method

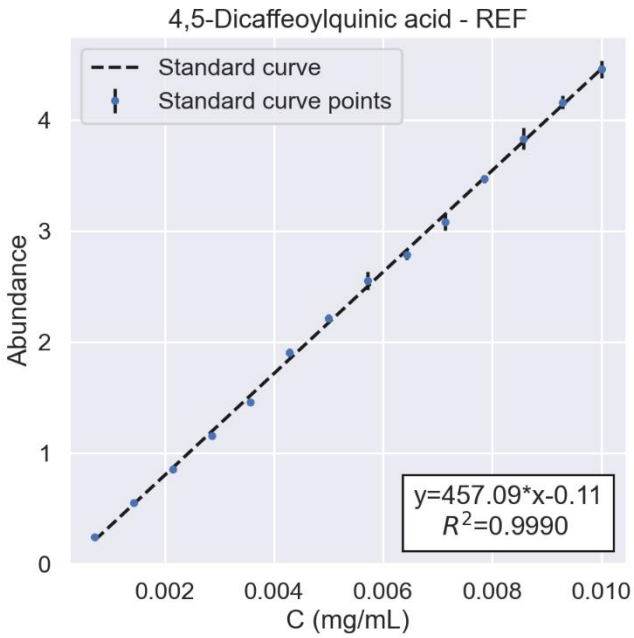



Figure N-5 Standard curve for 4,5-diCaffeoylquinic acid prepared without standard addition method

# Appendix O: MSI Level 2 annotation of chemical compounds significantly affected by roasting degree or instant coffee manufacture.

Table O.1 Chemical entities significantly decreased during roasting.

| Prec. m/z | Ret. time (min) | SIRIUS NAME | PUBCHEM ID | SIRIUS SCORE | CSI SCORE | Class | **Compound** |
|---|---|---|---|---|---|---|---|
| 110.0086 | 0.7270003 | CID 138969061 | 138969061 | 98.319 | -103.158 | Carboxylic acids and derivatives | **109.0014@0.7270003** |
| 187.0817 | 0.7280001 | 1-(Dihydroxyamino)-2-(3-hydroxypropyl)guanidine | 3708720 | 99.996 | -85.185 | Amino acids, peptides and analogues | **186.0742@0.7280001** |
| 175.1191 | 0.80699956 | N(5)-Acetyl-L-ornithine | 193343 | 100 | -30.831 | Amino acids, peptides and analogues | **174.1117@0.80699956** |
| 132.0306 | 0.8139995 | Aspartic Acid | 5960 | 99.595 | -8.442 | Amino acids, peptides and analogues | **133.0376@0.8139995** |
| 134.0449 | 0.82199943 | Aspartic Acid | 5960 | 100 | -3.217 | Amino acids, peptides and analogues | **133.0375@0.82199943** |
| 184.1081 | 0.82600015 | 3-[(1,3-Dimethyl-1H-imidazole-3-ium)-4-yl]-L-alanine | 101134202 | 100 | -53.452 | Amino acids, peptides and analogues | **183.1009@0.82600015** |
| 146.0461 | 0.82600015 | DL-Glutamic acid | 611 | 99.685 | -8.469 | Amino acids, peptides and analogues | **147.0535@0.82600015** |
| 222.064 | 0.82600015 | 1-Acetamido-3-pent-3-ynylurea | 130736707 | 100 | -145.893 | Tetriary amines | **183.1009@0.82600015** |
| 148.0604 | 0.83100057 | DL-Glutamic acid | 611 | 100 | -3.343 | Amino acids, peptides and analogues | **147.0532@0.83100057** |
| 195.0513 | 0.8330001 | Gluconic Acid | 10690 | 99.883 | -2.321 | Carbohydrate and carbohydrate conjugates | **136.0373@0.8330001** |
| 87.0439 | 0.8419999 | Butyne-1 diol | 22729408 | 100 | -72.813 | Aldehydes | **86.0367@0.8419999** |
| 477.1458 | 0.84600043 | (2R,3R,4S,5S,6R)-2-[(2S,3S,4S,5R)-3,4-dihydroxy-2,5-bis(hydroxymethyl)oxolan-2- | 87178436 | 42.003 | -135.485 | Carbohydrate and carbohydrate conjugates | **478.1531@0.84600043** |

Table O.1 cont.

| Prec. m/z | Ret. time (min) | SIRIUS NAME | PUBCHEM ID | SIRIUS SCORE | CSI SCORE | Class | **Compound** |
|---|---|---|---|---|---|---|---|
| | | yl]oxy-6-(2,3-dihydroxypropylperoxymethyl)oxane-3,4,5-triol | | | | | |
| 503.1618 | 0.84799963 | Maltotriose | 871 | 33.305 | -14.272 | Carbohydrate and carbohydrate conjugates | **504.1685@0.84799963** |
| 549.1668 | 0.84799963 | Gentianose | 117678 | 33.272 | -9.782 | Carbohydrate and carbohydrate conjugates | **504.1685@0.84799963** |
| 609.1881 | 0.8489993 | beta-D-Glc-(1->4)-[L-alpha-D-Hep-(1->3)]-L-alpha-D-Hep | 45480578 | 48.129 | -71.527 | Carbohydrate and carbohydrate conjugates | **550.1742@0.8489993** |
| 305.1346 | 0.8569998 | PEG-bis-amido-Succinic Acid, MW 10K | 51340888 | 85.507 | -131.943 | Amino acids, peptides and analogues | **304.1273@0.8569998** |
| 310.1135 | 0.857 | InChI=1S/C11H19NO9/c1-4(15)12-7-9(20-6(3-14)10(17)18)8(16)5(2-13)21-11(7)19/h5-9,11,13-14,16,19H,2-3H2,1H3,(H,12,15)(H,17,18) | N/A | 98.932 | -111.336 | Pyranoid amino acids and derivatives | **309.1062@0.857** |
| 266.1237 | 0.85800093 | D-1-[(3-Carboxypropyl)amino]-1-deoxyfructose | 131752417 | 99.994 | -70.579 | Carbohydrate and carbohydrate conjugates | **265.1164@0.85800093** |
| 521.1721 | 0.85900056 | Mannobiosylmannitol | 129670968 | 97.32 | -137.482 | Carbohydrate and carbohydrate conjugates | **522.1793@0.85900056** |
| 522.2033 | 0.86000043 | 1-[[(2S,3S,4S,5R,6R)-4,5-dihydroxy-2-(hydroxymethyl)-6-[(2R,3S,4R,5R)-4,5,6-trihydroxy-2-(hydroxymethyl)oxan-3-yl]oxyoxan-3-yl]amino]hexane-1,2,3,4,5,6-hexol | 56950099 | 95.55 | -111.355 | Carbohydrate and carbohydrate conjugates | **504.169@0.86000043** |
| 341.1092 | 0.8619996 | Trehalose | 7427 | 99.978 | -8.483 | Carbohydrate and carbohydrate conjugates | **342.1162@0.8619996** |
| 387.1147 | 0.8619996 | Trehalose | 7427 | 49.997 | -8.966 | Carbohydrate and carbohydrate conjugates | **342.1162@0.8619996** |
| 163.0602 | 0.8639991 | Idosan | 1742165 | 100 | -41.052 | Carbohydrate and carbohydrate conjugates | **162.0568@0.8639991** |

Table O.1 cont.

| Prec. m/z | Ret. time (min) | SIRIUS NAME | PUBCHEM ID | SIRIUS SCORE | CSI SCORE | Class | **Compound** |
|---|---|---|---|---|---|---|---|
| 127.039 | 0.8659997 | Maltol | 8369 | 100 | -55.269 | Phenols | **126.0317@0.8659997** |
| 747.1528 | 0.8660004 | Kaempferide 3-rhamnoside-7-(6''-succinylglucoside) | 44257993 | 99.879 | -131.104 | Flavonoids | **708.1917@0.8660004** |
| 97.0283 | 0.8740004 | trans-2-Penten-4-ynoic acid | 12487626 | 100 | -72.027 | Dihydrofurans | **74.0391@0.8740004** |
| 533.1725 | 0.875 | (2R,3S,4R,5S,6S)-2-[(2R,3S,4R,5R,6S)-5-hydroxy-2-(hydroxymethoxy)-6-(hydroxymethyl)-3-[(2S,3R,4S,5R,6R)-3,4,5-trihydroxy-6-(hydroxymethyl)oxan-2-yl]oxyoxan-4-yl]oxy-6-(hydroxymethyl)oxane-3,4,5-triol | 44429606 | 88.337 | -119.481 | Carbohydrate and carbohydrate conjugates | **534.1794@0.875** |
| 579.1776 | 0.875 | (2R,3S,4R,5S,6S)-2-[(2R,3S,4R,5R,6S)-5-hydroxy-2-(hydroxymethoxy)-6-(hydroxymethyl)-3-[(2S,3R,4S,5R,6R)-3,4,5-trihydroxy-6-(hydroxymethyl)oxan-2-yl]oxyoxan-4-yl]oxy-6-(hydroxymethyl)oxane-3,4,5-triol | 44429606 | 49.713 | -88.06 | Carbohydrate and carbohydrate conjugates | **534.1794@0.875** |
| 695.2251 | 0.8759996 | Gal(b1-4)Glc(b1-4)Glc(b1-4)a-LDManHep | 91855613 | 77.358 | -83.943 | Carbohydrate and carbohydrate conjugates | **636.211@0.8759996** |
| 104.107 | 0.89700043 | Choline | 305 | 100 | -27.093 | Organitrogen compounds | **103.0997@0.89700043** |
| 475.1302 | 0.9230002 | 3,3-bis[[(2S,3R,4S,5R,6R)-3,4,5-trihydroxy-6-(hydroxymethyl)oxan-2-yl]oxy]propanoic acid | 67742984 | 44.311 | -58.682 | Carbohydrate and carbohydrate conjugates | **430.132@0.9230002** |
| 133.0143 | 0.9359996 | Malic Acid | 525 | 100 | -3.991 | Hydroxy fatty acids | **88.0155@0.9359996** |
| 147.03 | 0.9359996 | Citramalic acid | 1081 | 99.981 | -13.395 | Hydroxy fatty acids | **88.0155@0.9359996** |
| 118.0862 | 0.94499975 | DL-Valine | 1182 | 100 | -21.621 | Amino acids, peptides and analogues | **117.079@0.94499975** |
| 409.0196 | 1.0429994 | InChI=1S/C15H14O11/c16-7-3-1-6(5-8(7)17)2-4-9(18)26-13(15(24)25)11(20)10(19)12(21)14(22)23/h1-5,10-11,13,16-17,19-20H,(H,22,23)(H,24,25) | N/A | 100 | -134.493 | Benzene and substituted derivatives | **408.0122@1.0429994** |
| 193.0343 | 1.0429994 | Citric Acid | 311 | 100 | -7.663 | Carboxylic acids and derivatives | **192.0271@1.0429994** |

Table O.1
cont.

| Prec. m/z | Ret. time (min) | SIRIUS NAME | PUBCHEM ID | SIRIUS SCORE | CSI SCORE | Class | **Compound** |
|---|---|---|---|---|---|---|---|
| 230.9901 | 1.0429994 | Citric Acid | 311 | 100 | -8.405 | Carboxylic acids and derivatives | **192.0271@1.0429994** |
| 147.0289 | 1.0429994 | Acetonedicarboxylate | 6950210 | 100 | -29.769 | Keto acids and derivatives | **146.0144@1.0429994** |
| 129.0183 | 1.0429994 | Pent-2-ynedioic acid | 15559550 | 100 | -107.717 | Pyranones and derivatives | **128.011@1.0429994** |
| 191.0199 | 1.0439992 | Citric Acid | 311 | 100 | -4.205 | Hydroxy fatty acids | **192.0272@1.0439992** |
| 138.0552 | 1.0439992 | Trigonelline | 5570 | 99.995 | -13.064 | Pyridines and derivatives | **137.0479@1.0439992** |
| 182.0461 | 1.0469995 | 4-Pyridoxic acid | 6723 | 100 | -83.448 | Amino acids, peptides and analogues | **123.0323@1.0469995** |
| 132.102 | 1.2580012 | DL-Isoleucine | 791 | 100 | -22.177 | Amino acids, peptides and analogues | **131.0947@1.2580012** |
| 147.03 | 1.4110011 | 3-Hydroxybutanedioic acid methyl ester | 14827202 | 33.311 | -33.031 | Hydroxy fatty acids | **148.0373@1.4110011** |
| 268.1041 | 1.6549991 | Adenosine | 60961 | 87.067 | -1.41 | Purine ribonucleotides | **267.0969@1.6549991** |
| 220.1195 | 2.0989993 | trans-Zeatin | 449093 | 99.997 | -34.471 | Purines and purine derivatives | **219.1121@2.0989993** |
| 210.0761 | 2.2509997 | 4-carboxyphenylalanine | 265273 | 99.895 | -49.837 | Amino acids, peptides and analogues | **209.0689@2.2509997** |
| 166.0863 | 2.4929976 | DL-Phenylalanine | 994 | 99.99 | -1.219 | Amino acids, peptides and analogues | **165.079@2.4929976** |
| 202.1801 | 2.5390012 | (3R,5S)-1-propan-2-yl-5-(propan-2-yloxymethyl)pyrrolidin-3-ol | 124113423 | 100 | -99.728 | Amino acids, peptides and analogues | **201.1729@2.5390012** |
| 220.1194 | 2.6820033 | trans-Zeatin | 449093 | 80.753 | -20.162 | Purines and purine derivatives | **219.1121@2.6820033** |
| 188.0706 | 4.729003 | (2E)-3-(1H-indol-2-yl)prop-2-enoic acid | 15030923 | 31.892 | -24.463 | Indoles | **187.0633@4.729003** |
| 203.0828 | 4.7539988 | DL-Tryptophan | 1148 | 99.869 | -2.855 | Amino acids, peptides and analogues | **204.0901@4.7539988** |
| 397.0712 | 5.1650023 | (2,3,4,5,6-pentahydroxycyclohexyl) (2R,3S,4R,5R)-2,3,4,5,6-pentahydroxyhexanoate | 123313679 | 99.555 | -125.46 | Carbohydrate and carbohydrate conjugates | **396.064@5.1650023** |
| 179.0352 | 7.6290073 | Caffeic acid | 689043 | 100 | -24.03 | Cinnamic acids and derivatives | **180.0423@7.6290073** |

Table O.1 cont.

| Prec. m/z | Ret. time (min) | SIRIUS NAME | PUBCHEM ID | SIRIUS SCORE | CSI SCORE | Class | **Compound** |
|---|---|---|---|---|---|---|---|
| 377.0845 | 8.224995 | Caffeoylquinic acid | | 91.229 | -3.391 | Cinnamic acids and derivatives | **354.0953@8.224995** |
| 393.0583 | 8.224995 | Caffeoylquinic acid | | 95.613 | -30.929 | Cinnamic acids and derivatives | **354.0953@8.224995** |
| 353.088 | 8.239994 | Caffeoylquinic acid | 9798666 | 99.996 | -4.384 | Cinnamic acids and derivatives | **354.0953@8.239994** |
| 375.0698 | 8.241008 | [(2R,3S,4R,5R)-3,4-dihydroxy-5-(6-oxo-1H-purin-9-yl)oxolan-2-yl]methyl dimethyl phosphate | 136187603 | 76.314 | -90.642 | Purine ribonucleotides | **376.077@8.241008** |
| 355.1029 | 8.60999 | Caffeoylquinic acid | | 47 | -2.69 | Cinnamic acids and derivatives | **354.0954@8.60999** |
| 377.0846 | 8.60999 | Caffeoylquinic acid | | 99.99 | -3.265 | Cinnamic acids and derivatives | **354.0954@8.60999** |
| 421.0752 | 8.614994 | InChI=1S/C18H16O9/c19-10-3-1-9(5-11(10)20)2-4-16(23)26-14(17(24)25)8-18-7-13(22)12(21)6-15(18)27-18/h1-7,14-15,19-22H,8H2,(H,24,25) | N/A | 46.898 | -149.306 | Cinnamic acids and derivatives | **376.0771@8.614994** |
| 353.0881 | 8.620991 | Caffeoylquinic acid | 9798666 | 99.999 | -3.527 | Cinnamic acids and derivatives | **354.0952@8.620991** |
| 191.0563 | 8.622991 | Quinic acid | 6508 | 99.999 | -8.281 | Cyclitols and derivatives | **192.0635@8.622991** |
| 425.1663 | 9.046003 | 1,1-Dimethyl-2-propenyl 6-O-[[(2R)-3alpha,4alpha-dihydroxy-4-(hydroxymethyl)tetrahydrofuran]-2beta-yl]-beta-D-glucopyranoside | 11794150 | 49.454 | -18.638 | Fatty acyl glycosides | **380.168@9.046003** |
| 369.1183 | 9.479003 | Feruloylquinic acid | | 96.899 | -8.656 | Cinnamic acids and derivatives | **368.1109@9.479003** |
| 197.0686 | 10.16499 | CID 58148343 | 58148343 | 98.769 | -115.707 | Pyridines and derivatives | **174.0793@10.16499** |
| 339.1078 | 10.84699 | Feruloylquinic acid | | 81.649 | -5.583 | Cinnamic acids and derivatives | **338.1002@10.84699** |
| 369.1184 | 11.294002 | Feruloylquinic acid | | 98.139 | -7.386 | Cinnamic acids and derivatives | **368.1109@11.294002** |
| 391.1003 | 11.752006 | Feruloylquinic acid | | 100 | -8.247 | Cinnamic acids and derivatives | **368.111@11.752006** |
| 177.0547 | 11.752997 | 3-(4-Hydroxy-3-methoxyphenyl)prop-2-ynal | 82362867 | 100 | -61.444 | Cinnamic acids and derivatives | **176.0474@11.752997** |

Table O.1 cont.

| Prec. m/z | Ret. time (min) | SIRIUS NAME | PUBCHEM ID | SIRIUS SCORE | CSI SCORE | Class | **Compound** |
|---|---|---|---|---|---|---|---|
| 367.1037 | 11.760007 | Feruloylquinic acids | 131850437 | 100 | -8.24 | Cinnamic acids and derivatives | **368.1109@11.760007** |
| 553.2623 | 11.872005 | (1R,2R,3S,4S,5R,9S,10S,13R,14R)-2,3-dihydroxy-14-(hydroxymethyl)-5,9-dimethyl-14-[(2S,3R,4S,5S,6R)-3,4,5-trihydroxy-6-(hydroxymethyl)oxan-2-yl]oxytetracyclo[11.2.1.01,10.04,9]hexadecane-5-carboxylic acid | 44179026 | 55.471 | -124.019 | Phenol lipids | **552.2547@11.872005** |
| 138.0662 | 12.057006 | 1,3-Dimethyl-2-oxoimidazole-4-carbonitrile | 84020630 | 100 | -63.115 | Alkyl aryl ethers | **137.0589@12.057006** |
| 195.088 | 12.057006 | Caffeine | 2519 | 100 | -5.846 | Purines and purine derivatives | **194.0806@12.057006** |
| 517.1344 | 12.619996 | di-Caffeoylquinic acid | | 56.568 | -6.865 | Cinnamic acids and derivatives | **516.1273@12.619996** |
| 539.1163 | 12.619996 | di-Caffeoylquinic acid | | 87.439 | -10.988 | Cinnamic acids and derivatives | **516.1273@12.619996** |
| 517.1344 | 12.629016 | di-Caffeoylquinic acid | | 87.07 | -6.968 | Cinnamic acids and derivatives | **516.1269@12.629016** |
| 355.1025 | 12.630992 | Caffeoylquinic acid | | 29.927 | -7.193 | Cinnamic acids and derivatives | **354.0953@12.630992** |
| 515.1196 | 12.633993 | di-Caffeoylquinic acid | 129316855 | 97.13 | -3.129 | Cinnamic acids and derivatives | **516.1268@12.633993** |
| 515.1196 | 12.63599 | di-Caffeoylquinic acid | 129316855 | 66.199 | -4.642 | Cinnamic acids and derivatives | **516.1266@12.63599** |
| 163.039 | 12.637003 | 6-Hydroxybenzofuran-5-carbaldehyde | 12269547 | 99.957 | -92.043 | Coumarins and derivatives | **162.0316@12.637003** |
| 353.0878 | 12.825008 | Caffeoylquinic acid | 9798666 | 99.94 | -3.326 | Cinnamic acids and derivatives | **354.0953@12.825008** |
| 355.1027 | 13.406005 | Caffeoylquinic acid | | 42.533 | -2.722 | Cinnamic acids and derivatives | **354.0953@13.406005** |
| 499.1242 | 13.411991 | 1alpha,3alpha-Dihydroxy-4alpha-(3,4-dihydroxycinnamoyloxy)-5beta-(4-hydroxycinnamoyloxy)cyclohexane-1-carboxylic acid | 102383780 | 99.313 | -17.058 | Cinnamic acids and derivatives | **500.1318@13.411991** |
| 529.1351 | 13.715002 | (1R,3R,4S,5R)-4-[(E)-3-(3,4-dihydroxyphenyl)prop-2-enoyl]oxy-1,3- | 42598867 | 96.513 | -4.476 | Cinnamic acids and derivatives | **530.1426@13.715002** |

Table O.1 cont.

| Prec. m/z | Ret. time (min) | SIRIUS NAME | PUBCHEM ID | SIRIUS SCORE | CSI SCORE | Class | **Compound** |
|---|---|---|---|---|---|---|---|
| | | dihydroxy-5-[(E)-3-(3-hydroxy-4-methoxyphenyl)prop-2-enoyl]oxycyclohexane-1-carboxylic acid | | | | | |
| 529.135 | 13.831995 | Caffeoyl-feruloyl-quinic acid | 131752147 | 99.337 | -4.328 | Cinnamic acids and derivatives | **530.1425@13.831995** |
| 509.2383 | 13.937008 | 14,17-Dihydroxy-12-methyl-17-[[3,4,5-trihydroxy-6-(hydroxymethyl)oxan-2-yl]oxymethyl]-8-oxapentacyclo[14.2.1.01,13.04,12.05,9]nonadeca-5(9),6-dien-10-one | 163059063 | 45.409 | -101.181 | Naphtofurans | **508.2309@13.937008** |
| 367.129 | 13.995983 | Caffeoyltryptophan | 15228042 | 99.99 | -38.785 | Amino acids, peptides and analogues | **366.1218@13.995983** |
| 365.1143 | 14.008997 | Caffeoyltryptophan | 15228042 | 99.678 | -56.909 | Amino acids, peptides and analogues | **366.1218@14.008997** |
| 529.1351 | 14.323987 | (1R,3R,4S,5R)-3-[(E)-3-(3,4-dihydroxyphenyl)prop-2-enoyl]oxy-1,5-dihydroxy-4-[(E)-3-(3-hydroxy-4-methoxyphenyl)prop-2-enoyl]oxycyclohexane-1-carboxylic acid | 75368781 | 85.171 | -4.795 | Cinnamic acids and derivatives | **530.1424@14.323987** |
| 795.3411 | 14.398994 | InChI=1S/C37H56O17/c1-16-31(54-33-29(46)27(44)26(43)22(14-38)53-33)28(45)30(47)32(51-16)52-18-3-9-36(23(39)12-24(40)41)20-4-7-34(2)19(17-11-25(42)50-15-17)6-10-37(34,49)21(20)5-8-35(36,48)13-18/h11,16,18-23,26-33,38-39,43-49H,3-10,12-15H2,1-2H3,(H,40,41) | N/A | 33.168 | -130.131 | Cardenolides and derivatives | **794.3334@14.398994** |
| 247.1177 | 14.398995 | 1-O-(4-Pentynyl)-alpha-D-glucopyranose | 87425972 | 100 | -66.053 | Carbohydrate and carbohydrate conjugates | **246.1103@14.398995** |
| 727.3549 | 14.412996 | 3-[14-hydroxy-3-[3-hydroxy-6-(hydroxymethyl)-4-methoxy-5-[3,4,5-trihydroxy-6-(hydroxymethyl)oxan-2-yl]oxyoxan-2-yl]oxy-10-(hydroxymethyl)-13-methyl-1,2,3,4,5,6,7,8,9,11,12,15,16,17-tetradecahydrocyclopenta[a]phenanthren-17-yl]-2H-furan-5-one | 162857418 | 78.031 | -93.597 | Steroid lactones | **772.3511@14.412996** |

Table O.1 cont.

| Prec. m/z | Ret. time (min) | SIRIUS NAME | PUBCHEM ID | SIRIUS SCORE | CSI SCORE | Class | **Compound** |
|---|---|---|---|---|---|---|---|
| 727.3549 | 14.412996 | 3-[14-hydroxy-3-[3-hydroxy-6-(hydroxymethyl)-4-methoxy-5-[3,4,5-trihydroxy-6-(hydroxymethyl)oxan-2-yl]oxyoxan-2-yl]oxy-10-(hydroxymethyl)-13-methyl-1,2,3,4,5,6,7,8,9,11,12,15,16,17-tetradecahydrocyclopenta[a]phenanthren-17-yl]-2H-furan-5-one | 162857418 | 78.031 | -93.597 | Steroid lactones | **728.3615@14.412996** |
| 385.1988 | 14.47 | InChI=1S/C21H30O5/c1-20-5-3-12(23)7-11(20)8-15(24)18-13(20)4-6-21(2)14(18)9-16(25)19(21)17(26)10-22/h7,13-16,18-19,22,24-25H,3-6,8-10H2,1-2H3 | N/A | 100 | -135.676 | Pyranones and derivatives | **384.1913@14.47** |
| 529.1351 | 14.487016 | (1R,3R,4S,5R)-3-[(E)-3-(3,4-dihydroxyphenyl)prop-2-enoyl]oxy-1,5-dihydroxy-4-[(E)-3-(3-hydroxy-4-methoxyphenyl)prop-2-enoyl]oxycyclohexane-1-carboxylic acid | 75368781 | 99.905 | -8.588 | Cinnamic acids and derivatives | **530.1425@14.487016** |
| 349.1194 | 14.579992 | p-Coumaroyl-L-tryptophan | 67130674 | 99.637 | -51.559 | Amino acids, peptides and analogues | **350.1268@14.579992** |
| 683.3253 | 14.973012 | 16-(beta-D-Glucopyranosyloxy)-17-hydroxy-kaurane-18-oic acid beta-D-glucopyranosyl ester | 10985203 | 81.969 | -65.468 | Diterpene glycosides | **682.3177@14.973012** |
| 543.1514 | 15.583006 | di-Feruloylquinic acid | 102036608 | 88.007 | -50.071 | Cinnamic acids and derivatives | **544.1586@15.583006** |
| 617.5098 | 19.741976 | 1-(9Z-tetradecenoyl)-2-eicosanoyl-sn-glycerol | 53477984 | 100 | -10.379 | Glycerolipids | **616.5054@19.741976** |

Table O.2 Chemical entities significantly increased during roasting.

| Prec. m/z | Ret. time (min) | SIRIUS NAME | PUBCHEM ID | SIRIUS SCORE | CSI SCORE | Class | Compound |
|---|---|---|---|---|---|---|---|
| 195.0872 | 0.84400105 | N-but-3-yn-2-yl-3-methyl-5-nitroimidazol-4-amine | 114382927 | 90.01 | -132.63 | Azoles | 194.0789@0.84400105 |
| 90.0912 | 0.84700006 | 2-(Methylamino)propan-1-ol | 12695785 | 100 | -54.471 | Amino acids, peptides and analogues | 89.0839@0.84700006 |

Table O.2 cont.

| Prec. m/z | Ret. time (min) | SIRIUS NAME | PUBCHEM ID | SIRIUS SCORE | CSI SCORE | Class | Compound |
|---|---|---|---|---|---|---|---|
| 371.1199 | 0.875 | 2-O-alpha-L-Rhamnopyranosyl-D-glucopyranose | 441426 | 49.99 | -26.144 | Carbohydrate and carbohydrate conjugates | 372.1268@0.875 |
| 185.0421 | 0.8759996 | InChI=1S/C6H10O5/c7-2-1-4(9)6(11)5(10)3-8/h4-11H,3H2 | N/A | 96.298 | -50.145 | Alcohols and polyols | 162.0528@0.8759996 |
| 163.0602 | 0.8759996 | 3,6-Anhydro-D-glucose | 16069993 | 100 | -51.284 | Carbohydrate and carbohydrate conjugates | 162.0528@0.8759996 |
| 325.1131 | 0.87799907 | InChI=1S/C12H20O10/c13-2-1-6(8(17)5(16)3-14)21-12-11(20)10(19)9(18)7(4-15)22-12/h5-20H,3-4H2 | N/A | 99.935 | -25.521 | Carbohydrate and carbohydrate conjugates | 324.1058@0.87799907 |
| 129.0546 | 0.8799996 | 2-Acetylbutanedial | 17765995 | 100 | -86.047 | Carboxylic acids and derivatives | 128.0473@0.8799996 |
| 161.0461 | 0.8809995 | Cerelose | 24749 | 100 | -19.795 | Carbohydrate and carbohydrate conjugates | 162.053@0.8809995 |
| 147.0652 | 0.8810003 | 5-Methoxy-5-oxopentanoic acid | 73917 | 100 | -65.765 | Carboxylic acids and derivatives | 146.0581@0.8810003 |
| 215.0528 | 0.8870005 | InChI=1S/C8H8N4O2/c1-11-6(12-3-2-9-5-12)4-10-7(11)8(13)14/h2-5H,1H3,(H,13,14) | N/A | 85.423 | -108.054 | Azoles | 192.0635@0.8870005 |
| 157.0496 | 0.8880004 | 2-(2-Methylprop-2-enylidene)propanedioic acid | 87996037 | 100 | -46.624 | Carboxylic acids and derivatives | 156.0423@0.8880004 |
| 473.1512 | 0.8979997 | 2,4,5-Trihydroxy-3-[3,4,5-trihydroxy-6-[[3,4,5-trihydroxy-6-(hydroxymethyl)oxan-2-yl]oxymethyl]oxan-2-yl]oxypentanal | 162888859 | 49.286 | -40.294 | Carbohydrate and carbohydrate conjugates | 474.1581@0.8979997 |
| 545.1721 | 0.9140003 | Gal6Ac(?1-6)Glc(?1-2b)Fruf | 90701676 | 49.516 | -58.484 | Carbohydrate and carbohydrate conjugates | 486.1581@0.9140003 |
| 515.1619 | 0.9290006 | (2R,3R,4S,5S,6R)-2-[(2S,3S,4R,5R)-4-hydroxy-2,5-bis(hydroxymethyl)-2-[(2R,3R,4S,5S,6R)-3,4,5-trihydroxy-6-(hydroxymethoxymethyl)oxan-2-yl]oxyoxolan-3-yl]oxy-6-(hydroxymethyl)oxane-3,4,5-triol | 57034926 | 98.671 | -97.149 | Carbohydrate and carbohydrate conjugates | 516.1688@0.9290006 |
| 163.0616 | 0.95500076 | CID 58100822 | 58100822 | 100 | -31.172 | Carbohydrate and carbohydrate conjugates | 164.0688@0.95500076 |

Table O.2 cont.

| Prec. m/z | Ret. time (min) | SIRIUS NAME | PUBCHEM ID | SIRIUS SCORE | CSI SCORE | Class | Compound |
|---|---|---|---|---|---|---|---|
| 200.0918 | 0.95800006 | 2'-Hydroxy-4'-O-methylpyridoxine | 101499959 | 100 | -115.668 | Benzene and substituted derivatives | 199.0846@0.95800006 |
| 337.0778 | 0.9810001 | (3R,4S,5S,6R)-6-[[(3R,4R,8R)-3,4-dihydroxy-2,6-dioxabicyclo[3.2.1]octan-8-yl]oxy]-3,4,5-trihydroxyoxane-2-carboxylic acid | 117661820 | 99.978 | -102.717 | Carbohydrate and carbohydrate conjugates | 338.0853@0.9810001 |
| 117.0546 | 0.9980003 | CID 57941047 | 57941047 | 99.911 | -43.434 | Carboxylic acids and derivatives | 116.0375@0.9980003 |
| 117.0546 | 1.0079997 | CID 57941047 | 57941047 | 100 | -51.33 | Carboxylic acids and derivatives | 116.0422@1.0079997 |
| 89.0244 | 1.0130004 | Glyceraldehyde | 751 | 100 | -18.017 | Carbohydrate and carbohydrate conjugates | 90.0317@1.0130004 |
| 117.0546 | 1.0299993 | CID 57941047 | 57941047 | 99.913 | -56.256 | Carboxylic acids and derivatives | 116.031@1.0299993 |
| 501.146 | 1.0309993 | InChI=1S/C18H30O16/c19-1-5-8(22)11(25)13(27)16(31-5)30-3-7-9(23)12(26)14(28)17(32-7)34-18(4-21)15(29)10(24)6(2-20)33-18/h4-17,19-20,22-29H,1-3H2 | N/A | 36.399 | -61.774 | Carbohydrate and carbohydrate conjugates | 456.1475@1.0309993 |
| 96.0443 | 1.0439993 | 3-Hydroxypyridine | 7971 | 100 | -11.602 | Pyrimidines and pyrimidine derivatives | 95.037@1.0439993 |
| 94.065 | 1.0520014 | beta-PICOLINE | 7970 | 99.996 | -13.018 | Pyrimidines and pyrimidine derivatives | 93.0578@1.0520014 |
| 94.065 | 1.2200006 | beta-PICOLINE | 7970 | 99.983 | -13.018 | Pyrimidines and pyrimidine derivatives | 93.0578@1.2200006 |
| 124.0393 | 1.2649995 | Nicotinic acid | 938 | 93.257 | -8.005 | Pyrimidines and pyrimidine derivatives | 123.032@1.2649995 |
| 126.0549 | 1.2919999 | 4-Methylidenepiperidine-2,6-dione | 18762684 | 100 | -115.383 | Heteroaromatic compounds | 125.0476@1.2919999 |
| 130.0499 | 1.3919988 | DL-Pyroglutamic acid | 499 | 100 | -12.888 | Amino acids, peptides and analogues | 129.0426@1.3919988 |
| 110.06 | 1.5640012 | 3-Hydroxy-2-methylpyridine | 70719 | 100 | -20.785 | Pyrimidines and pyrimidine derivatives | 109.0528@1.5640012 |
| 185.0921 | 1.738999 | (1S,2R)-1-(5-Methylpyrazin-2-yl)propane-1,2,3-triol | 45099925 | 100 | -61.286 | Carbohydrate and carbohydrate conjugates | 184.0848@1.738999 |

Table O.2 cont.

| Prec. m/z | Ret. time (min) | SIRIUS NAME | PUBCHEM ID | SIRIUS SCORE | CSI SCORE | Class | Compound |
|---|---|---|---|---|---|---|---|
| 110.06 | 1.8450007 | 3-Hydroxy-2-methylpyridine | 70719 | 100 | -18.425 | Pyrimidines and pyrimidine derivatives | 109.0528@1.8450007 |
| 124.0757 | 1.9879994 | 2,6-Dimethyl-3-hydroxypyridine | 70732 | 100 | -32.038 | Pyrimidines and pyrimidine derivatives | 123.0683@1.9879994 |
| 124.0757 | 2.2060006 | 2,6-Dimethyl-3-hydroxypyridine | 70732 | 99.999 | -32.798 | Pyrimidines and pyrimidine derivatives | 123.0684@2.2060006 |
| 110.06 | 2.432001 | 5-Hydroxy-2-methylpyridine | 14275 | 95.858 | -28.845 | Pyrimidines and pyrimidine derivatives | 109.0526@2.432001 |
| 235.1191 | 2.4980006 | 1-Crotyl theobromine | 252657 | 100 | -119.79 | Ethers | 234.1118@2.4980006 |
| 234.0763 | 2.9199986 | 1,3-Dimethylindole-2,5-dicarboxylic acid | 105492226 | 95.914 | -131.106 | Phenols | 233.0688@2.9199986 |
| 166.0862 | 3.378999 | N-(3-methoxy-4-methylphenyl)formamide | 138968417 | 91.739 | -78.096 | Benzene and substituted derivatives | 165.079@3.378999 |
| 199.1078 | 3.3999975 | 4-(3-Methylpyrazin-2-yl)butane-1,2,3-triol | 5319803 | 100 | -54.97 | Carbohydrate and carbohydrate conjugates | 198.1006@3.3999975 |
| 127.039 | 3.5899973 | 5-Hydroxymethylfurfural | 237332 | 100 | -41.13 | Phenols | 126.0318@3.5899973 |
| 355.1025 | 3.9360015 | Caffeoylquinic acid | | 43.49 | -2.427 | Cinnamic acids and derivatives | 354.0952@3.9360015 |
| 129.0544 | 5.391999 | 3,3a,6,6a-tetrahydro-1H-furo[3,4-c]furan-4-one | 54173531 | 100 | -68.322 | Carbonyl compounds | 128.047@5.391999 |
| 164.0683 | 5.931 | 2-Aminohept-6-ynoic acid | 71435968 | 99.999 | -75.221 | Amino acids, peptides and analogues | 141.079@5.931 |
| 227.1027 | 6.3680043 | Pyroglutamylproline | 13306588 | 99.556 | -79.3 | Amino acids, peptides and analogues | 226.0954@6.3680043 |
| 163.039 | 7.0260005 | 4,7-Dihydroxyinden-1-one | 86158727 | 99.997 | -75.435 | Coumarins and derivatives | 162.0317@7.0260005 |
| 247.0481 | 7.329003 | N,N'-(2-Hydroxy-1,4-phenylene)diacetamide | 13668863 | 100 | -146.44 | Ketones | 208.0849@7.329003 |
| 266.1388 | 7.7819986 | Caffeoylcholine | 6440794 | 99.993 | -66.415 | Cinnamic acids and derivatives | 265.1315@7.7819986 |
| 174.0913 | 9.0599985 | 2-ethyl-4(1H)-quinolinone | 10419657 | 99.999 | -68.771 | Pyrimidines and pyrimidine derivatives | 173.0841@9.0599985 |
| 244.097 | 9.391999 | 4-hydroxy-N-(4-hydroxy-3-methylphenyl)benzamide | 81566361 | 99.161 | -131.222 | Benzene and substituted derivatives | 243.0894@9.391999 |

Table O.2 cont.

| Prec. m/z | Ret. time (min) | SIRIUS NAME | PUBCHEM ID | SIRIUS SCORE | CSI SCORE | Class | Compound |
|---|---|---|---|---|---|---|---|
| 197.1285 | 9.733001 | Cyclo(D-Val-L-Pro) | 927560 | 99.649 | -17.196 | Amino acids, peptides and analogues | 196.1213@9.733001 |
| 337.0918 | 9.759001 | 5-Caffeoylshikimic acid | 5281762 | 59.735 | -51.176 | Cinnamic acids and derivatives | 336.0846@9.759001 |
| 195.1129 | 9.843996 | Cyclo(Pro-Pro) | 529063 | 100 | -45.199 | Amino acids, peptides and analogues | 194.1057@9.843996 |
| 197.1285 | 10.190996 | Cyclo(D-Val-L-Pro) | 927560 | 100 | -22.31 | Amino acids, peptides and analogues | 196.1212@10.190996 |
| 261.1237 | 10.455001 | N-(2-methoxyethyl)-4-morpholin-4-ylpyrimidin-2-amine | 112885845 | 51.016 | -137.912 | Pyrimidines and pyrimidine derivatives | 260.1173@10.455001 |
| 163.039 | 10.744002 | 7-Hydroxy-1-benzofuran-2-carbaldehyde | 83480306 | 85.886 | -81.786 | Pyrimidines and pyrimidine derivatives | 162.0317@10.744002 |
| 335.0773 | 10.866014 | 4-o-Caffeoylshikimic acid | 49821869 | 98.002 | -83.501 | Cinnamic acids and derivatives | 336.0846@10.866014 |
| 513.1368 | 10.875 | 4-O-(6-O-caffeylglucosyl) caffeic acid | 129711658 | 97.758 | -140.555 | Carbohydrate and carbohydrate conjugates | 490.148@10.875 |
| 533.2719 | 11.019997 | H-DL-Gln-DL-Glu-DL-xiThr-DL-Arg-OH | 18479083 | 68.469 | -70.15 | Amino acids, peptides and analogues | 532.2646@11.019997 |
| 337.092 | 11.060989 | 5-Caffeoylshikimic acid | 5281762 | 89.496 | -54.143 | Cinnamic acids and derivatives | 336.0847@11.060989 |
| 359.0738 | 11.060989 | N-(3-nitrophenyl)-6-oxo-2-phenyl-1H-pyrimidine-5-carboxamide | 92648668 | 61.655 | -140.389 | Organic nitro compounds | 336.0847@11.060989 |
| 323.0774 | 11.216002 | Skimmin | 99693 | 99.742 | -108.279 | Cinnamic acids and derivatives | 324.0847@11.216002 |
| 188.107 | 11.239996 | 5-Methyl-6-penta-1,3-dienylpyridine-2-carbaldehyde | 123147823 | 99.998 | -79.952 | Pyrimidines and pyrimidine derivatives | 187.0997@11.239996 |
| 337.0921 | 11.346004 | 5-Caffeoylshikimic acid | 5281762 | 77.434 | -50.966 | Cinnamic acids and derivatives | 336.0847@11.346004 |
| 211.1441 | 12.031004 | Cyclo(D-Leu-L-Pro) | 927565 | 100 | -4.482 | Amino acids, peptides and analogues | 210.1369@12.031004 |
| 675.3436 | 12.354003 | H-Ala-Pro-Pro-Leu-Gly-Gln-Ala-OH | 102210090 | 62.277 | -129.049 | Amino acids, peptides and analogues | 652.3543@12.354003 |
| 211.1442 | 12.440997 | Cyclo(D-Leu-L-Pro) | 927565 | 100 | -7.046 | Amino acids, peptides and analogues | 210.1369@12.440997 |

Table O.2 cont.

| Prec. m/z | Ret. time (min) | SIRIUS NAME | PUBCHEM ID | SIRIUS SCORE | CSI SCORE | Class | Compound |
|---|---|---|---|---|---|---|---|
| 505.241 | 13.153001 | [(2S,3S,4S,5S,6S)-5-acetamido-3,4-diacetyloxy-6-[5-(3-hydroxypropanoylamino)pentoxy]oxan-2-yl]methyl acetate | 117854909 | 45.123 | -137.624 | Carbohydrate and carbohydrate conjugates | 504.2339@13.153001 |
| 303.1956 | 13.155016 | InChI=1S/C19H26O3/c1-18-8-7-14-12(13(18)5-6-17(18)22)4-3-11-9-15(20)16(21)10-19(11,14)2/h3,12-14,16,21H,4-10H2,1-2H3 | N/A | 100 | -76.667 | Hydroxysteroids | 302.1883@13.155016 |
| 205.0857 | 13.419999 | 1-(4-Acetylphenyl)butane-1,3-dione | 101913461 | 99.993 | -88.046 | Benzene and substituted derivatives | 204.078@13.419999 |
| 541.2741 | 13.829999 | H-DL-His-DL-Glu-DL-Lys-DL-Gln-OH | 18494852 | 58.568 | -129.482 | Amino acids, peptides and analogues | 540.2671@13.829999 |
| 561.3372 | 14.219992 | H-Thr-DL-Lys-Pro-Pro-Nle-al | 117783685 | 99.987 | -149.756 | Amino acids, peptides and analogues | 538.3479@14.219992 |
| 540.3395 | 14.768997 | N-[(R)-3-[(L-Val-L-Pro-)Amino]-1,2-dioxopentyl]-D-Leu-L-Val-OH | 102000538 | 99.429 | -128.186 | Amino acids, peptides and analogues | 539.3321@14.768997 |
| 751.3513 | 15.33801 | H-Ala-Ala-Ala-Ala-Ala-Ala-Ala-Ala-Ala-Ala-al | 16040291 | 82.357 | -142.309 | Amino acids, peptides and analogues | 750.3437@15.33801 |
| 357.2038 | 15.770005 | InChI=1S/C20H30O4/c1-2-3-4-5-6-7-10-13-18(16-17-20(23)24)14-11-8-9-12-15-19(21)22/h6-8,10-11,13,16-18H,2-5,9,12,14-15H2,1H3,(H,21,22)(H,23,24) | N/A | 99.999 | -66.512 | Fatty acyls | 356.1965@15.770005 |

Table O.3 Chemical entities with maximum abundance in green beans

| Prec. m/z | Ret. time (min) | SIRIUS NAME | PUBCHEM ID | SIRIUS SCORE | CSI SCORE | Class | Compound |
|---|---|---|---|---|---|---|---|
| 175.1191 | 0.80699956 | N(5)-Acetyl-L-ornithine | 193343 | 100 | -32.612 | Amino acids, peptides and analogues | 174.1117@0.80699956 |
| 225.0619 | 0.8119996 | heptonic acid | 25588 | 90.708 | -12.495 | Hydroxy acids and derivatives | 226.069@0.8119996 |
| 181.072 | 0.8160011 | Mannitol | 6251 | 99.996 | -3.954 | Carbohydrates and carbohydrate conjugates | 182.0794@0.8160011 |

Table O.3 cont.

| Prec. m/z | Ret. time (min) | SIRIUS NAME | PUBCHEM ID | SIRIUS SCORE | CSI SCORE | Class | Compound |
|---|---|---|---|---|---|---|---|
| 184.1081 | 0.82600015 | 3-[(1,3-Dimethyl-1H-imidazole-3-ium)-4-yl]-L-alanine | 101134202 | 100 | -56.388 | Amino acids, peptides and analogues | 183.1009@0.82600015 |
| 146.0461 | 0.82600015 | DL-Glutamic acid | 611 | 100 | -14.187 | Amino acids, peptides and analogues | 147.0535@0.82600015 |
| 148.0604 | 0.83100057 | DL-Glutamic acid | 611 | 100 | -3.488 | Amino acids, peptides and analogues | 147.0532@0.83100057 |
| 195.0513 | 0.8330001 | Gluconic Acid | 10690 | 99.99 | -2.701 | Carbohydrates and carbohydrate conjugates | 136.0373@0.8330001 |
| 341.1092 | 0.8619996 | Trehalose | 7427 | 99.958 | -8.596 | Carbohydrates and carbohydrate conjugates | 342.1162@0.8619996 |
| 145.0496 | 0.8619996 | (2S)-2-(hydroxymethyl)-5,6-didehydro-3,4-dihydro-2H-pyran-3,4-diol | 145689814 | 99.999 | -71.892 | Carboxylic acids and derivatives | 144.0462@0.8619996 |
| 145.0496 | 0.8619996 | Triacetate | 5459844 | 100 | -61.368 | Carboxylic acids and derivatives | 144.047@0.8619996 |
| 127.039 | 0.8659997 | Maltol | 8369 | 100 | -66.649 | Pyrans | 126.0317@0.8659997 |
| 97.0283 | 0.8740004 | Protoanemonin | 66948 | 100 | -67.061 | Furans | 74.0391@0.8740004 |
| 533.1725 | 0.875 | (2R,3S,4R,5S,6S)-2-[(2R,3S,4R,5R,6S)-5-hydroxy-2-(hydroxymethoxy)-6-(hydroxymethyl)-3-[(2S,3R,4S,5R,6R)-3,4,5-trihydroxy-6-(hydroxymethyl)oxan-2-yl]oxyoxan-4-yl]oxy-6-(hydroxymethyl)oxane-3,4,5-triol | 44429606 | 54.134 | -121.133 | Carbohydrates and carbohydrate conjugates | 534.1794@0.875 |
| 475.1302 | 0.9230002 | 3,3-bis[[(2S,3R,4S,5R,6R)-3,4,5-trihydroxy-6-(hydroxymethyl)oxan-2-yl]oxy]propanoic acid | 67742984 | 49.252 | -59.298 | Carbohydrates and carbohydrate conjugates | 430.132@0.9230002 |
| 193.0343 | 1.0429994 | Citric Acid | 311 | 99.998 | -7.998 | Carboxylic acids and derivatives | 192.0271@1.0429994 |
| 147.0289 | 1.0429994 | 3-Oxopentanedioic acid | 68328 | 100 | -30.644 | Dicarboxylic acids | 146.0144@1.0429994 |
| 191.0199 | 1.0439992 | Citric acid | 311 | 100 | -3.933 | Carboxylix acids and derivatives | 194.0316@1.0439992 |
| 138.0552 | 1.0439992 | Trigonelline | 5570 | 99.998 | -13.161 | Pyridines and derivatives | 137.0479@1.0439992 |

Table O.3 cont.

| Prec. m/z | Ret. time (min) | SIRIUS NAME | PUBCHEM ID | SIRIUS SCORE | CSI SCORE | Class | Compound |
|---|---|---|---|---|---|---|---|
| 182.0461 | 1.0469995 | 2,4-Bis(hydroxymethyl)pyridine-3-carboxylic acid | 90450742 | 100 | -128.941 | Amino acids, peptides and analogues | 123.0323@1.0469995 |
| 220.1195 | 2.0989993 | trans-Zeatin | 449093 | 99.99 | -29.442 | Purine and purine derivatives | 219.1121@2.0989993 |
| 210.0761 | 2.2509997 | 2-[[(1R)-1-carboxyethyl]amino]benzoic acid | 92139622 | 100 | -83.869 | Amino acids, peptides and analogues | 209.0689@2.2509997 |
| 166.0863 | 2.4929976 | DL-Phenylalanine | 994 | 99.995 | -1.515 | Amino acids, peptides and analogues | 165.079@2.4929976 |
| 202.1801 | 2.5390012 | 4-[Cyclopentyl(2-hydroxyethyl)amino]butan-1-ol | 61584375 | 100 | -62.565 | Alkaloamines | 201.1729@2.5390012 |
| 220.1194 | 2.6820033 | trans-Zeatin | 449093 | 99.991 | -15.77 | Purine and purine derivatives | 219.1121@2.6820033 |
| 188.0706 | 4.729003 | 3-Indoleacrylic acid | 5375048 | 100 | -22.592 | Benzenoids | 187.0633@4.729003 |
| 203.0828 | 4.7539988 | DL-Tryptophan | 1148 | 99.99 | -3.213 | Amino acids, peptides and analogues | 204.0901@4.7539988 |
| 447.1475 | 6.3119993 | [(2R,3R,4S,5S,6S)-3,4,5-trihydroxy-6-[(2R,3R,4R,5S,6S)-3,4,5-trihydroxy-6-(hydroxymethyl)oxan-2-yl]oxyoxan-2-yl]methyl (E)-2-methylbut-2-enoate | 96355518 | 96.352 | -28.282 | Saccharolipids | 446.14@6.3119993 |
| 517.155 | 6.7359967 | (1S,3R,4R,5R)-1,3,4-trihydroxy-5-[(E)-3-[4-hydroxy-3-[(2S,3S,4R,5R,6S)-3,4,5-trihydroxy-6-(hydroxymethyl)oxan-2-yl]oxyphenyl]prop-2-enoyl]oxycyclohexane-1-carboxylic acid | 49821570 | 75.689 | -89.852 | Cinnamic acids and derivatives | 516.1482@6.7359967 |
| 539.1375 | 6.7359967 | 1-Amino-2-(2-methylsulfonylethyl)guanidine | 64866025 | 99.96 | -80.217 | Guanidines | 516.1482@6.7359967 |
| 462.1605 | 6.811002 | InChI=1S/C19H27NO12/c20-4-11(7-1-2-8(21)9(22)3-7)31-19-17(28)15(26)14(25)12(32-19)6-30-18-16(27)13(24)10(23)5-29-18/h1-3,8-19,21-28H,5-6H2 | N/A | 99.653 | -87.28 | Carbohydrate and carbohydrate conjugates | 461.1533@6.811002 |
| 179.0352 | 7.6290073 | Caffeic acid | 689043 | 100 | -21.727 | Cinnamic acids and derivatives | 180.0423@7.6290073 |
| 503.1401 | 7.838007 | Caffeic acid sucrose | 10346004 | 61.099 | -18.533 | Cinnamic acids and derivatives | 504.1475@7.838007 |
| 179.0576 | 7.990998 | Theophylline | 2153 | 100 | -8.136 | Imidazopyrimidines | 180.0648@7.990998 |

Table O.3 cont.

| Prec. m/z | Ret. time (min) | SIRIUS NAME | PUBCHEM ID | SIRIUS SCORE | CSI SCORE | Class | Compound |
|---|---|---|---|---|---|---|---|
| 265.1548 | 8.191994 | (+)-Abscisic acid | 5375200 | 100 | -103.816 | Phenol lipids | 264.1471@8.191994 |
| 377.0845 | 8.224995 | cis-Chlorogenic acid | 1794425 | 99.881 | -4.631 | Cinnamic acids and derivatives | 354.0953@8.224995 |
| 353.088 | 8.239994 | 4-O-Caffeoylquinic acid | 9798666 | 92.424 | -4.269 | Cinnamic acids and derivatives | 354.0953@8.239994 |
| 443.057 | 8.242003 | 5-[3-(beta-D-Glucopyranosyloxy)-1,5-dimethyl-8-hydroxy-6-oxabicyclo[3.2.1]octane-8-yl]-3-methyl-2,4-pentadienoic acid | 100966496 | 49.968 | -57.562 | Phenol lipids | 444.0644@8.242003 |
| 377.0846 | 8.60999 | cis-Chlorogenic acid | 1794425 | 99.997 | -3.139 | Cinnamic acids and derivatives | 354.0954@8.60999 |
| 429.0975 | 8.611005 | 4-[3-(6-Hydroxynaphthalene-2-carbonyl)oxybenzoyl]oxybenzoic acid | 53795003 | 99.958 | -138.821 | Catechols | 428.0902@8.611005 |
| 353.0881 | 8.620991 | Caffeoylquinic acid | 1794425 | 99.467 | -2.996 | Cinnamic acids and derivatives | 354.0952@8.620991 |
| 175.0867 | 10.16499 | Indole-3-acetamide | 397 | 100 | -20.487 | Benzenoids | 174.0793@10.16499 |
| 197.0686 | 10.16499 | 3-(5,6-Dimethylpyridin-3-yl)-3-oxopropanenitrile | 130438969 | 63.085 | -97.382 | Pyridines and derivatives | 174.0793@10.16499 |
| 361.0896 | 10.84699 | p-Coumaroylquinic acid | 6441280 | 70.908 | -15.611 | Cinnamic acids and derivatives | 338.1002@10.84699 |
| 339.1078 | 10.84699 | p-Coumaroylquinic acid | 6441280 | 98.144 | -3.364 | Cinnamic acids and derivatives | 338.1002@10.84699 |
| 337.093 | 10.856006 | 2-Coumaroylquinic acid | 6441280 | 100 | -5.115 | Cinnamic acids and derivatives | 338.1002@10.856006 |
| 499.1424 | 10.921998 | [(2R,3S,4S,5R,6S)-3,4,5-trihydroxy-6-[[(1S,2S,4S,5S,6R,10S)-5-hydroxy-2-(hydroxymethyl)-3,9-dioxatricyclo[4.4.0.02,4]dec-7-en-10-yl]oxy]oxan-2-yl]methyl 3,4-dihydroxybenzoate | 76683650 | 44.68 | -120.76 | Carbohydrate and carbohydrate conjugates | 498.1351@10.921998 |
| 367.1035 | 11.30299 | 4-O-Feruloylquinic acid | 4635494 | 99.984 | -7.044 | Cinnamic acids and derivatives | 368.1109@11.30299 |
| 369.1183 | 11.752006 | Feruloylquinic acid | 5317346 | 95.282 | -6.987 | Cinnamic acids and derivatives | 368.111@11.752006 |
| 177.0547 | 11.752997 | 3-(4-Hydroxy-3-methoxyphenyl)prop-2-ynal | 82362867 | 100 | -61.429 | Cinnamic acids and derivatives | 176.0474@11.752997 |

Table O.3 cont.

| Prec. m/z | Ret. time (min) | SIRIUS NAME | PUBCHEM ID | SIRIUS SCORE | CSI SCORE | Class | Compound |
|---|---|---|---|---|---|---|---|
| 367.1037 | 11.760007 | 3-O-Feruloylquinic acids | 131850437 | 100 | -6.163 | Cinnamic acids and derivatives | 368.1109@11.760007 |
| 138.0662 | 12.057006 | 5-hydroxy-1,3-dimethyl-1H-pyrazole-4-carbonitrile | 15145031 | 100 | -51.36 | Diazines | 137.0589@12.057006 |
| 195.088 | 12.057006 | Caffeine | 2519 | 100 | -5.767 | Purines and purine derivatives | 194.0806@12.057006 |
| 193.0508 | 12.07701 | Ferulic acid | 445858 | 92.67 | -8.229 | Cinnamic acids and derivatives | 194.0581@12.07701 |
| 537.2674 | 12.219985 | [(14R)-3beta,5,14,16-Tetrahydroxygrayanotoxa-10(20)-ene-6beta-yl]alpha-D-glucopyranoside | 101224094 | 48.107 | -74.573 | Carbohydrates and carbohydrate conjugates | 536.2598@12.219985 |
| 537.2672 | 12.4260025 | [(14R)-3beta,5,14,16-Tetrahydroxygrayanotoxa-10(20)-ene-6beta-yl]alpha-D-glucopyranoside | 101224094 | 66.986 | -90.559 | Phenol lipids | 536.2598@12.4260025 |
| 517.1344 | 12.629016 | di-Caffeoylquinic acid | 5281780 | 93.966 | -6.791 | Cinnamic acids and derivatives | 516.1269@12.629016 |
| 539.1164 | 12.629016 | di-Caffeoylquinic acid | 5281780 | 99.993 | -11.773 | Cinnamic acids and derivatives | 516.1269@12.629016 |
| 355.1025 | 12.630992 | cis-Chlorogenic acid | 1794425 | 92.008 | -4.569 | Cinnamic acids and derivatives | 354.0953@12.630992 |
| 515.1196 | 12.63599 | di-Caffeoylquinic acid | 134769983 | 99.697 | -4.468 | Cinnamic acids and derivatives | 516.1266@12.63599 |
| 163.039 | 12.814006 | 7-Hydroxy-1-benzofuran-2-carbaldehyde | 83480306 | 100 | -83.935 | Coumarines and derivatives | 162.0316@12.814006 |
| 473.1087 | 13.245987 | (1S,3R,4R,5R)-3-[(E)-3-(3,4-dihydroxyphenyl)prop-2-enoyl]oxy-1,5-dihydroxy-4-(4-hydroxybenzoyl)oxycyclohexane-1-carboxylic acid | 24094133 | 96.813 | -80.205 | Cinnamic acids and derivatives | 474.1162@13.245987 |
| 499.1246 | 13.29601 | 1alpha,3alpha-Dihydroxy-4alpha-(3,4-dihydroxycinnamoyloxy)-5beta-(4-hydroxycinnamoyloxy)cyclohexane-1-carboxylic acid | 102383780 | 89.643 | -12.277 | Cinnamic acids and derivatives | 500.1315@13.29601 |
| 355.1027 | 13.406005 | cis-Chlorogenic acid | 1794425 | 42.959 | -2.603 | Cinnamic acids and derivatives | 354.0953@13.406005 |
| 499.1242 | 13.411991 | 1alpha,5beta-Dihydroxy-3alpha-(3,4-dihydroxycinnamoyloxy)-4alpha-(4- | 102383774 | 99.631 | -15.208 | Cinnamic acids and derivatives | 500.1318@13.411991 |

Table O.3 cont.

| Prec. m/z | Ret. time (min) | SIRIUS NAME | PUBCHEM ID | SIRIUS SCORE | CSI SCORE | Class | Compound |
|---|---|---|---|---|---|---|---|
| | | hydroxycinnamoyloxy)cyclohexane-1-carboxylic acid | | | | | |
| 537.1016 | 13.413001 | Melitric acid A | 10459878 | 69.144 | -173.071 | Cinnamic acids and derivatives | 538.1087@13.413001 |
| 437.1452 | 13.645007 | Benzyl 2-O,3-O,4-O,6-O-tetraacetyl-D-mannopyranoside | 102364003 | 99.739 | -164.173 | Cinnamic acids and derivatives | 438.1524@13.645007 |
| 529.1351 | 13.715002 | (1R,3R,4S,5R)-4-[(E)-3-(3,4-dihydroxyphenyl)prop-2-enoyl]oxy-1,3-dihydroxy-5-[(E)-3-(3-hydroxy-4-methoxyphenyl)prop-2-enoyl]oxycyclohexane-1-carboxylic acid | 42598867 | 71.749 | -4.75 | Cinnamic acids and derivatives | 530.1426@13.715002 |
| 529.135 | 13.831995 | Caffeoyl-feruloyl quinic acid | 131752147 | 99.567 | -5.988 | Cinnamic acids and derivatives | 530.1425@13.831995 |
| 389.1111 | 13.995983 | (2S)-3-(5-hydroxy-1H-indol-3-yl)-2-[[(E)-3-(4-hydroxyphenyl)prop-2-enoyl]amino]propanoic acid | 68025994 | 78.328 | -112.545 | Amino acids, peptides and analogues | 366.1218@13.995983 |
| 365.1143 | 14.008997 | Caffeoyltryptophan | 15228042 | 99.99 | -48.995 | Amino acids, peptides and analogues | 366.1218@14.008997 |
| 247.1177 | 14.398995 | 1-O-(4-Pentynyl)-alpha-D-glucopyranose | 87425972 | 100 | -76.314 | Carbohydrate and carbohydrate conjugates | 246.1103@14.398995 |
| 529.1351 | 14.487016 | (1R,3R,4S,5R)-4-[(E)-3-(3,4-dihydroxyphenyl)prop-2-enoyl]oxy-1,3-dihydroxy-5-[(E)-3-(3-hydroxy-4-methoxyphenyl)prop-2-enoyl]oxycyclohexane-1-carboxylic acid | 42598867 | 99.91 | -8.313 | Cinnamic acids and derivatives | 530.1425@14.487016 |
| 279.0064 | 14.499012 | D-Cystine S-oxide | 13456552 | 89.484 | -68.092 | Amino acids, peptides and analogues | 256.0171@14.499012 |
| 351.1343 | 14.568981 | p-Coumaroyl-L-tryptophan | 67130674 | 92.672 | -72.703 | Amino acids, peptides and analogues | 350.1269@14.568981 |
| 349.1194 | 14.579992 | p-Coumaroyl-L-tryptophan | C20H18N2O4 | 100 | -46.855 | Amino acids, peptides and analogues | 350.1268@14.579992 |
| 379.1299 | 14.882997 | (2S)-2-[[(E)-3-(4-hydroxy-3-methoxyphenyl)prop-2-enoyl]amino]-3-(1H-indol-3-yl)propanoic acid | 7097585 | 100 | -39.558 | Amino acids, peptides and analogues | 380.1373@14.882997 |

Table O.3 cont.

| Prec. m/z | Ret. time (min) | SIRIUS NAME | PUBCHEM ID | SIRIUS SCORE | CSI SCORE | Class | Compound |
|---|---|---|---|---|---|---|---|
| 683.3253 | 14.973012 | 13-(beta-D-Glucopyranosyloxy)-16-hydroxykaurane-19-oic acid beta-D-glucopyranosyl ester | 102404144 | 61.467 | -99.191 | Fatty acyls glycosides | 682.3177@14.973012 |
| 227.1256 | 15.155019 | 2-[(4-Amino-6-methoxy-1,3,5-triazin-2-yl)amino]-2-methylpropanamide | 80818839 | 99.994 | -125.19 | Pyrimidines and pyrimidine derivatives | 204.1364@15.155019 |
| 633.2885 | 15.216002 | H-Gly-Gly-Gly-Gly-Glu-Glu-Lys-OH | 25185011 | 72.654 | -141.894 | Amino acids, peptides and analogues | 632.2812@15.216002 |
| 247.1307 | 15.59301 | 4,4'-(Hydroxymethylene)dicyclohexanone | 117698060 | 42.223 | -103.158 | Ketones | 224.1414@15.59301 |
| 225.1486 | 15.59301 | InChI=1S/C13H20O3/c1-8-5-10(15)7-13(3,4)12(8)11(16)6-9(2)14/h5-6,9,12,14,16H,7H2,1-4H3 | N/A | 100 | -127.671 | Ketones | 224.1414@15.59301 |
| 158.154 | 15.905019 | 3-methyl-N-(2-methylpropyl)butanamide | 233652 | 99.972 | -56.167 | Fatty amides | 157.1467@15.905019 |
| 198.1854 | 15.991984 | N-cyclopropylnonanamide | 3653265 | 100 | -58.587 | Fatty amides | 197.1781@15.991984 |
| 220.1673 | 15.991984 | 3-Methyl-1-(2-methylpyrrolidin-3-yl)hexan-1-one | 116592103 | 100 | -74.533 | Fatty amides | 197.1781@15.991984 |

Table O.4 Chemical entities with maximum abundance in roasted beans

| Prec. m/z | Ret. time (min) | SIRIUS NAME | PUBCHEM ID | SIRIUS SCORE | CSI SCORE | Class | Compound |
|---|---|---|---|---|---|---|---|
| 195.0872 | 0.84400105 | L-Quebrachitol | 151108 | 99.783 | -16.71 | Cyclitols and derivatives | 194.0789@0.84400105 |
| 90.0912 | 0.84700006 | 2-(Methylamino)propan-1-ol | 12695785 | 100 | -74.789 | Amines | 89.0839@0.84700006 |
| 163.0602 | 0.8759996 | Idosan | 1742165 | 100 | -55.19 | Carbohydrate and carbohydrate conjugates | 162.0528@0.8759996 |
| 147.0652 | 0.8810003 | (2R,3S,4R)-hex-5-yne-1,2,3,4-tetrol | 88101453 | 100 | -55.501 | Furofurans | 146.0581@0.8810003 |
| 157.0496 | 0.8880004 | (E)-2-methyl-4-methylidenepent-2-enedioic acid | 89835634 | 100 | -53.249 | Carboxylic acids and derivatives | 156.0423@0.8880004 |

Table O.4 cont.

| Prec. m/z | Ret. time (min) | SIRIUS NAME | PUBCHEM ID | SIRIUS SCORE | CSI SCORE | Class | Compound |
|---|---|---|---|---|---|---|---|
| 515.1619 | 0.9290006 | (2R,3R,4S,5S,6R)-2-[(2S,3S,4R,5R)-4-hydroxy-2,5-bis(hydroxymethyl)-2-[(2R,3R,4S,5S,6R)-3,4,5-trihydroxy-6-(hydroxymethoxymethyl)oxan-2-yl]oxyoxolan-3-yl]oxy-6-(hydroxymethyl)oxane-3,4,5-triol | 57034926 | 51.806 | -88.814 | Carbohydrate and carbohydrate conjugates | 516.1688@0.9290006 |
| 365.109 | 0.9440002 | [3,4,5-Trihydroxy-6-[3,4,5-trihydroxy-6-(hydroxymethyl)oxan-2-yl]oxyoxan-2-yl]methyl acetate | 59514402 | 95.659 | -152.691 | Shikimic acids and derivatives | 366.1164@0.9440002 |
| 337.0778 | 0.9810001 | (5R)-3-hydroxy-5-[(1S)-1-hydroxy-2-[(2R,3R,4S,5R,6R)-3,4,5-trihydroxy-6-(hydroxymethyl)oxan-2-yl]oxyethyl]oxolane-2,4-dione | 54391609 | 98.874 | -83.901 | Carbohydrate and carbohydrate conjugates | 338.0853@0.9810001 |
| 219.0513 | 0.9980006 | InChI=1S/C8H12O7/c9-3-5(11)8(15)7(14)4(10)1-2-6(12)13/h4-5,7-11,14-15H,3H2,(H,12,13) | N/A | 100 | -51.326 | Cyclitols and derivatives | 174.0531@0.9980006 |
| 233.0669 | 0.9980006 | O-acetyl-quinic acid | 129800630 | 100 | -90.001 | Cyclitols and derivatives | 174.0531@0.9980006 |
| 455.1405 | 1.0309993 | (2R,3S,4S)-2,4,5-trihydroxy-3-[(2S,3R,4S,5R,6R)-3,4,5-trihydroxy-6-[[(2R,3R,4S,5R,6R)-3,4,5-trihydroxy-6-(hydroxymethyl)oxan-2-yl]oxymethyl]oxan-2-yl]oxypentanal | 162888860 | 99.985 | -41.012 | Carbohydrate and carbohydrate conjugates | 456.1475@1.0309993 |
| 501.146 | 1.0309993 | InChI=1S/C18H30O16/c19-1-5-8(22)11(25)13(27)16(31-5)30-3-7-9(23)12(26)14(28)17(32-7)34-18(4-21)15(29)10(24)6(2-20)33-18/h4-17,19-20,22-29H,1-3H2 | N/A | 44.864 | -60.01 | Carbohydrate and carbohydrate conjugates | 456.1475@1.0309993 |
| 231.1129 | 1.0469995 | N-(4-acetamidophenyl)pent-4-ynamide | 82363198 | 99.834 | -109.785 | Amino acids, peptides and analogues | 230.1057@1.0469995 |
| 94.065 | 1.2200006 | beta-PICOLINE | 7970 | 99.99 | -13.013 | Pyridines and derivatives | 93.0578@1.2200006 |
| 124.0393 | 1.2649995 | Nicotinic acid | 938 | 85.956 | -15.614 | Pyridines and derivatives | 123.032@1.2649995 |
| 233.0668 | 1.7630004 | O-acetyl-quinic acid | 129800630 | 100 | -91.476 | Cyclitols and derivatives | 234.074@1.7630004 |

Table O.4 cont.

| Prec. m/z | Ret. time (min) | SIRIUS NAME | PUBCHEM ID | SIRIUS SCORE | CSI SCORE | Class | Compound |
|---|---|---|---|---|---|---|---|
| 323.0774 | 11.216002 | InChI=1S/C15H16O8/c16-7-10-12(19)13(20)14(21)15(22-10)23-11(18)6-3-8-1-4-9(17)5-2-8/h1-7,10,12-15,17,19-21H | N/A | 93.766 | -124.242 | Cinnamic acids and derivatives | 324.0847@11.216002 |
| 163.1328 | 12.741995 | 4-Methoxy-2,4-dimethylpentane-1,2-diol | 82712976 | 98.14 | -83.381 | Fatty acyls | 162.1257@12.741995 |
| 233.0785 | 14.00599 | 1-Butan-2-yl-3-pyrimidin-2-ylurea | 45369340 | 100 | -139.351 | Pyrimidines and pyrimidine derivatives | 232.0714@14.00599 |

Table O.5 Chemical entities with maximum abundance in instant coffee

| Prec. m/z | Ret. time (min) | SIRIUS NAME | PUBCHEM ID | SIRIUS SCORE | CSI SCORE | Class | Compound |
|---|---|---|---|---|---|---|---|
| 127.024 | 0.7270003 | 2-oxo-2-(2H-tetrazol-5-yl)acetaldehyde | 53927792 | 62.765 | -98.771 | Azoles | 126.0167@0.7270003 |
| 132.0306 | 0.8139995 | Aspartic Acid | 5960 | 99.997 | -6.487 | Amino acids, peptides and analogues | 133.0376@0.8139995 |
| 134.0449 | 0.82199943 | Aspartic Acid | 5960 | 100 | -3.402 | Amino acids, peptides and analogues | 133.0375@0.82199943 |
| 179.0566 | 0.843 | D-Glucose | 5793 | 100 | -12.014 | Carbohydrate and carbohydrate conjugates | 180.0633@0.843 |
| 355.0885 | 0.844001 | (2S,3S,4S,5R,6R)-3,4,5-trihydroxy-6-[(2R,3R,4R,5R)-1,2,4,5-tetrahydroxy-6-oxohexan-3-yl]oxyoxane-2-carboxylic acid | 87905756 | 99.925 | -27.452 | Carbohydrate and carbohydrate conjugates | 296.0744@0.844001 |
| 161.0458 | 0.84700006 | Cartose | 24749 | 100 | -20.873 | Carbohydrate and carbohydrate conjugates | 102.0315@0.84700006 |
| 101.0247 | 0.84700006 | Erythrulose | 162406 | 100 | -32.165 | Carbohydrate and carbohydrate conjugates | 102.0315@0.84700006 |

Table O.5
cont.

| Prec. m/z | Ret. time (min) | SIRIUS NAME | PUBCHEM ID | SIRIUS SCORE | CSI SCORE | Class | Compound |
|---|---|---|---|---|---|---|---|
| 549.1668 | 0.84799963 | 4-O-beta-D-Glucopyranosyl-beta-D-glucopyranosyl beta-D-fructofuranoside | 101924360 | 48.893 | -25.281 | Carbohydrate and carbohydrate conjugates | 504.1685@0.84799963 |
| 193.0357 | 0.84899926 | 2-Dehydro-D-galactonate | 17756738 | 100 | -16.77 | Carbohydrate and carbohydrate conjugates | 194.0432@0.84899926 |
| 185.0392 | 0.8639991 | InChI=1S/C6H10O5/c7-2-1-4(9)6(11)5(10)3-8/h4-11H,3H2 | N/A | 100 | -62.462 | Fatty acyls | 162.0568@0.8639991 |
| 85.0283 | 0.8639991 | Fumaraldehyde | 5287477 | 100 | -65.815 | Ketones | 84.021@0.8639991 |
| 191.0203 | 0.8719998 | Citric acid | 311 | 100 | -4.98 | Fatty acids and conjugates | 192.0272@0.8719998 |
| 371.1199 | 0.875 | (2R,3S,4S,5R)-2-(hydroxymethyl)-6-[[(3R,4S,5S,6R)-3,4,5-trihydroxy-6-(hydroxymethyl)oxan-2-yl]oxymethoxy]oxane-3,4,5-triol | 53722046 | 99.059 | -44.588 | Carbohydrate and carbohydrate conjugates | 372.1268@0.875 |
| 695.2251 | 0.8759996 | Gal(b1-4)Glc(b1-4)Glc(b1-4)a-LDManHep | 91855613 | 30.882 | -92.127 | Carbohydrate and carbohydrate conjugates | 636.211@0.8759996 |
| 289.033 | 0.8759996 | InChI=1S/C7H15O10P/c8-3(1-5(10)11)6(12)7(13)4(9)2-17-18(14,15)16/h3-4,6-9,12-13H,1-2H2,(H,10,11)(H2,14,15,16) | N/A | 99.996 | -107.674 | Quinic acids and derivatives | 290.0414@0.8759996 |
| 605.1931 | 0.87599975 | (1,3)-beta-Xylotetraose | 52940205 | 33.326 | -51.807 | Carbohydrate and carbohydrate conjugates | 606.2003@0.87599975 |
| 161.0461 | 0.8809995 | Inositol | 892 | 100 | -29.651 | Carbohydrate and carbohydrate conjugates | 162.053@0.8809995 |
| 443.1407 | 0.90900034 | 4-O-[4-O-(beta-D-Glucopyranosyl)-beta-D-xylopyranosyl]-D-xylopyranose | 101754096 | 49.913 | -95.949 | Carbohydrate and carbohydrate conjugates | 384.1265@0.90900034 |
| 485.1511 | 0.9140003 | InChI=1S/C18H30O15/c1-4-7(19)10(22)14(26)17(31-4)29-3-6-9(21)12(24)15(27)18(33-6)30-2-5- | N/A | 49.499 | -83.767 | Carbohydrate and carbohydrate conjugates | 486.1581@0.9140003 |

Table O.5 cont.

| Prec. m/z | Ret. time (min) | SIRIUS NAME | PUBCHEM ID | SIRIUS SCORE | CSI SCORE | Class | Compound |
|---|---|---|---|---|---|---|---|
| 531.1564 | 0.9140003 | 8(20)11(23)13(25)16(28)32-5/h4-6,8-18,20-28H,2-3H2,1H3 InChI=1S/C19H32O17/c20-1-6-11(25)16(30)19(4-21,35-6)36-18-15(29)13(27)10(24)8(34-18)3-32-17-14(28)12(26)9(23)7(33-17)2-31-5-22/h5-18,20-21,23-30H,1-4H2 | N/A | 48.041 | -63.98 | Carbohydrate and carbohydrate conjugates | 486.1581@0.9140003 |
| 545.1721 | 0.9140003 | (1,4)-beta-Xylotetraose | 5289594 | 36.299 | -53.853 | Carbohydrate and carbohydrate conjugates | 486.1581@0.9140003 |
| 133.0143 | 0.9359996 | Malic acid | 525 | 100 | -4.229 | Fatty acids and conjugates | 88.0155@0.9359996 |
| 147.03 | 0.9359996 | 2-Hydroxyglutaric acid | 43 | 100 | -32.114 | Fatty acids and conjugates | 88.0155@0.9359996 |
| 175.0252 | 0.9420008 | 2-[(3R,4S)-3,4-dihydroxy-5-oxooxolan-2-yl]-2-hydroxyacetaldehyde | 129627904 | 100 | -21.725 | Carbohydrate and carbohydrate conjugates | 116.0111@0.9420008 |
| 115.0037 | 0.9420008 | Malic acid | 525 | 99.99 | -8.965 | Fatty acids and conjugates | 116.0111@0.9420008 |
| 118.0862 | 0.94499975 | DL-Valine | 1182 | 100 | -38.664 | Amino acids, peptides and analogues | 117.079@0.94499975 |
| 707.2244 | 0.9459995 | alpha-D-mannopyranosyl-(1->5)-beta-D-arabinofuranosyl-(1->2)-alpha-D-arabinofuranosyl-(1->5)-alpha-D-arabinofuranosyl-(1->5)-D-arabinofuranose | 134160293 | 90.96 | -130.303 | Carbohydrate and carbohydrate conjugates | 708.2321@0.9459995 |
| 163.0616 | 0.95500076 | CID 58100822 | 58100822 | 100 | -24.108 | Carbohydrate and carbohydrate conjugates | 164.0688@0.95500076 |
| 267.1089 | 0.97999966 | PyroGlu-His | 3839181 | 99.865 | -73.695 | Amino acids, peptides and analogues | 266.1021@0.97999966 |
| 89.0244 | 1.0130004 | Glyceraldehyde | 751 | 100 | -29.207 | Carbohydrate and carbohydrate conjugates | 90.0317@1.0130004 |

Table O.5
cont.

| Prec. m/z | Ret. time (min) | SIRIUS NAME | PUBCHEM ID | SIRIUS SCORE | CSI SCORE | Class | Compound |
|---|---|---|---|---|---|---|---|
| 809.2567 | 1.0330006 | beta-Cellopentaose | 440949 | 98.355 | -49.313 | Carbohydrate and carbohydrate conjugates | 750.2427@1.0330006 |
| 111.0088 | 1.0439992 | Itaconic acid | 811 | 100 | -64.337 | Carbohydrate and carbohydrate conjugates | 112.0162@1.0439992 |
| 96.0443 | 1.0439993 | 3-Hydroxypyridine | 7971 | 100 | -11.989 | Pyridines and derivatives | 95.037@1.0439993 |
| 339.0935 | 1.0439997 | InChI=1S/C12H20O11/c13-1-4(16)7(17)8(18)5(2-14)22-12-11(21)10(20)9(19)6(3-15)23-12/h1-2,4-12,15-21H,3H2 | N/A | 49.488 | -43.306 | Carbohydrate and carbohydrate conjugates | 294.0951@1.0439997 |
| 247.1081 | 1.0460005 | 4-amino-3-hydroxy-N-[(5-methylfuran-2-yl)methyl]benzamide | 107075141 | 99.878 | -114.156 | Benzene and substituted derivatives | 246.1005@1.0460005 |
| 94.065 | 1.0520014 | beta-PICOLINE | 7970 | 100 | -13.923 | Pyridines and derivatives | 93.0578@1.0520014 |
| 243.0624 | 1.2419987 | Pyroglutamylaspartic acid | 81640562 | 100 | -95.045 | Amino acids, peptides and analogues | 244.0697@1.2419987 |
| 289.0677 | 1.2419987 | Uridine | 6029 | 99.337 | -62.448 | Amino acids, peptides and analogues | 244.0697@1.2419987 |
| 132.102 | 1.2580012 | DL-Leucine | 857 | 100 | -33.454 | Amino acids, peptides and analogues | 131.0947@1.2580012 |
| 126.0549 | 1.2919999 | 3,5-Dioxohexanenitrile | 14165401 | 100 | -98.475 | Carboxylic acid and derivatives | 125.0476@1.2919999 |
| 130.0499 | 1.3919988 | L-Pyroglutamic acid | 7405 | 100 | -8.72 | Amino acids, peptides and analogues | 129.0426@1.3919988 |
| 128.0354 | 1.3949987 | L-Pyroglutamic acid | 7405 | 100 | -37.847 | Amino acids, peptides and analogues | 129.0427@1.3949987 |
| 110.06 | 1.5640012 | 5-Hydroxy-2-methylpyridine | 14275 | 100 | -21.706 | Pyridines and derivatives | 109.0528@1.5640012 |
| 257.0781 | 1.6350002 | InChI=1S/C10H14N2O6/c11-6(2-1-5-13)9(16)12-7(10(17)18)3-4-8(14)15/h6-7,13H,2-4,11H2,(H,12,16)(H,14,15)(H,17,18) | N/A | 100 | -66.669 | Amino acids, peptides and analogues | 258.0852@1.6350002 |
| 268.1041 | 1.6549991 | Adenosine | 60961 | 97.664 | -2.425 | Purine nucleosides | 267.0969@1.6549991 |

Table O.5 cont.

| Prec. m/z | Ret. time (min) | SIRIUS NAME | PUBCHEM ID | SIRIUS SCORE | CSI SCORE | Class | Compound |
|---|---|---|---|---|---|---|---|
| 129.0194 | 1.663 | Mesaconic acid | 638129 | 100 | -17.13 | Fatty acids and conjugates | 130.0267@1.663 |
| 185.0921 | 1.738999 | (1S,2R)-1-(5-Methylpyrazin-2-yl)propane-1,2,3-triol | 45099925 | 100 | -61.683 | Carbohydrate and carbohydrate conjugates | 184.0848@1.738999 |
| 128.0706 | 1.7979984 | 6-Oxo-piperidine-2-carbaldehyde | 19903070 | 100 | -93.323 | Carboxylic acid and derivatives | 127.0633@1.7979984 |
| 235.1191 | 1.9729997 | Cyclo(-D-His-Pro) | 360579 | 100 | -145.326 | Amino acids, peptides and analogues | 234.1117@1.9729997 |
| 124.0757 | 1.9879994 | 2,6-Dimethyl-3-hydroxypyridine | 70732 | 100 | -55.832 | Pyridines and derivatives | 123.0683@1.9879994 |
| 220.1194 | 2.3569999 | trans-Zeatin | 449093 | 96.493 | -36.884 | Purines and purine derivatives | 219.1122@2.3569999 |
| 145.0496 | 2.365 | 3-Methylenepentanedioic acid | 13495591 | 100 | -40.812 | Carboxylic acid and derivatives | 144.0422@2.365 |
| 110.06 | 2.432001 | 5-Hydroxy-2-methylpyridine | 14275 | 100 | -24.866 | Pyridines and derivatives | 109.0526@2.432001 |
| 235.1191 | 2.4980006 | Cyclo(-D-His-Pro) | 360579 | 100 | -92.587 | Amino acids, peptides and analogues | 234.1118@2.4980006 |
| 167.0352 | 3.111 | 3,4-Dihydroxyphenylacetic acid | 547 | 100 | -16.686 | Cinnamic acids and derivatives | 168.0423@3.111 |
| 166.0862 | 3.378999 | N-(3-methoxy-4-methylphenyl)formamide | 138968417 | 99.34 | -79.17 | Benzene and substitided derivatives | 165.079@3.378999 |
| 199.1078 | 3.3999975 | 4-(3-Methylpyrazin-2-yl)butane-1,2,3-triol | 5319803 | 100 | -61.243 | Pyrazines | 198.1006@3.3999975 |
| 333.0826 | 3.473 | 3,5-Dihydroxyphenyl alpha-D-glucopyranoside | 54455264 | 49.919 | -36.084 | Carbohydrate and carbohydrate conjugates | 288.0848@3.473 |
| 155.0815 | 3.5789986 | CYCLO(-GLY-PRO) | 126154 | 100 | -23.906 | Amino acids, peptides and analogues | 154.0742@3.5789986 |
| 127.039 | 3.5899973 | 5-Hydroxymethylfurfural | 237332 | 100 | -39.825 | Phenols | 126.0318@3.5899973 |
| 353.0878 | 3.953002 | 4-O-Caffeoylquinic acid | 9798666 | 97.238 | -5.437 | Cinnamic acids and derivatives | 354.0948@3.953002 |

Table O.5 cont.

| Prec. m/z | Ret. time (min) | SIRIUS NAME | PUBCHEM ID | SIRIUS SCORE | CSI SCORE | Class | Compound |
|---|---|---|---|---|---|---|---|
| 274.1074 | 4.1340013 | 2-(4-hydroxyphenoxy)-N-(2-methoxyphenyl)acetamide | 43326297 | 99.697 | -114.286 | Phenol ehters | 273.1003@4.1340013 |
| 355.1026 | 4.3910007 | cis-Chlorogenic acid | 1794425 | 94.107 | -6.439 | Cinnamic acids and derivatives | 354.095@4.3910007 |
| 353.0879 | 4.3999968 | Isochlorogenic acid | 5315832 | 96.397 | -4.088 | Cinnamic acids and derivatives | 354.0951@4.3999968 |
| 163.0389 | 5.1650023 | 4-Hydroxyindene-1,3-dione | 59734489 | 99.996 | -89.269 | Coumarins and derivatives | 162.0318@5.1650023 |
| 226.144 | 5.2050004 | 1-[4-(2-Hydroxyethoxy)piperidin-1-yl]pent-4-yn-1-one | 108021304 | 100 | -137.712 | Piperidines | 225.1367@5.2050004 |
| 137.0245 | 5.3049946 | Protocatechualdehyde | 8768 | 100 | -10.916 | Catechols | 138.0317@5.3049946 |
| 129.0544 | 5.391999 | (R)-6-methyldihydro-2H-pyran-2,4(3H)-dione | 11804775 | 100 | -68.217 | Carboxylic acid and derivatives | 128.047@5.391999 |
| 164.0683 | 5.931 | InChI=1S/C7H11NO2/c1-2-8-6-4-3-5-7(9)10/h1,8H,3-6H2,(H,9,10) | N/A | 100 | -88.998 | Pyridines and derivatives | 141.079@5.931 |
| 171.1128 | 6.0820003 | 3,6-Diethylpiperazine-2,5-dione | 12206391 | 100 | -80.681 | Amino acids, peptides and analogues | 170.1056@6.0820003 |
| 227.1027 | 6.3680043 | Pyroglutamylproline | 13306588 | 57.317 | -48.526 | Amino acids, peptides and analogues | 226.0954@6.3680043 |
| 204.102 | 6.3909984 | (2E,4E)-5-(4-aminophenyl)-4-methylpenta-2,4-dienoic acid | 87494677 | 99.946 | -83.993 | Benzene and substituted derivatives | 203.0946@6.3909984 |
| 269.1133 | 6.748996 | 1-[2-(2,5-Dioxopyrrolidin-1-yl)acetyl]piperidine-4-carboxylic acid | 60644262 | 99.906 | -140.62 | Amino acids, peptides and analogues | 268.1059@6.748996 |
| 269.1133 | 6.934998 | 1-[2-(2,5-Dioxopyrrolidin-1-yl)acetyl]piperidine-4-carboxylic acid | 60644262 | 99.879 | -139.319 | Amino acids, peptides and analogues | 268.106@6.934998 |
| 355.1026 | 7.014005 | Caffeoylquinic acid | | 75.274 | -4.493 | Cinnamic acids and derivatives | 354.0952@7.014005 |
| 337.0929 | 7.2180004 | p-Coumaroylquinic acid | 92135638 | 48.849 | -13.936 | Cinnamic acids and derivatives | 338.1001@7.2180004 |
| 269.1132 | 7.3469925 | 1-[3-(2,5-Dioxopyrrolidin-1-yl)propanoyl]pyrrolidine-3-carboxylic acid | 63032159 | 99.997 | -148.523 | Carboxylic acid and derivatives | 268.106@7.3469925 |
| 353.0877 | 7.3569965 | Isochlorogenic acid | 5315832 | 99.908 | -4.428 | Cinnamic acids and derivatives | 354.0948@7.3569965 |

Table O.5
cont.

| Prec. m/z | Ret. time (min) | SIRIUS NAME | PUBCHEM ID | SIRIUS SCORE | CSI SCORE | Class | Compound |
|---|---|---|---|---|---|---|---|
| 151.0402 | 7.683998 | 2',5'-Dihydroxyacetophenone | 10279 | 100 | -19.216 | Simple phenolic acids | 152.0474@7.683998 |
| 359.0772 | 8.145997 | 3-(3,4-dihydroxyphenyl)-3-[(E)-3-(3,4-dihydroxyphenyl)prop-2-enoyl]oxypropanoic acid | 68980299 | 91.723 | -137.301 | Catechols | 360.0845@8.145997 |
| 375.0697 | 8.614994 | [(2R,3S,4R,5R)-3,4-dihydroxy-5-(6-oxo-1H-purin-9-yl)oxolan-2-yl]methyl dimethyl phosphate | 136187603 | 70.431 | -113.901 | Purine ribonucleotides | 376.0771@8.614994 |
| 355.1033 | 8.881003 | cis-2-Glucosyloxy-4-methoxycinnamic acid | 129707764 | 99.635 | -62.203 | Carbohydrate and carbohydrate conjugates | 356.1107@8.881003 |
| 369.118 | 8.967005 | 3-O-Feruloylquinic acid | 9799386 | 99.506 | -8.838 | Cinnamic acids and derivatives | 368.1109@8.967005 |
| 367.1034 | 8.977998 | Feruloylquinic acid | 101024370 | 65.633 | -6.201 | Cinnamic acids and derivatives | 368.1108@8.977998 |
| 235.0614 | 9.295999 | Diethyl 2,5-dihydroxyterephthalate | 79980 | 99.99 | -109.395 | Benzopyrans | 236.0686@9.295999 |
| 367.1035 | 9.495989 | Feruloylquinic acid | 73210496 | 99.993 | -6.37 | Cinnamic acids and derivatives | 368.1109@9.495989 |
| 265.116 | 9.593996 | 6-Oxo-6-[(5-oxopyrrolidin-2-yl)methylamino]hexanoic acid | 64431570 | 100 | -107.552 | Amino acids, peptides and analogues | 242.1269@9.593996 |
| 243.1341 | 9.593996 | Pyroglutamyl isoleucine | 22799706 | 75.842 | -45.383 | Amino acids, peptides and analogues | 242.1269@9.593996 |
| 241.1195 | 9.613 | Pyroglutamyl isoleucine | 22799706 | 100 | -37.561 | Amino acids, peptides and analogues | 242.1268@9.613 |
| 261.1238 | 9.729003 | Cyclo(L-pro-L-tyr) | 119404 | 45.469 | -16.049 | Amino acids, peptides and analogues | 260.1172@9.729003 |
| 197.1285 | 9.733001 | Cyclo(Pro-Val) |  | 99.999 | -13.658 | Amino acids, peptides and analogues | 196.1213@9.733001 |
| 335.0773 | 9.760994 | Caffeoylquinic acid | 124136972 | 99.593 | -7.09 | Cinnamic acids and derivatives | 336.0846@9.760994 |
| 195.1129 | 9.843996 | Cyclo(Pro-Pro) | 529063 | 99.936 | -26.718 | Amino acids, peptides and analogues | 194.1057@9.843996 |
| 533.1299 | 10.181009 | (1R,3S,4S,5S)-3-[(E)-3-(3,4-dihydroxyphenyl)prop-2-enoyl]oxy-1,5-dihydroxy-4-(4-hydroxy-3,5-dimethoxybenzoyl)oxycyclohexane-1-carboxylic acid | 46185340 | 77.889 | -143.49 | Cinnamic acids and derivatives | 534.1373@10.181009 |

Table O.5 cont.

| Prec. m/z | Ret. time (min) | SIRIUS NAME | PUBCHEM ID | SIRIUS SCORE | CSI SCORE | Class | Compound |
|---|---|---|---|---|---|---|---|
| 197.1285 | 10.190996 | Cyclo(Pro-Val) | | 100 | -20.146 | Amino acids, peptides and analogues | 196.1212@10.190996 |
| 337.0931 | 10.25 | p-Coumaroylquinic acid | 92135638 | 94.315 | -20.314 | Cinnamic acids and derivatives | 338.1001@10.25 |
| 287.0562 | 10.293003 | Eriodyctiol (flavanone) | 373261 | 99.87 | -98.975 | Catechols | 288.0635@10.293003 |
| 333.1558 | 10.474 | Glycinamide, 5-oxo-L-prolyl-L-phenylalanyl- | 7408721 | 99.062 | -140.281 | Amino acids, peptides and analogues | 332.1483@10.474 |
| 331.1413 | 10.480002 | Glycinamide, 5-oxo-L-prolyl-L-phenylalanyl- | 7408721 | 99.994 | -140.723 | Amino acids, peptides and analogues | 332.1484@10.480002 |
| 353.0878 | 10.526996 | Caffeoylquinic acid | 124136972 | 96.447 | -6.301 | Cinnamic acids and derivatives | 354.095@10.526996 |
| 219.1129 | 10.537999 | Cyclo(Ala-Phe) | 139767 | 100 | -122.259 | Amino acids, peptides and analogues | 218.1056@10.537999 |
| 241.1196 | 10.609002 | Pyroglutamylleucine | 152417 | 100 | -60.803 | Amino acids, peptides and analogues | 242.1268@10.609002 |
| 335.0774 | 10.744996 | Isodactylifric acid | 131751510 | 99.978 | -67.694 | Cinnamic acids and derivatives | 336.0847@10.744996 |
| 395.1035 | 10.744996 | 1beta-[(E)-3-(3,4-Dihydroxyphenyl)propenoyloxy]-3alpha,5alpha-dihydroxy-2alpha-acetoxycyclohexane-5beta-carboxylic acid | 102313807 | 97.73 | -38.241 | Cinnamic acids and derivatives | 336.0847@10.744996 |
| 135.0451 | 10.857991 | 4-vinylcatechol | 151398 | 100 | -54.35 | Catechols | 136.0525@10.857991 |
| 335.0773 | 10.866014 | Isodactylifric acid | 131751510 | 99.973 | -79.348 | Cinnamic acids and derivatives | 336.0846@10.866014 |
| 337.0918 | 10.956986 | 5-Caffeoylshikimic acid | 5281762 | 96.265 | -51.285 | Cinnamic acids and derivatives | 336.0847@10.956986 |
| 335.0774 | 11.067005 | Isodactylifric acid | 131751510 | 99.99 | -66.403 | Cinnamic acids and derivatives | 336.0847@11.067005 |
| 315.0874 | 11.170998 | 2-(3,4-Dihydroxyphenyl)-3,7-dimethoxy-2,3-dihydrochromen-4-one | 162972586 | 99.97 | -127.481 | Catechols | 316.0949@11.170998 |
| 361.0932 | 11.170998 | bis(4-methoxyphenyl) (2R,3R)-2,3-dihydroxybutanedioate | 89106310 | 49.499 | -147.623 | Phenol lipids | 316.0949@11.170998 |

Table O.5
cont.

| Prec. m/z | Ret. time (min) | SIRIUS NAME | PUBCHEM ID | SIRIUS SCORE | CSI SCORE | Class | Compound |
|---|---|---|---|---|---|---|---|
| 193.0508 | 11.226008 | 1,4-Phenylenediacetic acid | 81760 | 100 | -63.182 | Cinnamic acids and derivatives | 194.0581@11.226008 |
| 188.107 | 11.239996 | 5-Methyl-6-penta-1,3-dienylpyridine-2-carbaldehyde | 123147823 | 99.893 | -77.117 | Pyridines and derivatives | 187.0997@11.239996 |
| 391.1002 | 11.294002 | 3-O-Feruloylquinic acid | 9799386 | 97.418 | -12.566 | Cinnamic acids and derivatives | 368.1109@11.294002 |
| 703.1881 | 11.33399 | 3beta-[3-[4-[6-O-[3-(3,5-Dimethoxy-4-hydroxyphenyl)acryloyl]-beta-D-glucopyranosyloxy]-3-hydroxyphenyl]acryloyloxy]-1,4alpha,5alpha-trihydroxycyclohexane-1beta-carboxylic acid | 49788419 | 91.341 | -115.394 | Cinnamic acids and derivatives | 704.1951@11.33399 |
| 337.0921 | 11.346004 | 5-Caffeoylshikimic acid | 5281762 | 83.364 | -54.876 | Cinnamic acids and derivatives | 336.0847@11.346004 |
| 335.0774 | 11.354003 | 4-o-Caffeoylshikimic acid | 49821869 | 99.459 | -63.819 | Cinnamic acids and derivatives | 336.0846@11.354003 |
| 137.0608 | 11.691998 | 2-Methoxy-4-methylphenol | 7144 | 100 | -21.268 | Methoxyphenols | 138.0681@11.691998 |
| 211.1442 | 11.807005 | Cyclo(D-Leu-L-Pro) | 927565 | 32.083 | -15.151 | Amino acids, peptides and analogues | 210.1371@11.807005 |
| 335.0773 | 11.958991 | Isodactylifric acid | 131751510 | 99.36 | -65.193 | Cinnamic acids and derivatives | 336.0845@11.958991 |
| 233.1264 | 12.031004 | 2-[4-Amino-1-hydroxy-2-(methylamino)butyl]phenol | 83930490 | 42.703 | -127.291 | Alcohols and polyols | 210.1369@12.031004 |
| 211.1441 | 12.031004 | Cyclo(D-Leu-L-Pro) | 927565 | 100 | -6.712 | Amino acids, peptides and analogues | 210.1369@12.031004 |
| 369.1181 | 12.045996 | 3-O-Feruloylquinic acid | 9799386 | 95.884 | -10.524 | Cinnamic acids and derivatives | 368.1108@12.045996 |
| 367.1038 | 12.056011 | Methyl chlorogenate | 6476139 | 99.559 | -12.249 | Cinnamic acids and derivatives | 368.1105@12.056011 |
| 349.093 | 12.0750065 | Feruloylquinic acid | 139031501 | 99.97 | -8.719 | Cinnamic acids and derivatives | 350.1001@12.0750065 |
| 428.3235 | 12.1710005 | H-Leu-Leu-Leu-Ala-NH2 | 22839695 | 100 | -74.786 | Amino acids, peptides and analogues | 427.3159@12.1710005 |

Table O.5 cont.

| Prec. m/z | Ret. time (min) | SIRIUS NAME | PUBCHEM ID | SIRIUS SCORE | CSI SCORE | Class | Compound |
|---|---|---|---|---|---|---|---|
| 319.0826 | 12.356997 | 4-O-(p-coumaroyl)shikimic acid | 101712560 | 99.921 | -59.54 | Cinnamic acids and derivatives | 320.0897@12.356997 |
| 213.1599 | 12.390998 | Cyclo(Leu-Val) | 138543 | 100 | -40.027 | Amino acids, peptides and analogues | 212.1526@12.390998 |
| 211.1442 | 12.440997 | Cyclo(D-Leu-L-Pro) | 927565 | 100 | -13.325 | Amino acids, peptides and analogues | 210.1369@12.440997 |
| 349.0931 | 12.609005 | 3,4-dihydroxy-5-[(E)-3-(4-hydroxy-3-methoxyphenyl)prop-2-enoyl]oxycyclohexene-1-carboxylic acid | 131836358 | 98.62 | -90.445 | Cinnamic acids and derivatives | 350.1003@12.609005 |
| 351.1075 | 12.638998 | 3,4-dihydroxy-5-[(E)-3-(4-hydroxy-3-methoxyphenyl)prop-2-enoyl]oxycyclohexene-1-carboxylic acid | 131836358 | 98.586 | -67.669 | Cinnamic acids and derivatives | 350.1004@12.638998 |
| 351.1075 | 12.887008 | 3,4-dihydroxy-5-[(E)-3-(4-hydroxy-3-methoxyphenyl)prop-2-enoyl]oxycyclohexene-1-carboxylic acid | 131836358 | 99.374 | -87.25 | Cinnamic acids and derivatives | 350.1004@12.887008 |
| 349.093 | 12.893994 | 3,4-dihydroxy-5-[(E)-3-(4-hydroxy-3-methoxyphenyl)prop-2-enoyl]oxycyclohexene-1-carboxylic acid | 131836358 | 99.97 | -86.643 | Cinnamic acids and derivatives | 350.1005@12.893994 |
| 427.2551 | 12.923998 | H-DL-Leu-DL-xiThr-DL-Pro-DL-Pro-OH | 18301026 | 99.769 | -127.294 | Amino acids, peptides and analogues | 426.2479@12.923998 |
| 425.2406 | 12.937008 | H-DL-xiThr-DL-Pro-DL-Pro-DL-Leu-OH | 18750976 | 99.398 | -147.912 | Amino acids, peptides and analogues | 426.2478@12.937008 |
| 193.0508 | 12.9400015 | Isoferulic acid | 736186 | 99.998 | -15.818 | Cinnamic acids and derivatives | 194.058@12.9400015 |
| 481.2445 | 13.161991 | 3alpha-(beta-D-Glucopyranuronosyloxy)-6beta-hydroxy-5beta-androstane-17-one | 122381121 | 46.306 | -126.124 | Phenol lipids | 482.2515@13.161991 |
| 203.0715 | 13.427001 | p-Hydroxy-beta,beta-diacetylstyrene | 334612 | 100 | -68.494 | Shikimates and Phenylpropanoids | 204.0788@13.427001 |
| 583.3461 | 14.229003 | H-Pro-Leu-Leu-Asp-Lys-OH | 11592336 | 94.851 | -99.411 | Amino acids, peptides and analogues | 538.3474@14.229003 |
| 319.1915 | 14.231005 | 1,1'-[(Ethene-1,1-diyl)(ethene-1,1-diyl)]bis(1-cyclohexene 4-methanol) | 102113399 | 32.465 | -86.195 | Phenol lipids | 320.1989@14.231005 |
| 193.0872 | 15.363005 | trans-Anol | 5474441 | 33.299 | -43.276 | Cinnamic acids and derivatives | 194.0944@15.363005 |

# Appendix P: Relative abundance values of MS2 annotated polyphenols in coffee

Table P.1 Relative abundance values of MS2 annotated polyphenols in coffee at different roasted degree. Values were normalised against the abundance of internal standard (i.e.Sinapic acid)

| | Arabica Washed | | | | Arabica Unwashed | | | | Robusta Unwashed | | | |
|---|---|---|---|---|---|---|---|---|---|---|---|---|
| Compound | R0 min | R2 min | R4 min | R6 min | R0 min | R2 min | R4 min | R6 min | R0 min | R2 min | R4 min | R6 min |
| 3-Methylcatechol | 0.0000 | 0.0000 | 0.0000 | 0.0007 | 0.0003 | 0.0000 | 0.0000 | 0.0007 | 0.0000 | 0.0000 | 0.0000 | 0.0000 |
| 4-Ethylcatechol | 0.0001 | 0.0000 | 0.0000 | 0.0000 | 0.0000 | 0.0000 | 0.0000 | 0.0014 | 0.0000 | 0.0000 | 0.0000 | 0.0002 |
| 4-Vinylcatechol | 0.0023 | 0.0000 | 0.0000 | 0.0004 | 0.0000 | 0.0000 | 0.0000 | 0.0000 | 0.0036 | 0.0057 | 0.0035 | 0.0016 |
| 4-Vinylguaiacol | 0.0021 | 0.0011 | 0.0024 | 0.0000 | 0.0021 | 0.0015 | 0.0033 | 0.0000 | 0.0000 | 0.0015 | 0.0020 | 0.0000 |
| Caffeic acid | 0.0633 | 0.0472 | 0.0170 | 0.0075 | 0.0274 | 0.0426 | 0.0148 | 0.0062 | 0.2787 | 0.0784 | 0.0244 | 0.0129 |
| Caffeoyl quinolactone alpha | 0.0020 | 0.0025 | 0.0166 | 0.0277 | 0.0015 | 0.0021 | 0.0187 | 0.0259 | 0.0007 | 0.0029 | 0.0287 | 0.0455 |
| Caffeoyl quinolactone beta | 0.0009 | 0.0000 | 0.0040 | 0.0057 | 0.0000 | 0.0000 | 0.0043 | 0.0052 | 0.0000 | 0.0000 | 0.0051 | 0.0050 |
| Caffeoyl-feruloyl-quinic acid alpha | 0.2245 | 0.1294 | 0.0546 | 0.0178 | 0.1290 | 0.0877 | 0.0359 | 0.0120 | 0.5498 | 0.7761 | 0.4251 | 0.1381 |
| Caffeoyl-feruloyl-quinic acid beta | 0.0708 | 0.0470 | 0.0175 | 0.0060 | 0.0320 | 0.0352 | 0.0126 | 0.0061 | 0.1997 | 0.2977 | 0.1488 | 0.0631 |
| Caffeoyl-feruloyl-quinic acid gamma | 0.0011 | 0.0000 | 0.0018 | 0.0028 | 0.0011 | 0.0000 | 0.0000 | 0.0018 | 0.0011 | 0.0000 | 0.0034 | 0.0038 |
| Caffeoylquinic acid gamma | 0.0017 | 0.0168 | 0.0588 | 0.0479 | 0.0010 | 0.0190 | 0.0662 | 0.0455 | 0.0022 | 0.0189 | 0.0758 | 0.0720 |

| | Arabica Washed | | | | Arabica Unwashed | | | | Robusta Unwashed | | | |
|---|---|---|---|---|---|---|---|---|---|---|---|---|
| Compound | R0 min | R2 min | R4 min | R6 min | R0 min | R2 min | R4 min | R6 min | R0 min | R2 min | R4 min | R6 min |
| Catechol | 0.0000 | 0.0000 | 0.0000 | 0.0000 | 0.0001 | 0.0013 | 0.0000 | 0.0000 | 0.0000 | 0.0005 | 0.0016 | 0.0000 |
| di-Caffeoyl quinolactone alpha | 0.0000 | 0.0047 | 0.0134 | 0.0051 | 0.0000 | 0.0052 | 0.0128 | 0.0055 | 0.0000 | 0.0146 | 0.0475 | 0.0264 |
| di-Caffeoyl quinolactone beta | 0.0000 | 0.0000 | 0.0035 | 0.0007 | 0.0000 | 0.0000 | 0.0027 | 0.0017 | 0.0000 | 0.0017 | 0.0093 | 0.0059 |
| di-Caffeoylquinic acid beta | 0.0000 | 0.0000 | 0.0129 | 0.0104 | 0.0000 | 0.0000 | 0.0136 | 0.0098 | 0.0000 | 0.0000 | 0.0000 | 0.0287 |
| di-Feruloylquinic acid alpha | 0.0112 | 0.0026 | 0.0016 | 0.0019 | 0.0026 | 0.0044 | 0.0000 | 0.0000 | 0.0142 | 0.0261 | 0.0171 | 0.0081 |
| di-Feruloylquinic acid beta | 0.0221 | 0.0143 | 0.0066 | 0.0000 | 0.0027 | 0.0079 | 0.0000 | 0.0000 | 0.0251 | 0.0446 | 0.0172 | 0.0066 |
| Epigallocatechin gallate | 0.0016 | 0.0015 | 0.0015 | 0.0017 | 0.0010 | 0.0015 | 0.0013 | 0.0017 | 0.0017 | 0.0017 | 0.0019 | 0.0012 |
| Ferulic acid | 0.0110 | 0.0041 | 0.0056 | 0.0041 | 0.0057 | 0.0033 | 0.0052 | 0.0061 | 0.0296 | 0.0173 | 0.0054 | 0.0047 |
| Feruloylquinolactone alpha | 0.0021 | 0.0092 | 0.1053 | 0.1591 | 0.0007 | 0.0088 | 0.1001 | 0.1326 | 0.0000 | 0.0201 | 0.2270 | 0.4188 |
| Feruloylquinolactone beta | 0.0000 | 0.0000 | 0.0006 | 0.0024 | 0.0000 | 0.0017 | 0.0012 | 0.0006 | 0.0000 | 0.0000 | 0.0000 | 0.0025 |
| Guaiacol | 0.0000 | 0.0000 | 0.0002 | 0.0000 | 0.0000 | 0.0000 | 0.0000 | 0.0000 | 0.0000 | 0.0000 | 0.0000 | 0.0000 |
| p-Coumaroylquinic acid alpha | 0.2061 | 0.1331 | 0.0681 | 0.0412 | 0.2458 | 0.1632 | 0.0920 | 0.0446 | 0.0670 | 0.0941 | 0.0634 | 0.0349 |
| p-Coumaroylquinic acid beta | 0.0000 | 0.0002 | 0.0000 | 0.0004 | 0.0000 | 0.0000 | 0.0000 | 0.0000 | 0.0000 | 0.0000 | 0.0000 | 0.0000 |
| p-Coumaroylquinic acid gamma | 0.0435 | 0.0470 | 0.0393 | 0.0249 | 0.0503 | 0.0611 | 0.0534 | 0.0302 | 0.0172 | 0.0307 | 0.0321 | 0.0350 |
| p-Coumaroylquinolactone | 0.0000 | 0.0022 | 0.0243 | 0.0379 | 0.0007 | 0.0027 | 0.0334 | 0.0462 | 0.0000 | 0.0020 | 0.0148 | 0.0307 |
| Phenol | 0.0007 | 0.0009 | 0.0000 | 0.0049 | 0.0005 | 0.0005 | 0.0000 | 0.0052 | 0.0007 | 0.0007 | 0.0018 | 0.0054 |

| | Arabica Washed | | | | Arabica Unwashed | | | | Robusta Unwashed | | | |
|---|---|---|---|---|---|---|---|---|---|---|---|---|
| Compound | R0 min | R2 min | R4 min | R6 min | R0 min | R2 min | R4 min | R6 min | R0 min | R2 min | R4 min | R6 min |
| Pyrogallol | 0.0001 | 0.0001 | 0.0000 | 0.0000 | 0.0000 | 0.0002 | 0.0000 | 0.0000 | 0.0007 | 0.0000 | 0.0000 | 0.0000 |
| Quinic acid | 1.3525 | 1.0569 | 0.6333 | 0.2446 | 1.2493 | 0.9976 | 0.6151 | 0.2204 | 1.0235 | 1.2134 | 0.8257 | 0.3853 |
| Quinolactone | 0.0000 | 0.0000 | 0.0019 | 0.0021 | 0.0000 | 0.0000 | 0.0017 | 0.0019 | 0.0000 | 0.0006 | 0.0012 | 0.0024 |
| Roasted Caffeic Acid product alpha | 0.0000 | 0.0003 | 0.0014 | 0.0024 | 0.0005 | 0.0003 | 0.0015 | 0.0017 | 0.0000 | 0.0013 | 0.0022 | 0.0028 |
| Roasted Caffeic Acid product beta | 0.0000 | 0.0000 | 0.0003 | 0.0004 | 0.0000 | 0.0000 | 0.0014 | 0.0005 | 0.0000 | 0.0002 | 0.0003 | 0.0000 |
| Salicylic acid | 0.0105 | 0.0411 | 0.0970 | 0.0728 | 0.0136 | 0.0434 | 0.0868 | 0.0582 | 0.0283 | 0.1043 | 0.1152 | 0.0871 |

Table P.2 Relative abundance values of MS2 annotated polyphenols in Robusta and Arabica coffee at different manufacture stages (i.e. Green Bean, Roasted Bean, Instant coffee). Values were normalised against the abundance of internal standard (i.e.Sinapic acid).

| | Robusta | | | Arabica | | |
|---|---|---|---|---|---|---|
| Compound | Green Bean | Roasted Bean | Instant Coffee | Green Bean | Roasted Bean | Instant Coffee |
| 3-Methylcatechol | 0.0006 | 0.0008 | 0.0015 | 0.0003 | 0.0000 | 0.0017 |
| 4-Ethylcatechol | 0.0000 | 0.0021 | 0.0015 | 0.0002 | 0.0000 | 0.0028 |
| 4-Vinylcatechol | 0.0045 | 0.0000 | 0.0012 | 0.0000 | 0.0000 | 0.0006 |
| 4-Vinylguaiacol | 0.0023 | 0.0039 | 0.0008 | 0.0017 | 0.0019 | 0.0009 |
| Caffeic acid | 0.4689 | 0.0068 | 0.0646 | 0.0518 | 0.0077 | 0.0686 |
| Caffeoyl quinolactone alpha | 0.0013 | 0.0265 | 0.0500 | 0.0000 | 0.0260 | 0.0632 |
| Caffeoyl quinolactone beta | 0.0000 | 0.0039 | 0.0071 | 0.0000 | 0.0060 | 0.0108 |

| | Robusta | | | Arabica | | |
|---|---|---|---|---|---|---|
| Compound | Green Bean | Roasted Bean | Instant Coffee | Green Bean | Roasted Bean | Instant Coffee |
| Caffeoyl-feruloyl-quinic acid alpha | 0.9274 | 0.0216 | 0.1238 | 0.0831 | 0.0148 | 0.0588 |
| Caffeoyl-feruloyl-quinic acid beta | 0.3349 | 0.0111 | 0.0461 | 0.0242 | 0.0059 | 0.0172 |
| Caffeoyl-feruloyl-quinic acid gamma | 0.0019 | 0.0000 | 0.0043 | 0.0011 | 0.0000 | 0.0000 |
| Caffeoylquinic acid gamma | 0.0026 | 0.0201 | 0.0894 | 0.0011 | 0.0703 | 0.1768 |
| Catechol | 0.0000 | 0.0000 | 0.0024 | 0.0000 | 0.0002 | 0.0000 |
| di-Caffeoyl quinolactone alpha | 0.0017 | 0.0034 | 0.0211 | 0.0000 | 0.0068 | 0.0456 |
| di-Caffeoyl quinolactone beta | 0.0000 | 0.0000 | 0.0103 | 0.0000 | 0.0015 | 0.0205 |
| di-Caffeoylquinic acid beta | 0.0000 | 0.0059 | 0.0159 | 0.0000 | 0.0121 | 0.0241 |
| di-Feruloylquinic acid alpha | 0.0201 | 0.0057 | 0.0145 | 0.0202 | 0.0020 | 0.0065 |
| di-Feruloylquinic acid beta | 0.0314 | 0.0159 | 0.0077 | 0.0348 | 0.0000 | 0.0049 |
| Epigallocatechin gallate | 0.0025 | 0.0013 | 0.0016 | 0.0013 | 0.0017 | 0.0030 |
| Ferulic acid | 0.0735 | 0.0042 | 0.0175 | 0.0082 | 0.0068 | 0.0205 |
| Feruloylquinolactone alpha | 0.0012 | 0.2032 | 0.4159 | 0.0000 | 0.1058 | 0.2832 |
| Feruloylquinolactone beta | 0.0000 | 0.0007 | 0.0010 | 0.0000 | 0.0011 | 0.0034 |
| Guaiacol | 0.0000 | 0.0000 | 0.0018 | 0.0000 | 0.0007 | 0.0018 |

| | Robusta | | | Arabica | | |
|---|---|---|---|---|---|---|
| Compound | Green Bean | Roasted Bean | Instant Coffee | Green Bean | Roasted Bean | Instant Coffee |
| p-Coumaroylquinic acid alpha | 0.1341 | 0.0180 | 0.0331 | 0.2280 | 0.0600 | 0.1203 |
| p-Coumaroylquinic acid beta | 0.0000 | 0.0000 | 0.0000 | 0.0000 | 0.0000 | 0.0000 |
| p-Coumaroylquinic acid gamma | 0.0299 | 0.0123 | 0.0268 | 0.0267 | 0.0271 | 0.0590 |
| p-Coumaroylquinolactone | 0.0004 | 0.0186 | 0.0406 | 0.0000 | 0.0349 | 0.0865 |
| Phenol | 0.0006 | 0.0090 | 0.0075 | 0.0008 | 0.0039 | 0.0036 |
| Pyrogallol | 0.0000 | 0.0000 | 0.0292 | 0.0000 | 0.0000 | 0.0000 |
| Quinic acid | 1.3902 | 0.0762 | 0.2628 | 1.4549 | 0.4062 | 0.6722 |
| Quinolactone | 0.0002 | 0.0000 | 0.0018 | 0.0008 | 0.0018 | 0.0042 |
| Roasted Caffeic Acid product alpha | 0.0000 | 0.0031 | 0.0091 | 0.0000 | 0.0006 | 0.0077 |
| Roasted Caffeic Acid product beta | 0.0000 | 0.0036 | 0.0000 | 0.0000 | 0.0004 | 0.0000 |
| Salicylic acid | 0.0419 | 0.0581 | 0.2599 | 0.0104 | 0.0786 | 0.1869 |

# Appendix Q:Foam quality assessment of centrifuged and ultracentrifuged control instant coffee

The present thesis was focused on the influence of chemical compounds on foaming quality. However, it has been reported in the literature that also fine particulates can influence the foam ability and foam stability. For this reason, three instant coffee sample was prepared as per Chapter 3. One instant coffee sample was centrifuged @3739 g while the other was ultra centrifuged @ 18000g. The foaming ability was evaluated as per Chapter 3 of the present thesis. It is observed that the absence of particles, did not influence the foam ability but increased both the Drainage rate (i.e. b parameter) and the Disproportion/Coalescence rate (i.e. d parameter). It can be hypothesized that the absence of particles decreased the viscosity of continuous phase.

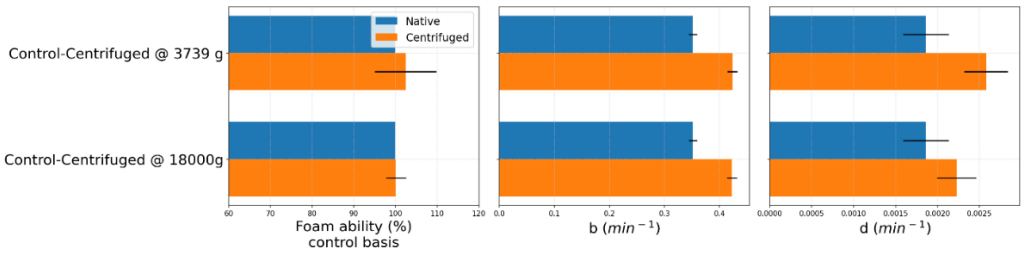



Figure Q.1 Foam quality parameters for native control instant coffee, centrifuged control instant coffee @ 3739g and control instant coffee centrifuged @ 18000g.